EPIGENETIC AND TRANSCRIPTIONAL DYSREGULATIONS IN CANCER AND THERAPEUTIC OPPORTUNITIES

EDITED BY: Ata Abbas and Rais Ahmad Ansari
PUBLISHED IN: Frontiers in Genetics and
Frontiers in Cell and Developmental Biology

frontiers Research Topics

ISSN 1664-8714
ISBN 978-2-88976-657-4
DOI 10.3389/978-2-88976-657-4

About Frontiers

Frontiers is more than just an open-access publisher of scholarly articles: it is a pioneering approach to the world of academia, radically improving the way scholarly research is managed. The grand vision of Frontiers is a world where all people have an equal opportunity to seek, share and generate knowledge. Frontiers provides immediate and permanent online open access to all its publications, but this alone is not enough to realize our grand goals.

Frontiers Journal Series

The Frontiers Journal Series is a multi-tier and interdisciplinary set of open-access, online journals, promising a paradigm shift from the current review, selection and dissemination processes in academic publishing. All Frontiers journals are driven by researchers for researchers; therefore, they constitute a service to the scholarly community. At the same time, the Frontiers Journal Series operates on a revolutionary invention, the tiered publishing system, initially addressing specific communities of scholars, and gradually climbing up to broader public understanding, thus serving the interests of the lay society, too.

Dedication to Quality

Each Frontiers article is a landmark of the highest quality, thanks to genuinely collaborative interactions between authors and review editors, who include some of the world's best academicians. Research must be certified by peers before entering a stream of knowledge that may eventually reach the public - and shape society; therefore, Frontiers only applies the most rigorous and unbiased reviews.
Frontiers revolutionizes research publishing by freely delivering the most outstanding research, evaluated with no bias from both the academic and social point of view. By applying the most advanced information technologies, Frontiers is catapulting scholarly publishing into a new generation.

What are Frontiers Research Topics?

Frontiers Research Topics are very popular trademarks of the Frontiers Journals Series: they are collections of at least ten articles, all centered on a particular subject. With their unique mix of varied contributions from Original Research to Review Articles, Frontiers Research Topics unify the most influential researchers, the latest key findings and historical advances in a hot research area! Find out more on how to host your own Frontiers Research Topic or contribute to one as an author by contacting the Frontiers Editorial Office: frontiersin.org/about/contact

EPIGENETIC AND TRANSCRIPTIONAL DYSREGULATIONS IN CANCER AND THERAPEUTIC OPPORTUNITIES

Topic Editors:
Ata Abbas, Case Western Reserve University, United States
Rais Ahmad Ansari, Nova Southeastern University, United States

Citation: Abbas, A., Ansari, R. A., eds. (2022). Epigenetic and Transcriptional Dysregulations in Cancer and Therapeutic Opportunities.
Lausanne: Frontiers Media SA. doi: 10.3389/978-2-88976-657-4

Table of Contents

frontiers in Genetics

EDITORIAL
published: 22 February 2022
doi: 10.3389/fgene.2022.857380

Editorial: Epigenetic and Transcriptional Dysregulations in Cancer and Therapeutic Opportunities

Rais A. Ansari[1] *and Ata Abbas*[2,3]*

[1]Department of Pharmaceutical Sciences, Nova Southeastern University, Fort Lauderdale, FL, United States, [2]Division of Hematology and Oncology, Department of Medicine, Case Western Reserve University, Cleveland, OH, United States, [3]Case Comprehensive Cancer Center, Case Western Reserve University School of Medicine, Cleveland, OH, United States

Keywords: epigenetics, transcription, transcriptional dysregultaion, cancer, cancer therapies

Editorial on the Research Topic

Epigenetic and Transcriptional Dysregulations in Cancer and Therapeutic Opportunities

Aberrations in epigenetic regulation at various levels, including DNA methylation, chromatin architecture, and regulatory RNAs, are often associated with, and significantly contribute in most carcinogenesis (Jones and Baylin, 2007; Baylin and Jones, 2016). Transcriptional dysregulation is another hallmark of nearly all kinds of cancers (Hanahan, 2022). Gene transcription is a complex process and highly regulated at various stages as well as at the post-transcriptional level (Corbett, 2018; Roeder, 2019). Epigenetic and transcriptional events often influence each other, e.g., DNA methylation and histone modifications regulate gene transcription, and transcriptional processes can modify chromatin architectures (Bonasio et al., 2010; Gibney and Nolan, 2010). Increasing numbers of evidence suggest epigenetic and transcriptional dysregulations play vital roles in carcinogenesis, including metastasis, aggressiveness, and recurrence of malignancies (Bradner et al., 2017; Hanahan, 2022). An in-depth understanding of both epigenetic and transcriptional processes and alterations in their regulations are needed to better understand tumor pathobiology and to improve clinical management (**Figure 1**). Epigenetic and transcriptional dysregulations also confer therapeutic vulnerabilities and remarkably, offer novel biomarkers and therapeutic targets (Gonda and Ramsay, 2015; Cheng et al., 2019; Lu et al., 2020; Vervoort et al., 2021).

Genome-wide transcriptional control is often dysregulated in cancer. In this research topic, Parrello et al. discussed the possibility of targeting factors that control global transcriptional regulation. Li et al. discussed the dual roles of CBX7, a component of polycomb repressive complex, in cancer where it can either help in cancer progression by downregulating tumor suppressor genes or help cancer suppression by modulating cell cycle related proteins. CBX7 interacts with various regulatory RNAs, including micro RNAs, long non-coding RNAs, circular RNAs. Regulatory RNAs play a significant role in carcinogenesis, including chemo-resistance (Lan et al., Gareev et al., and Zhang et al.). Sun et al. showed that plasma-derived exosomal micro RNA, miR-2276-5p in glioma patients could serve as a potential diagnostic and prognostic marker. Transcriptomics based gene signatures are emerging as promising biomarkers in cancer (Jin et al. and Fang et al.).

Epigenetic landscape is altered in cancer cells that results in transcriptional dysregulation. Various dietary components have ability to modulate epigenetic aberration (Fatima et al. and Raina et al.). Abbas et al. reported that maternal diet rich in omega-3 fatty acid can reprogram epigenetic and transcriptomic landscapes in F1 generation mice and provide resistance to breast cancer development. Pu et al. reported that methylation profiles of zinc finger genes, specially *ESR1* and *ZNF132*, could be potential biomarkers for the early diagnosis of colorectal cancer patients carrying KRAS mutations. Another study by Gua et al. showed that *APOA1* gene is downregulated by DNA methylation in

Edited and reviewed by:
Michael E. Symonds, University of Nottingham, United Kingdom

***Correspondence:**
Ata Abbas
ata.abbas@case.edu

Specialty section:
This article was submitted to Epigenomics and Epigenetics, a section of the journal Frontiers in Genetics

Received: *18 January 2022*
Accepted: *07 February 2022*
Published: *22 February 2022*

Citation:
Ansari RA and Abbas A (2022) Editorial: Epigenetic and Transcriptional Dysregulations in Cancer and Therapeutic Opportunities. Front. Genet. 13:857380. doi: 10.3389/fgene.2022.857380

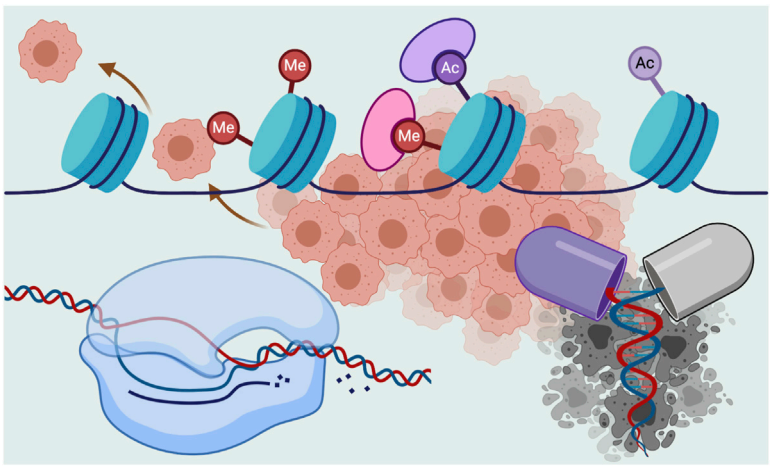

FIGURE 1 | Alteration of epigenetic and transcriptional processes often contribute in carcinogenic events. These alterations can also serve as novel therapeutic targets and biomarkers (created with BioRender.com).

hepatocellular carcinoma that could be a potential biomarker to predict survival. Role of NTPCR in epithelial ovarian cancer (Shang et al.) and FGFR1–GLI1 axis as a potential therapeutic target in breast cancer (Riaz et al.) were also reported.

Gazova et al. used CRISPR-Cas9 to generate homozygous inactivating mutation in *USP16* gene using leukemia cell line and studied how these cells adapt to the extreme selection pressure through compensatory pathways. Authors also cautioned targeting USP16 in leukemia as cancer could develop resistant to USP16 inhibitors. A timely review by Amir et al. discussed the usefulness of combination therapy of tyrosine kinase inhibitors with epigenetic drugs in chronic myeloid leukemia. Leszczynska et al. reviewed the emerging therapeutic approaches against pediatric high-grade gliomas, particularly those having mutations in genes coding for histone 3 variants that result in substitution of lysine at 27 to methionine.

In conclusion, epigenetic aberration and transcriptional homeostasis disruptions are associated with cancer. In-depth understanding of these processes and their interdependencies is needed to better understand carcinogenesis and to develop novel and effective therapeutic approaches.

AUTHOR CONTRIBUTIONS

RAA and AA wrote the manuscript.

REFERENCES

Baylin, S. B., and Jones, P. A. (2016). Epigenetic Determinants of Cancer. *Cold Spring Harb Perspect. Biol.* 8, a019505. doi:10.1101/cshperspect.a019505

Bonasio, R., Tu, S., and Reinberg, D. (2010). Molecular Signals of Epigenetic States. *Science* 330, 612–616. doi:10.1126/science.1191078

Bradner, J. E., Hnisz, D., and Young, R. A. (2017). Transcriptional Addiction in Cancer. *Cell* 168, 629–643. doi:10.1016/j.cell.2016.12.013

Cheng, Y., He, C., Wang, M., Ma, X., Mo, F., Yang, S., et al. (2019). Targeting Epigenetic Regulators for Cancer Therapy: Mechanisms and Advances in Clinical Trials. *Signal. Transduction Targeted Ther.* 4, 62. doi:10.1038/s41392-019-0095-0

Corbett, A. H. (2018). Post-transcriptional Regulation of Gene Expression and Human Disease. *Curr. Opin. Cell Biol.* 52, 96–104. doi:10.1016/j.ceb.2018.02.011

Gibney, E. R., and Nolan, C. M. (2010). Epigenetics and Gene Expression. *Heredity* 105, 4–13. doi:10.1038/hdy.2010.54

Gonda, T. J., and Ramsay, R. G. (2015). Directly Targeting Transcriptional Dysregulation in Cancer. *Nat. Rev. Cancer* 15, 686–694. doi:10.1038/nrc4018

Hanahan, D. (2022). Hallmarks of Cancer: New Dimensions. *Cancer Discov.* 12, 31–46. doi:10.1158/2159-8290.cd-21-1059

Jones, P. A., and Baylin, S. B. (2007). The Epigenomics of Cancer. *Cell* 128, 683–692. doi:10.1016/j.cell.2007.01.029

Lu, Y., Chan, Y. T., Tan, H. Y., Li, S., Wang, N., and Feng, Y. (2020). Epigenetic Regulation in Human Cancer: the Potential Role of Epi-Drug in Cancer Therapy. *Mol. Cancer* 19, 79. doi:10.1186/s12943-020-01197-3

Roeder, R. G. (2019). 50+ Years of Eukaryotic Transcription: an Expanding Universe of Factors and Mechanisms. *Nat. Struct. Mol. Biol.* 26, 783–791. doi:10.1038/s41594-019-0287-x

Vervoort, S. J., Devlin, J. R., Kwiatkowski, N., Teng, M., Gray, N. S., and Johnstone, R. W. (2021). Targeting Transcription Cycles in Cancer. *Nat. Rev. Cancer* 22, 5–24. doi:10.1038/s41568-021-00411-8

Conflict of Interest: The authors declare that the research was conducted in the absence of any commercial or financial relationships that could be construed as a potential conflict of interest.

Publisher's Note: All claims expressed in this article are solely those of the authors and do not necessarily represent those of their affiliated organizations, or those of the publisher, the editors and the reviewers. Any product that may be evaluated in this article, or claim that may be made by its manufacturer, is not guaranteed or endorsed by the publisher.

frontiers in Cell and Developmental Biology

ORIGINAL RESEARCH
published: 31 May 2021
doi: 10.3389/fcell.2021.679544

CRISPR-Cas9 Editing of Human Histone Deubiquitinase Gene *USP16* in Human Monocytic Leukemia Cell Line THP-1

Iveta Gažová[1†‡], Lucas Lefevre[1†‡], Stephen J. Bush[1†‡], Rocio Rojo[1†‡], David A. Hume[2‡], Andreas Lengeling[1†‡] and Kim M. Summers[1,2‡]*

[1] The Roslin Institute, University of Edinburgh, Easter Bush, United Kingdom, [2] Mater Research Institute - University of Queensland, Translational Research Institute, Woolloongabba, QLD, Australia

USP16 is a histone deubiquitinase which facilitates G2/M transition during the cell cycle, regulates DNA damage repair and contributes to inducible gene expression. We mutated the *USP16* gene in a high differentiation clone of the acute monocytic leukemia cell line THP-1 using the CRISPR-Cas9 system and generated four homozygous knockout clones. All were able to proliferate and to differentiate in response to phorbol ester (PMA) treatment. One line was highly proliferative prior to PMA treatment and shut down proliferation upon differentiation, like wild type. Three clones showed sustained expression of the progenitor cell marker *MYB*, indicating that differentiation had not completely blocked proliferation in these clones. Network analysis of transcriptomic differences among wild type, heterozygotes and homozygotes showed clusters of genes that were up- or down-regulated after differentiation in all cell lines. Prior to PMA treatment, the homozygous clones had lower levels than wild type of genes relating to metabolism and mitochondria, including *SRPRB*, encoding an interaction partner of USP16. There was also apparent loss of interferon signaling. In contrast, a number of genes were up-regulated in the homozygous cells compared to wild type at baseline, including other deubiquitinases (*USP12, BAP1*, and *MYSM1*). However, three homozygotes failed to fully induce *USP3* during differentiation. Other network clusters showed effects prior to or after differentiation in the homozygous clones. Thus the removal of USP16 affected the transcriptome of the cells, although all these lines were able to survive, which suggests that the functions attributed to USP16 may be redundant. Our analysis indicates that the leukemic line can adapt to the extreme selection pressure applied by the loss of USP16, and the harsh conditions of the gene editing and selection protocol, through different compensatory pathways. Similar selection pressures occur during the evolution of a cancer *in vivo*, and our results can be seen as a case study in leukemic cell adaptation. USP16 has been considered a target for cancer chemotherapy, but our results suggest that treatment would select for escape mutants that are resistant to USP16 inhibitors.

Keywords: histone deubiquitinases, epigenetic modifications, THP-1 cell line, genome editing, macrophage, monocyte, *USP16* gene

OPEN ACCESS

Edited by:
Ata Abbas,
Case Western Reserve University,
United States

Reviewed by:
Hengbin Wang,
University of Alabama at Birmingham,
United States
Tim M. Townes,
University of Alabama at Birmingham,
United States
Janani Kumar,
University of Texas MD Anderson Cancer Center, United States

****Correspondence:***
Kim M. Summers
kim.summers@mater.uq.edu.au

†Present address:
Iveta Gažová,
MRC HGU, Institute of Genetics and Cancer, University of Edinburgh, Western General Hospital, Edinburgh, United Kingdom
Lucas Lefevre,
Dementia Research Institute, University of Edinburgh, Little France, United Kingdom
Stephen J. Bush,
Nuffield Department of Clinical Medicine, John Radcliffe Hospital, University of Oxford, Oxford, United Kingdom
Rocio Rojo,
Tecnologico de Monterrey, Escuela de Medicina y Ciencias de la Salud, Monterrey, Mexico
Andreas Lengeling,
Max Planck Society Administrative Headquarters, Munich, Germany

Specialty section:
This article was submitted to Epigenomics and Epigenetics, a section of the journal Frontiers in Cell and Developmental Biology

Received: *12 March 2021*
Accepted: *27 April 2021*
Published: *31 May 2021*

INTRODUCTION

The development of a tumorigenic lineage from healthy cells is usually associated with a wide range of genetic changes, including point mutations, small and large deletions and insertions (indels) and chromosomal rearrangements (Vogelstein et al., 2013). A high level of genomic instability in cancer cells allows for novel forms of effector molecules to be produced, but also imposes a genetic load of potentially detrimental mutations. Cancer lineages are heterogeneous with many diverse sublineages arising over time (Heppner, 1984; Vogelstein et al., 2013), and these are subjected to intensive selection pressure as the tumor evolves (Fortunato et al., 2017).

One form of modification in cancer lines is alteration in the epigenetic status of the cells. Addition or removal of repressive marks on histone molecules is a major mechanism for altering gene expression, and a number of genes encoding enzymes associated with histone modifications have been identified as tumor suppressors, for example, the histone deubiquitinase *BAP1* (Abdel-Rahman et al., 2011) and the histone demethylase *KDM6A* (Ler et al., 2017). Ubiquitination of the lysine at position 119 in histone 2A (H2AK119) blocks transcription by preventing RNA polymerase from traveling along the DNA template (Lanzuolo and Orlando, 2012). During transcriptional activation, H2A deubiquitinases remove ubiquitin from H2AK119 (Abdel-Wahab et al., 2012). A small number of these enzymes have been identified, among as many as 100 deubiquitinases in the human genome (Komander et al., 2009; Belle and Nijnik, 2014). These are six ubiquitin specific proteases (USPs; USP3, USP12, USP16, USP21, USP22, and USP46), one ubiquitin C-terminal hydrolase (BAP1) and one Zn^{2+} metalloprotease (MYSM1) (Chen et al., 2015). The present study focused on the role of the histone deubiquitinase USP16.

USP16 (originally named UBP-M; Cai et al., 1999) is an 823 amino acid protein containing two domains; a zinc finger, ubiquitin-binding type domain (ZnF UBP domain; also called BUZ domain), which is also found in histone deacetylase 6 (HDAC6); and a catalytic site in the C19 family cysteine peptidase domain (**Figure 1A**). The ZnF UBP domain contains three zinc-binding sites consisting of 12 residues (Pai et al., 2007), which facilitate protein-protein and DNA-protein interactions, and the cysteine peptidase domain acts as a ubiquitin carboxyl-terminal hydrolase (Rawlings and Barrett, 1994). The protein was initially localized in cytoplasm (Cai et al., 1999). Subsequently it was found that USP16 functions as a homotetramer and is actively exported from the nucleus during interphase (Xu et al., 2013). At the onset of mitosis USP16 is phosphorylated at serine 552, by cyclin dependent kinase 1 (CDK1) (Xu et al., 2013) and localizes to the nucleus, where it is required for G2/M progression. The function of USP16 in mitosis is to deubiquitinate and therefore activate polo like kinase 1 (PLK1), which is needed for proper chromosome alignment, without which cell cycle progression is blocked at G2 (Joo et al., 2007).

USP16 can also act as a regulator of DNA damage repair. DNA double strand break damage induces H2A ubiquitination at the site of damage. The levels of *USP16* mRNA increase directly after DNA damage. After the break is repaired, the ubiquitin is removed by USP16 with the help of HERC2 (HECT and RLD domain containing E3 ubiquitin protein ligase 2) (Zhang et al., 2014). Over-expression of USP16 resulted in decreased ubiquitination of H2A immediately after the damage, while down-regulation resulted in increased and prolonged ubiquitination and failure to resolve the break (Zhang et al., 2014). The net result of either change was to reduce the cell's ability to repair DNA damage, either because the initial ubiquitination of H2A at the site of the break was suppressed (over-expression of USP16) or because the ubiquitin could not then be removed after the repair (down-regulation) (Zhang et al., 2014). There are examples where *USP16* was down-regulated or mutated in leukemias and other human cancers, such as lung adenocarcinoma and hepatocellular carcinoma, which might contribute to the inability of cancer cells to resolve the DNA repair process (Fernandez et al., 2004; Gelsi-Boyer et al., 2008; Qian et al., 2016), but these are rare and the gene is ubiquitously expressed (data from FANTOM5 project[1]) and only rarely mutated (data from The Cancer Genome Atlas[2]).

USP16 may also contribute to inducible gene expression. USP16 was shown to be bound to promoter regions of various genes on all chromosomes of embryonic stem cells (ESC), and this was correlated with low H2A ubiquitination levels and high gene expression (Yang et al., 2014). USP16 was also identified to bind to active genes and promoters and take part in a shift of mouse B-cells from quiescent to active state (Frangini et al., 2013). In addition, USP16 regulates developmental *Hox* genes in *Xenopus laevis* (Joo et al., 2007).

Homozygous knockout of the *Usp16* gene ($Usp16^{-/-}$) in mouse is embryonically lethal. Defects in development were found as early as 7.5 days after conception (E7.5) (Yang et al., 2014). USP16 catalytic function was required for ESC differentiation, but not ESC viability (Yang et al., 2014). Knock down of *USP16* in human HeLa cells caused slow cell growth rates, as there was a sharp decrease in cells in phase G2/M of the cell cycle (Joo et al., 2007). There was also a decrease in *HOX* gene expression. In *Usp16* conditional bone marrow knockout mice, the hematopoietic stem cells were reduced in maturity and lineage commitment and there were fewer mature cells in peripheral blood (Gu et al., 2016).

USP16 is located on human chromosome 21, which is trisomic in Down syndrome (Adorno et al., 2013). In mice triplication of *Usp16* was associated with accelerated senescence, consistent with the early aging phenomena in patients with Down syndrome (Adorno et al., 2013). Consequences of overexpression of *Usp16* in mice included reduction of hematopoietic stem cells and their self-renewal ability, cellular defects owing to increased removal of H2A ubiquitin and decreased proliferation (Adorno et al., 2013). Patients with Down syndrome also have increased incidence of leukemia and decreased rate of solid tumors (Mateos et al., 2015). A human Down syndrome cell line with

[1]https://fantom.gsc.riken.jp/zenbu/, accessed April 2021
[2]https://www.cancer.gov/tcga, accessed April 2021

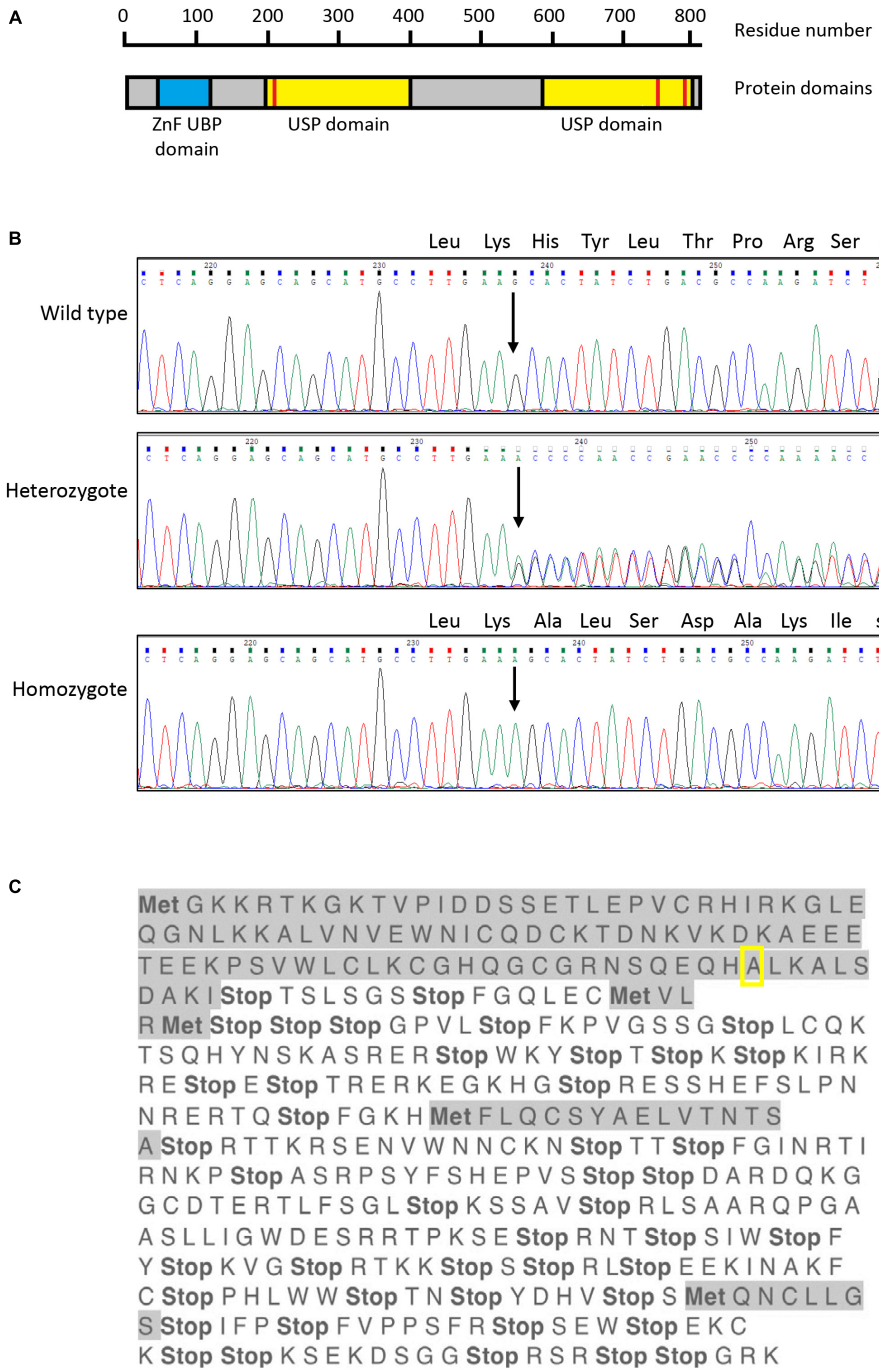

FIGURE 1 | Sanger sequencing of exon 4 of *USP16* clones. **(A)** Structure of the human *USP16* gene and protein. Blue – ZnF UBP domain; yellow – ubiquitin specific protease (USP) domains; red bars – cysteine (left) and histidine (right) boxes of the C19 family peptidase domain. Asparagine at position 200 and cysteine at position 205 are key residues of the cysteine box; histidine at position 758 and aspartate at position 798 are key residues of the histidine box. The peptidase unit extends from residue 141 to the C terminus at residue 823. The USP domains are members of the C19 family of cysteine peptidases. Drawn from data in Jones et al. (2013), Rawlings and Barrett (2013) and the MEROPS database at https://www.ebi.ac.uk/merops/index.shtml (Rawlings et al., 2018). **(B)** Sequence of *USP16* in edited clones. Upper panel shows the wild type, middle panel shows a heterozygote and lower panel shows a homozygous edited clone. The site of the insertion is indicated by the arrow and the amino acid codons of the wild type allele are shown above the sequence traces. All three founder heterozygous clones had the same insertion of adenine (A; green trace) in one allele. The four homozygous *USP16*$^{-/-}$ clones had the same insertion of one additional adenine, on both alleles. The nucleotide sequence before and after the insert was identical to wild type. (**C**) Translation of edited *USP16* in homozygous clones by the ExPaSy tool (single letter code). Insertion of the single nucleotide causes a frame shift, which introduces multiple stop codons in the translated sequence. The insert is present in the middle of the zinc finger domain, in codon 91 for the amino acid alanine (pictured here framed by yellow box). Ten codons later, translation would be terminated by an in frame stop codon. Met indicates potential start codons (amino acid methionine), and highlighted sequences show open reading frames. The first gray sequence up to the yellow box is the correct amino acid sequence.

a triplicated *USP16* gene had decreased DNA damage response (Zhang et al., 2014).

These results show that USP16 has three functions: cell cycle progression (Xu et al., 2013), DNA damage repair (Zhang et al., 2014) and gene activation by removal of H2A ubiquitin (Yang et al., 2014). Disruption of each of these activities could contribute to generation and progression of leukemia.

Here we report the creation of a loss of function mutation in the *USP16* gene using CRISPR-Cas9 technology in the THP-1 human acute monocytic leukemia (AML) cell line. The THP-1 cell line was isolated in 1980 from a 1-year old boy suffering from AML. The cells resemble human monocytes (Tsuchiya et al., 1980) but can be induced to differentiate into macrophage-like cells by administration of phorbol myristate acetate (PMA) (Tsuchiya et al., 1982). PMA initially inhibits cell growth prior to differentiation, by up-regulation of the cyclin-dependent kinase CDKN1A; this in turn inhibits the activating phosphorylation of CDK2 (Traore et al., 2005). In the parent THP-1 line available from the American Type Culture Collection (ATCC® TIB-202™), around 50% of cells become adherent in response to PMA, indicating that there is considerable phenotypic heterogeneity (see **Supplementary Figure 1** in Suzuki et al., 2009). To enable a detailed study of the transcriptomic response to PMA, the FANTOM consortium isolated a clonal line that was highly responsive to PMA and uniformly differentiated into a macrophage like state (Suzuki et al., 2009; Gazova et al., 2020). The karyotype of the clonal line was established by microarray-based comparative genomic hybridization to be 46XY, with minimal chromosomal aberrations (deletions at 6p, 12p, 17p, and on the X chromosome) (Adati et al., 2009). The THP-1 cells are also predisposed to mutations in tumor suppressor genes (for example *TP53* and *PTEN*) and *MLL* fusions (Adati et al., 2009).

We report the knockout of *USP16* in four homozygous cell lines derived from the high differentiation clone of THP-1. We observed heterogeneity amongst the homozygous knockout lines and examined their transcriptomic profiles to understand whether these cells have evolved mechanisms to compensate for the impact of the *USP16* mutation.

MATERIALS AND METHODS

THP-1 Cell Line and Differentiation Assay

THP-1 cells (high differentiation clone 5, from FANTOM4 consortium, passage number 8, provided by Dr. Mark Barnett, The Roslin Institute, United Kingdom) were cultured as described previously (Gazova et al., 2020). The day before the start of the differentiation assay, cells were counted by hemocytometer and between 3×10^6 and 5×10^6 cells were pelleted and resuspended in 10 ml fresh medium. THP-1 cells were then differentiated by adding 30 ng/ml (48.6 nM) phorbol 12-myristate 13-acetate (PMA; P1585, Sigma-Aldrich) in DMSO. The cells were plated on a Sterilin plate (without tissue culture treatment of the plastic), and after 24 h of differentiation, the cells were lifted off by flushing with a blunt-end needle syringe.

CRISPR-Cas9 Editing of *USP16* in THP-1 Cells

The CRISPR sequence guide was designed using an online website tool[3], and selected based upon base chemistry and possible off-target effects. Information about human USP16 protein and gene structures was taken from the Ensembl database[4] (Yates et al., 2016). Information was correct as of January 2021, based on transcript USP16-201 (ENST00000334352.8). The guide was designed to target exon 5 (5′-TGGCGTCAGATAGTGCTTCA-3′, score 79). *In silico* translation of the altered *USP16* DNA exonic sequence into protein was provided by the online ExPaSy tool[5]. Transcription start site (TSS) information was taken from the FANTOM5 database (Forrest et al., 2014) visualized on the ZENBU hg19 genome viewer[6] (Severin et al., 2014). The oligonucleotides were ordered through Sigma-Aldrich (0.025 μmol, DST purification) (Ran et al., 2013).

Annealing and phosphorylation of the CRISPR guides followed the protocol of Andersson-Rolf et al. (2016). The phosphorylated and annealed oligonucleotides were diluted 1:200 and then cloned into a plasmid vector containing the *Streptococcus pyogenes* Cas9 open reading frame sequence and a GFP reporter gene (pX458 from Addgene, plasmid#48138, kindly provided by Dr. Peter Hohenstein, The Roslin Institute) in one step. Cutting and ligation was done by adding together 100 ng of pX458, 2 μl of the diluted annealed oligonucleotide, 2 μl of 10X T4 ligase buffer with 10mM ATP (NEB, Ipswich, MA, United States), 1 μl of *Bbs*I restriction endonuclease (10 U/μl, NEB), 0.5 μl of ligase from Quick Ligation kit (NEB) made up to 20 μl with water. The mixture was incubated for 6 cycles of 37°C for 5 min and 21°C for 5 min. The plasmid with sgRNA sequence was treated using the Plasmid Safe Exonuclease kit (Epicentre, Madison, WI, United States) which digests any residual linear DNA, following manufacturer's instructions.

DH5α strain *E. coli* bacteria were then transformed with the plasmid using a heat shock at 42°C and the bacteria were streaked on an ampicillin plate (100 μg/ml ampicillin in LB (Lysogeny Broth) agar). Two colonies per plate were selected and grown overnight in 5 ml LB with 100 μg/ml ampicillin. To assess the presence of the appropriate insert, plasmid DNA was extracted using the Qiagen MiniPrep kit according to manufacturer's instructions (Qiagen, Hilden, Germany). The sequence was validated by chain termination sequencing using U6 FWD primer at Edinburgh Genomics (University of Edinburgh, United Kingdom). A large scale preparation of plasmid DNA was then made using the Endo-free Maxi Prep (Qiagen) according to manufacturer's instructions. It was important to use endotoxin-free (Endo-free) reagents to avoid activating the cells during the transfection step. The sequence of the maxi

[3]http://crispr.mit.edu

[4]https://www.ensembl.org

[5]http://web.expasy.org/translate/

[6]http://fantom.gsc.riken.jp/zenbu/

prep-prepared plasmid was again verified by sequencing at Edinburgh Genomics.

Nucleofection of CRISPR-Cas9 Plasmids Into THP-1 Cells

THP-1 cells were transfected using the 4D Nucleofector kit (Lonza, Cologne, Germany), with a Lonza protocol optimized for THP-1 cells. 1×10^6 THP-1 cells per sample were centrifuged at 400 *g* for 5 mins, the pellet resuspended in 100 μl of SG 4D Nucleofector solution with added supplement (SG Cell line 4D Nucleofector solution X kit, Lonza). 0.5 μg of DNA per sample of Endotoxin-free plasmid was added. The cell suspension was transferred to the Nucleocuvette vessels and the program FF-100 was executed on the 4D Nucleofector. 500 μl of pre-warmed THP-1 medium was then added and the cell suspension was transfered to a 12-well plate with 1 ml of THP-1 medium already in each well. Next day (∼24 h after nucleofection), the cells were spun down at 400 g for 5 min at room temperature, and the pellet resuspended in 300 μl of 10% fetal bovine serum in PBS and subjected to flow cytometry assisted cell sorting. Single GFP positive cells (which had taken up the plasmid) were sorted into 96-well plates with 200 μl THP-1 media per well, using a BD FACS Aria IIIu (BD Biosciences, San Jose, CA, United States).

Validation of Knockout Cell Lines

The single cell clones were left to grow in 96 well plates until there were enough cells to passage into a bigger vessel (multiple weeks). DNA was prepared from these potential knockout clones using phenol extraction. DNA was resuspended using a suitable volume of TE or water. The targeted region was then amplified by the polymerase chain reaction using High Fidelity Q5 Polymerase (NEB) according to manufacturer's instructions. The primer sequences were CCTAGCGAGTGCATGGTTTT (USP16 CRISPR site F) and ACCCAAGAGGCAGAGGAACT (USP16 CRISPR site R) and the T_m for both was 65°C (NEB Tm Calculator[7]). The samples were initially denatured at 98°C for 30 s, then incubated for 35 cycles of 98°C for 10 s, 65°C for 30 s and 72°C for 30 s. The final extension was at 72°C for 2 mins. The PCR product was run on a 1.5% agarose gel (Agarose Ultrapure, Invitrogen, Paisley, United Kingdom) in 1X TAE with 1X of SYBR Safe DNA stain (Invitrogen). 20 μl of the PCR product was purified using Charge Switch PCR clean-up kit (Invitrogen) according to manufacturer's instructions. For sequencing, 3 μl of water, 2 μl of the purified PCR product and 1 μl of 3.2 μM primer was mixed and sent for chain termination (Sanger) sequencing at Edinburgh Genomics. The results were viewed using FinchTV programme (Geospiza, Perkin Elmer, Waltham, MA, United States) or Chromas[8].

Gene Expression Analysis

RNA was extracted from pelleted cells using RNABee (AMS Biosciences, Friendswood, TX, United States) or TRIzol (Thermo Fisher Scientific, Waltham, MA, United States) according to the manufacturers' instructions. The RNA samples were then treated with DNase I according to manufacturer's instructions (Ambion DNase kit AM1906, Thermo Fisher Scientific). The concentration of RNA was measured using a NanoDrop spectrophotometer ND-1000 (Nanodrop Technologies, Wilmington, DE, United States) and quality was assessed using the Agilent RNA ScreenTape System (Agilent Technologies, Santa Clara, CA, United States) according to the manufacturer's instructions. 500 ng DNase I treated RNA was used to prepare cDNA, together with 2 μl random primers (50 ng/μl, Invitrogen) and 1 μl dNTPs (10 mM, Invitrogen), with water to 13 μl. The RNA with random primers was denatured at 65°C for 5 mins and then cooled at 4°C for at least 1 min. Afterward, 4 μl 5x first strand buffer (Invitrogen), 1 μl 0.1 M DTT (Invitrogen), 1 μl RNAsin Plus (Promega, Madison, WI, United States) and 1 μl Superscript III Reverse Transcriptase (RT; Invitrogen) were added to the mixture. An RT negative control was prepared using RNAse-free water instead of RT. The cDNA synthesis reaction was incubated at 25°C for 5 mins, 50°C for 60 mins, and finally 70°C for 15 mins to stop the reaction. Before quantitative polymerase chain reaction (qPCR), the cDNA was diluted 1:1 with 20 μl water. To establish standard curves, cDNA from THP-1 RNA was diluted three times. The first point of the standard curve was undiluted cDNA (estimated 12.5 ng/μl), then 1:1 (estimated 6.25 ng/μl), then 1:4 (estimated 3.125 ng/μl), and 1:8 (estimated 1.5625 ng/μl). qPCR was used to assess the levels of *USP16* expression using manufacturer's protocols for SYBR Green 1 Master Mix with Light Cycler 480 96-well white plates (Roche, Mannheim, Germany). The settings for all qPCR analyses (both quantification and melting curves for primers) were as follows: pre-incubation was carried out at 95°C for 5 mins (ramp rate 4.40°C/s), then amplification steps were repeated for 45 cycles. Amplification steps were as follows: 95°C for 10 s (ramp rate 4.40°C/s), 60°C for 15 s (ramp rate 2.20°C/s), and 70°C for 30 s (ramp rate 4.40°C/s). Afterward, the melting curve was measured by incubating at 95°C for 5 s (ramp rate 4.40°C/s), 65°C for 1 min (ramp rate 2.20°C/s) and then the temperature was increased to 97°C by 0.11C°/s. At the end, the plate was cooled for 30 s at 40°C. All reverse transcriptase-qPCR analysis was carried out using the Advanced Quantification setting of the Light Cycler 480 Roche software. ΔCt was calculated with previously established values of primer efficiencies from standard curves (calculated using the same software, by using Abs Quant/2nd Derivative Max setting).

Two sets of primers for two different housekeeping genes were used in this study. The first one was for the human beta actin gene (*ACTB*) (Maess et al., 2010); the second, for *GAPDH*, was purchased from Qiagen (QuantiTect Primer Assay QT0112646). The *USP16* primers were designed to span an intron, to have melting temperature (Tm) of 60°C and to generate a cDNA product of approximately 200 bp, using Primer3 program[9]. The ideal slope value from standard curves is around −3.345 when the primer efficiency is 2, but values from −3.0 to −3.5 were considered acceptable (**Table 1**).

CAGE (Cap Analysis Gene Expression)

Cap analysis gene expression libraries were made as described previously (Takahashi et al., 2012; Gazova et al., 2020). Libraries

[7]http://tmcalculator.neb.com

[8]https://technelysium.com.au/wp/chromas/

[9]http://primer3.ut.ee/

TABLE 1 | qPCR primers and efficiencies for *USP16* expression analysis.

Gene target	Sequence 5′ – 3′	Slope value
USP16_ex4-5_F	TGCCAAGACTGTAAGACTGACA	−3.543
USP16_ex4-5_R	TGGCGTCAGATAGTGCTTCA	
USP16_ex15-16_F	AGTATGCACACGGAGACAGT	−3.528
USP16_ex15-16_R	AGAGTAAGAACAGGAGGAGCA	
USP16_ex17-18_F	CCTACGCAAAGTTAACAAACACA	−3.014
USP16_ex17-18_R	GTGTAATGCCCCGACCTCAT	
ACTB_F	ATTGCCGACAGGATGCAGAA	−3.398
ACTB_R	GCTGATCCACATCTGCTGGAA	
GAPDH	Qiagen	−3.498

were sequenced by Edinburgh Genomics on an Illumina HiSeq 2500 machine in high throughput mode. One library consisting of eight pooled samples was sequenced per lane, with custom sequencing primer and inline barcodes. Quality control, quantification of expression levels and bioinformatic analysis were performed as described (Gazova et al., 2020). The final expression value for each CTSS (CAGE transcription start site) was provided as TPM (tags per million). The normalized data were then formatted into OSCtable[10], providing chromosome, start, end and strand coordinates and uploaded into ZENBU[11] (Severin et al., 2014). CTSS were clustered in each sample based on their distance apart using distclu option in CAGEr package (Haberle et al., 2015). The settings were as follows, the minimum CTSS TPM value was 1, the distance between CTSS was maximum of 20 bp and singletons (single CTSS not neighboring any other CTSS) were not removed. To compare the clustered CTSS across different samples, the CTSS range values were aggregated, retaining only the CTSS clusters with expression in at least one sample of higher than 5 TPM. The maximum distance between CTSS was kept at 100 bp. These commands created a single matrix file with cluster coordinates (start, end, strand) and normalized TPM values for the aggregated clusters. Normalized and annotated clusters of CTSS were allocated to the nearest downstream gene (Gazova et al., 2020). A matrix of gene annotations and expression values was uploaded into BioLayout software (Freeman et al., 2007; Theocharidis et al., 2009)[12]. Sample-to-sample correlation (equivalent to principal components analysis) was created by transposing the data in pre-processing and analyzed at a Pearson correlation coefficient (r) threshold of 0.88. Gene network analysis created a graph by visualizing each node as one aggregated cluster of CTSS. A correlation graph was created at $r \geq 0.92$ (**Supplementary Figure 1**) using Fast Multiple Multilevel Method (FMMM) format. The analysis was done by clustering using the Markov Cluster Algorithm (MCL) at inflation values indicated in the Results section. Differential gene expression was analyzed using the edge package for the R statistical environment[13]. GO enrichment analysis was performed with PANTHER (Protein Analysis Through Evolutionary Relationships, release of July 28, 2020; available through The Gene Ontology Resource[14]). The background was *Homo sapiens*, the test used was Fisher's Exact test and all results were corrected for multiple testing using the Bonferroni method.

Western Blot

For each sample, 2×10^6 cells were resuspended in 50 µl PBS, then 50 µl of 2X Laemmli loading buffer with 50 mM DTT (BioRAD, Hercules, CA, United States, prepared by mixing 950 µl Laemmli loading buffer + 50 µl 1M DTT (NEB) in water) was added and mixed thoroughly. Samples were then incubated at 95°C for 5 mins and stored at −20°C until needed. Samples were loaded on a precast Mini-Protean TGX 4-15% 12-well gel (Bio-Rad Laboratories, Herclues, CA, United States). A molecular weight marker (PageRuler Plus Prestained Protein Ladder, Thermo Fisher Scientific) was loaded in the outer lanes. The running buffer was 25 mM Tris (Thermo Fisher Scientific), 192 mM Glycine (Sigma-Aldrich) and 0.1% w/v SDS (Thermo Fisher Scientific) and the gel was run at 100V for 5 min and then 120V till the end of the gel. The gel was then rinsed in water. The protein was then transferred onto PVDF membrane (Immobilon-P, Sigma-Aldrich, St Louis, MO, United States), using a Bio-Rad transfer apparatus, according to manufacturers' instructions. The blotting was run at 50 V for 1 h at initial current of 400 mA. The membrane was blocked for 1 h in 5% milk powder (Marvel Dried Milk, Premier Foods Group Ltd., London, United Kingdom) in PBS-T (0.05% Tween in PBS). Primary anti-human antibodies (dilution of 1:1000 for rabbit anti-USP16 (ab121650, Abcam, Cambridge, United Kingdom); and 1:2000 dilution for mouse anti-ß-actin (C4) monoclonal IgG1 (sc-47778, Santa Cruz Biotech, Dallas, TX, United States) were diluted in 5% milk powder in PBS-T and the membrane immersed rotating overnight at room temperature. The next day, the membrane was washed six times for 5 min in PBS-T, and then secondary antibodies were diluted at 1:2000 in 5% milk powder in PBS-T (horse anti-mouse HRP-linked for β-actin and goat anti-rabbit HPR-linked for USP16; both from Cell Signaling Technology, Danvers, MA, United States), and the membrane immersed rotating for 1 h at room temperature. The membrane was again washed six times for 5 min in PBS-T, and then Pierce ECL western blotting substrate (Thermo Fisher Scientific) was applied according to manufacturer's instructions. The image was developed onto Amersham Hyperfilm (GE Healthcare, Little Chalfont, United Kingdom).

Analysis of Edited Cells

MTT assay was performed to assess metabolic activity and cell proliferation. A 96-well plate was seeded with 2×10^4 THP-1 cells in 100 µl of media per well. After 48 h, 10 µl MTT (3-(4,5-dimethylthiazol-2-yl)-2,5-diphenyltetrazolium bromide, 5 mg/ml, Sigma Aldrich) was added to each well and incubated for 3 h at 37°C in 5% CO_2. Then 100 µl solubilization solution (89% (v/v) Isopropanol, 10% (v/v) Triton 100x, 1% (v/v) HCl) was added and left at 37°C 5% CO_2 overnight. The following day, substrate conversion was determined via the optical densities

[10]https://zenbu-wiki.gsc.riken.jp/zenbu/wiki/index.php/OSCtable

[11]http://fantom.gsc.riken.jp/zenbu/gLyphs/#config=Gazova_USP16KO

[12]http://biolayout.org

[13]https://www.rdocumentation.org/packages/edge/versions/2.4.2

[14]http://geneontology.org/, Go Ontology database DOI: 10.5281/zenodo.4081749 Released 9 October 2020

which were measured using a plate reader at 570 nm. The phases of the cell cycle were determined using propidium iodide staining, as described previously (Gazova et al., 2020).

A phagocytosis assay was performed by incubating THP-1 macrophages that had been differentiated with PMA for 2 days with Zymosan A particles (Thermo Fisher Scientific, Z2841) coated with fluorescein isothiocyanate (FITC), at a ratio of 100 particles per cell; for 1 h at 37°C. Cells were washed five times with cold PBS and fixed with 4% paraformaldehyde (PFA, WVR, Radnor, PA, United States) for 10 min at room temperature and washed twice with PBS. Images were viewed using a fluorescent microscope (Zeiss Vert.A.1, Carl Zeiss Limited, Cambridge, United Kingdom).

Statistical Analysis

Results are presented as mean ± standard error. Significance of differences was assessed using a two tailed *t*-test where two groups were compared or a two tailed *Z*-test where a single sample was compared with the mean of multiple values.

RESULTS

Editing of the *USP16* Gene in THP-1 Cells

The guide was designed to make an indel in exon 5 of *USP16*, creating an out of frame mutation. Exon 5 (the third coding exon) codes for part of the zinc finger domain. Out of two 96 well plates, 15 clones survived the sorting and 3 clones proved to be heterozygous for the same single nucleotide insertion (adenine) into the expected site. The sequence is shown in **Figure 1B**. No homozygotes were present at the first targeting, so two of the heterozygotes were used for targeting a second time with the same guide. Out of 3 plates for each heterozygous parental cell line, 67 clones survived the sorting. 13 clones (19%) had reverted to the wild type sequence and 4 clones (6%) were homozygous for the same adenine insertion in exon 5 (**Figure 1B**). The insertion site of the adenine in exon 5 created a frame shift, with an in-frame stop codon ten amino acids downstream. Any resulting peptide would be small and contain only the start of the protein sequence with no functional domains (**Figure 1C**). One homozygous clone (Hom1) was derived from one heterozygote (HetC) and the other three (Hom2, Hom3, and Hom4) from a second heterozygote. Sequencing of the cDNA derived from the homozygous clones confirmed that the insertion was present in the transcript as well as the gene (not shown).

Impact of *USP16* Frame Shift on Gene Expression

Quantitative reverse transcriptase PCR experiments were conducted with the four homozygotes, a parental heterozygote (HetC), a heterozygote from the second targeting (HetdE) and wild type THP-1 cells for 3 sets of primers, each amplifying a different exon along the transcript (**Table 1**). Consistent with predicted nonsense-mediated decay, the *USP16* $^{-/-}$ homozygous clones had decreased level of mRNA compared to wild type THP-1 cells (**Figure 2A**) for all three sets of primers ($p < 10^{-7}$ for each set of primers). The *USP16* expression levels were also extracted from the transcriptomic data generated by CAGE analysis (see below) and found to be negligible in the homozygous edited clones after differentiation ($p = 0.004$) (**Figure 2B**).

The production of USP16 protein in the edited clones was assessed by western blotting. Previous studies reported an estimated molecular weight for USP16 of 110 - 120 kDa (Joo et al., 2007; Xu et al., 2013), although the antibody manufacturer predicted a band size of 94 kDa. A band of around 120 kDa was present in heterozygotes and wild type but absent in the homozygous clones (**Figure 2C**). There was no evidence of any bands between 70 and 130 kDa in the homozygotes. This suggests that the homozygous clones were not making full length USP16. Other bands on the gel (**Figure 2C**) that were not altered in the deleted clones may be from different deubiquitinases, since there is strong homology in the family.

Cellular Impact in *USP16* Knockout Cells

The *USP16* knockout clones retained active proliferation in the absence of PMA, indicating that USP16 is not absolutely required for mitosis in these leukemic cells. Upon addition of PMA the parent THP-1 *USP16*$^{+/+}$ high differentiation clone underwent growth arrest, with down-regulation of cell-cycle associated transcripts and *MYB*, and up-regulation of macrophage markers (Gazova et al., 2020). The absence of functional USP16 did not alter the ability of the cells to undergo this differentiation process. In control and USP16-deficient cells, addition of PMA generated a confluent layer of adherent macrophage-like cells after 48 h. These cells were able to phagocytose Zymosan A particles and there was no apparent difference between the control and USP-deficient clones (**Figure 3A**).

To analyze the requirement for USP16 in growth regulation of these cells, we first assessed proliferation based upon metabolic activity (MTT reduction). This was assessed on both early and late passage lines to determine whether there was any phenotypic drift. The results differed among *USP16*$^{-/-}$ homozygotes. The proliferative activity of wild type, heterozygotes and homozygote Hom1 was indistinguishable, as indicated by the level of metabolic activity after 48 h in culture. The remaining homozygotes (Hom2, Hom3, and Hom4, all derived from the same heterozygote) were also actively proliferative albeit with a marginal decrease in MTT reduction compared to WT (**Figure 3B**).

To assess the impact of *USP16* mutation on cell cycle regulation, the various clones were differentiated into macrophages with PMA over the course of 3 days and the proportions of cells in different phases of the cell cycle were assayed each day using propidium iodide staining and flow cytometry. This analysis confirmed that USP16 is not absolutely required for cell cycle progression. Before differentiation, edited and wild type cells were indistinguishable, with 20-30% of cells in S phase (**Figure 3C**). During differentiation of THP-1 *USP16*$^{+/+}$ monocytes to macrophages in response to PMA the proportion of cells in S phase was previously shown to decline as the cells differentiate (Gazova et al., 2020). This response was replicated here in wild type and in *USP16* heterozygous and homozygous cells, although the decline in Hom2 was not as marked. The proportion of cells in S phase was reduced to half or less in most

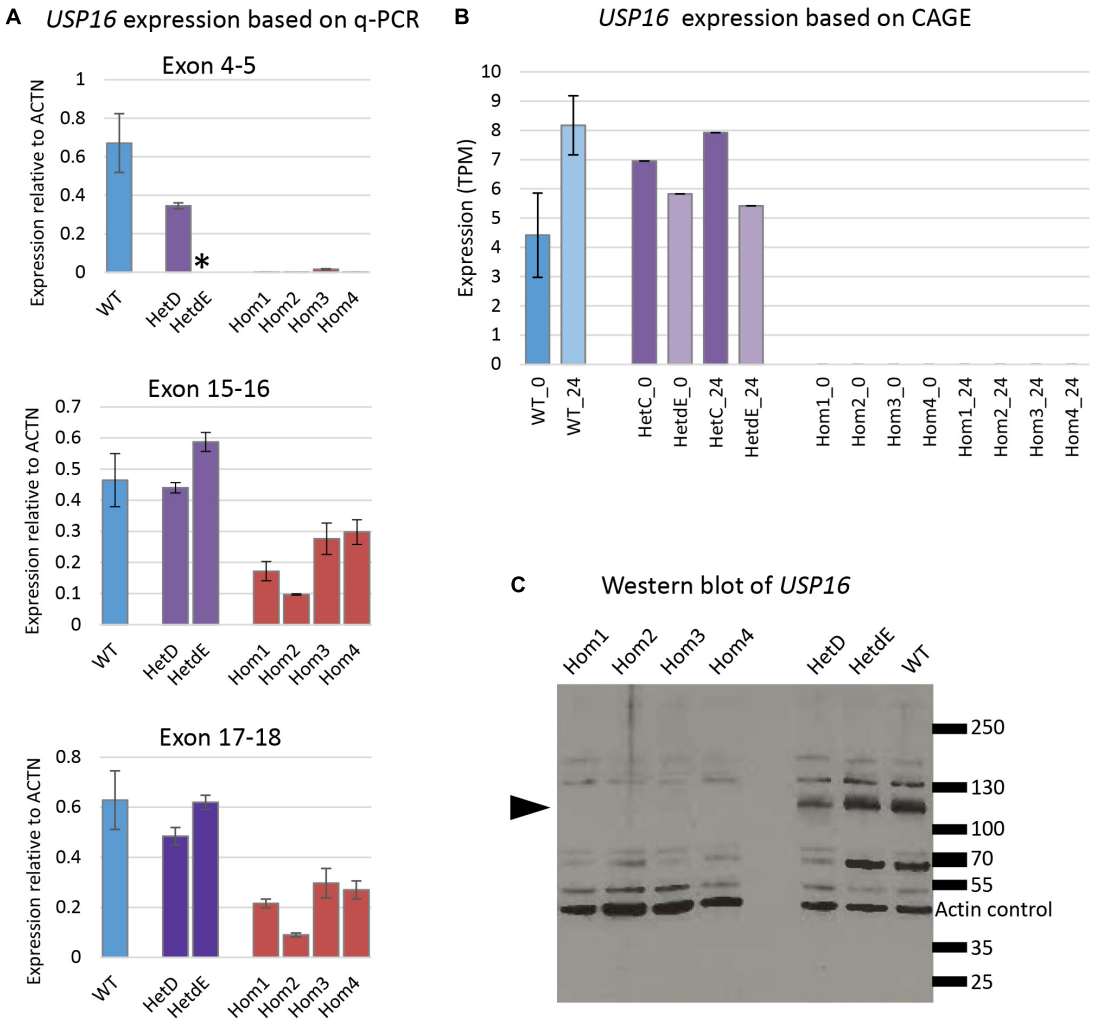

FIGURE 2 | *USP16* expression in edited clones. **(A)** Quantitative PCR for three sets of *USP16* primers, targeting different exons. RNA was from undifferentiated cells. Blue – wild type; purple – heterozygotes; red – homozygotes. *Y*-axis shows the Roche ratio normalized by *ACTB* expression with error rates calculated by Roche LightCycler480 software. Error bars show standard error. Asterisk shows technical failure of qPCR for HetdE. All assays were carried out in duplicate. Homozygotes were significantly different from wild type (all $p < 10^{-7}$); heterozygotes were not significantly different from wild type. **(B)** *USP16* expression derived from transcriptomic analysis using CAGE. Expression levels are shown for control untreated cells (darker columns) and cells after 24 h of PMA stimulation (lighter columns). Blue – wild type; purple – heterozygotes; values in homozygotes were all 0. Homozygotes were significantly different from wild type ($p = 0.03$ at 0 h and $p = 0.004$ at 24 h). Heterozygotes were not significantly different from wild type at either time point. **(C)** Western blotting for USP16 and actin in extracts of THP-1 clones. Lanes 1, 2, 3, and 4 are *USP16* knockout homozygotes; lanes 6 and 7 are *USP16* knockout heterozygotes, and lane 8 shows the wild type THP-1 cell line. Molecular weight ladder sizes (kDa) are shown to the right of the image. Actin loading control bands of 42 kDa are indicated. All other bands were detected by anti-USP16 antibody (ab121650). Bands of around 120 kDa (present in heterozygotes and wild type) were not present in the four homozygous *USP16* knockout THP-1 clones (arrowhead).

lines alongside an increased proportion in G1 phase by Day 2. In Hom2, the proportion of cells in S phase following PMA treatment was maintained around 30% (**Figure 3C**). As indicated by the error bars in **Figure 3C**, there was considerable variability between replicates.

Transcriptomic Analysis of Wild Type THP-1 and *USP16* Knockout Clones

The phenotypic analysis indicated that the impact of the *USP16* insertion is conditional; in one clone (Hom2) there was a reduced impact on proliferation though not on differentiation, whereas Hom1 was not different from its heterozygous parent HetC or the replicates from the original wild type THP-1 clone. To dissect the reasons for this variable impact, RNA from *USP16* knockout THP-1 cells was subjected to expression analysis using CAGE before and after 24 h PMA stimulation, and compared with results for wild type using CAGE sequencing results from the 0 and 24 h time points of the previous publication (Gazova et al., 2020). Sample-to-sample analysis (which provides similar information to a principal components analysis) using BioLayout network analysis software showed that prior to PMA treatment,

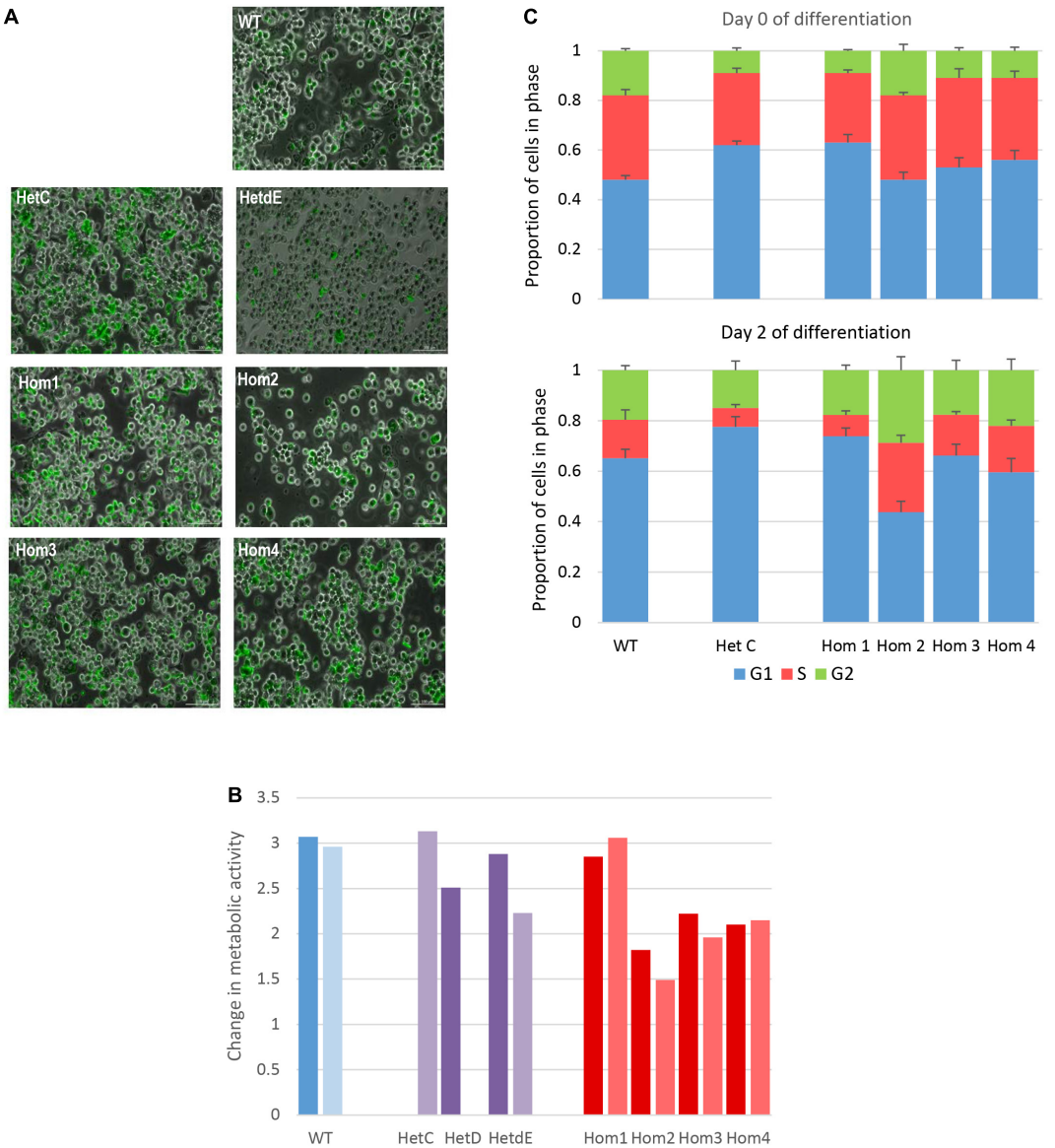

FIGURE 3 | Impact of *USP16* knockout on cellular functions. **(A)** Phagocytosis of Zymosan particles by wild type and edited clones. Adherent THP-1 cells differentiated with PMA were incubated with FITC-labeled Zymosan particles for 1 h at 37°C and washed as described in Methods. Images show that the large majority of cells in each culture contained labeled (green) particles. **(B)** Proliferation of individual THP-1 clones measured using the MTT reduction assay. Cells were plated at 2 × 10^5/ml and incubated for 48 h, prior to assay of viable cells as described in Methods section. Dark colors show an assay after initial expansion; light colors show a repeat assay of the same clones, after several passages. *Y*-axis shows the optical density after 48 h. Red – homozygotes; purple – heterozygotes; blue – wild type. HetD was only tested after the initial expansion and HetC was only tested after several passages. **(C)** Proportion of cells in different stages of the cell cycle in wild type and edited clones. Cell cycle was analyzed by flow cytometry of propidium iodide-stained cells as described in Methods. Results are the average of 3 (HetC) or 4 experiments. Upper panel – before differentiation; lower panel – after 2 days with PMA. Blue – G1 phase; orange – S phase; green – G2 phase. Error bars show standard error.

all cells had similar transcriptomic profiles (dark green in **Figure 4A**). All cell lines showed some change over the first 24 h of differentiation, with the transcriptome of the wild type cells changing most and Hom4 changing least (**Figure 4B**). One heterozygote (HetC) was similar to wild type and the other (HetdE, a heterozygous clone that had been through two rounds of targeting, from the same parent as Hom2, Hom3, and Hom4) was similar to the homozygotes, which were closest to undifferentiated cells in the network, indicating a reduced response to PMA (**Figure 4B**).

The differentiation of THP-1 cells is associated with up-regulation of a number of macrophage-specific genes, including *CSF1R*, which encodes the receptor for the lineage-specific growth factors CSF1 and IL34 (Hume et al., 2016; Gazova et al., 2020). The three related homozygous knockout lines (Hom2, Hom3, and Hom4) showed no increase of *CSF1R* mRNA after

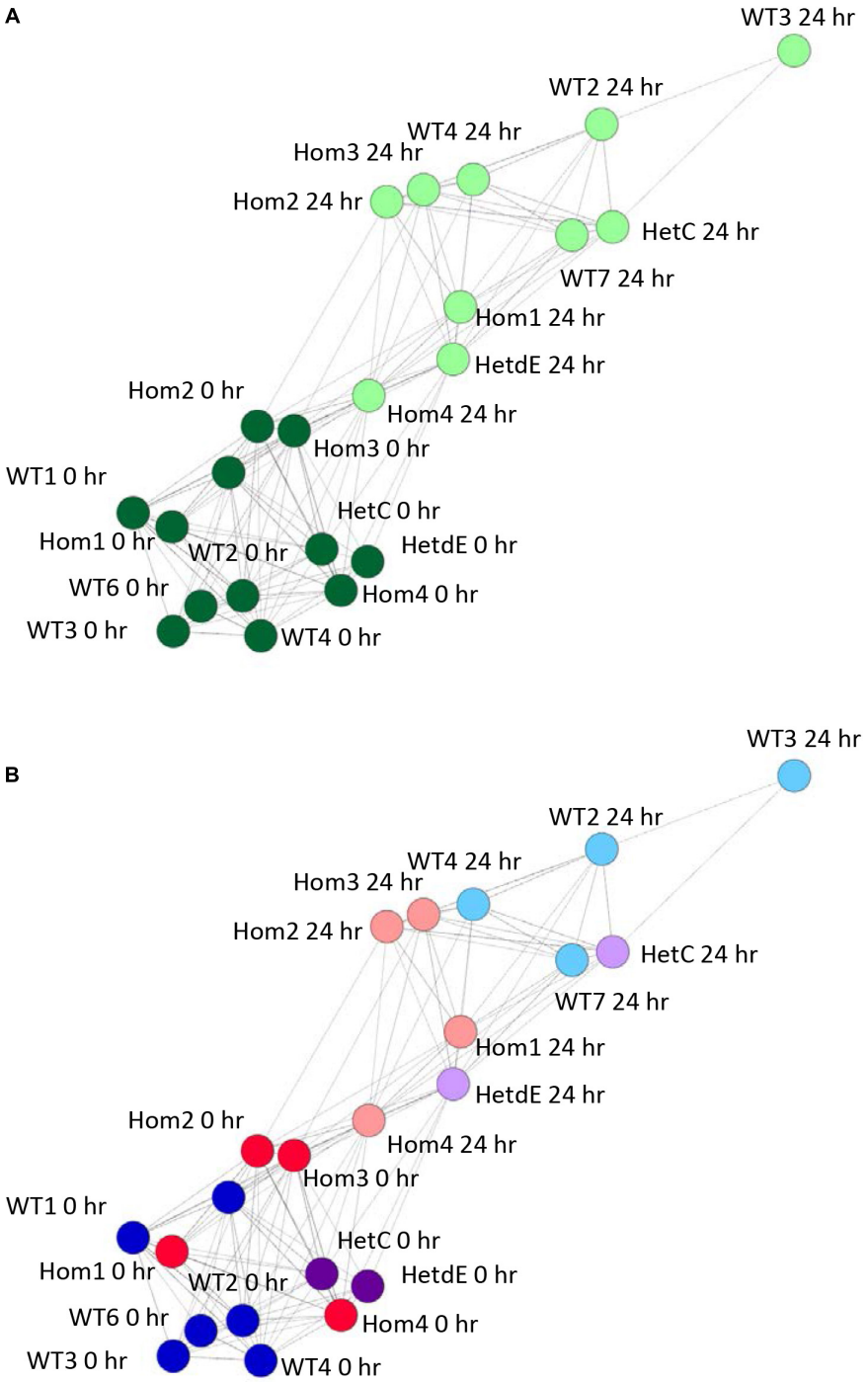

FIGURE 4 | Sample to sample network graph of edited clones. Circles represent clones and lines between them correlations of at least 0.88. Wild type results are from Gazova et al. (2020). **(A)** Analysis showing the transition from 0 h (dark green) to 24 h post PMA treatment (light green). **(B)** The same network as in panel **(A)**, colored to show the effect of genotype on the transition following PMA treatment. Dark colors show cells prior to treatment, light colors show cells 24 h after PMA treatment. Red – homozygotes; purple – heterozygotes; blue – wild type.

PMA treatment ($p = 0.19$; **Figure 5A**), while their double targeted "sibling" HetdE showed a small (3-fold) increase. In contrast, Hom1 and its parental heterozygote HetC showed approximately 10-fold increase in *CSF1R*, greater than the 5-fold increase seen in wild type. The progenitor cell marker *MYB* decreased to about 15% in wild type after PMA treatment. This marker was higher in Hom1 and HetC than in wild type prior to treatment and decreased to less than 15% 1 day after PMA treatment.

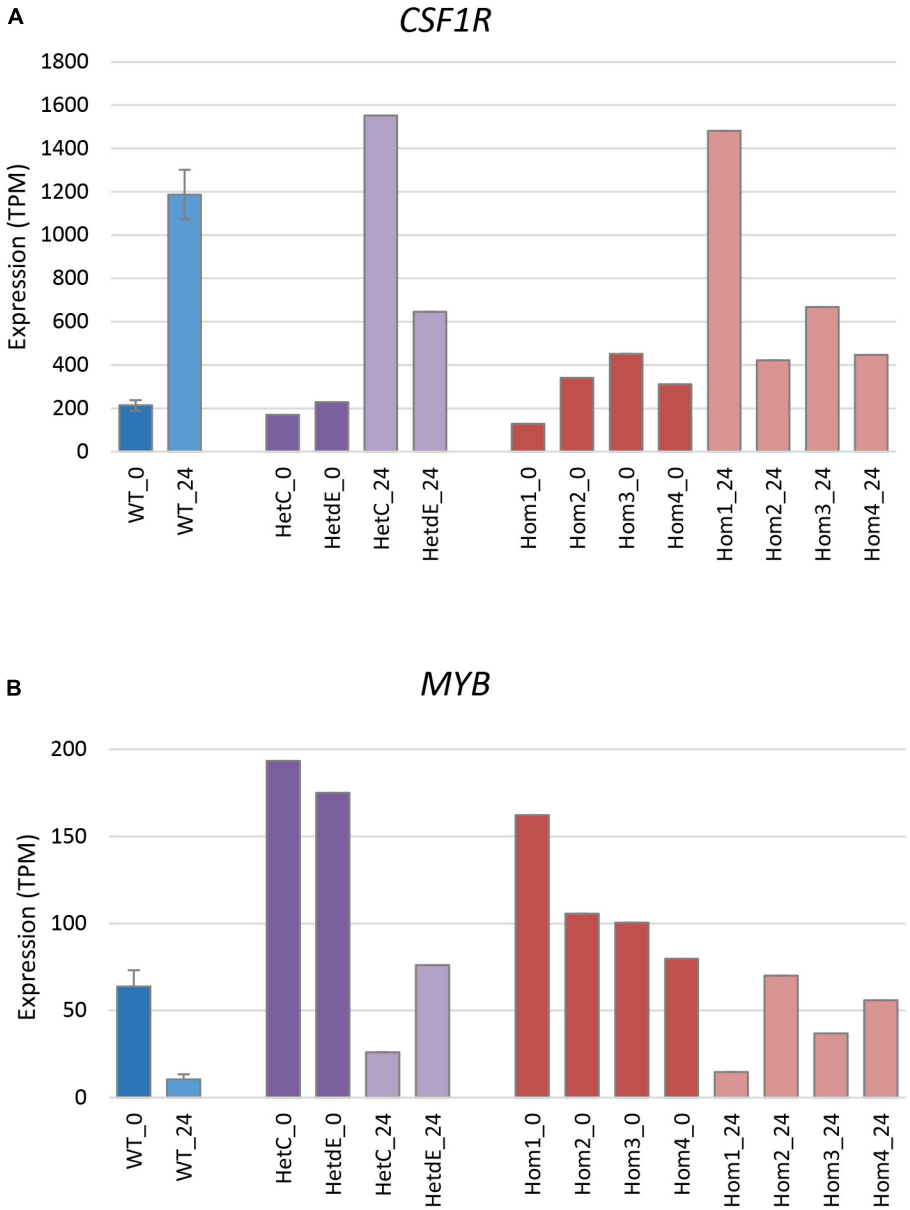

FIGURE 5 | Expression of signature genes in edited clones. Results are based on expression levels extracted from CAGE data. Wild type samples are from Gazova et al. (2020); results are the mean of 6 (0 time point) and 4 (24 h time point) replicates and standard error is shown by the bars. (**A**) Expression of *CSF1R* (total of three promoters), a marker of monocyte to macrophage transition. At 0 h, Hom1 was significantly lower than wild type ($p = 0.0006$) while at 24 h it was significantly higher ($p = 0.01$). The mean value for Hom2-4 was slightly higher than wild type at 0 h ($p = 0.04$) but did not change after PMA stimulation and was then significantly lower than wild type ($p = 0.005$). (**B**) Expression of *MYB* (total of two promoters), a marker of cell proliferation. At 0 h, Hom1 was significantly higher than wild type ($p = 0$) while at 24 h it was not significantly different ($p = 0.15$). The mean value for Hom2-4 was slightly higher than wild type at both 0 and 24 h ($p = 0.04$ in both cases).

In the double targeted HetdE, Myb expression prior to PMA treatment was similar to HetC, but only decreased to about 40%. In Hom2, Hom3 and Hom4, *MYB* expression was lower prior to differentiation and dropped up to 50% after PMA treatment ($p = 0.03$) indicating that cell proliferation persisted in these clones (**Figure 5B**).

To explain the apparent redundancy of USP16 for cell proliferation and differentiation, and inconsistency between the mutant clones, we examined expression of other histone deubiquitinase genes. Because Hom1 was different from the other homozygotes, it was analyzed separately. All homozygotes had higher levels of expression prior to differentiation for *USP12, BAP1*, and *MYSM1* (**Figure 6** and **Table 2**). *USP12* and *MYSM1* were induced in wild type cells upon PMA treatment, reaching the same level as the homozygotes. *BAP1* did not change following PMA treatment and was significantly elevated in Hom1 regardless of time point. Hom1 was also higher than wild type for *USP21* both before and after treatment but lower than wild type

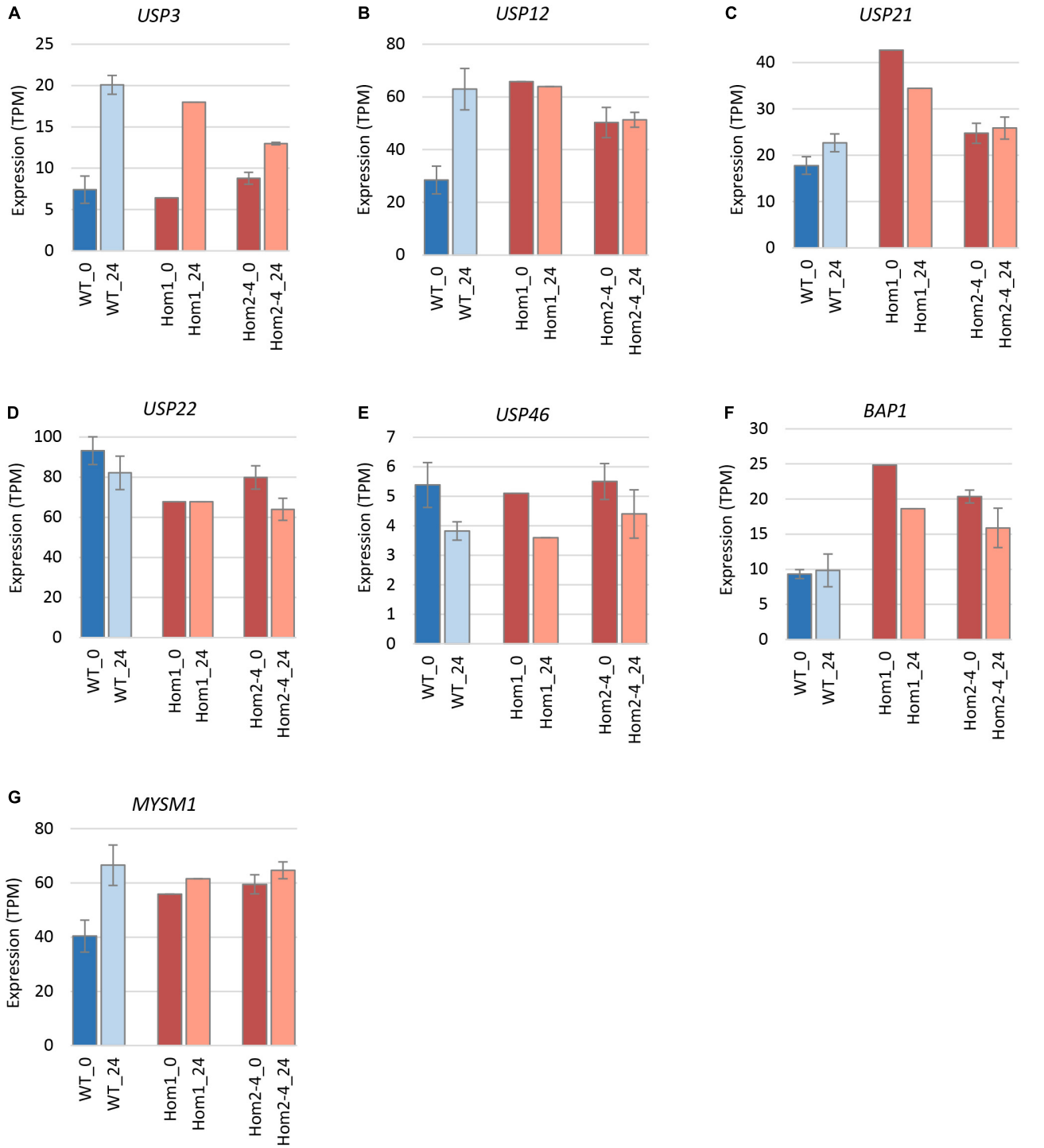

FIGURE 6 | Expression of deubiquitinase genes in edited clones. Results are based on expression levels extracted from CAGE data. Wild type samples are from Gazova et al. (2020). Results for wild type are the mean of 6 (0 h time point) and 4 (24 h time point) replicates. Results for Hom2, Hom3, and Hom4 were averaged. Standard error is shown by the bars. Significance of differences between genotypes can be seen in **Table 2**. **(A)** Expression of *USP3*. **(B)** Expression of *USP12*. **(C)** Expression of *USP21*. **(D)** Expression of *USP22*. **(E)** Expression of *USP46*. **(F)** Expression of *BAP1*. **(G)** Expression of *MYSM1*.

for *USP22* prior to treatment (**Figure 6** and **Table 2**). Expression of *USP3* in Hom2, Hom3, and Hom4 was lower than wild type after 24 h of PMA treatment, suggesting that these clones failed to fully induce *USP3* during differentiation. There was no effect of the *USP16* knockout on *USP46*, which had relatively low expression in these cells.

TABLE 2 | Expression of deubiquitinases in USP16 edited cells.

Gene	Time point	Wild type	Hom 1	Hom 2–4	All homozygotes	P (Hom 1 vs. wild type) (2-tailed *Z*-test)	P (Hom 2–4 vs. wild type) (2 tailed *T*-test)	P (all homozygotes vs. wild type) (2-tailed *T*-test)
USP3	Day 0	7.40 ± 1.66	6.42	8.78 ± 0.71	8.19 ± 0.78	0.56	0.47	0.68
	Day 1	20.08 ± 1.14	17.98	12.99 ± 0.16	14.23 ± 1.25	0.07	0.008	0.01
USP12	Day 0	28.50 ± 5.27	65.80	50.29 ± 5.75	54.17 ± 5.62	1.53E–12	0.04	0.01
	Day 1	62.96 ± 7.84	63.96	51.33 ± 2.81	54.49 ± 3.73	0.90	0.24	0.38
USP21	Day 0	17.78 ± 1.89	42.68	24.73 ± 2.14	29.22 ± 4.74	0	0.06	0.09
	Day 1	22.65 ± 1.92	34.43	25.85 ± 2.39	28.00 ± 2.73	9.33E–10	0.35	0.17
USP22	Day 0	93.16 ± 6.95	67.78	79.80 ± 5.83	76.80 ± 5.10	2.62E–4	0.19	0.09
	Day 1	82.15 ± 8.37	67.74	63.93 ± 5.47	64.88 ± 3.98	0.09	0.13	0.13
USP46	Day 0	5.38 ± 0.76	5.10	5.50 ± 0.61	5.40 ± 0.44	0.71	0.91	0.99
	Day 1	3.83 ± 0.31	3.60	4.40 ± 0.82	4.20 ± 0.61	0.47	0.56	0.61
BAP1	Day 0	9.31 ± 0.62	24.84	20.37 ± 0.92	21.49 ± 1.29	0	6.45E–04	6.90E–04
	Day 1	9.84 ± 2.32	18.63	15.88 ± 2.80	16.57 ± 2.10	1.52E–4	0.17	0.08
MYSM1	Day 0	40.41 ± 5.93	55.91	59.49 ± 3.55	58.59 ± 2.67	8.89E–3	0.03	0.03
	Day 1	66.55 ± 7.45	61.59	64.66 ± 3.10	63.89 ± 2.32	0.50	0.83	0.75

Data were taken from expression levels derived from CAGE analysis. Results for homozygotes are a single replicate for Hom1 and the average of the three lines for Hom2, Hom3, and Hom4. Results for wild type are the average of six experiments for day 0 and four experiments for day 1. Results are shown as mean ± standard error. Cells are colored by significance level: deep orange $P \leq 0.001$; mid orange $0.001 < P \leq 0.01$; light orange $0.01 < P \leq 0.05$. Two-tailed tests were used.

Network Analysis of *USP16* Edited Clones

The analysis of differentially expressed genes and determination of the phenotypes of the edited clones indicated that there were impacts of the lack of USP16 in both homozygotes and heterozygotes, and that the edited lines had adapted to the knockout in different ways. To dissect the differences further, the CAGE-based transcriptional profiles of the *USP16* knockout homozygous, heterozygous and wild type clones were analyzed using BioLayout network analysis software. A gene-to-gene analysis was performed with a relatively stringent Pearson correlation coefficient threshold of 0.92 and MCL clustering with an inflation coefficient of 2.0 (**Figure 7A**). This included 5640 nodes (representing CTSS, equivalent to gene promoters) making 109,930 edges (correlation of at least 0.92 between nodes). The majority of the nodes (4474 nodes, 105,618 edges) were in two distinct regions, which were associated with high expression either in THP-1 cells prior to treatment with PMA (monocytic cells), or in THP-1 cells after 24 h treatment (macrophage-like cells) (**Figure 7A**). The remaining nodes were in smaller elements of 2 to 154 nodes. Cluster lists for clusters discussed below are available in **Supplementary Figure 2** and show groups of genes whose expression patterns were more similar to each other than to others in the analysis, as identified by the MCL clustering method. The largest cluster was Cluster 1 with 850 nodes (CTSS), which included the main *CSF1R* promoter and contained genes which were upregulated after differentiation (**Figure 7B**). Genes in this and other smaller clusters showing high expression 24 h after induction of differentiation tended to be associated with immunity, cell-cell adhesion and migration, neutrophil degranulation and the lysosome (analyzed by PANTHER – see **Supplementary Figure 2**), although there was a wide variety of GO terms found for these genes. The second most abundant cluster was Cluster 2 with 286 nodes, which contained genes highly expressed in monocytic THP-1 cells prior to differentiation (**Figure 7B**). A number of smaller clusters also showed this pattern and contained genes associated with cell division, the cell cycle and DNA replication and repair (Giotti et al., 2019). Notably cluster 6 (80 nodes) showed this pattern and contained the majority of the detected histone genes. There was little indication of an effect of absence of functional USP16 on genes in these clusters, showing that homozygous and heterozygous *USP16* knockout cells maintain most of the gene expression patterns of monocyte and macrophage-like wild type cells, consistent with the ability to phagocytose and differentiate shown above.

To understand how the edited clones are able to maintain these functions, we looked for clusters where the expression pattern was different from wild type. As we have seen previously for cell lines (Gazova et al., 2020) and inbred animals (Summers et al., 2020), there was considerable variation among replicates, reflected in clusters with idiosyncratic profiles usually dependent on a single sample (shown in **Supplementary Table 1**). The wild type replicates were all generated from the parent THP-1 clone 5, so these differences may reflect phenotypic drift or phenotypic heterogeneity of the parent clone. The edited samples represent different clonal lines, each of which may have responded to the effect of the knockout differently. In particular, Hom1 and its parental heterozygote HetC showed a different phenotype from the other heterozygote and homozygotes (**Figures 3**, **5**). However, there were several clusters where there was a clear difference between the wild type replicates and the edited clones, enabling some insight into the mechanisms used by the cells to escape the effects of the absence of USP16.

Genes in Cluster 13 (38 nodes), Cluster 31 (15 nodes), Cluster 37 (13 nodes) and Cluster 44 (12 nodes) were high in most wild type replicates prior to PMA stimulation. These genes were low in wild type after 24 h of PMA treatment and low in all heterozygous and homozygous clones at both time

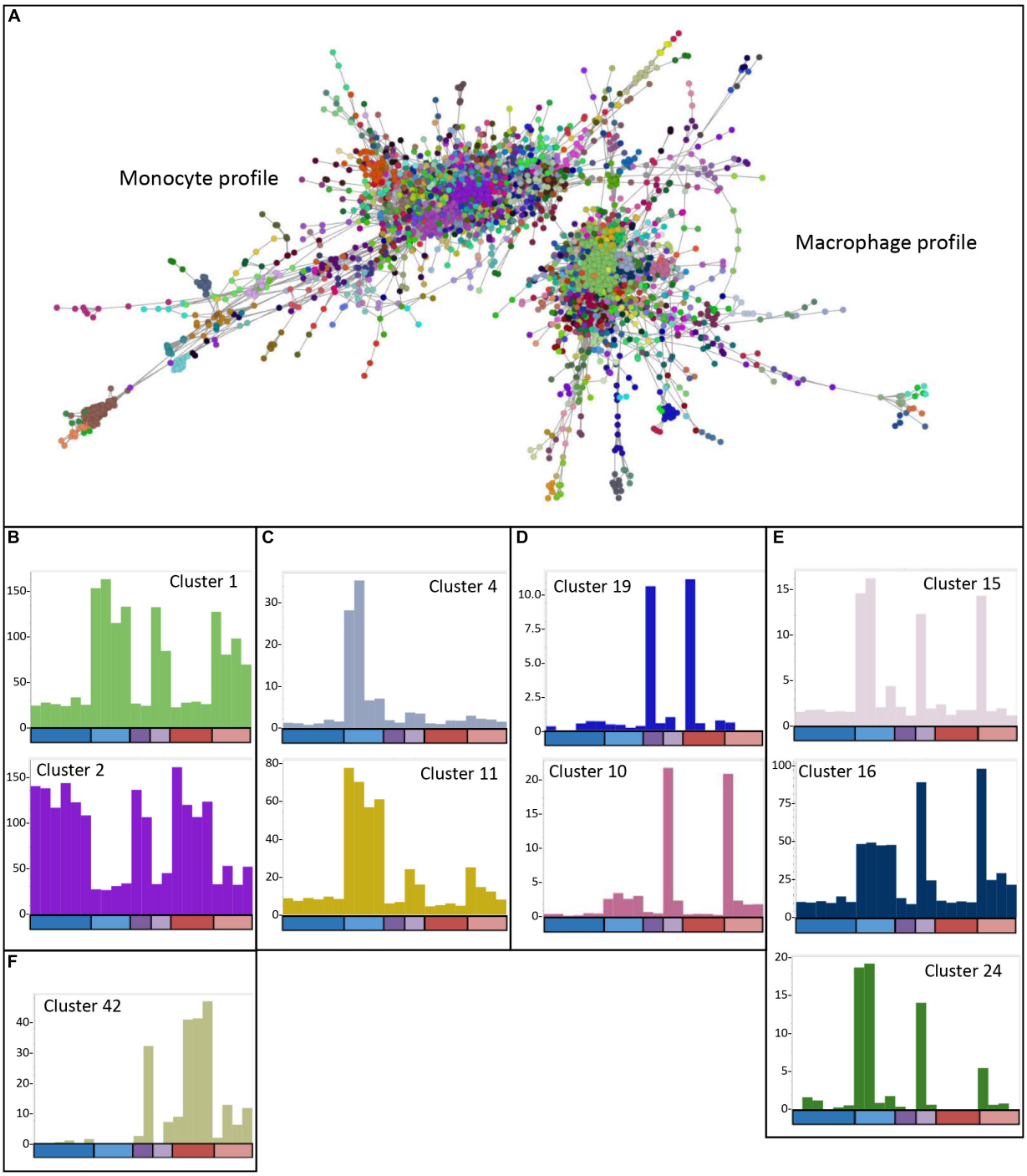

FIGURE 7 | Network analysis of edited cells. **(A)** Gene-to-gene 2D network graph. Image taken from BioLayout output showing CTSS-CTSS correlations (nodes = CTSS; edges = correlations of ≥0.92 between them). The analysis included all four *USP16* knockout lines, HetC and HetdE and wild type samples; raw data for wild type are from (Gazova et al., 2020), 0 h and 24 h time points. Nodes in the same cluster have the same color. **(B)** Average expression profiles for Clusters 1 and 2, showing up- or down-regulation in response to PMA in all cells. **(C)** Average expression profiles for Clusters 4 and 11 showing very small effect of PMA in the edited homozygous and heterozygous cells. **(D)** Average expression profiles for Clusters 10 and 19, showing specific expression in Hom1 and its parent HetC at 0 h (cluster 19) or 24 h post PMA treatment (Cluster 10). **(E)** Average expression profiles for Clusters 15, 16, and 24 showing expression in some or all wild type samples as well as HetC and Hom1. **(F)** Average expression profile for Cluster 42, showing high expression only in HetdE, Hom2, Hom3, and Hom4. In panels (**B**-**F**), *Y*-axis shows the average expression of genes in the cluster in TPM. *X*-axis shows the samples. The bar along the X axis shows the time point, colored as for **Figure 5**: dark colors 0 h, light colors – 24 h after PMA stimulation; blue – wild type, purple – heterozygotes, red – homozygotes. Samples are in the order wild type (6 samples at 0 h and 4 at 24 h), heterozygotes (HetC, HetdE), homozygotes (Hom1, Hom2, Hom3, and Hom4). Columns have the same color as the clustered nodes in panel **(A)**.

points. Because of the small number of genes in the clusters, GO enrichment analysis was performed on the combined list of genes to increase the power. With Bonferroni correction, the only enriched terms were GO Cellular Component (GO CC) terms relating to the mitochondrial matrix. For ontology terms, the Bonferroni adjustment is considered conservative since the terms are not independent (PANTHER documentation[15]). Therefore we used a reduced stringency (raw *P*-value < 0.001) to look for possible enrichment. GO Biological Process (GO BP) terms relating to metabolic processes and mitochondrial functions were enriched at this level (**Supplementary Table 2**). In contrast, genes in Cluster 33 (14 nodes) were low in wild type prior to PMA stimulation and increased in wild type after treatment and were high in all homozygotes and heterozygotes at both time points. This group was too small for meaningful GO enrichment analysis. These clusters indicate genes which may be affected by the absence of USP16, either in the monocyte state or after the cells are triggered to differentiate. Notably, the group which is low in the edited clones contains the *SRPRB* gene (Cluster 13), which encodes a protein thought to be an interaction partner of USP16 (BioGRID database of protein, genetic and chemical interactions[16]).

There were several other clusters which contained genes that were differently expressed in wild type and the edited clones. The average expression of genes in Cluster 4 (140 nodes) was up-regulated 8 to 30-fold during differentiation of wild type THP-1 cells (**Figure 7C**) but only increased up to two-fold in the heterozygous and homozygous knockout clones. These genes are likely dependent on USP16 for expression. This cluster contained known interferon inducible genes, and a promoter for the gene encoding the key transcription factor IRF9. GO annotations for genes within this clusters were enriched for terms involved with interferon signaling and response to virus.

Cluster 11 (44 nodes) contained genes that were increased 6 to 8 fold in wild type 24 h after PMA treatment. These genes were also increased at 24 h in heterozygotes and homozygotes, but only 4- to 5-fold (HetC and Hom1) or 2- to 3-fold (HetdE and Homs 2-4) (**Figure 7C**). These genes appear to be impacted by the loss of USP16, even in the heterozygotes which had wild type levels of expression of *USP16* mRNA (**Figure 2**). There was no significant GO term enrichment for these genes using the stringent Bonferroni correction. As above, to gain further insight into the impact of USP16 absence, we therefore looked at GO terms using a less stringent uncorrected significance threshold of $P < 0.001$. At this significance threshold, enriched GO Biological Process (GO BP) terms were related to regulation of immune system processes and membrane transporter activity (**Supplementary Table 2**).

Cluster 19 (23 nodes) contained genes that were high only in HetC and Hom1 prior to PMA treatment (**Figure 7D**). Although there were no significant GO terms for this small cluster using the Bonferroni correction, genes included several involved in the cell cycle (*BUB1, ESPL1B*, and *FANCA*) (Giotti et al., 2019). This was reflected in the GO BP terms enriched at lower stringency (uncorrected $P < 0.001$) which included terms relating to chromosome separation (**Supplementary Table 2**). In all cases of genes with multiple promoters, a minor promoter was found in this cluster, suggesting that one way Hom1 escapes the lack of USP16 and maintains the ability to proliferate (shown by the high level of *MYB* seen in **Figure 5B**) is to up-regulate minor promoters of other genes to compensate.

Cluster 10 (52 nodes) was the reciprocal of Cluster 19, where average expression increased around 5-fold in most samples at 24 h, but in HetC and Hom1 these genes were increased 27- and 53-fold respectively (**Figure 7D**). Most promoters in this cluster were expressed only in these two samples. As for Cluster 19, where genes had more than one promoter in the analysis, promoters in this cluster were almost all minor (usually low expression) promoters, including the third promoter for *CSF1R*. There was no GO terms enrichment at the stringent Bonferroni corrected significance level, but there was enrichment for genes associated with the PANTHER *integrin signaling* pathway. To examine the adaptations of HetC and Hom1 we therefore looked at GO terms using an uncorrected significance threshold of $P < 0.001$, which showed enrichment for GO BP terms related to tumor necrosis factor production, negative regulation of cell death, positive regulation of macrophage proliferation, cytokine production, regulation of histone phosphorylation and morphogenesis (**Supplementary Table 2**).

Several other clusters contained genes that were up-regulated in at least some wild type samples and in HetC and Hom1 at 24 h. Genes in Cluster 15 (29 nodes) were up-regulated after PMA stimulation in three wild type samples and in Hom1 and HetC (**Figure 7E**). The cluster included the gene for CSF1, the major effector of macrophage differentiation. Cluster 16 genes were also up-regulated at 24 h in wild type, HetC and Hom1 (**Figure 7E**). Genes in Cluster24 were increased in two wild type samples at 24 h and to a lesser extent in HetC and Hom1 but not in the other homozygous and heterozygous cells (**Figure 7E**). GO enrichment analysis of the combined gene list from these clusters included terms related to mesodermal cell differentiation, inflammation and cell motility.

Since their phenotype showed greater difference to wild type, and their differentiation appeared less complete than Hom1 (**Figures 3**, **5**), we also looked for clusters of genes that distinguished Hom2, Hom3 and Hom4 and the double-edited HetdE (from the same parent heterozygote) from wild type and HetC/Hom1. One small cluster (Cluster 42, 12 nodes; **Figure 7F**) contained genes that were increased in these cells prior to differentiation and slightly increased after 24 h with PMA. At the reduced stringency, enriched GO terms were related to biosynthetic processes and activation of plasma proteins involved in acute inflammation. However the major effects on these cells appeared to be reduction in expression of genes whose levels were maintained in HetC and Hom1.

DISCUSSION

This paper describes the impact of generating a homozygous inactivating mutation of the *USP16* gene in a high differentiation

[15] pantherdb.org/tips/tips_bonferroni.jsp, accessed February 2021

[16] https://thebiogrid.org, accessed February 2021

clone of the THP-1 acute monocytic leukemia cell line, using the CRISPR-Cas9 genome editing technique. The fact that we generated independent subclonal lines that proliferated in culture and were able to differentiate in response to PMA might imply that the many functions attributed to USP16 described in the introduction are redundant. However, our detailed analysis rather points to the ability of the leukemic line to adapt to the extreme selection pressure applied by the loss of USP16 through different compensatory pathways.

The generation of homozygous *USP16* knockout cells required two rounds of CRISPR-Cas9 mutagenesis. There were no homozygotes after the first round. After a second round using heterozygotes from the first round, 4 out of 67 viable clones were homozygous mutants, whereas 13 reverted back to wild type, presumably by homology-directed repair from the wild-type allele. This pattern strongly suggests that the survival and growth of homozygous $USP16^{-/-}$ cells was compromised, consistent with the observation that *Usp16* knockout is embryonic lethal in mice (Yang et al., 2014). The THP-1 $USP16^{-/-}$ survivors had likely up-regulated compensatory mechanisms (genetic or epigenetic) to overcome the deficiency. Since the surviving homozygotes had different phenotypes, depending on the heterozygote from which they originated, we conclude that different mechanisms were responsible for the viability of these clones. Aside from the loss of USP16, additional selection pressures derived from the harsh conditions of electroporation, FACS sorting and single cell cloning. For this reason, it is important to use controls that have also been subjected to the same process. We present results from heterozygote cells that had been through the same two rounds of CRISPR-Cas9 treatment. We also assessed doubly targeted cells which had reverted to wild type, for cell cycle characteristics; they showed no difference from the parental wild type cells.

Arguably, selection pressures similar to those of CRISPR-Cas9 treated cultures occur during the evolution of a cancer *in vivo* (Fortunato et al., 2017). Although our starting population was a clonal line selected for high differentiation potential (Suzuki et al., 2009), THP-1 cells have deficient mutation repair (Bauer et al., 2011) and the original clonal population is likely by now to contain divergent lines characterized by different mutations. The heterozygous mutant lines from the first round may have been derived from cells that had accumulated other mutations or epigenetic modifications that compensated at least in part for the loss of *USP16* and allowed the survival of the homozygotes after the second round of selection.

The simple MTT viable cell assay suggested that three of the homozygous mutant clones (Hom2, Hom3, and Hom4) grew marginally more slowly than the parent (**Figure 3B**) but this was not supported by cell cycle analysis (**Figure 3C**). There were some differences in down-regulation of *MYB* and up-regulation of *CSF1R* between wild type and homozygous clones (**Figure 5**). However, in overview the loss of USP16 did not prevent THP-1 cells from proliferating or differentiating to become adherent phagocytic macrophages in response to PMA (**Figure 3A**).

To dissect the transcriptome of THP-1 wild type cells with the *USP16* knockout clones we used CAGE, a promoter based approach that provides expression levels by capturing mRNA with the 5′ modified guanine cap (Balwierz et al., 2009; Forrest et al., 2014). The CAGE data (**Figure 2B**) confirmed reduction of *USP16* mRNA in the homozygous knockout clones both before and after PMA treatment, presumably due to nonsense-mediated decay. Combined with the lack of effect of heterozygous mutation on USP16 protein (**Figure 2C**) the data suggest there is dosage compensation.

The H2AK119 deubiquitinases are collectively involved in cell cycle progression and DNA repair (Atanassov et al., 2011; Chen et al., 2015; Aquila and Atanassov, 2020), and the most obvious potential mechanism to escape the impacts of loss of USP16 would be to up-regulate related deubiquitinases. Other studies have observed interdependence of deubiquitinase mRNA levels. For example, *USP12* down-regulation resulted in *USP46* up-regulation (Joo et al., 2011). Indeed, mRNA encoding USP12, BAP1 and MYSM1 was increased in all USP16-deficient lines and Hom1 also had increased *USP21* mRNA, encoding another H2AK119 deubiquitinase. *USP3* and *USP22* mRNA showed distinct patterns of down-regulation by PMA in the different homozygous lines. Both over- and under-expression of *USP3* have been shown to have effects consistent with tumorigenesis. For example, USP3 promoted proliferation in a number of cancers (Fang et al., 2018; Wu et al., 2019; Das et al., 2020; Li et al., 2020; Liao et al., 2020) while other reports show that depletion of USP3 can increase the incidence of spontaneous tumors (Lancini et al., 2016), promote metastasis (Wang et al., 2017), inhibit leukemia cell differentiation (Chae et al., 2019), and accelerate degradation of TP53 leading to enhanced proliferation and transformation (Fu et al., 2017).

Our transcriptional network analysis of individual clones in the presence and absence of PMA complements our recent high-density time course analysis of the differentiation response in the parent line (Gazova et al., 2020). In effect it is a perturbation analysis in which intrinsic plasticity and genetic-epigenetic instability of THP-1 and clonal heterogeneity, as well as the specific loss of USP16, all contribute to the phenotype. Genes in Clusters 4 and 11 were reduced in all edited cells, both homozygotes and heterozygotes, and were associated with interferon signaling and immune responses. Transfection with plasmid DNA to generate mutations activates the AIM2 inflammasome and cGAS pathways in THP-1 cells (Burckstummer et al., 2009; Paijo et al., 2016) leading to interferon induction and inhibition of proliferation as well as cell death. It is very likely that the generation of mutants selects against interferon responsiveness. Conversely, other clusters of genes were greatly increased in the edited cells, albeit not tightly correlated with *USP16* genotype. HetC and Hom1, where the phenotype was closer to wild type, up-regulated the key regulator, *MYB* (Suzuki et al., 2009) which may overcome a partial block on proliferation caused by the loss of USP16.

Despite the subtle differences in gene expression amongst the clones, irrespective of the loss of USP16 and the apparent loss of interferon signaling, all of the lines were able to undergo macrophage-specific cellular differentiation and some degree of growth inhibition in response to PMA, indicated by the coordinated regulation of transcripts within Clusters

1 and 2 respectively. They each expressed the macrophage-specific transcription factor *SPI1* (encoding PU.1) constitutively with a similar signal from the upstream enhancer identified previously (Suzuki et al., 2009; Gazova et al., 2020). The 24 h time point occurs before induction of surface markers such as ITGAM (CD11B) and APOE, but the inducible genes in Cluster 1 include *SPP1* (encoding osteopontin) and *CSF1R*, both of which were highlighted in earlier analyses (Suzuki et al., 2009) as well as genes encoding macrophage surface receptors and lysosomal enzymes. Each clone showed similar massive induction of the key cell cycle inhibitor, *CDKN1A* (p21WAF) highlighted previously (Gazova et al., 2020) and Cluster 2, down-regulated in all lines, contains numerous S-phase cell cycle-related transcripts including *CDK2, E2F1*, and *PCNA*.

A limitation of this study is that it used an immortalized cell line derived from an acute myeloid leukemia 40 years ago. The compensation phenomenon we have described is specific to cells under the intense selection of USP16 deletion. Generation of homozygous knockout clones was a rare event in our study, with strong selection in the second targeting for cells that had reverted to wild type. To better understand the role of USP16 and possible compensatory mechanisms, cells from newly diagnosed tumors could be examined. In particular, changes in expression of the histone deubiquitinases over the evolution of the tumor and during relapses would reveal whether the mechanism proposed here is also found in primary tumors. There are some examples of apparent down-regulation of USP16 in cancer (Fernandez et al., 2004; Gelsi-Boyer et al., 2008; Qian et al., 2016) but *USP16* mutation is rare in primary cancers (data from TCGA Project[17]) which may be consistent with its important role in the cell cycle and DNA repair, and a reason why it has been considered as a cancer drug target. The gene is actually expressed ubiquitously in every tumor cell line (leukemias, sarcomas, adenocarcinomas) and proliferating primary cell population that was analyzed in the large FANTOM5 project (Forrest et al., 2014). A study of those rare cancers which have inactivating *USP16* mutations would reveal whether the compensatory mechanisms proposed here are also operating *in vivo*.

In conclusion, this communication is a case study in leukemic cell adaptation. The original functional analysis of USP16 (Joo et al., 2007) reported a 3-fold slowing of proliferation, M phase arrest and increased basal H2A ubiquitination in HeLa cells with a stable 90% knock down of the USP16 protein. On that basis one might consider USP16 as a target for cancer chemotherapy and indeed that has been proposed (Harrigan et al., 2018). Our study shows clearly that USP16 is potentially redundant and with sufficient selection pressure, leukemic cells would give rise to escape mutants that are resistant to USP16 inhibitors.

‡ORCID:

Iveta Gažová
orcid.org/0000-0002-0787-9463
Lucas Lefevre
orcid.org/0000-0003-0925-7411
Stephen J. Bush
orcid.org/0000-0001-9341-2562
Rocio Rojo
orcid.org/0000-0001-9686-3377
David A. Hume
orcid.org/0000-0002-2615-1478
Andreas Lengeling
orcid.org/0000-0002-7992-2563
Kim M. Summers
orcid.org/0000-0002-7084-4386

[17]https://www.cancer.gov/about-nci/organization/ccg/research/structural-genomics/tcga, accessed April 2021

DATA AVAILABILITY STATEMENT

The datasets presented in this study can be found in an online repository at https://www.ebi.ac.uk/ena, PRJEB43087. The results can be visualised using the ZENBU browser at http://fantom.gsc.riken.jp/zenbu/gLyphs/#config=Gazova_USP16KO.

AUTHOR CONTRIBUTIONS

KS, AL, and DH designed and supervised the project. IG, LL, and RR performed the laboratory work. IG, SB, and KS performed the bioinformatic analysis. IG and KS wrote the manuscript. All authors read and approved the manuscript.

FUNDING

IG is grateful for a scholarship from the Lady Tata Memorial Trust, London, United Kingdom. RR is supported by a doctoral scholarship (application number: 314413, file number: 218819) granted by the CONACyT Nuevo Leon—I2T2, Mexico. DH and KS are supported by the Mater Foundation, Brisbane, QLD, Australia. The Translational Research Institute receives funding from the Australian Government. The Roslin Institute receives core strategic funding from the Biotechnology and Biological Sciences Research Council of the United Kingdom (BB/J004235/1, BB/E/D/20211552, BB/J004227/1, and BB/E/D/20231762).

SUPPLEMENTARY MATERIAL

The Supplementary Material for this article can be found online at: https://www.frontiersin.org/articles/10.3389/fcell.2021.679544/full#supplementary-material

Supplementary Figure 1 | Graph size vs correlation threshold for BioLayout analysis.

Supplementary Figure 2 | Image of CAGE tags mapping to *USP16* taken from the ZENBU viewer.

Supplementary Table 1 | Clusters of coexpressed genes.

Supplementary Table 2 | GO term enrichment analysis for selected clusters.

REFERENCES

Abdel-Rahman, M. H., Pilarski, R., Cebulla, C. M., Massengill, J. B., Christopher, B. N., Boru, G., et al. (2011). Germline *BAP1* mutation predisposes to uveal melanoma, lung adenocarcinoma, meningioma, and other cancers. *J. Med. Genet.* 48, 856–859. doi: 10.1136/jmedgenet-2011-100156

Abdel-Wahab, O., Adli, M., Lafave, L. M., Gao, J., Hricik, T., Shih, A. H., et al. (2012). *ASXL1* mutations promote myeloid transformation through loss of PRC2-mediated gene repression. *Cancer Cell* 22, 180–193. doi: 10.1016/j.ccr.2012.06.032

Adati, N., Huang, M. C., Suzuki, T., Suzuki, H., and Kojima, T. (2009). High-resolution analysis of aberrant regions in autosomal chromosomes in human leukemia THP-1 cell line. *BMC Res. Notes* 2:153. doi: 10.1186/1756-0500-2-153

Adorno, M., Sikandar, S., Mitra, S. S., Kuo, A., Nicolis Di Robilant, B., Haro-Acosta, V., et al. (2013). USP16 contributes to somatic stem-cell defects in Down's syndrome. *Nature* 501, 380–384. doi: 10.1038/nature12530

Andersson-Rolf, A., Merenda, A., Mustata, R. C., Li, T., Dietmann, S., and Koo, B. K. (2016). Simultaneous paralogue knockout using a CRISPR-concatemer in mouse small intestinal organoids. *Dev. Biol.* 420, 271–277. doi: 10.1016/j.ydbio.2016.10.016

Aquila, L., and Atanassov, B. S. (2020). Regulation of histone ubiquitination in response to DNA double strand breaks. *Cells* 9:1699. doi: 10.3390/cells9071699

Atanassov, B. S., Koutelou, E., and Dent, S. Y. (2011). The role of deubiquitinating enzymes in chromatin regulation. *FEBS Lett.* 585, 2016–2023. doi: 10.1016/j.febslet.2010.10.042

Balwierz, P. J., Carninci, P., Daub, C. O., Kawai, J., Hayashizaki, Y., Van Belle, W., et al. (2009). Methods for analyzing deep sequencing expression data: constructing the human and mouse promoterome with deepCAGE data. *Genome Biol.* 10:R79. doi: 10.1186/gb-2009-10-7-r79

Bauer, M., Goldstein, M., Christmann, M., Becker, H., Heylmann, D., and Kaina, B. (2011). Human monocytes are severely impaired in base and DNA double-strand break repair that renders them vulnerable to oxidative stress. *Proc. Natl. Acad. Sci. U.S.A.* 108, 21105–21110. doi: 10.1073/pnas.1111919109

Belle, J. I., and Nijnik, A. (2014). H2A-dubbing the mammalian epigenome: expanding frontiers for histone H2A deubiquitinating enzymes in cell biology and physiology. *Int. J. Biochem. Cell. Biol.* 50, 161–174. doi: 10.1016/j.biocel.2014.03.004

Burckstummer, T., Baumann, C., Bluml, S., Dixit, E., Durnberger, G., Jahn, H., et al. (2009). An orthogonal proteomic-genomic screen identifies AIM2 as a cytoplasmic DNA sensor for the inflammasome. *Nat. Immunol.* 10, 266–272. doi: 10.1038/ni.1702

Cai, S. Y., Babbitt, R. W., and Marchesi, V. T. (1999). A mutant deubiquitinating enzyme (Ubp-M) associates with mitotic chromosomes and blocks cell division. *Proc. Natl. Acad. Sci. U.S.A.* 96, 2828–2833.

Chae, Y. C., Jung, H., Kim, J. Y., Lee, D. H., and Seo, S. B. (2019). Ubiquitin-specific peptidase 3 induces TPA-mediated leukemia cell differentiation via regulating H2AK119ub. *Anim. Cells Syst. (Seoul)* 23, 311–317. doi: 10.1080/19768354.2019.1661283

Chen, D., Dai, C., and Jiang, Y. (2015). Histone H2A and H2B deubiquitinase in developmental disease and cancer. *Cancer Transl. Med.* 1, 170–175. doi: 10.4103/2395-3977.168578

Das, S., Chandrasekaran, A. P., Suresh, B., Haq, S., Kang, J. H., Lee, S. J., et al. (2020). Genome-scale screening of deubiquitinase subfamily identifies USP3 as a stabilizer of Cdc25A regulating cell cycle in cancer. *Cell Death Differ.* 27, 3004–3020. doi: 10.1038/s41418-020-0557-5

Fang, C. L., Lin, C. C., Chen, H. K., Hseu, Y. C., Hung, S. T., Sun, D. P., et al. (2018). Ubiquitin-specific protease 3 overexpression promotes gastric carcinogenesis and is predictive of poor patient prognosis. *Cancer Sci.* 109, 3438–3449. doi: 10.1111/cas.13789

Fernandez, P., Carretero, J., Medina, P. P., Jimenez, A. I., Rodriguez-Perales, S., Paz, M. F., et al. (2004). Distinctive gene expression of human lung adenocarcinomas carrying LKB1 mutations. *Oncogene* 23, 5084–5091. doi: 10.1038/sj.onc.1207665

Forrest, A. R., Kawaji, H., Rehli, M., Baillie, J. K., De Hoon, M. J., Haberle, V., et al. (2014). A promoter-level mammalian expression atlas. *Nature* 507, 462–470. doi: 10.1038/nature13182

Fortunato, A., Boddy, A., Mallo, D., Aktipis, A., Maley, C. C., and Pepper, J. W. (2017). Natural selection in cancer biology: from molecular snowflakes to trait hallmarks. *Cold Spring Harb. Perspect. Med.* 7:a029652. doi: 10.1101/cshperspect.a029652

Frangini, A., Sjoberg, M., Roman-Trufero, M., Dharmalingam, G., Haberle, V., Bartke, T., et al. (2013). The aurora B kinase and the polycomb protein ring1B combine to regulate active promoters in quiescent lymphocytes. *Mol. Cell* 51, 647–661. doi: 10.1016/j.molcel.2013.08.022

Freeman, T. C., Goldovsky, L., Brosch, M., Van Dongen, S., Maziere, P., Grocock, R. J., et al. (2007). Construction, visualisation, and clustering of transcription networks from microarray expression data. *PLoS Comput. Biol.* 3, 2032–2042. doi: 10.1371/journal.pcbi.0030206

Fu, S., Shao, S., Wang, L., Liu, H., Hou, H., Wang, Y., et al. (2017). USP3 stabilizes p53 protein through its deubiquitinase activity. *Biochem. Biophys. Res. Commun.* 492, 178–183. doi: 10.1016/j.bbrc.2017.08.036

Gazova, I., Lefevre, L., Bush, S. J., Clohisey, S., Arner, E., De Hoon, M., et al. (2020). The transcriptional network that controls growth arrest and macrophage differentiation in the human myeloid leukemia cell line THP-1. *Front. Cell. Dev. Biol.* 8:498. doi: 10.3389/fcell.2020.00498

Gelsi-Boyer, V., Trouplin, V., Adelaide, J., Aceto, N., Remy, V., Pinson, S., et al. (2008). Genome profiling of chronic myelomonocytic leukemia: frequent alterations of RAS and RUNX1 genes. *BMC Cancer* 8:299. doi: 10.1186/1471-2407-8-299

Giotti, B., Chen, S. H., Barnett, M. W., Regan, T., Ly, T., Wiemann, S., et al. (2019). Assembly of a parts list of the human mitotic cell cycle machinery. *J. Mol. Cell Biol.* 11, 703–718. doi: 10.1093/jmcb/mjy063

Gu, Y., Jones, A. E., Yang, W., Liu, S., Dai, Q., Liu, Y., et al. (2016). The histone H2A deubiquitinase Usp16 regulates hematopoiesis and hematopoietic stem cell function. *Proc. Natl. Acad. Sci. U.S.A.* 113, E51–E60. doi: 10.1073/pnas.1517041113

Haberle, V., Forrest, A. R., Hayashizaki, Y., Carninci, P., and Lenhard, B. (2015). CAGEr: precise TSS data retrieval and high-resolution promoterome mining for integrative analyses. *Nucleic Acids Res.* 43:e51. doi: 10.1093/nar/gkv054

Harrigan, J. A., Jacq, X., Martin, N. M., and Jackson, S. P. (2018). Deubiquitylating enzymes and drug discovery: emerging opportunities. *Nat. Rev. Drug Discov.* 17, 57–78. doi: 10.1038/nrd.2017.152

Heppner, G. H. (1984). Tumor heterogeneity. *Cancer Res.* 44, 2259–2265.

Hume, D. A., Summers, K. M., and Rehli, M. (2016). Transcriptional regulation and macrophage differentiation. *Microbiol. Spectr.* 4:MCHD-0024-2015. doi: 10.1128/microbiolspec.MCHD-0024-2015

Jones, A., Xu, C., Min, J., and Wang, H. (2013). Ubiquitin specific peptidase 16. *Handb. Proteolytic Enzymes* 2, 2090–2094. doi: 10.1016/B978-0-12-382219-2.00470-1

Joo, H. Y., Jones, A., Yang, C., Zhai, L., Smith, A. D. T., Zhang, Z., et al. (2011). Regulation of histone H2A and H2B deubiquitination and xenopus development by USP12 and USP46. *J. Biol. Chem.* 286, 7190–7201. doi: 10.1074/jbc.M110.158311

Joo, H. Y., Zhai, L., Yang, C., Nie, S., Erdjument-Bromage, H., Tempst, P., et al. (2007). Regulation of cell cycle progression and gene expression by H2A deubiquitination. *Nature* 449, 1068–1072. doi: 10.1038/nature06256

Komander, D., Clague, M. J., and Urbe, S. (2009). Breaking the chains: structure and function of the deubiquitinases. *Nat. Rev. Mol. Cell Biol.* 10, 550–563. doi: 10.1038/nrm2731

Lancini, C., Gargiulo, G., Van Den Berk, P. C., and Citterio, E. (2016). Quantitative analysis by next generation sequencing of hematopoietic stem and progenitor cells (LSK) and of splenic B cells transcriptomes from wild-type and Usp3-knockout mice. *Data Brief.* 6, 556–561. doi: 10.1016/j.dib.2015.12.049

Lanzuolo, C., and Orlando, V. (2012). Memories from the polycomb group proteins. *Annu. Rev. Genet.* 46, 561–589. doi: 10.1146/annurev-genet-110711-155603

Ler, L. D., Ghosh, S., Chai, X., Thike, A. A., Heng, H. L., Siew, E. Y., et al. (2017). Loss of tumor suppressor KDM6A amplifies PRC2-regulated transcriptional repression in bladder cancer and can be targeted through inhibition of EZH2. *Sci. Transl. Med.* 9:eaai8312. doi: 10.1126/scitranslmed.aai8312

Li, B., Jin, M., Cao, F., Li, J., Wu, J., Xu, L., et al. (2020). Hsa_circ_0017639 expression promotes gastric cancer proliferation and metastasis by sponging miR-224-5p and upregulating USP3. *Gene* 750:144753. doi: 10.1016/j.gene.2020.144753

Liao, X. H., Wang, Y., Zhong, B., and Zhu, S. Y. (2020). USP3 promotes proliferation of non-small cell lung cancer through regulating RBM4. *Eur.*

Rev. Med. Pharmacol. Sci. 24, 3143–3151. doi: 10.26355/eurrev_202003_20681

Maess, M. B., Sendelbach, S., and Lorkowski, S. (2010). Selection of reliable reference genes during THP-1 monocyte differentiation into macrophages. *BMC Mol. Biol.* 11:90. doi: 10.1186/1471-2199-11-90

Mateos, M. K., Barbaric, D., Byatt, S. A., Sutton, R., and Marshall, G. M. (2015). Down syndrome and leukemia: insights into leukemogenesis and translational targets. *Transl. Pediatr.* 4, 76–92. doi: 10.3978/j.issn.2224-4336.2015.03.03

Pai, M. T., Tzeng, S. R., Kovacs, J. J., Keaton, M. A., Li, S. S., Yao, T. P., et al. (2007). Solution structure of the Ubp-M BUZ domain, a highly specific protein module that recognizes the C-terminal tail of free ubiquitin. *J. Mol. Biol.* 370, 290–302. doi: 10.1016/j.jmb.2007.04.015

Paijo, J., Doring, M., Spanier, J., Grabski, E., Nooruzzaman, M., Schmidt, T., et al. (2016). cGAS senses human cytomegalovirus and induces type I interferon responses in human monocyte-derived cells. *PLoS Pathog.* 12:e1005546. doi: 10.1371/journal.ppat.1005546

Qian, Y., Wang, B., Ma, A., Zhang, L., Xu, G., Ding, Q., et al. (2016). USP16 downregulation by carboxyl-terminal truncated HBx promotes the growth of hepatocellular carcinoma cells. *Sci. Rep.* 6:33039. doi: 10.1038/srep33039

Ran, F. A., Hsu, P. D., Wright, J., Agarwala, V., Scott, D. A., and Zhang, F. (2013). Genome engineering using the CRISPR-Cas9 system. *Nat. Protoc.* 8, 2281–2308. doi: 10.1038/nprot.2013.143

Rawlings, N. D., and Barrett, A. J. (1994). Families of cysteine peptidases. *Methods Enzymol.* 244, 461–486. doi: 10.1016/0076-6879(94)44034-4

Rawlings, N. D., and Barrett, A. J. (2013). "Introduction: the clans and families of cysteine peptidases," in *Handbook of Proteolytic Enzymes*, eds N. C. Rawlings and G. Salvesen (Amsterdam: Academic Press), 1743–1773.

Rawlings, N. D., Barrett, A. J., Thomas, P. D., Huang, X., Bateman, A., and Finn, R. D. (2018). The MEROPS database of proteolytic enzymes, their substrates and inhibitors in 2017 and a comparison with peptidases in the PANTHER database. *Nucleic Acids Res.* 46, D624–D632. doi: 10.1093/nar/gkx1134

Severin, J., Lizio, M., Harshbarger, J., Kawaji, H., Daub, C. O., Hayashizaki, Y., et al. (2014). Interactive visualization and analysis of large-scale sequencing datasets using ZENBU. *Nat. Biotechnol.* 32, 217–219. doi: 10.1038/nbt.2840

Summers, K. M., Bush, S. J., and Hume, D. A. (2020). Network analysis of transcriptomic diversity amongst resident tissue macrophages and dendritic cells in the mouse mononuclear phagocyte system. *PLoS Biol.* 18:e3000859. doi: 10.1371/journal.pbio.3000859

Suzuki, H., Forrest, A. R., Van Nimwegen, E., Daub, C. O., Balwierz, P. J., Irvine, K. M., et al. (2009). The transcriptional network that controls growth arrest and differentiation in a human myeloid leukemia cell line. *Nat. Genet.* 41, 553–562. doi: 10.1038/ng.375

Takahashi, H., Lassmann, T., Murata, M., and Carninci, P. (2012). 5' end-centered expression profiling using cap-analysis gene expression and next-generation sequencing. *Nat. Protoc.* 7, 542–561. doi: 10.1038/nprot.2012.005

Theocharidis, A., Van Dongen, S., Enright, A. J., and Freeman, T. C. (2009). Network visualization and analysis of gene expression data using biolayout express(3d). *Nat. Protoc.* 4, 1535–1550. doi: 10.1038/nprot.2009.177

Traore, K., Trush, M. A., George, M. Jr., Spannhake, E. W., Anderson, W., and Asseffa, A. (2005). Signal transduction of phorbol 12-myristate 13-acetate (PMA)-induced growth inhibition of human monocytic leukemia THP-1 cells is reactive oxygen dependent. *Leuk Res.* 29, 863–879. doi: 10.1016/j.leukres.2004.12.011

Tsuchiya, S., Kobayashi, Y., Goto, Y., Okumura, H., Nakae, S., Konno, T., et al. (1982). Induction of maturation in cultured human monocytic leukemia cells by a phorbol diester. *Cancer Res.* 42, 1530–1536.

Tsuchiya, S., Yamabe, M., Yamaguchi, Y., Kobayashi, Y., Konno, T., and Tada, K. (1980). Establishment and characterization of a human acute monocytic leukemia cell line (tTHP-1). *Int. J. Cancer* 26, 171–176.

Vogelstein, B., Papadopoulos, N., Velculescu, V. E., Zhou, S., Diaz, L. A. Jr., and Kinzler, K. W. (2013). Cancer genome landscapes. *Science* 339, 1546–1558. doi: 10.1126/science.1235122

Wang, Z., Yang, J., Di, J., Cui, M., Xing, J., Wu, F., et al. (2017). Downregulated USP3 mRNA functions as a competitive endogenous RNA of SMAD4 by sponging miR-224 and promotes metastasis in colorectal cancer. *Sci. Rep.* 7:4281. doi: 10.1038/s41598-017-04368-3

Wu, Y., Qin, J., Li, F., Yang, C., Li, Z., Zhou, Z., et al. (2019). USP3 promotes breast cancer cell proliferation by deubiquitinating KLF5. *J. Biol. Chem.* 294, 17837–17847. doi: 10.1074/jbc.RA119.009102

Xu, Y., Yang, H., Joo, H. Y., Yu, J. H., Smith, A. D. T., Schneider, D., et al. (2013). Ubp-M serine 552 phosphorylation by cyclin-dependent kinase 1 regulates cell cycle progression. *Cell Cycle* 12, 3219–3227. doi: 10.4161/cc.26278

Yang, W., Lee, Y. H., Jones, A. E., Woolnough, J. L., Zhou, D., Dai, Q., et al. (2014). The histone H2A deubiquitinase USP16 regulates embryonic stem cell gene expression and lineage commitment. *Nat. Commun.* 5:3818. doi: 10.1038/ncomms4818

Yates, A., Akanni, W., Amode, M. R., Barrell, D., Billis, K., Carvalho-Silva, D., et al. (2016). Ensembl 2016. *Nucleic Acids Res.* 44, D710–D716. doi: 10.1093/nar/gkv1157

Zhang, Z., Yang, H., and Wang, H. (2014). The histone H2A deubiquitinase USP16 interacts with HERC2 and fine-tunes cellular response to DNA damage. *J. Biol. Chem.* 289, 32883–32894. doi: 10.1074/jbc.M114.599605

Conflict of Interest: The authors declare that the research was conducted in the absence of any commercial or financial relationships that could be construed as a potential conflict of interest.

Citation: Gažová I, Lefevre L, Bush SJ, Rojo R, Hume DA, Lengeling A and Summers KM (2021) CRISPR-Cas9 Editing of Human Histone Deubiquitinase Gene USP16 in Human Monocytic Leukemia Cell Line THP-1. Front. Cell Dev. Biol. 9:679544. doi: 10.3389/fcell.2021.679544

frontiers in Cell and Developmental Biology

ORIGINAL RESEARCH
published: 01 June 2021
doi: 10.3389/fcell.2021.671202

Exosomal miR-2276-5p in Plasma Is a Potential Diagnostic and Prognostic Biomarker in Glioma

Jingxian Sun[1,2†], Zhenying Sun[1,2†], Ilgiz Gareev[3†], Tao Yan[1,2], Xin Chen[1,2], Aamir Ahmad[4], Daming Zhang[1,2], Boxian Zhao[1,2], Ozal Beylerli[3], Guang Yang[1,2]* and Shiguang Zhao[1,2]**

[1] Department of Neurosurgery, The First Affiliated Hospital of Harbin Medical University, Harbin, China, [2] Institute of Brain Science, Harbin Medical University, Harbin, China, [3] Central Research Laboratory, Bashkir State Medical University, Ufa, Russia, [4] University of Alabama at Birmingham, Birmingham, AL, United States

OPEN ACCESS

Edited by:
Ata Abbas,
Case Western Reserve University,
United States

Reviewed by:
Atrayee Bhattacharya,
Dana–Farber Cancer Institute,
United States
Khalid Timani,
Rosalind Franklin University of Medicine and Science,
United States

***Correspondence:**
Guang Yang
yangguang@163.com
Shiguang Zhao
guangsz@hotmail.com
Aamir Ahmad
aamirahmad100@gmail.com

† These authors have contributed equally to this work

Specialty section:
This article was submitted to Epigenomics and Epigenetics, a section of the journal Frontiers in Cell and Developmental Biology

Received: *23 February 2021*
Accepted: *23 April 2021*
Published: *01 June 2021*

Citation:
Sun J, Sun Z, Gareev I, Yan T, Chen X, Ahmad A, Zhang D, Zhao B, Beylerli O, Yang G and Zhao S (2021) Exosomal miR-2276-5p in Plasma Is a Potential Diagnostic and Prognostic Biomarker in Glioma. Front. Cell Dev. Biol. 9:671202. doi: 10.3389/fcell.2021.671202

Introduction: Exosomal microRNAs (miRNAs) play an essential role in near and distant intercellular communication and are potential diagnostic and prognostic biomarkers for various cancers. This study focused on evaluation of exosomal miR-2276-5p in plasma as a diagnostic and prognostic biomarker for glioma.

Methods: Plasma exosomes from 124 patients with glioma and 36 non-tumor controls were collected and subjected to quantitative real-time polymerase chain reaction (qRT-PCR) analysis for the exosomal miR-2276-5p expression. Bioinformatic analyses were performed to identify a gene target, and CGGA and TCGA databases were checked for evaluation of prognostic relevance.

Results: The exosomal miR-2276-5p in glioma patients had a significantly decreased expression, compared with non-glioma patients ($p < 0.01$). Receiver operating characteristics (ROC) curve analyses were observed to regulate the diagnostic sensitivity and specificity of miR-2276-5p in glioma; the area under the curve (AUC) for miR-2276-5p was 0.8107. The lower expression of exosomal miR-2276-5p in patients with glioma correlated with poorer survival rates. RAB13 was identified as the target of miR-2276-5p which was high in glioma patients, especially those with higher tumor grades and correlated with poor survival.

Conclusion: The circulating exosomal miR-2276-5p is significantly reduced in the plasma of glioma patients, and thus, it could be a potential biomarker for patients with glioma for diagnostic and/or prognostic purposes.

Keywords: miRNA-2276-5p, circulating exosomes, glioma, RAB13, prognosis

INTRODUCTION

Glioma is a malignant disease with a high rate of mortality and morbidity. In 2018, there were 296,851 new glioma cases and 241,037 glioma patients' deaths worldwide (Ferlay et al., 2019). According to the World Health Organization (WHO), glioma is classified as grades I–IV, with glioblastoma (GBM, grade IV) as the most malignant type (Ostrom et al., 2017; Capper et al., 2018).

The primary treatment for GBM is surgical resection with radiotherapy and chemotherapy, and the median survival of patients is around 14–17 months (Reifenberger et al., 2017).

Exosomes, the small extracellular vesicles, are prevalent in biological fluids (Yoshimura et al., 2018) and can be invaluable biomarkers in cancer. The data for such role of exosomes in glioma are emerging (Huang et al., 2018). Exosomes contain nucleic acids and proteins, which play an essential role during glioma intercellular communication(s) (Qian et al., 2019). Exosomes' concentration has been suggested as a biomarker in glioma, and it has been reported that Rabs, located on the specific organelle membranes, regulate each step of membrane transport. There are 60 Rabs or Rab-like proteins in cells (Hutagalung and Novick, 2011) that are all involved in the regulation of membrane transport. Rab proteins are also involved in the process of exosome formation (D'Souza-Schorey and Clancy, 2012), and their targeted knockdown can negatively impact the secretion of exosomes (Hoshino et al., 2013). Although miR-2276-5p is rarely reported in glioma, wherein it exists as an endogenous competitive RNA impacting glioma cells (Wang Z. et al., 2019), there has been no report on its possible evaluation as a potential biomarker in the exosomes for the diagnosis (or prognosis) of glioma patients. Furthermore, RAB13 has been reported as a novel biomarker in cancer (Chen et al., 2019a) with its expression correlating negatively with gastric cancer patients' overall survival (OS) and progression-free survival (PFS). However, the role, if any, of RAB13 in glioma is unclear. Our study reports exosomal miR-2276-5p in GBM for the first time and further establishes RAB13 as the downstream of the miR-2276-5p. RAB13 could also predict the prognosis in glioma patients. This novel information should help design future studies to further explore the role of miR-2276-5p and its target RAB13 in glioma progression, with the aim to exploit this knowledge for development of targeted therapies against GBM.

MATERIALS AND METHODS

Patients and Sample Preparation

The study was approved by the First Affiliated Hospital of the Harbin Medical University and implemented by the principles of the Helsinki Declaration. Patients signed informed consent forms before blood draw and surgery. We collected blood samples and clinical dates from 124 glioma patients, including three WHO grade I patients, 30 grade II patients, 34 grade III patients, and 57 grade IV patients who underwent treatment in the Department of Neurosurgery at the First Affiliated Hospital of Harbin Medical University in China between July 2015 and July 2017. The patients were diagnosed with glioma by postoperative pathological section according to the WHO criteria, and pathological diagnosis was performed by two independent pathologists. Non-glioma patients who had no medical history of another cancer were recruited into this study as controls ($n = 36$), matched by sex and age with the glioma group. Clinical characteristics of the glioma patients are summarized in **Table 1**. All plasma samples for glioma and non-tumor patients were collected in EDTA-K3 tubes before the start of any treatment. After the first centrifugation for 10 min at 3,000 × *g*, the supernatants were carefully moved to a new tube and snap frozen at −80°C to isolate the exosomes.

TABLE 1 | The Baseline Characteristics of Glioma Patients.

Characteristics	*n* = 124
Age, y	50.7 ± 14.1
Grade	
I	3 (2.4)
II	30 (24.2)
III	34 (27.4)
IV	57 (46.0)
Gender	
Male	54 (43.5)
Female	70 (56.5)
Survival Time (Month)	13.18 ± 11.30
Location of Glioma	
Frontal	66 (53.2)
Temporal	40 (32.3)
Parietal	10 (8.1)
Occipital	5 (4.0)
Infratentorial	3 (2.4)
Extent of Surgery	
Complete resection	85 (78.5)
Biopsy or partial resection	39 (31.5)

Cell Lines and Transfections

Human glioblastoma cell lines (LN229 and U87) were obtained from China Infrastructure of Cell Line Resource (National Science and Technology Infrastructure, NSTI). They were maintained in DMEM medium, and 10% fetal bovine serum (Biological Industries, Israel) was added to the medium. The miR-2276-5p mimics and negative control (NC) were purchased from the General Biosystems (Anhui, China), and Lipofectamine 2000 was purchased from Invitrogen (United States). Before transfection, the glioma cells LN229 and U87 were cultured in six-well plates at a density of 6×10^4 cells per well, and transfections were performed according to the manufacturer's instructions.

Exosome Isolation From Plasma

Five hundred microliters of plasma samples was centrifuged at 4°C at 300 × *g* for 10 min, 1,000 × *g* for 10 min, and 10,000 × *g* for 30 min to remove cells and debris. Then, supernatants were subjected to ultracentrifugation at 100,000 × *g* for 70 min. Next, we discarded the supernatants and used phosphate-buffered saline (PBS) to wash exosomes. Finally, the exosomes were pelleted by ultracentrifugation at 100,000 × *g* for 70 min again and resuspended in 100 μl of PBS for RNA isolation and follow-up use.

Transmission Electron Microscope

The use of transmission electron microscopy was consistent with that of previous reports, and the experimental procedures used in previous experiments were used (Wang et al., 2018).

The exosome resuspension was loaded onto a carbon-coated 300 mesh copper grid and dried at room temperature for 5 min. Then, the grid was dyed with the 2% phosphotungstic acid at room temperature for 10 min, and the morphology of exosomes was checked using an electron microscope (JEM-1220, JEOL Ltd., Japan).

Protein Extraction and Western Blot

Extraction of proteins and Western blot (WB) analysis was performed as reported earlier (Wang et al., 2018). CD63 antibody (25682-1-AP, 1:1,000), CD9 antibody (20597-1-AP, 1:1,000), and GAPDH (60004-1-LG, 1:5,000) were purchased from Proteintech. RAB13 antibody (DF9813, 1:1,000) was purchased from Affinity Biosciences. Polyclonal goat anti-rabbit antibody (SA00001-2, Proteintech) was used as the secondary antibody, and the WB detection system (Gene Sys) was used for generation of data.

MTT

Transfected glioma cells LN229 and U87 were seeded in 96-well plates at a cell density of 1×10^4 cells per well, and 20 μl of MTT was added at 24, 48, and 72 h. The test conditions were similar to our previous studies (Zhong et al., 2019).

RNA Extraction and Quantitative Real-Time Polymerase Chain Reaction

Total exosome RNA was isolated from 100 μl of exosome samples using Trizol and stored in a −80°C freezer until use. U6 was used as an endogenous control miRNA that is stably expressed in exosomes. qRT-PCR was performed as described earlier (Gareev et al., 2019). The relative expression of miR-2276-5p was calculated using the equation $2^{-\Delta Ct}$, in which ΔCt = Ct miR-2276-5p-Ct U6. The primer sequences used in this study are reported in **Supplementary Table 1**.

Bioinformatic Tools

We consulted GEPIA[1], GEO[2], and GlioVis[3] to check the expression level of RAB13 in the glioma patients and the outcome survival of RAB13 expression. TargetScan[4], mirDIP[5], and mirtargetbase[6] were checked to calculate the gene targets of miR-2276-5p.

Statistical Analyses

Statistical analyses were analyzed by SPSS 13.0. Data were expressed as mean ± SEM. Kaplan–Meier analysis was used to generate and analyze survival time data. The univariate Cox proportional hazards regression was performed on SPSS 13.0. The differences were considered statistically significant at $p < 0.05$.

[1]http://gepia.cancer-pku.cn

[2]https://www.ncbi.nlm.nih.gov/geo

[3]http://gliovis.bioinfo.cnio.es/

[4]http://www.targetscan.org/vert_72

[5]http://ophid.utoronto.ca/mirDIP/

[6]http://mirdb.org/

RESULTS

Identification of Plasma Exosomes

To confirm the extraction of exosomes from the plasma of glioma and control patients, the markers of exosomes (CD63 and CD9) were evaluated by WB analysis. The result showed CD63 and CD9 expression in the samples, thus, establishing the presence of exosomes (**Figure 1A**). Then, we checked the diameter of exosomes using Nano-Sight (**Figure 1B**) and found the size of exosomes to be distributed below 100 nm. We further examined the morphology of exosomes and verified our findings using transmission electron microscope (**Figure 1C**). Thus, we concluded that we had successfully extracted exosomes from plasma samples.

Exosomal miR-2276-5p Is Unconventionally Expressing in Glioma Patients and Could Be a Potential Diagnostic Biomarker in Glioma

As shown in **Figures 2A,B**, GSE139031, GSE113740, GSE113486, and GSE112246 reported a significantly reduced expression of miR-2276 in glioma. To further understand whether miR-2276-5p is also differentially expressed in the plasma exosomes of glioma patients, we checked miR-2276-5p in the exosomes isolated from the plasma of glioma patients and controls. The expression of exosomal miR-2276-5p was found to be differential between glioma and non-glioma patients' plasma (**Figure 2C**). The results showed that plasma exosomal miR-2276-5p in glioma is significantly lower, compared with the non-glioma controls (**Figure 2C**). Another interesting revelation was that the exosomal miR-2276-5p expression levels were lower in patients with high-grade glioma (HGG, including grade III and grade IV) than in patients with low-grade glioma (LGG, including grade I and grade II) (**Figure 2D**). The result of univariate logistic regression analysis of factors associated with a risk factor for glioma (**Table 2**). Then a receiver operating characteristics (ROC) analysis curve was used to analyze the predictive diagnostic capability of exosomal miR-2276-5p for glioma patients. Admission exosomal miR-2276-5p had a good area under curve with an AUC value of 0.8107 (**Figure 2E**). These results suggested that the exosomal miR-2276-5p expression levels are markedly decreased in glioma patients and further correlate negatively with the tumor grade.

Exosomal miR-2276-5p in Plasma Could Be a Potential Prognostic Biomarker in Glioma

We further explored whether there existed a relationship between these differences in expression and the survival outcome of the patients. The relative expression of exosomal miR-2276-5p in patients was divided into a high-expression group and a low-expression group, and our analysis showed that glioma patients in the low-expression group of exosomal miR-2276-5p had lower overall survival (**Figure 2F**). We used the univariate and multivariable Cox proportional hazards regression to confirm

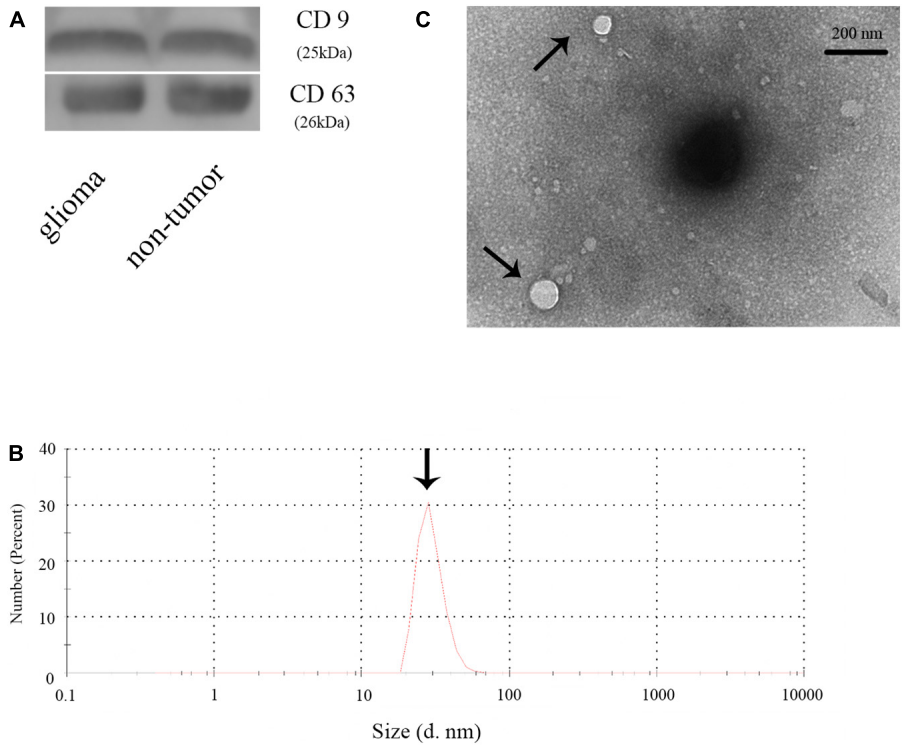

FIGURE 1 | Identification of plasma exosomes. **(A)** The expression of CD9 and CD63 in plasma exosomes in glioma and non-glioma patients. **(B)** Determination of the exosome diameter by Nano-Sight. **(C)** Transmission electron microscope image of the plasma exosomes.

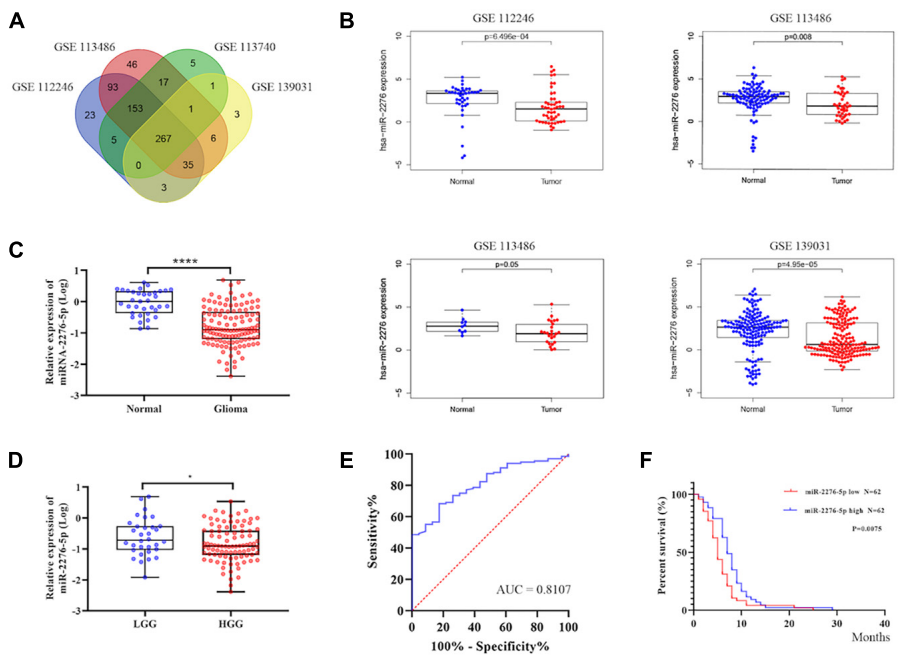

FIGURE 2 | Exosomal miR-2276-5p could be a potential diagnostic and prognostic biomarker in glioma. **(A,B)** The relative expression of miR-2276-5p in glioma patients' plasma in GSE139031, GSE113740, GSE113486, and GSE112246. **(C)** The relative expression of miR-2276-5p in glioma patients' plasma exosomes. **(D)** The relative expression of miR-2276-5p in LGG and HGG patients' plasma exosomes. **(E)** The receiver operating characteristics analysis curve of the miR-2276-5p and the AUC was 0.8107. **(F)** Correlation of expression level of exosomal miR-2276-5p with the overall survival rate of glioma patients. *$p < 0.05$, ****$p < 0.0001$.

our findings (**Table 3**). Based on these findings, we suggest that plasma exosomal miR-2276-5p expression can be used as an independent factor to predict the survival of patients with glioma.

RAB13 May Be the Target Gene of the Plasma Exosomal miR-2276-5p Which Also Predicts the Glioma Patients' Survival

To better understand which genes are the targets of miR-2276-5p in glioma, we used mirDIP, mirtargetbase, and TargetScan to predict the target genes and found that RAB13 and PLEKHG48 might be the target of miR-2276-5p (**Figure 3A**). However, PLEKHG48 had no difference in expression in glioma patients, and it was not necessarily related to the prognosis of patients in the TCGA database (**Supplementary Figure 1**). We transfected miR-2276-5p mimics and negative control (NC) miRNA into the LN229 and U87 human glioma cell lines and found that when miR-2276-5p was ectopically highly expressed in LN229 and U87 glioma cells, the expression of RAB13 mRNA in cells was decreased, as evaluated by RT-PCR (**Figure 3B**). We further confirmed these results with Western blotting (**Figure 3C**); the protein expression of RAB13 also decreased in both the glioma cell lines. Furthermore, the survival of miR-2276-5p-transfected LN229 as well as U87 cells was worse than in the NC group (**Figure 3D**). Moreover, we evaluated the tumor tissues obtained from our hospital and obtained the results that showed that the expression of RAB13 mRNA was negatively correlated with miR-2276-5p (**Figure 3E**). Based on these results, we speculate that RAB13 may be a target gene for miR-2276-5p. We used GSEA to analyze the TCGA-related data and analyzed the cell signaling pathways related to RAB13. Our analysis revealed that RAB13 was enriched in IL2-STAT5 signaling pathway, TGF-β signaling pathway, IL6-JAK-STAT3 signaling pathway, angiogenesis signaling pathway, TNF-α signaling pathway, and epithelial–mesenchymal transition (**Figure 4A**). Furthermore, in order to clarify that RAB13 was correlated with the overall survival of patients, the expression level of RAB13 was checked in the CGGA and TCGA databases. The expression level of RAB13 in HGG patients was significantly higher than in LGG patients (**Figure 4B**). Next, we classified the patients in the CGGA and TCGA database via IDH1 and 1p19q status; RAB13 was highly expressed in IDH1 wild-type and 1p19q non-codel patients (**Figure 4B**). We verified using the GlioVis database that the prognosis of patients with high RAB13 expression was significantly worse than that of patients with low RAB13 expression in both the CGGA and TCGA patients (**Figure 4C**). Thus, we conclude that RAB13 is a genuine target of miR-2276-5p, which is differentially expressed in glioma patients, relative to the controls, as well as in LGG vs. HGG patients, making it a putative indicator to predict the prognosis of glioma patients.

TABLE 2 | The result of univariate logistic regression analysis in glioma patients.

	Univariable analysis OR	95% CI	*P*-value
Relative expression of miR-2276-5p	0.334	0.204-0.548	<0.01

TABLE 3 | The univariate and multivariable Cox proportional hazards regression in glioma patients.

	Univariate		Multivariable	
	Hazard ratio (95% CI)	*P*-value	Hazard ratio (95% CI)	*P*-value
Relative expression of miR-2276-5p	0.619 (0.408–0.940)	0.024	0.573 (0.354–0.926)	0.023
Grade	4.379 (3.066–6.252)	<0.001	3.987 (2.738–5.806)	<0.001
Age	1.047 (1.031–1.063)	<0.001	1.021 (1.004–1.037)	0.014
Gender (VS Female)	0.791 (0.523–1.197)	0.268	0.895 (0.584–1.374)	0.613
Total cut	0.813 (0.530–1.249)	0.345	0.907 (0.579–1.420)	0.669

DISCUSSION

In our current study, we found that exosomal miR-2276-5p in plasma may be a diagnostic biomarker in glioma patients and that this miRNA is associated with a poor prognosis in patients with lower expression levels. Moreover, we conclude that miR-2276-5p is likely to target RAB13 and inhibit glioma cell growth. In published literature, miR-2276-5p has been reported dysregulated in breast cancer (Torkashvand et al., 2016) and colorectal cancer (Chen et al., 2019a), and the researchers used the predictive tools to suggest a relationship between miR-2276 and PIWIL2. In another report, there was a 4.5-fold high expression of miR-2276 in colorectal cancer cells that were silenced for STAT3. STAT3 is a well characterized tumor promotor in glioma (Zhang et al., 2014; Lv et al., 2017; Almiron Bonnin et al., 2018; Man et al., 2018). It can promote glioma cell proliferation and glioma stem-like cell self-renewal. Thus, suppression of miR-2276 by oncogenic STAT3 establishes it as a tumor suppressive miRNA in gliomas.

Exosomes are 40–150 nm small extracellular vesicles, which are involved in the regulation of cellular microenvironment. They carry cargo such as RNA (including mRNAs, microRNAs, and non-coding RNAs), DNA, protein, and lipids to facilitate communications between cancer cells (Jeppesen et al., 2019; Khan et al., 2020). During the past several years, there have been many reports on miRNAs in glioma. Not only the miRNAs, such as, miR-21 (Masoudi et al., 2018), miR-454-3p (Van Meir et al., 2010), and miR-9 (Chen et al., 2019b), but even reports on non-coding RNAs, such as long non-coding RNA HOTAIR (Tan et al., 2018), have suggested a possible role of non-coding RNAs as biomarkers in glioma and asserted that they were a risk factor for the prognosis in glioma patients. This fits wells with the increasing realization of a role of non-coding RNAs in the pathogenesis of human cancers (Ahmad, 2016; Kim, 2019). It has been reported that miR-26a promotes tumor angiogenesis; it activates PI3K/Akt signaling pathway by targeting PTEN, thus, promoting glioma cells' proliferation (Wang Z.F. et al.,

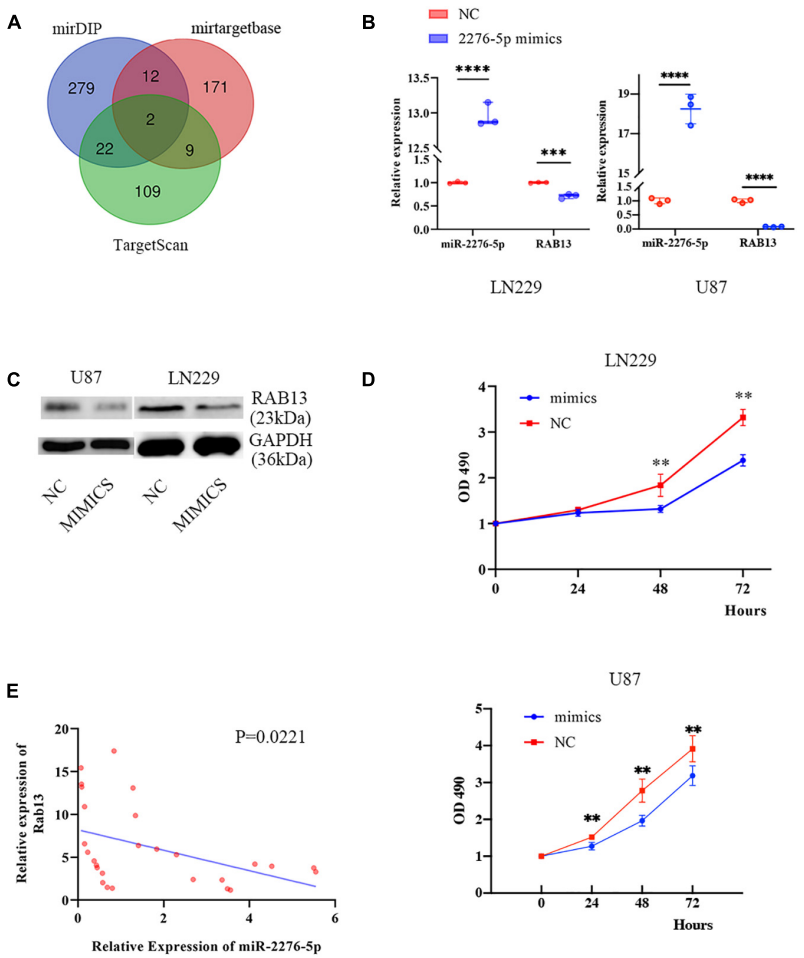

FIGURE 3 | RAB13 may be the target gene of miR-2276-5p. **(A)** The predicted result of target genes of miR-2276-5p, as determined by consultation with mirDIP, mirtargetbase, and TargetScan. **(B)** The relative expression of miR-2276-5p and RAB13 mRNA in LN229 and U87 glioma cell lines transfected with miR-2276-5p or the negative control (NC) mimics. **(C)** Western blotting results showing the expression levels of RAB13 protein in miR-2276-5p/NC- transfected LN229 and U87 glioma cell lines. **(D)** The cell proliferation state of miR-2276-5p/NC-transfected LN229 and U87 glioma cells, as determined by MTT. **(E)** The correlation of expression level of miR-2276-5p with the expression levels of RAB13 in glioma tissues. $^{**}p < 0.01$; $^{***}p < 0.001$; $^{****}p < 0.0001$.

2019). Previous studies have found that the concentration of extracellular vesicles can be a factor in predicting the prognosis of patients with glioma (Osti et al., 2019), but it was not clear as to why the glioma patients had high concentration of extracellular vesicles. According to our findings, as reported here, we suspect that the low expression of miR-2276-5p would promote the expression of RAB13, which in turn can positively regulate the secretion of transport vesicles between glioma cells, and finally lead to the secretion of a large number of extracellular vesicles. Our work also links miR-2276-5p to glioma through exosomes for the first time, and we found a relationship between the expression of this exosomal miRNA and the diagnosis and prognosis of glioma patients.

RAB13 regulates transport and location function proteins. These include integrin transport during cell proliferation and migration, GLUT4 and VEGFR during angiogenesis (Munn et al., 1998; Sun et al., 2010; Nishikimi et al., 2014). RAB13 regulates the proliferation of cancer cells and tumor growth *in vivo*. Therefore, RAB13 is involved in the regulation of several key determinants of cancer cells aggressiveness (Ioannou et al., 2015). We found, through bioinformatics analysis, that RAB13 is mainly enriched in the JAK/STAT3 signaling pathway. The JAK/STAT3 signaling pathway has previously been shown to be critical in glioma. By inhibiting the JAK-STAT3 signaling pathway, the growth and invasion of glioma cells could be significantly inhibited, primarily through the inhibition of cell cycle in the G0/G1 phase (Lu et al., 2017). We also found that RAB13 is significantly enriched in the signaling pathway of angiogenesis. Angiogenesis is a significant feature of gliomas, and inhibition of the formation of blood vessels has direct effect on the treatment and prognosis of gliomas (Shi et al., 2014). Studies have also found that activation of STAT3 could induce tumor angiogenesis (Yu and Jove, 2004). Therefore, we infer that the low expression of miR-2276-5p leads to the differential expression of RAB13, and RAB13 may promote glioma angiogenesis through the JAK/STAT3 signaling pathway,

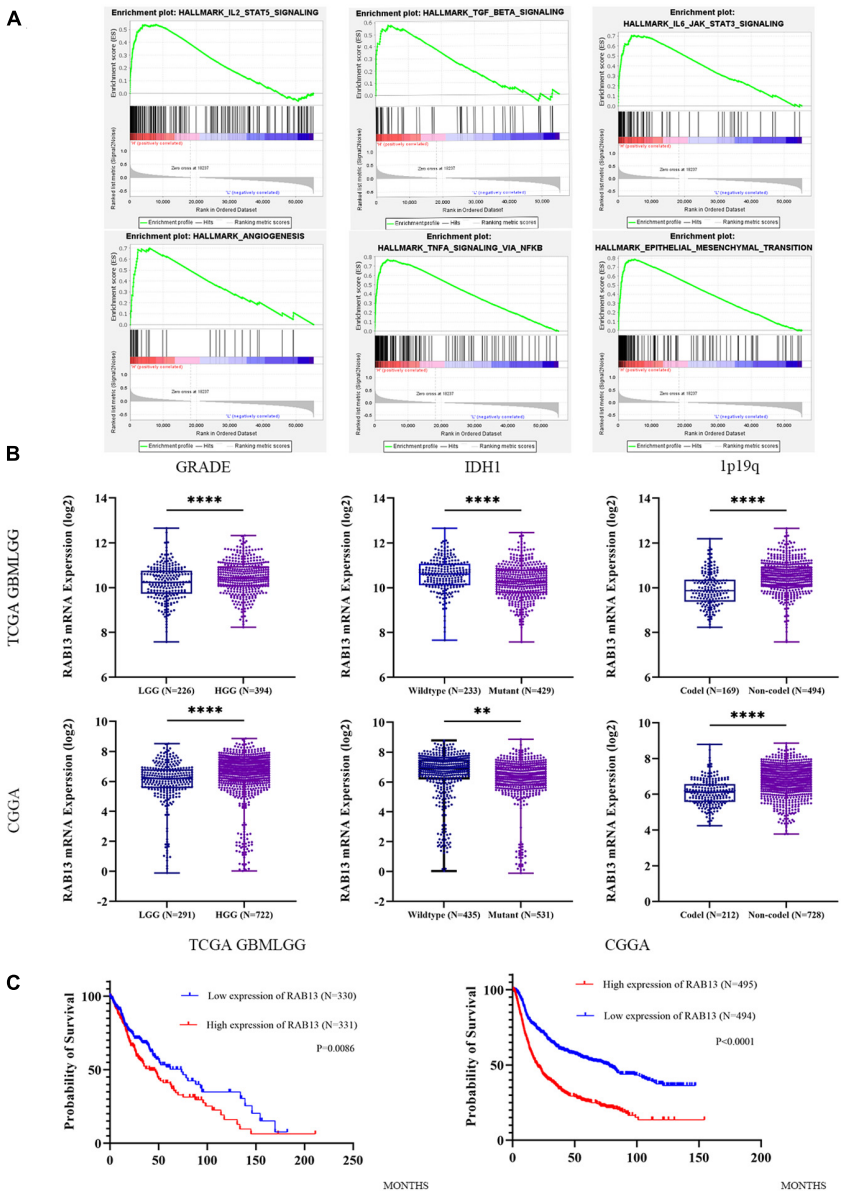

FIGURE 4 | The expression of RAB13 in the glioma database is correlated with the clinical indicators of the patient. **(A)** The enrichment result of RAB13 by GSEA analysis, using the TCGA database. **(B)** The relative expression of RAB13 mRNA in the TCGA and CGGA databases by grouping according to the grade, IDH1, and 1p19q status. **(C)** Correlation of expression level of RAB13 with the overall survival rate of glioma patients in the TCGA and CGGA databases. $^{**}p < 0.01$; $^{****}p < 0.0001$.

leading to tumor proliferation and poor prognosis. Clearly, more experimental proof is needed to verify this and should be the focus of future studies.

In conclusion, we report that miR-2276-5p is reduced in the plasma-derived exosomes of patients with glioma, and its low expression associates with poor prognosis of patients. Additionally, we found, using bioinformatic tools, that RAB13 is differentially expressed in patients with glioma, and predicted and verified it as a target of miR-2276-5p. Our findings suggest that exosomal miR-2276-5p in plasma is a potential diagnostic and prognostic biomarker for glioma.

DATA AVAILABILITY STATEMENT

The original contributions presented in the study are included in the article/**Supplementary Material**, further inquiries can be directed to the corresponding author/s.

ETHICS STATEMENT

The studies involving human participants were reviewed and approved by the First Affiliated Hospital of the Harbin Medical

University. The patients/participants provided their written informed consent to participate in this study.

AUTHOR CONTRIBUTIONS

JS, ZS, IG, and TY performed the experiments. JS, ZS, IG, OB, DZ, BZ, and GY analyzed the data. GY and SZ provided the funds. OB, AA, GY, and SZ conceptualized the study. OB, GY, and SZ drafted the manuscript. All authors read and approved the manuscript.

FUNDING

This work was supported by the National Natural Science Foundations of China (81971135), the Natural Science Foundations of Heilongjiang (YQ2020H014), the "Chunhui Plan" of the Ministry of Education (HLJ2019009), and the Distinguished Young Foundations of the First Affiliated Hospital of Harbin Medical University (HYD2020JQ0014).

SUPPLEMENTARY MATERIAL

The Supplementary Material for this article can be found online at: https://www.frontiersin.org/articles/10.3389/fcell.2021.671202/full#supplementary-material

Supplementary Figure 1 | The relationship between the expression of PLEKHG48 and the diagnosis and prognosis of patients with glioma.

Supplementary Table 1 | The detailed sequence of miRNAs.

REFERENCES

Ahmad, A. (2016). Non-coding RNAs: a tale of junk turning into treasure. *Noncoding RNA Res.* 1, 1–2. doi: 10.1016/j.ncrna.2016.12.001

Almiron Bonnin, D. A., Havrda, M. C., Lee, M. C., Liu, H., Zhang, Z., Nguyen, L. N., et al. (2018). Secretion-mediated STAT3 activation promotes self-renewal of glioma stem-like cells during hypoxia. *Oncogene* 37, 1107–1118. doi: 10.1038/onc.2017.404

Capper, D., Jones, D. T. W., Sill, M., Hovestadt, V., Schrimpf, D., Sturm, D., et al. (2018). DNA methylation-based classification of central nervous system tumours. *Nature* 555, 469–474.

Chen, P., Chen, G., Wang, C., and Mao, C. (2019a). RAB13 as a novel prognosis marker promotes proliferation and chemotherapeutic resistance in gastric cancer. *Biochem. Biophys. Res. Commun.* 519, 113–120. doi: 10.1016/j.bbrc.2019.08.141

Chen, X., Yang, F., Zhang, T., Wang, W., Xi, W., Li, Y., et al. (2019b). MiR-9 promotes tumorigenesis and angiogenesis and is activated by MYC and OCT4 in human glioma. *J. Exp. Clin. Cancer Res.* 38:99.

D'Souza-Schorey, C., and Clancy, J. W. (2012). Tumor-derived microvesicles: shedding light on novel microenvironment modulators and prospective cancer biomarkers. *Genes Dev.* 26, 1287–1299. doi: 10.1101/gad.192351.112

Ferlay, J., Colombet, M., Soerjomataram, I., Mathers, C., Parkin, D. M., Pineros, M., et al. (2019). Estimating the global cancer incidence and mortality in 2018: GLOBOCAN sources and methods. *Int. J. Cancer* 144, 1941–1953. doi: 10.1002/ijc.31937

Gareev, I., Yang, G., Sun, J., Beylerli, O., Chen, X., Zhang, D., et al. (2019). Circulating microRNAs as potential noninvasive biomarkers of spontaneous intracerebral hemorrhage. *World Neurosurg.* 133, e369–e375.

Hoshino, D., Kirkbride, K. C., Costello, K., Clark, E. S., Sinha, S., Grega-Larson, N., et al. (2013). Exosome secretion is enhanced by invadopodia and drives invasive behavior. *Cell Re.p* 5, 1159–1168. doi: 10.1016/j.celrep.2013.10.050

Huang, S. W., Ali, N. D., Zhong, L., and Shi, J. (2018). MicroRNAs as biomarkers for human glioblastoma: progress and potential. *Acta Pharmacol. Sin* 39, 1405–1413. doi: 10.1038/aps.2017.173

Hutagalung, A. H., and Novick, P. J. (2011). Role of Rab GTPases in membrane traffic and cell physiology. *Physiol. Rev.* 91, 119–149. doi: 10.1152/physrev.00059.2009

Ioannou, M. S., Bell, E. S., Girard, M., Chaineau, M., Hamlin, J. N., Daubaras, M., et al. (2015). DENND2B activates Rab13 at the leading edge of migrating cells and promotes metastatic behavior. *J. Cell Biol.* 208, 629–648. doi: 10.1083/jcb.201407068

Jeppesen, D. K., Fenix, A. M., Franklin, J. L., Higginbotham, J. N., Zhang, Q., Zimmerman, L. J., et al. (2019). Reassessment of exosome composition. *Cell* 177, 428–445.e18.

Khan, A. Q., Akhtar, S., Prabhu, K. S., Zarif, L., Khan, R., Alam, M., et al. (2020). Exosomes: emerging diagnostic and therapeutic targets in cutaneous diseases. *Int. J. Mol. Sci.* 21:9264. doi: 10.3390/ijms21239264

Kim, M. Y. (2019). Long non-coding RNAs in cancer. *Noncoding RNA Res.* 4:45. doi: 10.1016/j.ncrna.2019.02.003

Lu, L., Zhang, S., Li, C., Zhou, C., Li, D., Liu, P., et al. (2017). Cryptotanshinone inhibits human glioma cell proliferation in vitro and in vivo through SHP-2-dependent inhibition of STAT3 activation. *Cell Death Dis.* 8:e2767. doi: 10.1038/cddis.2017.174

Lv, D., Li, Y., Zhang, W., Alvarez, A. A., Song, L., Tang, J., et al. (2017). TRIM24 is an oncogenic transcriptional co-activator of STAT3 in glioblastoma. *Nat. Commun.* 8:1454.

Man, J., Yu, X., Huang, H., Zhou, W., Xiang, C., Huang, H., et al. (2018). Hypoxic induction of vasorin regulates notch1 turnover to maintain glioma stem-like cells. *Cell Stem Cell* 22, 104–118e6.

Masoudi, M. S., Mehrabian, E., and Mirzaei, H. (2018). MiR-21: a key player in glioblastoma pathogenesis. *J. Cell. Biochem.* 119, 1285–1290. doi: 10.1002/jcb.26300

Munn, D. H., Zhou, M., Attwood, J. T., Bondarev, I., Conway, S. J., Marshall, B., et al. (1998). Prevention of allogeneic fetal rejection by tryptophan catabolism. *Science* 281, 1191–1193. doi: 10.1126/science.281.5380.1191

Nishikimi, A., Ishihara, S., Ozawa, M., Etoh, K., Fukuda, M., Kinashi, T., et al. (2014). Rab13 acts downstream of the kinase Mst1 to deliver the integrin LFA-1 to the cell surface for lymphocyte trafficking. *Sci. Signal.* 7:ra72. doi: 10.1126/scisignal.2005199

Osti, D., Del Bene, M., Rappa, G., Santos, M., Matafora, V., Richichi, C., et al. (2019). Clinical significance of extracellular vesicles in plasma from glioblastoma patients. *Clin. Cancer Res.* 25, 266–276. doi: 10.1158/1078-0432.ccr-18-1941

Ostrom, Q. T., Gittleman, H., Liao, P., Vecchione-Koval, T., Wolinsky, Y., Kruchko, C., et al. (2017). Primary brain and other central nervous system tumors diagnosed in the United States in 2010-2014. *Neuro Oncol.* 19:v1–v88.

Qian, M., Wang, S., Guo, X., Wang, J., Zhang, Z., Qiu, W., et al. (2019). Hypoxic glioma-derived exosomes deliver microRNA-1246 to induce M2 macrophage polarization by targeting TERF2IP via the STAT3 and NF-kappaB pathways. *Oncogene* 39, 1–15.

Reifenberger, G., Wirsching, H. G., Knobbe-Thomsen, C. B., and Weller, M. (2017). Advances in the molecular genetics of gliomas - implications for classification and therapy. *Nat. Rev. Clin. Oncol.* 14, 434–452. doi: 10.1038/nrclinonc.2016.204

Shi, Z., Chen, Q., Li, C., Wang, L., Qian, X., Jiang, C., et al. (2014). MiR-124 governs glioma growth and angiogenesis and enhances chemosensitivity by targeting R-Ras and N-Ras. *Neuro Oncol.* 16, 1341–1353. doi: 10.1093/neuonc/nou084

Sun, Y., Bilan, P. J., Liu, Z., and Klip, A. (2010). Rab8A and Rab13 are activated by insulin and regulate GLUT4 translocation in muscle cells. *Proc. Natl. Acad. Sci. U.S.A.* 107, 19909–19914. doi: 10.1073/pnas.1009523107

Tan, S. K., Pastori, C., Penas, C., Komotar, R. J., Ivan, M. E., Wahlestedt, C., et al. (2018). Serum long noncoding RNA HOTAIR as a novel diagnostic and prognostic biomarker in glioblastoma multiforme. *Mol. Cancer* 17:74.

Torkashvand, S., Damavandi, Z., Mirzaei, B., Tavallaei, M., Vasei, M., and Mowla, S. J. (2016). Decreased expression of bioinformatically predicted piwil2-targetting microRNAs, miR-1267 and miR-2276 in Breast Cancer. *Arch. Iran Med.* 19, 420–425.

Van Meir, E. G., Hadjipanayis, C. G., Norden, A. D., Shu, H. K., Wen, P. Y., and Olson, J. J. (2010). Exciting new advances in neuro-oncology: the avenue to a cure for malignant glioma. *CA Cancer J. Clin.* 60, 166–193. doi: 10.3322/caac.20069

Wang, X., Shen, C., Liu, Z., Peng, F., Chen, X., Yang, G., et al. (2018). Nitazoxanide, an antiprotozoal drug, inhibits late-stage autophagy and promotes ING1-induced cell cycle arrest in glioblastoma. *Cell Death Dis* 9, 1032.

Wang, Z., Wang, L., Liang, Z., and Xi, Y. (2019). Long non-coding RNA BCAR4 promotes growth, invasion and tumorigenicity by targeting miR-2276 to Upregulate MMP7 expression in glioma. *Onco Targets Ther.* 12, 10963–10973. doi: 10.2147/ott.s226026

Wang, Z. F., Liao, F., Wu, H., and Dai, J. (2019). Glioma stem cells-derived exosomal miR-26a promotes angiogenesis of microvessel endothelial cells in glioma. *J. Exp. Clin. Cancer Res.* 38, 201.

Yoshimura, A., Sawada, K., Nakamura, K., Kinose, Y., Nakatsuka, E., Kobayashi, M., et al. (2018). Exosomal miR-99a-5p is elevated in sera of ovarian cancer patients and promotes cancer cell invasion by increasing fibronectin and vitronectin expression in neighboring peritoneal mesothelial cells. *BMC Cancer* 18:1065. doi: 10.1186/s12885-018-4974-5

Yu, H., and Jove, R. (2004). The STATs of cancer–new molecular targets come of age. *Nat. Rev. Cancer* 4, 97–105. doi: 10.1038/nrc1275

Zhang, J., Luo, X., Li, H., Deng, L., and Wang, Y. (2014). Genome-wide uncovering of STAT3-mediated miRNA expression profiles in colorectal cancer cell lines. *Biomed. Res. Int.* 2014, 187105.

Zhong, C., Shu, M., Ye, J., Wang, X., Chen, X., Liu, Z., et al. (2019). Oncogenic Ras is downregulated by ARHI and induces autophagy by Ras/AKT/mTOR pathway in glioblastoma. *BMC Cancer* 19:441. doi: 10.1186/s12885-019-5643-z

Conflict of Interest: The authors declare that the research was conducted in the absence of any commercial or financial relationships that could be construed as a potential conflict of interest.

frontiers in Cell and Developmental Biology

ORIGINAL RESEARCH
published: 10 June 2021
doi: 10.3389/fcell.2021.682593

Epigenetic Reprogramming Mediated by Maternal Diet Rich in Omega-3 Fatty Acids Protects From Breast Cancer Development in F1 Offspring

Ata Abbas[1,2†], Theodore Witte[3], William L. Patterson III[2,3], Johannes F. Fahrmann[3†], Kai Guo[4], Junguk Hur[4], W. Elaine Hardman[3] and Philippe T. Georgel[1,2,3]*

[1] Department of Biological Sciences, Marshall University, Huntington, WV, United States, [2] Cell Differentiation and Development Center, Marshall University, Huntington, WV, United States, [3] Department of Biochemistry and Microbiology, Marshall University School of Medicine, Huntington, WV, United States, [4] Department of Biomedical Sciences, University of North Dakota School of Medicine and Health Sciences, Grand Forks, ND, United States

Diets rich in omega-3 fatty acids (FA) have been associated with lowered risks of developing certain types of cancers. We earlier reported that in transgenic mice prone to develop breast cancer (BCa), a diet supplemented with canola oil, rich in omega-3-rich FA (as opposed to an omega-6-rich diet containing corn oil), reduced the risk of developing BCa, and also significantly reduced the incidence of BCa in F1 offspring. To investigate the underlying mechanisms of the cancer protective effect of canola oil in the F1 generation, we designed and performed the present study with the same diets using BALB/c mice to remove any possible effect of the transgene. First, we observed epigenetic changes at the genome-wide scale in F1 offspring of mothers fed diets containing omega-3 FAs, including a significant increase in acetylation of H3K18 histone mark and a decrease in H3K4me2 mark on nucleosomes around transcription start sites. These epigenetic modifications contribute to differential gene expressions associated with various pathways and molecular mechanisms involved in preventing cancer development, including p53 pathway, G2M checkpoint, DNA repair, inflammatory response, and apoptosis. When offspring mice were exposed to 7,12-Dimethylbenz(a)anthracene (DMBA), the group of mice exposed to a canola oil (with omega 3 FAs)-rich maternal diet showed delayed mortality, increased survival, reduced lateral tumor growth, and smaller tumor size. Remarkably, various genes, including BRCA genes, appear to be epigenetically re-programmed to poise genes to be ready for a rapid transcriptional activation due to the canola oil-rich maternal diet. This ability to respond rapidly due to epigenetic potentiation appeared to contribute to and promote protection against breast cancer after carcinogen exposure.

Keywords: epigenetic changes, histone post-translational modification (PTM), maternal diet, breast cancer prevention, omega-3 fatty acids

OPEN ACCESS

Edited by:
Trygve Tollefsbol, University of Alabama at Birmingham, United States

Reviewed by:
Alyson Ashe, The University of Sydney, Australia
Alice Hudder, Lake Erie College of Osteopathic Medicine, United States

***Correspondence:**
Philippe T. Georgel
georgel@marshall.edu

†Present address:
Ata Abbas, Division of Hematology and Oncology, Department of Medicine, Case Western Reserve University, Cleveland, OH, Untied States
Johannes F. Fahrmann, Department of Clinical Cancer Prevention, University of Texas MD Anderson Cancer Center, Houston, TX, Untied States

Specialty section:
This article was submitted to Epigenomics and Epigenetics, a section of the journal Frontiers in Cell and Developmental Biology

Received: *18 March 2021*
Accepted: *19 May 2021*
Published: *10 June 2021*

Citation:
Abbas A, Witte T, Patterson WL III, Fahrmann JF, Guo K, Hur J, Hardman WE and Georgel PT (2021) Epigenetic Reprogramming Mediated by Maternal Diet Rich in Omega-3 Fatty Acids Protects From Breast Cancer Development in F1 Offspring. Front. Cell Dev. Biol. 9:682593. doi: 10.3389/fcell.2021.682593

INTRODUCTION

Alpha-linolenic acid (ALA), eicosapentaenoic acid (EPA), and docosahexaenoic acid (DHA) are the three important omega-3 (ω-3) fatty acids (FA) (Lunn and Theobald, 2006; Glick and Fischer, 2013). ALA is an essential FA mainly found in plant oils such as canola oils, flaxseed, and soybean. Linoleic acid (LA) is an omega-6 (ω-6) FA and is also an essential FA that our body could not synthesize. The primary dietary sources of ω-6 FA are vegetable oils, including corn oil, sunflower oil, and soybean oil. Both ω-3 and ω-6 FA are essential structural components of cell membranes and are precursors for various important biochemical conversions. Considering both the benefits and adverse effects of ω-6 FA, a balance between ω-6 and ω-3 FA (optimal ω-6/ω-3 ratio between 1:1 to 1:3) is critical for a healthy lifestyle (Simopoulos, 2009; Gomez Candela et al., 2011; DiNicolantonio and O'Keefe, 2018). Numerous studies provide preclinical evidence linking the ω-3 to ω-6 FA ratio in the diet with cancer development (Pizato et al., 2005; Hardman, 2007; Kang and Liu, 2013; Abel et al., 2014; Diorio and Dumas, 2014; Zanoaga et al., 2018).

Over the last 15 years, an increasing number of publications have linked various dietary compounds to the long-term protection of individuals against multiple types of cancers (Syed et al., 2008; Turati et al., 2015; Vanamala, 2017; Koh et al., 2020; Saini et al., 2020; Steck and Murphy, 2020). Notably, both maternal and paternal diets contribute, in a trans-generational manner, to this observed protective effect (Ion et al., 2010; Fleming et al., 2018; Li et al., 2018). Among the dietary compounds investigated, ω-3 and ω-6 FA have received significant interest, as using oil high in ω-3 and low in ω-6 FA may provide an easy and affordable way to reduce the incidence of several types of cancer, including breast cancer (BCa) (Karmali et al., 1993; Huang et al., 1996; Hardman et al., 1999; Hardman, 2004), possibly through ω-3 FA's anti-inflammatory properties (Patterson and Georgel, 2014). More recently, as nutrients are unlikely to trigger mutations, researchers have shifted their interest to a potential epigenetic mode of action to explain the diet-mediated gene expression changes (Choi and Friso, 2010; Abbas et al., 2013, 2016; Bishop and Ferguson, 2015; Remely et al., 2015).

It is evident that ω-3 FA can reduce the risk of developing various complex diseases, including cancer (Hardman, 2014; Witte and Hardman, 2015; Simopoulos, 2016). An earlier report from our group using BCa transgenic C3(1)-TAg mice indicated that a canola oil supplemented maternal diet (ω-3 FA rich) significantly reduced the incidence of BCa in F1 offspring (Ion et al., 2010). Here, we sought to comprehensively investigate the effect of a canola oil-rich maternal diet compared to that of a corn oil-rich maternal diet and the underlying protective mechanisms preventing BCa development after DMBA treatment using non-transgenic BALB/c mice. The use of normal BALB/c mice allowed us to remove any possible effects of the transgene or of a developing mammary gland tumor from the genetic profile of the mice.

RESULTS

Maternal Diet Induces Genome-Wide Epigenetic Changes in the Mammary Tissue of F1 Generation Mice

To understand if maternal diets enriched with either canola oil or corn oil can modulate histone post-translational modification (PTM) in the F1 generation, we first screened the global changes in histone PTMs known to affect gene expression, such as H3K9me2, H3K9me3, H3K18ac, and H3K4me2, as well as H4K5ac, H4K8ac, H4K12ac, H4K16ac, and panH4ac using western blot (**Supplementary Figure 1**). We observed a statistically significant increase in acetylation of histone 3 at lysine 18 in mammary tissue of the F1 mice from mothers fed a canola oil-rich diet (Ca/Co) compared to mothers fed a corn oil-rich diet (Co/Co) (P-value = 0.005) along with an increase in H4K12ac and H4K16ac marks (**Supplementary Figure 1**). Since the increase in global H3K18ac was statistically significant, and its association with gene transcription is well-known, we decided to perform chromatin immunoprecipitation-sequencing (ChIP-seq) to elucidate genome-wide changes. We also noted an increase in H3K4me2, and though it was not statistically significant, we included it in our ChIP-seq experiments due to its role in gene expression and regulation. We performed H3K4me2 and H3K18ac ChIP-seq using mammary gland tissue samples of F1 mice whose mothers were fed either corn (Co/Co) or the canola (Ca/Co) oil-rich diets (**Figure 1** and **Supplementary Figure 2**). We observed a slight decrease in the H3K4Me2 signal around the transcription start site (TSS) in our Ca/Co mice compared to Co/Co mice (**Figures 1A–C**). Remarkably, the H3K18ac signal was enriched around TSS in F1 mice from Ca/Co group compare to the Co/Co mice (**Figures 1D–F**). Next, we analyzed H3K4me2 and H3K18ac ChIP-seq for lincRNA genes, microRNA genes, and enhancers and compared them between Ca/Co and Co/Co mice. We observed a notable increase in H3K18ac histone marks around TSS of lincRNA genes with a slight decrease in H3K4me2 level (**Supplementary Figure 3A**). Surprisingly, H3K18ac histone PTM was decreased at enhancer regions, but no noticeable change in H3K4me2 PTM level over enhancer regions was observed (**Supplementary Figure 3B**). We did not observe any noteworthy changes in micro RNA (miRNA) genes (**Supplementary Figure 3C**). These observations, altogether, suggest that the maternal ω-3 FA rich diet can significantly impact the genome-wide epigenetic landscape changes in offspring and potentially modulate gene expression patterns in F1 mice.

Maternal Diets Modulate Global Gene Expression Patterns in F1 Offspring

We performed microarray analysis to measure the differentially expressed genes in mammary gland tissues of Ca/Co mice compared to Co/Co mice (**Figure 2** and **Supplementary Figure 4**). Among the observed differentially expressed genes, 2,767 genes were over-expressed (≥2-fold, P-adj < 0.05), and 759 genes were under-expressed (≥2-fold, P-adj < 0.05) (**Figure 2A**). Next, we performed Gene Set Enrichment

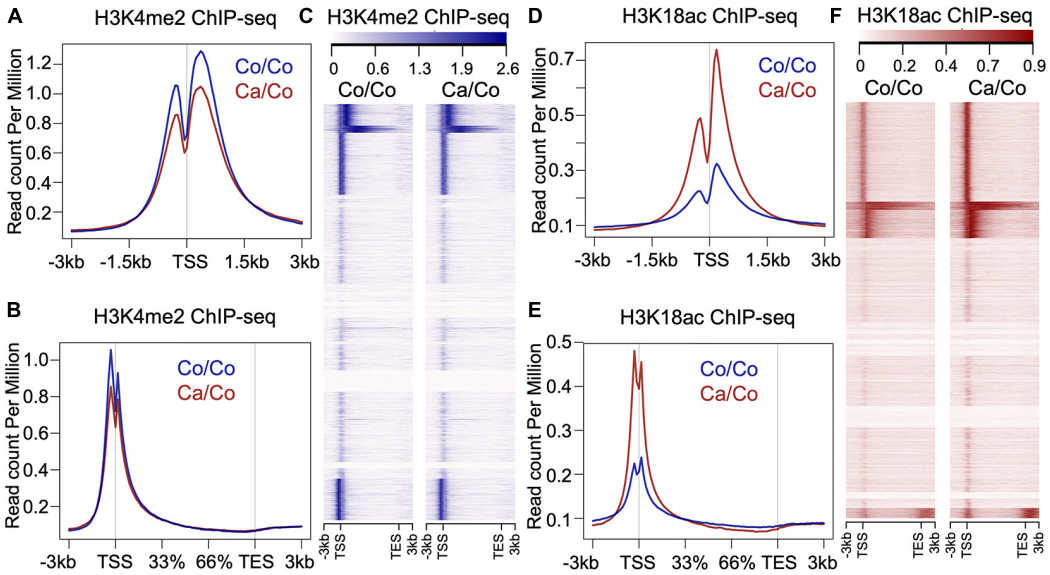

FIGURE 1 | Effects of maternal diets on histone post-translational modifications (PTMs) in offspring breast tissue. **(A)** Metagene plot showing histone H3K4me2 ChIP-seq signals around transcription start site (TSS, ±3 kb) in the breast tissue of F1 generation mice whose mothers were fed either corn (Co/Co) or canola (Ca/Co) oil-rich diets. **(B)** Metagene plot and **(C)** heatmap showing histone H3K4me2 ChIP-seq signals at gene bodies (–3 kb from TSS to +3 kb beyond TES, transcription end site) in the breast tissue of F1 generation mice whose mothers were fed either corn (Co/Co) or canola (Ca/Co) oil-rich diets. **(D)** Metagene plot showing histone H3K18ac signals around TSS (±3 kb) in the breast tissue of F1 generation mice whose mothers were fed either corn (Co/Co) or canola (Ca/Co) oil-rich diets. **(E)** Metagene plot and **(F)** heatmap showing histone H3K18ac ChIP-seq signals at gene bodies in the breast tissue of F1 generation mice whose mothers were fed either corn (Co/Co) or canola (Ca/Co) oil-rich diets.

Analysis (GSEA) using Molecular Signatures Database (MSigDB) for our normalized microarray gene expression datasets. Several pathways were significantly upregulated in Ca/Co mice (**Supplementary Figure 5**) such as IL2-STAT5 signaling pathway involved in mammary gland development and lactogenesis (Liu et al., 1997; **Supplementary Figure 5B**); however, no significantly downregulated pathways were observed. Remarkably, among the top significantly enriched pathways in Ca/Co mice were interferon-gamma response, apoptosis, p53 pathway, G2M checkpoint, DNA repair, and inflammatory response (**Figure 2B**). Activation of these pathways in Ca/Co mice compared to Co/Co mice suggest better homeostatic controls that suppress aberrant cell proliferation in tumorigenesis. These observations signify anti-cancer properties of omega-3 FA and further provide the first line of evidence for transcriptomic changes favoring the blockade of neoplastic cells in F1 offspring.

Maternal ω-3 FA Diet Induces Epigenetic Changes in Nucleosomes Around TSS of Differentially Expressed Genes

Epigenetic changes, especially specific subsets of histone PTMs have been shown to be associated with genes' transcriptional status (Jenuwein, 2001). We, therefore, analyzed H3K4me2 and H3K18ac ChIP-seq signals at TSS of differentially expressed genes to better understand the impact of maternal diets induced epigenetic changes on gene transcription in F1 mice mammary tissue. As expected, overall H3K4me2 histone marks around TSS were higher in over-expressed genes compare to under-expressed genes in both Ca/Co and Co/Co mice (**Figure 3A**). However, enrichment of H3K4me2 marks was slightly decreased in both over-expressed and under-expressed genes around TSS in mammary tissue of Ca/Co mice compare to Co/Co mice (**Figure 3A**). Next, we looked at H3K18ac ChIP-seq signals around TSS of differentially expressed genes. We observed a large noticeable increase in acetylation of histone H3K18 around TSS in over-expressed genes in mammary tissue of F1 generation of Ca/Co mice compare to Co/Co mice (**Figure 3B**). Note that the increase that we observed was often at TSS which already displayed H3K18ac signal. The Ca/Co seemed to accentuate the signal. There was a slight increase in H3K18ac ChIP-seq signals around TSS of under-expressed genes as well. An examination of representative genes, *Pten* (over-expressed), *Hdac2* (unchanged), and *Elk3* (under-expressed) using the UCSC genome browser further corroborates our observations of maternal diet-induced alterations of histone marks around TSS (**Figure 3C**). To understand if there were any specific patterns or correlations of non-differentially expressed genes (Ca/Co vs. Co/Co) with H3K4me2 and H3K18ac histones marks around TSS, we calculated H3K4me2 and H3K18ac counts around TSS (±500 bp) to plot cumulative frequency and scattered plots (**Supplementary Figure 6**). Although there was a subset of genes that was differentially expressed and showed alterations in histone marks (**Figure 3** and **Supplementary Figure 6**), no specific patterns were observed in the histone modulations of the remaining genes that exhibited no change in expression level (**Supplementary Figures 6A,B**). Since the increase in H3K18ac level is not absolutely correlated with enhanced expression (only a subset

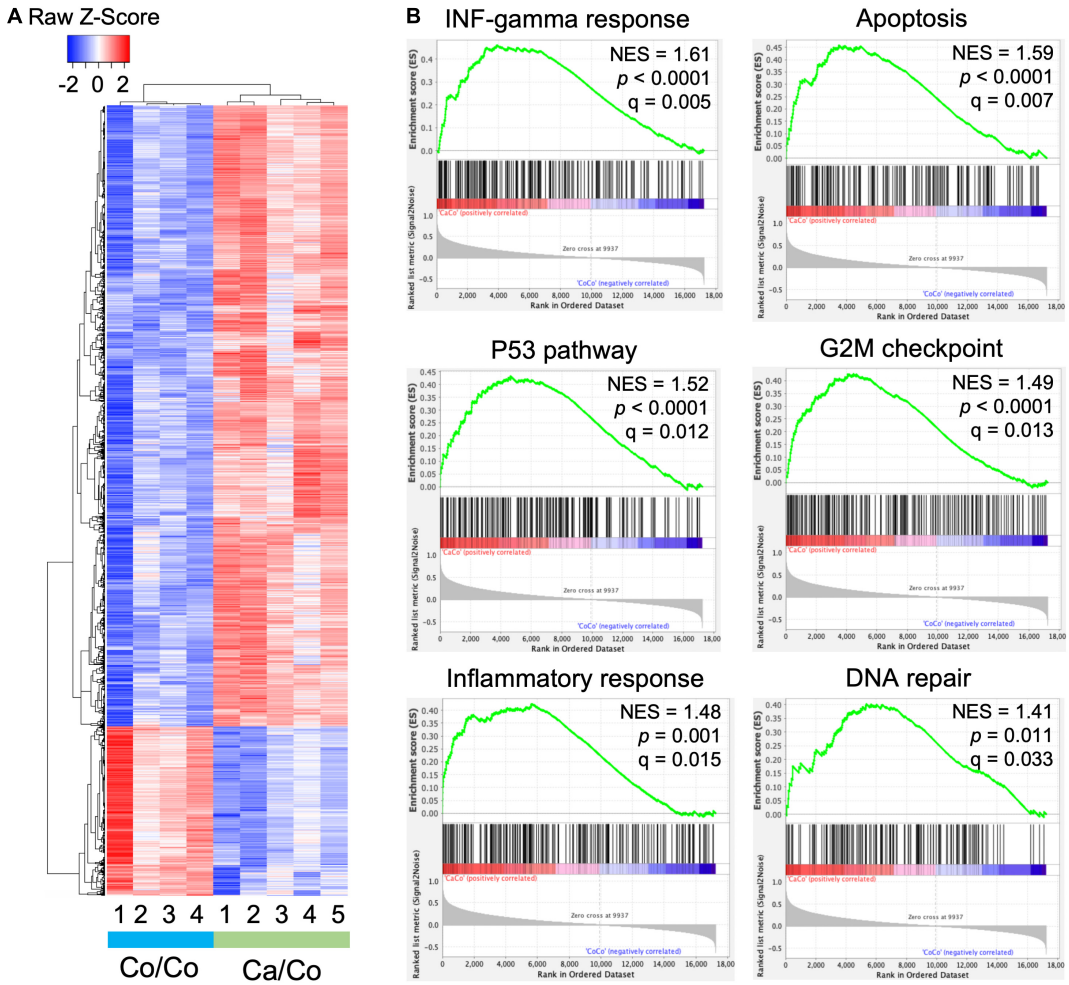

FIGURE 2 | Maternal diets modulate genome-wide gene expression patterns in offspring. **(A)** Heatmap showing differential gene expression in breast tissue samples in offspring mice whose mothers were fed either corn (Co/Co) or canola (Ca/Co) oil-rich diets by microarray analysis. We observed 2,767 and 759 genes that exhibited twofold or more over-expression or under-expression, respectively (*P*-adj < 0.05). **(B)** GSEA analysis showing enrichment of various pathways due to differential gene expression (Ca/Co vs. Co/Co; NES, normalized enrichment score).

of genes was over-expressed), this raises the possibility that the canola oil-rich maternal diet induces epigenetic potentiation in these genes in a context-dependent manner, possibly contributing to maintenance of cellular homeostasis.

Maternal Diets Modulate the Carcinogenic Effects of DMBA on Offspring Mammary Glands

To test the effect of maternal diets (canola vs. corn oil-rich diets) on the protection against DMBA induced carcinogenesis, F1 mice were treated with DMBA (weekly dose of 1 mg for 6 weeks). Surprisingly, we observed a 3-week delay in DMBA induced mortality in F1 generation mice whose mothers were fed canola oil (Ca/Co) in comparison to corn (Co/Co) oil-rich diets (**Figure 4A**). This early delay in mortality in Ca/Co group was statistically significant (*P*-value < 0.0001), however, the overall survivals were not statistically different. Eventually, all of the mice developed tumors and became moribund; still, tumor development in Co/Co mice was faster than in Ca/Co mice (**Supplementary Figure 7A**). The lateral growth rate of mammary tumors was slower (**Figure 4B**) and size of mammary tumors was relatively less in Ca/Co mice compared to Co/Co mice, albeit not statistically significant (**Figure 4C**). Since maternal diets epigenetically modulated various gene promoters, we performed protein expression analysis using western blotting to determine if the expression of proteins responsible for DNA damage repair and epigenetic remodeling were altered after carcinogen exposure. We found that increased H3K18ac levels around TSS were correlated with slightly increased levels of BRCA1, BRCA2, RAD51, and FAN1 proteins in the Ca/Co mice compared to the Co/Co mice in response to DMBA; however, changes in protein levels were not statistically significant (**Figures 4D–G** and **Supplementary Figure 7B**). Notably, the transcriptional expression of *Brca1* was decreased (*P*-value < 0.01), and *Fan1* was unchanged in the

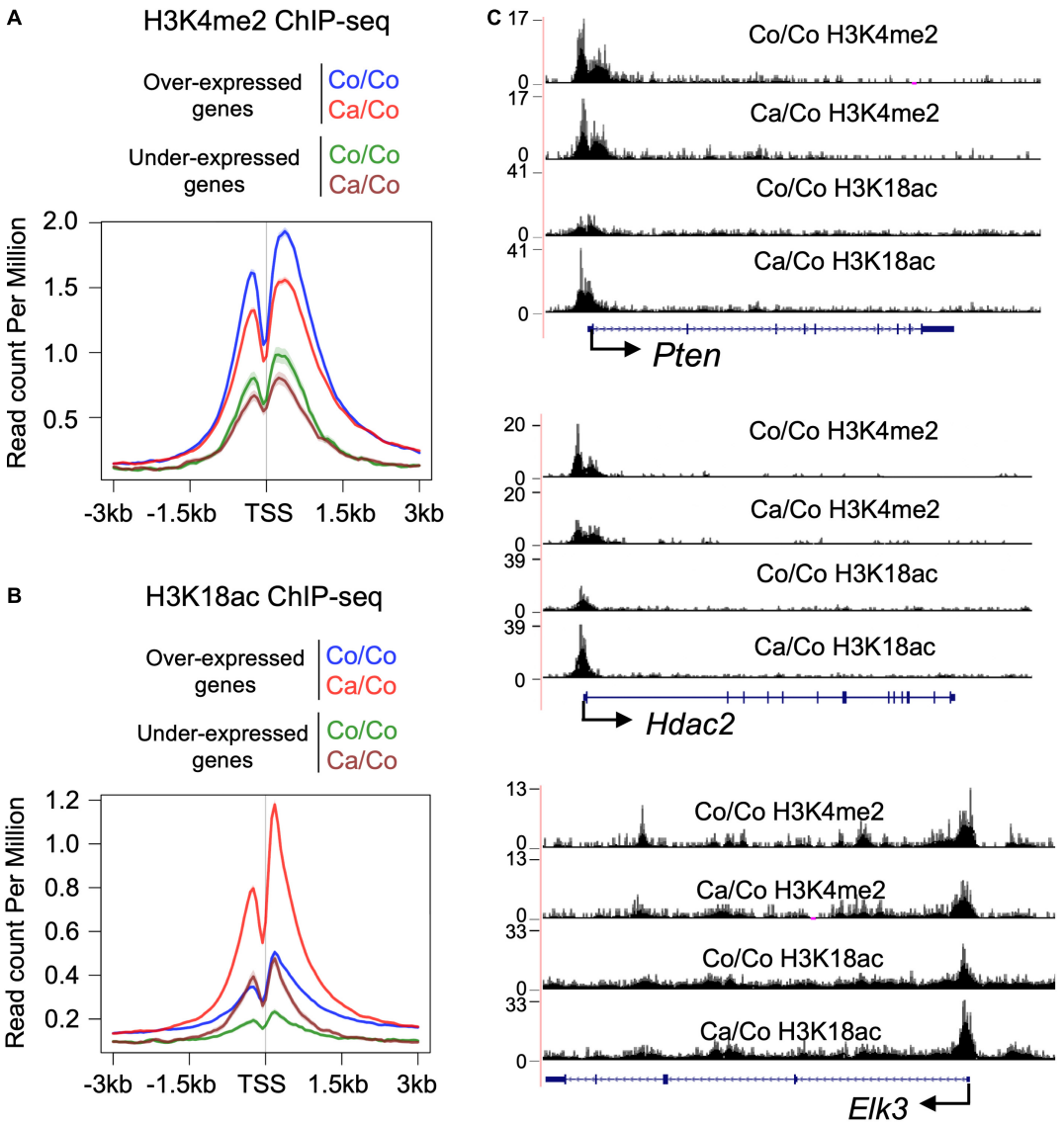

FIGURE 3 | Histone PTMs at TSS of the differentially expressed genes. Metagene plot showing histone H3K4me2 **(A)** and H3K18ac **(B)** ChIP-seq signals at TSS (±3 kb) of differentially expressed genes in the breast tissue of F1 generation mice whose mothers were fed either corn (Co/Co) or canola (Ca/Co) oil-rich diets. **(C)** UCSC genome browser tracks representing the changes in H3K4me2 and H3K18ac signals around TSS due to maternal diets are shown for *Pten* (over-expressed), *Hdac2* (unchanged), and *Elk3* (under-expressed) genes.

Ca/Co mice compared to Co/Co mice before DMBA treatment (basal level in F1, **Supplementary Figure 8**). Furthermore, protein expression of PRMT2 was relatively increased (*P*-value, ns) but CHD1 and SMARCA5 was unchanged in Ca/Co compared to Co/Co mice (**Supplementary Figure 7C**); however, transcriptional levels of *Prmt2* and *Chd1* genes were unchanged and *Smarca5* was significantly increased (P-value < 0.01) in the Ca/Co mice before DMBA treatment (**Supplementary Figure 8**). Altogether, these findings suggest that the canola oil-rich maternal diets epigenetically modulate transcriptional expression and epigenetically potentiate various genes, possibly for rapid activation to protect from mammary tumor development in the event of carcinogenic insult.

DISCUSSION

Epigenetic inheritance in plants, nematodes, and *Drosophila* has already been demonstrated, but how environmental cues transmit to offspring in mammals, if they do, is controversial (Heard and Martienssen, 2014; Boskovic and Rando, 2018; Horsthemke, 2018). However, it is apparent that the environment, including diets, certainly affects gene expression patterns and influences physiopathology. Recently, Xavier et al. (2019) reviewed the impact of various environmental factors, including diets on epigenetic states, and how they can be hereditably transmitted. More precisely, recent evidence has shown that parental diets can

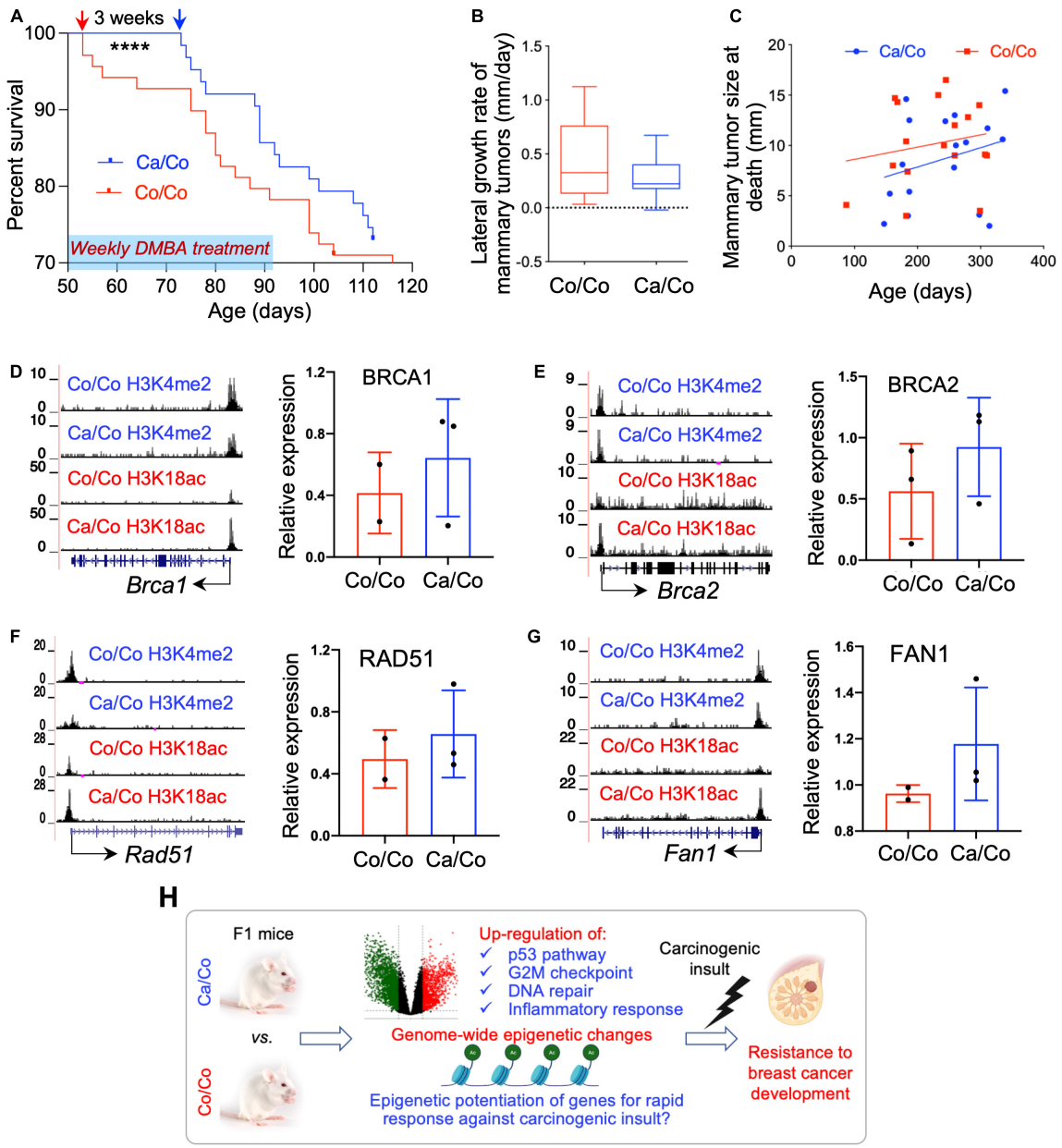

FIGURE 4 | Maternal diets modulate the effects of DMBA on offspring mammary tissue. **(A)** Survival curve showing 3 weeks delay in mortality (***P-value < 0.0001) after DMBA treatment in F1 generation mice whose mothers were fed canola (Ca/Co) oil in comparison to corn (Co/Co) oil-rich diets, however, overall survival is not statistically significant. Red and blue arrows showing the time of first mortality in Co/Co and Ca/Co mice respectively after DMBA treatment. **(B)** Lateral growth rate of mammary tumors (mm/day) after DMBA treatment in F1 mice (Tukey; P-value, ns). **(C)** Mammary tumor size at the time of death (P-value, ns). **(D)** UCSC genome browser tracks showing maternal diets induced epigenetic changes (potentiation) in the *Brca1* gene (left, no DMBA) and BRCA1 protein expression (right, quantified using ImageJ) after DMBA treatment (t-test; P-value, ns). **(E)** UCSC genome browser tracks showing maternal diets induced epigenetic changes (potentiation) in the *Brca2* gene (left, no DMBA) and BRCA2 protein expression (right, quantified using ImageJ) after DMBA treatment (t-test; P-value, ns). **(F)** UCSC genome browser tracks showing maternal diets induced epigenetic changes (potentiation) in the *Rad51* gene (left, no DMBA) and RAD51 protein expression (right, quantified using ImageJ) after DMBA treatment (t-test; P-value, ns). **(G)** UCSC genome browser tracks showing maternal diets induced epigenetic changes (potentiation) in the *Fan1* gene (left, no DMBA) and FAN1 protein expression (right, quantified using ImageJ) after DMBA treatment (t-test; P-value, ns). **(H)** Carton describing differential gene expression and epigenetic potentiation providing resistance to BCa development in F1 generation mice whose mothers were fed canola rich diet (Ca/Co). ns, not significant.

influence the outcome of BCa through transgenerational epigenetic inheritance (da Cruz et al., 2020). The present study evaluated the influence of maternal diet on BCa development in F1 offspring using BALB/c mice and investigated the associated genome-wide epigenetic and transcriptional changes.

There is a large body of evidence suggesting the chemo-preventive effect of ω-3 FA against BCa and other cancer development [see recent reviews and meta-analysis (Mokbel and Mokbel, 2019; Nindrea et al., 2019a,b; Donovan et al., 2020; Yurko-Mauro et al., 2020)]. Hardman's group earlier reported that maternal diet supplemented with canola oil (ω-3 FA-rich) reduced tumor incidence and growth in C3(1)-TAg mice offspring (Ion et al., 2010), suggesting the involvement of possible transgenerational epigenetic mechanisms. Our data, showing the effect of maternal diet on genome-wide histone modifications (**Figure 1**) in F1 BALB/c mice, provides first-hand evidence corroborating the above findings. Remarkably, the transcriptomic changes involve the differential expression of ∼3,500 genes, enriched in multiple molecular pathways associated with preventing/suppressing cancer incidence/growth (**Figure 2** and **Supplementary Figure 5**). The unpredicted large number of genes affected suggest a nearly genome-wide impact of ω-3 FA-rich maternal diet. Consistent with our results, it has been shown that a high ω-3 FA-rich diet can lead to the inhibition of the enzyme acetyl-CoA carboxylase (Willumsen et al., 1993), in turn leading to an increased pool of acetyl-CoA, a acetyl donor for histone acetylation. An increased acetyl-CoA level due to attenuation of acetyl-CoA carboxylase enzyme can lead to the global increase in histone acetylation (Galdieri and Vancura, 2012). This change in global histone acetylation is congruent with the observed increase in H3K18ac that we reported in this study, But, importantly, our results suggest that the change in global histone acetylation that is of maternal origin appears to be passed onto the F1 mice of our Ca/Co group.

Histone modifications around TSS play a crucial role in gene transcription. An open chromatin state (euchromatin) around the TSS is created or maintained for the recruitment of the general transcriptional machinery, as well as various gene-specific transcriptional factors necessary to regulate transcriptional homeostasis. A large increase of H3K18ac with a decrease in H3K4me2 marks around TSS of over-expressed genes (**Figure 3**, ∼80% of total differentially expressed genes are over-expressed) indicates that epigenetic regulation is a primary driver of the effects of ω-3 FA rich maternal diets. These results are consistent with recent studies that demonstrate the epigenetic modifying potential of ω-3 FA (Tremblay et al., 2017; Amatruda et al., 2019; Gonzalez-Becerra et al., 2019; Ceccarelli et al., 2020); however, to the best of our knowledge, this is the first study comprehensively showing the global impact of ω-3 FA-rich maternal diets on F1 offspring's epigenome and transcriptome.

The ω-3 FA-rich maternal diets in addition to modulating F1 offspring's epigenome, it also incredibly provides protection again early carcinogenic insults (**Figure 4** and **Supplementary Figure 7**). As our data indicated, epigenetic changes, more specifically the increase in H3K18ac at TSS were located over a subset of important DNA damage response genes. The activation of such genes is likely to be associated with an early response against DMBA induced carcinogenesis (**Figures 4D–G**). These results suggest that the ω-3 FA-rich maternal diet causes epigenetic potentiation of genes in F1 offspring, setting them ready to rapidly express DNA repair and cell cycle controlling genes after a carcinogenic insult.

In conclusion, our study provides an in-depth analysis of mechanisms of action involving genome-wide epigenetic changes mediated by the ω-3 FA-rich maternal diet onto F1 offspring. These changes in both expression and epigenetics potentiation of genes important in cancer-fighting pathways contribute to providing resistance to BCa development (**Figure 4H**). However, future studies are needed to further pin-point the diet-induced specific transgenerational epigenetic effects, and also extend the results to F2 and F3 generations, and their role in preventing various chronic illnesses, including cancers.

MATERIALS AND METHODS

Animal Experiments

BALB/c mice (around 4 weeks old) were purchased from the Jackson Laboratory (Bar Harbor, ME, United States). The animal protocol describing the mouse treatment and use was reviewed and approved by the Marshall University Institutional Animal Care and Use Committee (IACUC). Mice were used in compliance with the National Institutes of Health (NIH) recommendations published in the "Guide for the Care and Use of Laboratory Animals"[1]. Mice were randomized and 15 female mice were placed on AIN-93 diet containing 10% corn oil, 15 female mice were placed on a diet containing 10% canola oil. After 2 weeks, mice were bred with male BALB/c mice to produce 200 experimental female mice (100 from corn oil and 100 from canola oil supplemented maternal diet group). At weaning, all pups were placed on the corn oil diet, thus the only time any pups were exposed to the canola oil diet was during gestation and lactation. At 50 days of age, the female pups were randomized, half of each maternal diet group were treated with 7,12-Dimethylbenz(a)anthracene (DMBA). Mammary gland tumors were induced using DMBA, beginning at 50 days of age. DMBA (10 mg/ml in sesame seed oil) treated pups (n = 50) received 0.1 ml of DMBA by gavage once per week for 6 weeks. Control pups (n = 50) without DMBA received only 0.1 ml of vehicle (sesame seed oil). After 6 weeks, non-DMBA control pups provided mammary tissue for transcriptomic (microarray) and epigenetic (ChIP-seq) studies to examine genome-wide differences that are the result of the maternal diet and that are not influenced by the carcinogen nor by a tumor. DMBA-treated pups were palpated weekly until a tumor was detected. We followed DMBA-treated pups for the time of the first detection of tumor incidence and multiplicity. After detection, all tumors were measured three times weekly to develop tumor growth curves.

Microarray for Gene Expression

Total RNA was extracted from cells using the RNeasy kit (Qiagen, Germantown, MD, United States). On-column DNase treatment was given following the procedure provided by the manufacturer. RNA quality was assessed via the Agilent 2100 Bioanalyzer (Agilent Technologies, Santa Clara, CA,

[1]https://grants.nih.gov/grants/olaw/guide-for-the-care-and-use-of-laboratory-animals.pdf

United States). Microarray analysis was performed using Agilent Gene Expression Microarray Platform (SurePrint G3 Mouse GE 8 × 60K Microarray) at Marshall University Genomics and Bioinformatics Core following the manufacturer recommendations. Processing of the microarray, including normalization and differential expression analysis, was performed using GeneSpring GX (Agilent Techonolgies, United States). Principal component analysis (PCA) was performed to examine the overall similarity among the samples at the gene expression level. *t*-test was used to identify differential gene expression between the Ca/Co and Co/Co groups with Benjamini–Hochberg multiple testing corrected *P*-value < 0.05 as the significant cut-off. Differentially expressed genes were further curated by removing "unknown" genes, cDNA clones, etc. GSEA (Subramanian et al., 2005) was performed to identify over-represented biological functions in the differential gene expression in terms of the signatures in MSigDB (Liberzon et al., 2011).

ChIP-Sequencing and Analysis

Chromatin immunoprecipitation-sequencing was performed on pooled samples. Briefly, mammary tissues were dissected into small pieces and crosslinked using formaldehyde (1% w/v, methanol-free) followed by homogenization and chromatin preparation using a Covaris sonicator (Covaris, Woburn, MA, United States). Chromatin was immunoprecipitated using an appropriate antibody, washed, reverse-crosslinked, and DNA isolated using the phenol-chloroform method. Precipitated DNA was QC'ed by quantitative PCR using Mouse ChIP Control qPCR Primer Sets (Active Motiff, Carlsbad, CA United States). For ChIP-seq, 10 ng precipitated DNA was used to prepare the library using Illumina TruSeq ChIP library preparation kit following the manufacturer recommendations. Libraries were quantified for cluster generation using KAPA Library Quantification Kit (Kapa Biosystems, Wilmington, MA, United States). Sequencing was performed using Illumina HiSeq2500 using 50-bp single-end rapid run format. Sequencing quality was initially checked by running FastQC. Sequencing reads were aligned against mm9 by using Bowtie2. BAM files were normalized by depth after removal of PCR duplicates and blacklisted regions. Peaks were called using MACS2 with default parameters. For heatmap and metagene plots, ngs.plot program was used. UCSC genome browser was used to visualize individual gene tracks.

Western Blot

Protein lysates were prepared from mammary tissues using a standard RIPA lysis buffer containing a protease inhibitor cocktail (Roche). Lysates were electrophoresed using SDS-PAGE, transferred to ECL nitrocellulose membranes (Amersham), and probed using specific antibodies. HRP-conjugated secondary antibodies were used, and our blots were developed using the ECL detection system (Thermo Scientific) combined with ECL hypersensitive films. The densitometry analysis was performed using the Alpha Innotech FluorChem™ IS 9000 software.

Statistics

Prism™ was used for analyses of data and graph preparation. Time-to-death or to-detection of mammary gland tumors was analyzed by a log-rank (Mantel–Cox) test. These "survival" curves also provided calculation of median times. Prism™ was used to further analyze the survival curve data to generate linear regression analyses of portions of the data. For box plot, box and whiskers graphs were plotted using the Tukey method (two-tailed Mann–Whitney U test was used to calculate *P*-value). The middle line in the box indicates the median, whiskers indicate the highest and lowest values within 1.5 × IQR (inter-quartile distance between the 25th and 75th percentiles) up and down from the box. Bar graphs are plotted using mean with SD, and *t*-tests were used to calculate *P*-values.

DATA AVAILABILITY STATEMENT

The datasets presented in this study can be found in online repositories. The names of the repository/repositories and accession number(s) can be found below: NCBI GEO; GSE169115.

ETHICS STATEMENT

The animal study was reviewed and approved by the Marshall University School of Medicine Institutional Animal Care and Use Committee.

AUTHOR CONTRIBUTIONS

PG and WH conceptualized the study. AA, TW, WP, and JF performed the experiments. AA, KG, and JH performed bioinformatic data analyses. AA and PG drafted the manuscript. All authors critically revised the manuscript and gave final approval.

FUNDING

This work was supported in part by a DOD grant # BC096996P1 – "Maternal Consumption of Omega 3 Fatty Acids to Reduce Breast Cancer Risk in Offspring" (WH, AA, TW, WP, JF, and PG) and NIH grants CA90890 and CA122906, and NIH COBRE grant 5P20RR-020180 (PG).

ACKNOWLEDGMENTS

The authors thank to Goran Boskovic and James Denvir for help in design and analysis of the gene expression profiling experiments. The authors also thank to Tanner Bahkshi for his critical reading of the manuscript.

SUPPLEMENTARY MATERIAL

The Supplementary Material for this article can be found online at: https://www.frontiersin.org/articles/10.3389/fcell.2021.682593/full#supplementary-material

REFERENCES

Abbas, A., Hall, J. A., Patterson, W. L. III, Ho, E., Hsu, A., Al-Mulla, F., et al. (2016). Sulforaphane modulates telomerase activity via epigenetic regulation in prostate cancer cell lines. *Biochem. Cell Biol.* 94, 71–81. doi: 10.1139/bcb-2015-0038

Abbas, A., Patterson, W. III, and Georgel, P. T. (2013). The epigenetic potentials of dietary polyphenols in prostate cancer management. *Biochem. Cell Biol.* 91, 361–368. doi: 10.1139/bcb-2012-0044

Abel, S., Riedel, S., and Gelderblom, W. C. (2014). Dietary PUFA and cancer. *Proc. Nutr. Soc.* 73, 361–367. doi: 10.1017/s0029665114000585

Amatruda, M., Ippolito, G., Vizzuso, S., Vizzari, G., Banderali, G., Verduci, E., et al. (2019). Epigenetic effects of n-3 LCPUFAs: a role in pediatric metabolic syndrome. *Int. J. Mol. Sci.* 20:2118. doi: 10.3390/ijms20092118

Bishop, K. S., and Ferguson, L. R. (2015). The interaction between epigenetics, nutrition and the development of cancer. *Nutrients* 7, 922–947. doi: 10.3390/nu7020922

Boskovic, A., and Rando, O. J. (2018). Transgenerational epigenetic inheritance. *Annu. Rev. Genet.* 52, 21–41.

Ceccarelli, V., Ronchetti, S., Marchetti, M. C., Calvitti, M., Riccardi, C., Grignani, F., et al. (2020). Molecular mechanisms underlying eicosapentaenoic acid inhibition of HDAC1 and DNMT expression and activity in carcinoma cells. *Biochim. Biophys. Acta Gene Regul. Mech.* 1863:194481. doi: 10.1016/j.bbagrm.2020.194481

Choi, S. W., and Friso, S. (2010). Epigenetics: a new bridge between nutrition and health. *Adv. Nutr.* 1, 8–16. doi: 10.3945/an.110.1004

da Cruz, R. S., Chen, E., Smith, M., Bates, J., and de Assis, S. (2020). Diet and transgenerational epigenetic inheritance of breast cancer: the role of the paternal germline. *Front. Nutr.* 7:93. doi: 10.3389/fnut.2020.00093

DiNicolantonio, J. J., and O'Keefe, J. H. (2018). Importance of maintaining a low omega-6/omega-3 ratio for reducing inflammation. *Open Heart* 5:e000946. doi: 10.1136/openhrt-2018-000946

Diorio, C., and Dumas, I. (2014). Relations of omega-3 and omega-6 intake with mammographic breast density. *Cancer Causes Control* 25, 339–351. doi: 10.1007/s10552-013-0335-5

Donovan, M. G., Selmin, O. I., Stillwater, B. J., Neumayer, L. A., and Romagnolo, D. F. (2020). Do olive and fish oils of the mediterranean diet have a role in triple negative breast cancer prevention and therapy? An exploration of evidence in cells and animal models. *Front. Nutr.* 7:571455. doi: 10.3389/fnut.2020.571455

Fleming, T. P., Watkins, A. J., Velazquez, M. A., Mathers, J. C., Prentice, A. M., Stephenson, J., et al. (2018). Origins of lifetime health around the time of conception: causes and consequences. *Lancet* 391, 1842–1852. doi: 10.1016/s0140-6736(18)30312-x

Galdieri, L., and Vancura, A. (2012). Acetyl-CoA carboxylase regulates global histone acetylation. *J. Biol. Chem.* 287, 23865–23876. doi: 10.1074/jbc.m112.380519

Glick, N. R., and Fischer, M. H. (2013). The role of essential fatty acids in human health. *J. Evidence Based Complement. Altern. Med.* 18, 268–289.

Gomez Candela, C., Bermejo Lopez, L. M., and Loria Kohen, V. (2011). Importance of a balanced omega 6/omega 3 ratio for the maintenance of health: nutritional recommendations. *Nutr. Hosp.* 26, 323–329.

Gonzalez-Becerra, K., Ramos-Lopez, O., Barrón-Cabrera, E., Riezu-Boj, J. I., Milagro, F. I., Martínez-López, E., et al. (2019). Fatty acids, epigenetic mechanisms and chronic diseases: a systematic review. *Lipids Health Dis.* 18:178.

Hardman, W. E. (2004). (n-3) fatty acids and cancer therapy. *J. Nutr.* 134(12 Suppl.), 3427S–3430S.

Hardman, W. E. (2007). Dietary canola oil suppressed growth of implanted MDA-MB 231 human breast tumors in nude mice. *Nutr. Cancer* 57, 177–183. doi: 10.1080/01635580701277445

Hardman, W. E. (2014). Diet components can suppress inflammation and reduce cancer risk. *Nutr. Res. Pract.* 8, 233–240. doi: 10.4162/nrp.2014.8.3.233

Hardman, W. E., Moyer, M. P., and Cameron, I. L. (1999). Fish oil supplementation enhanced CPT-11 (irinotecan) efficacy against MCF7 breast carcinoma xenografts and ameliorated intestinal side-effects. *Br. J. Cancer* 81, 440–448. doi: 10.1038/sj.bjc.6690713

Heard, E., and Martienssen, R. A. (2014). Transgenerational epigenetic inheritance: myths and mechanisms. *Cell* 157, 95–109. doi: 10.1016/j.cell.2014.02.045

Horsthemke, B. (2018). A critical view on transgenerational epigenetic inheritance in humans. *Nat. Commun.* 9:2973.

Huang, Y. C., Jessup, J. M., Forse, R. A., Flickner, S., Pleskow, D., Anastopoulos, H. T., et al. (1996). n-3 fatty acids decrease colonic epithelial cell proliferation in high-risk bowel mucosa. *Lipids* 31(Suppl.), S313–S317.

Ion, G., Akinsete, J. A., and Hardman, W. E. (2010). Maternal consumption of canola oil suppressed mammary gland tumorigenesis in C3(1) TAg mice offspring. *BMC Cancer* 10:81. doi: 10.1186/1471-2407-10-81

Jenuwein, T. (2001). Translating the histone code. *Science* 293, 1074–1080. doi: 10.1126/science.1063127

Kang, J. X., and Liu, A. (2013). The role of the tissue omega-6/omega-3 fatty acid ratio in regulating tumor angiogenesis. *Cancer Metastasis Rev.* 32, 201–210. doi: 10.1007/s10555-012-9401-9

Karmali, R. A., Adams, L., and Trout, J. R. (1993). Plant and marine n-3 fatty acids inhibit experimental metastasis of rat mammary adenocarcinoma cells. *Prostag. Leukot Ess. Fatty Acids* 48, 309–314. doi: 10.1016/0952-3278(93)90221-h

Koh, Y. C., Ho, C. T., and Pan, M. H. (2020). Recent advances in cancer chemoprevention with phytochemicals. *J. Food Drug Anal.* 28, 14–37. doi: 10.1016/j.jfda.2019.11.001

Li, J., Li, K., Gao, J., Guo, X., Lu, M., Li, Z., et al. (2018). Maternal exposure to an n-3 polyunsaturated fatty acid diet decreases mammary cancer risk of female offspring in adulthood. *Food Funct.* 9, 5768–5777. doi: 10.1039/c8fo01006d

Liberzon, A., Subramanian, A., Pinchback, R., Thorvaldsdóttir, H., Tamayo, P., Mesirov, J. P., et al. (2011). Molecular signatures database (MSigDB) 3.0. *Bioinformatics* 27, 1739–1740. doi: 10.1093/bioinformatics/btr260

Liu, X., Robinson, G. W., Wagner, K. U., Garrett, L., Wynshaw-Boris, A., Hennighausen, L., et al. (1997). Stat5a is mandatory for adult mammary gland development and lactogenesis. *Genes Dev.* 11, 179–186. doi: 10.1101/gad.11.2.179

Lunn, J., and Theobald, H. E. (2006). The health effects of dietary unsaturated fatty acids. *Nutr. Bull.* 31, 178–224. doi: 10.1111/j.1467-3010.2006.00571.x

Mokbel, K., and Mokbel, K. (2019). Chemoprevention of breast cancer with vitamins and micronutrients: a concise review. *In Vivo* 33, 983–997. doi: 10.21873/invivo.11568

Nindrea, R. D., Aryandono, T., Lazuardi, L., and Dwiprahasto, I. (2019a). Association of dietary intake ratio of n-3/n-6 polyunsaturated fatty acids with breast cancer risk in western and asian countries: a meta-analysis. *Asian Pac. J. Cancer Prev.* 20, 1321–1327. doi: 10.31557/apjcp.2019.20.5.1321

Nindrea, R. D., Aryandono, T., Lazuardi, L., and Dwiprahasto, I. (2019b). Protective effect of Omega-3 fatty acids in fish consumption against breast cancer in asian patients: a meta-analysis. *Asian Pac. J. Cancer Prev.* 20, 327–332. doi: 10.31557/apjcp.2019.20.2.327

Patterson, W. L. III, and Georgel, P. T. (2014). Breaking the cycle: the role of omega-3 polyunsaturated fatty acids in inflammation-driven cancers. *Biochem. Cell Biol.* 92, 321–328. doi: 10.1139/bcb-2013-0127

Pizato, N., Bonatto, S., Yamazaki, R. K., Aikawa, J., Nogata, C., Mund, R. C., et al. (2005). Ratio of n6 to n-3 fatty acids in the diet affects tumor growth and cachexia in Walker 256 tumor-bearing rats. *Nutr. Cancer* 53, 194–201. doi: 10.1207/s15327914nc5302_8

Remely, M., Lovrecic, L., de la Garza, A. L., Migliore, L., Peterlin, B., Milagro, F. I., et al. (2015). Therapeutic perspectives of epigenetically active nutrients. *Br. J. Pharmacol.* 172, 2756–2768. doi: 10.1111/bph.12854

Saini, R. K., Keum, Y.-S., Daglia, M., and Rengasamy, K. R. R. (2020). Dietary carotenoids in cancer chemoprevention and chemotherapy: a review of emerging evidence. *Pharmacol. Res.* 157:104830. doi: 10.1016/j.phrs.2020.104830

Simopoulos, A. P. (2009). Evolutionary aspects of the dietary omega-6:omega-3 fatty acid ratio: medical implications. *World Rev. Nutr. Diet.* 100, 1–21. doi: 10.1159/000235706

Simopoulos, A. P. (2016). An increase in the Omega-6/Omega-3 fatty acid ratio increases the risk for obesity. *Nutrients* 8:128. doi: 10.3390/nu8030128

Steck, S. E., and Murphy, E. A. (2020). Dietary patterns and cancer risk. *Nat. Rev. Cancer* 20, 125–138. doi: 10.1038/s41568-019-0227-4

Subramanian, A., Tamayo, P., Mootha, V. K., Mukherjee, S., Ebert, B. L., Gillette, M. A., et al. (2005). Gene set enrichment analysis: a knowledge-based approach for interpreting genome-wide expression profiles. *Proc. Natl. Acad. Sci. U.S.A.* 102, 15545–15550. doi: 10.1073/pnas.0506580102

Syed, D. N., Suh, Y., Afaq, F., and Mukhtar, H. (2008). Dietary agents for chemoprevention of prostate cancer. *Cancer Lett.* 265, 167–176. doi: 10.1016/j.canlet.2008.02.050

Tremblay, B. L., Guénard, F., Rudkowska, I., Lemieux, S., Couture, P., Vohl, M. C., et al. (2017). Epigenetic changes in blood leukocytes following an omega-3 fatty acid supplementation. *Clin. Epigenetics* 9:43.

Turati, F., Rossi, M., Pelucchi, C., Levi, F., and La Vecchia, C. (2015). Fruit and vegetables and cancer risk: a review of southern European studies. *Br. J. Nutr.* 113(Suppl. 2), S102–S110.

Vanamala, J. (2017). Food systems approach to cancer prevention. *Crit. Rev. Food Sci. Nutr.* 57, 2573–2588. doi: 10.1080/10408398.2015.1028023

Willumsen, N., Skorve, J., Hexeberg, S., Rustan, A. C., and Berge, R. K. (1993). The hypotriglyceridemic effect of eicosapentaenoic acid in rats is reflected in increased mitochondrial fatty acid oxidation followed by diminished lipogenesis. *Lipids* 28, 683–690. doi: 10.1007/bf02535987

Witte, T. R., and Hardman, W. E. (2015). The effects of omega-3 polyunsaturated Fatty Acid consumption on mammary carcinogenesis. *Lipids* 50, 437–446. doi: 10.1007/s11745-015-4011-2

Xavier, M. J., Roman, S. D., Aitken, R. J., and Nixon, B. (2019). Transgenerational inheritance: how impacts to the epigenetic and genetic information of parents affect offspring health. *Hum. Reprod. Update* 25, 518–540.

Yurko-Mauro, K., Van Elswyk, M., and Teo, L. (2020). A scoping review of interactions between Omega-3 long-chain polyunsaturated fatty acids and genetic variation in relation to cancer risk. *Nutrients* 12:1647. doi: 10.3390/nu12061647

Zanoaga, O., Jurj, A., Raduly, L., Cojocneanu-Petric, R., Fuentes-Mattei, E., Wu, O., et al. (2018). Implications of dietary omega-3 and omega-6 polyunsaturated fatty acids in breast cancer. *Exp. Ther. Med.* 15, 1167–1176.

Conflict of Interest: The authors declare that the research was conducted in the absence of any commercial or financial relationships that could be construed as a potential conflict of interest.

frontiers in Cell and Developmental Biology

ORIGINAL RESEARCH
published: 27 July 2021
doi: 10.3389/fcell.2021.685120

Analysis of Ferroptosis-Mediated Modification Patterns and Tumor Immune Microenvironment Characterization in Uveal Melanoma

Yi Jin[1,2,3†], Zhanwang Wang[1†], Dong He[4], Yuxing Zhu[1], Lian Gong[1], Mengqing Xiao[1], Xingyu Chen[1] and Ke Cao[1]*

[1] Department of Oncology, Third Xiangya Hospital of Central South University, Changsha, China, [2] Department of Radiation Oncology, Hunan Cancer Hospital, The Affiliated Cancer Hospital of Xiangya School of Medicine, Central South University, Changsha, China, [3] Department of Radiation Oncology, Hunan Key Laboratory of Translational Radiation Oncology, Hunan Cancer Hospital and The Affiliated Cancer Hospital of Xiangya School of Medicine, Central South University, Changsha, China, [4] Department of Respiratory, The Second People's Hospital of Hunan Province, Changsha, China

OPEN ACCESS

Edited by:
Rais Ahmad Ansari, Nova Southeastern University, United States

Reviewed by:
Yusra Shao, Wayne State University, United States
Babu Roshan Padmanabhan, University Hospitals Cleveland Medical Center, United States

***Correspondence:**
Ke Cao
csucaoke@163.com

[†] These authors have contributed equally to this work

Specialty section:
This article was submitted to Epigenomics and Epigenetics, a section of the journal Frontiers in Cell and Developmental Biology

Received: *24 March 2021*
Accepted: *24 May 2021*
Published: *27 July 2021*

Citation:
Jin Y, Wang Z, He D, Zhu Y, Gong L, Xiao M, Chen X and Cao K (2021) Analysis of Ferroptosis-Mediated Modification Patterns and Tumor Immune Microenvironment Characterization in Uveal Melanoma. Front. Cell Dev. Biol. 9:685120. doi: 10.3389/fcell.2021.685120

Uveal melanoma (UVM) is an intraocular malignancy in adults in which approximately 50% of patients develop metastatic disease and have a poor prognosis. The need for immunotherapies has rapidly emerged, and recent research has yielded impressive results. Emerging evidence has implicated ferroptosis as a novel type of cell death that may mediate tumor-infiltrating immune cells to influence anticancer immunity. In this study, we first selected 11 ferroptosis regulators in UVM samples from the training set (TCGA and GSE84976 databases) by Cox analysis. We then divided these molecules into modules A and B based on the STRING database and used consensus clustering analysis to classify genes in both modules. According to the Gene Ontology (GO), Kyoto Encyclopedia of Genes and Genomes (KEGG), and Gene Set Enrichment Analysis (GSEA), the results revealed that the clusters in module A were remarkably related to immune-related pathways. Next, we applied the ESTIMATE and CIBERSORT algorithms and found that these ferroptosis-related patterns may affect a proportion of TME infiltrating cells, thereby mediating the tumor immune environment. Additionally, to further develop the prognostic signatures based on the immune landscape, we established a six-gene-regulator prognostic model in the training set and successfully verified it in the validation set (GSE44295 and GSE27831). Subsequently, we identified the key molecules, including ABCC1, CHAC1, and GSS, which were associated with poor overall survival, progression-free survival, disease-specific survival, and progression-free interval. We constructed a competing endogenous RNA network to further elucidate the mechanisms, which consisted of 29 lncRNAs, 12 miRNAs, and 25 ferroptosis-related mRNAs. Our findings indicate that the ferroptosis-related genes may be suitable potential biomarkers to provide novel insights into UVM prognosis and decipher the underlying mechanisms in tumor microenvironment characterization.

Keywords: Uveal melanoma, ferroptosis, tumor-infiltrating immune cells, tumor immune environment, prognostic model

INTRODUCTION

Uveal melanoma (UVM), which represents 85% of ocular melanomas, is the most common primary intraocular malignancy in adults and arises from melanocytes of the iris (3–5%), ciliary body (5–8%), or choroid (∼85%) (Chang et al., 1998; McLaughlin et al., 2005). Analysis of the Surveillance, Epidemiology, and End Results program database in the USA and the European Cancer Registry-based study on survival and care of cancer patients revealed an overall incidence of 1.3–8.6 cases per million per year (Virgili et al., 2007; Singh et al., 2011). Currently, the management of surgical options mainly depends on tumor location, extent, and size, adverse effects, and systemic status, including partial iridectomy, iridotrabeculectomy of the iris, and iridocyclectomy (Henderson and Margo, 2008). Radiotherapy can also achieve high local control in most cases with extensive seeding and in non-resectable tumors (Shields et al., 2013; Rahmi et al., 2014). However, approximately 50% of patients develop metastatic disease, predominantly in the liver, which is refractory to traditional treatments such as chemotherapy and surgical metastasectomy (Achberger et al., 2014). Due to the lack of standard therapies to significantly improve survival, newer fields of targeted treatments and immunotherapies have rapidly emerged and yielded impressive results by targeting specific regulators or immune system checkpoints (Chang et al., 1998; de Vries et al., 1998; Chen et al., 2017). However, there are few reports on oncogenes underlying UVM. Therefore, unraveling genomic properties is crucial for the development of effective treatments and prediction of individual survival.

Previous studies have confirmed that programmed cell death (PCD) is related to tumorigenesis, progression, and metastasis processes (Labi and Erlacher, 2015; Lee et al., 2018). Efficient cancer treatment ultimately aims to induce cell-specific PCD. Ferroptosis is a novel form of PCD that is driven by lethal iron-dependent accumulation of lipid reactive oxygen species (ROS). Cytological changes, including decreased mitochondrial cristae, a ruptured outer mitochondrial membrane, or a condensed mitochondrial membrane, ferroptosis gradually plays a pivotal role in the mediation of the carcinogenic environment and suppression of tumor progression in various cancer cells (Yagoda et al., 2007; Cao and Dixon, 2016; Latunde-Dada, 2017; Yu et al., 2017). For instance, results from NCI-60, a panel of different cancer cell lines from eight different tissue types, showed that ferroptosis with excess iron overload was found in several types of tumor cells such as breast cancer, ovarian cancer, lung cancer, diffuse large B-cell lymphoma, and renal cell carcinoma (Xie et al., 2016). Moreover, further investigations revealed that radiotherapy and chemotherapeutic drugs such as cisplatin and temozolomide, combined with ferroptosis-induction therapy, had a more significant effect than traditional treatments alone (Mou et al., 2019). Currently, no studies have focused on the role of ferroptosis in UVM patients and rare therapies inducing ferroptosis-induction therapy; thus, we first performed a set of studies to identify the clinical importance of ferroptosis in UVM and estimate the relationship between the microenvironment and specific ferroptosis-related biomarkers, aiming to explore the essential function of ferroptosis.

Checkpoint inhibitors, which promote immune function and induce anti-tumor immunity, are among the most successful agents for treating advanced melanoma. Regarding UVM, statistics from a phase II trial of metastasized patients showed a satisfactory outcome with a disease control rate (DCR) of 47% and a durable DCR of 21% ([DCR] = complete response [CR] + partial response [PR] + stable disease [SD], durable DCR [DCR $\geq$ 6 months]) (Schank and Hassel, 2019; Pelster et al., 2021; Piulats et al., 2021). Despite sharing similar clinical characteristics, patients with UVM may invariably exhibit different clinical survival rates (Polak et al., 2007). The underlying molecular mechanisms that elucidate this phenomenon may be attributed to the tumor microenvironment (TME), which includes cancer cells, stromal cells, distant recruited cells, bone marrow-derived cells, and secreted factors (Topalian et al., 2012; Wang et al., 2017). Thus, identifying TME characteristics is crucial to improving clinical survival outcomes in patients with UVM. Emerging evidence suggests that ferroptosis may be an adaptive process for achieving better treatment effects, such as exerting an obvious synergistic effect with PD1/PD-L1/CTLA4 inhibitors by generating lipid-derived mediators to modulate intracellular and intercellular signaling pathways, including receptor tyrosine kinase signaling in the TME (Friedmann et al., 2019; Hoefsmit et al., 2020). Moreover, some efficient treatments, including radiotherapy and immunotherapy, control ferroptosis and promote immunotherapy-activated CD8+ T cells, and radiotherapy-activated ATM can effectively kill cancer cells and prevent cancer cells from escaping immune surveillance (Lang et al., 2019). However, little is known about the relationship between ferroptosis in the tumor immune microenvironment and UVM.

In this study, we performed a retrospective analysis based on The Cancer Genome Atlas (TCGA) database and the Gene Expression Omnibus Database (GEO) to estimate the effect of ferroptosis-related genes on the prognostic value. We further verified its prognostic significance and explored the underlying mechanisms between ferroptosis-related genes and individual TME characterizations.

Abbreviations: UVM, uveal melanoma; SEER, Surveillance, Epidemiology, and End Results; EUROCARE, European Cancer Registry-based study on survival and care of cancer patients; PCD, programmed cell death; RCD, regulated cell death; ROS, reactive oxygen species; DCR, disease control rate; TME, tumor microenvironment; TCGA, The Cancer Genome Atlas; GEO, Gene Expression Omnibus Database; PPI, protein-protein interaction; OS, overall survival; DEGs, differentially expressed genes; GSEA, Gene set enrichment analysis; HR, hazard ratio; ROC, receiver operating characteristic; ceRNA, competing endogenous RNA; PFS, progression-free survival; DSS, disease-specific survival; PFI, progression-free interval; ICIs, immune checkpoint inhibitors.

MATERIALS AND METHODS

Data Processing of UVM Dataset

We downloaded the RNA sequencing, mutation expression, and clinical information of UVM from TCGA and GEO databases. The RNA sequencing data (FPKM value) and somatic mutation data from TCGA-UVM were downloaded from the Genomic Data Commons[1]. In total, three eligible GEO

[1]https://portal.gdc.cancer.gov/

datasets (GSE27831, GSE44295, GSE84976) were downloaded and received background adjustment and quantile normalization using affy and simpleaffy packages. Data from TCGA and GEO are publicly available.

Selection of Potential Ferroptosis-Related Genes

We first selected 60 ferroptosis-related genes (**Supplementary Table 1**) from previously published articles (Stockwell et al., 2017; Bersuker et al., 2019; Doll et al., 2019; Hassannia et al., 2019). Cox proportional hazard regression analysis was used to select the prognostic regulators positively or negatively based on the TCGA dataset and GSE84976. Finally, we considered the intersection of these regulators from different databases as potential functional molecules.

Clustering of Ferroptosis-Related Regulators

The STRING database[2] was used to analyze protein–protein interactions (PPI) among ferroptosis modulators. In this study, we propose an MCL cluster to identify cancer driver modules that combine mutex, functional similarity, and connectivity in the PPI network (Zhang et al., 2020). Pearson correlation analysis was used to reveal the associations among different regulators in different modules. Next, differentially expressed prognostic ferroptosis-related genes in specific modules were classified into different clusters using the ConsensusClusterPlus R package with optimal k-means clustering (Wilkerson and Hayes, 2010), which aimed to precisely gather genes with similar expression, and we performed 1,000 iterations (50 iterations, resampling rate of 80%) to ensure the stability of the classification. Overall survival (OS) analysis between different clusters was calculated using the Kaplan–Meier method.

Identification of Signaling Pathways in Ferroptosis-Related Patterns

To identify the function regulated by diverse patterns, we obtained the differentially expressed genes (DEGs) with $|\log FC \text{ (fold change)}| \geq 2$ and adj. $p < 0.05$ by applying the empirical Bayesian approach of limma R package in the standard comparison mode. To further investigate the signaling pathways in ferroptosis-related patterns, we implemented the clusterProfiler R package to perform the Kyoto Encyclopedia of Genes and Genomes (KEGG) pathway, Gene Ontology (GO) biological processes, and Gene Set Enrichment Analysis (GSEA) analysis, which aimed to evaluate all DEGs and assess the functions associated with subtypes.

Estimation of Immune Cell Infiltration in Ferroptosis-Related Patterns

In this study, we applied the ESTIMATE algorithm. The R script was downloaded from the website[3] and applied to estimate the ratio of the immune stromal components in the TME and further explore differences in the TME scores, including ESTIMATE, immune, and stromal scores (Newman et al., 2015). We utilized the CIBERSORT package to assess the distribution of 22 immune cell types based on TCGA-UVM samples. Results with $p < 0.05$ obtained from the ESTIMATE algorithm and CIBERSORT analysis were used in further analysis.

Construction of Prognostic Ferroptosis Signatures and Validation

Univariate Cox regression analysis was performed to examine the relationship between ferroptosis-related genes and OS in the TCGA UVM cohort. Moreover, two prognostic models were constructed, and the risk score was generated as follows: risk score = $\text{Expression}_{\text{mRNA1}} \times \text{Coefficient}_{\text{mRNA1}} + \text{Expression}_{\text{mRNA2}} \times \text{Coefficient}_{\text{mRNA2}} + \ldots \text{Expression}_{\text{mRNAn}} \times \text{Coefficient}_{\text{mRNAn}}$. The patients from TCGA and GEO databases were divided into high-risk and low-risk groups according to the median cutoff of the risk score. Next, to determine independent prognostic factors in UVM, univariate and multivariate Cox analyses were utilized to distinguish the clinicopathological parameters positively or negatively with the hazard ratio (HR). Subsequently, the Kaplan–Meier survival method was used to screen the availability of the prognostic model, and the receiver operating characteristic (ROC) curve was used to evaluate the prediction accuracy of 3-year and 5-year OS. To enhance prediction accuracy and interpretability, three GEO cohorts were further presented as validation sets to re-verify the prognostic model and selection of key ferroptosis modulators.

Building of ceRNA Network Based on Key Genes

To further understand how the ferroptosis-related mRNAs regulate tumorigenesis along with miRNA and lncRNA, we obtained differentially expressed lncRNAs and miRNAs based on the TCGA cohort with the standards of $|\log2(\text{Fold change})| > 1$ and $p < 0.05$ by using the R package "limma." Furthermore, we used the miRcode database to target experimentally validated lncRNA (Jeggari et al., 2012) and miRTarBase[4], miRDB[5], and TargetScan[6] datasets (Li et al., 2014; Agarwal et al., 2015; Chou et al., 2018; Chen and Wang, 2020) to predict miRNA–mRNA interactions. The competing endogenous RNA (ceRNA) network was visualized using the Cytoscape software (Shannon et al., 2003).

Statistical Analysis

Most analyses were performed using the R software (version 3.6.1[7]). Kaplan–Meier curves were used to compare OS based

[2]http://string-db.org

[3]https://sourceforge.net/projects/estimateproject/

[4]http://mirtarbase.mbc.nctu.edu.tw/

[5]http://www.mirdb.org/

[6]http://www.targetscan.org/

[7]http://www.R-project.org

on the risk score of subgroups and expression of ferroptosis-related genes. The comparison of the ESTIMATE algorithm between the two subgroups was performed using the Wilcoxon rank sum test. Cox proportional hazard regression analyses were used to select the independent prognostic value of OS, including clinical characteristics and ferroptosis regulators. All statistical p values were bilateral, and $p < 0.05$ was considered statistically significant.

RESULTS

Selection of Prognostic Ferroptosis-Related Regulators

In this study, the expression of 60 ferroptosis-related regulators and clinicopathological characteristics associated with UM patients were obtained from the TCGA and GEO databases. First, 80 UM patients from TCGA and 28 UM patients from GSE84976 with OS were identified as the training set for selecting potential ferroptosis-related modulators. We then utilized Cox analysis to identify these genes and found 11 genes, including 9 upregulated genes (CHAC1, NQO1, SQLE, SLC1A5, GSS, LPCAT3, GPX4, AIFM2, and ABCC1) and 2 downregulated genes (ACSF2 and FDFT1) that were overlapped in TCGA and GSE84976 datasets (**Figure 1A** and **Supplementary Table 2**). The workflow is illustrated in **Figure 1B**.

Clustering of Ferroptosis-Related Genes With Prognostic Value of Clinical Outcomes

Based on the STRING database, differentially expressed or prognostic ferroptosis-related genes were selected for MCL clustering and divided into cancer driver modules A and B (**Figure 2A**). Pearson correlation analysis showed that genes in both functional modules were highly correlated (**Figure 2B** and **Supplementary Figure 1A**). To better understand the interrelations among these regulators, a consensus clustering analysis using the Consensus Cluster Plus package was implemented in the TCGA UVM cohort, and $k = 2$ seemed to be the most appropriate selection in both modules (**Figure 2C** and **Supplementary Figure 1B**). Next, the Kaplan–Meier method showed a significant difference in OS when cluster1 with low risk was compared to cluster2 with high risk (**Figure 2D** and **Supplementary Figure 1C**). Moreover, to clearly visualize the expression of these regulators, we plotted a boxplot based on module A and found that the expression of CHAC1, ABCC1,

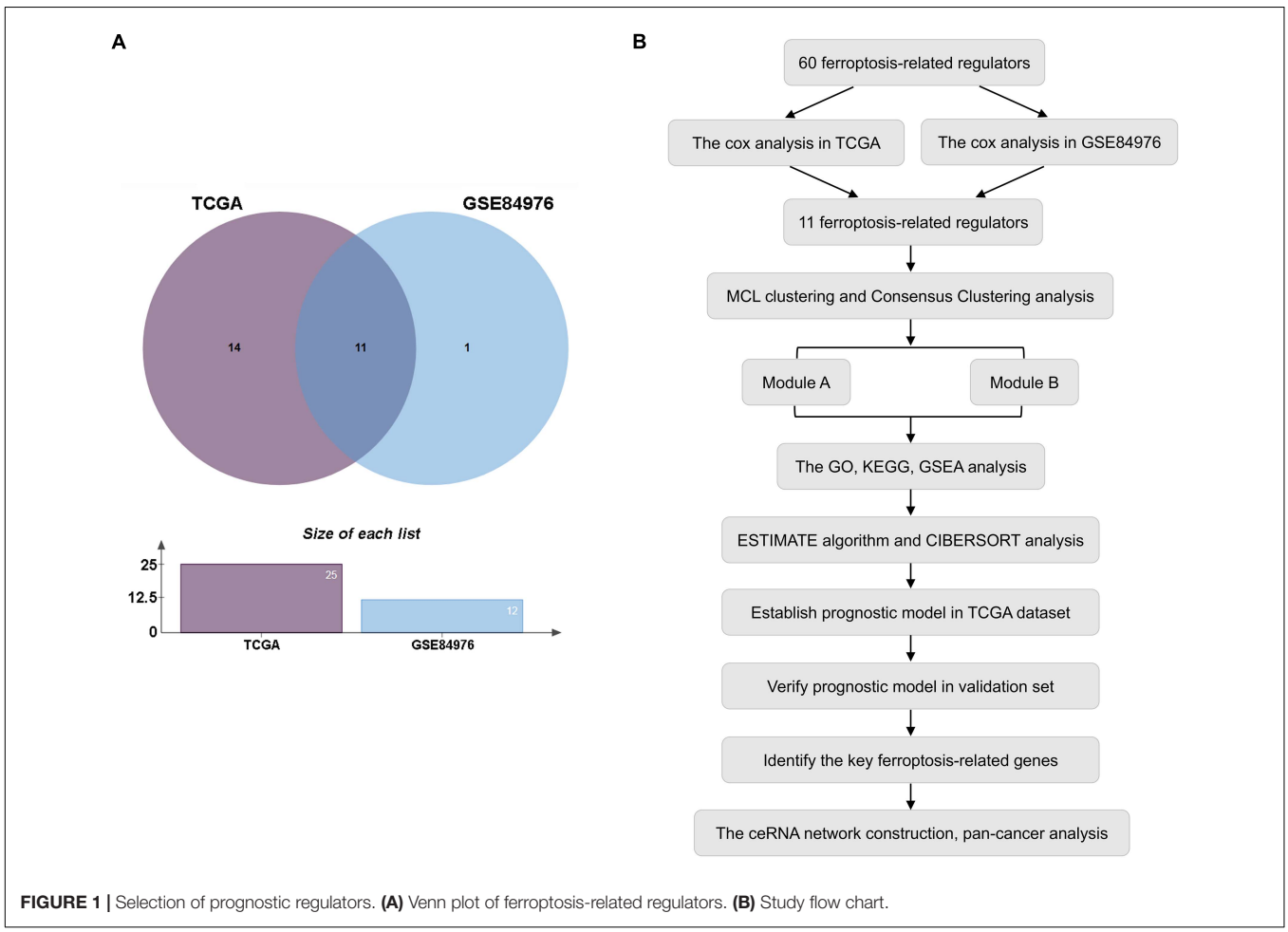

FIGURE 1 | Selection of prognostic regulators. **(A)** Venn plot of ferroptosis-related regulators. **(B)** Study flow chart.

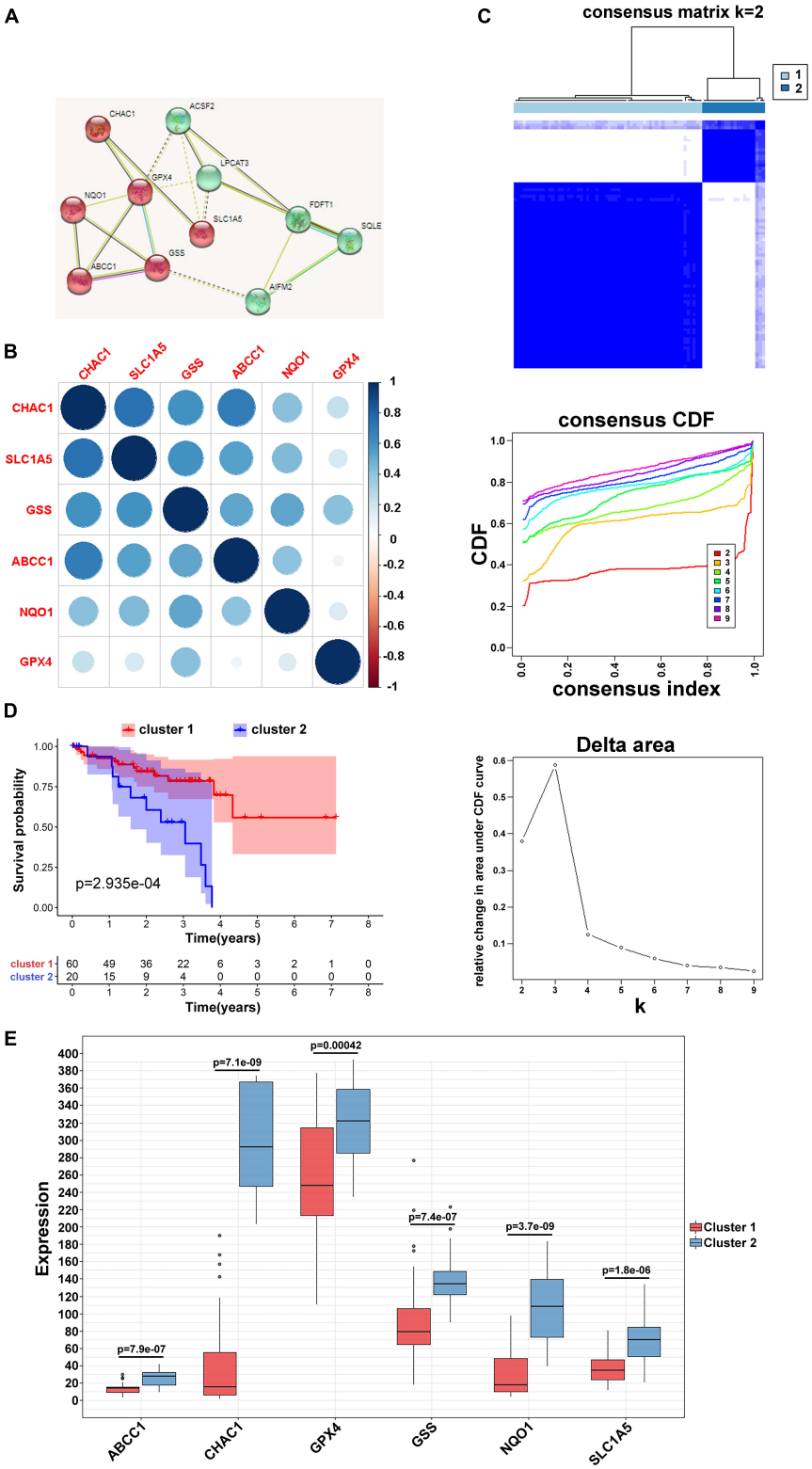

FIGURE 2 | Clustering of ferroptosis-related genes. **(A)** MCL clustering of ferroptosis-related genes. **(B)** Pearson correlation analysis among ferroptosis-related regulators in module A. **(C)** Consensus clustering cumulative distribution function (CDF) and relative change in area under CDF curve for k = 2 in module A. **(D)** Kaplan–Meier curves of two clusters in UVM about OS in module A. **(E)** The different expression of the ferroptosis-related mediators in two clusters based on module A.

NQO1, GPX4, SLC1A5, and GSS in cluster2 was higher than that in cluster1 ($p < 0.01$) (**Figure 2E**), while in module B, the expression of FDFT1 and ACSF2 was higher in cluster2 than in the other clusters (**Supplementary Figure 1D**).

Interaction of Ferroptosis-Related Regulators in Two Patterns

To investigate the potential biological processes involved in the molecular heterogeneity between the clusters, we identified DEGs with | log2 (fold change) |>2 and adj. $p < 0.05$, in the TCGA cohort. In module A, the biological process of GO analysis showed that the DEGs were enriched in response to interferon-gamma, T-cell activation, and cellular response to interferon-gamma. Cellular component analysis indicated that DEGs were abundant on the side of the membrane and on the external side of the plasma membrane. The molecular function indicated that DEGs were mainly located in receptor regulator activity and ligand activity. KEGG analysis showed that the DEGs were enriched in primary immunodeficiency, Th1, Th2, Th17 cell differentiation, and so on (**Figure 3A**). Furthermore, according to the results from GSEA analysis, these DEGs were primarily enriched in these terms, which were significantly related to cluster1: cell adhesion molecules, Th1 and Th2 cell differentiation, and Th17 cell differentiation. These results have been confirmed to be remarkably related to immunotherapy, giving us some insights into the ferroptosis-regulating effects on the tumor immune microenvironment (**Figure 3B**; Im et al., 2016; Garcia-Diaz et al., 2017; Zhang et al., 2017). However, the GO, KEGG, and GSEA analyses in module B failed to target meaningful pathways associated with the immune landscape (**Figure 3C**).

Characteristics of Tumor Immune Microenvironment in UVM Patients

To reveal the potential role and explore the potential mechanism of ferroptosis modification-related phenotypes in the TME, we used the ESTIMATE algorithm to apply stromal scores, immune scores, and ESTIMATE scores for all UVM samples. As shown in **Figure 4A**, we found that all enrolled genes in module A showed a similar expression trend along with immune and ESTIMATE scores. Moreover, in this study, when compared to cluster1, the ESTIMATE ($p = 0.043$) and immune scores ($p = 0.52e^{-6}$) were significantly higher in cluster2, indicating that ferroptosis-related patterns may be involved in regulating the immune landscape and play a central role in immune regulation (**Figure 4B**). However, the mechanism by which ferroptosis-related patterns affect immune-related molecules (especially TMEs) is unclear. Therefore, we quantified the level of immune cell infiltration to evaluate the immune landscape of clusters using the CIBERSORT algorithm. The results revealed that naïve B cells, CD8 T cells, CD4 memory resting T cells, CD4 memory activated T cells, follicular helper T cells, and gamma delta T cells accounted for a large proportion of immune cell infiltration. Particularly, we observed that cluster1 with better survival showed higher levels of naïve B cells, resting T cells CD4 memory, resting NK cells, resting monocytes, and resting mast cells compared to cluster2. On the contrary, the outcome revealed that the proportion of CD8 + T cells, CD4 memory activated T cells, follicular helper T cells, gamma delta T cells, macrophages M0, and resting dendritic cells were higher in cluster2 (**Figure 4C**). However, we failed to unravel the relationship between module B and the immune microenvironment (**Supplementary Figure 2B**). These results suggest that specific multiple ferroptosis-related modulators may combine to affect the type of TME infiltrating cells to mediate the TME and change the clinical survival in UVM.

Prognostic Analysis of Risk Model and Ferroptosis-Related Genes

To develop a predictive signature based on the immune landscape of UVM patients, we performed Cox regression analysis on six modulators in module A using the TCGA database. Next, we calculated the risk score as follows: risk score = CHAC1 × 0.0037 + ABCC1 × 0.067 + NQO1 × 0.0067 + GPX4 × 0.0043 + SLC1A5 × 0.021 + GSS × 0.012. The risk score distribution, survival status, and expression profile of the six prognostic regulators are shown in **Figure 5A**. Patients were separated into the low-risk or high-risk groups with the median cutoff, and we found that the high-risk group had a significantly poorer OS ($p = 1.6e^{-08}$) (**Figure 5B**). Univariate and multivariate analyses showed that clinical characteristics, including age, sex, and T stage, were unable to predict OS, except for the risk score, which was viewed as an independent prognostic factor ($p < 0.001$, HR = 1.276, 95% CI = 1.106–1.472) (**Figure 5C**). The results from the ROC curve indicated that the risk score has strong predictive ability, with an AUC of 0.832 and 0.907 at 3 and 5 years, respectively (**Figure 5D**). These results indicate that the ferroptosis-related risk model from module A may serve as an important indicator for evaluating the prognosis of UVM. Additionally, in module B, we also constructed the risk score as follows: risk score = FDFT1 × (−0.012) + SQLE × 0.016 + AIFM2 × 0.05 + LPCAT3 × 0.17 + ACSF2 × (−0.19). As shown in **Supplementary Figures 3A,B**, we found that as the risk score increased, more patients died. The ROC curve showed that the risk score risk score had a better efficiency in predicting 3- and 5-year OS, with AUC values of 0.828 and 0.792, respectively (**Supplementary Figure 3C**). Furthermore, in one of the training sets GSE84976, we also obtained satisfactory outcomes, and both ferroptosis-related models could be regarded as independent risk factors for predicting OS (**Figure 5E** and **Supplementary Figure 3D**).

Verification of Ferroptosis Regulators–Based Risk Model

To verify the predictive ability of both risk models, validation analysis was performed in two GEO datasets, including 57 UM from GSE44295 with OS and 29 patients from GSE27831 with progression-free survival (PFS). In GSE44295, which contained the largest sample of UVM in the Genomic Data Commons, the Kaplan–Meier curve revealed that there was a significant difference between the high-risk and low-risk groups with a log-rank test of $p = 0.026$ (**Figure 6A**). The risk formula from module A was exactly suitable for predicting OS by using

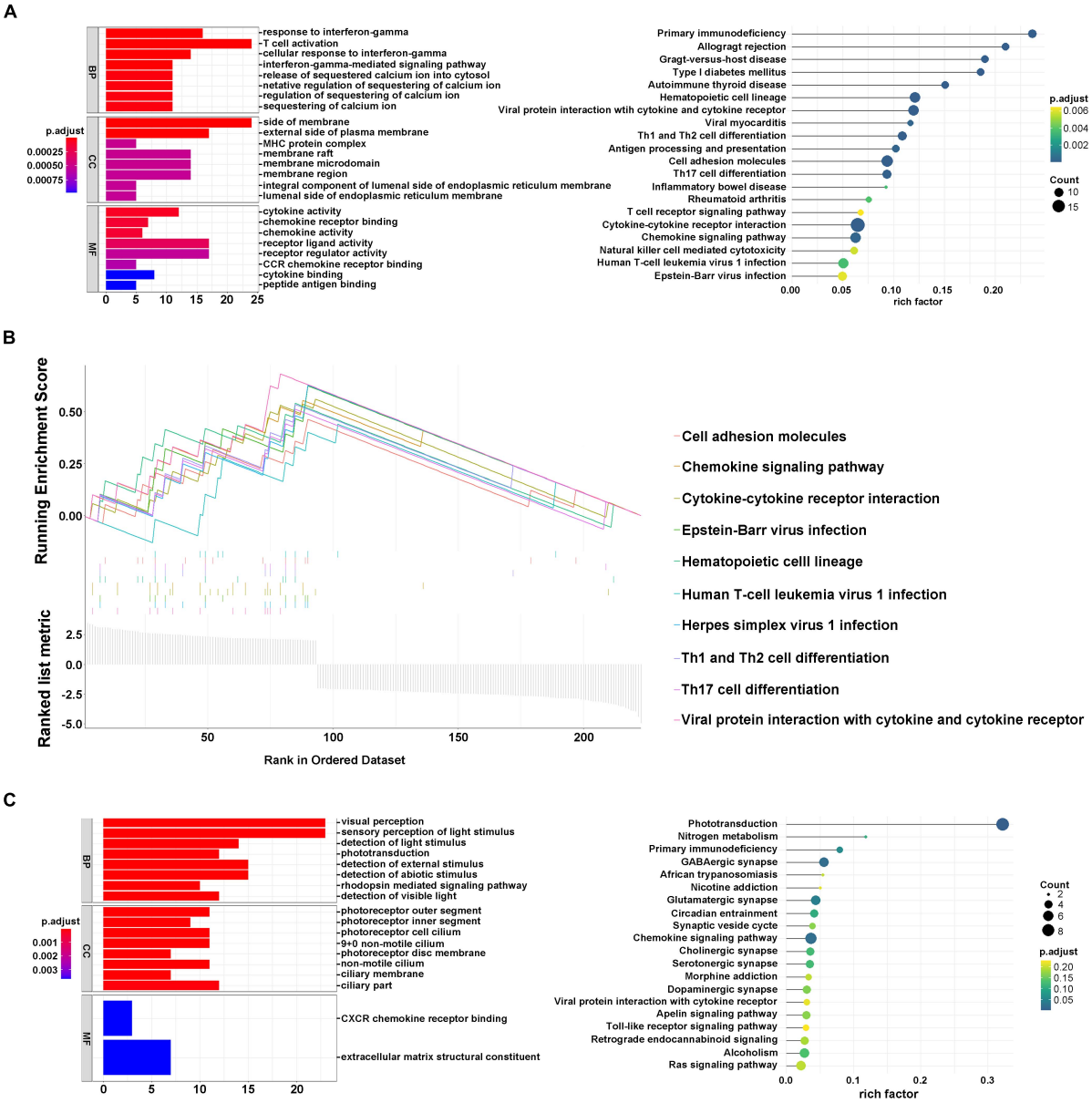

FIGURE 3 | Interaction of ferroptosis-related genes. **(A)** GO and KEGG analyses of DEGs in module A. **(B)** GSEA analysis of DEGs in module A. **(C)** GO and KEGG analysis of DEGs in module B.

the median value as the cutoff. Similarly, in GSE27831, the Kaplan–Meier analysis indicated that this risk formula can be predictive of a high risk of disease progression with a log-rank test of $p = 0.0007$ by using the best cutoff (**Figure 6B**). However, the risk formula from module B failed to be re-verified in both GEO databases. To further select the key prognostic ferroptosis modification-related genes, we continued to calculate the prognostic values of six genes in all GEO datasets and believed that the overlapping molecules might be significantly meaningful. As shown in **Figures 6C–F**, ABCC1, CHAC1, and GSS were successfully re-verified as crucial biomarkers to induce poor OS and PFS in TCGA and all GEO datasets. Additionally, data from the UCSC Cancer Genomics Browser[8] showed that high ABCC1, CHAC1, and GSS expression was associated with decreased disease-specific survival (DSS) and progression-free interval (PFI) ($p < 0.001$) (**Supplementary Figure 4**).

Construction of ceRNA Based on Key Genes

To elucidate the mechanism underlying the ferroptosis-related pathway combined with miRNAs and lncRNAs, we obtained 316 differentially expressed lncRNAs and 126 miRNAs using

[8]https://genome-cancer.ucsc.edu

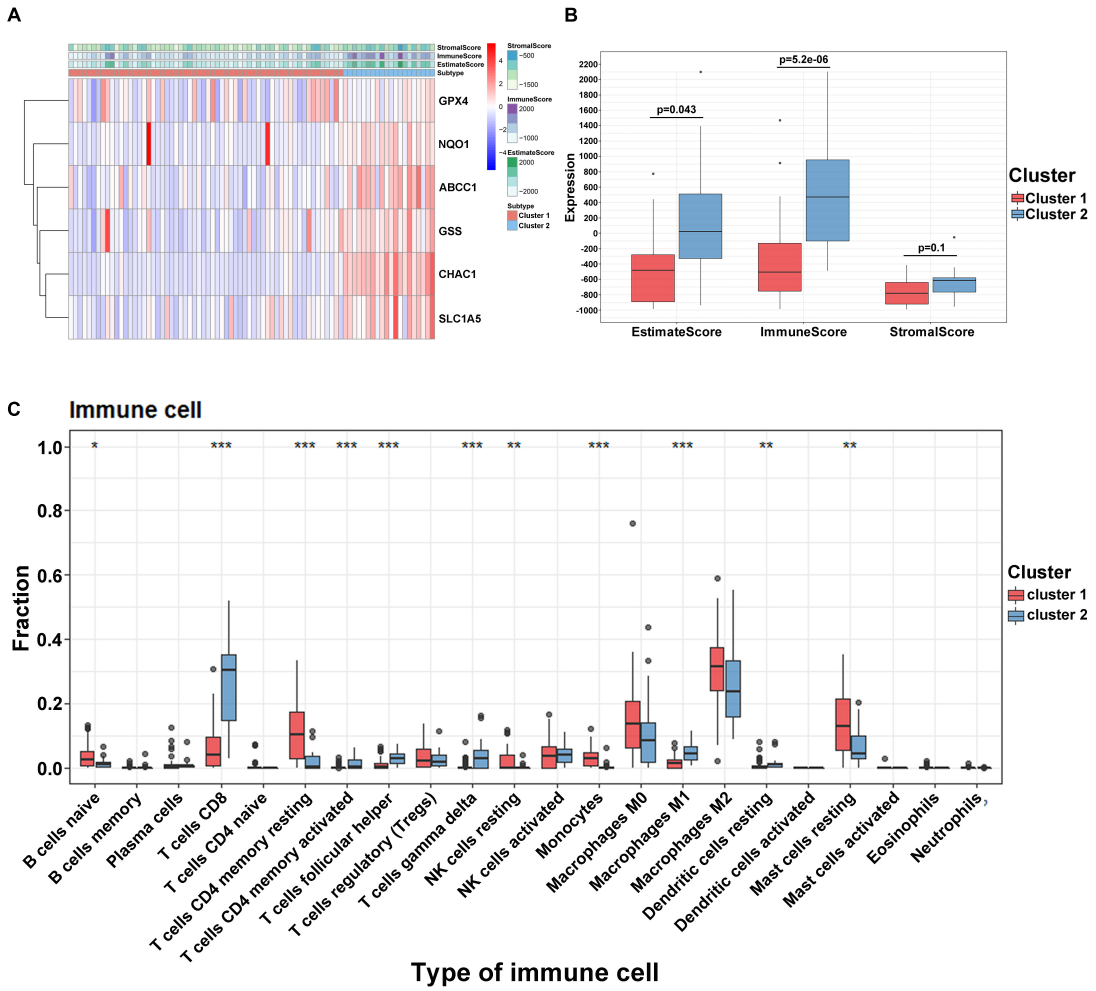

FIGURE 4 | Tumor immune microenvironment in module A. **(A)** The heatmap of ferroptosis-related regulators in two clusters. **(B)** The different expression of ESTIMATE score in two clusters. **(C)** The different distribution of 22 TME infiltrating cells in two patterns (***$p < 0.001$; **$p < 0.01$; *$p < 0.05$).

the TCGA database (**Supplementary Tables 3, 4**). We drew the heatmaps (**Figures 7A,C**) and volcano plots (**Figures 7B,D**) to visualize the distribution of DEGs with | logFC (fold change) |≥2 and FDR < 0.05. To further identify the pathway by which lncRNAs mediate mRNA expression by sponging miRNAs, we selected 29 lncRNAs from the miRcode database, which targeted 20 miRNAs and enrolled a total of 679 mRNAs based on three databases (miRTarBase, miRDB, and TargetScan) (**Supplementary Table 5**). We then calculated the top 200 genes that were highly associated with ABCC1, CHAC1, and GSS to take the intersection of the enrolled mRNAs (**Figure 7E**); finally, we constructed a ceRNA regulatory network containing 25 ferroptosis-related mRNAs, 12 miRNAs, and 29 lncRNAs and then used Cytoscape for visualization (**Figure 7F**).

Evaluation of Key Genes in Immune Landscape and Pan-Cancer

To further evaluate the role of key genes in mediating the immune signature, we analyzed the correlation between the expression of ABCC1, CHAC1, GSS, and ESTIMATE scores and infiltrating immune cells. The results showed that ABCC1, CHAC1, and GSS levels had a significantly positive correlation with immune score, stromal score, and ESTIMATE score (**Figures 8A–C**). In addition, we found that the proportion of diverse types of T cell and B cell naïve dendritic cells, which have been proven to coordinately trigger successful immune reactions and positive costimulatory signals, had an intimate relationship with the expression of three key genes (Sharpe and Pauken, 2018; **Supplementary Figure 5A**). It is well known that the expression of PD1 (PDCD1 or CD279) and PD-L1 (CD274) serves as a potential marker for predicting the response to immunotherapy. In our study, we found an important correlation between ABCC1 and CHAC1 expression and the levels of PD1 and PD-L1 (**Supplementary Figure 5B**). The GSEA analysis of these regulators also targeted meaningful immune-related pathways, such as immune response regulating cell surface receptor signaling, B cell-mediated immunity, and adaptive immune response (**Figure 8D**). In pan-cancer analysis of 32 cancer species, ABCC1, CHAC1, and GSS may act as

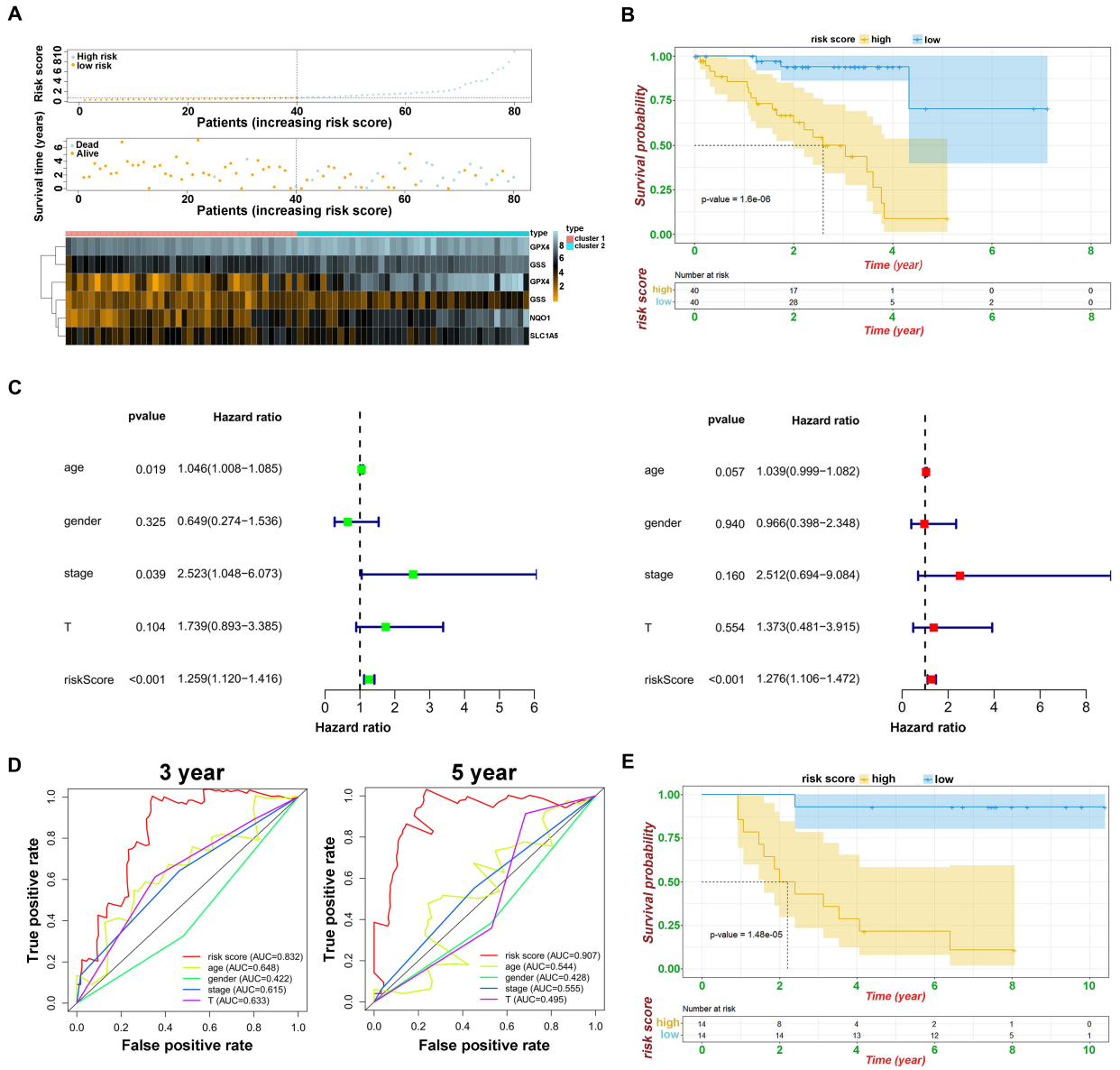

FIGURE 5 | Prognostic analysis of risk model and ferroptosis-related genes. **(A)** The distributions of risk scores, alive/dead status, and expression of ferroptosis-related genes in module A. **(B)** Kaplan–Meier curves of patients in high/low risk about OS in module A. **(C)** Univariate (above) and multivariate analysis (below) of clinical characteristics. **(D)** ROC curve of risk score and clinical characteristics in module A. **(E)** Kaplan–Meier curves of patients in high/low risk about OS based on GSE84976.

hallmarks to activate tumor immune reactions and reshape the tumor environment in LGG, LIGC, BRAC, LUAD, LUSC, and UVM (**Figure 8E**).

In addition to novel immunotherapies, multiple mRNA inhibitors, including BRAF, also showed an astonishing effect in a large number of patients with sustained efficacy (Luke et al., 2017). Simultaneously, we also identified four mRNAs (AIMP1, TMEM33, ITGB5, and PSPH) with positive polymorphisms in UVM based on the SNP2APA database. The correlation between the three ferroptosis-related modulators and the above mRNA was observed (**Supplementary Figure 6**).

DISCUSSION

Uveal melanoma is considered rare but is the most common malignant primary intraocular tumor among adults. Most UVMs are usually treated with surgery or radiotherapy, resulting in similar short-term survival outcomes. With distinct biological and clinical behavior, half of patients will suffer from a poor prognosis, including recurrence and metastatic disease (Marseglia et al., 2021). To date, standard approaches have not provided a survival benefit or precise prognostic prediction for these patients; however, newer systemic therapies, particularly

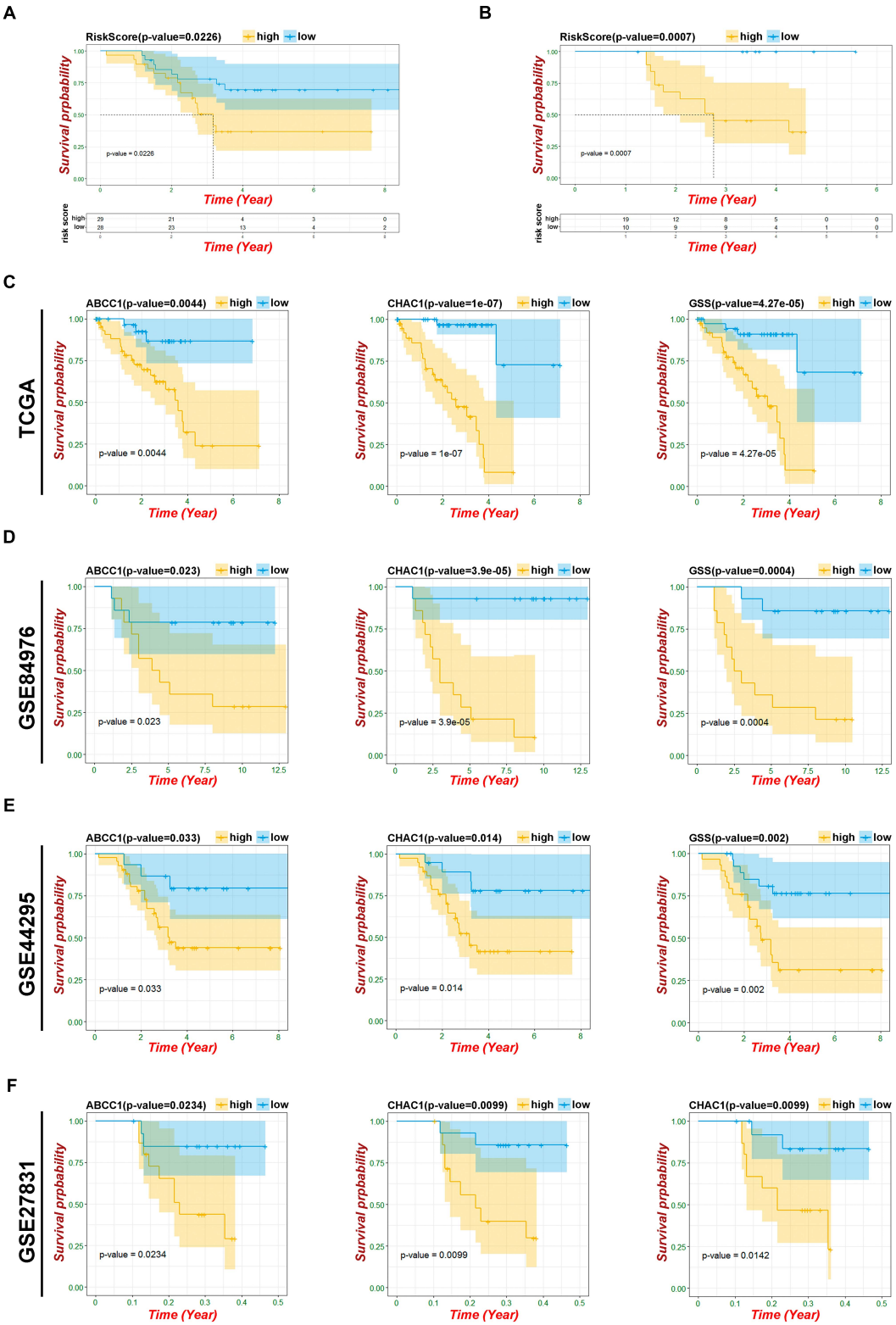

FIGURE 6 | Verification of risk model and ferroptosis-related genes. **(A)** Kaplan–Meier curves of patients in risk model about OS based on GSE44295. **(B)** Kaplan–Meier curves of patients in risk model about PFS based on GSE27831. **(C)** Kaplan–Meier OS curves for patients in key ferroptosis-related genes based on TCGA. **(D)** Kaplan–Meier OS curves for patients in key ferroptosis-related genes based on GSE84976. **(E)** Kaplan–Meier OS curves for patients in key ferroptosis-related genes based on GSE44295. **(F)** Kaplan–Meier PFS curves for patients in key ferroptosis-related genes based on GSE27831.

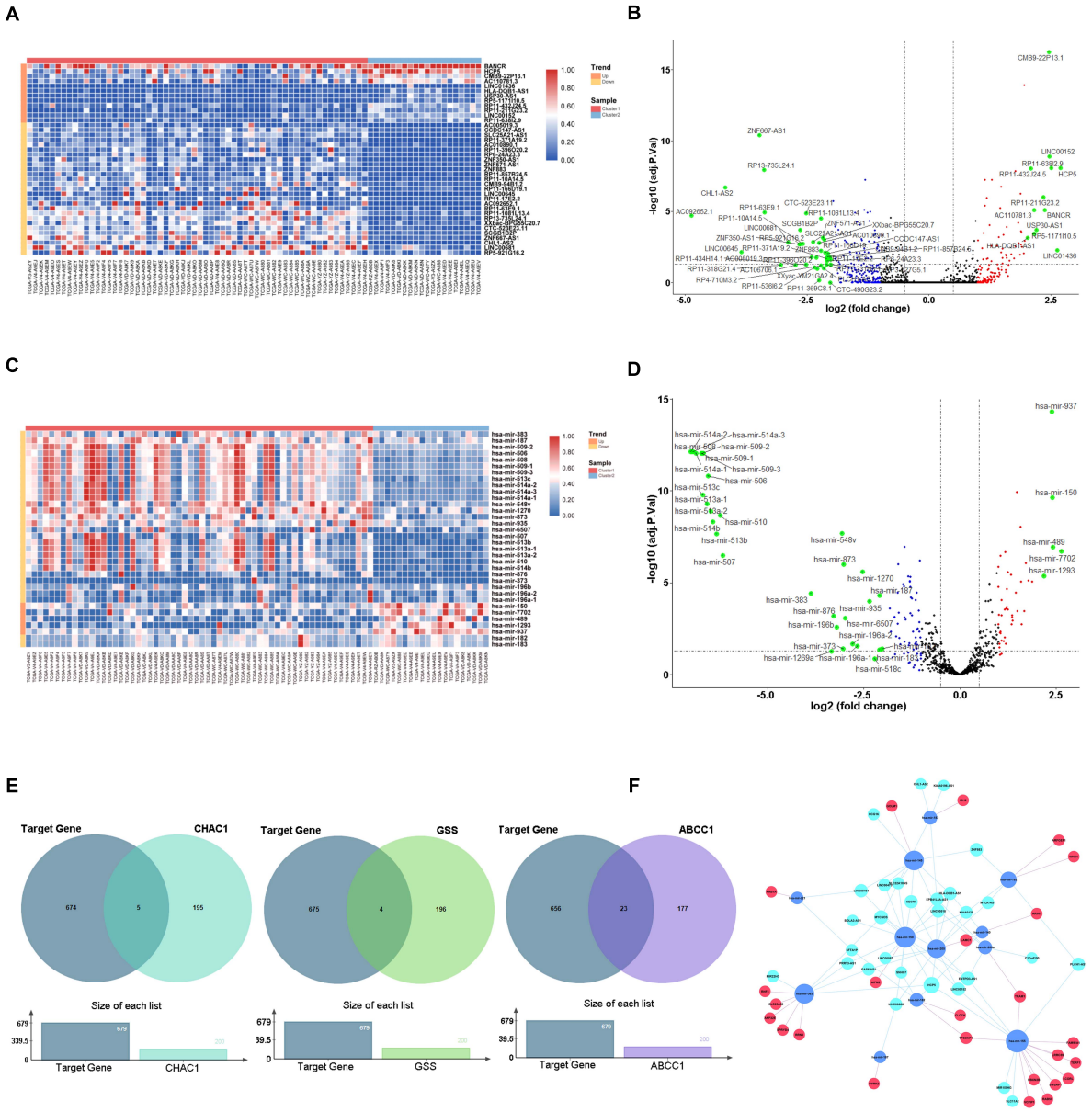

FIGURE 7 | Construction of ceRNA network key genes. **(A)** Heatmap of differential expression lncRNAs. **(B)** Volcano plot of differential expression lncRNAs. **(C)** Heatmap of differential expression miRNAs. **(D)** Volcano plot of differential expression miRNAs. **(E)** Venn plot of target mRNAs and highly associated ferroptosis-related regulators. **(F)** ceRNA building of the 29 lncRNAs (light blue) and 12 miRNAs (dark blue) and 25 mRNAs (red).

immunotherapies and targeted therapy, have significantly improved patient survival. Furthermore, previous studies have shown that several tumor-infiltrating immune cells, T cells, and dendritic cells are abundant in UVM (de Waard-Siebinga et al., 1996; Polak et al., 2007), indicating that UVM may be a possible target for immunotherapy. However, immune checkpoint inhibitors (ICIs) are remarkably limited by the fact that only a subset of patients with most types of cancer respond to these agents and the unknown mechanisms of innate ICI resistance. In our study, we found that the current TNM classification system is not applicable for predicting prognosis. We performed a retrospective analysis to select biomarkers correlated with the tumor immune microenvironment to predict prognosis and locate that part of the population to benefit most from ICIs.

Ferroptosis is a novel type of cell death that was first proposed by Dixon in 2012 (Dixon, 2017). Many studies have reported that induction of ferroptosis effectively represses tumor development, even in specific drug-resistant tumors (Friedmann et al., 2019; Xu et al., 2019). Notably, the synergistic effect of ferroptosis inducers and PD1/PDL-1 inhibitors resulted in more obvious tumor inhibition. Direct evidence was reported by Wang et al. (2019)

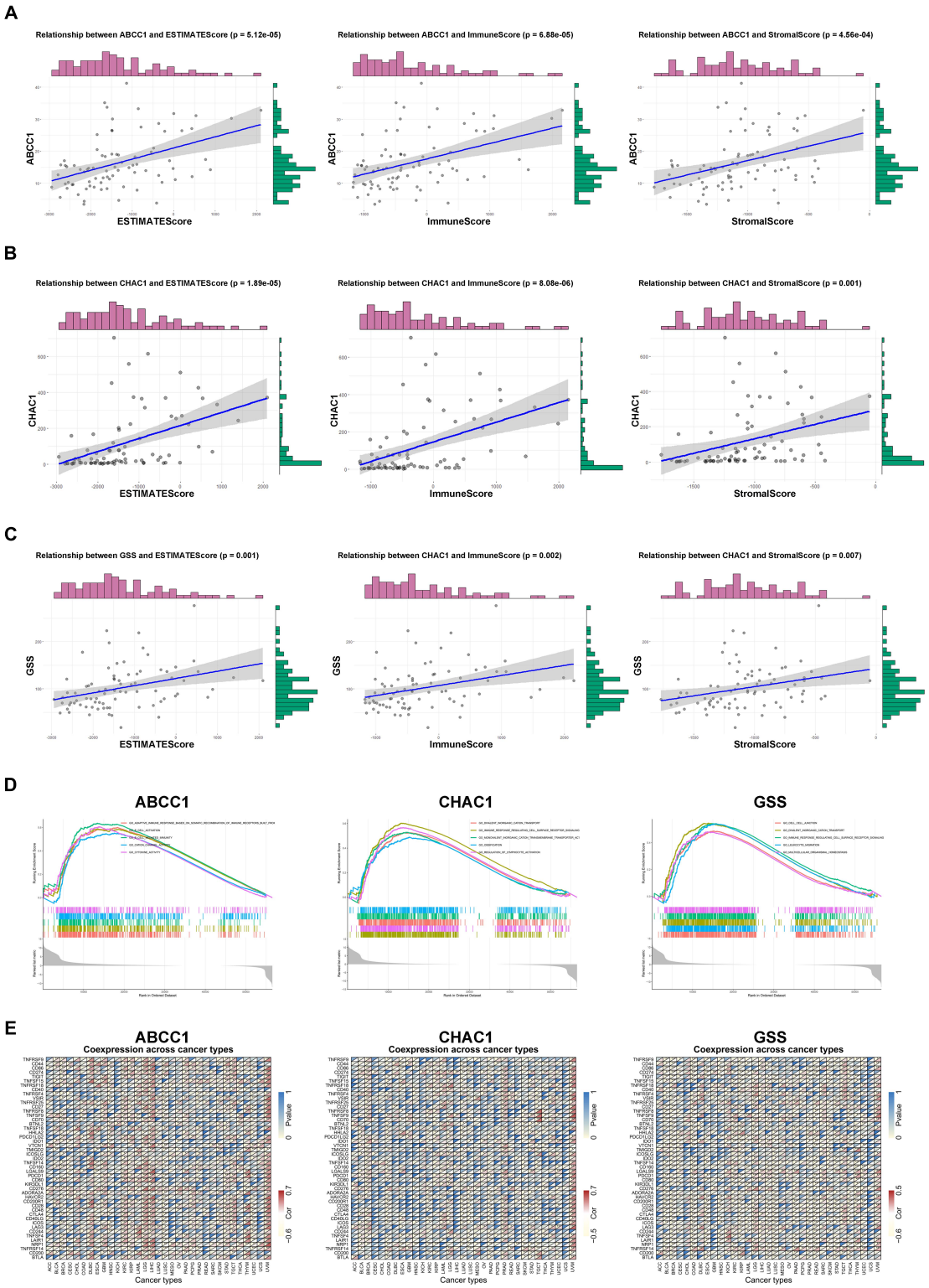

FIGURE 8 | Evaluation of key genes in immune landscape. **(A)** Relationship between ABCC1 expression and ESTIMATEScore, ImmuneScore, as well as StromalScore. **(B)** Relationship between CHAC1 expression and ESTIMATEScore, ImmuneScore, as well as StromalScore. **(C)** Relationship between GSS expression and ESTIMATEScore, ImmuneScore, as well as StromalScore. **(D)** GSEA analysis of ABCC1, CHAC1, and GSS in UVM. **(E)** Correlation among ABCC1, CHAC1, and GSS expression and immune-related mRNAs.

that CD8+ T cells have the ability to induce ferroptosis *in vivo* and downregulate the expression of ferroptosis-related genes (SLC7A11). Furthermore, Lang et al. (2019) reported that IFN-γ derived from immunotherapy-activated CD8+ T cells combined with radiotherapy-activated ataxia-telangiectasia mutated (ATM) can strengthen ferroptosis in fibrosarcoma and melanoma cells, which underpins the crosstalk between ferroptosis and anticancer immunity. In contrast, ferroptosis-resistant or ferroptosis-inhibitor-treated tumor cells are insensitive to PDL1 inhibitor treatment (Wang et al., 2019). Thus, based on accumulating evidence, we systematically investigated the expression of 60 ferroptosis-related genes in UVM tumor tissues and their association with OS. Subsequently, we identified 11 regulators by utilizing the Cox analysis in the training set and divided these genes into two modules by MCL clustering in the STRING database. To further verify the biologically plausible hypothesis, UVM cells can communicate with immune cells through a set of ferroptosis-related signals; when clustering by using a consensus clustering analysis according to the expression of genes, the GO, KEGG, and GSEA analyses were implemented to evaluate the function of clusters in two modules; the results revealed that the function of module A was enriched in the primary immunodeficiency, Th1, Th2, and Th17 cell differentiation, which is remarkably related to the immune landscape. Therefore, we confirmed that module A is a key ferroptosis modification in the tumor immune microenvironment. Some researchers have identified the phenomenon through which T cells trigger tumor killing by activating ferroptosis pathways. Nevertheless, the mechanism underlying UVM remains unclear. In the current study, we found that the ESTIMATE score, especially the immune score, was significantly associated with the expression of clusters. Similarly, we validated that the crosstalk of CD8+ T cells and ferroptosis pathways and diverse types of T cells and other TMEs, including B cells, NK cells, macrophages, and dendritic cells, were observed to increase or decrease to have a combined effect on the clinical survival. These results suggest that this module consists of six ferroptosis-related modulators, especially ABCC1, CHAC1, and GSS, which may change the status of TME and exert selective induction of cancer cell death. By focusing on the specific role of the three key ferroptotic genes in TME, results have shown that the level of CD4 memory activated T cells, CD8 T cells, and gamma delta T cells was positively associated with key ferroptotic regulators, which tend to have poor survival. In contrast, naive B cells, resting memory of CD4 T cells, and monocytes were negatively related to these regulators with better survival, suggesting that the sensitivity to ferroptosis is parallel to anticancer immunity.

In our study, we comprehensively explored the predictive value of ferroptosis regulators and constructed two predictive signatures based on the TCGA database. After verifying the validation set, the prognostic model from module A was successfully built; unfortunately, module B failed to be constructed. Compared with the previous clinical characteristics (age, gender, T stage), our prognostic risk signature can achieve an AUC of more than 0.8. Although most GEO databases have limited amounts of samples, this model was re-confirmed, and the overlapping regulators, including ABCC1, CHAC1, and GSS, acted as crucial biomarkers associated with poor OS, PFS, DSS, and PFS.

ABCC1 multidrug resistance protein (1/MRP1) is a member of the C subfamily of ABC transporters that is capable of contributing to chemotherapeutic failure in various cancers by regulating the efflux of chemotherapeutic drugs (Sharom, 2008; Robey et al., 2018). Previous reports have shown that ABCC1 is a negative biomarker associated with a decreased survival rate and an increased risk of relapse in colorectal cancer (Zhao et al., 2020), lung cancer (Fan et al., 2020), and breast cancer (Low et al., 2020). However, the relationship with UVM has not been investigated in detail. Our data showed that the expression of ABCC1 was upregulated in UVM with poor survival, and had a similar trend to the immune score, ESTIMATE score, stromal score, and diverse types of T cells, especially the levels of PD1 and PD-L1, implying that ABCC1 may play a non-negligible role in shaping the TME landscape to affect the therapeutic efficacy of immune checkpoint blockade. CHAC1 is a new pro-apoptotic member of the unfolded protein response pathway and is intimately related to failed chemotherapy (Shuda et al., 2003; Scriven et al., 2009; Goebel et al., 2012). Previously, only Yanchen Liu indicated that the mRNA expression of CHAC1 was associated with poor OS and high risk of metastasis in a limited number of samples from 34 patients (Liu et al., 2019). In the present study, we re-validated the conclusion above in four datasets and further discovered a relationship between CHAC1 and the immune signature of UVM, illustrating the innate mechanisms by which CHAC1 exerts a harmful influence on clinical outcomes. Glutathione synthetase (GSS), which plays a key role in metabolism, catalyzes the last step of glutathione (GSH) synthesis, which is an important antioxidant that protects cancer cells against potential ferroptosis (Proneth and Conrad, 2019; Chen et al., 2020). In liver cancer, researchers found that RRM2 was capable of sustaining intracellular GSH by protecting GSS from degradation (Yang et al., 2020). To the best of our knowledge, this is the first study to explore the correlation between the expression of GSS and the carcinogenic environment of UVM. Interestingly, our findings suggest that the expression of GSS, combined with CHAC1 and ABCC1, mediates the TME infiltration patterns to accelerate UVM progression partly by regulating T cells and other types of immune cells. Tumor burden is considered a promising indicator to promote tumorigenesis in malignant cells and exhibits predictive utility in identifying responders to ICIs. According to the SNP2APA database, we identified positive polymorphisms from four mRNAs and found that all mRNAs were highly correlated with the levels of ABCC1, CHAC1, and GSS, indicating that high expression of key ferroptosis regulators was related to the sharp accumulation of gene mutations, thus becoming a promising therapeutic target and prediction for UVM.

Furthermore, to determine how ferroptosis-related genes act in a lncRNA–miRNA dependent manner in the process of UVM progression, we built a ceRNA network consisting of 25 ferroptosis-related mRNAs, 12 miRNAs, and 29 lncRNAs. In this network, many intersections have been verified in experiments; for example, miR-155 was upregulated, blocking the translation of TP53INP1 to induce cell migration during pancreatic cancer

evolution (Seux et al., 2011). Hence, we plan to take the next step to explore the interaction of these molecules *in vitro*.

CONCLUSION

This study is the first to comprehensively explore the role of ferroptosis-related genes in UVM and extensively profile the immune landscape based on ferroptosis pathways. Ferroptosis modification clusters, which have different clinical survival, have become an important mediator in the heterogeneity and complexity of the TME. After analyzing the correlation among clusters, we developed and validated a six-gene signature prognostic model to precisely predict the clinical outcome of UVM. Finally, we further evaluated the function of three key prognostic ferroptosis-related regulators, including ABCC1, CHAC1, and GSS, and constructed a ceRNA network to elucidate the molecular mechanisms based on these key regulators. Our findings suggest that ferroptosis-related genes may act as promising indicators for determining effective therapeutic strategies and providing novel insights into immunotherapy.

DATA AVAILABILITY STATEMENT

The datasets presented in this study can be found in online repositories. The names of the repository/repositories and accession number(s) can be found in the article/ **Supplementary Material**.

AUTHOR CONTRIBUTIONS

KC designed the study. YJ and WZW analyzed, interpreted the data, and wrote original draft. WZW, DH, and YZ wrote this manuscript. LG, MX, and XC edited and revised the manuscript. All authors have seen and approved the final version of the manuscript.

FUNDING

This work was supported by the National Natural Science Foundation of China (81874137), the Outstanding Youth Foundation of Hunan Province (2018JJ1047), the Hunan Province Science and Technology Talent Promotion Project (2019TJ-Q10), Hunan Cancer Hospital Climb Plan (No. QH201905), the Special Foundation for Cancer Research from the National Cancer Center (NCC2017L01 and NCC2017A17), China, and the Independent Exploration and Innovation Project of Central South University (2021zzts0401).

SUPPLEMENTARY MATERIAL

The Supplementary Material for this article can be found online at: https://www.frontiersin.org/articles/10.3389/fcell.2021.685120/full#supplementary-material

Supplementary Figure 1 | Clustering of ferroptosis-related genes in module B. **(A)** Pearson correlation analysis among ferroptosis-related regulators in module B. **(B)** Consensus clustering cumulative distribution function (CDF) and relative change in area under CDF curve for $k = 2$ in module B. **(C)** Kaplan–Meier curves of two clusters in UVM about OS in module B. **(D)** Different expression of the ferroptosis-related mediators in two clusters based on module B (***$p < 0.001$; **$p < 0.01$; *$p < 0.05$).

Supplementary Figure 2 | Tumor immune microenvironment in module B. **(A)** Different expression of ESTIMATE score in two clusters. **(B)** Different distribution of 22 TME infiltrating cells in two patterns (***$p < 0.001$; **$p < 0.01$; *$p < 0.05$).

Supplementary Figure 3 | Prognostic analysis of risk model and ferroptosis-related genes in module B. **(A)** Kaplan–Meier curves of patients in high/low risk about OS in module B. **(B)** Distributions of risk scores, alive/dead status, and expression of ferroptosis-related genes in module B. **(C)** ROC curve of risk score and clinical characteristics in module B. **(D)** Kaplan–Meier curves of patients in high/low risk about OS based on GSE84976.

Supplementary Figure 4 | Prognostic value of ferroptosis-related genes. **(A)** Kaplan–Meier DSS curves of patients in key ferroptosis-related genes. **(B)** Kaplan–Meier PFI curves of patients in key ferroptosis-related genes.

Supplementary Figure 5 | Evaluation of key ferroptosis-related genes in immune cell infiltration. **(A)** Relationship between ABCC1, CHAC1, and GSS expression and infiltrating immune cells. **(B)** Relationship between key genes expression and level of CD274 and CD279.

Supplementary Figure 6 | Correlation of key ferroptosis-related genes and mRNAs with positive polymorphisms. **(A)** Correlation of ABCC1 and mRNAs with positive polymorphisms. **(B)** Correlation of CHAC1 and mRNAs with positive polymorphisms. **(C)** Correlation of GSS and mRNAs with positive polymorphisms.

Supplementary Table 1 | Sixty ferroptosis-related genes list.

Supplementary Table 2 | Cox analysis of ferroptosis-related genes in TCGA and GSE84976.

Supplementary Table 3 | Differential expression lncRNAs based on TCGA.

Supplementary Table 4 | Differential expression miRNAs based on TCGA.

Supplementary Table 5 | Targeted mRNAs base on miRTarBase, miRDB, and TargetScan databases.

REFERENCES

Achberger, S., Aldrich, W., Tubbs, R., Crabb, J. W., Singh, A. D., and Triozzi, P. L. (2014). Circulating immune cell and microRNA in patients with uveal melanoma developing metastatic disease. *Mol. Immunol.* 58, 182–186. doi: 10.1016/j.molimm.2013.11.018

Agarwal, V., Bell, G., Nam, J., and Bartel, D. (2015). Predicting effective microRNA target sites in mammalian mRNAs. *Elife* 12:e05005.

Bersuker, K., Hendricks, J., Li, Z., Magtanong, L., Ford, B., Tang, P., et al. (2019). The CoQ oxidoreductase FSP1 acts parallel to GPX4 to inhibit ferroptosis. *Nature* 575, 688–692. doi: 10.1038/s41586-019-1705-2

Cao, J., and Dixon, S. (2016). Mechanisms of ferroptosis. *Cell. Mol. Life. Sci.* 73, 2195–2209. doi: 10.1007/s00018-016-2194-1

Chang, A. E., Karnell, L. H., and Menck, H. R. (1998). The national cancer data base report on cutaneous and noncutaneous melanoma: a summary of 84,836 cases from the past decade. the american college of surgeons commission on cancer and the american cancer society. *Cancer* 83, 1664–1678. doi: 10.1002/(sici)1097-0142(19981015)83:8<1664::aid-cncr23>3.0.co;2-g

Chen, X., Li, J., Kang, R., Klionsky, D., and Tang, D. (2020). Ferroptosis: machinery and regulation. *Autophagy* 26, 1–28. doi: 10.1080/15548627.2020.1810918

Chen, X., Wu, Q., Depeille, P., Chen, P., Thornton, S., Kalirai, H., et al. (2017). RasGRP3 mediates MAPK pathway activation in GNAQ mutant uveal melanoma. *Cancer. Cell.* 31, 685–696e. doi: 10.1016/j.ccell.2017.04.002

Chen, Y., and Wang, X. (2020). miRDB: an online database for prediction of functional microRNA targets. *Nucleic. Acids. Res.* 48, D127–D131.

Chou, C., Shrestha, S., Yang, C., Chang, N., Lin, Y., Liao, K., et al. (2018). miRTarBase update 2018: a resource for experimentally validated microRNA-target interactions. *Nucleic. Acids. Res.* 46, D296–D302. doi: 10.1093/nar/gkx1067

de Vries, T. J., Trancikova, D., Ruiter, D. J., and van Muijen, G. N. (1998). High expression of immunotherapy candidate proteins gp100, MART-1, tyrosinase and TRP-1 in uveal melanoma. *Br. J. Cancer.* 78, 1156–1161. doi: 10.1038/bjc.1998.646

de Waard-Siebinga, I., Hilders, C., Hansen, B., van Delft, J., and Jager, M. (1996). HLA expression and tumor-infiltrating immune cells in uveal melanoma. *Graefes. Arch. Clin. Exp. Ophthalmol.* 234, 34–42. doi: 10.1007/BF00186516

Dixon, S. (2017). Ferroptosis: bug or feature? *Immunol. Rev.* 277, 150–151. doi: 10.1111/imr.12533

Doll, S., Freitas, F., Shah, R., Aldrovandi, M., da Silva, M., Ingold, I., et al. (2019). FSP1 is a glutathione-independent ferroptosis suppressor. *Nature* 575, 693–696. doi: 10.1038/s41586-019-1707-0

Fan, C., Tsai, S., Lin, C., Chang, L., Yang, J., Chen, G., et al. (2020). EFHD2 contributes to non-small cell lung cancer cisplatin resistance by the activation of NOX4-ROS-ABCC1 axis. *Redox. Biol.* 34:1015.

Friedmann, J., Krysko, D., and Conrad, M. (2019). Ferroptosis at the crossroads of cancer- acquired drug resistance and immune evasion. *Nat. Rev. Cancer.* 19, 405–414. doi: 10.1038/s41568-019-0149-1

Garcia-Diaz, A., Shin, D., Moreno, B., Saco, J., Escuin-Ordinas, H., Rodriguez, G., et al. (2017). Interferon receptor signaling pathways regulating PD-L1 and PD-L2 expression. *Cell. Rep.* 19, 1189–1201. doi: 10.1016/j.celrep.2017.04.031

Goebel, G., Berger, R., Strasak, A., Egle, D., Müller-Holzner, E., Schmidt, S., et al. (2012). Elevated mRNA expression of CHAC1 splicing variants is associated with poor outcome for breast and ovarian cancer patients. *Br. J. Cancer.* 106, 189–198. doi: 10.1038/bjc.2011.510

Hassannia, B., Vandenabeele, P., and Vanden Berghe, T. (2019). Targeting ferroptosis to iron out cancer. *Cancer. Cell.* 35, 830–838. doi: 10.1016/j.ccell.2004.002

Henderson, E., and Margo, C. E. (2008). Iris melanoma. *Arch. Pathol. Lab. Med.* 132, 268–272.

Hoefsmit, E. P., Rozeman, E. A., Van, T. M., Dimitriadis, P., Krijgsman, O., Conway, J. W., et al. (2020). Comprehensive analysis of cutaneous and uveal melanoma liver metastases. *J. Immunother. Cancer.* 8:e0015. doi: 10.1136/jitc-2020-001501

Im, S., Hashimoto, M., Gerner, M., Lee, J., Kissick, H., Burger, M., et al. (2016). Defining CD8+ T cells that provide the proliferative burst after PD-1 therapy. *Nature* 537, 417–421. doi: 10.1038/nature19330

Jeggari, A., Marks, D., and Larsson, E. (2012). miRcode: a map of putative microRNA target sites in the long non-coding transcriptome. *Bioinformatics* 28, 2062–2063. doi: 10.1093/bioinformatics/bts344

Labi, V., and Erlacher, M. (2015). How cell death shapes cancer. *Cell. Death. Dis.* 6, e16. doi: 10.1038/cddis.2015.20

Lang, X., Green, M., Wang, W., Yu, J., Choi, J., Jiang, L., et al. (2019). Radiotherapy and immunotherapy promote tumoral lipid oxidation and ferroptosis via synergistic repression of SLC7A11. *Cancer. Discov.* 9, 1673–1685. doi: 10.1158/2159-8290.cd-19-0338

Latunde-Dada, G. (2017). Ferroptosis: role of lipid peroxidation, iron and ferritinophagy. *Biochim. Biophys. Acta. Gen. Subj.* 1861, 1893–1900. doi: 10.1016/j.bbagen.2017.05.019

Lee, S., Ju, K., Jeon, H., Jeong, E., Lee, Y., Kim, C., et al. (2018). Regulation of tumor progression by programmed necrosis. *Oxid. Med. Cell. Longev.* 2018:35374. doi: 10.1155/2018/3537471

Li, J., Liu, S., Zhou, H., Qu, L., and Yang, J. (2014). starBase v2.0: decoding miRNA-ceRNA, miRNA-ncRNA and protein-RNA interaction networks from large-scale CLIP-Seq data. *Nucleic. Acids. Res.* 42, D92–D97.

Liu, Y., Li, M., Shi, D., and Zhu, Y. (2019). Higher expression of cation transport regulator-like protein 1 (CHAC1) predicts of poor outcomes in uveal melanoma (UM) patients. *Int. Ophthalmol.* 39, 2825–2828. doi: 10.1007/s10792-019-01129-1

Low, F., Shabir, K., Brown, J., Bill, R., and Rothnie, A. (2020). Roles of ABCC1 and ABCC4 in proliferation and migration of breast cancer cell lines. *Int. J. Mol. Sci.* 21:76. doi: 10.3390/ijms21207664

Luke, J., Flaherty, K., Ribas, A., and Long, G. (2017). Targeted agents and immunotherapies: optimizing outcomes in melanoma. *Nat. Rev. Clin. Oncol.* 14, 463–464. doi: 10.1038/nrclinonc.2017.43

Marseglia, M., Amaro, A., Solari, N., Gangemi, R., Croce, E., Tanda, E. T., et al. (2021). How to make immunotherapy an effective therapeutic choice for uveal melanoma. *Cancers (Basel)* 13:20. doi: 10.3390/cancers13092043

McLaughlin, C. C., Wu, X. C., Jemal, A., Martin, H. J., Roche, L. M., and Chen, V. W. (2005). Incidence of noncutaneous melanomas in the U.S. *Cancer* 103, 1000–1007. doi: 10.1002/cncr.20866

Mou, Y., Wang, J., Wu, J., He, D., Zhang, C., and Duan, C. (2019). Ferroptosis, a new form of cell death: opportunities and challenges in cancer. *J. Hematol. Oncol.* 12:34. doi: 10.1186/s13045-019-0720-y

Newman, A., Liu, C., Green, M., Gentles, A., Feng, W., Xu, Y., et al. (2015). Robust enumeration of cell subsets from tissue expression profiles. *Nat. Methods.* 12, 453–454. doi: 10.1038/nmeth.3337

Pelster, M. S., Gruschkus, S. K., Bassett, R., Gombos, D. S., Shephard, M., Posada, L., et al. (2021). Nivolumab and ipilimumab in metastatic uveal melanoma: results from a single-arm phase II study. *J. Clin. Oncol.* 39, 599–607. doi: 10.1200/JCO.00605

Piulats, J. M., Espinosa, E., de la Cruz Merino, L., Varela, M., Alonso Carrión, L., Martín-Algarra, S., et al. (2021). Nivolumab plus ipilimumab for treatment-naïve metastatic uveal melanoma: an open-label, multicenter, phase II trial by the spanish multidisciplinary melanoma group (GEM-1402). *J. Clin. Oncol.* 39, 586–598. doi: 10.1200/JCO.20.00550

Polak, M., Borthwick, N., Johnson, P., Hungerford, J., Higgins, B., Di Palma, S., et al. (2007). Presence and phenotype of dendritic cells in uveal melanoma. *Br. J. Ophthalmol.* 91, 971–979. doi: 10.1136/bjo.2006.110908

Proneth, B., and Conrad, M. (2019). Ferroptosis and necroinflammation, a yet poorly explored link. *Cell. Death. Differ.* 26, 14–24. doi: 10.1038/s41418-018-0173-9

Rahmi, A., Mammar, H., Thariat, J., Angellier, G., Herault, J., Chauvel, P., et al. (2014). Proton beam therapy for presumed and confirmed iris melanomas: a review of 36 cases. *Graefes. Arch. Clin. Exp. Ophthalmol.* 252, 1515–1521. doi: 10.1007/s00417-014-2735-y

Robey, R., Pluchino, K., Hall, M., Fojo, A., Bates, S., and Gottesman, M. (2018). Revisiting the role of ABC transporters in multidrug-resistant cancer. *Nat. Rev. Cancer.* 8, 452–454. doi: 10.1038/s41568-018-0005-8

Schank, T., and Hassel, J. (2019). Immunotherapies for the treatment of uveal melanoma-history and future. *Cancers (Basel)* 11: 10.

Scriven, P., Coulson, S., Haines, R., Balasubramanian, S., Cross, S., and Wyld, L. (2009). Activation and clinical significance of the unfolded protein response in breast cancer. *Br. J. Cancer.* 101, 1692–1698. doi: 10.1038/sj.bjc.6605365

Seux, M., Peuget, S., Montero, M., Siret, C., Rigot, V., Clerc, P., et al. (2011). TP53INP1 decreases pancreatic cancer cell migration by regulating SPARC expression. *Oncogene* 30, 3049–3061. doi: 10.1038/onc.2011.25

Shannon, P., Markiel, A., Ozier, O., Baliga, N., Wang, J., Ramage, D., et al. (2003). Cytoscape: a software environment for integrated models of biomolecular interaction networks. *Genome. Res.* 13, 2498–2504. doi: 10.1101/gr.1239303

Sharom, F. (2008). ABC multidrug transporters: structure, function and role in chemoresistance. *Pharmacogenomics* 9, 105–127. doi: 10.2217/14622416.9.1.105

Sharpe, A., and Pauken, K. (2018). The diverse functions of the PD1 inhibitory pathway. *Nat. Rev. Immunol.* 18, 153–167. doi: 10.1038/nri.2017.108

Shields, C. L., Shah, S. U., Bianciotto, C. G., Emrich, J., Komarnicky, L., and Shields, J. A. (2013). Iris melanoma management with iodine-125 plaque radiotherapy in 144 patients: impact of melanoma-related glaucoma on outcomes. *Ophthalmology* 120, 55–61. doi: 10.1016/j.ophtha.2012.06.053

Shuda, M., Kondoh, N., Imazeki, N., Tanaka, K., Okada, T., Mori, K., et al. (2003). Activation of the ATF6, XBP1 and grp78 genes in human hepatocellular carcinoma: a possible involvement of the ER stress pathway in hepatocarcinogenesis. *J. Hepatol.* 38, 605–614. doi: 10.1016/s0168-8278(03)00029-1

Singh, A. D., Turell, M. E., and Topham, A. K. (2011). Uveal melanoma: trends in incidence, treatment, and survival. *Ophthalmology* 118, 1881–1885. doi: 10.1016/j.ophtha.2011.01.040

Stockwell, B., Friedmann, J., Bayir, H., Bush, A., Conrad, M., Dixon, S. J., et al. (2017). Ferroptosis: a regulated cell death nexus linking metabolism, redox biology, and disease. *Cell* 171, 273–285. doi: 10.1016/j.cell.2017.09.021

Topalian, S., Hodi, F., Brahmer, J., Gettinger, S., Smith, D., McDermott, D., et al. (2012). Safety, activity, and immune correlates of anti-PD-1 antibody in cancer. *N. Engl. J. Med.* 366, 2443–2454. doi: 10.1056/NEJMoa1200690

Virgili, G., Gatta, G., Ciccolallo, L., Capocaccia, R., Biggeri, A., Crocetti, E., et al. (2007). Incidence of uveal melanoma in Europe. *Ophthalmology* 114, 2309–2315. doi: 10.1016/j.ophtha.2007.01.032

Wang, Q., Hu, B., Hu, X., Kim, H., Squatrito, M., Scarpace, L., et al. (2017). Tumor evolution of glioma-intrinsic gene expression subtypes associates with immunological changes in the microenvironment. *Cancer. Cell.* 32, 42–56.e6.

Wang, W., Green, M., Choi, J., Gijón, M., Kennedy, P., Johnson, J., et al. (2019). CD8+ T cells regulate tumour ferroptosis during cancer immunotherapy. *Nature* 569, 270–272. doi: 10.1038/s41586-019-1170-y

Wilkerson, M. D., and Hayes, D. N. (2010). Consensus cluster plus: a class discovery tool with confidence assessments and item tracking. *Bioinformatics* 26, 1572–1573. doi: 10.1093/bioinformatics/btq170

Xie, Y., Hou, W., Song, X., Yu, Y., Huang, J., Sun, X., et al. (2016). Ferroptosis: process and function. *Cell. Death. Differ.* 23, 369–379. doi: 10.1038/cdd.2015.158

Xu, T., Ding, W., Ji, X., Ao, X., Liu, Y., Yu, W., et al. (2019). Molecular mechanisms of ferroptosis and its role in cancer therapy. *J. Cell. Mol. Med.* 23, 4900–4949. doi: 10.1111/jcmm.14511

Yagoda, N., von Rechenberg, M., Zaganjor, E., Bauer, A., Yang, W., Fridman, D., et al. (2007). RAS-RAF-MEK-dependent oxidative cell death involving voltage- dependent anion channels. *Nature* 447, 864–868. doi: 10.1038/nature05859

Yang, Y., Lin, J., Guo, S., Xue, X., Wang, Y., Qiu, S., et al. (2020). RRM2 protects against ferroptosis and is a tumor biomarker for liver cancer. *Cancer. Cell. Int.* 20:587. doi: 10.1186/s12935-020-0 1689-1688

Yu, H., Guo, P., Xie, X., Wang, Y., and Chen, G. (2017). Ferroptosis, a new form of cell death, and its relationships with tumourous diseases. *J. Cell. Mol. Med.* 21, 648–657. doi: 10.1111/jcmm.13008

Zhang, W., Zeng, Y., Wang, L., Liu, Y., and Cheng, Y. (2020). An effective graph clustering method to identify cancer driver modules. *Front. Bioeng. Biotechnol.* 8:2. doi: 10.3389/fbioe.2020.00271

Zhang, Y., Ma, C., Lawrence, M., Break, T., O'Connell, M., Lyons, J., et al. (2017). PD-L1 up-regulation restrains Th17 cell differentiation in STAT3 loss- and STAT1 gain-of-function patients. *J. Exp. Med.* 214, 2523–2525. doi: 10.1084/jem.20161427

Zhao, H., Chen, S., and Fu, Q. (2020). Exosomes from CD133+ cells carrying circ-ABCC1 mediate cell stemness and metastasis in colorectal cancer. *J. Cell. Biochem.* 121, 3286–3297. doi: 10.1002/jcb.29600

Conflict of Interest: The authors declare that the research was conducted in the absence of any commercial or financial relationships that could be construed as a potential conflict of interest.

Publisher's Note: All claims expressed in this article are solely those of the authors and do not necessarily represent those of their affiliated organizations, or those of the publisher, the editors and the reviewers. Any product that may be evaluated in this article, or claim that may be made by its manufacturer, is not guaranteed or endorsed by the publisher.

frontiers in Genetics

REVIEW
published: 20 August 2021
doi: 10.3389/fgene.2021.693259

The Emerging Role of Non-coding RNAs in Drug Resistance of Ovarian Cancer

Hua Lan, Jing Yuan, Da Zeng, Chu Liu, Xiaohui Guo, Jiahui Yong, Xiangyang Zeng and Songshu Xiao**

Department of Obstetrics and Gynecology, Third Xiangya Hospital of Central South University, Changsha, China

Ovarian cancer is one of the most common gynecological malignancies with highest mortality rate among all gynecological malignant tumors. Advanced ovarian cancer patients can obtain a survival benefit from chemotherapy, including platinum drugs and paclitaxel. In more recent years, the administration of poly-ADP ribose polymerase inhibitor to patients with BRCA mutations has significantly improved the progression-free survival of ovarian cancer patients. Nevertheless, primary drug resistance or the acquisition of drug resistance eventually leads to treatment failure and poor outcomes for ovarian cancer patients. The mechanism underlying drug resistance in ovarian cancer is complex and has not been fully elucidated. Interestingly, different non-coding RNAs (ncRNAs), such as circular RNAs, long non-coding RNAs and microRNAs, play a critical role in the development of ovarian cancer. Accumulating evidence has indicated that ncRNAs have important regulatory roles in ovarian cancer resistance to chemotherapy reagents and targeted therapy drugs. In this review, we systematically highlight the emerging roles and the regulatory mechanisms by which ncRNAs affect ovarian cancer chemoresistance. Additionally, we suggest that ncRNAs can be considered as potential diagnostic and prognostic biomarkers as well as novel therapeutic targets for ovarian cancer.

Keywords: ovarian cancer, drug resistance, microRNA, long non-coding RNA, circular RNA

OPEN ACCESS

Edited by:
Rais Ahmad Ansari,
Nova Southeastern University,
United States

Reviewed by:
Nabab Khan,
University of North Dakota,
United States
Yilin Zhang,
University of Chicago, United States

****Correspondence:***
Songshu Xiao
xiaosongshu@csu.edu.cn
Xiangyang Zeng
441783907@qq.com

Specialty section:
This article was submitted to Cancer Genetics and Oncogenomics, a section of the journal Frontiers in Genetics

Received: *10 April 2021*
Accepted: *28 June 2021*
Published: *20 August 2021*

Citation:
Lan H, Yuan J, Zeng D, Liu C, Guo X, Yong J, Zeng X and Xiao S (2021) The Emerging Role of Non-coding RNAs in Drug Resistance of Ovarian Cancer. Front. Genet. 12:693259. doi: 10.3389/fgene.2021.693259

Abbreviations: PTX, paclitaxel; ADR, adriamycin; PARPi, poly-ADP ribose polymerase inhibitor; PFS, progression-free survival; ncRNAs, non-coding RNAs; miRNAs, microRNAs; lncRNAs, long non-coding RNAs; circRNAs, circular RNAs; MDR, multidrug resistance; EMT, epithelial-mesenchymal transition; piRNAs, PIWI-interacting RNAs; snoRNAs, small nucleolar RNAs; snRNAs, small nuclear RNAs; 3′-UTR, 3′-untranslated region; mRNAs, messenger RNAs; DDP, cisplatin; PRKC, protein kinase C; PTEN, phosphatase and tensin homolog; PPP1R12A, protein phosphatase 1 regulatory subunit 12A; MST, STE20-like kinase; SAV1, protein salvador homolog 1; SFRP1, secreted frizzled-related protein 1; KCNMA1, potassium calcium-activated channel subfamily M alpha 1; FOXO3, forkhead box O3; TRIM31, tripartite motif containing 31; EZH2, zeste homolog 2; PTPN3, protein tyrosine phosphatase non-receptor type 3; ITGB8, integrin subunit beta 8; DDR1, discoidin domain receptor 1; NOTCH1, notch receptor 1; HMGA1, high mobility group AT-hook 1; RAD51, RAD51 recombinase; DNMT, DNA methyltransferase; AXL, AXL Receptor Tyrosine Kinase; APAF1, apoptotic peptidase activating factor 1; CIC, capicua transcriptional repressor; ING5, inhibitor of growth family member 5; XIAP, X-linked inhibitor of apoptosis; STAT3, signal transducer and activator of transcription; TRIM27, tripartite motif containing 27; SIK2, salt inducible kinase 2; DSB, double-strand breaks; RNASEH2A, ribonuclease H2 subunit A; FEN1, flap structure-specific endonuclease 1; SSRP1, structure specific recognition protein 1; SSA, single-strand annealing; HGSOCs, high-grade serous ovarian carcinomas; NHEJ, non-homologous end joining; NRP1, Neuropilin 1; RNAP II, RNA Polymerase II; ceRNA, competitive endogenous RNA; UCA1, urothelial cancer associated 1; ABC, ATP binding cassette; HOTAIR, HOX antisense intergenic RNA; ATG7, autophagy related 7; VPA, valproic acid; CCAT1, colon cancer associated transcript 1; MALAT1, metastasis-associated lung adenocarcinoma transcript 1; ZEB1, zinc finger E-box binding homeobox 1; Gal-1, galectin 1; FOXR2, forkhead box R2; SCAI, suppressor of cancer cell invasion.

BACKGROUND

Ovarian cancer is one of the most deadly gynecologic malignancy, there are approximately 313,959 new cases and more than 207,252 deaths annually worldwide (Sung et al., 2021). Unfortunately, due to lack of effective early screening methods, 5-year survival rate was only 20–40% (Lheureux et al., 2019). Currently, the main methods used for clinical treatment of ovarian cancer are still based on cytoreductive surgery and multidrug combination chemotherapy based on platinum drugs (Armstrong et al., 2021). Chemotherapy is the main treatment option available for advanced or recurrent ovarian cancers, and the commonly used chemotherapeutic agents include platinum drugs and paclitaxel (PTX). In addition, the administration of poly-ADP ribose polymerase inhibitor (PARPi) to BRCA mutation patients has significantly improved the progression-free survival (PFS) of ovarian cancer (Tew et al., 2020). Although chemotherapy in combination with targeted therapy prolongs the overall survival of ovarian cancer patients, acquired multidrug resistance (MDR) hinders its clinical benefits. Therefore, patients with ovarian cancer frequently have a poor prognosis. The complicated mechanisms involved in MDR ovarian cancer include decreased drug uptake into the cell, increased drug efflux, intracellular drug inactivation, DNA damage repair, resistance to drug-induced apoptosis, activation of cancer stem cells, and epithelial-mesenchymal transition (EMT) (Christie et al., 2019; Liang et al., 2019; Belur Nagaraj et al., 2021; Chiappa et al., 2021). While progress has been made in understanding the pathogenesis of ovarian cancer, the detailed mechanisms of MDR remain elusive.

Non-coding RNAs (ncRNAs) are a kind of DNA transcription product that cannot be encoded into proteins. NcRNAs can be classified according to their length and shape into tiny/short ncRNAs, long ncRNAs (lncRNAs) which is larger than 200 nucleotides (nt), and circular RNA (circRNAs). Various small ncRNAs have been identified, such as microRNAs (miRNAs), PIWI-interacting RNAs (piRNAs), small nucleolar RNAs (snoRNAs), and small nuclear RNAs (snRNAs) (Kristensen et al., 2019; Shuai et al., 2019; Jin et al., 2020; Cui et al., 2021; Han et al., 2021; Luo et al., 2021; Tsitsipatis et al., 2021). NcRNAs have been proven to have important regulatory potential, both in transcription and post transcription, instead of just being "transcription noise" or "transcription garbage." There is ample evidence that ncRNAs are of crucial importance in the regulation of gene expression. Meanwhile, ncRNAs participate in many biological functions, such as cell proliferation, cell cycle progression, and apoptosis (Cocquerelle et al., 1993; Memczak et al., 2013; Cech and Steitz, 2014; Li et al., 2021; Ramat and Simonelig, 2021; Statello et al., 2021). In addition, a large number of studies have shown that abnormally expressed ncRNAs participate in tumor cell invasion, metastasis, drug resistance and radiotherapy resistance (Bi et al., 2020; Chen et al., 2020; Wang P. et al., 2020). Similarly, previous research suggested that ncRNAs are dysregulated when drug resistance develops, which indicates that in ovarian cancer, multiple ncRNAs might play a vital role in drug resistance.

In this review, we summarized the detailed mechanisms by which miRNAs, lncRNAs, and circRNAs affect ovarian cancer drug resistance. The potential mechanisms of ncRNAs related to drug-resistance in ovarian cancer are summarized in **Figure 1**. NcRNAs have potential as diagnostic and prognostic biomarkers as well as novel therapeutic targets for ovarian cancer in the future.

MiRNAs AND DRUG RESISTANCE

MicroRNAs are a class of small ncRNAs containing 20–24 nt that can post transcriptionally suppress gene expression by binding to the 3′-untranslated region (3′-UTR) of multiple target messenger RNAs (mRNAs) and/or other RNAs (Wang X. et al., 2021). MiRNAs are key molecules that are involved in many different kinds of fundamental cellular processes, including cell differentiation and proliferation, cell cycle regulation, angiogenesis, metabolic stress, and other functions (He et al., 2019; Komoll et al., 2021; Xing et al., 2021). It has been found that multiple miRNAs are dysregulated in ovarian cancer and are closely related to its occurrence, development, metastasis and drug resistance (Mak et al., 2017; Tung et al., 2020; Zhang Z. et al., 2020). Significant changes in miRNA expression profiles have been observed in drug-resistant cancer cells in comparison with parental drug-sensitive cancer cells. The involvement of miRNAs in ovarian cancer resistance to platinum drugs, PTX, ADR, and PARPi is summarized below.

MiRNAs AND RESISTANCE TO PLATINUM

Platinum drugs are cell cycle non-specific drugs that are widely used in the clinic. They induce DNA damage or ribosome biosynthesis stress and activate tumor cell death by apoptosis or necrosis. However, a series of complex mechanisms lead to platinum resistance (Bruno et al., 2017; Huang et al., 2019). The commonly used platinum drugs include the first generation of drug cisplatin (DDP), the second generation of drug carboplatin, as well as the third-generation drugs oxaliplatin and Lopatin. Many miRNAs are related to the resistance to platinum drugs in ovarian cancer (**Table 1**).

Several oncogenic miRNAs can promote resistance to platinum drugs in ovarian cancer cells. For example, miR-205-5p and miR-216a confer DDP resistance by suppressing the PTEN (phosphatase and tensin homolog)/Akt signaling pathway in ovarian cancer cells (Jin et al., 2018; Shi et al., 2018). Similarly, miR-483-3p and miR-224-5p have also been found to promote DDP resistance by silencing protein kinase C (PRKC) family members (Zhao et al., 2014; Arrighetti et al., 2016). Studies have shown that miR-30b and miR-149-5p are involved in the Hippo signaling pathway and promote DDP resistance by downregulating the target genes protein phosphatase 1 regulatory subunit 12A (PPP1R12A), STE20-like kinase 1 (MST1), and protein salvador homolog 1 (SAV1), respectively (Xu M. et al., 2018;

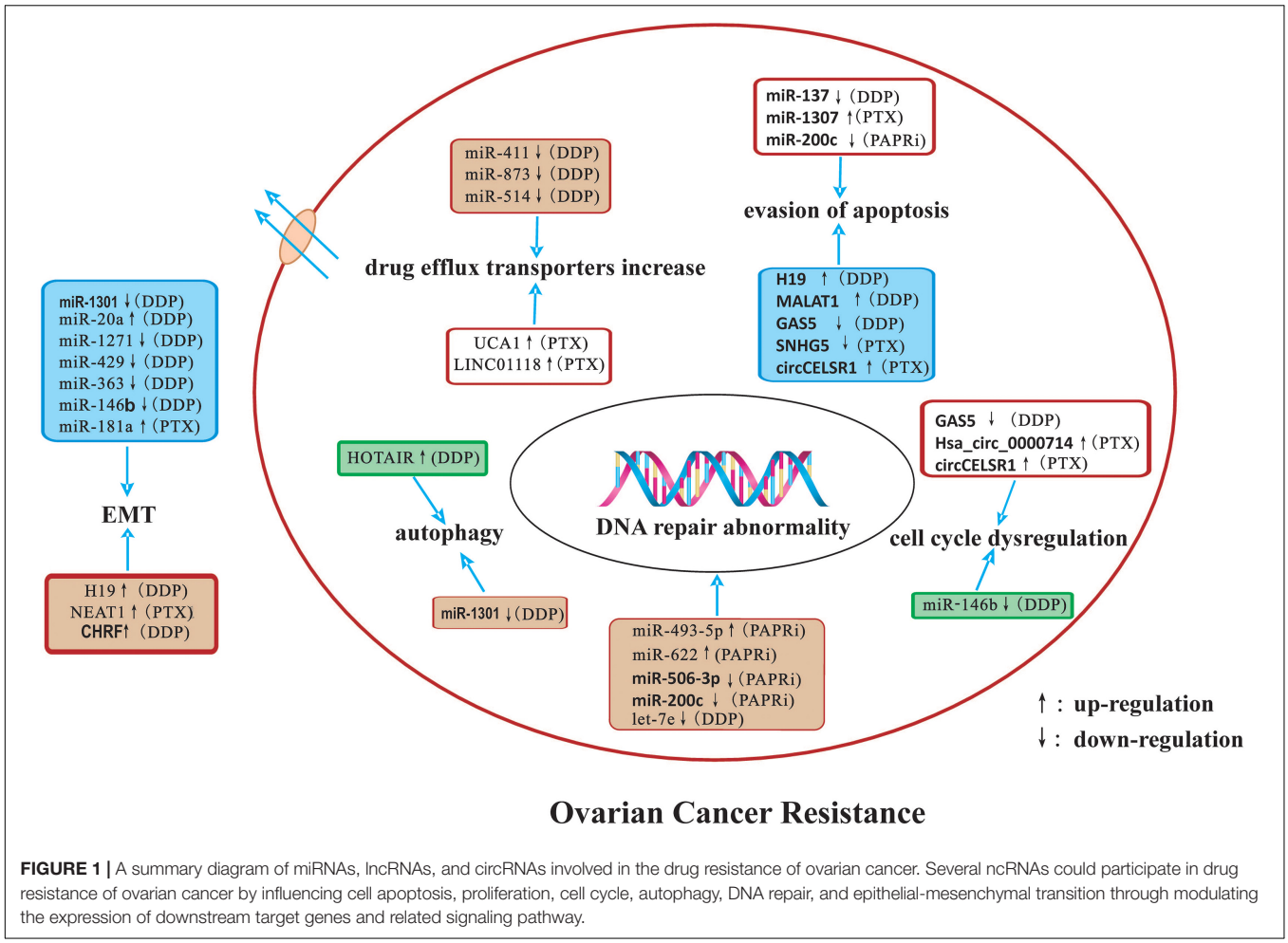

FIGURE 1 | A summary diagram of miRNAs, lncRNAs, and circRNAs involved in the drug resistance of ovarian cancer. Several ncRNAs could participate in drug resistance of ovarian cancer by influencing cell apoptosis, proliferation, cell cycle, autophagy, DNA repair, and epithelial-mesenchymal transition through modulating the expression of downstream target genes and related signaling pathway.

Munoz-Galvan et al., 2020). In addition, oncogenic miR-1180, miR-493-5p, and miR-31 confer DDP resistance to ovarian cancer cells through silencing secreted frizzled-related protein 1(SFRP1), BRCA2, and potassium calcium-activated channel subfamily M alpha 1 (KCNMA1), respectively (Samuel et al., 2016; Meghani et al., 2018; Gu et al., 2019). In animal models, miR-98-5p can potentiate the resistance of ovarian cancer to DDP, suggesting that miR-98-5p is a possible therapeutic target of ovarian cancer (Wang Y. et al., 2018; Guo et al., 2019). MiR-551b functions through the suppression of forkhead box O3 (FOXO3) and tripartite motif containing 31 (TRIM31), two important tumor suppressors. It was also found that elevated expression of miR-551b is significantly associated with worse survival of xenograft ovarian cancer models (Wei et al., 2016). Additionally, miR-20a could enhance DDP resistance of OVCAR3 ovarian cancer cells by altering the expression of EMT markers (E-cadherin, N-cadherin, and vimentin) (Liu et al., 2017).

In contrast, multiple tumor suppressor miRNAs have been found to be able to reverse DDP resistance in ovarian cancer. For instance, tumor suppressors miR-411, miR-873, and miR-514 have been confirmed to be involved in DDP resistance of ovarian cancer by modulating the expression/function of the ABC transporters family members (Wu et al., 2016; Chen et al., 2018; Xiao et al., 2018). In the meantime, miR-1301, miR-1271, miR-429, miR-363, and miR-146b can sensitize ovarian cancer cells to DDP by inhibiting the expression of multiple EMT-related genes (Zou et al., 2017; Cao et al., 2018; Yan et al., 2018; Chen Y. et al., 2019; Yu and Gao, 2020). By inhibiting the Bcl-2 signaling pathway, several tumor suppressor miRNAs, including miR-142-5p, miR-335-5p, miR-146a-5p, and miR-137 have been confirmed to sensitize ovarian cancer cells to DDP (Li et al., 2017a,b; Liu R. et al., 2018; Li X. et al., 2019). In addition, exogenous expression of miR-137 can also strongly promote DDP chemosensitivity through downregulating the expression of X-linked inhibitor of apoptosis (XIAP) and the zeste homolog 2 (EZH2) (Sun et al., 2019). Similarly, miR-708 and miR-503 can modulate ovarian cancer resistance to cisplatin through regulating the Akt pathway (Qin et al., 2017; Wu et al., 2018).Recently, emerging evidence has shown that miRNAs are aberrantly expressed in ovarian cancer, and some of them regulate different mRNAs and inhibit cisplatin resistance. Abnormal expression of the miR-199 cluster, for example, has been confirmed to increase the sensitivity of ovarian cancer cells to DDP through silencing the expression of protein tyrosine phosphatase non-receptor type 3 (PTPN3), integrin subunit beta 8 (ITGB8) and discoidin

TABLE 1 | MiRNAs and platinum resistance in ovarian cancer.

MiRNAs	Expression[1]	Genes and pathways	Drugs	References
miR-205-5p	↑	PTEN/Akt	Cisplatin	Jin et al., 2018
miR-216a	↑	PTEN	Cisplatin	Shi et al., 2018
miR-483-3p	↑	PKC-alpha	Cisplatin	Arrighetti et al., 2016
miR-224-5p	↑	PRKCD	Cisplatin	Zhao et al., 2014
miR-30b	↑	MYPT1	Cisplatin	Munoz-Galvan et al., 2020
miR-149-5p	↑	MST1, SAV1	Cisplatin	Xu M. et al., 2018
miR-1180	↑	SFRP1	Cisplatin	Gu et al., 2019
miR-493-5p	↑	BRCA2	Cisplatin	Meghani et al., 2018
miR-31	↑	KCNMA1	Cisplatin	Samuel et al., 2016
miR-98-5p	↑	CDKN1A, Dicer1	Cisplatin	Wang Y. et al., 2018; Guo et al., 2019
miR-551b	↑	FOXO3, TRIM31	Cisplatin	Wei et al., 2016
miR-20a	↑	Vimentin, E-cadherin, N-cadherin	Cisplatin	Liu et al., 2017
miR-411	↓	ABCG2	Cisplatin	Chen et al., 2018
miR-873	↓	ABCB1	Cisplatin	Wu et al., 2016
miR-514	↓	ABCA1, ABCA10, ABCF2	Cisplatin	Xiao et al., 2018
miR-1301	↓	E-cadherin, N-cadherin, ATG5, Beclin1	Cisplatin	Yu and Gao, 2020
miR-1271	↓	E-cadherin, N-cadherin, α-SMA	Cisplatin	Chen Y. et al., 2019
miR-429	↓	ZEB1	Cisplatin	Zou et al., 2017
miR-363	↓	Snai1	Cisplatin	Cao et al., 2018
miR-146b	↓	Vimentin, ZEB1, cyclin D1	Cisplatin	Yan et al., 2018
miR-142-5p	↓	XIAP, BIRC3, BCL2, BCL2L2, MCL1	Cisplatin	Li X. et al., 2019
miR-335-5p	↓	BCL2L2	Cisplatin	Li et al., 2017a
miR-146a-5p	↓	XIAP, BCL2L2, BIRC5	Cisplatin	Li et al., 2017b
miR-137	↓	XIAP, EZH2	Cisplatin	Liu R. et al., 2018; Sun et al., 2019
miR-708	↓	IGF2BP1/Akt	Cisplatin	Qin et al., 2017
miR-503	↓	PI3K/Akt	Cisplatin	Wu et al., 2018
miR-199	↓	PTPN3	Cisplatin	Li S. et al., 2016
miR-199a-3p	↓	ITGB8, DDR1	Cisplatin	Deng et al., 2017; Cui et al., 2018
let-7d-5p	↓	HMGA1	Cisplatin	Chen Y. N. et al., 2019
let-7e	↓	BRCA1, Rad51	Cisplatin	Xiao et al., 2017
miR-200b/c	↓	DNMT3A/DNMT3B/DNMT1	Cisplatin	Liu et al., 2019
miR-515-3p	↓	AXL	Oxaliplatin	Hisamatsu et al., 2019
let-7d-3p	↑	ABC transporters, HIF-1, RAS, ErbB	Carboplatin	Garcia-Vazquez et al., 2018
miR-34c-5p	↓	AREG-EGFR-ERK	Carboplatin	Tung et al., 2017

[1]*MiRNAs either up-regulated (↑) or down-regulated (↓) in platinum resistant ovarian cancer cells. This table shows 34 miRNAs whose expression levels and potential targets in platinum resistance of ovarian cancer.*

domain receptor 1 (DDR1) (Li S. et al., 2016; Deng et al., 2017; Cui et al., 2018). Additionally, ectopic miR-let-7 cluster expression can weaken DDP resistance in ovarian cancer cells by inhibiting high mobility group AT-hook 1 (HMGA1), RAD51 recombinase (RAD51), and BRCA1, indicating that the miR-let-7 cluster might be a candidate biomarker to predict ovarian cancer responders to DDP treatment (Xiao et al., 2017; Chen Y. N. et al., 2019). Moreover, the miR-200b/c cluster can improve the sensitivity of ovarian cancer cells to cisplatin by inhibiting the expression of DNA methyltransferase (DNMT) (Liu et al., 2019).

Studies on carboplatin and oxaliplatin are far less extensive than cisplatin. Tumor suppressor miR-515-3p can regulate oxaliplatin sensitivity by targeting AXL Receptor Tyrosine Kinase (AXL) (Hisamatsu et al., 2019). Similarly, let-7d-3p could enhance carboplatin-resistance (Garcia-Vazquez et al., 2018). Tumor suppressors miR-634 and miR-34c-5p have been proven to be involved in the regulation of carboplatin sensitivity through the MAPK pathway (Tung et al., 2017).

MiRNAs AND PTX RESISTANCE

Paclitaxel is one of the first-line chemotherapy drugs used to treat ovarian cancer. It is highly cytotoxic against tubulin. It induces and promotes the polymerization of tubulin and microtubule assembly, and it prevents depolymerization, stabilizing microtubules, and inhibiting the mitosis of cancer cells, leading to cell cycle arrest in G2/M. This effectively prevents the proliferation of cancer cells. It has been reported that various miRNAs are involved in PTX-resistance of ovarian cancer (**Table 2**).

Several oncogenic miRNAs can facilitate PTX resistance, such as miR-21 and miR-630. Exogenous expression of miR-21 and

TABLE 2 | MiRNAs and paclitaxel resistance in ovarian cancer.

MiRNAs	Expression[1]	Genes and pathways	References
miR-21	↑	APAF1	Au Yeung et al., 2016
miR-630	↑	APAF1	Eoh et al., 2018
miR-1307	↑	CIC, ING5	Chen W. T. et al., 2017; Zhou et al., 2019
miR-181a	↑	E-cadherin, N-cadherin	Li L. et al., 2016
miR-215	↓	XIAP	Ge et al., 2016
miR-200bc/141	↓	EMT	Duran et al., 2017
miR-92	↓	DKK1	Chen M. W. et al., 2017
miR-503-5p	↓	CD97	Park and Kim, 2019
miR-136	↓	NOTCH3	Jeong et al., 2017
miR-383-5p	↓	TRIM27	Jiang et al., 2019
miR-874	↓	SIK2	Xia et al., 2018

[1]MiRNAs either up-regulated (↑) or down-regulated (↓) in paclitaxel resistant ovarian cancer cells. This table shows 11 miRNAs whose expression levels and potential targets in paclitaxel resistance of ovarian cancer.

miR-630 enhanced PTX resistance of ovarian cancer cells by silencing apoptotic peptidase activating factor 1 (APAF1) (Au Yeung et al., 2016; Eoh et al., 2018). Similarly, miR-1307, a highly expressed miRNA in ovarian cancer tissues and cell lines, has been demonstrated to be positively correlated with PTX resistance. By targeting the capicua transcriptional repressor (CIC) and the inhibitor of growth family member 5 (ING5), miR-1307 could dramatically inhibit apoptosis induced by PTX (Chen W. T. et al., 2017; Zhou et al., 2019). Moreover, the miR-181a level in chemoresistant cancer tissues is significantly higher than in chemosensitive cancer tissues and in normal tissue, and its upregulation is associated with an increased level of EMT and decreased cell apoptosis induced by PTX treatment (Li L. et al., 2016).

In contrast, several tumor suppressor miRNAs may reverse PTX resistance in ovarian cancer. The Bcl-2 family participates in the chemoresistance of malignancies, including ovarian cancer. Tumor suppressors miR-215 can promote PTX-induced apoptosis of ovarian cancer cells by silencing the expression of XIAP (Ge et al., 2016). Activation of the EMT pathway has also been observed to regulate PTX resistance of ovarian cancer. A variety of miRNAs, such as miR-200b and miR-200c, have been observed to be involved in the EMT pathway mediated PTX resistance of ovarian cancer (Duran et al., 2017). By inhibiting the signal transducer and activator of transcription 3 (STAT3) signaling pathway, several tumor suppressor miRNAs, including miR-92 and miR-503-5p, have been found to sensitize ovarian cancer cells to PTX. In animal models, targeting STAT3 in combination with paclitaxel can synergistically reduce intraperitoneal dissemination and prolong the survival of mice with ovarian cancer (Chen M. W. et al., 2017; Park and Kim, 2019). Similarly, tumor suppressors miR-136, miR-383-5p, and miR-874 have been reported to conquer PTX resistance of ovarian cancer cells by silencing NOTCH3, tripartite motif containing 27 (TRIM27), and salt inducible kinase 2 (SIK2), respectively (Jeong et al., 2017; Xia et al., 2018; Jiang et al., 2019).

MiRNAs AND PARPi RESISTANCE

Poly-ADP ribose polymerase inhibitor have emerged as exciting new chemotherapy options for women with ovarian cancer, especially for patients with BRCA1 or BRCA2 mutations or non-functional homologous recombination repair pathways. The most advantageous feature of PARPi is its mechanism of action. PARPi is able to eliminate the function of PARP, leading to the accumulation of single-stranded breaks (SSB), which in turn can be converted into double-strand breaks (DSB) that the cell cannot repair, leading to cancer cell death (Wiltshire et al., 2010). Moreover, PARPi can enhance the efficacy of radiotherapy and chemotherapy with docetaxel and platinum drugs. Three PARPis have been approved for the treatment of recurrent epithelial ovarian cancer in the United States: olaparib, rucaparib, and niraparib. However, long-term use of PARPis may cause PARPi resistance. In ovarian cancer cells, multiple miRNAs were found to be involved in PARPi resistance (**Table 3**).

Multiple oncogene miRNAs can promote PARPi resistance. According to a recent report, miR-493-5p is significantly upregulated in BRCA2-mutated ovarian cancer cells and it participates in the PARPi resistance process by regulating ribonuclease H2 subunit A (RNASEH2A), flap structure-specific endonuclease 1 (FEN1), and structure specific recognition protein 1 (SSRP1). miR-493-5p can reduce single-strand annealing (SSA), stabilize the replication fork, and thus induce PARPi tolerance (Meghani et al., 2018). In addition, miR-622 is highly expressed in BRCA1-deficient high-grade serous ovarian carcinomas (HGSOCs), which can rescue the homologous recombination repair (HRR) defect of BRCA1 mutant ovarian cancer and promote PARPi resistance by regulating the expression of Ku complex and inhibiting HR and non-homologous end joining (NHEJ) (Choi et al., 2016).

In contrast, multiple tumor suppressor miRNAs can reverse the PARPi resistance of ovarian cancer. For instance, miR-506-3p acts as a vital regulator in the sensitivity to PARPis and

TABLE 3 | MiRNAs and PARPi resistance in ovarian cancer.

MiRNAs	Expression[1]	Genes and pathways	References
miR-493-5p	↑	RNASEH2A, FEN1, SSRP1	Meghani et al., 2018
miR-622	↑	Ku	Choi et al., 2016
miR-506-3p	↓	EZH2/β-catenin	Sun et al., 2021
miR-200c	↓	NRP1	Vescarelli et al., 2020

[1]MiRNAs either up-regulated (↑) or down-regulated (↓) in paclitaxel resistant ovarian cancer cells. This table shows four miRNAs whose expression levels and potential targets in PARPi resistance of ovarian cancer.

cisplatin by targeting EZH2/β-catenin pathway in ovarian cancers (Sun et al., 2021). Additionally, ectopic miR-200c expression can increase apoptosis and weaken the resistance to olaparib in the ovarian cancer cells SKOV3/PARPi by silencing Neuropilin 1 (NRP1) (Vescarelli et al., 2020).

LncRNAs AND THERAPY RESISTANCE

Long non-coding RNAs are a category of RNA transcripts longer than 200 nt without coding capacity, which are transcribed by RNA Polymerase II (RNAP II) and expressed in a tissue-specific manner (Quinn and Chang, 2016). At present, it is known that lncRNAs can regulate the malignant biological behavior of cells by acting as a competitive endogenous RNA (ceRNA), recruiting downstream molecules, serving as protein scaffolds, transmitting regulatory signals (Wong et al., 2018), and regulating endolysosome pH (Miller et al., 2018). A number of lncRNAs have a close relationship to the development of ovarian cancer metastasis, recurrence, and chemotherapy resistance (Winham et al., 2019; Zhang M. et al., 2019; Sun et al., 2020). Aberrantly expressed lncRNAs may participate in ovarian cancer progression through various mechanisms, including inducing autophagy, increasing DNA damage repair, changing cell cycle progression and checkpoints, inducing anti-apoptosis, regulating cell signaling pathways, and promoting EMT (Liu et al., 2015; Yan et al., 2017; Xu Q. F. et al., 2018; Wu et al., 2019). Several lncRNAs have been found to be involved in drug resistance in ovarian cancer (**Tables 4**, **5**).

It has been reported that lncRNA UCA1 (urothelial cancer associated 1) is significantly upregulated in PTX-resistant ovarian cancer tissues and cell lines and confers ovarian cancer resistance to PTX. UCA1 promote tumor progression both *in vitro* and *in vivo*. SIK2 protein is involved in the separation of centrosomes during mitosis, which can lead to ovarian cancer drug resistance (Ahmed et al., 2010; Zhou et al., 2017). In ovarian cancer cells, UCA1 can induce SIK2 expression *via* endogenous sponging of miR-654-5p and thus antagonize chemosensitivity to PTX (Li Z. Y. et al., 2020). Additionally, ABCB1 (ATP binding cassette subfamily B member 1) is one of the members of the superfamily of ABC transporters that are involved in MDR. In ovarian cancer cells, UCA1 can also induce ABCB1 expression though endogenous sponging of miR-129 to enhance PTX tolerance (Wang J. et al., 2018). In recent years, lncRNA UCA1 has also been found to be involved in cisplatin resistance in ovarian cancer and blood UCA1 levels are upregulated in patients after cisplatin treatment. *Via* binding to the 3′-UTRs of FOS-like 2 (FOSL2), miR-143 can negatively regulate FOSL2 expression, suggesting that the UCA1/miR-143 axis may have potential therapeutic value for the treatment of cisplatin resistance in ovarian cancer patients (Li Z. et al., 2019).

Long non-coding RNAs HOTAIR (HOX antisense intergenic RNA) is one of the most well-studied lncRNAs, which is transcribed from the antisense strand of the HOXC gene cluster present on chromosome 12 with a length of 2.2 kb. HOTAIR, a highly expressed lncRNA in ovarian cancer tissues and cell lines, has been found to be positively correlated with advanced tumor stages, high histological grade, lymph node metastasis, drug resistance, and poor prognosis of ovarian cancer patients (Qiu et al., 2014; Wang et al., 2015). Moreover, it has been reported that exogenous HOTAIR overexpression in ovarian cancer cells significantly promoted cisplatin resistance by regulating the Wnt/β-catenin signaling pathway as well as the NF-κB-HOTAIR axis, indicating that HOTAIR may act as a regulator of cisplatin resistance (Li J. et al., 2016; Ozes et al., 2016). Similarly, knockdown of HOTAIR can inhibit autophagy *via* decreasing autophagy related 7 (ATG7) expression, and the inhibition of cisplatin-induced autophagy by silencing HOTAIR has been shown to enhance the chemotherapeutic efficacy of cisplatin in ovarian cancer (Yu et al., 2018).

Increasing findings indicate that lncRNA H19 plays an important role in chemotherapy drug resistance of ovarian cancer. In the OVCAR3/DDP resistant ovarian cancer cell, silencing lncRNA H19 can significantly increase E-cadherin

TABLE 4 | LncRNAs and platinum resistance in ovarian cancer.

LncRNAs	Expression[1]	Genes and pathways	Drugs	References
UCA1	↑	miR-143/FOSL2	Cisplatin	Li Z. et al., 2019
HOTAIR	↑	Wnt/β-catenin pathway	Cisplatin	Li J. et al., 2016
		NF-κB pathway	Cisplatin	Ozes et al., 2016
		ATG7	Cisplatin	Yu et al., 2018
H19	↑	EMT	Cisplatin	Liu et al., 2015
		GSH metabolism	Cisplatin	Zheng et al., 2016
		EZH2/p21/PTEN pathway	Cisplatin	Sajadpoor et al., 2018
NEAT1	↑	miR-770-5p/PARP1	Cisplatin	Zhu et al., 2020
CCAT1	↑	miR-454/survivin	Cisplatin	Wang D. Y. et al., 2020
MALAT1	↑	NOTCH1	Cisplatin	Bai et al., 2018
	↑	miR-1271-5p/E2F5	Cisplatin	Wang Y. et al., 2020
Linc00161	↑	miR-128/MAPK1	Cisplatin	Xu et al., 2019
CHRF	↑	EMT and STAT3 pathway	Cisplatin	Tan et al., 2020
ANRIL	↑	miR-324-5p/Ran axis	Cisplatin	Wang K. et al., 2021
SNHG22	↑	miR-2467/Gal-1	Cisplatin	Zhang P. F. et al., 2019
GAS5	↓	E2F4/PARP1/MAPK	Cisplatin	Long et al., 2019
PANDAR	↓	SFRS2-p53	Cisplatin	Wang H. et al., 2018
LINC01125	↓	miR-1972	Cisplatin	Guo and Pan, 2019
MEG3	↓	miR-214	Cisplatin	Zhang et al., 2017

[1] *LncRNAs either up-regulated (↑) or down-regulated (↓) in platinum resistant ovarian cancer cells. This table shows 14 lncRNAs whose expression levels and potential targets in platinum resistance of ovarian cancer.*

TABLE 5 | LncRNAs and paclitaxel resistance in ovarian cancer.

LncRNAs	Expression[1]	Genes and pathways	References
UCA1	↑	miR-654-5p/SIK2	Li Z. Y. et al., 2020
		miR-129/ABCB1	Wang J. et al., 2018
NEAT1	↑	miR-194/ZEB1	An et al., 2017
LINC01118	↑	miR-134/ABCC1	Shi and Wang, 2018
PRLB	↑	RSF1/NF-κB	Zhao and Hong, 2021
SNHG22	↑	miR-2467/Gal-1	Zhang P. F. et al., 2019
FER1L4	↓	MAPK	Liu S. et al., 2018
SNHG5	↓	miR-23a	Lin et al., 2020

[1]*LncRNAs either up-regulated (↑) or down-regulated (↓) in paclitaxel resistant ovarian cancer cells. This table shows seven lncRNAs whose expression levels and potential targets in paclitaxel resistance of ovarian cancer.*

expression and reduce twist, slug, and snail expression, indicating that lncRNA H19 induces cisplatin resistance *via* EMT (Wu et al., 2019). In addition, lncRNA H19 can also confer resistance to cisplatin to ovarian cancer cells by promoting glutathione (GSH) metabolism (Zheng et al., 2016). It has been reported that valproic acid (VPA) acts on A2780/CP resistant cells, which negatively regulates the expression of lncRNA H19, and then induces cell apoptosis and inhibits cell proliferation, thereby making A2780 resistant cells sensitive to cisplatin (Sajadpoor et al., 2018). These findings suggest that lncRNA H19 has potential as a new target for overcoming drug resistance in ovarian cancer.

Long non-coding RNAs NEAT1 (nuclear paraspeckle assembly transcript 1) was reported to be correlated with clinically poor paclitaxel response ovarian cancer. It has been found that lncRNA NEAT1 promotes paclitaxel resistance *via* competitively binding miR-194 to facilitate ZEB1 expression in ovarian cancer cells (An et al., 2017). Recently, LncRNA NEAT1 is also found to play a part in cisplatin resistance of ovarian cancer. NEAT1 is significantly upregulated in ovarian cancer, associates with cisplatin resistance and FIGO stage. Knockdown of NEAT1 suppresses cisplatin resistance of ovarian cancer cells *in vitro* and *in vivo*. LncRNA NEAT1 contributes to DDP resistance of ovarian cancer cells by regulating PARP1 expression *via* miR-770-5p (Zhu et al., 2020).

In addition, some other lncRNAs were found to be involved in platinum-based chemotherapy resistance in ovarian cancer. On the one hand, lncRNAs can promote platinum resistance. For instance, lncRNA CCAT1 (colon cancer associated transcript 1) is upregulated in A2780/DDP and SKOV3/DDP resistant ovarian cancer cells, and it can confer resistance to DDP by modulating the miR-454/survivin axis (Wang D. Y. et al., 2020). LncRNA metastasis-associated lung adenocarcinoma transcript 1 (MALAT1) has been reported to be upregulated and to contribute to ovarian cancer tumorigenesis. Knockdown of MALAT1 could enhance cisplatin-induced apoptosis and improve the chemosensitivity of ovarian cancer cells to cisplatin through inhibiting the notch1 signaling pathway (Bai et al., 2018). Besides, MALAT1 could regulate ovarian cancer progression and DDP-resistance by miR-1271-5p/E2F5 Axis (Wang Y. et al., 2020). Moreover, it has been found that lncRNA linc0161 functions as a ceRNA of microRNA-128 and promotes drug resistance through blocking MAPK1 (Xu et al., 2019). In addition, CHRF contributes to cisplatin resistance of ovarian cancer cells by regulating EMT and STAT3 signaling *via* miR-10b (Tan et al., 2020). ANRIL could modulate the progression, drug resistance and tumor stem cell-like characteristics of ovarian cancer cells *via* miR-324-5p/Ran Axis (Wang K. et al., 2021).

Some tumor suppressor lncRNAs can reverse platinum drug resistance of ovarian cancer. LncRNA GAS5 expression in SKOV3/DDP cells has been found to be significantly reduced compared to that in drug-sensitive cells, and it has been reported that GAS5 can sensitize ovarian cancer cells to DDP by leading to G0/G1 cell cycle arrest and increasing apoptosis. Further research showed that GAS5 could inhibit DDP-resistance and tumor progression of ovarian cancer *via* the GAS5-E2F4-PARP1-MAPK axis (Long et al., 2019). It has been reported that lncRNA PANDAR dictates the chemoresistance of ovarian cancer by regulating SFRS2-mediated p53 phosphorylation (Wang H. et al., 2018). Interestingly, lncRNA linc01125 can inhibit ovarian cancer cell proliferation and it enhances the cytotoxicity of DDP in ovarian cancer cells. Tumor suppressor linc01125 has been shown to enhance the cisplatin sensitivity of ovarian cells by sponging miR-1972 (Guo and Pan, 2019). In addition, the literature shows that curcumin inhibits cisplatin resistance development partly by regulating extracellular vesicle-mediated transfer of MEG3 and miR-214 in ovarian cancer (Zhang et al., 2017).

There are several novel lncRNAs that have been found to play crucial functions in ovarian cancer PTX resistance. For instance, it has been reported that lncRNA linc0118 is significantly upregulated in PTX-resistant ovarian cancer tissues and cell lines and confers ovarian cancer resistance to PTX. Linc0118 can promote tumor progression *in vitro* and *in vivo*. In ovarian cancer cells, linc0118 can induce ABCC1 expression *via* endogenous sponging of miR-134 and, thus, antagonize chemosensitivity to PTX (Shi and Wang, 2018). In ovarian cancer cells, lncRNA-PRLB have been found to promote TAX resistance by suppressing miR-150-5p and activating NF-κB signaling. Moreover, PRLB has been found to inhibit TAX in ovarian cancer cells through enhancing RSF1 expression, whereas elevated PRLB expression has been found to be associated with a poor response to TAX treatment (Zhao and Hong, 2021). LncRNA SNHG22 is another chemoresistance-related gene and it has been found to promote DDP resistance and PTX resistance through regulating the miR-2467/galectin 1 (Gal-1) axis and it is correlated with poor patient outcomes (Zhang P. F. et al., 2019).

In contrast, a number of tumor suppressor lncRNAs can reverse PTX drug resistance in ovarian cancer. In comparison with normal ovarian epithelial cells, lncRNA FER1L4 is downregulated in SKOV3/PTX resistant cells. Overexpression of the lncRNA FER1L4 can inhibit paclitaxel tolerance of ovarian cancer cells through regulating MAPK signaling pathway (Liu S. et al., 2018). Recently, significantly diminished expression of lncRNA SNHG5 was observed in SKOV3/PTX and HeyA-8/PTX PTX-resistant ovarian cancer cells. Exogenous expression of lncRNA SNHG5 has been found to promote apoptosis, inhibit cell proliferation and enhance PTX sensitivity of ovarian cancer cells by sponging miR-23a (Lin et al., 2020).

TABLE 6 | CircRNAs and drug resistance in ovarian cancer.

CircRNAs	Expression[1]	Genes and pathways	Drugs	References
circTNPO3	↑	miR-1299/NEK2	Paclitaxel	Xia et al., 2020
circNRIP1	↑	miR-211-5p/HOXC8	Paclitaxel	Li M. et al., 2020
Hsa_circ_0000714	↑	miR-370-3p/RAB17	Paclitaxel	Guo et al., 2020
CELSR1	↑	miR-1252/FOXR2	Paclitaxel	Zhang S. et al., 2020
circEXOC6B	↓	miR-376c-3p/FOXO3	Paclitaxel	Zheng et al., 2020
Cdr1as	↓	miR-1270/SCAI	Cisplatin	Zhao et al., 2019
circFoxp1	↑	miR-22/CEBPG, miR-150-3p/FMNL3	Cisplatin	Luo and Gui, 2020

[1]*CircRNAs either up-regulated (↑) or down-regulated (↓) in chemo-resistant ovarian cancer cells. This table shows seven circRNAs whose expression levels and underlying pathways in chemoresistance of ovarian cancer.*

CircRNAs AND CHEMORESISTANCE IN OVARIAN CANCER

Circular RNAs are crucial members of the ncRNA family, and those related to animal physiologies have been widely studied in recent years. CircRNAs have a closed-loop structure because of a covalent junction between their 3′ and 5′ ends. CircRNAs show stability, conservation, abundance, and tissue and cell specificity (Salzman et al., 2013; Ashwal-Fluss et al., 2014; Maass et al., 2017; Xia et al., 2017). CircRNAs play important roles in biological functions by acting as a "microRNA sponge," regulating gene transcription and interacting with RNA binding proteins in most cases (Fan et al., 2021; Shen et al., 2021; Zeng et al., 2021). Accumulating evidences have shown that circRNAs are abnormally expressed in various malignant tumors, and circRNAs can act as both proto-oncogenes and tumor suppressors. It has been reported that circRNAs in tumors not only contribute to multiple processes of malignancy, including cell differentiation, proliferation, invasion, and metastasis but are also involved in the mechanism of chemotherapy resistance (Ding et al., 2020; Hong et al., 2020; Ou et al., 2020; **Table 6**).

Several circRNAs are known to be involved in PTX-resistant ovarian cancer. The cancer-related circTNPO3 has, for example, been found to function as an oncogene in ovarian cancer and confer PTX resistance. CircTNPO3 associates with advanced FIGO stage and histological type. CircTNPO3 promotes PTX resistance of ovarian cancer cells *in vitro* and *in vivo*. CircTNPO3 promotes PTX resistance *via* competitively binding miR-1299 to upregulate NEK2 (Xia et al., 2020). Moreover, circNRIP1 was up-regulated in PTX-resistant ovarian cancer tissues and cells. Silencing of circNRIP1 suppressed the PTX resistance of ovarian cancer cells *in vitro* and *in vivo*. Oncogenic CircNRIP1 could contribute to PTX resistance of ovarian cancer by modulating expression of the miR-211-5p/HOXC8 axis (Li M. et al., 2020). Additionally, Hsa_circ_0000714 is an up-regulated circRNA in PTX resistant cells SKOV3/PTX and A2780/PTX, which is contributed to PTX resistance by influencing cell cycle G1/S transition and colony formation. Hsa_circ_0000714 mediates PTX resistance in ovarian cancer cells by sponging miR-370-3p and regulating the expression of RAB17 (Guo et al., 2020). Meanwhile, the cancer-related circCELSR1 (hsa_circ_0063809) has also been identified to be upregulated in SKOV3/PTX and HeyA-8/PTX PTX-resistant ovarian cancer cell lines. Inhibiting circCELSR1 can cause ovarian cancer cell cycle G0/G1 arrest and an increase in apoptosis. CircCELSR1 has been shown to contribute to PTX resistance by modulating forkhead box R2 (FOXR2) expression through miR-1252 (Zhang S. et al., 2020). On the contrary, tumor suppressor circRNAs can reverse PTX resistance in ovarian cancer. circEXOC6B shows notably decreased expression in ovarian cancer tissues and is associated with long survival time of ovarian cancer patients. In ovarian cancer cells, circEXOC6B could suppress FOXO3 expression *via* endogenous sponging miR-376c-3p and, thus, elevate chemosensitivity to PTX (Zheng et al., 2020).

Also, several circRNAs have been found to be involved in ovarian cancer DDP chemoresistance. Significantly decreased expression levels of circRNA Cdr1as have been observed in both tissues and serum exosomes of Cisplatin-Resistant ovarian cancer patients. It has been confirmed that downregulating suppressor of cancer cell invasion (SCAI) by sponging miR-1270, Cdr1as can conquer DDP resistance of ovarian cancer cells (Zhao et al., 2019). Recently, circulating exosomal circFoxp1, whose expression is positively associated with International Federation of Gynecology and Obstetrics stage, primary tumor size, lymphatic metastasis, distant metastasis, residual tumor diameter, and clinical response, has been reported to promote resistance to DDP of ovarian cancer cells through up-regulating expression of CCAAT enhancer binding protein gamma (CEBPG) and formin like 3 (FMNL3) through miR-22 and miR-150-3p (Luo and Gui, 2020).

CONCLUSION AND FUTURE PERSPECTIVES

Ovarian cancer is a comprehensive disease, but the pathogenesis has not been completely elucidated. Although substantial progress has been made in the diagnosis and treatment of ovarian cancer, unfortunately, the prognosis remains unsatisfactory. A growing number of ncRNAs have been identified to be involved in chemoresistance of ovarian cancer. Targeting ncRNAs, in combination with traditional chemotherapy or targeted therapy, may be a promising choice to combat drug resistance in advanced ovarian cancers. NcRNAs affect cell drug resistance through multiple mechanisms. In ovarian cancer, we reviewed EMT,

drug efflux transporters, autophagy, cell cycle dysregulation, and DNA repair abnormality. At present, it has also received widespread attention that ncRNAs mediate exosomes to cause cell drug resistance.

A variety of methods are used to identify ncRNA that affect drug resistance, and the more commonly used methods include high-throughput analysis, silicon analysis, integrated analysis, bioinformatics, and expression arrays (Hartmaier et al., 2017; Cen et al., 2021). These technologies enable researchers to target the direction of tumor research, explore the mechanism of tumor occurrence and development, and explore the mechanism of clinical drug resistance. However, it is still a great challenge to select the critical target ncRNAs from the large number of candidates and there is still a long way to go for ncRNA to be used as clinical drug targets. Further translational studies or clinical trials are indispensable to develop ncRNAs-based therapeutics, which may ultimately provide potential approaches for overcoming ovarian cancer drug resistance.

AUTHOR CONTRIBUTIONS

XZ and SX designed the study. HL analyzed and interpreted the data, and wrote the original draft. JYu wrote this manuscript. DZ, CL, XG, and JYo edited and revised the manuscript. All authors have seen and approved the final version of the manuscript.

FUNDING

This work was supported by the Independent Exploration and Innovation Project for Graduate Students of Central South University (2021zzts1080), Philosophy and Social Science Foundation Project of Hunan Province (19YBA349), Clinical Medical Technology Innovation Guidance Plan of Hunan Province (2020SK53607), and Natural Science Foundation of Changsha (kq2014261).

REFERENCES

Ahmed, A. A., Lu, Z., Jennings, N. B., Etemadmoghadam, D., Capalbo, L., Jacamo, R. O., et al. (2010). SIK2 is a centrosome kinase required for bipolar mitotic spindle formation that provides a potential target for therapy in ovarian cancer. *Cancer Cell* 18, 109–121. doi: 10.1016/j.ccr.2010.06.018

An, J., Lv, W., and Zhang, Y. (2017). LncRNA NEAT1 contributes to paclitaxel resistance of ovarian cancer cells by regulating ZEB1 expression via miR-194. *Onco Targets Ther.* 10, 5377–5390. doi: 10.2147/OTT.S147586

Armstrong, D. K., Alvarez, R. D., Bakkum-Gamez, J. N., Barroilhet, L., Behbakht, K., Berchuck, A., et al. (2021). Ovarian cancer, version 2.2020, NCCN clinical practice guidelines in oncology. *J. Natl. Compr. Cancer Netw.* 19, 191–226. doi: 10.6004/jnccn.2021.0007

Arrighetti, N., Cossa, G., De Cecco, L., Stucchi, S., Carenini, N., Corna, E., et al. (2016). PKC-alpha modulation by miR-483-3p in platinum-resistant ovarian carcinoma cells. *Toxicol. Appl. Pharmacol.* 310, 9–19. doi: 10.1016/j.taap.2016.08.005

Ashwal-Fluss, R., Meyer, M., Pamudurti, N. R., Ivanov, A., Bartok, O., Hanan, M., et al. (2014). circRNA biogenesis competes with pre-mRNA splicing. *Mol. Cell* 56, 55–66. doi: 10.1016/j.molcel.2014.08.019

Au Yeung, C. L., Co, N. N., Tsuruga, T., Yeung, T. L., Kwan, S. Y., Leung, C. S., et al. (2016). Exosomal transfer of stroma-derived miR21 confers paclitaxel resistance in ovarian cancer cells through targeting APAF1. *Nat. Commun.* 7:11150. doi: 10.1038/ncomms11150

Bai, L., Wang, A., Zhang, Y., Xu, X., and Zhang, X. (2018). Knockdown of MALAT1 enhances chemosensitivity of ovarian cancer cells to cisplatin through inhibiting the Notch1 signaling pathway. *Exp. Cell Res.* 366, 161–171. doi: 10.1016/j.yexcr.2018.03.014

Belur Nagaraj, A., Knarr, M., Sekhar, S., Connor, R. S., Joseph, P., Kovalenko, O., et al. (2021). The miR-181a-SFRP4 axis regulates Wnt activation to drive stemness and platinum resistance in ovarian cancer. *Cancer Res.* 81, 2044–2055. doi: 10.1158/0008-5472.CAN-20-2041

Bi, Z., Li, Q., Dinglin, X., Xu, Y., You, K., Hong, H., et al. (2020). Nanoparticles (NPs)-meditated LncRNA AFAP1-AS1 silencing to block Wnt/beta-catenin signaling pathway for synergistic reversal of radioresistance and effective cancer radiotherapy. *Adv. Sci.* 7:2000915. doi: 10.1002/advs.202000915

Bruno, P. M., Liu, Y., Park, G. Y., Murai, J., Koch, C. E., Eisen, T. J., et al. (2017). A subset of platinum-containing chemotherapeutic agents kills cells by inducing ribosome biogenesis stress. *Nat. Med.* 23, 461–471. doi: 10.1038/nm.4291

Cao, L., Wan, Q., Li, F., and Tang, C. E. (2018). MiR-363 inhibits cisplatin chemoresistance of epithelial ovarian cancer by regulating snail-induced epithelial-mesenchymal transition. *BMB Rep.* 51, 456–461.

Cech, T. R., and Steitz, J. A. (2014). The noncoding RNA revolution-trashing old rules to forge new ones. *Cell* 157, 77–94. doi: 10.1016/j.cell.2014.03.008

Cen, J., Liang, Y., Huang, Y., Pan, Y., Shu, G., Zheng, Z., et al. (2021). Circular RNA circSDHC serves as a sponge for miR-127-3p to promote the proliferation and metastasis of renal cell carcinoma via the CDKN3/E2F1 axis. *Mol. Cancer* 20:19. doi: 10.1186/s12943-021-01314-w

Chen, F. D., Chen, H. H., Ke, S. C., Zheng, L. R., and Zheng, X. Y. (2018). SLC27A2 regulates miR-411 to affect chemo-resistance in ovarian cancer. *Neoplasma* 65, 915–924. doi: 10.4149/neo_2018_180122N48

Chen, L. Y., Wang, L., Ren, Y. X., Pang, Z., Liu, Y., Sun, X. D., et al. (2020). The circular RNA circ-ERBIN promotes growth and metastasis of colorectal cancer by miR-125a-5p and miR-138-5p/4EBP-1 mediated cap-independent HIF-1alpha translation. *Mol. Cancer* 19:164. doi: 10.1186/s12943-020-01272-9

Chen, M. W., Yang, S. T., Chien, M. H., Hua, K. T., Wu, C. J., Hsiao, S. M., et al. (2017). The STAT3-miRNA-92-Wnt signaling pathway regulates spheroid formation and malignant progression in ovarian cancer. *Cancer Res.* 77, 1955–1967. doi: 10.1158/0008-5472.CAN-16-1115

Chen, W. T., Yang, Y. J., Zhang, Z. D., An, Q., Li, N., Liu, W., et al. (2017). MiR-1307 promotes ovarian cancer cell chemoresistance by targeting the ING5 expression. *J. Ovarian Res.* 10:1. doi: 10.1186/s13048-016-0301-4

Chen, Y., Wang, L., and Zhou, J. (2019). Effects of microRNA-1271 on ovarian cancer via inhibition of epithelial-mesenchymal transition and cisplatin resistance. *J. Obstet. Gynaecol. Res.* 45, 2243–2254. doi: 10.1111/jog.14079

Chen, Y. N., Ren, C. C., Yang, L., Nai, M. M., Xu, Y. M., Zhang, F., et al. (2019). MicroRNA let7d5p rescues ovarian cancer cell apoptosis and restores chemosensitivity by regulating the p53 signaling pathway via HMGA1. *Int. J. Oncol.* 54, 1771–1784. doi: 10.3892/ijo.2019.4731

Chiappa, M., Guffanti, F., Bertoni, F., Colombo, I., and Damia, G. (2021). Overcoming PARPi resistance: preclinical and clinical evidence in ovarian cancer. *Drug Resist. Updat.* 55:100744. doi: 10.1016/j.drup.2021.100744

Choi, Y. E., Meghani, K., Brault, M. E., Leclerc, L., He, Y. J., Day, T. A., et al. (2016). Platinum and PARP inhibitor resistance due to overexpression of MicroRNA-622 in BRCA1-mutant ovarian cancer. *Cell Rep.* 14, 429–439. doi: 10.1016/j.celrep.2015.12.046

Christie, E. L., Pattnaik, S., Beach, J., Copeland, A., Rashoo, N., Fereday, S., et al. (2019). Multiple ABCB1 transcriptional fusions in drug resistant high-grade serous ovarian and breast cancer. *Nat. Commun.* 10:1295. doi: 10.1038/s41467-019-09312-9

Cocquerelle, C., Mascrez, B., Hetuin, D., and Bailleul, B. (1993). Mis-splicing yields circular RNA molecules. *FASEB J.* 7, 155–160. doi: 10.1096/fasebj.7.1.7678559

Cui, C., Liu, Y., Gerloff, D., Rohde, C., Pauli, C., Kohn, M., et al. (2021). NOP10 predicts lung cancer prognosis and its associated small nucleolar RNAs drive proliferation and migration. *Oncogene* 40, 909–921. doi: 10.1038/s41388-020-01570-y

Cui, Y., Wu, F., Tian, D., Wang, T., Lu, T., Huang, X., et al. (2018). miR-199a-3p enhances cisplatin sensitivity of ovarian cancer cells by targeting ITGB8. *Oncol. Rep.* 39, 1649–1657. doi: 10.3892/or.2018.6259

Deng, Y., Zhao, F., Hui, L., Li, X., Zhang, D., Lin, W., et al. (2017). Suppressing miR-199a-3p by promoter methylation contributes to tumor aggressiveness and cisplatin resistance of ovarian cancer through promoting DDR1 expression. *J. Ovarian Res.* 10:50. doi: 10.1186/s13048-017-0333-4

Ding, C., Yi, X., Wu, X., Bu, X., Wang, D., Wu, Z., et al. (2020). Exosome-mediated transfer of circRNA CircNFIX enhances temozolomide resistance in glioma. *Cancer Lett.* 479, 1–12. doi: 10.1016/j.canlet.2020.03.002

Duran, G. E., Wang, Y. C., Moisan, F., Francisco, E. B., and Sikic, B. I. (2017). Decreased levels of baseline and drug-induced tubulin polymerisation are hallmarks of resistance to taxanes in ovarian cancer cells and are associated with epithelial-to-mesenchymal transition. *Br. J. Cancer* 116, 1318–1328. doi: 10.1038/bjc.2017.102

Eoh, K. J., Lee, S. H., Kim, H. J., Lee, J. Y., Kim, S., Kim, S. W., et al. (2018). MicroRNA-630 inhibitor sensitizes chemoresistant ovarian cancer to chemotherapy by enhancing apoptosis. *Biochem. Biophys. Res. Commun.* 497, 513–520. doi: 10.1016/j.bbrc.2018.02.062

Fan, Y., Wang, J., Jin, W., Sun, Y., Xu, Y., Wang, Y., et al. (2021). CircNR3C2 promotes HRD1-mediated tumor-suppressive effect via sponging miR-513a-3p in triple-negative breast cancer. *Mol. Cancer* 20:25. doi: 10.1186/s12943-021-01321-x

Garcia-Vazquez, R., Gallardo Rincon, D., Ruiz-Garcia, E., Meneses Garcia, A., Hernandez De La Cruz, O. N., Astudillo-De La Vega, H., et al. (2018). let-7d-3p is associated with apoptosis and response to neoadjuvant chemotherapy in ovarian cancer. *Oncol. Rep.* 39, 3086–3094. doi: 10.3892/or.2018.6366

Ge, G., Zhang, W., Niu, L., Yan, Y., Ren, Y., and Zou, Y. (2016). miR-215 functions as a tumor suppressor in epithelial ovarian cancer through regulation of the X-chromosome-linked inhibitor of apoptosis. *Oncol. Rep.* 35, 1816–1822. doi: 10.3892/or.2015.4482

Gu, Z. W., He, Y. F., Wang, W. J., Tian, Q., and Di, W. (2019). MiR-1180 from bone marrow-derived mesenchymal stem cells induces glycolysis and chemoresistance in ovarian cancer cells by upregulating the Wnt signaling pathway. *J. Zhejiang Univ. Sci. B* 20, 219–237. doi: 10.1631/jzus.B1800190

Guo, H., Ha, C., Dong, H., Yang, Z., Ma, Y., and Ding, Y. (2019). Cancer-associated fibroblast-derived exosomal microRNA-98-5p promotes cisplatin resistance in ovarian cancer by targeting CDKN1A. *Cancer Cell. Int.* 19:347. doi: 10.1186/s12935-019-1051-3

Guo, J., and Pan, H. (2019). Long noncoding RNA LINC01125 enhances cisplatin sensitivity of ovarian cancer via miR-1972. *Med. Sci. Monit.* 25, 9844–9854. doi: 10.12659/MSM.916820

Guo, M., Li, S., Zhao, X., Yuan, Y., Zhang, B., and Guan, Y. (2020). Knockdown of circular RNA Hsa_circ_0000714 can regulate RAB17 by sponging miR-370-3p to reduce paclitaxel resistance of ovarian cancer through CDK6/RB pathway. *Onco Targets Ther.* 13, 13211–13224. doi: 10.2147/OTT.S285153

Han, H., Fan, G., Song, S., Jiang, Y., Qian, C., Zhang, W., et al. (2021). piRNA-30473 contributes to tumorigenesis and poor prognosis by regulating m6A RNA methylation in DLBCL. *Blood* 137, 1603–1614. doi: 10.1182/blood.2019003764

Hartmaier, R. J., Albacker, L. A., Chmielecki, J., Bailey, M., He, J., Goldberg, M. E., et al. (2017). High-throughput genomic profiling of adult solid tumors reveals novel insights into cancer pathogenesis. *Cancer Res.* 77, 2464–2475. doi: 10.1158/0008-5472.CAN-16-2479

He, L., Zhu, W., Chen, Q., Yuan, Y., Wang, Y., Wang, J., et al. (2019). Ovarian cancer cell-secreted exosomal miR-205 promotes metastasis by inducing angiogenesis. *Theranostics* 9, 8206–8220. doi: 10.7150/thno.37455

Hisamatsu, T., McGuire, M., Wu, S. Y., Rupaimoole, R., Pradeep, S., Bayraktar, E., et al. (2019). PRKRA/PACT expression promotes chemoresistance of mucinous ovarian cancer. *Mol. Cancer Ther.* 18, 162–172. doi: 10.1158/1535-7163.MCT-17-1050

Hong, X., Liu, N., Liang, Y., He, Q., Yang, X., Lei, Y., et al. (2020). Circular RNA CRIM1 functions as a ceRNA to promote nasopharyngeal carcinoma metastasis and docetaxel chemoresistance through upregulating FOXQ1. *Mol. Cancer* 19:33. doi: 10.1186/s12943-020-01149-x

Huang, X., Li, Z., Zhang, Q., Wang, W., Li, B., Wang, L., et al. (2019). Circular RNA AKT3 upregulates PIK3R1 to enhance cisplatin resistance in gastric cancer via miR-198 suppression. *Mol. Cancer* 18:71. doi: 10.1186/s12943-019-0969-3

Jeong, J. Y., Kang, H., Kim, T. H., Kim, G., Heo, J. H., Kwon, A. Y., et al. (2017). MicroRNA-136 inhibits cancer stem cell activity and enhances the anti-tumor effect of paclitaxel against chemoresistant ovarian cancer cells by targeting Notch3. *Cancer Lett.* 386, 168–178. doi: 10.1016/j.canlet.2016.11.017

Jiang, J., Xie, C., Liu, Y., Shi, Q., and Chen, Y. (2019). Up-regulation of miR-383-5p suppresses proliferation and enhances chemosensitivity in ovarian cancer cells by targeting TRIM27. *Biomed. Pharmacother.* 109, 595–601. doi: 10.1016/j.biopha.2018.10.148

Jin, H., Ma, J., Xu, J., Li, H., Chang, Y., Zang, N., et al. (2020). Oncogenic role of MIR516A in human bladder cancer was mediated by its attenuating PHLPP2 expression and BECN1-dependent autophagy. *Autophagy* 17, 840–854. doi: 10.1080/15548627.2020.1733262

Jin, P., Liu, Y., and Wang, R. (2018). STAT3 regulated miR-216a promotes ovarian cancer proliferation and cisplatin resistance. *Biosci. Rep.* 38:BSR20180547. doi: 10.1042/BSR20180547

Komoll, R. M., Hu, Q., Olarewaju, O., von Dohlen, L., Yuan, Q., Xie, Y., et al. (2021). MicroRNA-342-3p is a potent tumour suppressor in hepatocellular carcinoma. *J. Hepatol.* 74, 122–134. doi: 10.1016/j.jhep.2020.07.039

Kristensen, L. S., Andersen, M. S., Stagsted, L. V. W., Ebbesen, K. K., Hansen, T. B., and Kjems, J. (2019). The biogenesis, biology and characterization of circular RNAs. *Nat. Rev. Genet.* 20, 675–691. doi: 10.1038/s41576-019-0158-7

Lheureux, S., Braunstein, M., and Oza, A. M. (2019). Epithelial ovarian cancer: evolution of management in the era of precision medicine. *CA Cancer J. Clin.* 69, 280–304. doi: 10.3322/caac.21559

Li, B., Zhu, L., Lu, C., Wang, C., Wang, H., Jin, H., et al. (2021). circNDUFB2 inhibits non-small cell lung cancer progression via destabilizing IGF2BPs and activating anti-tumor immunity. *Nat. Commun.* 12:295. doi: 10.1038/s41467-020-20527-z

Li, J., Yang, S., Su, N., Wang, Y., Yu, J., Qiu, H., et al. (2016). Overexpression of long non-coding RNA HOTAIR leads to chemoresistance by activating the Wnt/beta-catenin pathway in human ovarian cancer. *Tumour Biol.* 37, 2057–2065. doi: 10.1007/s13277-015-3998-6

Li, L., Xu, Q. H., Dong, Y. H., Li, G. X., Yang, L., Wang, L. W., et al. (2016). MiR-181a upregulation is associated with epithelial-to-mesenchymal transition (EMT) and multidrug resistance (MDR) of ovarian cancer cells. *Eur. Rev. Med. Pharmacol. Sci.* 20, 2004–2010.

Li, M., Cai, J., Han, X., and Ren, Y. (2020). Downregulation of circNRIP1 suppresses the paclitaxel resistance of ovarian cancer via regulating the miR-211-5p/HOXC8 axis. *Cancer Manag. Res.* 12, 9159–9171. doi: 10.2147/CMAR.S268872

Li, S., Cao, J., Zhang, W., Zhang, F., Ni, G., Luo, Q., et al. (2016). Protein tyrosine phosphatase PTPN3 promotes drug resistance and stem cell-like characteristics in ovarian cancer. *Sci. Rep.* 6:36873. doi: 10.1038/srep36873

Li, X., Chen, W., Jin, Y., Xue, R., Su, J., Mu, Z., et al. (2019). miR-142-5p enhances cisplatin-induced apoptosis in ovarian cancer cells by targeting multiple anti-apoptotic genes. *Biochem. Pharmacol.* 161, 98–112. doi: 10.1016/j.bcp.2019.01.009

Li, X., Chen, W., Zeng, W., Wan, C., Duan, S., and Jiang, S. (2017a). microRNA-137 promotes apoptosis in ovarian cancer cells via the regulation of XIAP. *Br. J. Cancer* 116, 66–76. doi: 10.1038/bjc.2016.379

Li, X., Jin, Y., Mu, Z., Chen, W., and Jiang, S. (2017b). MicroRNA146a5p enhances cisplatininduced apoptosis in ovarian cancer cells by targeting multiple antiapoptotic genes. *Int. J. Oncol.* 51, 327–335. doi: 10.3892/ijo.2017.4023

Li, Z., Niu, H., Qin, Q., Yang, S., Wang, Q., Yu, C., et al. (2019). lncRNA UCA1 mediates resistance to cisplatin by regulating the miR-143/FOSL2-signaling pathway in ovarian cancer. *Mol. Ther. Nucleic Acids* 17, 92–101. doi: 10.1016/j.omtn.2019.05.007

Li, Z. Y., Wang, X. L., Dang, Y., Zhu, X. Z., Zhang, Y. H., Cai, B. X., et al. (2020). Long non-coding RNA UCA1 promotes the progression of paclitaxel resistance in ovarian cancer by regulating the miR-654-5p/SIK2 axis. *Eur. Rev. Med. Pharmacol. Sci.* 24, 591–603. doi: 10.26355/eurrev_202001_20035

Liang, F., Ren, C., Wang, J., Wang, S., Yang, L., Han, X., et al. (2019). The crosstalk between STAT3 and p53/RAS signaling controls cancer cell metastasis and cisplatin resistance via the Slug/MAPK/PI3K/AKT-mediated regulation of EMT and autophagy. *Oncogenesis* 8:59. doi: 10.1038/s41389-019-0165-8

Lin, H., Shen, L., Lin, Q., Dong, C., Maswela, B., Illahi, G. S., et al. (2020). SNHG5 enhances Paclitaxel sensitivity of ovarian cancer cells through sponging miR-23a. *Biomed. Pharmacother.* 123:109711. doi: 10.1016/j.biopha.2019.109711

Liu, E., Liu, Z., Zhou, Y., Mi, R., and Wang, D. (2015). Overexpression of long non-coding RNA PVT1 in ovarian cancer cells promotes cisplatin resistance by regulating apoptotic pathways. *Int. J. Clin. Exp. Med.* 8, 20565–20572.

Liu, J., Zhang, X., Huang, Y., Zhang, Q., Zhou, J., Zhang, X., et al. (2019). miR-200b and miR-200c co-contribute to the cisplatin sensitivity of ovarian cancer cells by targeting DNA methyltransferases. *Oncol. Lett.* 17, 1453–1460. doi: 10.3892/ol.2018.9745

Liu, R., Guo, H., and Lu, S. (2018). MiR-335-5p restores cisplatin sensitivity in ovarian cancer cells through targeting BCL2L2. *Cancer Med.* 7, 4598–4609. doi: 10.1002/cam4.1682

Liu, S., Zou, B., Tian, T., Luo, X., Mao, B., Zhang, X., et al. (2018). Overexpression of the lncRNA FER1L4 inhibits paclitaxel tolerance of ovarian cancer cells via the regulation of the MAPK signaling pathway. *J. Cell Biochem.* [Epub ahead of print]. doi: 10.1002/jcb.28032

Liu, Y., Han, S., Li, Y., Liu, Y., Zhang, D., Li, Y., et al. (2017). MicroRNA-20a contributes to cisplatin-resistance and migration of OVCAR3 ovarian cancer cell line. *Oncol. Lett.* 14, 1780–1786. doi: 10.3892/ol.2017.6348

Long, X., Song, K., Hu, H., Tian, Q., Wang, W., Dong, Q., et al. (2019). Long non-coding RNA GAS5 inhibits DDP-resistance and tumor progression of epithelial ovarian cancer via GAS5-E2F4-PARP1-MAPK axis. *J. Exp. Clin. Cancer Res.* 38:345. doi: 10.1186/s13046-019-1329-2

Luo, Y., and Gui, R. (2020). Circulating exosomal circFoxp1 confers cisplatin resistance in epithelial ovarian cancer cells. *J. Gynecol. Oncol.* 31:e75. doi: 10.3802/jgo.2020.31.e75

Luo, Y., Zheng, S., Wu, Q., Wu, J., Zhou, R., Wang, C., et al. (2021). Long noncoding RNA (lncRNA) EIF3J-DT induces chemoresistance of gastric cancer via autophagy activation. *Autophagy* [Epub ahead of print]. doi: 10.1080/15548627.2021.1901204

Maass, P. G., Glazar, P., Memczak, S., Dittmar, G., Hollfinger, I., Schreyer, L., et al. (2017). A map of human circular RNAs in clinically relevant tissues. *J. Mol. Med.* 95, 1179–1189. doi: 10.1007/s00109-017-1582-9

Mak, C. S., Yung, M. M., Hui, L. M., Leung, L. L., Liang, R., Chen, K., et al. (2017). MicroRNA-141 enhances anoikis resistance in metastatic progression of ovarian cancer through targeting KLF12/Sp1/survivin axis. *Mol. Cancer* 16:11. doi: 10.1186/s12943-017-0582-2

Meghani, K., Fuchs, W., Detappe, A., Drane, P., Gogola, E., Rottenberg, S., et al. (2018). Multifaceted impact of MicroRNA 493-5p on genome-stabilizing pathways induces platinum and parp inhibitor resistance in BRCA2-mutated carcinomas. *Cell Rep.* 23, 100–111. doi: 10.1016/j.celrep.2018.03.038

Memczak, S., Jens, M., Elefsinioti, A., Torti, F., Krueger, J., Rybak, A., et al. (2013). Circular RNAs are a large class of animal RNAs with regulatory potency. *Nature* 495, 333–338. doi: 10.1038/nature11928

Miller, C. M., Wan, W. B., Seth, P. P., and Harris, E. N. (2018). Endosomal escape of antisense oligonucleotides internalized by stabilin receptors is regulated by Rab5C and EEA1 during endosomal maturation. *Nucleic Acid Ther.* 28, 86–96. doi: 10.1089/nat.2017.0694

Munoz-Galvan, S., Felipe-Abrio, B., Verdugo-Sivianes, E. M., Perez, M., Jimenez-Garcia, M. P., Suarez-Martinez, E., et al. (2020). Downregulation of MYPT1 increases tumor resistance in ovarian cancer by targeting the Hippo pathway and increasing the stemness. *Mol. Cancer* 19:7. doi: 10.1186/s12943-020-1130-z

Ou, R., Mo, L., Tang, H., Leng, S., Zhu, H., Zhao, L., et al. (2020). circRNA-AKT1 Sequesters miR-942-5p to upregulate AKT1 and promote cervical cancer progression. *Mol. Ther. Nucleic Acids* 20, 308–322. doi: 10.1016/j.omtn.2020.01.003

Ozes, A. R., Miller, D. F., Ozes, O. N., Fang, F., Liu, Y., Matei, D., et al. (2016). NF-kappaB-HOTAIR axis links DNA damage response, chemoresistance and cellular senescence in ovarian cancer. *Oncogene* 35, 5350–5361. doi: 10.1038/onc.2016.75

Park, G. B., and Kim, D. (2019). MicroRNA-503-5p inhibits the CD97-mediated JAK2/STAT3 pathway in metastatic or paclitaxel-resistant ovarian cancer cells. *Neoplasia* 21, 206–215. doi: 10.1016/j.neo.2018.12.005

Qin, X., Sun, L., and Wang, J. (2017). Restoration of microRNA-708 sensitizes ovarian cancer cells to cisplatin via IGF2BP1/Akt pathway. *Cell Biol. Int.* 41, 1110–1118. doi: 10.1002/cbin.10819

Qiu, J. J., Lin, Y. Y., Ye, L. C., Ding, J. X., Feng, W. W., Jin, H. Y., et al. (2014). Overexpression of long non-coding RNA HOTAIR predicts poor patient prognosis and promotes tumor metastasis in epithelial ovarian cancer. *Gynecol. Oncol.* 134, 121–128. doi: 10.1016/j.ygyno.2014.03.556

Quinn, J. J., and Chang, H. Y. (2016). Unique features of long non-coding RNA biogenesis and function. *Nat. Rev. Genet.* 17, 47–62. doi: 10.1038/nrg.2015.10

Ramat, A., and Simonelig, M. (2021). Functions of PIWI proteins in gene regulation: new arrows added to the piRNA quiver. *Trends Genet.* 37, 188–200. doi: 10.1016/j.tig.2020.08.011

Sajadpoor, Z., Amini-Farsani, Z., Teimori, H., Shamsara, M., Sangtarash, M. H., Ghasemi-Dehkordi, P., et al. (2018). Valproic acid promotes apoptosis and cisplatin sensitivity through downregulation of H19 noncoding RNA in ovarian A2780 cells. *Appl. Biochem. Biotechnol.* 185, 1132–1144. doi: 10.1007/s12010-017-2684-0

Salzman, J., Chen, R. E., Olsen, M. N., Wang, P. L., and Brown, P. O. (2013). Cell-type specific features of circular RNA expression. *PLoS Genet.* 9:e1003777. doi: 10.1371/journal.pgen.1003777

Samuel, P., Pink, R. C., Caley, D. P., Currie, J. M., Brooks, S. A., and Carter, D. R. (2016). Over-expression of miR-31 or loss of KCNMA1 leads to increased cisplatin resistance in ovarian cancer cells. *Tumour Biol.* 37, 2565–2573. doi: 10.1007/s13277-015-4081-z

Shen, P., Yang, T., Chen, Q., Yuan, H., Wu, P., Cai, B., et al. (2021). CircNEIL3 regulatory loop promotes pancreatic ductal adenocarcinoma progression via miRNA sponging and A-to-I RNA-editing. *Mol. Cancer* 20:51. doi: 10.1186/s12943-021-01333-7

Shi, C., and Wang, M. (2018). LINC01118 modulates paclitaxel resistance of epithelial ovarian cancer by regulating miR-134/ABCC1. *Med. Sci. Monit.* 24, 8831–8839. doi: 10.12659/MSM.910932

Shi, X., Xiao, L., Mao, X., He, J., Ding, Y., Huang, J., et al. (2018). miR-205-5p mediated downregulation of PTEN contributes to cisplatin resistance in C13K human ovarian cancer cells. *Front. Genet.* 9:555. doi: 10.3389/fgene.2018.00555

Shuai, S., Suzuki, H., Diaz-Navarro, A., Nadeu, F., Kumar, S. A., Gutierrez-Fernandez, A., et al. (2019). The U1 spliceosomal RNA is recurrently mutated in multiple cancers. *Nature* 574, 712–716. doi: 10.1038/s41586-019-1651-z

Statello, L., Guo, C. J., Chen, L. L., and Huarte, M. (2021). Gene regulation by long non-coding RNAs and its biological functions. *Nat. Rev. Mol. Cell Biol.* 22, 96–118. doi: 10.1038/s41580-020-00315-9

Sun, J., Cai, X., Yung, M. M., Zhou, W., Li, J., Zhang, Y., et al. (2019). miR-137 mediates the functional link between c-Myc and EZH2 that regulates cisplatin resistance in ovarian cancer. *Oncogene* 38, 564–580. doi: 10.1038/s41388-018-0459-x

Sun, Y., Wu, J., Dong, X., Zhang, J., Meng, C., and Liu, G. (2021). MicroRNA-506-3p increases the response to PARP inhibitors and cisplatin by targeting EZH2/beta-catenin in serous ovarian cancers. *Transl. Oncol.* 14:100987. doi: 10.1016/j.tranon.2020.100987

Sun, Z., Gao, S., Xuan, L., and Liu, X. (2020). Long non-coding RNA FEZF1-AS1 induced progression of ovarian cancer via regulating miR-130a-5p/SOX4 axis. *J. Cell. Mol. Med.* 24, 4275–4285. doi: 10.1111/jcmm.15088

Sung, H., Ferlay, J., Siegel, R. L., Laversanne, M., Soerjomataram, I., Jemal, A., et al. (2021). Global cancer statistics 2020: GLOBOCAN estimates of incidence and mortality worldwide for 36 cancers in 185 countries. *CA Cancer J. Clin.* 71, 209–249. doi: 10.3322/caac.21660

Tan, W. X., Sun, G., Shangguan, M. Y., Gui, Z., Bao, Y., Li, Y. F., et al. (2020). Novel role of lncRNA CHRF in cisplatin resistance of ovarian cancer is mediated by miR-10b induced EMT and STAT3 signaling. *Sci. Rep.* 10:14768. doi: 10.1038/s41598-020-71153-0

Tew, W. P., Lacchetti, C., Ellis, A., Maxian, K., Banerjee, S., Bookman, M., et al. (2020). PARP inhibitors in the management of ovarian cancer: ASCO guideline. *J. Clin. Oncol.* 38, 3468–3493. doi: 10.1200/JCO.20.01924

Tsitsipatis, D., Grammatikakis, I., Driscoll, R. K., Yang, X., Abdelmohsen, K., Harris, S. C., et al. (2021). AUF1 ligand circPCNX reduces cell proliferation by competing with p21 mRNA to increase p21 production. *Nucleic Acids Res.* 49, 1631–1646. doi: 10.1093/nar/gkaa1246

Tung, C. H., Kuo, L. W., Huang, M. F., Wu, Y. Y., Tsai, Y. T., Wu, J. E., et al. (2020). MicroRNA-150-5p promotes cell motility by inhibiting c-Myb-mediated Slug suppression and is a prognostic biomarker for recurrent ovarian cancer. *Oncogene* 39, 862–876. doi: 10.1038/s41388-019-1025-x

Tung, S. L., Huang, W. C., Hsu, F. C., Yang, Z. P., Jang, T. H., Chang, J. W., et al. (2017). miRNA-34c-5p inhibits amphiregulin-induced ovarian cancer stemness and drug resistance via downregulation of the AREG-EGFR-ERK pathway. *Oncogenesis* 6:e326. doi: 10.1038/oncsis.2017.25

Vescarelli, E., Gerini, G., Megiorni, F., Anastasiadou, E., Pontecorvi, P., Solito, L., et al. (2020). MiR-200c sensitizes Olaparib-resistant ovarian cancer cells by targeting Neuropilin 1. *J. Exp. Clin. Cancer Res.* 39:3. doi: 10.1186/s13046-019-1490-7

Wang, D. Y., Li, N., and Cui, Y. L. (2020). Long non-coding RNA CCAT1 sponges miR-454 to promote chemoresistance of ovarian cancer cells to cisplatin by regulation of surviving. *Cancer Res. Treat.* 52, 798–814. doi: 10.4143/crt.2019.498

Wang, H., Fang, L., Jiang, J., Kuang, Y., Wang, B., Shang, X., et al. (2018). The cisplatin-induced lncRNA PANDAR dictates the chemoresistance of ovarian cancer via regulating SFRS2-mediated p53 phosphorylation. *Cell Death Dis.* 9:1103. doi: 10.1038/s41419-018-1148-y

Wang, J., Ye, C., Liu, J., and Hu, Y. (2018). UCA1 confers paclitaxel resistance to ovarian cancer through miR-129/ABCB1 axis. *Biochem. Biophys. Res. Commun.* 501, 1034–1040. doi: 10.1016/j.bbrc.2018.05.104

Wang, K., Hu, Y. B., Zhao, Y., and Ye, C. (2021). LncRNA ANRIL regulates ovarian cancer progression and tumor stem cell-like characteristics via miR-324-5p/Ran axis. *Onco Targets Ther.* 14, 565–576. doi: 10.2147/OTT.S273614

Wang, P., Yang, Z., Ye, T., Shao, F., Li, J., Sun, N., et al. (2020). lncTUG1/miR-144-3p affect the radiosensitivity of esophageal squamous cell carcinoma by competitively regulating c-MET. *J. Exp. Clin. Cancer Res.* 39:7. doi: 10.1186/s13046-019-1519-y

Wang, X., He, Y., Mackowiak, B., and Gao, B. (2021). MicroRNAs as regulators, biomarkers and therapeutic targets in liver diseases. *Gut* 70, 784–795. doi: 10.1136/gutjnl-2020-322526

Wang, Y., Bao, W., Liu, Y., Wang, S., Xu, S., Li, X., et al. (2018). miR-98-5p contributes to cisplatin resistance in epithelial ovarian cancer by suppressing miR-152 biogenesis via targeting Dicer1. *Cell Death Dis.* 9:447. doi: 10.1038/s41419-018-0390-7

Wang, Y., Wang, H., Song, T., Zou, Y., Jiang, J., Fang, L., et al. (2015). HOTAIR is a potential target for the treatment of cisplatinresistant ovarian cancer. *Mol. Med. Rep.* 12, 2211–2216. doi: 10.3892/mmr.2015.3562

Wang, Y., Wang, X., Han, L., and Hu, D. (2020). LncRNA MALAT1 regulates the progression and cisplatin resistance of ovarian cancer cells via modulating miR-1271-5p/E2F5 axis. *Cancer Manag. Res.* 12, 9999–10010. doi: 10.2147/CMAR.S261979

Wei, Z., Liu, Y., Wang, Y., Zhang, Y., Luo, Q., Man, X., et al. (2016). Downregulation of Foxo3 and TRIM31 by miR-551b in side population promotes cell proliferation, invasion, and drug resistance of ovarian cancer. *Med. Oncol.* 33:126. doi: 10.1007/s12032-016-0842-9

Wiltshire, T. D., Lovejoy, C. A., Wang, T., Xia, F., O'Connor, M. J., and Cortez, D. (2010). Sensitivity to poly(ADP-ribose) polymerase (PARP) inhibition identifies ubiquitin-specific peptidase 11 (USP11) as a regulator of DNA double-strand break repair. *J. Biol. Chem.* 285, 14565–14571. doi: 10.1074/jbc.M110.104745

Winham, S. J., Larson, N. B., Armasu, S. M., Fogarty, Z. C., Larson, M. C., McCauley, B. M., et al. (2019). Molecular signatures of X chromosome inactivation and associations with clinical outcomes in epithelial ovarian cancer. *Hum. Mol. Genet.* 28, 1331–1342. doi: 10.1093/hmg/ddy444

Wong, C. M., Tsang, F. H., and Ng, I. O. (2018). Non-coding RNAs in hepatocellular carcinoma: molecular functions and pathological implications. *Nat. Rev. Gastroenterol. Hepatol.* 15, 137–151. doi: 10.1038/nrgastro.2017.169

Wu, D., Lu, P., Mi, X., and Miao, J. (2018). Downregulation of miR-503 contributes to the development of drug resistance in ovarian cancer by targeting PI3K p85. *Arch. Gynecol. Obstet.* 297, 699–707. doi: 10.1007/s00404-018-4649-0

Wu, D. D., Li, X. S., Meng, X. N., Yan, J., and Zong, Z. H. (2016). MicroRNA-873 mediates multidrug resistance in ovarian cancer cells by targeting ABCB1. *Tumour Biol.* 37, 10499–10506. doi: 10.1007/s13277-016-4944-y

Wu, Y., Zhou, Y., He, J., Sun, H., and Jin, Z. (2019). Long non-coding RNA H19 mediates ovarian cancer cell cisplatin-resistance and migration during EMT. *Int. J. Clin. Exp. Pathol.* 12, 2506–2515.

Xia, B., Lin, M., Dong, W., Chen, H., Li, B., Zhang, X., et al. (2018). Upregulation of miR-874-3p and miR-874-5p inhibits epithelial ovarian cancer malignancy via SIK2. *J. Biochem. Mol. Toxicol.* 32:e22168. doi: 10.1002/jbt.22168

Xia, B., Zhao, Z., Wu, Y., Wang, Y., Zhao, Y., and Wang, J. (2020). Circular RNA circTNPO3 regulates paclitaxel resistance of ovarian cancer cells by miR-1299/NEK2 signaling pathway. *Mol. Ther. Nucleic Acids* 21, 780–791. doi: 10.1016/j.omtn.2020.06.002

Xia, S., Feng, J., Lei, L., Hu, J., Xia, L., Wang, J., et al. (2017). Comprehensive characterization of tissue-specific circular RNAs in the human and mouse genomes. *Brief Bioinform.* 18, 984–992. doi: 10.1093/bib/bbw081

Xiao, M., Cai, J., Cai, L., Jia, J., Xie, L., Zhu, Y., et al. (2017). Let-7e sensitizes epithelial ovarian cancer to cisplatin through repressing DNA double strand break repair. *J. Ovarian Res.* 10, 24. doi: 10.1186/s13048-017-0321-8

Xiao, S., Zhang, M., Liu, C., and Wang, D. (2018). MiR-514 attenuates proliferation and increases chemoresistance by targeting ATP binding cassette subfamily in ovarian cancer. *Mol. Genet. Genomics* 293, 1159–1167. doi: 10.1007/s00438-018-1447-0

Xing, S., Tian, Z., Zheng, W., Yang, W., Du, N., Gu, Y., et al. (2021). Hypoxia downregulated miR-4521 suppresses gastric carcinoma progression through regulation of IGF2 and FOXM1. *Mol. Cancer* 20:9. doi: 10.1186/s12943-020-01295-2

Xu, M., Xiao, J., Chen, M., Yuan, L., Li, J., Shen, H., et al. (2018). miR1495p promotes chemotherapeutic resistance in ovarian cancer via the inactivation of the Hippo signaling pathway. *Int. J. Oncol.* 52, 815–827. doi: 10.3892/ijo.2018.4252

Xu, M., Zhou, K., Wu, Y., Wang, L., and Lu, S. (2019). Linc00161 regulated the drug resistance of ovarian cancer by sponging microRNA-128 and modulating MAPK1. *Mol. Carcinog.* 58, 577–587. doi: 10.1002/mc.22952

Xu, Q. F., Tang, Y. X., and Wang, X. (2018). LncRNA EBIC promoted proliferation, metastasis and cisplatin resistance of ovarian cancer cells and predicted poor survival in ovarian cancer patients. *Eur. Rev. Med. Pharmacol. Sci.* 22, 4440–4447. doi: 10.26355/eurrev_201807_15495

Yan, H., Xia, J. Y., and Feng, F. Z. (2017). Long non-coding RNA ENST00000457645 reverses cisplatin resistance in CP70 ovarian cancer cells. *Genet. Mol. Res.* 16:gmr16019411. doi: 10.4238/gmr16019411

Yan, M., Yang, X., Shen, R., Wu, C., Wang, H., Ye, Q., et al. (2018). miR-146b promotes cell proliferation and increases chemosensitivity, but attenuates cell migration and invasion via FBXL10 in ovarian cancer. *Cell Death Dis.* 9:1123. doi: 10.1038/s41419-018-1093-9

Yu, J. L., and Gao, X. (2020). MicroRNA 1301 inhibits cisplatin resistance in human ovarian cancer cells by regulating EMT and autophagy. *Eur. Rev. Med. Pharmacol. Sci.* 24, 1688–1696. doi: 10.26355/eurrev_202002_20343

Yu, Y., Zhang, X., Tian, H., Zhang, Z., and Tian, Y. (2018). Knockdown of long non-coding RNA HOTAIR increases cisplatin sensitivity in ovarian cancer by inhibiting cisplatin-induced autophagy. *J. BUON* 23, 1396–1401.

Zeng, Z., Xia, L., Fan, S., Zheng, J., Qin, J., Fan, X., et al. (2021). Circular RNA CircMAP3K5 acts as a MicroRNA-22-3p sponge to promote resolution of intimal hyperplasia via TET2-mediated smooth muscle cell differentiation. *Circulation* 143, 354–371. doi: 10.1161/CIRCULATIONAHA.120.049715

Zhang, J., Liu, J., Xu, X., and Li, L. (2017). Curcumin suppresses cisplatin resistance development partly via modulating extracellular vesicle-mediated transfer of MEG3 and miR-214 in ovarian cancer. *Cancer Chemother. Pharmacol.* 79, 479–487. doi: 10.1007/s00280-017-3238-4

Zhang, M., Liu, S., Fu, C., Wang, X., Zhang, M., Liu, G., et al. (2019). LncRNA KB-1471A8.2 overexpression suppresses cell proliferation and migration and antagonizes the paclitaxel resistance of ovarian cancer cells. *Cancer Biother. Radiopharm.* 34, 316–324. doi: 10.1089/cbr.2018.2698

Zhang, P. F., Wu, J., Luo, J. H., Li, K. S., Wang, F., Huang, W., et al. (2019). SNHG22 overexpression indicates poor prognosis and induces chemotherapy resistance via the miR-2467/Gal-1 signaling pathway in epithelial ovarian carcinoma. *Aging* 11, 8204–8216. doi: 10.18632/aging.102313

Zhang, S., Cheng, J., Quan, C., Wen, H., Feng, Z., Hu, Q., et al. (2020). circCELSR1 (hsa_circ_0063809) contributes to paclitaxel resistance of ovarian cancer cells by regulating FOXR2 expression via miR-1252. *Mol. Ther. Nucleic Acids* 19, 718–730. doi: 10.1016/j.omtn.2019.12.005

Zhang, Z., Zhang, L., Wang, B., Wei, R., Wang, Y., Wan, J., et al. (2020). MiR-337-3p suppresses proliferation of epithelial ovarian cancer by targeting PIK3CA and PIK3CB. *Cancer Lett.* 469, 54–67. doi: 10.1016/j.canlet.2019.10.021

Zhao, H., Bi, T., Qu, Z., Jiang, J., Cui, S., and Wang, Y. (2014). Expression of miR-224-5p is associated with the original cisplatin resistance of ovarian papillary serous carcinoma. *Oncol. Rep.* 32, 1003–1012. doi: 10.3892/or.2014.3311

Zhao, Y., and Hong, L. (2021). lncRNA-PRLB confers paclitaxel resistance of ovarian cancer cells by regulating RSF1/NF-kappaB signaling pathway. *Cancer Biother. Radiopharm.* 36, 202–210. doi: 10.1089/cbr.2019.3363

Zhao, Z., Ji, M., Wang, Q., He, N., and Li, Y. (2019). Circular RNA Cdr1as upregulates SCAI to suppress cisplatin resistance in ovarian cancer via miR-1270 suppression. *Mol. Ther. Nucleic Acids* 18, 24–33. doi: 10.1016/j.omtn.2019.07.012

Zheng, Y., Li, Z., Yang, S., Wang, Y., and Luan, Z. (2020). CircEXOC6B suppresses the proliferation and motility and sensitizes ovarian cancer cells to paclitaxel through miR-376c-3p/FOXO3 axis. *Cancer Biother. Radiopharm.* [Epub ahead of print]. doi: 10.1089/cbr.2020.3739

Zheng, Z. G., Xu, H., Suo, S. S., Xu, X. L., Ni, M. W., Gu, L. H., et al. (2016). The essential role of H19 contributing to cisplatin resistance by regulating glutathione metabolism in high-grade serous ovarian cancer. *Sci. Rep.* 6:26093. doi: 10.1038/srep26093

Zhou, J., Alfraidi, A., Zhang, S., Santiago-O'Farrill, J. M., Yerramreddy Reddy, V. K., Alsaadi, A., et al. (2017). A novel compound ARN-3236 inhibits salt-inducible kinase 2 and sensitizes ovarian cancer cell lines and xenografts to paclitaxel. *Clin. Cancer Res.* 23, 1945–1954. doi: 10.1158/1078-0432.CCR-16-1562

Zhou, Y., Wang, M., Shuang, T., Liu, Y., Zhang, Y., and Shi, C. (2019). MiR-1307 influences the chemotherapeutic sensitivity in ovarian cancer cells through the regulation of the CIC transcriptional repressor. *Pathol. Res. Pract.* 215:152606. doi: 10.1016/j.prp.2019.152606

Zhu, M., Yang, L., and Wang, X. (2020). NEAT1 knockdown suppresses the cisplatin resistance in ovarian cancer by regulating miR-770-5p/PARP1 axis. *Cancer Manag. Res.* 12, 7277–7289. doi: 10.2147/CMAR.S257311

Zou, J., Liu, L., Wang, Q., Yin, F., Yang, Z., Zhang, W., et al. (2017). Downregulation of miR-429 contributes to the development of drug resistance in epithelial ovarian cancer by targeting ZEB1. *Am. J. Transl. Res.* 9, 1357–1368.

Conflict of Interest: The authors declare that the research was conducted in the absence of any commercial or financial relationships that could be construed as a potential conflict of interest.

Publisher's Note: All claims expressed in this article are solely those of the authors and do not necessarily represent those of their affiliated organizations, or those of the publisher, the editors and the reviewers. Any product that may be evaluated in this article, or claim that may be made by its manufacturer, is not guaranteed or endorsed by the publisher.

frontiers in Genetics

ORIGINAL RESEARCH
published: 01 September 2021
doi: 10.3389/fgene.2021.695245

Characterization of the Potential Role of NTPCR in Epithelial Ovarian Cancer by Integrating Transcriptomic and Metabolomic Analysis

*Hongkai Shang[1,2,3], Huizhi Zhang[1,2], Ziyao Ren[2,3], Hongjiang Zhao[1,2], Zhifen Zhang[4] and Jinyi Tong[1,4]**

[1] Department of the Fourth Clinical Medical College, Zhejiang Chinese Medical University, Hangzhou, China, [2] Department of Gynecology, Hangzhou First People's Hospital, Hangzhou, China, [3] Department of Gynecology, Zhejiang University School of Medicine, Hangzhou, China, [4] Department of Gynecology, Hangzhou Women's Hospital (Maternity and Child Health Care Hospital), Hangzhou, China

Background: Epithelial ovarian carcinoma (EOC) is a malignant tumor with high motility in women. Our previous study found that dysregulated nucleoside-triphosphatase cancer-related (NTPCR) was associated with the prognosis of EOC patients, and thus, this present study attempted to explore the potential roles of NTPCR in disease progression.

Methods: Expressed level of NTPCR was investigated in EOC tissues by RT-qPCR and Western blot analysis. NTPCR shRNA and overexpression vector were generated and transfected into OVCAR-3 or SKOV3 cells to detect the effect of NTPCR on cell proliferation, cell cycle, cell migration, and invasion. Transcriptomic sequencing and metabolite profiling analysis were performed in shNTPCR groups to identify transcriptome or metabolite alteration that might contribute to EOC. Finally, we searched the overlapped signaling pathways correlated with differential metabolites and differentially expressed genes (DEGs) by integrating analysis.

Results: Comparing para-cancerous tissues, we found that NTPCR is highly expressed in cancer tissues ($p < 0.05$). Overexpression of NTPCR inhibited cell proliferation, migration, and invasion and reduced the proportion of S- and G2/M-phase cells, while downregulation of NTPCR showed the opposite results. RNA sequencing analysis demonstrated cohorts of DEGs were identified in shNTPCR samples. Protein–protein interaction networks were constructed for DEGs. STAT1 (degree = 43) and OAS2 (degree = 36) were identified as hub genes in the network. Several miRNAs together with target genes were predicted to be crucial genes related to disease progression, including *hsa-miR-124-3p*, *hsa-miR-30a-5p*, *hsa-miR-146a-5*, *EP300*, *GATA2,* and *STAT3*. We also screened the differential metabolites from shNTPCR samples, including 22 upregulated and 22 downregulated metabolites. By integrating transcriptomics and metabolomics analysis, eight overlapped pathways were correlated with these DEGs and differential metabolites, such as primary bile acid biosynthesis, protein digestion, and absorption, pentose, and glucuronate interconversions.

OPEN ACCESS

Edited by:
Rais Ahmad Ansari,
Nova Southeastern University,
United States

Reviewed by:
Atrayee Bhattacharya,
Dana-Farber Cancer Institute,
United States
Jalal K. Siddiqui,
The Ohio State University,
United States

***Correspondence:**
Jinyi Tong
tongjinyi252@zju.edu.cn

Specialty section:
This article was submitted to Cancer Genetics and Oncogenomics, a section of the journal Frontiers in Genetics

Received: *14 April 2021*
Accepted: *27 July 2021*
Published: *01 September 2021*

Citation:
Shang H, Zhang H, Ren Z, Zhao H, Zhang Z and Tong J (2021) Characterization of the Potential Role of NTPCR in Epithelial Ovarian Cancer by Integrating Transcriptomic and Metabolomic Analysis. Front. Genet. 12:695245. doi: 10.3389/fgene.2021.695245

Conclusion: NTPCR might serve as a tumor suppressor in EOC progression. Our results demonstrated that DEGs and differential metabolites were mainly related to several signaling pathways, which might be a crucial role in the progression of NTPCR regulation of EOC.

Keywords: epithelial ovarian cancer, transcriptome sequencing, metabolomics sequencing, NTPCR, nucleoside-triphosphatase cancer-related

INTRODUCTION

Epithelial ovarian carcinoma (EOC) is a leading cause of cancer death and accounts for a high incidence rate in women more than 50 years old. Surgery and platinum-based chemotherapy have been confirmed as a standard treatment method for advanced EOCs. However, the 5 years survival rate of advanced EOC is still less than 30% for platinum resistance or disease relapse (Holschneider and Berek, 2000). Thus, understanding the mechanism of disease progression will promote an effective therapeutic method for EOC.

As the cost becomes more affordable in next-generation sequencing (NGS) technology, transcriptomic analysis has been extensively utilized to identify novel biomarkers for early detection, diagnosis, and therapeutics in cancers. A recent study of systematic transcriptome analysis has revealed tumor-specific mRNA isoforms for ovarian cancer diagnosis and therapy by using RNA-seq methods (Barrett et al., 2015). Another paper showed NGS was used to identify transcriptome changes and hypermethylation associated with cisplatin resistance in high-grade serous ovarian cancer (Lund et al., 2017). Although findings promoted a better understanding of ovarian cancer, disease progression still could not be explained only on the transcriptomic alteration. More efforts should be directed to elucidate complicated genetic network and its interactions with biomolecules, such as metabolites. Recently, integrating transcriptome profiling with metabolic profiling analysis has been demonstrated to be an effective method to identify differential genetic and metabolic pathways in various cancer types (Zhang G. et al., 2013; Popławski et al., 2017).

Our previous study has reported that high expression levels of nucleoside-triphosphatase cancer-related (NTPCR) were related to better prognosis in EOC patients (Shang et al., 2020). Thus, this present study aimed to explore the potential roles of NTPCR in disease progression. Based on transcriptomic profiling analysis, we screened differentially expressed genes (DEGs) between shNTPCR groups and shNC groups in EOC cells, and following performed functional analysis, interaction network analysis, prediction of miRNAs, and target transcription factors (TFs). Integrating the transcriptomic and metabolomic profiling analysis revealed crucial overlapped pathways correlated with DEGs and metabolites in EOC. The integrative analysis of our study promoted a better understanding of NTPCR roles in EOC, which might facilitate therapeutic or prognosis discovery of biomarkers.

Abbreviations: EOC, epithelial ovarian carcinoma; NTPCR, nucleoside-triphosphatase cancer-related; DEGs, differential expressed genes; NGS, next-generation sequencing; TFs, transcription factors; GO, Gene Oncology; KEGG, Kyoto Encyclopedia of Genes and Genomes; GATA2, GATA-binding factor 2; EP300, histone acetyltransferase p300; STK, serine-threonine kinases; PI, propidium iodide; FPKM, fragments per kilobase of exon per million fragments mapped; GSEA, Gene Set Enrichment Analysis; UPLC, ultra performance liquid chromatography; PCA, principal component analysis; PLS-DA, partial least-square discriminant analysis.

MATERIALS AND METHODS

Cell Lines and Culture Conditions

Epithelial ovarian carcinoma cell lines (SKOV3, CAOV-3, OV-1063, and OVCAR-3) and human ovarian epithelium cell line IOSE80 were purchased from Chinese Academy of Sciences (Beijing, China). The cells were cultured in RPMI-1640 medium supplement with 10% fetal bovine serum and maintained in a condition of 37°C and 5% CO_2.

Samples

Approved by the Ethics Committee of Hangzhou First People's Hospital (approval no. IRB#2021-20210406-01), with informed consent by patients, we collected 22 tissue samples from 11 patients. These specimens were human tissue specimens that were pathologically diagnosed as epithelial ovarian cancer during staging ovarian cancer surgery, including cancerous tissues and para-cancerous tissues.

RT-PCR Analysis

The total RNA was extracted from EOC cells and tissues using TRIzol (TaKaRa Inc. Tokyo, Japan). Reverse transcription kit (TaKaRa Inc., Tokyo, Japan) was used to transform RNA to cDNA. The mRNA levels of NTPCR in tumor cells and tissues were detected using SYBR Green kit (Thermo Inc., Waltham, MA, United States), and GAPDH was set as an endogenous control. The relative expression levels of NTPCR in different samples were determined by the method of comparing CT values ($\Delta\Delta$CT) and normalization with internal reference. The primers were NTPCR-hF: ACCCGTCTTGAGGAATGTGA and NTPCR-hR: CTCTTGAACTGGGCACTCCT, and GAPDH-hF: TGACAACTTTGGTATCGTGGAAGG and GAPDH-hR: AGGCAGGGATGATGTTCTGGAGAG.

Cell Transfection

The overexpression vector of NTPCR used a commercial vector (Sino Biological, Beijing, China, cat: HG17161-NY); shRNA was synthesized by Shanghai Gima Biopharmaceutical Technology (sequence as follows): shRNA1, 5′-GGCCTTTATCGAGAGTTGGGTTAGA-3′; shRNA2, 5′-CCTCTGGTGTGCCTGTTGATGGATT-3′; and shRNA3, 5′-CAGTATGTGGTCGACCTGACTTCTT-3′. shRNA was

inserted into pGPU6/Neo to obtain the corresponding plasmid. SKOV3 and OVCAR-3 cells were taken in the logarithmic growth phase and transfected with Lipofectamine^{TM} 2000. Six hours later, the mixture was aspirated and changed to a normal medium to continue culturing. After 72 h, the cells were harvested and used to detect molecular expression by RT-PCR.

Cell Viability

Cell viability was evaluated using a CCK-8 kit (Beyotime Biotechnology, China) following the protocol of the manufacturers. SKOV3 and OVCAR-3 cells were seeded into 96-well plates with 3,000 cells per well. After transfecting the overexpression vector or interference shRNA vector of NTPCR for 24, 48, 72, and 96 h, a total of 10 μl CCK-8 solution was added to wells, and the optical density (OD) values were read at 450 nm using a microplate reader system.

5-Ethynyl-2′-deoxyuridine (EdU)

Cell proliferation was detected by BeyoClick^{TM} eyoClick cell proliferation detection kit (Biyuntian, C0078S). The following are the general steps. Add EdU to the cell culture medium at a final concentration of 10 μM, incubate for 10 h, and fix with 4% paraformaldehyde for 15 min after phosphate-buffered saline (PBS) immersion. Remove the fixative solution by PBS immersion, and then incubate with 0.5% Triton X-100 at room temperature for 15 min to permeate the membrane. After removing the permeabilization solution, immerse in PBS, add 0.5 ml of Click reaction solution, and incubate for 30 min at room temperature in the dark. Remove the reaction solution, after immersion in PBS, add Hoechst 33342 reaction solution dropwise and incubate at room temperature for 15 min in the dark. Mount the slide with mounting solution containing anti-fluorescence quencher, and then observe and collect the images under a fluorescence microscope (Olympus, BX53).

Flow Cytometry Analysis

After cell transfection, SKOV3 and OVCAR-3 cells were harvested for flow cytometry analysis. Differential groups of cells were washed with PBS three times and then stained with propidium iodide (PI)/RNase solution following the protocol of the manufacturer. Cell cycles were detected by using FACScan flow cytometer (BD Biosciences) and analyzed using FlowJo software.

Transwell Assay

We evaluated the effect of NTPCR on the cell invasion and migration abilities by using the Transwell system. The membranes of inserts were precoated with Matrigel for invasion assay overnight. After that, SKOV3 and OVCAR-3 cells were harvested and suspended using serum-free RPMI-1640 medium. Thus, 200 μl of cell suspension including 2.0×10^4 cells was added into the upper chamber, while 500 μl of culture medium with 10% fetal bovine serum (FBS) was added into the lower chamber. Following incubation for 24 h, the cells were fixed with 4% paraformaldehyde and stained with 0.1% crystal violet for 10 min. The results were analyzed by using a microscope (Olympus IX73; Olympus Corporation, Tokyo, Japan).

Western Blotting

The protein samples prepared in ice-cold RIPA buffer were separated on SDS-PAGE gels and then transferred onto polyvinylidene fluoride (PVDF) membranes. The membranes were then blocked in 5% skimmed milk at room temperature for 1 h and then incubated with the primary antibody solution (NTPCR: Biodragon BD-PT3202 anti-rabbit monoclonal, 1:1,000; GAPDH: Proteintech 60004-1-lg mouse monoclonal, 1:1,000) at 4°C overnight. The following day, the secondary antibodies (Peroxidase AffiniPure Goat Anti-Rabbit IgG (H + L), 1:10,000; Peroxidase AffiniPure Goat Anti-Mouse IgG (H + L), 1:5,000) were added and then incubated at room temperature for 2 h. For chemiluminescence development, Millipore ECL system was used; to perform grayscale analysis on the data, TanonImage was used, and then statistical analysis was performed on the grayscale analysis results. The data mapping software is GraphPad Prism5.

Transcriptomic Sequencing

We performed RNA-sequencing on an Illumina system for shNTPCR and control shNC group with three duplications per group. Firstly, Trimmomatic version 3.6 (Bolger et al., 2014) tool was used to clean up the reads by removing adapters and low-quality reads (quality value less than 20), and the reads with N ratio exceeding 10% or length less than 50 bp were also removed. Hisat2 software (v2.05) (Siren et al., 2014) was used for the alignment of clean reads to human genomic database (GRCH38, Gencode) (Harrow et al., 2012). Moreover, human genome annotation in the resulting files was mapped to corresponding read count by using featureCounts tools (Liao et al., 2014). Further filtering was performed for different results according to the fragments per kilobase of exon per million fragments mapped (FPKM) method, and the genes with FPKM value less than 0.1 in any samples were removed.

Quasi-likelihood *F*-tests in edgeR software (Lun et al., 2016) were used to analyze DEGs between shNTPCR and shNC samples by setting $|\log FC| > 1.585$ and false discovery rate (FDR) < 0.05 as cutoff criteria. Two-dimensional clustering analysis and functional enrichment analysis were conducted for these DEGs.

We further screened the gene–disease associations from the DisGeNET database (Piñero et al., 2016), a comprehensive platform containing information on human disease genes and related variants. As for the DEGs screened from the database, the expression status in EOC was investigated by using Gene Set Enrichment Analysis (GSEA) algorithm, a computational algorithm to assess significant differences of defined gene sets among biological phenotypes (Subramanian et al., 2007).

We analyzed the interactions of protein–protein according to the STRING online tool and constructed the protein–protein interaction (PPI) network using Cytoscape software. It has been shown that proteins with similar functions tend to cluster together in the PPI network, and thus, we mined the functional modules using MCODE tool (Bader and Hogue, 2003; Davis, 2015).

To further explored the regulation mechanism of EOC, we screened the miRNA–gene and TF–gene pairs using Enrichr

(Chen et al., 2013) and ENCODE tools (Rosenbloom et al., 2011) and constructed an miRNA–TF–gene network.

Metabolomics Sequencing

The EOC cell extract samples derived from the shNTPCR and shNC groups were analyzed by the ultra performance liquid chromatography (UPLC) method on a quadrupole time-of-flight (Q-TOF) liquid chromatography–mass spectrometry (LC-MS) system. Duplicates from 10 controls together with five QC samples were obtained to evaluate the assay reproducibility.

Metabolomics data under positive ion mode and negative ion mode were obtained and first normalized before multivariate analysis. We performed unsupervised principal component analysis (PCA) and supervised partial least-square discriminant analysis (PLS-DA) to explore the metabolic differences in NTPCR samples.

As for the differential performance of metabolites between two groups, metabolite analysis was conducted using MBROLE 2.0, which is a web server designed to permit systemic analysis for metabolomic data (Chong et al., 2018). Corresponding KEGG pathways were screened with $p < 0.05$ as cutoff criteria.

Integrated Transcriptomic Analysis and Metabolomics Analysis

We used the KEGG pathway-based method to analyze differential metabolites and genes in a biological process. The thresholds were set as num-overlapping-metabolites/genes > 0 and p joint/metabolites < 0.05.

Statistical Analysis

Prism9.0 statistical software was used for data analysis. All data were expressed as mean ± standard deviation (±S). Pairwise comparisons between different groups were performed by one-way analysis of variance, and $p < 0.05$ was considered statistically significant.

RESULTS

NTPCR Was Upregulated in EOC Tissues

The expressed status of NTPCR was detected in EOC tissues via RT-qPCR analysis and Western blot analysis. The results showed that the expression of NTPCR in cancer tissues was significantly increased compared to para-cancerous tissues (**Figure 1**, $p < 0.05$).

NTPCR Inhibits Cell Proliferation, Cell Cycle, and Cell Migration and Invasion in the EOC Cell Line

To further investigate the potential role of NTPCR on the biological function of EOC, we first constructed the overexpression and interference vector of NTPCR, and qRT-PCR verified its effect (**Figure 2A**). Simultaneously, analysis of NTPCR expression levels in different EOC cell lines (SKOV3, CAOV-, OV-1063, and OVCAR-3), and normal ovarian epithelial cell line IOSE80 as a control, found that the expression levels of NTPCR in SKOV3 and OVCAR-3 cells were higher (**Figure 2B**, $p < 0.05$); hence, we chose these two strains of cells for follow-up experiments.

In the CCK-8 assays, cell viability exhibited significant differences between NTPCR over expression (OE) and shNTPCR groups (**Figure 2C**, $p < 0.01$), indicating that overexpression of NTPCR inhibited EOC cell viability and interference with NTPCR expression increased cell viability. EdU results showed that NTPCR downregulation of NTPCR expression promotes the DNA replication process (**Figure 2D**), which shows that knockdown of NTPCR promoted cell proliferation in EOC cells. The effect of NTPCR on the cell cycle was also analyzed by flow cytometry analysis, and we found that overexpression of NTPCR increased the proportions of G0/G1phase cells and decreased the proportions of S- and G2/M-phase cells, while downregulating NTPCR expression was just the opposite (**Figure 2E**). Finally, through the Transwell chamber experiment, we found that NTPCR inhibited the metastatic and invasive abilities of EOC cells (**Figures 2F,G**). On the whole, we have enough reasons to believe that NTPCR can inhibit the biological process of EOC and act as a tumor suppressor.

Transcriptomic Analysis on the Effect of NTPCR Expression in EOC

On the basis of clarifying that NTPCR inhibits the biological process of EOC, we intended to initially explore the mechanism of NTPCR regulating the progress of EOC. First, we analyzed the mRNA expression profile of the shNTPCR and shNC groups through transcriptomics and screen out DEGs, and under the cutoff criteria of $|\log_2 FC| > 1.585$ and FDR < 0.05, we screened a total of 1,408 DEGs between the shNTPCR group and shNC group, including 783 upregulated and 625 downregulated genes. Bidirectional clustering analysis and Volcano Plot for DEGs are shown in **Figure 3A**.

We performed the Gene Oncology (GO) and Kyoto Encyclopedia of Genes and Genomes (KEGG) pathway enrichment analysis for DEGs in shNTPCR groups. The results showed that these genes were mainly related to biological processes of response to the virus, viral genome replication, response to lipopolysaccharide, and extracellular matrix organization. The signaling pathway categories included NOD-like receptor signaling pathway, IL-17 signaling pathway, hepatitis C, and cytokine–cytokine receptor interaction (**Figure 3B**).

Moreover, we analyzed the dysregulated gene sets in the shNTPCR group samples by using the GSEA algorithm. The results are shown in **Figure 3C** (enrichment score = 0.221325, $p < 0.05$). The enrichment score for upregulated genes is slightly higher than that of downregulated genes, indicating that the expression status of gene sets might exhibit a similar effect on EOC.

PPI Network Analysis

We constructed the PPI networks for these DEGs and screened the top 10 node genes with the higher scores based on the three topological properties (**Figure 4A** and **Table 1**). There

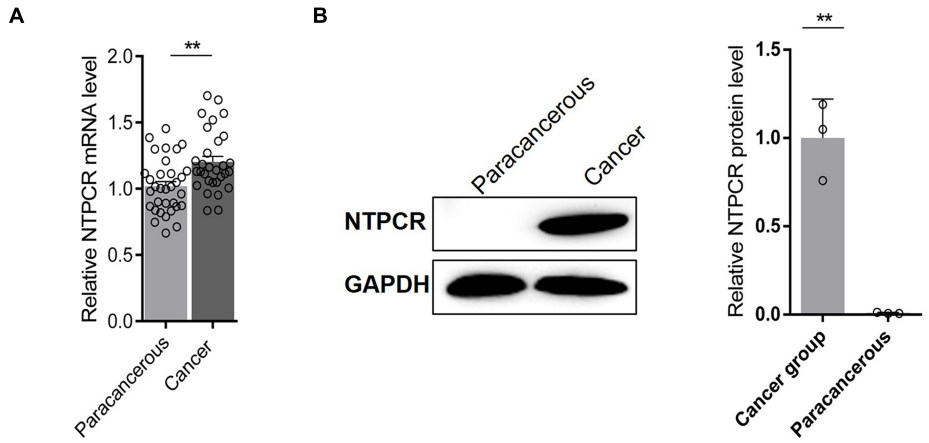

FIGURE 1 | *Via* **(A)** RT-qPCR analysis and **(B)** Western blot analysis, the expression of NTPCR in cancer tissues was significantly increased compared to para-cancerous tissues (**$p < 0.01$).

were 348 nodes and 1,154 edges in the network. Several genes obtained higher degree values, such as STAT1 (degree = 43), OAS2 (degree = 36), OAS1 (degree = 36), IFIT3 (degree = 36), OASL (degree = 36), and MX1 (degree = 36).

Furthermore, we used MCODE plug to screen subnetwork modules related to PPI networks. By setting the score $\geq$ 10 and node $\geq$ 10 as cutoff criteria, two subnetwork modules were screened (**Figure 4B**). Several signaling pathways were identified as associated with these DEGs, including human papillomavirus infection, TNF signaling pathway, and Kaposi sarcoma-associated herpesvirus infection (**Figure 4C**).

Prediction of miRNA and TFs Associated With EOC

The miRNAs and TFs correlated with DEGs were predicated by using Enrichr tools (**Table 2**). The top five miRNAs and TFs with the higher scores (combine score) were selected to establish a regulatory network of an miRNA–TF–target gene (**Figure 4D**). *Hsa-miR-124-3p* and EP300 obtained the highest count compared with other miRNAs or genes (*Hsa-miR-124-3p*, gene number = 195, $p < 0.01$; EP300, gene number = 27, $p < 0.01$), indicating the two genes were hub genes in the regulatory network.

Differential Metabolites Between NTPCR and Normal Samples

Metabolism is the downstream of gene regulatory network and protein action network and is closely related to the phenotype of organisms. DEGs may ultimately affect the composition and level of intracellular metabolic spectrum. We used mass spectrometry to detect metabolite difference between the shNTPCR and shNC groups; by the threshold of FDR < 0.01, $|\log2FC|$, and VIP > 1, we screened a total of 44 differential metabolites, including 26 metabolites in ESI + ion mode and 18 metabolites in the ESI− ion mode. Among these metabolites, there were 22 upregulated and 22 downregulated metabolites. Hierarchical cluster analysis and volcano plot results showed that these dysregulated metabolites can be significantly classified into two differential groups (**Figures 5A,B**).

Functional analysis results showed that a total of 12 signaling pathways were screened, including metabolic pathways, glycine, serine and threonine metabolism, glycerophospholipid metabolism, and ABC transporters (**Figure 5C**).

Integrated Transcriptomic and Metabolomic Analysis

The integrated transcriptomic and metabolomic analysis showed that DEGs and differential metabolites in the NTPCR groups were associated with eight overlapped pathways, such as primary bile acid biosynthesis, protein digestion and absorption, pentose, and glucuronate interconversions (**Figure 6**). Of these pathways, pentose and glucuronate interconversions obtained a higher overlapped gene number than other pathways, including 10 overlapped genes (SLC7A7, SLC7A8, COL4A5, etc.) and one metabolite (L-threonine).

DISCUSSION

In this study, we demonstrated the potential roles of NTPCR in EOC. It was observed that NTPCR was downregulated in EOC tissues and NTPCR can inhibit cell proliferation, migration, and invasion, and decrease the proportions of S- and G2/M-phase cells, indicating that NTPCR might serve as a tumor suppressor in ovarian cancer.

NTPCR (THEP 1, C1orf57, or HCR-NTPase) is a non-specific nucleoside triphosphatase exhibiting a slow hydrolyzed activity *in vitro*. It is overexpressed in several tumor tissues including neuroblastoma and liver cholangiocarcinoma (Placzek et al., 2007; Pasdziernik et al., 2009). A previous study reported there was no effect observed in NTPCR-silencing neuroblastoma cells, while overexpression of NTPCR led to the cytotoxicity of this protein (Pasdziernik et al., 2009). However, the expressed status

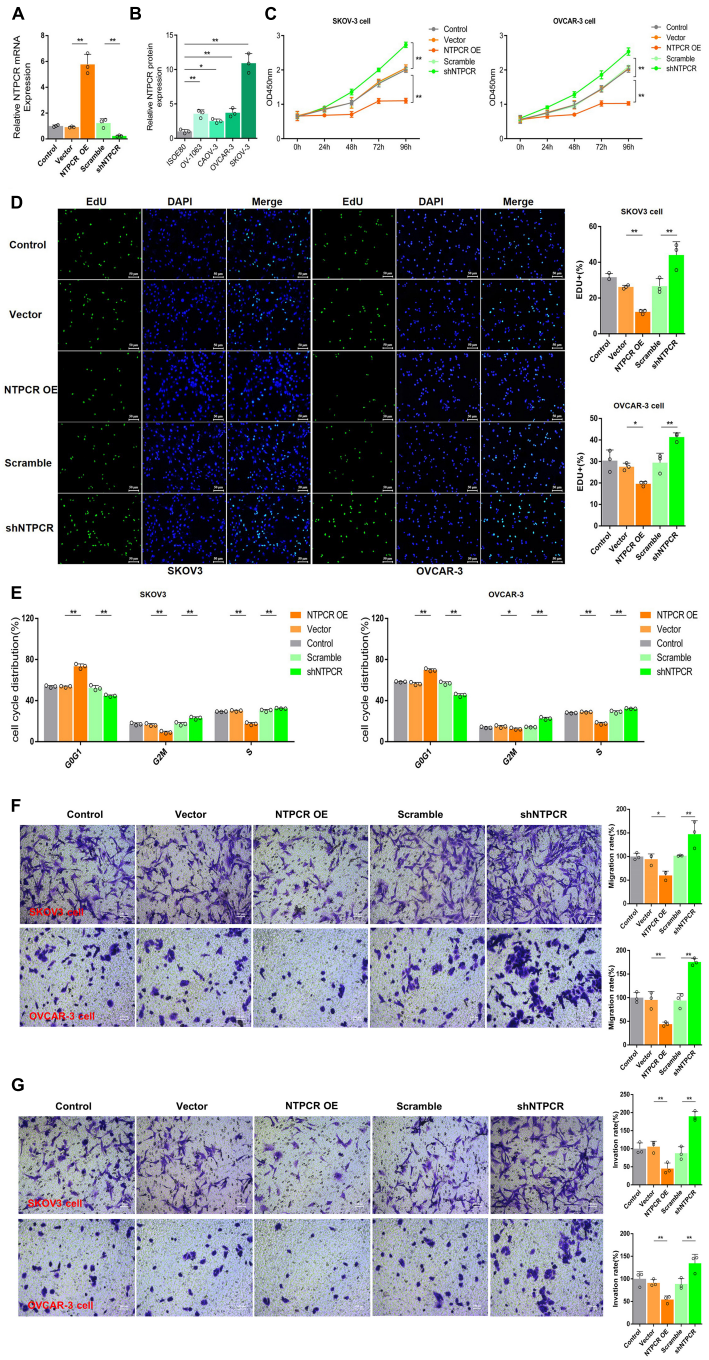

FIGURE 2 | Knocking out of NTPCR-induced cell proliferation, S phase arrest, promoted cell invasion, and migration in SKOV3 cell line. **(A)** The construction of the overexpression vector and interference shRNA vector of NTPCR. It can be seen from the left figure that compared with Scramble groups, the expression of NTPCR in shRNA groups was significantly reduced, and shRNA1 was more obvious. That is why we previously chose shRNA1 for the subsequent experimental studies. It also can be seen from the right figure that compared with the vector groups, the expression of NTPCR in NTPCR OE groups was significantly increased, and compared to the Scramble groups, shNTPCR groups were significantly reduced (*$p < 0.05$, **$p < 0.01$). **(B)** NTPCR expression levels were significantly upregulated in four ovarian cancer cell lines (SKOV3 vs. IOSE80, $p < 0.01$; CAOV-3 vs. IOSE80, $p < 0.05$; OV-1063 vs. IOSE80, $p < 0.01$; and OVCAR-3 vs. IOSE80, $p < 0.01$) compared with the human ovarian epithelium cell line IOSE80. **(C)** The effect of NTPCR on the viability of epithelial ovarian cancer cells. The CCK-8 assays were performed to evaluate the cell proliferation after being cultured at 24, 48, 72, and 96 h (**$p < 0.01$). **(D)** The effect of NTPCR on the DNA replication ability of epithelial ovarian cancer cell lines SKOV3 and OVCAR-3. In the figure, EdU detects the DNA replication ability (*$p < 0.05$, **$p < 0.01$). **(E)** The picture shows the distribution of the cell cycle detected by PI. NTPCR increased the proportion of G0/G1-phase cells in epithelial ovarian cancer cells and decreased the proportion of S-phase and G2/M-phase cells (*$p < 0.05$, **$p < 0.01$). **(F,G)** Transwell assesses the effect of NTPCR on the migration and invasion of epithelial ovarian cancer cells. In SKOV3 cells and OVCAR-3 cells, overexpression of NTPCR reduced cell migration ability, and downregulation of NTPCR increased cell migration ability. The results show the same in the cell invasion experiment (*$p < 0.05$, **$p < 0.01$).

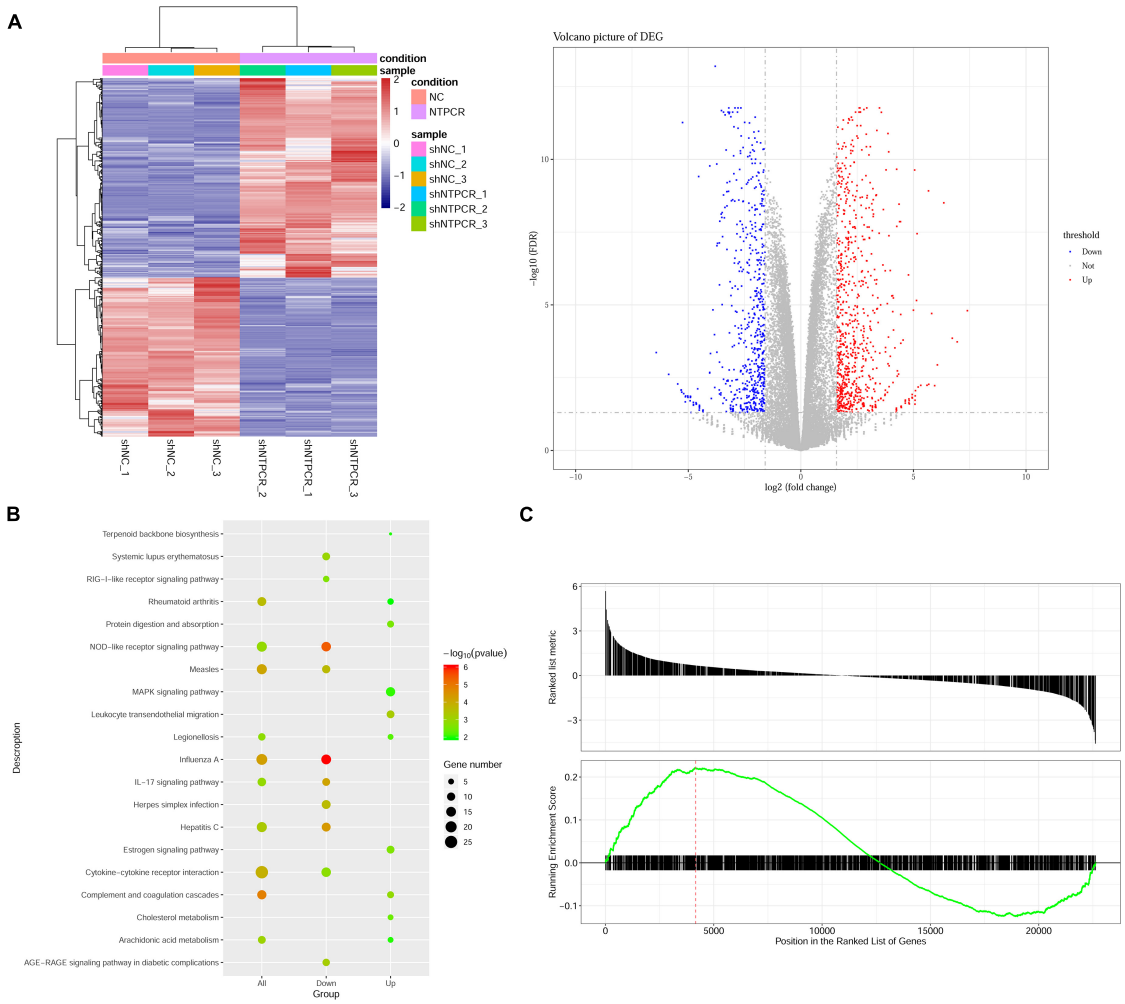

FIGURE 3 | Identification of DEGs between shNTPCR ovarian cancer groups and control shNC groups. **(A)** Two-dimensional clustering analysis (left) and volcano plot (right) for DEGs. Columns in the clustering analysis results represent different samples, while rows refer to differential genes; red and blue color represent upregulated and downregulated expression. Dots in the volcano plot diagram represent differential genes. Red and blue dots refer to upregulated and downregulated genes. **(B)** KEGG pathway enrichment analysis results for DEGs. The pathway with a smaller *p*-value represented a significant enrichment degree. The dot sizes refer to the count number of genes enriched by the pathway category. **(C)** GSEA results of dysregulated genes in ovarian cancer.

and physiological role of NTPCR is still unknown in other cancer types, especially in ovarian cancer. Our study firstly reported that NTPCR might serve as a tumor suppressor in ovarian cancer progression.

RNA sequencing results revealed that disturbance of transcriptome was observed in shNTPCR ovarian cancer cells, and several miRNAs and TFs were predicted to be hub genes correlated with ovarian cancer, including hsa-miR-124-3p, hsa-miR-146a-5p, hsa-miR-30a-5p, EP300, GATA2, and STAT3. MicroRNAs are endogenous small RNAs that function as pivotal roles in tumorigenesis, and they execute the posttranscriptional regulation process by interacting with target genes (Iorio et al., 2007; Kasinski and Slack, 2011). miR-124 s highly conserved in humans. Abnormally expressed has-miR-124 has been reported in multiple cancers, such as gastrointestinal carcinomas (Xia et al., 2012; Zhang et al., 2014) and hepatocellular carcinoma (Chen et al., 2018). Down-regulation of miR-124 was identified in highly metastatic ovarian cancer cells and human tissue specimens (Zhang H. et al., 2013). Consistent with the role in gastric cancer, it could inhibit invasive and migratory abilities of ovarian cancer cells according to interaction with the 3′-untranslated (3′-UTR) regions of SphK1 mRNA. Similarly, another paper showed miR-124 might serve as a tumor suppressor in malignant tumors, and thus, upregulated miR-124 could inhibit cell proliferation and migration by decreasing PDCD6 expression in SKOV3 and OCVAR3 cells (Yuan et al., 2017). A recent paper revealed miRNA-124-3p targeting gene Gata2 might be a novel biomarker related to ovarian cancer progression based on multiomics analysis of the tumor microenvironment (Gov et al., 2017). GATA-binding factor 2 (GATA2) is a TF that is critical for many physical processes, such as embryonic development, blood forming,

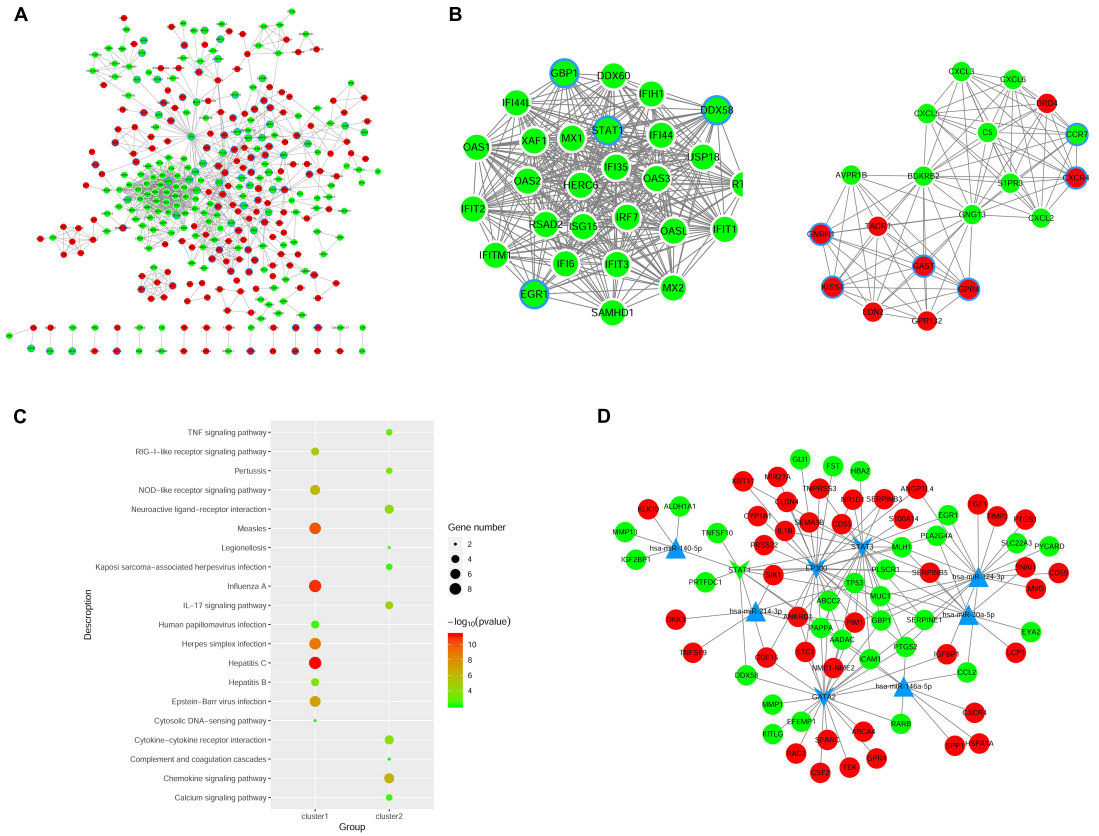

FIGURE 4 | Regulatory network analysis to predict miRNAs and TFs associated with ovarian cancer. **(A)** PPI network construction to analyze DEGs in shNTPCR ovarian cancer groups. The red node represent upregulated genes, while the green dot refer to downregulated genes. The node with blue aperture indicates genes related to ovarian carcinoma. **(B)** Two clusters of functional modules were identified from the PPI network. **(C)** Functional enrichment analysis results for DEGs in subnetwork modules, and the top 10 pathway categories were sorted according to the *p*-value. **(D)** Regulatory network of miRNA–TF–gene was constructed to predict crucial genes correlated with ovarian cancer progression. Dots in red and green color represent upregulated and downregulated genes, respectively; triangular nodes and V-shaped nodes represent miRNA and TFs.

and tissue-forming stem cells. Abnormal GATA2 epigenetic dysregulation can induce unfavorable phenotypes in human gastric cancer by decreasing expression of GATA6, which has a vital role in gastrointestinal development (Song et al., 2018).

TABLE 1 | The top 10 hub genes in PPI network were identified as candidate genes related to ovarian cancer according to topological properties (degree centrality, betweenness centrality, and closeness centrality).

Gene	Degree	Gene	Betweenness	Gene	Closeness
STAT1	43	TP53	30206.2	TP53	0.015058
OAS2	36	STAT1	14016.98	STAT1	0.015041
OAS1	36	SPP1	9019.094	ICAM1	0.01504
IFIT3	36	IL1B	8083.106	CCL2	0.015017
OASL	36	ICAM1	7465.445	PTGS2	0.015003
MX1	36	ITGB2	6537.538	SPP1	0.015002
OAS3	35	CMPK2	6499.484	IL1B	0.014997
TP53	34	NME1-NME2	5982	CXCR4	0.014997
IRF7	34	CYP1A1	5829.825	TLR3	0.014992
RSAD2	33	TIMP2	5323.395	EGR1	0.014985

Considering this, our study is consistent with a previous study that miR-124 might interact with target gene GATA2 to regulate the progression of ovarian cancer.

As for miR-146a, Wilczyński et al. (2017) analyzed the expression of miRNAs in ovarian cancer patients undergoing surgery and found miR-146a was increased in primary tumors compared with normal ovarian tissue (p = 0.02); lower levels of miR-146a in patients were correlated with shorter survival times. Many ovarian cancer patients with a strong family history had mutations of BRCA1/BRCA2, and a previous study demonstrated miR-146a can bind to the 3′-UTR region of the two genes and regulated their expression (Pastrello et al., 2010); patients who had polymorphism of hsa-mir-146a (rs2910164) may be diagnosed at a younger age than patients without a variant allele. Histone acetyltransferase p300 (EP300) is also known as p300, and it functions as a histone acetyltransferase that regulates cell growth and division. Somatic missense alterations of EP300 have been identified in gastrointestinal cancer, such as colorectal and gastric cancer (Muraoka et al., 1996). Six truncating mutations were identified in various human cancer types, including ovarian carcinoma (Gayther et al., 2000).

TABLE 2 | The top five miRNAs and transcription factors with higher combined scores were predicted to be crucial factors associated with ovarian cancer.

Term	Gene num	*P*-value	Combined score	Genes
hsa-miR-124-3p	195	0.000706	70.998557	IGFBP1, SLC22A3, EGR1, SERPINE1, PLA2G4A, PTGS2, FGF1, PTGS1, PYCARD, MUC1, SNAI1, PIM1, TIMP3, CCL2, MVD, CD59, ANGPTL4, GBP1, CD55
hsa-miR-146a-5p	7	0.000182	20.229601	STAT1, SPP1, CXCR4, RARB, PTGS2, ICAM1, HSPA1A
hsa-miR-30a-5p	9	0.028172	19.442688	PLSCR1, EYA2, SERPINE1, SNAI1, PLA2G4A, LCP1, MLH1, TP53, SERPINB5
hsa-miR-140-5p	5	0.000304	17.247252	MMP13, STAT1, ALDH1A1, IGF2BP1, KLK10
hsa-miR-214-3p	6	0.001346	17.236654	PAPPA, PIM1, TNFSF9, SIK1, TP53, DKK3
EP300	27	$2.87E-06$	22.275263	TMPRSS3, SERPINE1, SEMA3B, STC1, PTGS2, GLI1, PIM1, ANKRD1, GBP1, CD55, SERPINB3, ABCC2, GDF15, FST, PLA2G4A, NR1D1, MLH1, SERPINB5, CLDN4, AADAC, KRT17, IL1B, PAPPA, CYP1A1, SIK1, ANGPTL4, TP53
GATA2	25	0.000196	14.549745	CSF2, SPARC, SERPINE1, STC1, PTGS2, ICAM1, NME1-NME2, EFEMP1, RAC2, PIM1, ANKRD1, CCL2, GBP1, IGFBP1, ABCC2, GDF15, DDX58, MMP1, ABCA4, GPR4, KITLG, AADAC, PAPPA, RARB, TEK
EP300	6	0.000578	14.452685	STAT1, SEMA3B, ANKRD1, MIR27A, PRSS22, CD55
STAT3	24	0.000407	13.263751	SERPINB3, EGR1, ABCC2, STAT1, TMPRSS3, SERPINE1, SEMA3B, HBA2, NR1D1, PTGS2, MLH1, SERPINB5, ICAM1, NME1-NME2, MUC1, PLSCR1, KRT17, IL1B, PAPPA, PIM1, ANKRD1, S100A14, GBP1, CD55
STAT1	8	0.000966	12.789136	MUC1, PLSCR1, GDF15, STAT1, DDX58, TNFSF10, PRTFDC1, ICAM1

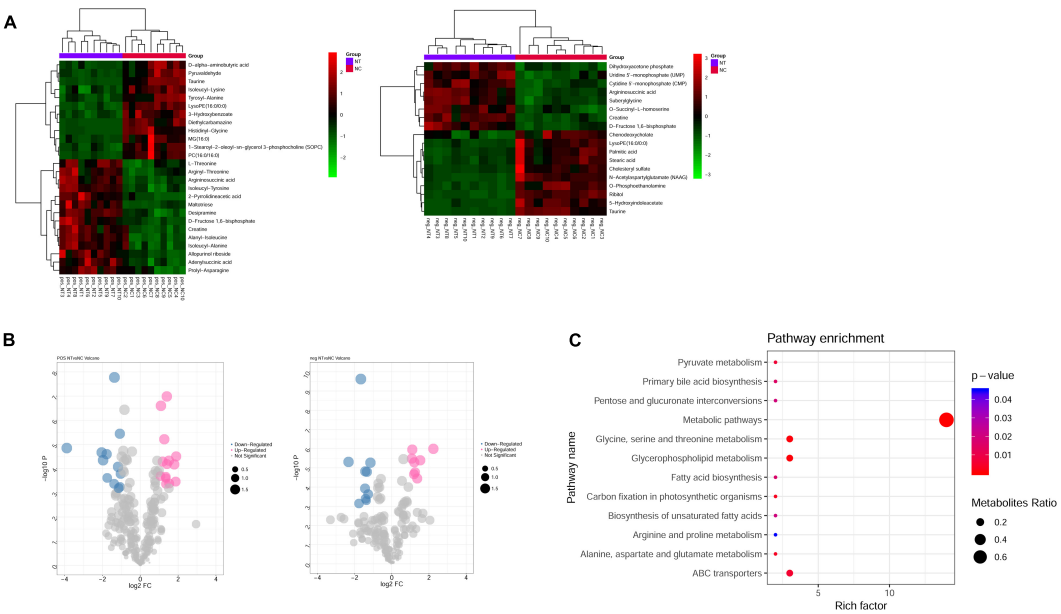

FIGURE 5 | Identification of differential metabolites between NTPCR groups and normal groups. **(A)** Hierarchical clustering analysis was performed for differential metabolites in NTPCR vs. normal control samples under ESI + ion (left) and ESI- ion (right) modes. Green represent downregulated metabolites, while red refer to upregulated metabolites. **(B)** Volcano plot of differential metabolites in NTPCR vs. normal control samples under ESI + ion (left) and ESI- ion (right) modes. Blue dots are downregulated metabolites, pink dots refer to upregulated metabolites, and gray dots represent normal metabolites. The dot size was correlated with VIP values. **(C)** Functional enrichment results of differential metabolites in NTPCR vs. control groups. The horizontal axis is the count number of pathways, while the vertical axis is the pathway names. The dot size represents the ratio of pathways enriched by metabolites. The color change from blue to red means a smaller *p*-value.

Moreover, EP300 can be targeted by the miR-106b∼25 cluster and be involved in regulating multidrug resistance in an ABC transporter-independent manner (Hu et al., 2016). Prevalent evidence uncovered the roles of STAT3 in ovarian cancer. Elevated STAT3 expression was identified in ovarian cancer ascites and could promote invasion and metastasis (Saini et al., 2017). STAT3 also interacting with miRNA-92 promoted malignant progression in ovarian cancer, and the potential mechanism was associated with regulation of the Wnt signaling pathway (Chen et al., 2017). Multiomics profiling reveals STAT3 regulated several biological processes in ovarian cancer, including epithelial–mesenchymal transition, cell cycle progression, and E2F signaling (Lu et al., 2019).

In addition, metabolites were final products in biological processes and can be disturbed by genetic factors. The integrated transcriptomic and metabolomic analysis demonstrated that significant alterations of eight pathways were identified in the NTPCR group, such as pentose and glucuronate

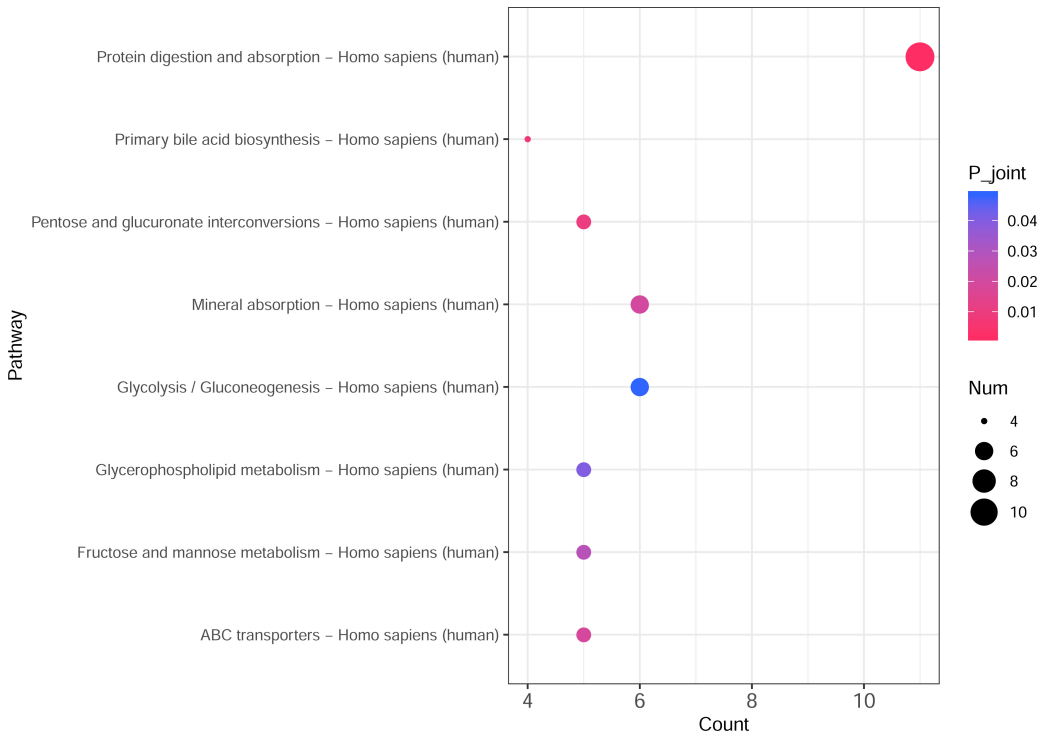

FIGURE 6 | Integrated transcriptomic and metabolomic analysis results to identify crucial KEGG pathways related to ovarian cancer. The horizontal axis is the pathway categories, and the vertical axis is the count number of differential genes and metabolites. A $p < 0.05$ represents a significant difference, and the dots with the color changing from pink to red represents a smaller *p*-value.

interconversions, primary bile acid biosynthesis, protein digestion, and absorption. A total of 10 overlapped genes (SLC7A7, SLC7A8, COL4A5, etc.) and one metabolite (L-threonine) were significantly correlated with the pathway of protein digestion and absorption in ovarian cancer. AKT serine/threonine kinase 1 can be target by microRNA-215 to regulate the progression of breast cancer (Yao et al., 2017). Moreover, serine–threonine kinases (STK) were also reported as attractive therapeutic targets in EOC; the combination of STK inhibitors with cytotoxic agents or other class biological agents significantly improved clinical benefit rates (Ciccone et al., 2016).

In summary, our study provided an experimental foundation that decreased NTPCR can affect cell proliferation, cell cycle, cell migration, and invasion in SKOV3 cells. Further experimental foundations should be conducted to investigate the mechanism of NTPCR in ovarian cancer progression. Integrative analysis of transcriptomic and metabolic profiling identified crucial pathways related to differential metabolites and genes. This study might provide attractive targets for the potential treatment of ovarian cancer patients.

DATA AVAILABILITY STATEMENT

The data can be found in online repositories: Gene Expression Omnibus GSE178486.

ETHICS STATEMENT

The studies involving human participants were reviewed and approved by Ethics Committee of Hangzhou First People's Hospital. The patients/participants provided their written informed consent to participate in this study.

AUTHOR CONTRIBUTIONS

JT: conception and design of the research. HS and ZR: acquisition of data. HZZ and ZR: analysis and interpretation of data. HS, HZZ, and HJZ: drafting the manuscript. ZZ and JT: revision of manuscript for important intellectual content. HS: conducting experiments. All authors read and approved the final manuscript.

FUNDING

This work was supported by the Research Fund of China National Health Commission (Grant No. WKJ-ZJ-2010) and Medical Scientific Research Foundation of Zhejiang Province (Grant No. 2019KY495).

REFERENCES

Bader, G. D., and Hogue, C. W. (2003). An automated method for finding molecular complexes in large protein interaction networks. *BMC Bioinformat.* 4:2. doi: 10.1186/1471-2105-4-2

Barrett, C. L., Deboever, C., Jepsen, K., Saenz, C. C., and Frazer, K. A. (2015). Systematic transcriptome analysis reveals tumor-specific isoforms for ovarian cancer diagnosis and therapy. *Proc. Natl. Acad. Sci. U S A.* 112:E3050. doi: 10.1073/pnas.1508057112

Bolger, A. M., Lohse, M., and Usadel, B. (2014). Trimmomatic: a flexible trimmer for Illumina sequence data. *Bioinformatics* 30, 2114–2120. doi: 10.1093/bioinformatics/btu170

Chen, E. Y., Tan, C. M., Kou, Y., Duan, Q., and Ayan, A. M. (2013). Enrichr: Interactive and collaborative HTML5 gene list enrichment analysis tool. *BMC Bioinformatics* 14:128. doi: 10.1186/1471-2105-14-128

Chen, G., Shi, Y., Liu, M., and Sun, J. (2018). circHIPK3 regulates cell proliferation and migration by sponging miR-124 and regulating AQP3 expression in hepatocellular carcinoma. *Cell Death Dis.* 9, 017–0204. doi: 10.1038/s41419-017-0204-3

Chen, M.-W., Yang, S.-T., Chien, M.-H., Hua, K.-T., Wu, C.-J., Hsiao, S., et al. (2017). The STAT3-miRNA-92-Wnt signaling pathway regulates spheroid formation and malignant progression in ovarian cancer. *Cancer Res.* 77, 1955–1967. doi: 10.1158/0008-5472.CAN-16-1115

Chong, J., Othman, S., Li, C., Iurie, C., Li, S., Guillaume, B., et al. (2018). MetaboAnalyst 4.0: towards more transparent and integrative metabolomics analysis. *Nucleic Acids Res.* 2018:W1. doi: 10.1093/nar/gky310

Ciccone, M. A., Maoz, A., Casabar, J. K., Machida, H., Mabuchi, S., and Matsuo, K. (2016). Clinical outcome of treatment with serine-threonine kinase inhibitors in recurrent epithelial ovarian cancer: a systematic review of literature. *Expert Opin. Investig. Drugs* 25, 781–796. doi: 10.1080/13543784.2016.1181748

Davis, D. (2015). Yavero?lu ON, Malod-Dognin N, Stojmirovic A, Pr?ulj N. Topology-function conservation in protein-protein interaction networks. *Bioinformatics* 31, 1632–1639. doi: 10.1093/bioinformatics/btv026

Gayther, S. A., Batley, S. J., Linger, L., Bannister, A., Thorpe, K., Chin, S. F., et al. (2000). Mutations truncating the EP300 acetylase in human cancers. *Nat. Genet.* 24, 300–303. doi: 10.1038/73536

Gov, E., Kori, M., and Arga, K. Y. (2017). Multiomics Analysis of Tumor Microenvironment Reveals Gata2 and miRNA-124-3p as Potential Novel Biomarkers in Ovarian Cancer. *OMICS* 21, 603–615. doi: 10.1089/omi.2017.0115

Harrow, J. F. A., Gonzalez, J. M., et al. (2012). GENCODE: The reference human genome annotation for The ENCODE Project. *Genome Res.* 22, 1760–1774. doi: 10.1101/gr.135350.111

Holschneider, C. H., and Berek, J. S. (2000). Ovarian cancer: epidemiology, biology, and prognostic factors. *Semin. Surg. Oncol.* 19, 3–10. doi: 10.1002/1098-2388(200007/08)19:1<3::AID-SSU2>3.0.CO;2-S

Hu, Y., Li, K., Asaduzzaman, M., Cuella, R., Shi, H., Raguz, S., et al. (2016). miR-106b˜25 cluster regulates multidrug resistance in an ABC transporter-independent manner via downregulation of EP300. *Oncol. Rep.* 35, 1170–1178. doi: 10.3892/or.2015.4412

Iorio, M. V., Visone, R., Di Leva, G., Donati, V., Petrocca, F., Casalini, P., et al. (2007). MicroRNA signatures in human ovarian cancer. *Cancer Res.* 67, 8699–8707. doi: 10.1158/0008-5472.CAN-07-1936

Kasinski, A. L., and Slack, F. J. (2011). Epigenetics and genetics. MicroRNAs en route to the clinic: progress in validating and targeting microRNAs for cancer therapy. *Nat. Rev. Cancer* 11, 849–864. doi: 10.1038/nrc3166

Liao, Y., Smyth, G. K., and Shi, W. (2014). featureCounts: an efficient general purpose program for assigning sequence reads to genomic features. *Bioinformatics* 30, 923–930. doi: 10.1093/bioinformatics/btt656

Lu, T., Bankhead, I. I. I. A., Ljungman, M., and Neamati, N. (2019). Multi-omics profiling reveals key signaling pathways in ovarian cancer controlled by STAT3. *Theranostics* 9:5478. doi: 10.7150/thno.33444

Lun, A. T. L., Chen, Y., and Smyth, G. K. (2016). It's DE-licious: A Recipe for Differential Expression Analyses of RNA-seq Experiments Using Quasi-Likelihood Methods in edgeR Methods. *Mol. Biol.* 1418, 391–416. doi: 10.1007/978-1-4939-3578-9_19

Lund, R. J., Huhtinen, K., Salmi, J., Rantala, J., and Carpén, O. D. N. A. (2017). methylation and Transcriptome Changes Associated with Cisplatin Resistance in Ovarian Cancer OPEN. *Sci. Rep.* 7:1469. doi: 10.1038/s41598-017-01624-4

Muraoka, M., Konishi, M., Kikuchi-Yanoshita, R., Tanaka, K., Shitara, N., Chong, J. M., et al. (1996). p300 gene alterations in colorectal and gastric carcinomas. *Oncogene* 12, 1565–1569.

Pasdziernik, M., Kaltschmidt, B., Kaltschmidt, C., Klinger, C., and Kaufmann, M. (2009). On the cytotoxicity of HCR-NTPase in the neuroblastoma cell line SH-SY5Y. *BMC Res. Notes* 2, 1756–1500. doi: 10.1186/1756-0500-2-102

Pastrello, C., Polesel, J., Della Puppa, L., Viel, A., and Maestro, R. (2010). Association between hsa-mir-146a genotype and tumor age-of-onset in BRCA1/BRCA2-negative familial breast and ovarian cancer patients. *Carcinogenesis* 31, 2124–2126. doi: 10.1093/carcin/bgq184

Piñero, J., Bravo, À, Queralt-Rosinach, N., Gutiérrez-Sacristán, A., Deu-Pons, J., Centeno, E., et al. (2016). DisGeNET: a comprehensive platform integrating information on human disease-associated genes and variants. *Nucleic Acids Res.* 45, D833–D839. doi: 10.1093/nar/gkw943

Placzek, W. J., Almeida, M. S., and Wuthrich, K. (2007). NMR structure and functional characterization of a human cancer-related nucleoside triphosphatase. *J. Mol. Biol.* 367, 788–801. doi: 10.1016/j.jmb.2007.01.001

Popławski, P., Tohge, T., Bogusławska, J., Rybicka, B., Tański, Z., Treviño, V., et al. (2017). Integrated transcriptomic and metabolomic analysis shows that disturbances in metabolism of tumor cells contribute to poor survival of RCC patients. *Biochim. Biophys. Acta Mol. Basis Dis.* 1863, 744–752. doi: 10.1016/j.bbadis.2016.12.011

Rosenbloom, K. R., Dreszer, T. R., Long, J. C., Malladi, V. S., Sloan, C. A., Raney, B. J., et al. (2011). ENCODE whole-genome data in the UCSC Genome Browser: update 2012. *Nucleic Acids Res.* 2011, D912–D917. doi: 10.1093/nar/gkr1012

Saini, U., Naidu, S., ElNaggar, A. C., Bid, H. K., Wallbillich, J. J., Bixel, K., et al. (2017). Elevated STAT3 expression in ovarian cancer ascites promotes invasion and metastasis: a potential therapeutic target. *Oncogene* 36:168. doi: 10.1038/onc.2016.197

Shang, H., Zheng, J., and Tong, J. (2020). Integrated analysis of transcriptomic and metabolomic data demonstrates the significant role of pyruvate carboxylase in the progression of ovarian cancer. *Aging* 12, 21874–21889. doi: 10.18632/aging.104004

Siren, J., Valimaki, N., and Makinen, V. (2014). Indexing Graphs for Path Queries with Applications in Genome Research. *IEEE/ACM Trans. Comput. Biol. Bioinform.* 11, 375–388. doi: 10.1109/TCBB.2013.2297101

Song, S. H., Jeon, M. S., Nam, J. W., Kang, J. K., Lee, Y. J., Kang, J. Y., et al. (2018). Aberrant GATA2 epigenetic dysregulation induces a GATA2/GATA6 switch in human gastric cancer. *Oncogene* 37, 993–1004. doi: 10.1038/onc.2017.397

Subramanian, A., Kuehn, H., Gould, J., Tamayo, P., and Mesirov, J. P. (2007). GSEA-P. *Bioinformatics* 23, 3251–3253. doi: 10.1093/bioinformatics/btm369

Wilczyński, M., Żytko, E., Szymańska, B., Dzieniecka, M., Nowak, M., Danielska, J., et al. (2017). Expression of miR-146a in patients with ovarian cancer and its clinical significance. *Oncol. Lett.* 14, 3207–3214. doi: 10.3892/ol.2017.6477

Xia, J., Wu, Z., Yu, C., He, W., Zheng, H., He, Y., et al. (2012). miR-124 inhibits cell proliferation in gastric cancer through down-regulation of SPHK1. *J. Pathol.* 227, 470–480. doi: 10.1002/path.4030

Yao, J., Zhang, P., Li, J., and Xu, W. (2017). MicroRNA-215 acts as a tumor suppressor in breast cancer by targeting AKT serine/threonine kinase 1. *Oncol. Lett.* 14, 1097–1104. doi: 10.3892/ol.2017.6200

Yuan, L., Li, S., Zhou, Q., Wang, D., Zou, D., Shu, J., et al. (2017). MiR-124 inhibits invasion and induces apoptosis of ovarian cancer cells by targeting programmed cell death 6. *Oncol. Lett.* 14, 7311–7317. doi: 10.3892/ol.2017.7157

Zhang, G., He, P., Tan, H., Budhu, A., Gaedcke, J., Ghadimi, B. M., et al. (2013). Integration of metabolomics and transcriptomics revealed a fatty acid network exerting growth inhibitory effects in human pancreatic cancer. *Clin. Cancer Res.* 19, 4983–4993. doi: 10.1158/1078-0432.CCR-13-0209

Zhang, H., Wang, Q., Zhao, Q., and Di, W. (2013). MiR-124 inhibits the migration and invasion of ovarian cancer cells by targeting SphK1. *J. Ovarian Res.* 6:84. doi: 10.1186/1757-2215-6-84

Zhang, Y., Lin, Z., Jing, H., Fei, G., Xiaoshan, L., Lian, H., et al. (2014). MiR-124 Radiosensitizes Human Colorectal Cancer Cells by Targeting PRRX1. *PLoS One* 9:e93917. doi: 10.1371/journal.pone.0093917

Conflict of Interest: The authors declare that the research was conducted in the absence of any commercial or financial relationships that could be construed as a potential conflict of interest.

Publisher's Note: All claims expressed in this article are solely those of the authors and do not necessarily represent those of their affiliated organizations, or those of the publisher, the editors and the reviewers. Any product that may be evaluated in this article, or claim that may be made by its manufacturer, is not guaranteed or endorsed by the publisher.

frontiers in Genetics

REVIEW
published: 16 September 2021
doi: 10.3389/fgene.2021.749850

Targeting the Transcriptome Through Globally Acting Components

Damien Parrello[1], *Maria Vlasenok*[2], *Lincoln Kranz*[1] *and Sergei Nechaev*[1]*

[1]Department of Biomedical Sciences, University of North Dakota School of Medicine, Grand Forks, ND, United States, [2]Skolkovo Institute of Science and Technology, Moscow, Russia

Transcription is a step in gene expression that defines the identity of cells and its dysregulation is associated with diseases. With advancing technologies revealing molecular underpinnings of the cell with ever-higher precision, our ability to view the transcriptomes may have surpassed our knowledge of the principles behind their organization. The human RNA polymerase II (Pol II) machinery comprises thousands of components that, in conjunction with epigenetic and other mechanisms, drive specialized programs of development, differentiation, and responses to the environment. Parts of these programs are repurposed in oncogenic transformation. Targeting of cancers is commonly done by inhibiting general or broadly acting components of the cellular machinery. The critical unanswered question is how globally acting or general factors exert cell type specific effects on transcription. One solution, which is discussed here, may be among the events that take place at genes during early Pol II transcription elongation. This essay turns the spotlight on the well-known phenomenon of promoter-proximal Pol II pausing as a step that separates signals that establish pausing genome-wide from those that release the paused Pol II into the gene. Concepts generated in this rapidly developing field will enhance our understanding of basic principles behind transcriptome organization and hopefully translate into better therapies at the bedside.

Keywords: transcriptome regulation, epigenetics, transcription elongation, RNA pol II pausing, NELF model

OPEN ACCESS

Edited by:
Rais Ahmad Ansari,
Nova Southeastern University,
United States

Reviewed by:
Rong Li,
George Washington University,
United States
Pabitra Parua,
Albert Einstein College of Medicine,
United States

***Correspondence:**
Sergei Nechaev
sergei.nechaev@UND.edu

Specialty section:
This article was submitted to Epigenomics and Epigenetics, a section of the journal Frontiers in Genetics

Received: *30 July 2021*
Accepted: *02 September 2021*
Published: *16 September 2021*

Citation:
Parrello D, Vlasenok M, Kranz L and Nechaev S (2021) Targeting the Transcriptome Through Globally Acting Components. Front. Genet. 12:749850. doi: 10.3389/fgene.2021.749850

INTRODUCTION

Treatments of cancers should ideally be tailored to their specific molecular signatures. The central place and complexity of transcription regulation in normal and cancer cells offer tantalizing opportunities for precise targeting (Bushweller, 2019; Van Hoeck et al., 2019; Malone et al., 2020). Many anticancer drugs in use and in development today target the transcriptional machinery or epigenetic regulators (Villicaña et al., 2014; Mohammad et al., 2019; Park and Han, 2019; Laham-Karam et al., 2020). However, rather than specific transcription factors, many drugs work against factors with broad-spectrum functionality including epigenome modifiers and components of the basal transcriptional machinery (Bywater et al., 2013). This targeting strategy draws from long-standing observations that perturbation of general or globally acting factors often results in distinct cell type specific effects for reasons that remain poorly understood (Ptashne, 2013). Because many targets of anti-cancer therapies have broad or essential roles in normal cells, their use remains heavily based on empirical findings. Targeting specific factors such as transcription factors causative of certain cancers is becoming feasible (Sievers et al., 2018; Duffy and Crown, 2021), but is limited by an uncertainty in how these and other factors may function in different cellular contexts.

Transcription is the first step in expression of genes and genomes. The combined activity of some 20,000 human genes results in genome-wide RNA transcriptome patterns that reflect the biology and define the identity of every cell. Despite the flood of technologies describing the transcriptomes with increasing precision, our understanding of gene regulation remains fundamentally based on the knowledge gained from studies of individual genes. A long-standing gene-centric paradigm describes regulation by sequence-specific transcription factors that serve as repressors and activators, in contrast to factors broadly involved in the process of transcription that are considered basal or general (Nikolov and Burley, 1997; Juven-Gershon and Kadonaga, 2010). This paradigm does not explain network-level events especially the molecular rules governing interactions among thousands of genes in different cell types.

Two features of Pol II transcription are of note. On the one hand, the Pol II machinery is constantly modulated by a host of activating and repressing inputs that connect transcription to the environment within and outside the cell. These second to minute-scale events underlie rapid responses to stimuli and have generated the bulk of our understanding of transcription regulation in cellular responses to environmental triggers such as heat shock, hormones such as estrogen, or innate immune responses (Adelman et al., 2009; Hah et al., 2011; Mahat et al., 2016). In addition, metazoan cells have a special ability to form distinct stable steady states and undergo regulated transitions between them. These transitions take place on longer timescales, lasting hours to years, and involve predefined programs that are commonly visualized through the concept of the epigenetic landscape (Waddington, 1957). These transitions underlie development and differentiation of normal cells and involve transcriptional and epigenetic control mechanisms and factors that can be ectopically activated in cancers (Rousseaux et al., 2013).

Targeting strategies should benefit from better understanding of principles that govern the transcriptomes. This problem can be conceptually narrowed down to defining the molecular interactions that link individual genes within transcriptional networks. Given the overall conservation of the RNA polymerase II machinery (Hampsey, 1998), mechanisms that drive this quantum leap in complexity in higher organisms presumably do not involve too many additional players and instead must rely on repurposing of existing components. In this essay, we discuss some of the challenges in targeting the transcriptional machinery and suggest a potential avenue for improving the precision of broad-stroke interventions.

PERVASIVE UNCERTAINTY IN TARGETING CELLULAR COMPONENTS

In this section we describe some of the challenges in targeting the transcriptional machinery. These arise not only from unintended effects of drugs, which can be improved by identifying better targets and better drug design, but also from the inherent uncertainty of transcription regulation in different cellular contexts.

Targeting the Transcription Machinery: Knocking on the Black Box

Transcription is the ultimate target of numerous anticancer drugs that act on Pol II or the epigenetic machinery. Cancer targeting aims to either kill or reprogram cells into more benign states (Gong et al., 2019). To gain selectivity over normal cells, targeting strategies exploit distinct properties of cancer cells. One property is addiction to transcription (Bradner et al., 2017), which increases the demands of cancer cells for Pol II activity and makes them more sensitive to its inhibition. Inhibitors of general transcription factors such as TFIIH and P-TEFb have been used (Villicaña et al., 2014; Wang et al., 2015; Sava et al., 2020). Known oncogene transcription factors such as c-Myc, KRAS, etc, are tempting targets because of their key roles in cancer initiation and progression (Hallin et al., 2020; Madden et al., 2021). However, some of these factors have been considered undruggable or difficult to target for various reasons including their critical roles in normal cells and/or difficulty to specifically target interactors as compared to enzymes (Lazo and Sharlow, 2016; Zhang et al., 2018). Recent studies suggest that these challenges will be at least to some extent overcome (Duffy and Crown, 2021; Trkulja et al., 2021; Wang et al., 2021). However, the highly changeable nature of cancers that can outselect therapies will always remain a formidable caveat.

A second property of cancer cells is broad dysregulation of the transcriptional machinery (Bywater et al., 2013; Lee and Young, 2013), which alters the requirements of cancer cells for its components and leads to unusual sensitivity to inhibition of certain factors. Several classes of epigenetic drugs are in development or already on the market, with the more common including Histone Deacetylase (HDAC) Inhibitors, Histone Acetyltransferase (HAT) inhibitors, Bromodomain Inhibitors, DNA methylation inhibitors, etc. These and others are described in detail in reviews elsewhere, for example, in (Heerboth et al., 2014; Mohammad et al., 2019; Nepali and Liou, 2021). Broad-stroke targeting has been rather successful in generating drugs, placing a burden on better understanding of when to target distinct components.

A third property of cancer cells is altered expression of genes outside of those involved in transcription. Differentially expressed genes are often marked as sources for therapeutic targets. Identifying therapeutic targets is perhaps the most common justification for basic studies over the years. Increasing our understanding of how different types of cancers work has indeed resulted in identification of targets including surface and nuclear receptors, kinases, etc (Kannaiyan and Mahadevan, 2018; Zhao et al., 2019; Skidmore et al., 2020). While revealing molecular mechanisms of various processes and perhaps holding the keys to successful therapies in a long run, translation of these findings into therapies takes years with no guaranteed success. The ability to tailor a drug to a living cancer patient therefore remains limited (Krzyszczyk et al., 2018).

Ambiguous Roles of Transcription Factors

Identifying causative factors for precise targeting of cancers is an attractive goal that has met serious challenges (Vishnoi et al.,

2020). Cancers with well-known etiology such as fusion protein driven pediatric cancers remain difficult to target (Uren and Toretsky, 2005; Brien et al., 2019). This uncertainty is only amplified in adult cancers (Dawson et al., 2011; Fung et al., 2015; Shan et al., 2017; Winters and Bernt, 2017). One major reason behind this uncertainty is that the functions of individual factors can be dramatically altered across cell types and different individuals. This property may be inherent to transcription factors themselves and might not always be controllable.

DNA-binding transcription factors are commonly labeled as either activators or repressors (Wolffe et al., 1997). It is becoming increasingly clear, however, that most if not all transcription factors can, and likely do, function both as repressors and activators. There are several possible reasons for this duality. First, a factor itself may play different roles at the same loci. A number of transcription factors involved in *Drosophila* development and stimulus responses in human cells show default repression of target genes unless activated, usually by a co-factor, thereby appearing both as repressors and activators (Barolo and Posakony, 2002). In *E. coli* bacteriophage T4, the transcription factor gp33 causes default repression of late promoters, but becomes their potent co-activator in the presence of its specific co-factors (Kolesky et al., 2002; Nechaev and Geiduschek, 2006). *Drosophila* Hunchback and Dorsal (Pan and Courey, 1992; Dubnicoff et al., 1997; Bauer et al., 2010) serve as repressors or activators depending on co-factors on different promoters to drive highly coordinated embryo development (Staller et al., 2015). These well studied examples show that switching between a repressor and an activator in principle does not require complex changes.

Dual functions of transcription factors may arise through other mechanisms. One involves distinct activities for different isoforms of the same gene. Given a large number of known gene isoforms and frequent creation of new gene isoforms in cancers (Belluti et al., 2020), alternative splicing may be a significant contributor to the ambiguity of transcription factor designation, at least at the level of a gene (Walker et al., 1996). The same factors may also have different roles because they function in distinct complexes. The Polycomb Repressive Complex 2, PRC2, introduces the H3K27 histone mark with essential roles in development, cell differentiation, and cancer (Aranda et al., 2015; Schuettengruber et al., 2017; Healy et al., 2019). Ezh2 is the catalytic component of PRC2 responsible for introducing the mark. Ezh2 has been also shown to activate transcription in a separate role that does not involve its catalytic activity and is independent of PRC2 complex (Kim et al., 2018). Ezh2 role as an activator involves the binding at a promoter of a target (AR) gene as a DNA-binding transcription factor.

While the *Drosophila* factors have been well known to have dual roles, as more studies become available in human systems, even long-studied factors "acquire" opposing functions (Ip, 1995). For example, Snail is a conserved member of a family of E-box motif binding transcription factors that is involved in development though its role in the epithelial-mesenchymal transition with close relevance to cancer metastasis (Alberga et al., 1991; Carver et al., 2001; Peinado et al., 2004). Snail was initially considered to be exclusively a transcriptional repressor that binds to target gene promoters such as E-Cadherin. However, Snail was later shown to also activate genes in *Drosophila* during mesoderm development (Wu et al., 2017). Conversion of Snail from a repressor to an activator was shown to involve acetylation of Snail by the CREB-binding protein (CBP) (Hsu et al., 2014). Post-translational modifications can convert transcriptional repressors to activators (Mosley et al., 2003; Zhang et al., 2012), suggesting that this mechanism may be used in cancers as well. The duality of transcription factor roles as activators and repressors, therefore, is likely to be their inherent property rather than an exception.

Another major mechanism that can contribute to dual roles of transcription factors has to do not with their direct function, but with compensatory changes in the rest of the cell. On a short time scale, such as during rapid responses to stimuli, these changes may be driven by redistribution of cellular machinery components (Bregman et al., 1995). Such effects are considered secondary or nonspecific and are not well understood, but are pervasive and may be just as important as direct roles of transcription factors. For example, it is common for experimental perturbation of a factor by assays such as RNA-interference to cause both activation and repression of gene cohorts regardless of its actual mechanism of action. One possible exception is the transcriptional amplifier c-Myc that supports unbiased amplification of gene activity from all promoters genome-wide (Lin et al., 2012; Nie et al., 2012). Which genes are indirectly activated or repressed through secondary interactions should depend on the cellular context of individual cancers. The apparent dual roles of P53 tumor suppressor may fall into a similar category. The transcription factor p53 is widely considered to be an activator. Several studies, however, have proposed p53 as a direct repressor of genes (Banerjee et al., 2009; Allen et al., 2014). Its repressor role is controversial and has been suggested to be indirect (Fischer et al., 2014).

The ambiguity of functional designations for transcription factors extends to their phenotypic classification as oncogenes versus tumor suppressors (Shen et al., 2018; Datta et al., 2020), which may or may not be connected to their molecular mechanisms of action. The duality of transcriptional effects as well as cancer targeting outcomes persists through all levels of transcription factor function. These opposing functions are inherent to transcription factors and might not be separable even by specific targeting.

Epigenetic Marks – A Knot Around Transcription

Epigenetic marks are known to be frequently altered in cancers (Jones and Baylin, 2007; Baylin and Jones, 2011; Bennett and Licht, 2018), making potentially reversible epigenetic reprogramming an attractive targeting strategy (Jin and Kim, 2017). There are caveats, however. First, known epigenetic marks have a broad scope, either covering large regions of the genome or distributed across multiple punctate regions, limiting the specificity of direct targeting. Second, many known histone marks are closely tied to transcription, either associated with

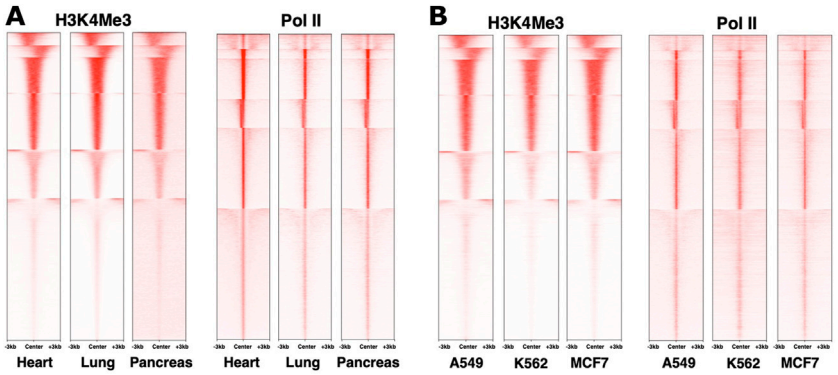

FIGURE 1 | Similarity in genome-wide distributions of Pol II and histone marks across distinct systems. ChIP-sequencing datasets from the ENCODE database (Davis et al., 2018) for human heart, lung and pancreas normal tissues **(A)** and A549, MCF7 and K562 cancer cell lines **(B)** were used to plot density heatmaps around peak regions ± 3 kb from a peak center using *computeMatrix reference-point* (version 3.3.0) and *plotHeatmap* (version 3.3.0) with k-means clustering (k = 6). The numbers of peaks are 22,944 for Pol II and 28,287 for H3K4Me3. The datasets used were ENCSR901SIL, ENCSR701FGA, ENCSR876DCP, ENCSR336YRS, ENCSR033NHF, ENCSR610EFT, ENCSR000DMZ, ENCSR388QZF, ENCSR000DMT, ENCSR203XPU, ENCSR668LDD, ENCSR985MIB, respectively.

repressed or active states of the nearby genes or regulatory elements such as enhancers (Henikoff and Shilatifard, 2011; Li et al., 2012; Kang et al., 2020) through mechanisms that remain to be fully understood. For example, histone H3 Lysine 4 trimethylation (H3K4Me3) preferentially marks active promoters, whereas monomethylation (H3K4Me1) mark appears to prefer regions outside of promoters including active and poised enhancers (Heintzman et al., 2007), and might have to do with transcriptional memory (Saeed et al., 2014; Bae and Lesch, 2020). Even with these well studied marks there are overlaps between distinct elements such as promoters and enhancers and the rules behind their deposition merit further studies (Pekowska et al., 2011; Scruggs et al., 2015; Soares et al., 2017). Histone H3K27 acetylation is commonly used to profile open genomic regions including active enhancers (Creyghton et al., 2010), but its functional roles remain not fully clear (Zhang et al., 2020). Acetylation patterns of various histones may be a good predictor for various types of regulatory elements (Rajagopal et al., 2014). Because genes and other regulatory regions are hotspots for multiple epigenetic marks with at least partial redundancy (Takeshima et al., 2009; Benveniste et al., 2014; Ahsendorf et al., 2017), targeting individual marks inevitably affects other marks and possibly the entire transcriptome.

The histone code hypothesis (Strahl and Allis, 2000) implies that the patterns of covalent histone modifications on a gene should reflect its dynamic regulatory state, likely contributing to widespread interest in epigenetics. Indeed, some histone modifications can be uncoupled from transcription activity. The conserved Polycomb Group (PcG) and Tritorax group of genes (trxG) complexes play crucial roles in development and introduce, respectively, repressive and activating histone modifications. The so-called bivalent genes that simultaneously harbor repressive and activating marks are poised for fate commitment in development and differentiation (Bernstein et al., 2006; Vastenhouw and Schier, 2012). The histone H3K36 modifications in the gene body regions may regulate alternative splicing (Kim et al., 2011). The histone H3K9 methylation, a repressive mark associated with heterochromatin, may be involved in arranging chromatin domains at the nuclear periphery (Towbin et al., 2012; Bian et al., 2020), protection against mechanical damage of the nucleus (Nava et al., 2020), remodeling of chromatin domains during differentiation (Wang et al., 2018; Burton et al., 2020) and maintenance of cell identity (Nicetto and Zaret, 2019). Many known histone modifications do not have clearly assigned functions yet, and will likely generate new findings (Tan et al., 2011).

When considering the dynamics of chromatin modifications, it is important to distinguish differences across loci within a cell type from differences at the same locus across cell types. Different genes in the same cell type clearly show distinct epigenomic patterns (Ernst and Kellis, 2010). However, across cell types, genome-wide patterns for histone modifications that we examined (ENCODE et al., 2020), at least in bulk experiments, appear to be similar for the same loci (**Figure 1** and not shown). This is mirrored in Pol II distribution as well (**Figure 1**), consistent with an earlier study, for example, (Day et al., 2016). Even examining a study that highlighted differences between epigenomes, most of the epigenomic features on a given gene are quantitatively similar (Yen and Kellis, 2015). Differences in epigenome patters between cell types may therefore be in relatively subtle shifts in balance among different marks (Gopi and Kidder, 2021), for example, in the breadth of regions harboring the marks (Benayoun et al., 2014), possibly representing distinct overall states of the nucleus or its compartments (Zhao et al., 2007), or distinct signaling pathways (Yen and Kellis, 2015). Comparing epigenetic marks remains difficult at this level due to quantitative limitations of omics technologies. Future studies employing emerging technologies and better integration of datasets should reveal new insights into the tightly interconnected workings of epigenetic marks. For

example, recent work using a mouse model identified epigenetic reprogramming as an essential step for the initiation of pancreatic cancer, wherein cells carrying certain oncogenic mutations require an environmental insult that causes epigenetic changes and triggers cancer cell fate (Alonso-Curbelo et al., 2021). To the best of our knowledge, this study is among the first to directly demonstrate a role for an epigenetic "hit" to trigger carcinogenesis. Finding the reasons behind why some cells are more sensitive to epigenetic reprogramming by drugs or environment, and identifying the weak points for their reprogramming, is an exciting direction to explore.

Multiple Sides of the Cellular Context

Cancers readily repurpose mechanisms that normally govern cell state transitions in differentiation, development, and responses to stimuli. Targeting of cancers borrows some of the overall concepts from the stem cells. Despite major advances in the stem cell field, reprogramming of stem cells rarely if ever approaches one hundred percent and can generate heterogeneous populations (Paik et al., 2018; Terryn et al., 2018). This heterogeneity, which is expected to be even higher in cancer cells, is likely to affect reprogramming and/or response to drugs. A recent study compared the effect of c-Myc on distinct fates of murine pre-B cells: transdifferentiating into macrophages and their reprogramming into iPSCs (Francesconi et al., 2019). Cells with high Myc activity reprogrammed to iPSCs more efficiently than transdifferentiated into macrophages, whereas cells with low Myc, in contrast, transdifferentiated readily, but failed to reprogram. That the levels of one factor can dramatically influence cell fate decisions highlights the importance and complexity of the cellular context.

Despite sharing certain features such as immortality and tendency for dedifferentiation, even recently transformed cells, without high if any mutation load, can readily deviate from normal cellular programs. A recent study showed that overexpression of the RAS oncogene in wild type mouse embryonic fibroblasts (MEFs) enhanced their dedifferentiation, but transformation of the same cells by deleting p53 or Arf tumor suppressors precluded it (Ferreirós et al., 2019). Similar interactions and context dependency were observed for histone marks as well (Nagaraja et al., 2019; Vidal et al., 2020). These data indicate that cancer cells diverge into distinct epigenetic programs, and likely change their cellular context, at the early stages of transformation. Thus, relatively small changes can lead to different responses to the same signal. These and other studies highlight the uncertainty that the cellular context can affect the apparent mechanism of transcription factor action as well as functional outcomes of its targeting.

A COMMON FRAMEWORK OF TRANSCRIPTOME ORGANIZATION

In this section we discuss a genome-wide view of transcription noting overall similarities in gene expression and highlighting potential mechanisms that might be pertinent for understanding transcriptome regulation.

The Transcriptome Rests on DNA

mRNA profiling has been widely used to identify genes with differential expression. Genome-wide gene expression patterns have been proposed as a basis to classify cancers (Perou et al., 2000). RNA-sequencing is arguably the easiest omics tool from the user's point of view today, and some thousands of mRNA datasets are publicly available. Comparing RNA profiles of publicly available datasets of human tissues, a majority of transcripts are classified as present in all or in most tissues (Uhlén et al., 2016), indicating that, at least in bulk experiments, most genes show similar patterns of expression across distinct cell types. Despite substantial differences, cancer cells and primary tumors show unexpectedly high correlation of RNA signal even among distant cancer types (for example, (Yu et al., 2019)). Comparison of RNA profiles showed that the group of genes that are differentially expressed is rather similar between distant cell lines (Crow et al., 2019). Analysis of gene expression across several species showed that variation in expression among different genes exceeds that of the same gene in different conditions (Zrimec et al., 2020). Accordingly, genes that account for differential transcriptome profiles are relatively few and seem to fall into categories related to stress responses and immune function regardless of the cell type (Crow et al., 2019). A small number of genes may be sufficient to classify cancer subtypes as, for example, is done for breast cancers (Parker et al., 2009). RNA-sequencing in cancers is just as, if not more frequently used for the detection of exonic mutations (PCAWG et al., 2020). These observations point to overall similarity of gene expression states across the genome, that is, imply a fundamentally common transcriptome structure in human cells.

One way to breach the boundaries of transcription control is through changing gene copy numbers. Local and chromosome-wide changes of DNA copy number is a frequent occurrence and is one of the hallmarks of cancer (Hanahan and Weinberg, 2011). Changes in copy number enable cancer cells to alter expression of genes without any other regulatory inputs (Shao et al., 2019). This may reflect a fundamental property of mammalian transcriptomes wherein changes in gene copy numbers are not by default compensated (Disteche, 2016) and can alter the entire transcriptome. Indeed, genetic haploinsufficiency is associated with many diseases (Han et al., 2018). Dosage compensation is best known in X-chromosome inactivation (Brockdorff and Turner, 2015). Forced reactivation of the inactive X-chromosome copy by knocking down Xist levels in mice results in an increase of total X-linked gene expression (Yang et al., 2016) that can lead to cancer (Yildirim et al., 2013). Interestingly, autosomal polysomy in human cells can be compensated at the level of protein, but not at the level of RNA (Stingele et al., 2012). Sensitivity to DNA copy number raises an intriguing possibility that the transcriptome may be fundamentally structured by the process of transcription rather than its products.

Pol II Pausing – A Common Step in Complex Organisms

Widespread accumulation of Pol II signal at promoter regions of genes has been well documented (Kim et al., 2005). Rather than preinitiation complexes, this signal comes largely from elongating Pol II that began RNA synthesis, but paused within the first ~50

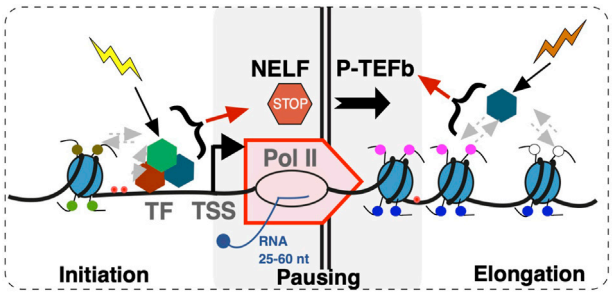

FIGURE 2 | A scheme of events during early transcription elongation. Early transcription elongation within 25–60 nucleotides (nt) from the Transcription Start Site (TSS) is a step integrating upstream and downstream regulatory inputs. Upstream inputs from multiple factors including transcription factors (TF) and epigenetic marks result in transcription initiation at the promoter and culminate in NELF-dependent pausing. DSIF complex is not included in the model. Pause release into transcription elongation is dependent on P-TEFb. Uncoupling of transcription initiation and elongation at the site of pausing through mechanisms such as promoter proximal termination contributes to transcriptome organization.

nucleotides (Pugh and Venters, 2016) (**Figure 2**). Because of its proximity to gene transcription start sites, the prevalence of Pol II pausing across the genome became clear only as technologies attained sufficient resolution (Muse et al., 2007; Zeitlinger et al., 2007; Nechaev et al., 2010). Perhaps because Pol II pausing was originally described on inducible genes such as MYC and heat shock HSP70 (O'Brien and Lis, 1991; Spencer and Groudine, 1990; Krumm et al., 1995), it was long believed to be a specialized mechanism that prepares highly inducible genes for activation. However, based on analyses of short RNA transcripts, Pol II pausing signatures are not confined to inducible genes, but are present on all genes, and likely accompany all transcription, whether initiating at or outside of promoters, including divergent transcription, intergenic transcription, enhancers, etc (Scheidegger et al., 2019). This makes pausing unlikely to be a mechanism that universally prepares genes for activation, although it likely contributes to it (see below) (Muse et al., 2007). Many details of Pol II pausing such as its relationship with the burst mode of transcription (Corrigan and Chubb, 2014; Fukaya et al., 2016; Tunnacliffe and Chubb, 2020) and its dynamics remain to be established. Whether Pol II pausing can be bypassed for individual transcription events or not, at least a certain percentage of Pol II complexes appear to undergo pausing at every start site of transcription (Scheidegger et al., 2019). The so-called "nonpaused" genes still show the same small RNA pausing signatures in terms of their size distributions, but are either less active or have a lower pausing index (Muse et al., 2007; Zeitlinger et al., 2007) (or higher traveling ratio (Rahl et al., 2010)) compared to other genes (Nechaev et al., 2010; Scheidegger et al., 2019). Examination of genome-wide datasets shows that different genes within a dataset show higher or lower pausing index, but these signatures, just like some histone marks, are overall stable across cell lines (**Figure 1**). These observations reinforce a notion on fundamental conservation of the human transcriptome and also raise a question about roles of pausing in regulation.

In considering potential biological roles of promoter-proximal Pol II pausing, it might be of significance that Pol II activity at this site is controlled by at least two distinct groups of factors: those that establish pausing and, on the other hand, those that release the Pol II from the paused state (**Figure 2**). The Negative Elongation Factor (NELF) is a five-subunit complex (Yamaguchi et al., 1999) that in conjunction with 5,6-dichloro-1-β-d-ribofuranosylbenzimidazole sensitivity-inducing factor (DSIF) (Yamaguchi et al., 2001) is sufficient to cause Pol II pausing *in vitro* (Renner et al., 2001; Wu et al., 2003). NELF is absent from yeast and *C. elegans*, indicating that NELF-dependent pausing is a function of higher organisms. Budding yeast *S. cerevisiae* do show Pol II accumulation at promoter regions at least at some genes (Radonjic et al., 2005). High-resolution nascent RNA analysis shows major differences between budding and fission (*S. pombe*) yeast, with the latter showing pausing signatures at a significant proportion of genes (Booth et al., 2016). However, fission yeast show clear differences from *Drosophila* and mammals in terms of the +1 nucleosome positioning presumably due to absence of NELF. These observations indicate that Pol II pausing is more prevalent and may be more tightly regulated in higher organisms.

Targeting of individual NELF subunit alters the levels of its other subunits (Sun et al., 2008), indicating that NELF components function as a complex. NELF is downregulated in breast cancers (Sun et al., 2008), but is potentially oncogenic in other cancers including prostate (Yun et al., 2018), liver (Dang et al., 2017; El Zeneini et al., 2017) and pancreas (Han et al., 2019). These observations indicate that the functional outcome of NELF perturbation is defined by the cellular context. The Positive Transcription Elongation factor B (P-TEFb) (Marshall and Price, 1995) is a two-component complex consisting of a cyclin T1, which can be substituted with cyclin T2 or possibly cyclin K, and a cyclin-dependent kinase 9 (CDK9) (Peng et al., 1998; Peterlin and Price, 2006; Kohoutek, 2009). P-TEFb releases the paused complex into productive elongation by phosphorylation of several proteins including DSIF subunit Spt5 at several sites (Wada et al., 1998; Kim and Sharp, 2001; Yamada et al., 2006; Parua et al., 2020), NELF (Fujinaga et al., 2004; Lu et al., 2016) and Pol II C-terminal domain at Ser-2 residues (Marshall et al., 1996). P-TEFb appears to be more conserved than NELF. Yeast may have more than one kinase (Hsin and Manley, 2012), although mammalian homologs of these kinases such as CDK12 appear to phosphorylate Pol II Ser-2 during elongation downstream of pause release by P-TEFb (Bartkowiak et al., 2010; Tellier et al., 2020). Neither NELF nor P-TEFb are essential for Pol II enzymatic function *in vitro*, but do appear to be essential for proper transcription *in vivo* (Sun et al., 2011; Aoi et al., 2020; Fujinaga, 2020). P-TEFb is a hub for regulatory inputs for multiple factors including c-MYC and NF-kB, and possibly many others (Zhou et al., 2012; Mahat et al., 2016; Aoi et al., 2020). The requirement for distinct essential factors individually controlling the on and off rates of a Pol II complex that is already committed to elongation is notable.

REGULATION BY GLOBALLY ACTING FACTORS

Here we discuss how transcription can be regulated by essential factors at the site of promoter-proximal Pol II pausing.

Encoding the Change in the Static Genome

One genome must specify the entire structure and dynamics of the transcriptomes for in every cell, but the rules of how it does so remain obscure. It is evident, however, that promoters, including core promoter basal sequence elements such as the TATA box, initiator motif, Downstream Promoter Element, etc, do not merely serve as a passive platform for the binding of regulatory factors, but actively shape the outcomes of regulatory inputs (Butler and Kadonaga, 2002). Flexibility of promoters is fundamental and starts with bacteria: in *E. coli*, no single promoter, including for the highest expressed rRNA genes, contains a full consensus sequence of basal elements (Bervoets and Charlier, 2019). Instead, promoters are pre-wired to require additional inputs for highest-level transcription and thus to be inherently controllable. In eukaryotes, properties of promoters depend on the presence of distinct basal sequence elements (Butler and Kadonaga, 2002). Mechanisms for such selectivity may include preference for distinct cohorts of general transcription factors, localization within the nucleus, or interaction with enhancers (Juven-Gershon and Kadonaga, 2010; Zabidi et al., 2015; Russo et al., 2018). Differences in core promoter properties should lead to differences in their responses to the same signal, thereby creating patterns that can be complex especially with multiple signals. In this regard, about ~350 human genes were recently noted to contain 5′-untranslated regions (UTRs) that show conservation across vertebrates, especially among specific categories of homeobox genes, kinases and genes involved in neurogenesis (Zuccotti et al., 2020).

Apart from differences between promoters, another question is whether and how the genome enables the same promoters to assume distinct regulatory states. In *Drosophila*, transcription start sites of regulatory genes contain sequences that favor both Pol II pausing and nucleosome binding at their transcription start sites (Gilchrist et al., 2010), which result in, respectively, active and repressed gene states. Housekeeping gene promoters, in contrast, do not contain these marks. By favoring mutually exclusive marks leading to distinct regulatory states, some promoters are intrinsically primed to be regulated. How these dynamic states are encoded in human promoters, which are highly enriched in CpG sequences, remains to be determined.

Transcriptional Responses Expose the Transcriptome

Global requirement for NELF- and P-TEFb raises a question about their functional relationship at the site of Pol II pausing. It has been proposed that activation of genes should proceed through pause "release," that is, relatively increased P-TEFb activity (Boehm et al., 2003; Hah et al., 2011; Liu et al., 2015; Mahat et al., 2016). Sustained transcription activation must also recruit additional Pol II, leaving a question as to how Pol II recruitment and pause release are related. A consistently rigid connection between pausing establishment and release would not be conducive for regulation. Evidence suggests that promoter Pol II recruitment and pause release can indeed be uncoupled. Chemical inhibition of P-TEFb - dependent Pol II pause release by flavopiridol causes accumulation of Pol II at promoters of active genes (Rahl et al., 2010; Henriques et al., 2013; Jonkers et al., 2014). Work by the Lis lab on heat shock response demonstrated that genes repressed by heat shock can accumulate Pol II signal at promoters (Mahat et al., 2016). Global Pol II accumulation at promoters has also been shown during acute oxidative stress response (Nilson et al., 2017). By demonstrating that Pol II pausing takes place even when P-TEFb activity is perturbed, these studies show that pausing establishment and release can be functionally uncoupled, and that this connection can be regulatory. Conversely, changes in Pol II recruitment without affecting pause release are possible as well. First, gene activation can take place through increased Pol II recruitment to promoters without changes in pause release (Samarakkody et al., 2015). Second, the Shilatifard lab showed that pause release can take place without additional Pol II recruitment when Pol II is being cleared from promoters prior to mitosis (Liang et al., 2015). Overall, these and other observations suggest that processes upstream of pausing, such as Pol II recruitment to promoters and formation of preinitiation complexes, can be functionally decoupled from pause release. Furthermore, the function of Pol II pausing as a limiting step for transcription may be more significant not at the steady state, but during rapid responses to stimuli (Gressel et al., 2019). Observing cells during rapid responses to stimuli outside of the steady state may help reveal their regulatory architecture (Danko et al., 2013; Vihervaara et al., 2017).

A study from the Young lab showed that overexpression of c-Myc causes uniform amplification of all genes (Lin et al., 2012; Nie et al., 2012). Since c-Myc was shown to function through recruitment of P-TEFb to promoters (Rahl et al., 2010), this amplification is likely due to uniformly increased genome-wide pause release. These findings are important because they imply that the transcriptome is fundamentally modular. Throttling up of pause release siphons Pol II traffic through all available transcription start sites without altering the upstream steps such as promoter architecture. These observations reveal pausing as a central step that can globally separate regulatory inputs at distinct points of the transcription cycle. In this view, rather than integrating regulatory signals, Pol II pausing separates them.

Regulation of the Transcriptome at the Level of Pol II Pausing

Either NELF or P-TEFb activities may become limiting at certain circumstances such as during rapid responses to stimuli. This raises a question of how these factors are redistributed across the genome when limited amounts or activity are available. This question is broadly related to an earlier concept of enhancer insufficiency (Barolo and Posakony, 2002) wherein restriction of

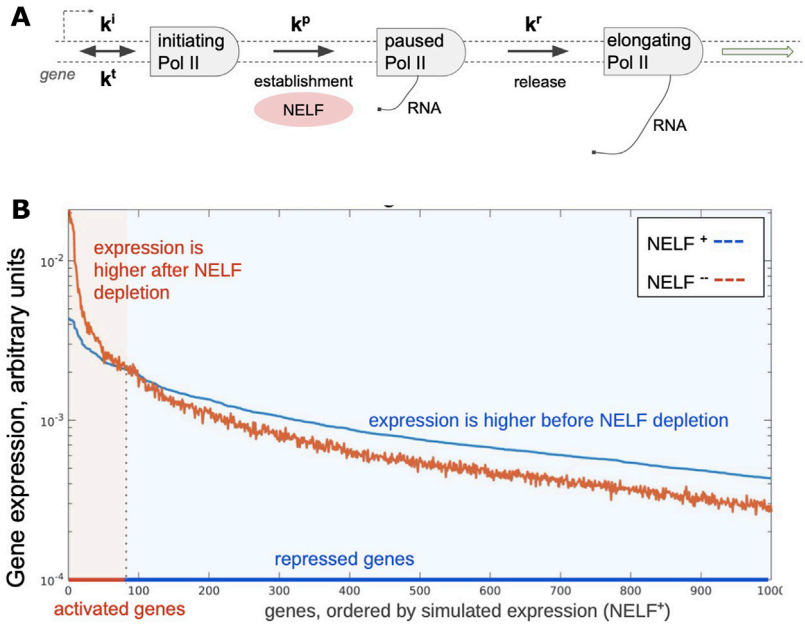

FIGURE 3 | Simulated changes in gene expression upon depletion of a pausing factor. **(A)** A scheme of steps in Pol II pausing. Initiation (ki), pausing (kp), and release (kr) constants were randomly distributed for 1000 simulated genes (with cauchy and two gaussian probability distribution functions, respectively); termination constant (kt) was the same for all simulated genes. **(B)** Results of simulation showing steady-state distribution of gene expression (light colored arrow) levels with two different amounts of total available NELF in the system, which results in activation and repression of genes.

the activator availability limits transcription from certain genes such as those with low activity promoters, thereby reducing noise. Simple simulation of a closed cell containing promoters with randomly distributed strengths shows that restricting a factor that is essential for transcription at a post-recruitment step, such as NELF, is sufficient to generate pools of genes that appear as activated and repressed (**Figure 3**). Addition of a second post-recruitment step such as that controlled by P-TEFb should likewise prioritize pause release among Pol II complexes that had reached the previous step. Prioritization of essential factors at multiple steps of the transcription cycle may lead to nonlinear effects including cooperativity and stabilization of transcription output. Prioritization of essential factors, we suggest, is a key principle organizing the transcriptome.

Step-wise prioritization of essential factors retrospectively accounts for known features of mammalian transcriptomes. Some transcription factors such as HSF1 and NF-kB have been shown to act on pause release by directly or indirectly recruiting P-TEFb (Zhou et al., 2012; Mahat et al., 2016; Aoi et al., 2020). P-TEFb function can be either global across the genome or involve specific groups of genes (Luo et al., 2012). Secondly, the model is agnostic to the exact promoter activity patterns and can work in all cells wherein promoter activity defines the network structure while pausing factors stabilize it. Notably, this regulation should be highly sensitive to gene copy numbers but does not require lateral interactions between gene products. This model is in principle similar to the concept of phase separation (Hnisz et al., 2017), except that the phases here are defined not spatially, but through availability of a factor that may be governed by diffusion or over-representation in different nuclear compartments. In this view, transcription of every gene must involve transitions between phases. Multiple inputs upstream and downstream of pausing including epigenetic and other broad-stroke mechanisms may form additional layers of regulation or converge on the two major limiting steps at the site of pausing. A caveat to our view is that a complex makeup of the cell is essentially reduced to a binary readout, which is certainly an oversimplification. However, the concept of binary readouts distinguishing complex systems such as cancers is gaining experimental ground (Pearson et al., 2021) and may form a paradigm for understanding and targeting these complex diseases. Transcriptional superenhancers (Hnisz et al., 2013; Hnisz et al., 2015) as well as the recently reported partitioning of small molecule drugs at distinct nuclear loci (Klein et al., 2020) must affect the specificity of globally acting factors and outcomes of their targeting through principles that remain to be explored. We note that our model is readily compatible with transcriptional bursting (Rodriguez and Larson, 2020) because bursting creates local and transient demand for transcriptional machinery components. Lastly, despite the prevalence of pause release during responses to stimuli, Pol II recruitment to promoters may still be the step limiting for overall transcription.

DISCUSSION

Substantial advances are made in targeting cancers based on transcription and epigenetic signatures (Malone et al., 2020). However, progress remains complicated by the inherent uncertainty in the roles of transcription machinery

components and critical yet poorly understood contribution of the cellular context. Pausing regulators including NELF and P-TEFb have been proposed (Yun et al., 2018) or used as therapeutic targets including P-TEFb (CDK9) small molecule inhibitors in clinical trials (Morales and Giordano, 2016; Cassandri et al., 2020). However, the main value of pausing factors may be not in serving as therapy targets, but in providing a conceptual platform to better understand targeting of other components. Dividing the myriad factors directly or indirectly affecting transcription into those that act upstream or downstream of Pol II pausing (**Figure 2**) highlights the balance between these steps as an important readout of cancers that can help expose their vulnerabilities.

The process of Pol II pausing is much more granular at the molecular level than described above (Elrod et al., 2019) and includes multiple additional steps such as premature transcription termination likely involving multiple mechanisms (London et al., 1991; Brannan et al., 2012; Huang et al., 2020; Rimel et al., 2020). These and other steps should affect the balance between Pol II functions upstream and downstream of pausing. The model of transcriptome regulation by stepwise restriction of globally acting factors proposed here is agnostic to the actual nature of its components and does not need to be limited to Pol II pausing. Additional transcription elongation checkpoints such as those controlled by CDK12 (Tellier et al., 2020) may define new steps where a balance would need to be considered. Despite the ongoing quest for therapeutics targeting specific factors, cancer treatments largely rely on broad-stroke interventions and are expected to do so for the foreseeable future. Studies that integrate experiments with refined models should reveal new insights into cancer transcriptomes to improve the treatments targeting the cellular machinery *via* globally acting or general factors.

AUTHOR CONTRIBUTIONS

DP - analyzed data, prepared figures and wrote the manuscript; MV - analyzed data and prepared figures; LK - analyzed data; SN, conceived the manuscript and wrote the manuscript.

FUNDING

Funding for this work was provided by the National Science Foundation CAREER award 1750379 to SN.

ACKNOWLEDGMENTS

We thank Motoki Takaku and Archana Dhasarathy for critical reading of the manuscript as well as Eda Yildirim and Al Courey for helpful suggestions.

REFERENCES

Adelman, K., Kennedy, M. A., Nechaev, S., Gilchrist, D. A., Muse, G. W., Chinenov, Y., et al. (2009). Immediate Mediators of the Inflammatory Response Are Poised for Gene Activation Through RNA Polymerase II Stalling. *Proc. Natl. Acad. Sci. U S A.* 106 (43), 18207–18212. doi:10.1073/pnas.0910177106

Ahsendorf, T., Müller, F. J., Topkar, V., Gunawardena, J., and Eils, R. (2017). Transcription Factors, Coregulators, and Epigenetic Marks Are Linearly Correlated and Highly Redundant. *PLoS One* 12, e0186324. doi:10.1371/journal.pone.0186324

Alberga, A., Boulay, J. L., Kempe, E., Dennefeld, C., and Haenlin, M. (1991). The Snail Gene Required for Mesoderm Formation in Drosophila Is Expressed Dynamically in Derivatives of All Three Germ Layers. *Development* 111 (4), 983–992. doi:10.1242/dev.111.4.983

Allen, M. A., Andrysik, Z., Dengler, V. L., Mellert, H. S., Guarnieri, A., Freeman, J. A., et al. (2014). Global Analysis of P53-Regulated Transcription Identifies its Direct Targets and Unexpected Regulatory Mechanisms. *Elife* 3, e02200. doi:10.7554/eLife.02200

Alonso-Curbelo, D., Ho, Y. J., Burdziak, C., Maag, J. L. V., Morris, J. P., Chandwani, R., et al. (2021). A Gene-Environment-Induced Epigenetic Program Initiates Tumorigenesis. *Nature* 590 (7847), 642–648. doi:10.1038/s41586-020-03147-x

Aoi, Y., Smith, E. R., Shah, A. P., Rendleman, E. J., Marshall, S. A., Woodfin, A. R., et al. (2020). NELF Regulates A Promoter-Proximal Step Distinct from RNA Pol II Pause-Release. *Mol. Cel.* 78 (2), 261–274.e5. doi:10.1016/j.molcel.2020.02.014

Aranda, S., Mas, G., and Di Croce, L. (2015). Regulation of Gene Transcription by Polycomb Proteins. *Sci. Adv.* 1 (11), e1500737. doi:10.1126/sciadv.1500737

Bae, S., and Lesch, B. J. (2020). H3K4me1 Distribution Predicts Transcription State and Poising at Promoters. *Front Cel. Dev. Biol.* 8, 289. doi:10.3389/fcell.2020.00289

Banerjee, T., Nath, S., and Roychoudhury, S. (2009). DNA Damage Induced P53 Downregulates Cdc20 by Direct Binding to its Promoter Causing Chromatin Remodeling. *Nucleic Acids Res.* 37 (8), 2688–2698. doi:10.1093/nar/gkp110

Barolo, S., and Posakony, J. W. (2002). Three Habits of Highly Effective Signaling Pathways: Principles of Transcriptional Control by Developmental Cell Signaling. *Genes Dev.* 16 (10), 1167–1181. doi:10.1101/gad.976502

Bartkowiak, B., Liu, P., Phatnani, H. P., Fuda, N. J., Cooper, J. J., Price, D. H., et al. (2010). CDK12 Is a Transcription Elongation-Associated CTD Kinase, the Metazoan Ortholog of Yeast Ctk1. *Genes Dev.* 24 (20), 2303–2316. doi:10.1101/gad.1968210

Bauer, D. C., Buske, F. A., and Bailey, T. L. (2010). Dual-functioning Transcription Factors in the Developmental Gene Network of *Drosophila melanogaster*. *BMC Bioinformatics* 11, 366. doi:10.1186/1471-2105-11-366

Baylin, S. B., and Jones, P. A. (2011). A Decade of Exploring the Cancer Epigenome - Biological and Translational Implications. *Nat. Rev. Cancer* 11 (10), 726–734. doi:10.1038/nrc3130

Belluti, S., Rigillo, G., and Imbriano, C. (2020). Transcription Factors in Cancer: When Alternative Splicing Determines Opposite Cell Fates. *Cells* 9 (3), E760. doi:10.3390/cells9030760

Benayoun, B. A., Pollina, E. A., Ucar, D., Mahmoudi, S., Karra, K., Wong, E. D., et al. (2014). H3K4me3 Breadth Is Linked to Cell Identity and Transcriptional Consistency. *Cell* 158 (3), 673–688. doi:10.1016/j.cell.2014.06.027

Bennett, R. L., and Licht, J. D. (2018). Targeting Epigenetics in Cancer. *Annu. Rev. Pharmacol. Toxicol.* 58, 187–207. doi:10.1146/annurev-pharmtox-010716-105106

Benveniste, D., Sonntag, H. J., Sanguinetti, G., and Sproul, D. (2014). Transcription Factor Binding Predicts Histone Modifications in Human Cell Lines. *Proc. Natl. Acad. Sci. U S A.* 111 (37), 13367–13372. doi:10.1073/pnas.1412081111

Bernstein, B. E., Mikkelsen, T. S., Xie, X., Kamal, M., Huebert, D. J., Cuff, J., et al. (2006). A Bivalent Chromatin Structure Marks Key Developmental Genes in Embryonic Stem Cells. *Cell* 125 (2), 315–326. doi:10.1016/j.cell.2006.02.041

Bervoets, I., and Charlier, D. (2019). Diversity, Versatility and Complexity of Bacterial Gene Regulation Mechanisms: Opportunities and Drawbacks for Applications in Synthetic Biology. *FEMS Microbiol. Rev.* 43 (3), 304–339. doi:10.1093/femsre/fuz001

Bian, Q., Anderson, E. C., Yang, Q., and Meyer, B. J. (2020). Histone H3K9 Methylation Promotes Formation of Genome Compartments in

Caenorhabditis elegans via Chromosome Compaction and Perinuclear Anchoring. *Proc. Natl. Acad. Sci. U S A.* 117 (21), 11459–11470. doi:10.1073/pnas.2002068117

Boehm, A. K., Saunders, A., Werner, J., and Lis, J. T. (2003). Transcription Factor and Polymerase Recruitment, Modification, and Movement on Dhsp70 In Vivo in the Minutes Following Heat Shock. *Mol. Cel Biol.* 23 (21), 7628–7637. doi:10.1128/mcb.23.21.7628-7637.2003

Booth, G. T., Wang, I. X., Cheung, V. G., and Lis, J. T. (2016). Divergence of a Conserved Elongation Factor and Transcription Regulation in Budding and Fission Yeast. *Genome Res.* 26 (6), 799–811. doi:10.1101/gr.204578.116

Bradner, J. E., Hnisz, D., and Young, R. A. (2017). Transcriptional Addiction in Cancer. *Cell* 168 (4), 629–643. doi:10.1016/j.cell.2016.12.013

Brannan, K., Kim, H., Erickson, B., Glover-Cutter, K., Kim, S., Fong, N., et al. (2012). mRNA Decapping Factors and the Exonuclease Xrn2 Function in Widespread Premature Termination of RNA Polymerase II Transcription. *Mol. Cel* 46 (3), 311–324. doi:10.1016/j.molcel.2012.03.006

Bregman, D. B., Du, L., van der Zee, S., and Warren, S. L. (1995). Transcription-dependent Redistribution of the Large Subunit of RNA Polymerase II to Discrete Nuclear Domains. *J. Cel Biol.* 129 (2), 287–298. doi:10.1083/jcb.129.2.287

Brien, G. L., Stegmaier, K., and Armstrong, S. A. (2019). Targeting Chromatin Complexes in Fusion Protein-Driven Malignancies. *Nat. Rev. Cancer* 19 (5), 255–269. doi:10.1038/s41568-019-0132-x

Brockdorff, N., and Turner, B. M. (2015). Dosage Compensation in Mammals. *Cold Spring Harb Perspect. Biol.* 7 (3), a019406. doi:10.1101/cshperspect.a019406

Burton, A., Brochard, V., Galan, C., Ruiz-Morales, E. R., Rovira, Q., Rodriguez-Terrones, D., et al. (2020). Heterochromatin Establishment During Early Mammalian Development Is Regulated by Pericentromeric RNA and Characterized by Non-repressive H3K9me3. *Nat. Cel Biol.* 22 (7), 767–778. doi:10.1038/s41556-020-0536-6

Bushweller, J. H. (2019). Targeting Transcription Factors in Cancer - From Undruggable to Reality. *Nat. Rev. Cancer* 19 (11), 611–624. doi:10.1038/s41568-019-0196-7

Butler, J. E., and Kadonaga, J. T. (2002). The RNA Polymerase II Core Promoter: A Key Component in the Regulation of Gene Expression. *Genes Dev.* 16 (20), 2583–2592. doi:10.1101/gad.1026202

Bywater, M. J., Pearson, R. B., McArthur, G. A., and Hannan, R. D. (2013). Dysregulation of the Basal RNA Polymerase Transcription Apparatus in Cancer. *Nat. Rev. Cancer* 13 (5), 299–314. doi:10.1038/nrc3496

Carver, E. A., Jiang, R., Lan, Y., Oram, K. F., and Gridley, T. (2001). The Mouse Snail Gene Encodes a Key Regulator of the Epithelial-Mesenchymal Transition. *Mol. Cel Biol.* 21 (23), 8184–8188. doi:10.1128/mcb.21.23.8184-8188.2001

Cassandri, M., Fioravanti, R., Pomella, S., Valente, S., Rotili, D., Del Baldo, G., et al. (2020). CDK9 as a Valuable Target in Cancer: From Natural Compounds Inhibitors to Current Treatment in Pediatric Soft Tissue Sarcomas. *Front. Pharmacol.* 11, 1230. doi:10.3389/fphar.2020.01230

Corrigan, A. M., and Chubb, J. R. (2014). Regulation of Transcriptional Bursting by a Naturally Oscillating Signal. *Curr. Biol.* 24 (2), 205–211. doi:10.1016/j.cub.2013.12.011

Creyghton, M. P., Cheng, A. W., Welstead, G. G., Kooistra, T., Carey, B. W., Steine, E. J., et al. (2010). Histone H3K27ac Separates Active from Poised Enhancers and Predicts Developmental State. *Proc. Natl. Acad. Sci. U S A.* 107 (50), 21931–21936. doi:10.1073/pnas.1016071107

Crow, M., Lim, N., Ballouz, S., Pavlidis, P., and Gillis, J. (2019). Predictability of Human Differential Gene Expression. *Proc. Natl. Acad. Sci. U S A.* 116 (13), 6491–6500. doi:10.1073/pnas.1802973116

Dang, H., Takai, A., Forgues, M., Pomyen, Y., Mou, H., Xue, W., et al. (2017). Oncogenic Activation of the RNA Binding Protein NELFE and MYC Signaling in Hepatocellular Carcinoma. *Cancer Cell* 32 (1), 101–114.e8. doi:10.1016/j.ccell.2017.06.002

Danko, C. G., Hah, N., Luo, X., Martins, A. L., Core, L., Lis, J. T., et al. (2013). Signaling Pathways Differentially Affect RNA Polymerase II Initiation, Pausing, and Elongation Rate in Cells. *Mol. Cel.* 50 (2), 212–222. doi:10.1016/j.molcel.2013.02.015

Datta, N., Chakraborty, S., Basu, M., and Ghosh, M. K. (2020). Tumor Suppressors Having Oncogenic Functions: The Double Agents. *Cells* 10 (1), E46. doi:10.3390/cells10010046

Davis, C. A., Hitz, B. C., Sloan, C. A., Chan, E. T., Davidson, J. M., Gabdank, I., et al. (2018). The Encyclopedia of DNA Elements (ENCODE): Data portal Update. *Nucleic Acids Res.* 46 (D1), D794–D801. doi:10.1093/nar/gkx1081

Dawson, M. A., Prinjha, R. K., Dittmann, A., Giotopoulos, G., Bantscheff, M., Chan, W. I., et al. (2011). Inhibition of BET Recruitment to Chromatin as an Effective Treatment for MLL-Fusion Leukaemia. *Nature* 478 (7370), 529–533. doi:10.1038/nature10509

Day, D. S., Zhang, B., Stevens, S. M., Ferrari, F., Larschan, E. N., Park, P. J., et al. (2016). Comprehensive Analysis of Promoter-Proximal RNA Polymerase II Pausing Across Mammalian Cell Types. *Genome Biol.* 17 (1), 120. doi:10.1186/s13059-016-0984-2

Disteche, C. M. (2016). Dosage Compensation of the Sex Chromosomes and Autosomes. *Semin. Cel Dev Biol.* 56, 9–18. doi:10.1016/j.semcdb.2016.04.013

Dubnicoff, T., Valentine, S. A., Chen, G., Shi, T., Lengyel, J. A., Paroush, Z., et al. (1997). Conversion of Dorsal from an Activator to a Repressor by the Global Corepressor Groucho. *Genes Dev.* 11 (22), 2952–2957. doi:10.1101/gad.11.22.2952

Duffy, M. J., and Crown, J. (2021). Drugging "Undruggable" Genes for Cancer Treatment: Are We Making Progress. *Int. J. Cancer* 148 (1), 8–17. doi:10.1002/ijc.33197

El Zeneini, E., Kamel, S., El-Meteini, M., and Amleh, A. (2017). Knockdown of COBRA1 Decreases the Proliferation and Migration of Hepatocellular Carcinoma Cells. *Oncol. Rep.* 37 (3), 1896–1906. doi:10.3892/or.2017.5390

Elrod, N. D., Henriques, T., Huang, K. L., Tatomer, D. C., Wilusz, J. E., Wagner, E. J., et al. (2019). The Integrator Complex Attenuates Promoter-Proximal Transcription at Protein-Coding Genes. *Mol. Cel.* 76 (5), 738–752.e7. doi:10.1016/j.molcel.2019.10.034

Encode, P. C., Moore, J. E., Purcaro, M. J., Pratt, H. E., Epstein, C. B., Shoresh, N., et al. (2020). Expanded Encyclopaedias of DNA Elements in the Human and Mouse Genomes. *Nature* 583 (7818), 699–710. doi:10.1038/s41586-020-2493-4

Ernst, J., and Kellis, M. (2010). Discovery and Characterization of Chromatin States for Systematic Annotation of the Human Genome. *Nat. Biotechnol.* 28 (8), 817–825. doi:10.1038/nbt.1662

Ferreirós, A., Pedrosa, P., Da Silva-Álvarez, S., Triana-Martínez, F., Vilas, J. M., Picallos-Rabina, P., et al. (2019). Context-Dependent Impact of RAS Oncogene Expression on Cellular Reprogramming to Pluripotency. *Stem Cel Rep.* 12 (5), 1099–1112. doi:10.1016/j.stemcr.2019.04.006

Fischer, M., Steiner, L., and Engeland, K. (2014). The Transcription Factor P53: Not a Repressor, Solely an Activator. *Cell Cycle* 13 (19), 3037–3058. doi:10.4161/15384101.2014.949083

Francesconi, M., Di Stefano, B., Berenguer, C., de Andrés-Aguayo, L., Plana-Carmona, M., Mendez-Lago, M., et al. (2019). Single Cell RNA-Seq Identifies the Origins of Heterogeneity in Efficient Cell Transdifferentiation and Reprogramming. *Elife* 8, e41627. doi:10.7554/eLife.41627

Fujinaga, K. (2020). P-TEFb as A Promising Therapeutic Target. *Molecules* 25 (4), E838. doi:10.3390/molecules25040838

Fujinaga, K., Irwin, D., Huang, Y., Taube, R., Kurosu, T., and Peterlin, B. M. (2004). Dynamics of Human Immunodeficiency Virus Transcription: P-TEFb Phosphorylates RD and Dissociates Negative Effectors from the Transactivation Response Element. *Mol. Cel Biol.* 24 (2), 787–795. doi:10.1128/mcb.24.2.787-795.2004

Fukaya, T., Lim, B., and Levine, M. (2016). Enhancer Control of Transcriptional Bursting. *Cell* 166 (2), 358–368. doi:10.1016/j.cell.2016.05.025

Fung, J. J., Kosaka, A., Shan, X., Danet-Desnoyers, G., Gormally, M., Owen, K., et al. (2015). Registered Report: Inhibition of BET Recruitment to Chromatin as an Effective Treatment for MLL-Fusion Leukemia. *Elife* 4, e08997. doi:10.7554/eLife.08997

Gilchrist, D. A., Dos Santos, G., Fargo, D. C., Xie, B., Gao, Y., Li, L., et al. (2010). Pausing of RNA Polymerase II Disrupts DNA-Specified Nucleosome Organization to Enable Precise Gene Regulation. *Cell* 143 (4), 540–551. doi:10.1016/j.cell.2010.10.004

Gong, L., Yan, Q., Zhang, Y., Fang, X., Liu, B., and Guan, X. (2019). Cancer Cell Reprogramming: A Promising Therapy Converting Malignancy to Benignity. *Cancer Commun. (Lond)* 39 (1), 48. doi:10.1186/s40880-019-0393-5

Gopi, L. K., and Kidder, B. L. (2021). Integrative Pan Cancer Analysis Reveals Epigenomic Variation in Cancer Type and Cell Specific Chromatin Domains. *Nat. Commun.* 12 (1), 1419. doi:10.1038/s41467-021-21707-1

Gressel, S., Schwalb, B., and Cramer, P. (2019). The Pause-Initiation Limit Restricts Transcription Activation in Human Cells. *Nat. Commun.* 10 (1), 3603. doi:10.1038/s41467-019-11536-8

Hah, N., Danko, C. G., Core, L., Waterfall, J. J., Siepel, A., Lis, J. T., et al. (2011). A Rapid, Extensive, and Transient Transcriptional Response to Estrogen Signaling in Breast Cancer Cells. *Cell* 145 (4), 622–634. doi:10.1016/j.cell.2011.03.042

Hallin, J., Engstrom, L. D., Hargis, L., Calinisan, A., Aranda, R., Briere, D. M., et al. (2020). The $KRAS^{G12C}$ Inhibitor MRTX849 Provides Insight Toward Therapeutic Susceptibility of KRAS-Mutant Cancers in Mouse Models and Patients. *Cancer Discov.* 10 (1), 54–71. doi:10.1158/2159-8290.CD-19-1167

Hampsey, M. (1998). Molecular Genetics of the RNA Polymerase II General Transcriptional Machinery. *Microbiol. Mol. Biol. Rev.* 62 (2), 465–503. doi:10.1128/MMBR.62.2.465-503.1998

Han, L., Zan, Y., Huang, C., and Zhang, S. (2019). NELFE Promoted Pancreatic Cancer Metastasis and the Epithelial-To-Mesenchymal Transition by Decreasing the Stabilization of NDRG2 mRNA. *Int. J. Oncol.* 55 (6), 1313–1323. doi:10.3892/ijo.2019.4890

Han, X., Chen, S., Flynn, E., Wu, S., Wintner, D., and Shen, Y. (2018). Distinct Epigenomic Patterns Are Associated with Haploinsufficiency and Predict Risk Genes of Developmental Disorders. *Nat. Commun.* 9 (1), 2138. doi:10.1038/s41467-018-04552-7

Hanahan, D., and Weinberg, R. A. (2011). Hallmarks of Cancer: The Next Generation. *Cell* 144 (5), 646–674. doi:10.1016/j.cell.2011.02.013

Healy, E., Mucha, M., Glancy, E., Fitzpatrick, D. J., Conway, E., Neikes, H. K., et al. (2019). PRC2.1 and PRC2.2 Synergize to Coordinate H3K27 Trimethylation. *Mol. Cel* 76 (3), 437–452.e6. doi:10.1016/j.molcel.2019.08.012

Heerboth, S., Lapinska, K., Snyder, N., Leary, M., Rollinson, S., and Sarkar, S. (2014). Use of Epigenetic Drugs in Disease: An Overview. *Genet. Epigenet* 6, 9–19. doi:10.4137/GEG.S12270

Heintzman, N. D., Stuart, R. K., Hon, G., Fu, Y., Ching, C. W., Hawkins, R. D., et al. (2007). Distinct and Predictive Chromatin Signatures of Transcriptional Promoters and Enhancers in the Human Genome. *Nat. Genet.* 39 (3), 311–318. doi:10.1038/ng1966

Henikoff, S., and Shilatifard, A. (2011). Histone Modification: Cause or Cog. *Trends Genet.* 27 (10), 389–396. doi:10.1016/j.tig.2011.06.006

Henriques, T., Gilchrist, D. A., Nechaev, S., Bern, M., Muse, G. W., Burkholder, A., et al. (2013). Stable Pausing by RNA Polymerase II Provides an Opportunity to Target and Integrate Regulatory Signals. *Mol. Cel* 52 (4), 517–528. doi:10.1016/j.molcel.2013.10.001

Hnisz, D., Abraham, B. J., Lee, T. I., Lau, A., Saint-André, V., Sigova, A. A., et al. (2013). Super-enhancers in the Control of Cell Identity and Disease. *Cell* 155 (4), 934–947. doi:10.1016/j.cell.2013.09.053

Hnisz, D., Schuijers, J., Lin, C. Y., Weintraub, A. S., Abraham, B. J., Lee, T. I., et al. (2015). Convergence of Developmental and Oncogenic Signaling Pathways at Transcriptional Super-enhancers. *Mol. Cel* 58 (2), 362–370. doi:10.1016/j.molcel.2015.02.014

Hnisz, D., Shrinivas, K., Young, R. A., Chakraborty, A. K., and Sharp, P. A. (2017). A Phase Separation Model for Transcriptional Control. *Cell* 169 (1), 13–23. doi:10.1016/j.cell.2017.02.007

Hsin, J. P., and Manley, J. L. (2012). The RNA Polymerase II CTD Coordinates Transcription and RNA Processing. *Genes Dev.* 26 (19), 2119–2137. doi:10.1101/gad.200303.112

Hsu, D. S., Wang, H. J., Tai, S. K., Chou, C. H., Hsieh, C. H., Chiu, P. H., et al. (2014). Acetylation of Snail Modulates the Cytokinome of Cancer Cells to Enhance the Recruitment of Macrophages. *Cancer Cell* 26 (4), 534–548. doi:10.1016/j.ccell.2014.09.002

Huang, K. L., Jee, D., Stein, C. B., Elrod, N. D., Henriques, T., Mascibroda, L. G., et al. (2020). Integrator Recruits Protein Phosphatase 2A to Prevent Pause Release and Facilitate Transcription Termination. *Mol. Cel.* 80 (2), 345–358.e9. doi:10.1016/j.molcel.2020.08.016

Ip, Y. T. (1995). Transcriptional Regulation. Converting an Activator into a Repressor. *Curr. Biol.* 5 (1), 1–3. doi:10.1016/s0960-9822(95)00001-7

Jin, X., and Kim, H. (2017). Cancer Stem Cells and Differentiation Therapy. *Tumour Biol.* 39 (10), 1010428317729933. doi:10.1177/1010428317729933

Jones, P. A., and Baylin, S. B. (2007). The Epigenomics of Cancer. *Cell* 128 (4), 683–692. doi:10.1016/j.cell.2007.01.029

Jonkers, I., Kwak, H., and Lis, J. T. (2014). Genome-wide Dynamics of Pol II Elongation and its Interplay with Promoter Proximal Pausing, Chromatin, and Exons. *Elife* 3, e02407. doi:10.7554/eLife.02407

Juven-Gershon, T., and Kadonaga, J. T. (2010). Regulation of Gene Expression via the Core Promoter and the Basal Transcriptional Machinery. *Dev. Biol.* 339 (2), 225–229. doi:10.1016/j.ydbio.2009.08.009

Kang, H., Shokhirev, M. N., Xu, Z., Chandran, S., Dixon, J. R., and Hetzer, M. W. (2020). Dynamic Regulation of Histone Modifications and Long-Range Chromosomal Interactions During Postmitotic Transcriptional Reactivation. *Genes Dev.* 34 (13-14), 913–930. doi:10.1101/gad.335794.119

Kannaiyan, R., and Mahadevan, D. (2018). A Comprehensive Review of Protein Kinase Inhibitors for Cancer Therapy. *Expert Rev. Anticancer Ther.* 18 (12), 1249–1270. doi:10.1080/14737140.2018.1527688

Kim, J. B., and Sharp, P. A. (2001). Positive Transcription Elongation Factor B Phosphorylates hSPT5 and RNA Polymerase II Carboxyl-Terminal Domain Independently of Cyclin-dependent Kinase-Activating Kinase. *J. Biol. Chem.* 276 (15), 12317–12323. doi:10.1074/jbc.m010908200

Kim, J., Lee, Y., Lu, X., Song, B., Fong, K. W., Cao, Q., et al. (2018). Polycomb- and Methylation-independent Roles of EZH2 as a Transcription Activator. *Cell Rep.* 25 (10), 2808–2820.e4. doi:10.1016/j.celrep.2018.11.035

Kim, S., Kim, H., Fong, N., Erickson, B., and Bentley, D. L. (2011). Pre-mRNA Splicing Is a Determinant of Histone H3K36 Methylation. *Proc. Natl. Acad. Sci. U S A.* 108 (33), 13564–13569. doi:10.1073/pnas.1109475108

Kim, T. H., Barrera, L. O., Zheng, M., Qu, C., Singer, M. A., Richmond, T. A., et al. (2005). A High-Resolution Map of Active Promoters in the Human Genome. *Nature* 436 (7052), 876–880. doi:10.1038/nature03877

Klein, I. A., Boija, A., Afeyan, L. K., Hawken, S. W., Fan, M., Dall'Agnese, A., et al. (2020). Partitioning of Cancer Therapeutics in Nuclear Condensates. *Science* 368 (6497), 1386–1392. doi:10.1126/science.aaz4427

Kohoutek, J. (2009). P-TEFb- the Final Frontier. *Cell Div.* 4, 19. doi:10.1186/1747-1028-4-19

Kolesky, S. E., Ouhammouch, M., and Geiduschek, E. P. (2002). The Mechanism of Transcriptional Activation by the Topologically DNA-Linked Sliding Clamp of Bacteriophage T4. *J. Mol. Biol.* 321 (5), 767–784. doi:10.1016/s0022-2836(02)00732-5

Krumm, A., Hickey, L. B., and Groudine, M. (1995). Promoter-proximal Pausing of RNA Polymerase II Defines a General Rate-Limiting Step After Transcription Initiation. *Genes Dev.* 9 (5), 559–572. doi:10.1101/gad.9.5.559

Krzyszczyk, P., Acevedo, A., Davidoff, E. J., Timmins, L. M., Marrero-Berrios, I., Patel, M., et al. (2018). The Growing Role of Precision and Personalized Medicine for Cancer Treatment. *Technology (Singap World Sci)* 6 (3-4), 79–100. doi:10.1142/S2339547818300020

Laham-Karam, N., Pinto, G. P., Poso, A., and Kokkonen, P. (2020). Transcription and Translation Inhibitors in Cancer Treatment. *Front. Chem.* 8, 276. doi:10.3389/fchem.2020.00276

Lazo, J. S., and Sharlow, E. R. (2016). Drugging Undruggable Molecular Cancer Targets. *Annu. Rev. Pharmacol. Toxicol.* 56, 23–40. doi:10.1146/annurev-pharmtox-010715-103440

Lee, T. I., and Young, R. A. (2013). Transcriptional Regulation and its Misregulation in Disease. *Cell* 152 (6), 1237–1251. doi:10.1016/j.cell.2013.02.014

Li, G., Ruan, X., Auerbach, R. K., Sandhu, K. S., Zheng, M., Wang, P., et al. (2012). Extensive Promoter-Centered Chromatin Interactions Provide a Topological Basis for Transcription Regulation. *Cell* 148 (1-2), 84–98. doi:10.1016/j.cell.2011.12.014

Liang, K., Woodfin, A. R., Slaughter, B. D., Unruh, J. R., Box, A. C., Rickels, R. A., et al. (2015). Mitotic Transcriptional Activation: Clearance of Actively Engaged Pol II via Transcriptional Elongation Control in Mitosis. *Mol. Cel.* 60 (3), 435–445. doi:10.1016/j.molcel.2015.09.021

Lin, C. Y., Loven, J., Rahl, P. B., Paranal, R. M., Burge, C. B., Bradner, J. E., et al. (2012). Transcriptional Amplification in Tumor Cells with Elevated C-Myc. *Cell* 151 (1), 56–67. doi:10.1016/j.cell.2012.08.026

Liu, X., Kraus, W. L., and Bai, X. (2015). Ready, Pause, Go: Regulation of RNA Polymerase II Pausing and Release by Cellular Signaling Pathways. *Trends Biochem. Sci.* 40 (9), 516–525. doi:10.1016/j.tibs.2015.07.003

London, L., Keene, R. G., and Landick, R. (1991). Analysis of Premature Termination in C-Myc During Transcription by RNA Polymerase II in a

HeLa Nuclear Extract. *Mol. Cel Biol.* 11 (9), 4599–4615. doi:10.1128/mcb.11.9.4599-4615.1991

Lu, X., Zhu, X., Li, Y., Liu, M., Yu, B., Wang, Y., et al. (2016). Multiple P-TEFbs Cooperatively Regulate the Release of Promoter-Proximally Paused RNA Polymerase II. *Nucleic Acids Res.* 44, 6853–6867. doi:10.1093/nar/gkw571

Luo, Z., Lin, C., Guest, E., Garrett, A. S., Mohaghegh, N., Swanson, S., et al. (2012). The Super Elongation Complex Family of RNA Polymerase II Elongation Factors: Gene Target Specificity and Transcriptional Output. *Mol. Cel Biol.* 32 (13), 2608–2617. doi:10.1128/MCB.00182-12

Madden, S. K., de Araujo, A. D., Gerhardt, M., Fairlie, D. P., and Mason, J. M. (2021). Taking the Myc Out of Cancer: Toward Therapeutic Strategies to Directly Inhibit C-Myc. *Mol. Cancer* 20 (1), 3. doi:10.1186/s12943-020-01291-6

Mahat, D. B., Salamanca, H. H., Duarte, F. M., Danko, C. G., and Lis, J. T. (2016). Mammalian Heat Shock Response and Mechanisms Underlying its Genome-wide Transcriptional Regulation. *Mol. Cel.* 62 (1), 63–78. doi:10.1016/j.molcel.2016.02.025

Malone, E. R., Oliva, M., Sabatini, P. J. B., Stockley, T. L., and Siu, L. L. (2020). Molecular Profiling for Precision Cancer Therapies. *Genome Med.* 12 (1), 8. doi:10.1186/s13073-019-0703-1

Marshall, N. F., Peng, J., Xie, Z., and Price, D. H. (1996). Control of RNA Polymerase II Elongation Potential by A Novel Carboxyl-Terminal Domain Kinase. *J. Biol. Chem.* 271 (43), 27176–27183. doi:10.1074/jbc.271.43.27176

Marshall, N. F., and Price, D. H. (1995). Purification of P-TEFb, A Transcription Factor Required for the Transition into Productive Elongation. *J. Biol. Chem.* 270 (21), 12335–12338. doi:10.1074/jbc.270.21.12335

Mohammad, H. P., Barbash, O., and Creasy, C. L. (2019). Targeting Epigenetic Modifications in Cancer Therapy: Erasing the Roadmap to Cancer. *Nat. Med.* 25 (3), 403–418. doi:10.1038/s41591-019-0376-8

Morales, F., and Giordano, A. (2016). Overview of CDK9 as a Target in Cancer Research. *Cell Cycle* 15 (4), 519–527. doi:10.1080/15384101.2016.1138186

Mosley, A. L., Lakshmanan, J., Aryal, B. K., and Ozcan, S. (2003). Glucose-mediated Phosphorylation Converts the Transcription Factor Rgt1 from a Repressor to an Activator. *J. Biol. Chem.* 278 (12), 10322–10327. doi:10.1074/jbc.M212802200

Muse, G. W., Gilchrist, D. A., Nechaev, S., Shah, R., Parker, J. S., Grissom, S. F., et al. (2007). RNA Polymerase Is Poised for Activation Across the Genome. *Nat. Genet.* 39 (12), 1507–1511. doi:10.1038/ng.2007.21

Nagaraja, S., Quezada, M. A., Gillespie, S. M., Arzt, M., Lennon, J. J., Woo, P. J., et al. (2019). Histone Variant and Cell Context Determine H3K27M Reprogramming of the Enhancer Landscape and Oncogenic State. *Mol. Cel.* 76 (6), 965–980.e12. doi:10.1016/j.molcel.2019.08.030

Nava, M. M., Miroshnikova, Y. A., Biggs, L. C., Whitefield, D. B., Metge, F., Boucas, J., et al. (2020). Heterochromatin-Driven Nuclear Softening Protects the Genome Against Mechanical Stress-Induced Damage. *Cell* 181 (4), 800–817.e22. doi:10.1016/j.cell.2020.03.052

Nechaev, S., Fargo, D. C., dos Santos, G., Liu, L., Gao, Y., and Adelman, K. (2010). Global Analysis of Short RNAs Reveals Widespread Promoter-Proximal Stalling and Arrest of Pol II in Drosophila. *Science* 327 (5963), 335–338. doi:10.1126/science.1181421

Nechaev, S., and Geiduschek, E. P. (2006). The Role of an Upstream Promoter Interaction in Initiation of Bacterial Transcription. *EMBO J.* 25 (8), 1700–1709. doi:10.1038/sj.emboj.7601069

Nepali, K., and Liou, J. P. (2021). Recent Developments in Epigenetic Cancer Therapeutics: Clinical Advancement and Emerging Trends. *J. Biomed. Sci.* 28 (1), 27. doi:10.1186/s12929-021-00721-x

Nicetto, D., and Zaret, K. S. (2019). Role of H3K9me3 Heterochromatin in Cell Identity Establishment and Maintenance. *Curr. Opin. Genet. Dev.* 55, 1–10. doi:10.1016/j.gde.2019.04.013

Nie, Z., Hu, G., Wei, G., Cui, K., Yamane, A., Resch, W., et al. (2012). c-Myc Is a Universal Amplifier of Expressed Genes in Lymphocytes and Embryonic Stem Cells. *Cell* 151 (1), 68–79. doi:10.1016/j.cell.2012.08.033

Nikolov, D. B., and Burley, S. K. (1997). RNA Polymerase II Transcription Initiation: A Structural View. *Proc. Natl. Acad. Sci. U S A.* 94 (1), 15–22. doi:10.1073/pnas.94.1.15

Nilson, K. A., Lawson, C. K., Mullen, N. J., Ball, C. B., Spector, B. M., Meier, J. L., et al. (2017). Oxidative Stress Rapidly Stabilizes Promoter-Proximal Paused Pol II Across the Human Genome. *Nucleic Acids Res.* 45 (19), 11088–11105. doi:10.1093/nar/gkx724

O'Brien, T., and Lis, J. T. (1991). RNA Polymerase II Pauses at the 5' End of the Transcriptionally Induced Drosophila Hsp70 Gene. *Mol. Cel Biol.* 11 (10), 5285–5290. doi:10.1128/mcb.11.10.5285

Paik, D. T., Tian, L., Lee, J., Sayed, N., Chen, I. Y., Rhee, S., et al. (2018). Large-Scale Single-Cell RNA-Seq Reveals Molecular Signatures of Heterogeneous Populations of Human Induced Pluripotent Stem Cell-Derived Endothelial Cells. *Circ. Res.* 123 (4), 443–450. doi:10.1161/CIRCRESAHA.118.312913

Pan, D., and Courey, A. J. (1992). The Same Dorsal Binding Site Mediates Both Activation and Repression in a Context-dependent Manner. *EMBO J.* 11 (5), 1837–1842. doi:10.1002/j.1460-2075.1992.tb05235.x

Park, J. W., and Han, J. W. (2019). Targeting Epigenetics for Cancer Therapy. *Arch. Pharm. Res.* 42 (2), 159–170. doi:10.1007/s12272-019-01126-z

Parker, J. S., Mullins, M., Cheang, M. C., Leung, S., Voduc, D., Vickery, T., et al. (2009). Supervised Risk Predictor of Breast Cancer Based on Intrinsic Subtypes. *J. Clin. Oncol.* 27 (8), 1160–1167. doi:10.1200/JCO.2008.18.1370

Parua, P. K., Kalan, S., Benjamin, B., Sansó, M., and Fisher, R. P. (2020). Distinct Cdk9-Phosphatase Switches Act at the Beginning and End of Elongation by RNA Polymerase II. *Nat. Commun.* 11 (1), 4338. doi:10.1038/s41467-020-18173-6

Pcawg, T. C. G., Calabrese, C., Davidson, N. R., Demircioğlu, D., Fonseca, N. A., He, Y., et al. (2020). Genomic Basis for RNA Alterations in Cancer. *Nature* 578 (7793), 129–136. doi:10.1038/s41586-020-1970-0

Pearson, J. D., Huang, K., Pacal, M., McCurdy, S. R., Lu, S., Aubry, A., et al. (2021). Binary Pan-Cancer Classes with Distinct Vulnerabilities Defined by Pro- or Anti-cancer YAP/TEAD Activity. *Cancer Cell* 39 (8), 1115–1134.e12. doi:10.1016/j.ccell.2021.06.016

Peinado, H., Ballestar, E., Esteller, M., and Cano, A. (2004). Snail Mediates E-Cadherin Repression by the Recruitment of the Sin3A/histone Deacetylase 1 (HDAC1)/HDAC2 Complex. *Mol. Cel Biol.* 24 (1), 306–319. doi:10.1128/mcb.24.1.306-319.2004

Pekowska, A., Benoukraf, T., Zacarias-Cabeza, J., Belhocine, M., Koch, F., Holota, H., et al. (2011). H3K4 Tri-methylation Provides an Epigenetic Signature of Active Enhancers. *EMBO J.* 30 (20), 4198–4210. doi:10.1038/emboj.2011.295

Peng, J., Zhu, Y., Milton, J. T., and Price, D. H. (1998). Identification of Multiple Cyclin Subunits of Human P-TEFb. *Genes Dev.* 12 (5), 755–762. doi:10.1101/gad.12.5.755

Perou, C. M., Sørlie, T., Eisen, M. B., van de Rijn, M., Jeffrey, S. S., Rees, C. A., et al. (2000). Molecular Portraits of Human Breast Tumours. *Nature* 406 (6797), 747–752. doi:10.1038/35021093

Peterlin, B. M., and Price, D. H. (2006). Controlling the Elongation Phase of Transcription with P-TEFb. *Mol. Cel.* 23 (3), 297–305. doi:10.1016/j.molcel.2006.06.014

Ptashne, M. (2013). Epigenetics: Core Misconcept. *Proc. Natl. Acad. Sci. U S A.* 110 (18), 7101–7103. doi:10.1073/pnas.1305399110

Pugh, B. F., and Venters, B. J. (2016). Genomic Organization of Human Transcription Initiation Complexes. *PLoS One* 11 (2), e0149339. doi:10.1371/journal.pone.0149339

Radonjic, M., Andrau, J. C., Lijnzaad, P., Kemmeren, P., Kockelkorn, T. T., van Leenen, D., et al. (2005). Genome-wide Analyses Reveal RNA Polymerase II Located Upstream of Genes Poised for Rapid Response upon *S. cerevisiae* Stationary Phase Exit. *Mol. Cel.* 18 (2), 171–183. doi:10.1016/j.molcel.2005.03.010

Rahl, P. B., Lin, C. Y., Seila, A. C., Flynn, R. A., McCuine, S., Burge, C. B., et al. (2010). c-Myc Regulates Transcriptional Pause Release. *Cell* 141 (3), 432–445. doi:10.1016/j.cell.2010.03.030

Rajagopal, N., Ernst, J., Ray, P., Wu, J., Zhang, M., Kellis, M., et al. (2014). Distinct and Predictive Histone Lysine Acetylation Patterns at Promoters, Enhancers, and Gene Bodies. *G3 (Bethesda)* 4 (11), 2051–2063. doi:10.1534/g3.114.013565

Renner, D. B., Yamaguchi, Y., Wada, T., Handa, H., and Price, D. H. (2001). A Highly Purified RNA Polymerase II Elongation Control System. *J. Biol. Chem.* 276 (45), 42601–42609. doi:10.1074/jbc.m104967200

Rimel, J. K., Poss, Z. C., Erickson, B., Maas, Z. L., Ebmeier, C. C., Johnson, J. L., et al. (2020). Selective Inhibition of CDK7 Reveals High-Confidence Targets and New Models for TFIIH Function in Transcription. *Genes Dev.* 34 (21-22), 1452–1473. doi:10.1101/gad.341545.120

Rodriguez, J., and Larson, D. R. (2020). Transcription in Living Cells: Molecular Mechanisms of Bursting. *Annu. Rev. Biochem.* 89, 189–212. doi:10.1146/annurev-biochem-011520-105250

Rousseaux, S., Debernardi, A., Jacquiau, B., Vitte, A. L., Vesin, A., Nagy-Mignotte, H., et al. (2013). Ectopic Activation of Germline and Placental Genes Identifies Aggressive Metastasis-Prone Lung Cancers. *Sci. Transl Med.* 5 (186), 186ra66. doi:10.1126/scitranslmed.3005723

Russo, M., Natoli, G., and Ghisletti, S. (2018). Housekeeping and Tissue-specific Cis-Regulatory Elements: Recipes for Specificity and Recipes for Activity. *Transcription* 9 (3), 177–181. doi:10.1080/21541264.2017.1378158

Saeed, S., Quintin, J., Kerstens, H. H., Rao, N. A., Aghajanirefah, A., Matarese, F., et al. (2014). Epigenetic Programming of Monocyte-To-Macrophage Differentiation and Trained Innate Immunity. *Science* 345 (6204), 1251086. doi:10.1126/science.1251086

Samarakkody, A., Abbas, A., Scheidegger, A., Warns, J., Nnoli, O., Jokinen, B., et al. (2015). RNA Polymerase II Pausing Can Be Retained or Acquired During Activation of Genes Involved in the Epithelial to Mesenchymal Transition. *Nucleic Acids Res.* 43 (8), 3938–3949. doi:10.1093/nar/gkv263

Sava, G. P., Fan, H., Coombes, R. C., Buluwela, L., and Ali, S. (2020). CDK7 Inhibitors as Anticancer Drugs. *Cancer Metastasis Rev.* 39 (3), 805–823. doi:10.1007/s10555-020-09885-8

Scheidegger, A., Dunn, C. J., Samarakkody, A., Koney, N. K., Perley, D., Saha, R. N., et al. (2019). Genome-wide RNA Pol II Initiation and Pausing in Neural Progenitors of the Rat. *BMC Genomics* 20 (1), 477. doi:10.1186/s12864-019-5829-4

Schuettengruber, B., Bourbon, H. M., Di Croce, L., and Cavalli, G. (2017). Genome Regulation by Polycomb and Trithorax: 70 Years and Counting. *Cell* 171 (1), 34–57. doi:10.1016/j.cell.2017.08.002

Scruggs, B. S., Gilchrist, D. A., Nechaev, S., Muse, G. W., Burkholder, A., Fargo, D. C., et al. (2015). Bidirectional Transcription Arises from Two Distinct Hubs of Transcription Factor Binding and Active Chromatin. *Mol. Cel.* 58 (6), 1101–1112. doi:10.1016/j.molcel.2015.04.006

Shan, X., Fung, J. J., Kosaka, A., Danet-Desnoyers, G., and Reproducibility, P. C. B. (2017). Replication Study: Inhibition of BET Recruitment to Chromatin as an Effective Treatment for MLL-Fusion Leukaemia. *Elife* 6, e25306. doi:10.7554/eLife.25306

Shao, X., Lv, N., Liao, J., Long, J., Xue, R., Ai, N., et al. (2019). Copy Number Variation Is Highly Correlated with Differential Gene Expression: A Pan-Cancer Study. *BMC Med. Genet.* 20 (1), 175. doi:10.1186/s12881-019-0909-5

Shen, L., Shi, Q., and Wang, W. (2018). Double Agents: Genes with Both Oncogenic and Tumor-Suppressor Functions. *Oncogenesis* 7 (3), 25. doi:10.1038/s41389-018-0034-x

Sievers, Q. L., Petzold, G., Bunker, R. D., Renneville, A., Słabicki, M., Liddicoat, B. J., et al. (2018). Defining the Human C2H2 Zinc Finger Degrome Targeted by Thalidomide Analogs Through CRBN. *Science* 362 (6414), eaat0572. doi:10.1126/science.aat0572

Skidmore, L., Sakamuri, S., Knudsen, N. A., Hewet, A. G., Milutinovic, S., Barkho, W., et al. (2020). ARX788, A Site-specific Anti-HER2 Antibody-Drug Conjugate, Demonstrates Potent and Selective Activity in HER2-Low and T-DM1-Resistant Breast and Gastric Cancers. *Mol. Cancer Ther.* 19 (9), 1833–1843. doi:10.1158/1535-7163.MCT-19-1004

Soares, L. M., He, P. C., Chun, Y., Suh, H., Kim, T., and Buratowski, S. (2017). Determinants of Histone H3K4 Methylation Patterns. *Mol. Cel.* 68 (4), 773–785.e6. doi:10.1016/j.molcel.2017.10.013

Spencer, C. A., and Groudine, M. (1990). Transcription Elongation and Eukaryotic Gene Regulation. *Oncogene* 5 (6), 777–785.

Staller, M. V., Vincent, B. J., Bragdon, M. D., Lydiard-Martin, T., Wunderlich, Z., Estrada, J., et al. (2015). Shadow Enhancers Enable Hunchback Bifunctionality in the Drosophila Embryo. *Proc. Natl. Acad. Sci. U S A.* 112 (3), 785–790. doi:10.1073/pnas.1413877112

Stingele, S., Stoehr, G., Peplowska, K., Cox, J., Mann, M., and Storchova, Z. (2012). Global Analysis of Genome, Transcriptome and Proteome Reveals the Response to Aneuploidy in Human Cells. *Mol. Syst. Biol.* 8, 608. doi:10.1038/msb.2012.40

Strahl, B. D., and Allis, C. D. (2000). The Language of Covalent Histone Modifications. *Nature* 403 (6765), 41–45. doi:10.1038/47412

Sun, J., Pan, H., Lei, C., Yuan, B., Nair, S. J., April, C., et al. (2011). Genetic and Genomic Analyses of RNA Polymerase II-Pausing Factor in Regulation of Mammalian Transcription and Cell Growth. *J. Biol. Chem.* 286 (42), 36248–36257. doi:10.1074/jbc.M111.269167

Sun, J., Watkins, G., Blair, A. L., Moskaluk, C., Ghosh, S., Jiang, W. G., et al. (2008). Deregulation of Cofactor of BRCA1 Expression in Breast Cancer Cells. *J. Cel Biochem* 103 (6), 1798–1807. doi:10.1002/jcb.21568

Takeshima, H., Yamashita, S., Shimazu, T., Niwa, T., and Ushijima, T. (2009). The Presence of RNA Polymerase II, Active or Stalled, Predicts Epigenetic Fate of Promoter CpG Islands. *Genome Res.* 19 (11), 1974–1982. doi:10.1101/gr.093310.109

Tan, M., Luo, H., Lee, S., Jin, F., Yang, J. S., Montellier, E., et al. (2011). Identification of 67 Histone Marks and Histone Lysine Crotonylation as a New Type of Histone Modification. *Cell* 146 (6), 1016–1028. doi:10.1016/j.cell.2011.08.008

Tellier, M., Zaborowska, J., Caizzi, L., Mohammad, E., Velychko, T., Schwalb, B., et al. (2020). CDK12 Globally Stimulates RNA Polymerase II Transcription Elongation and Carboxyl-Terminal Domain Phosphorylation. *Nucleic Acids Res.* 48 (14), 7712–7727. doi:10.1093/nar/gkaa514

Terryn, J., Tricot, T., Gajjar, M., and Verfaillie, C. (2018). Recent Advances in Lineage Differentiation from Stem Cells: Hurdles and Opportunities. *F1000Res* 7, 220. doi:10.12688/f1000research.12596.1

Towbin, B. D., González-Aguilera, C., Sack, R., Gaidatzis, D., Kalck, V., Meister, P., et al. (2012). Step-wise Methylation of Histone H3K9 Positions Heterochromatin at the Nuclear Periphery. *Cell* 150 (5), 934–947. doi:10.1016/j.cell.2012.06.051

Trkulja, C. L., Jungholm, O., Davidson, M., Jardemark, K., Marcus, M. M., Hägglund, J., et al. (2021). Rational Antibody Design for Undruggable Targets Using Kinetically Controlled Biomolecular Probes. *Sci. Adv.* 7 (16), eabe6397. doi:10.1126/sciadv.abe6397

Tunnacliffe, E., and Chubb, J. R. (2020). What Is a Transcriptional Burst. *Trends Genet.* 36 (4), 288–297. doi:10.1016/j.tig.2020.01.003

Uhlén, M., Hallström, B. M., Lindskog, C., Mardinoglu, A., Pontén, F., and Nielsen, J. (2016). Transcriptomics Resources of Human Tissues and Organs. *Mol. Syst. Biol.* 12 (4), 862. doi:10.15252/msb.20155865

Uren, A., and Toretsky, J. A. (2005). Pediatric Malignancies Provide Unique Cancer Therapy Targets. *Curr. Opin. Pediatr.* 17 (1), 14–19. doi:10.1097/01.mop.0000147904.84978.ae

Van Hoeck, A., Tjoonk, N. H., van Boxtel, R., and Cuppen, E. (2019). Portrait of a Cancer: Mutational Signature Analyses for Cancer Diagnostics. *BMC Cancer* 19 (1), 457. doi:10.1186/s12885-019-5677-2

Vastenhouw, N. L., and Schier, A. F. (2012). Bivalent Histone Modifications in Early Embryogenesis. *Curr. Opin. Cel Biol.* 24 (3), 374–386. doi:10.1016/j.ceb.2012.03.009

Vidal, S. E., Polyzos, A., Chatterjee, K., Ee, L. S., Swanzey, E., Morales-Valencia, J., et al. (2020). Context-Dependent Requirement of Euchromatic Histone Methyltransferase Activity During Reprogramming to Pluripotency. *Stem Cel Rep.* 15 (6), 1233–1245. doi:10.1016/j.stemcr.2020.08.011

Vihervaara, A., Mahat, D. B., Guertin, M. J., Chu, T., Danko, C. G., Lis, J. T., et al. (2017). Transcriptional Response to Stress Is Pre-wired by Promoter and Enhancer Architecture. *Nat. Commun.* 8 (1), 255. doi:10.1038/s41467-017-00151-0

Villicaña, C., Cruz, G., and Zurita, M. (2014). The Basal Transcription Machinery as a Target for Cancer Therapy. *Cancer Cel Int* 14 (1), 18. doi:10.1186/1475-2867-14-18

Vishnoi, K., Viswakarma, N., Rana, A., and Rana, B. (2020). Transcription Factors in Cancer Development and Therapy. *Cancers (Basel)* 12 (8), E2296. doi:10.3390/cancers12082296

Wada, T., Takagi, T., Yamaguchi, Y., Ferdous, A., Imai, T., Hirose, S., et al. (1998). DSIF, A Novel Transcription Elongation Factor that Regulates RNA Polymerase II Processivity, Is Composed of Human Spt4 and Spt5 Homologs. *Genes Dev.* 12 (3), 343–356. doi:10.1101/gad.12.3.343

Waddington, C. H. (1957). *The Strategy of the Genes A Discussion of Some Aspects of Theoretical Biology with an Appendix by H Kacser*. London: George Allen & Unwin, Ltd., 262.

Walker, W. H., Girardet, C., and Habener, J. F. (1996). Alternative Exon Splicing Controls a Translational Switch from Activator to Repressor Isoforms of Transcription Factor CREB During Spermatogenesis. *J. Biol. Chem.* 271 (33), 20145–21050. doi:10.1074/jbc.271.33.20219

Wang, C., Liu, X., Gao, Y., Yang, L., Li, C., Liu, W., et al. (2018). Reprogramming of H3K9me3-dependent Heterochromatin During Mammalian Embryo Development. *Nat. Cel Biol.* 20 (5), 620–631. doi:10.1038/s41556-018-0093-4

Wang, C., Zhang, J., Yin, J., Gan, Y., Xu, S., Gu, Y., et al. (2021). Alternative Approaches to Target Myc for Cancer Treatment. *Signal. Transduct Target. Ther.* 6 (1), 117. doi:10.1038/s41392-021-00500-y

Wang, Y., Zhang, T., Kwiatkowski, N., Abraham, B. J., Lee, T. I., Xie, S., et al. (2015). CDK7-dependent Transcriptional Addiction in Triple-Negative Breast Cancer. *Cell* 163 (1), 174–186. doi:10.1016/j.cell.2015.08.063

Winters, A. C., and Bernt, K. M. (2017). MLL-rearranged Leukemias-An Update on Science and Clinical Approaches. *Front. Pediatr.* 5, 4. doi:10.3389/fped.2017.00004

Wolffe, A. P., Wong, J., and Pruss, D. (1997). Activators and Repressors: Making Use of Chromatin to Regulate Transcription. *Genes Cells* 2 (5), 291–302. doi:10.1046/j.1365-2443.1997.1260323.x

Wu, C. H., Yamaguchi, Y., Benjamin, L. R., Horvat-Gordon, M., Washinsky, J., Enerly, E., et al. (2003). NELF and DSIF Cause Promoter Proximal Pausing on the Hsp70 Promoter in Drosophila. *Genes Dev.* 17 (11), 1402–1414. doi:10.1101/gad.1091403

Wu, W. S., You, R. I., Cheng, C. C., Lee, M. C., Lin, T. Y., and Hu, C. T. (2017). Snail Collaborates with EGR-1 and SP-1 to Directly Activate Transcription of MMP 9 and ZEB1. *Sci. Rep.* 7 (1), 17753. doi:10.1038/s41598-017-18101-7

Yamada, T., Yamaguchi, Y., Inukai, N., Okamoto, S., Mura, T., and Handa, H. (2006). P-TEFb-mediated Phosphorylation of hSpt5 C-Terminal Repeats Is Critical for Processive Transcription Elongation. *Mol. Cel.* 21 (2), 227–237. doi:10.1016/j.molcel.2005.11.024

Yamaguchi, Y., Filipovska, J., Yano, K., Furuya, A., Inukai, N., Narita, T., et al. (2001). Stimulation of RNA Polymerase II Elongation by Hepatitis Delta Antigen. *Science* 293 (5527), 124–127. doi:10.1126/science.1057925

Yamaguchi, Y., Takagi, T., Wada, T., Yano, K., Furuya, A., Sugimoto, S., et al. (1999). NELF, A Multisubunit Complex Containing RD, Cooperates with DSIF to Repress RNA Polymerase II Elongation. *Cell* 97 (1), 41–51. doi:10.1016/s0092-8674(00)80713-8

Yang, L., Kirby, J. E., Sunwoo, H., and Lee, J. T. (2016). Female Mice Lacking Xist RNA Show Partial Dosage Compensation and Survive to Term. *Genes Dev.* 30 (15), 1747–1760. doi:10.1101/gad.281162.116

Yen, A., and Kellis, M. (2015). Systematic Chromatin State Comparison of Epigenomes Associated with Diverse Properties Including Sex and Tissue Type. *Nat. Commun.* 6, 7973. doi:10.1038/ncomms8973

Yildirim, E., Kirby, J. E., Brown, D. E., Mercier, F. E., Sadreyev, R. I., Scadden, D. T., et al. (2013). Xist RNA Is a Potent Suppressor of Hematologic Cancer in Mice. *Cell* 152 (4), 727–742. doi:10.1016/j.cell.2013.01.034

Yu, K., Chen, B., Aran, D., Charalel, J., Yau, C., Wolf, D. M., et al. (2019). Comprehensive Transcriptomic Analysis of Cell Lines as Models of Primary Tumors Across 22 Tumor Types. *Nat. Commun.* 10 (1), 3574. doi:10.1038/s41467-019-11415-2

Yun, H., Bedolla, R., Horning, A., Li, R., Chiang, H. C., Huang, T. H., et al. (2018). BRCA1 Interacting Protein COBRA1 Facilitates Adaptation to Castrate-Resistant Growth Conditions. *Int. J. Mol. Sci.* 19 (7), E2104. doi:10.3390/ijms19072104

Zabidi, M. A., Arnold, C. D., Schernhuber, K., Pagani, M., Rath, M., Frank, O., et al. (2015). Enhancer-core-promoter Specificity Separates Developmental and Housekeeping Gene Regulation. *Nature* 518 (7540), 556–559. doi:10.1038/nature13994

Zeitlinger, J., Stark, A., Kellis, M., Hong, J. W., Nechaev, S., Adelman, K., et al. (2007). RNA Polymerase Stalling at Developmental Control Genes in the *Drosophila melanogaster* Embryo. *Nat. Genet.* 39 (12), 1512–1516. doi:10.1038/ng.2007.26

Zhang, G., Andersen, J., and Gerona-Navarro, G. (2018). Peptidomimetics Targeting Protein-Protein Interactions for Therapeutic Development. *Protein Pept. Lett.* 25 (12), 1076–1089. doi:10.2174/0929866525666181101100842

Zhang, L. J., Vogel, W. K., Liu, X., Topark-Ngarm, A., Arbogast, B. L., Maier, C. S., et al. (2012). Coordinated Regulation of Transcription Factor Bcl11b Activity in Thymocytes by the Mitogen-Activated Protein Kinase (MAPK) Pathways and Protein Sumoylation. *J. Biol. Chem.* 287 (32), 26971–26988. doi:10.1074/jbc.M112.344176

Zhang, T., Zhang, Z., Dong, Q., Xiong, J., and Zhu, B. (2020). Histone H3K27 Acetylation Is Dispensable for Enhancer Activity in Mouse Embryonic Stem Cells. *Genome Biol.* 21 (1), 45. doi:10.1186/s13059-020-01957-w

Zhao, L., Zhou, S., and Gustafsson, J. Å. (2019). Nuclear Receptors: Recent Drug Discovery for Cancer Therapies. *Endocr. Rev.* 40 (5), 1207–1249. doi:10.1210/er.2018-00222

Zhao, X. D., Han, X., Chew, J. L., Liu, J., Chiu, K. P., Choo, A., et al. (2007). Whole-genome Mapping of Histone H3 Lys4 and 27 Trimethylations Reveals Distinct Genomic Compartments in Human Embryonic Stem Cells. *Cell Stem Cell* 1 (3), 286–298. doi:10.1016/j.stem.2007.08.004

Zhou, Q., Li, T., and Price, D. H. (2012). RNA Polymerase II Elongation Control. *Annu. Rev. Biochem.* 81, 119–143. doi:10.1146/annurev-biochem-052610-095910

Zrimec, J., Börlin, C. S., Buric, F., Muhammad, A. S., Chen, R., Siewers, V., et al. (2020). Deep Learning Suggests that Gene Expression Is Encoded in All Parts of a Co-evolving Interacting Gene Regulatory Structure. *Nat. Commun.* 11 (1), 6141. doi:10.1038/s41467-020-19921-4

Zuccotti, P., Peroni, D., Potrich, V., Quattrone, A., and Dassi, E. (2020). Hyperconserved Elements in Human 5'UTRs Shape Essential Post-transcriptional Regulatory Networks. *Front. Mol. Biosci.* 7, 220. doi:10.3389/fmolb.2020.00220

Conflict of Interest: The authors declare that the research was conducted in the absence of any commercial or financial relationships that could be construed as a potential conflict of interest.

Publisher's Note: All claims expressed in this article are solely those of the authors and do not necessarily represent those of their affiliated organizations, or those of the publisher, the editors and the reviewers. Any product that may be evaluated in this article, or claim that may be made by its manufacturer, is not guaranteed or endorsed by the publisher.

frontiers in Genetics

ORIGINAL RESEARCH
published: 17 September 2021
doi: 10.3389/fgene.2021.702072

Characterization of Modification Patterns, Biological Function, Clinical Implication, and Immune Microenvironment Association of m^{6}A Regulators in Pancreatic Cancer

Kun Fang[1], Hairong Qu[2], Jiapei Wang[3], Desheng Tang[4], Changsheng Yan[5], Jiamin Ma[5] and Lei Gao[5]*

[1]Department of Surgery, Yinchuan Maternal and Child Health Hospital, Yinchuan, China, [2]Department of Gynaecology, Yinchuan Maternal and Child Health Hospital, Yinchuan, China, [3]Department of Pathology, Yinchuan Maternal and Child Health Hospital, Yinchuan, China, [4]Central Laboratory, Department of Gastroenterology, First Affiliated Hospital of Harbin Medical University, Harbin, China, [5]Central Laboratory, Department of Pancreatic and Biliary Surgery, The First Affiliated Hospital of Harbin Medical University, Harbin, China

OPEN ACCESS

Edited by:
Rais Ahmad Ansari,
Nova Southeastern University,
United States

Reviewed by:
Zitong Gao,
University of Hawaii at Manoa,
United States
Mehrdad Zarei,
Case Western Reserve University,
United States
Deli Liu,
Weill Cornell Medicine, United States

***Correspondence:**
Kun Fang
k99ftl@163.com

Specialty section:
This article was submitted to Cancer Genetics and Oncogenomics, a section of the journal Frontiers in Genetics

Received: 29 April 2021
Accepted: 06 September 2021
Published: 17 September 2021

Citation:
Fang K, Qu H, Wang J, Tang D, Yan C, Ma J and Gao L (2021) Characterization of Modification Patterns, Biological Function, Clinical Implication, and Immune Microenvironment Association of m^{6}A Regulators in Pancreatic Cancer. Front. Genet. 12:702072. doi: 10.3389/fgene.2021.702072

Objective: N^6-methyladenosine (m^{6}A) modification may modulate various biological processes. Nonetheless, clinical implications of m^{6}A modification in pancreatic cancer are undefined. Herein, this study comprehensively characterized the m^{6}A modification patterns in pancreatic cancer based on m^{6}A regulators.

Methods: Genetic mutation and expression pattern of 21 m^{6}A regulators and their correlations were assessed in pancreatic cancer from TCGA dataset. m^{6}A modification patterns were clustered using unsupervised clustering analysis in TCGA and ICGC datasets. Differences in survival, biological functions and immune cell infiltrations were assessed between modification patterns. A m^{6}A scoring system was developed by principal component analysis. Genetic mutations and TIDE scores were compared between high and low m^{6}A score groups.

Results: ZC3H13 (11%), RBM15B (9%), YTHDF1 (8%), and YTHDC1 (6%) frequently occurred mutations among m^{6}A regulators. Also, most of regulators were distinctly dysregulated in pancreatic cancer. There were tight crosslinks between regulators. Two m^{6}A modification patterns were constructed, with distinct prognoses, immune cell infiltration and biological functions. Furthermore, we quantified m^{6}A score in each sample. High m^{6}A scores indicated undesirable clinical outcomes. There were more frequent mutations in high m^{6}A score samples. Lower TIDE score was found in high m^{6}A score group, with AUC = 0.61, indicating that m^{6}A scores might be used for predicting the response to immunotherapy.

Abbreviations: OS, overall survival; m6A, N6-methyladenosine; TCGA, the cancer genome atlas; GSVA, gene set variation analysis; MSigDB, molecular signatures database; ssGSEA, single sample gene set enrichment analysis; DEGs, differentially expressed genes; EMT, epithelial-mesenchymal transition; CNV, copy number variation; TIDE, T cell dysfunction and exclusion; ICB, immune checkpoint blockade; ROC, receiver operating characteristic curve; AUC, area under the curve.

Conclusion: Collectively, these data demonstrated that m^{6}A modification participates pancreatic cancer progress and ornaments immune microenvironment, providing an insight into pancreatic cancer pathogenesis and facilitating precision medicine development.

Keywords: pancreatic cancer, N6-methyladenosine regulators, prognosis, immune microenvironment, immunotherapy

INTRODUCTION

Pancreatic cancer represents the most lethal malignancy globally, characterized by high intra-tumoral heterogeneity and undesirable survival outcomes (Jain and Dudeja, 2021). Despite the improvement in standard of care, survival outcomes are extremely undesirable with a 5 year survival rate <10% and median survivals <1 year (Qin et al., 2020). The existing therapies provide only limited efficacy. Despite surgical resection as the main therapeutic strategy for pancreatic cancer, merely 10–15% of newly diagnosed patients are qualified (Peng et al., 2019). Over 50% of subjects are diagnosed at locally advanced or metastatic stages (O'Reilly et al., 2020). Specially, traditional chemotherapy for advanced or metastatic patients merely provides months of overall survival (OS) benefit (Ho et al., 2020). Due to the undesirable clinical outcomes, novel treatment strategies are urgently required. Pancreatic cancer with similar morphology usually displays distinct clinical characteristics, response to therapies and survival outcomes (Bailey et al., 2016). Currently, molecular subtypes have been proposed for guidance of preclinical and clinical management, prediction of first-rank treatment strategies and minimum of treatment-relevant death risk and cost in pancreatic cancer (Collisson et al., 2019). Nevertheless, so far, molecular subtyping does not inform therapeutic decisions.

N^6-methyladenosine (m^{6}A), a dynamic and reversible process, represents the most plentiful posttranscriptional methylation modification of mRNAs in eukaryotic species (Zhang et al., 2020). It occurs in the RRACH sequence (where R = A or G, H = A, C, or U). m^{6}A methylation modulates nearly each step of RNA metabolism like RNA splicing, stability, decay, and translation. Aberrant m^{6}A levels alters target gene expression and cellular processes and physiological functions, thereby affecting cancer progression (He et al., 2019). This modification is mainly controlled by three kinds of regulators: methyltransferases ("writers"), demethylases ("erasers") as well as binding proteins ("readers"). Accumulating evidence has reported the carcinogenesis of m^{6}A regulators in pancreatic cancer. For instance, upregulating m^{6}A writer METTL14 may promote growth and metastases of pancreatic cancer by mediating PERP mRNA m^{6}A (Wang et al., 2020). Nevertheless, it remains limited understanding on the global landscape and dynamic changes of m^{6}A regulators in pancreatic cancer. Immune microenvironment exerts an important role in tumor progress and treatment effects for pancreatic cancer (Hegde et al., 2020). Comprehending immune microenvironment and its regulators assist enhance immunotherapy (Torphy et al., 2020). For example, targeting m^{6}A eraser ALKBH5 enhances the responsiveness to anti-PD-1 therapy through modulating tumor immune microenvironment (Li et al., 2020). Associations between m^{6}A regulators and immune microenvironment have been preliminarily characterized in pancreatic cancer (Xu et al., 2021). Nonetheless, m^{6}A regulators-mediated methylation modification patterns and immune microenvironment are ambiguous in pancreatic cancer.

Here, this study systematically assessed m^{6}A modification patterns in pancreatic cancer according to m^{6}A regulatory genes and their correlations to immune microenvironment. Also, we developed a m^{6}A scoring system for quantifying the m^{6}A modification patterns in each specimen. These findings might enhance the comprehension on immune microenvironment characteristics as well as make more effective immunotherapeutic strategy.

MATERIALS AND METHODS

Data Acquisition and Preprocessing

RNA sequencing profiling and copy number variation of pancreatic cancer were retrieved from The Cancer Genome Atlas (TCGA) via the UCSC Xena (https://gdc.xenahubs.net/). Meanwhile, the matched clinical data were acquired via cgdsr package. Genomic mutation data of pancreatic cancer containing somatic mutation were also obtained from TCGA database via TCGAbiolinks package (Colaprico et al., 2016). Use Mutation landscape of patients was characterized by maftools package. Also, expression profiles of two pancreatic cancer cohorts (PACA-AU and PACA-AU) were downloaded from ICGC cohort (https://dcc.icgc.org/projects). Specific clinical information was listed in **Table 1**. To maintain data consistency, sva package was applied for performing batch correction on the pancreatic cancer transcriptome data from TCGA and ICGC

TABLE 1 | Specific clinical information of pancreatic cancer patients.

Characteristics	TCGA	ICGC: PACA-AU	ICGC: PACA-AU
Sex			
Female	80	88	43
Male	97	109	47
NA	0	37	1
Age			
≥60	123	115	67
<60	54	53	22
Status			
Dead	92	152	58
Alive	85	45	32
NA	0	37	1

databases (Leek et al., 2012). The GSE79668 dataset containing RNA-seq and clinical information of 51 pancreatic cancer patients was downloaded from the Gene Expression Omnibus (GEO) repository (https://www.ncbi.nlm.nih.gov/gds/) (Kirby et al., 2016).

Unsupervised Clustering Analysis

Expression profiles of 21 m^{6}A regulators were extracted from TCGA and ICGC datasets as well as GSE79668 dataset. RCircos package was utilized for plotting the chromosome distribution of these regulators in chromosomes. Distinct m^{6}A modification patterns were clustered according to expression of m^{6}A regulators using unsupervised clustering analysis by ConsensusClusterPlus package (Wilkerson and Hayes, 2010). Patients were classified for distinct molecular subtypes for further analysis. The distance used for clustering was the Euclidean distance. This analysis was repeated 1,000 times to ensure the stability of clustering. Principal component analysis was applied for validating the accuracy of this classification.

Gene Set Variation Analysis

GSVA, a non-parametric, unsupervised method, is primarily utilized for estimating activity changes in pathway or biological process in a sample (Hänzelmann et al., 2013). For studying the differences in biological processes of distinct m^{6}A modification patterns, GSVA package was applied to perform GSVA enrichment analysis based on gene expression profiles. The "c2.cp.kegg.v6.2" gene set from the Molecular Signatures Database (MSigDB) database (https://www.gsea-msigdb.org/gsea/index.jsp) was set as the reference set (Liberzon et al., 2015).

Single Sample Gene Set Enrichment Analysis

The infiltration levels of 24 immune cells were estimated in each sample by ssGSEA package. Then, the differences between m^{6}A modification patterns were compared with Wilcox test. Univariate cox regression analysis was separately presented for assessing the associations between immune cells and prognosis of pancreatic cancer in each cluster.

Development of m^{6}A Score System

Differentially expressed genes (DEGs) were screened between m^{6}A modification patterns from TCGA and ICGC databases by limma package (Ritchie et al., 2015). The thresholds were set as adjusted p value < 0.05 and log2 |fold-change| > 0.5. The random forest method was utilized for removing redundant genes based on DEGs using randomForest, ROCR and Hmisc packages. The "meandecreaseaccuracy" parameter was set as the standard selection. Then, survival analysis on the remaining genes was performed. Genes with $p < 0.05$ were significantly related to survival outcomes of pancreatic cancer. By cox regression model, genes were separated into two categories according to positive or negative coefficients. m^{6}A score was determined using the following formula: m^{6}A score = scale($\sum$X−$\sum$Y). X represented the expression value of the gene set for which regression coefficient was positive. Meanwhile, Y represented the expression value of the gene set for which regression coefficient was negative. Based on the median of m^{6}A score, pancreatic cancer specimens were stratified into high and low m^{6}A score groups. Kaplan-Meier curves and log-rank tests were performed for assessing the overall survival (OS) differences between groups.

Association Between m^{6}A Score and Biological Pathways

Pearson analysis was performed for assessing associations between m^{6}A score and several key biological pathways including immune checkpoints, antigen processing and presentation, EMT1, EMT2, EMT3, and other epithelial-mesenchymal transition (EMT) markers, DNA damage repair, mismatch repair, nucleotide excision repair, and the like.

Copy Number Variation Analysis

The GISTIC method was employed for detecting the shared copy number change area in all samples based on the SNP6 CopyNumber segment data. The parameters were set as: Q ≤ 0.05 was the change significance standard and the confidence level was 0.95 when determining the peak interval. The analysis was presented through MutSigCV function of GenePattern (https://cloud.genepattern.org/gp/pages/index.jsf) online tool.

Assessment of T Cell Dysfunction and Exclusion

TIDE (http://tide.dfci.harvard.edu) was employed for assessing the response to immune checkpoint blockade (ICB) (Jiang et al., 2018). TIDE score of each specimen was determined. Receiver operating characteristic curve (ROC) was then carried out for evaluating the efficacy of m^{6}A scores for predicting the response to immunotherapy, and the area under the curve (AUC) was quantified with pROC package.

Statistical Analysis

Statistical analysis was achieved with R language (version 3.6.1) and appropriate packages. Wilcox test was applied for comparing the differences between groups. $p < 0.05$ indicated statistically significance.

RESULTS

Landscape of Genetic Mutation and Expression of m^{6}A Regulators in Pancreatic Cancer

Totally, 21 m^{6}A regulators were analyzed in our study. **Figure 1A** showed the locations of these regulators on the chromosomes. Also, we summarized frequencies of CNV and somatic mutation. In **Figure 1B**, CNV was common in all regulators. Among them, ALKBH5, FMR1, HNRNPA2B1, IGF2BP1 and KIAA1429 had high frequencies of gain, while other regulators occurred high frequencies of loss. Among 185 pancreatic cancer specimens in TCGA dataset, 61 occurred somatic mutations (**Figure 1C**). Among them, ZC3H13 (11%), RBM15B (9%), YTHDF1 (8%), and YTHDC1 (6%) displayed higher genetic mutation frequencies.

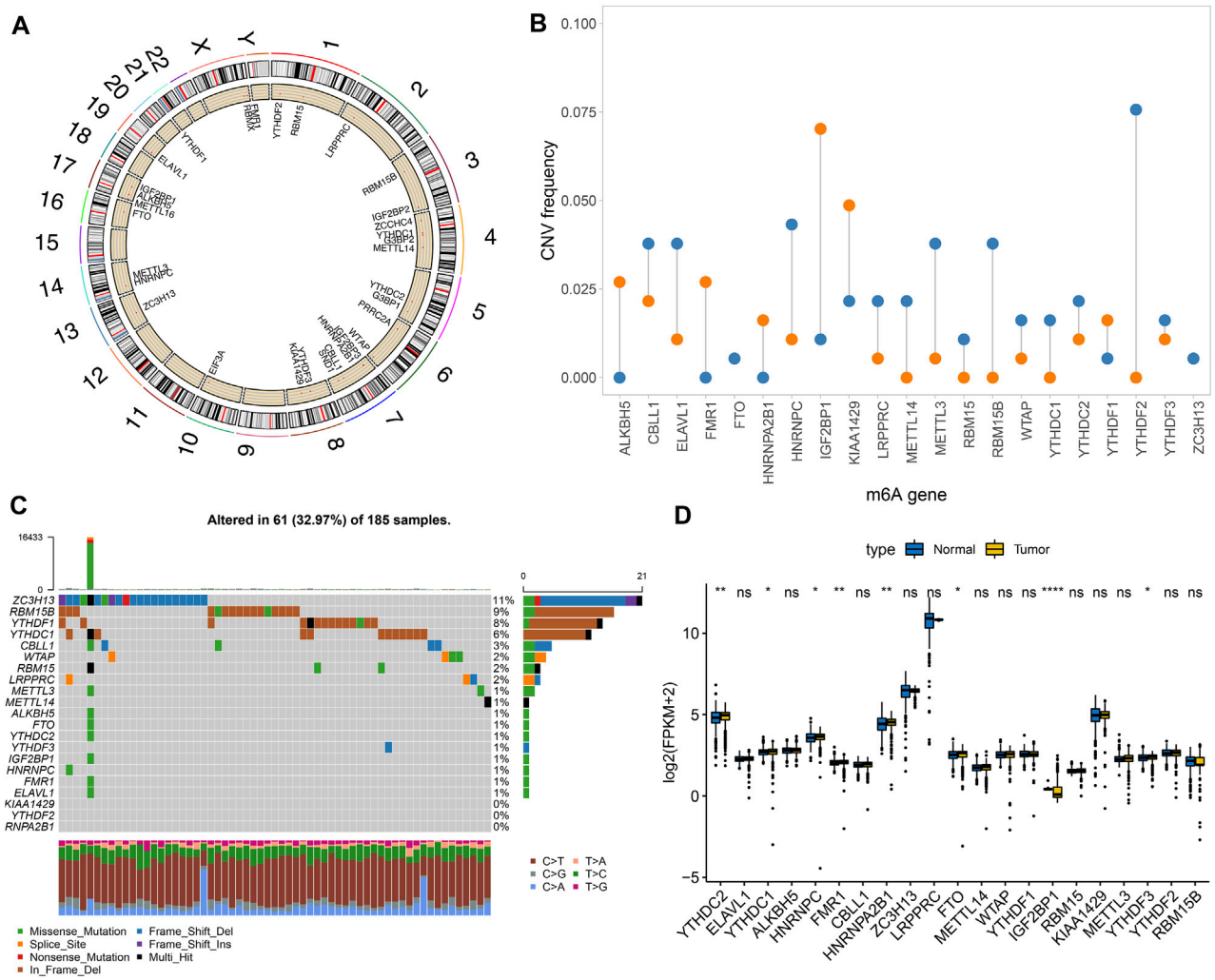

FIGURE 1 | Landscape of genetic mutation and expression patterns of m^{6}A regulators in pancreatic cancer. **(A)** The locations of m^{6}A regulators on the chromosomes. **(B)** The distribution of CNV frequency of m^{6}A regulators. Blue indicates deletion and orange indicates amplification. The height of bar indicates the variation frequency. **(C)** Landscape of somatic mutation of m^{6}A regulators. **(D)** Box plot of expression patterns of m^{6}A regulators in normal and pancreatic cancer. Ns: not significant; *p < 0.05; **p < 0.01; ****p < 0.0001.

Also, we compared the expression patterns of these regulators in pancreatic cancer and normal tissues. In **Figure 1D**, YTHDC2, YTHDC1, HNRNPC, FMR1, FTO, IGF2BP1, and YTHDF3 were significantly dysregulated in pancreatic cancer.

Characterization of Two m^{6}A Methylation Modification Patterns in Pancreatic Cancer

This study integrated RNA-seq data from TCGA and ICGC datasets and batch effects were removed by sva package (**Figure 2A**). By univariate cox regression analyses, associations between m^{6}A regulators and prognoses of pancreatic cancer were evaluated. As a result, ELAVL1, ALKBH5, and KIAA1429 were distinctly correlated to the patients' prognoses (**Table 2**). **Figure 2B** depicted the crosslinks between writers, erasers, and readers, indicating that the interactions between m^{6}A regulators might exert a critical role in forming distinct m^{6}A modification patterns. Multivariate cox regression analyses revealed that KIAA1429 served as an independent risk factor of pancreatic cancer prognosis among m^{6}A regulators (**Figure 2C**). After extracting the expression profiles of 21 regulators in pancreatic cancer specimens from TCGA and ICGC datasets, unsupervised clustering analysis was carried out with ConsensusClusterPlus package. As a result, 2 modification patterns were clustered (m^{6}A cluster A and m^{6}A cluster B; **Figure 2D**; **Supplementary Table S1**). PCA results demonstrated the prominent differences between clusters based on the expression profiles of m^{6}A regulators (**Figure 2E**). In **Figure 2F**, samples in m^{6}A cluster B displayed poorer OS duration in comparison to those in m^{6}A cluster A (p = 0.01). However, no significant differences in KRAS mutation (**Figure 2G**), TP53 (**Figure 2H**), metastasis (**Figure 2I**) and diabetes (**Figure 2J**) were found between clusters. The m^{6}A

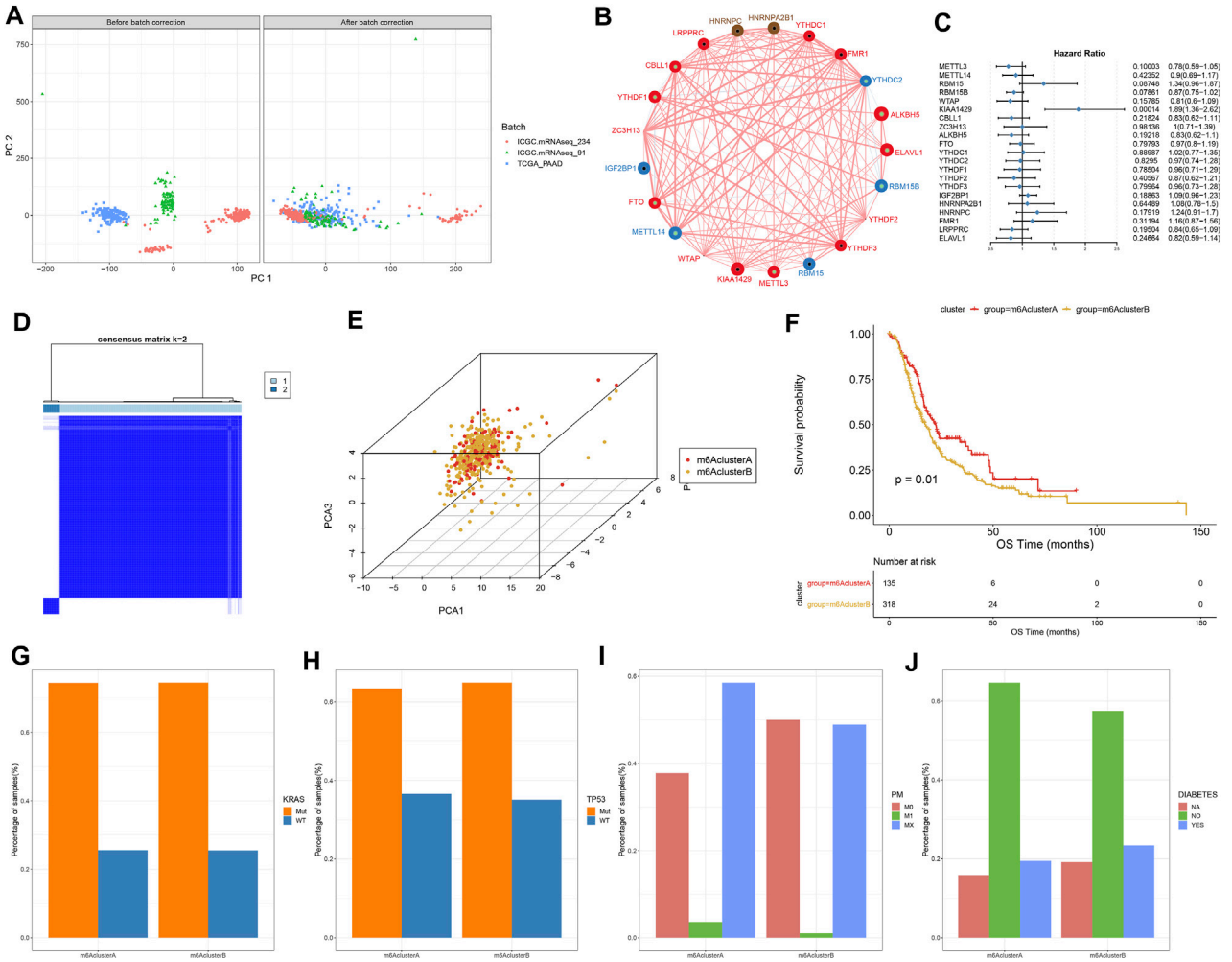

FIGURE 2 | Construction of two m^{6}A methylation modification patterns in pancreatic cancer from TCGA and ICGC datasets. **(A)** PCA plots showing before and after batch correction of TCGA and ICGC datasets. **(B)** An interaction network of m^{6}A regulators. The size of the circle indicates the impact of each regulator on survival, and the larger the circle, the more relevant its expression is to the prognosis. The green dot in the circle indicates that the regulator is a protective factor for prognosis, and the black dot in the circle indicates that the regulator is a risk factor for prognosis. The lines connecting regulators indicate their interactions, negative correlations are marked in blue, and positive correlations are marked in red. **(C)** Multivariate cox regression analyses for assessing associations of m^{6}A regulators with pancreatic cancer prognoses. **(D)** Consensus matrix heatmap when $k = 2$. **(E)** PCA plots showing the differences between m^{6}A cluster A and B based on the expression profiling of m^{6}A regulators. **(F)** Kaplan-Meier curves of two m^{6}A clusters. P was determined with log-rank test. Distributions of **(G)** KRAS mutation, **(H)** TP53 mutation, **(I)** metastasis, and **(J)** diabetes in two m^{6}A clusters.

clustering results and survival differences were confirmed in the GSE79668 dataset (**Supplementary Figures S1A,B**).

Two m^{6}A Methylation Modification Patterns Characterized by Distinct Immune Cell Infiltration, Biological Functions, and Genetic Mutations

Figure 3A depicted the expression patterns of 21 m^{6}A regulators in two m^{6}A methylation modification patterns. By ssGSEA algorithm, we estimated the infiltration levels of 24 immune cells in pancreatic cancer. Univariate cox regression analyses identified that activated CD4 T cell, activated dendritic cell, CD56bright natural killer cell, central memory CD4 T cell, gamma delta T cell and type 2 T helper cell were risk factors of pancreatic cancer prognoses in m^{6}A cluster A (**Figure 3B**). In contrast, we observed that activated B cell, activated CD8 T cell, eosinophil, immature B cell, and macrophage were protective factors of pancreatic cancer prognoses in m^{6}A cluster B (**Figure 3B**). In **Figure 3C**, m^{6}A cluster B was charactered by higher infiltration levels of activated CD4 T cells, activated dendritic cells, central memory CD8 T cells, Effector memory CD4 T cells, eosinophils, immature B cells, immature dendritic cells, mast cells, neutrophils, regulatory T cells and type 2 T helper cells, indicating that there was higher immunogenicity in m^{6}A cluster B. T explore the biological behaviors between these different m^{6}A modification patterns, GSVA enrichment analysis was carried out. As a result, there were distinct differences

TABLE 2 | Associations between m^{6}A regulators and prognoses of pancreatic cancer.

Regulators	Hazard ratio	Lower 0.95% CI	Upper 0.95% CI	*p*
YTHDC2	0.945573	0.804418	1.111497	0.501143
METTL14	0.87198	0.759141	1.001591	0.057076
IGF2BP1	1.102124	0.987532	1.230014	0.095858
RBM15	1.165283	0.893101	1.520415	0.256693
RBM15B	0.895478	0.794545	1.009233	0.06895
ELAVL1	0.745107	0.585853	0.947651	0.020395
YTHDC1	1.034719	0.880397	1.21609	0.677174
ALKBH5	0.755901	0.631814	0.904358	0.002477
FMR1	1.111698	0.934534	1.322447	0.222155
CBLL1	0.943543	0.786501	1.131941	0.534774
ZC3H13	0.992526	0.822421	1.197816	0.937711
LRPPRC	1.066698	0.898443	1.266463	0.456897
FTO	0.938485	0.838581	1.050291	0.276089
WTAP	0.984003	0.784578	1.234117	0.889144
YTHDF1	0.882007	0.721275	1.078557	0.229438
KIAA1429	1.326562	1.066612	1.649864	0.010711
METTL3	0.820477	0.65659	1.025272	0.083879
YTHDF3	1.087143	0.909575	1.299375	0.351575
YTHDF2	0.988164	0.777414	1.256047	0.922555
HNRNPC	1.147295	0.943431	1.395212	0.155486
HNRNPA2B1	1.129765	0.946279	1.348829	0.166181

in activation of glycosaminoglycan biosynthesis chondroitin sulfate, glycosaminoglycan biosynthesis keratan sulfate, one carbon pool by folate, RNA degradation, homologous recombination, propanoate metabolism, valine leucine and isoleucine degradation, non-homologous end joining, citrate cycle TCA cycle, olfactory transduction, purine metabolism, regulation of autophagy, ubiquitin mediated proteolysis, oocyte meiosis, endometrial cancer, adherens junction, starch and sucrose metabolism, lysine degradation, vasopressin regulated water reabsorption and lysosome between m^{6}A clusters (**Figure 3D**). Furthermore, we found that DNA replication, nucleotide excision repair, homologous recombination and mismatch repair were significantly activated in m^{6}A cluster A than cluster B (**Figure 3E**). However, EMT3 was distinctly activated in cluster B. We also compared the differences in genetic mutations between m^{6}A clusters (**Figures 3F,G**). Higher frequency of mutation was found in cluster B (38.61%) than cluster A (32.91%).

Construction of m^{6}A Gene Clusters in Pancreatic Cancer

To further study the potential mechanisms of m^{6}A clusters, limma package was applied for determining 140 m^{6}A-related DEGs with the cutoff values of $p = 0.05$, $|\log2\text{fold-change}| = 0.5$ (**Supplementary Table S2**). By clusterProfiler package, we analyzed KEGG pathways based on the DEGs. Only ribosome was significantly enriched by the DEGs. Furthermore, we performed unsupervised cluster analysis based on the obtained m^{6}A-related genes, and stratified the patients into two different m^{6}A gene clusters named as m^{6}A gene cluster A and B (**Figure 4A**; **Supplementary Table S3**). The expression patterns of the m^{6}A-related genes were visualized, as shown in **Figure 4B**. METTL14, WTAP, CBLL1, ZC3H13, FTO, YTHDC1, YTHDC2, YTHDF3, HNRNPC, FMR1, and LRPPRC were distinctly up-regulated in m^{6}A gene cluster B while RBM15B, ALKBH5, YTHDF1, and ELAVL1 were significantly up-regulated in m^{6}A gene cluster A (**Figure 4C**).

Development of a m^{6}A Scoring System in Pancreatic Cancer

For the m^{6}A-related genes, the random forest algorithm was used for eliminating the redundancy of DEGs. The characteristic genes that were most relevant to the classification were screened out, including RABAC1, ALKBH7, DPM3, POLR2I, MBD3, ISOC2, WBSCR16, CUTA, C17orf89, MRPL41, ZNF787, C19orf60, and C19orf43. By cox regression model, we determined the relationships between these genes and prognoses. According to the coefficients, the genes were divided into two categories. With the m^{6}A score calculation formula, each pancreatic cancer was scored (**Supplementary Table S4**). Based on m^{6}A score median, we stratified samples into high and low m^{6}A score groups (**Figure 5A**). Higher m^{6}A scores were detected in m^{6}A cluster B (**Figure 5B**) and m^{6}A gene cluster B (**Figure 5C**). There were not significant differences in primary sites (**Figure 5D**), sex (**Figure 5E**), age (**Figure 5F**) and stage (**Figure 5G**) between high and low m^{6}A score groups. However, patients with dead status exhibited higher m^{6}A score than those with alive status (**Figure 5H**).

m^{6}A Scores as a Prognostic Factor of Pancreatic Cancer

As shown in **Figure 6A**, patients in high m^{6}A score group displayed a poor prognosis, while those in low m^{6}A score group had a good prognosis, indicating that the m^{6}A scoring system can provide a good characterization of the prognosis of pancreatic cancer. The prognostic implication of m^{6}A score was confirmed in the GSE79668 dataset (**Supplementary Figure S1C**). In **Figure 6B**, m^{6}A scores were distinctly correlated to

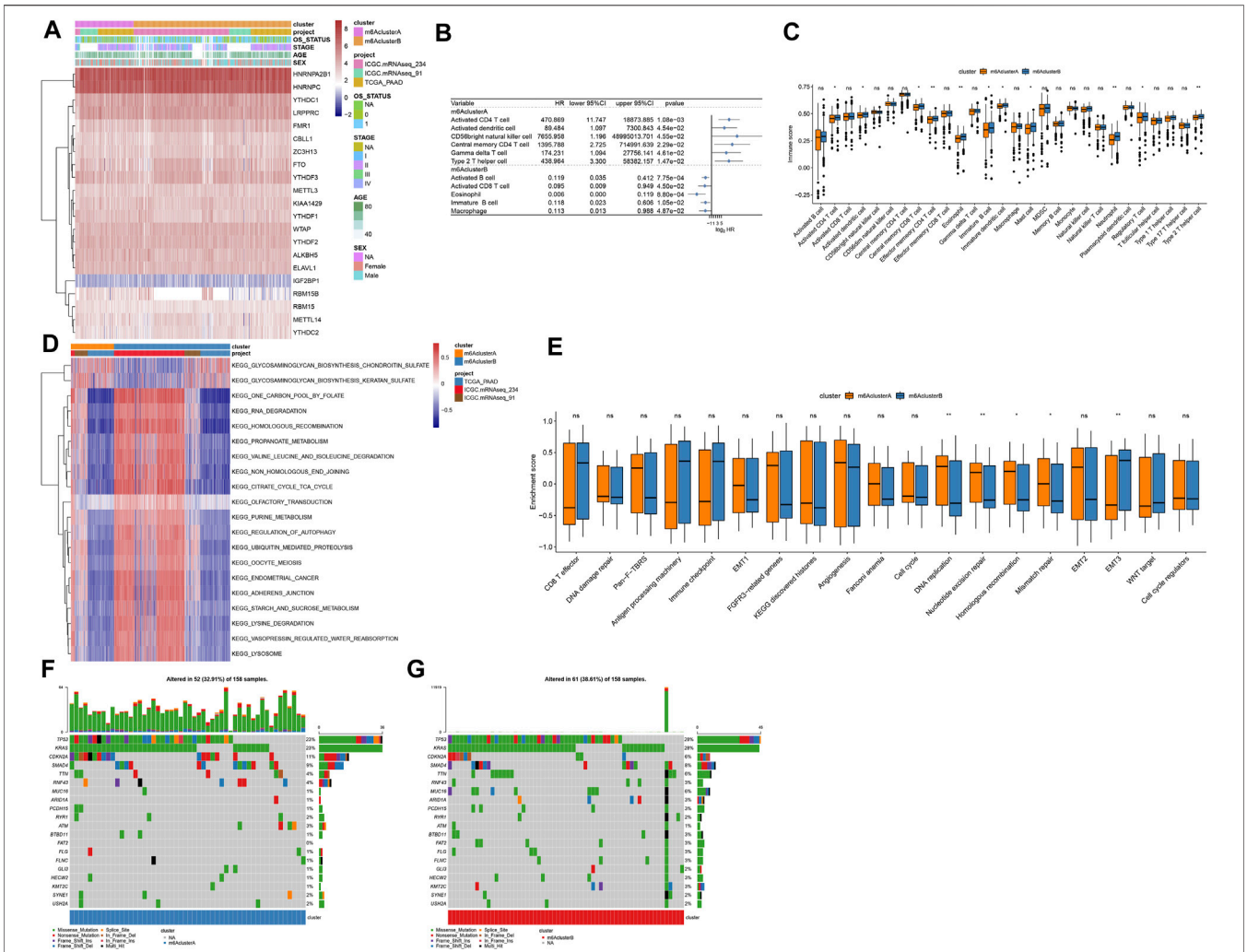

FIGURE 3 | Two m^{6}A methylation modification patterns with distinct immune cell infiltration, biological functions, and genetic mutation. **(A)** Heatmap of expression patterns of m^{6}A regulators in m^{6}A clusters (cluster A and B), OS status, stage, age, and sex. **(B)** Associations between immune cells and prognoses of pancreatic cancer. HR: hazard ratio and CI: confidence interval. **(C)** Box plot of the infiltration levels of immune cells in two m^{6}A clusters. Ns: not significant; *$p < 0.05$; **$p < 0.01$. **(D)** GSVA enrichment analysis for the activation status of biological pathways in two m^{6}A clusters. **(E)** Box plots of the enrichment scores of key biological processes in two m^{6}A clusters. **(F)** The somatic mutation landscape of samples in m^{6}A cluster A. **(G)** The somatic mutation landscape of samples in m^{6}A cluster B.

DNA replication, nucleotide excision repair, homologous recombination, EMT2, EMT3, WNT target and cell cycle regulators. Furthermore, high m^{6}A scores were characterized by activation of histones, EMT3, WNT target and cell cycle regulators, while low m^{6}A scores were characterized by angiogenesis, cell cycle, DNA replication, nucleotide excision repair, homologous recombination, and mismatch repair (**Figure 6C**).

Assessment of Genetic Mutation Characteristics of High and Low m^{6}A Scores

Our analysis found that m6A scores had no significant differences in KRAS mutation (**Figure 7A**) and TP53 mutation (**Figure 7B**). We applied maftools package for analyzing the differences in somatic mutations between high and low m^{6}A score groups. **Figures 7C,D** showed the frequencies of genetic mutations in two groups. Both in high and low m^{6}A score groups, FRG1B, KRAS, TP53, TCF20, MED12L, PRG4, OTUD4, and MYH9 were the eight most frequently mutated genes. Missense mutation was the main mutation type in pancreatic cancer. **Figures 7E,F** showed the distributions of CNV regions in two groups.

m^{6}A Score as a Predictive Tool of Immunotherapy Response

We further employed pRRophetic package for estimating IC50 values of chemotherapy drugs (Cisplatin, Gemcitabine) based on the expression profile. There were no significant differences in IC50 values of Cisplatin and Gemcitabine between high and low m6A scores (**Figures 8A,B**). Furthermore, TIDE scores were determined for evaluating the clinical effects of ICB treatment

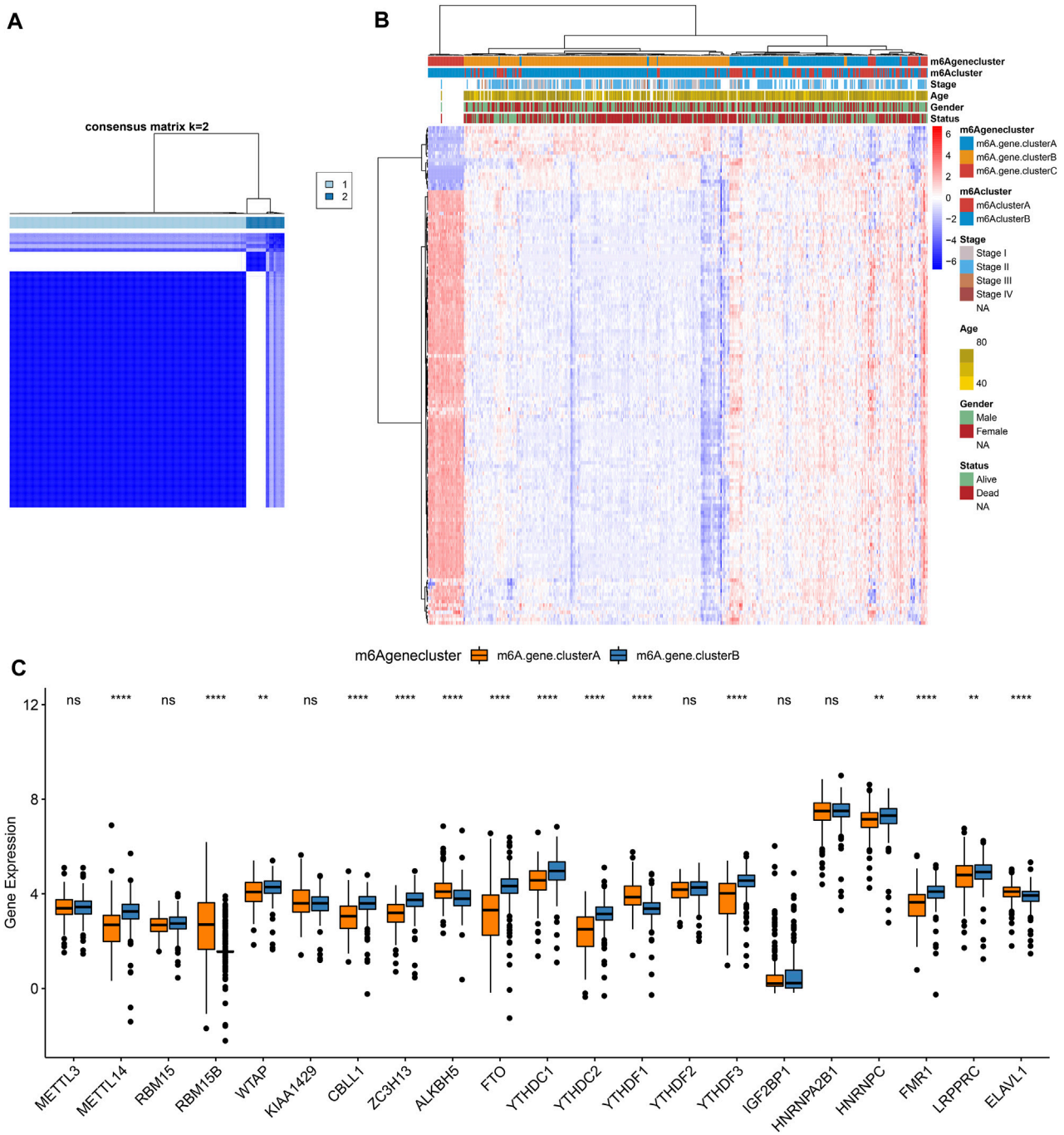

FIGURE 4 | Construction of m^{6}A gene clusters in pancreatic cancer. **(A)** Consensus matrix heatmap when $k = 2$. **(B)** Heatmap of two m^{6}A gene clusters and expression patterns of m^{6}A-related genes. **(C)** Box plot of expression patterns of 21 m^{6}A regulators in m^{6}A gene cluster A and B. Ns: not significant; $^{**}p < 0.01$; $^{****}p < 0.0001$.

in high and low m6A score groups based on the mRNA expression profiles. As shown in **Figure 8C**, TIDE scores of the high m^{6}A score group were distinctly lower than low m^{6}A score group. AUC reached 0.62, indicating that the m^{6}A score might be utilized for predicting the response of immunotherapy (**Figure 8D**). Difference in TIDE scores between high and low m^{6}A score groups was confirmed in the GSE79668 dataset (**Figure 8E**).

DISCUSSION

Pancreatic cancer represents a highly lethal malignancy with limited therapeutic options (Liang et al., 2020). Aberrant m^{6}A levels participate in modulating cancer malignant phenotypes through affecting the expression of tumor-related genes (Guo et al., 2020). Pancreatic cancer patients with genetic alterations of

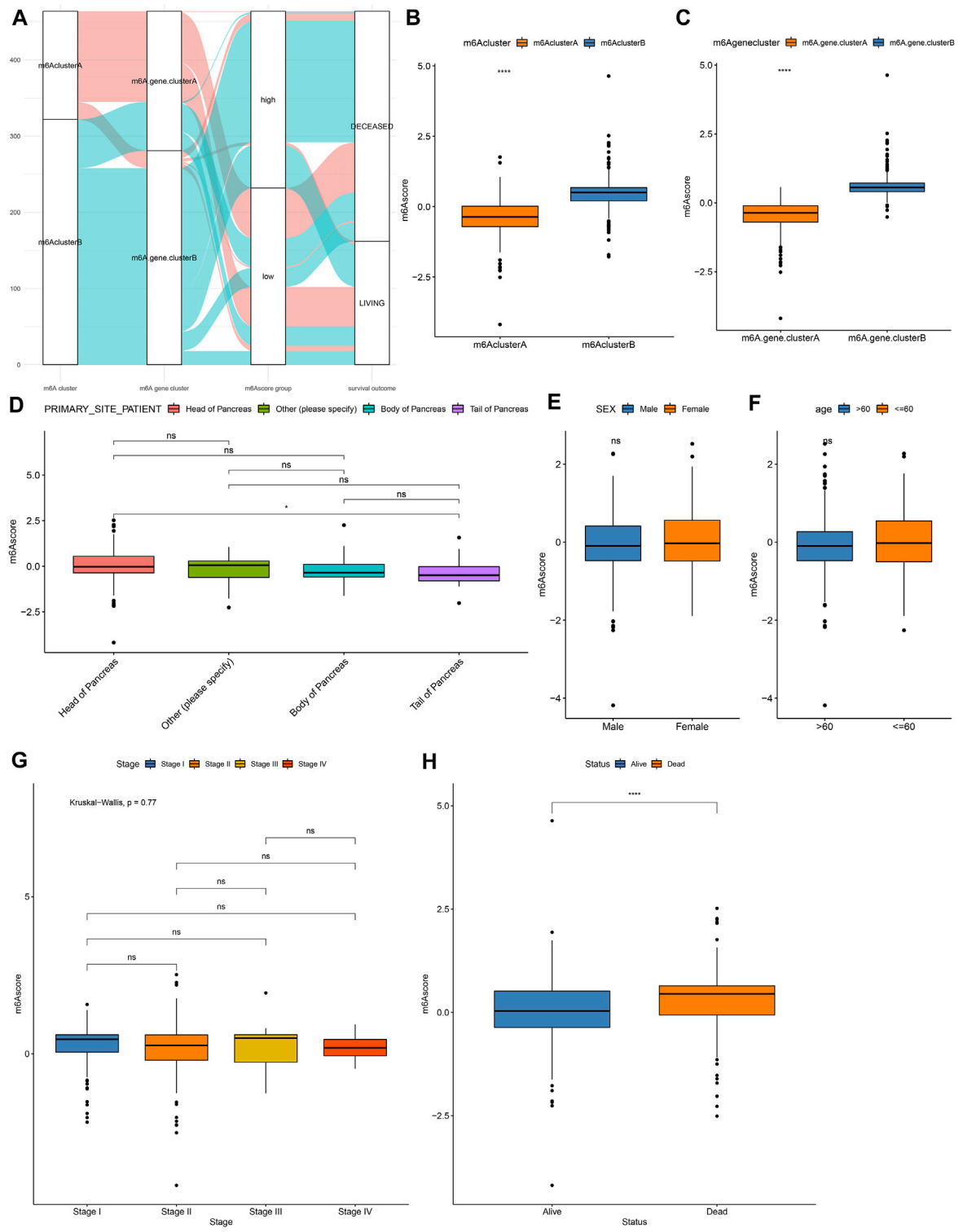

FIGURE 5 | Development of a m^{6}A scoring system in pancreatic cancer. **(A)** Alluvial diagram for the relationships of m^{6}A modification patterns, m^{6}A gene clusters and m^{6}A scores. **(B)** Distribution of m^{6}A scores in m^{6}A cluster A and B. **(C)** Distribution of m^{6}A scores in m^{6}A gene cluster A and B. Distributions of m^{6}A scores in **(D)** different primary sites, **(E)** sex, **(F)** age, **(G)** stage, and **(H)** survival status. Ns: not significant; ****$p < 0.0001$.

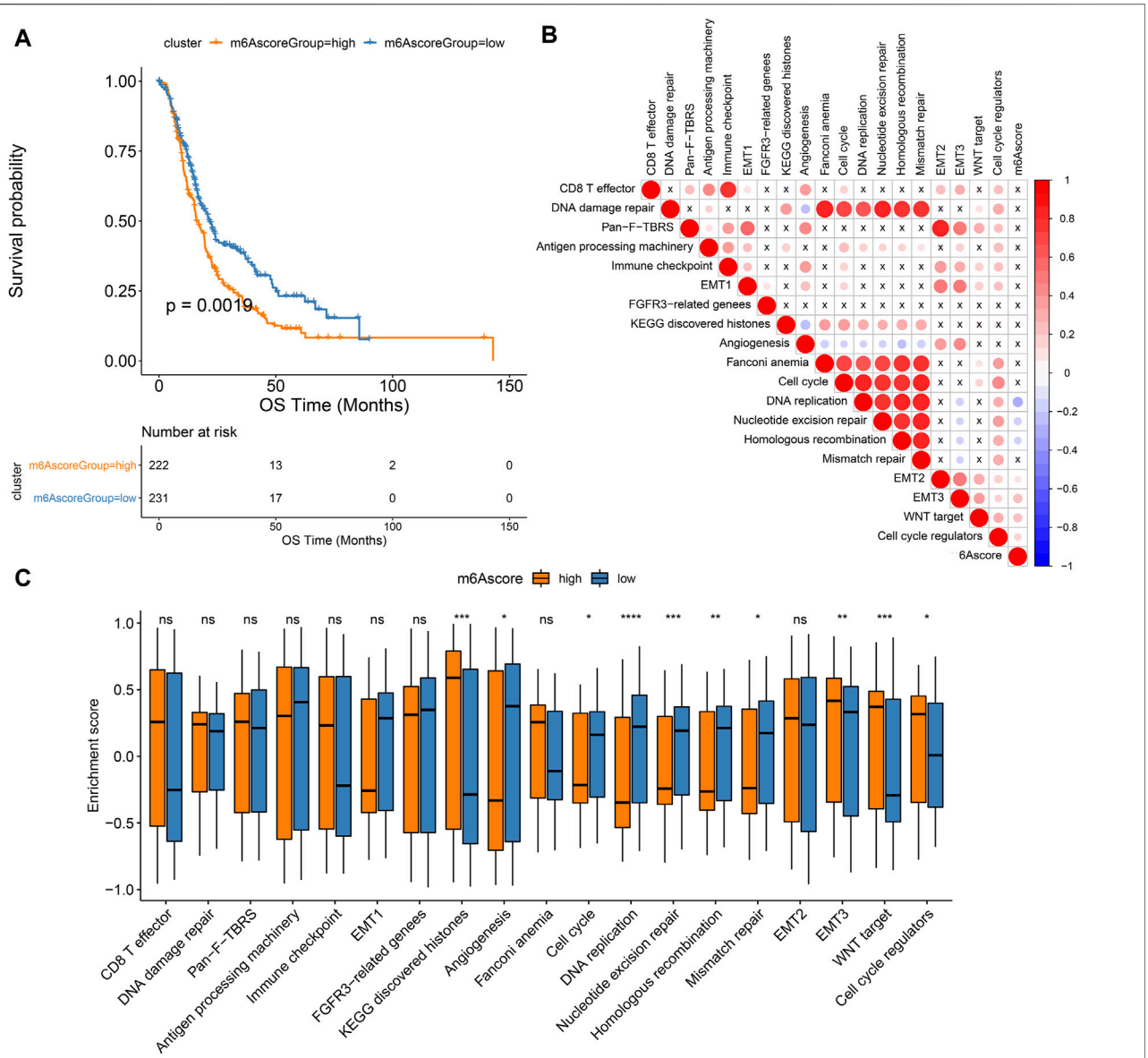

FIGURE 6 | Associations between m^{6}A scores and pancreatic cancer prognoses. **(A)** Kaplan-Meier curves of patients with high and low m^{6}A scores. **(B)** Correlation between key biological processes and m^{6}A scores. **(C)** Box plot of the enrichment scores of key biological processes in high and low m^{6}A score groups. Ns: not significant; *p < 0.05; **p < 0.01; ***p < 0.001; ****p < 0.0001.

m^{6}A regulators exhibit worse disease-free and OS (Meng et al., 2020). Despite the anti-cancer effects of several m^{6}A enzyme inhibitors, more effective m^{6}A-related drugs and treatment options required to be further probed. Here, we constructed two m^{6}A modification patterns, characterized by different survival outcomes, biological functions, and immune cell infiltration. To individually quantify the m^{6}A modification, we developed a m^{6}A scoring system. High m^{6}A scores indicated undesirable clinical outcomes and predicted high sensitivity to respond to immunotherapy in pancreatic cancer.

32.97% pancreatic cancer samples occurred genetic mutations. ZC3H13 (11%), RBM15B (9%), YTHDF1 (8%), and YTHDC1 (6%) frequently occurred genetic mutations in pancreatic cancer. Frame shift deletion was the most mutation type of ZC3H13 and in-frame deletion was the most mutation classification of RBM15B, YTHDF1, and YTHDC1. Crosslink among writers, erasers. and readers participates in cancer pathogenesis and progress (Ma et al., 2019). Here, tight crosslinks between m^{6}A regulators were found in pancreatic cancer. Based on the expression profiles of m^{6}A regulators, we constructed two m^{6}A clusters with distinct OS duration. Compared with m^{6}A cluster A, we observed that m^{6}A cluster B was characterized by higher infiltration levels of activated CD4 T cells, activated dendritic cells, central memory CD8 T cells, Effector memory CD4 T cells, eosinophils, immature B cells, immature dendritic cells, mast cells, neutrophils, regulatory

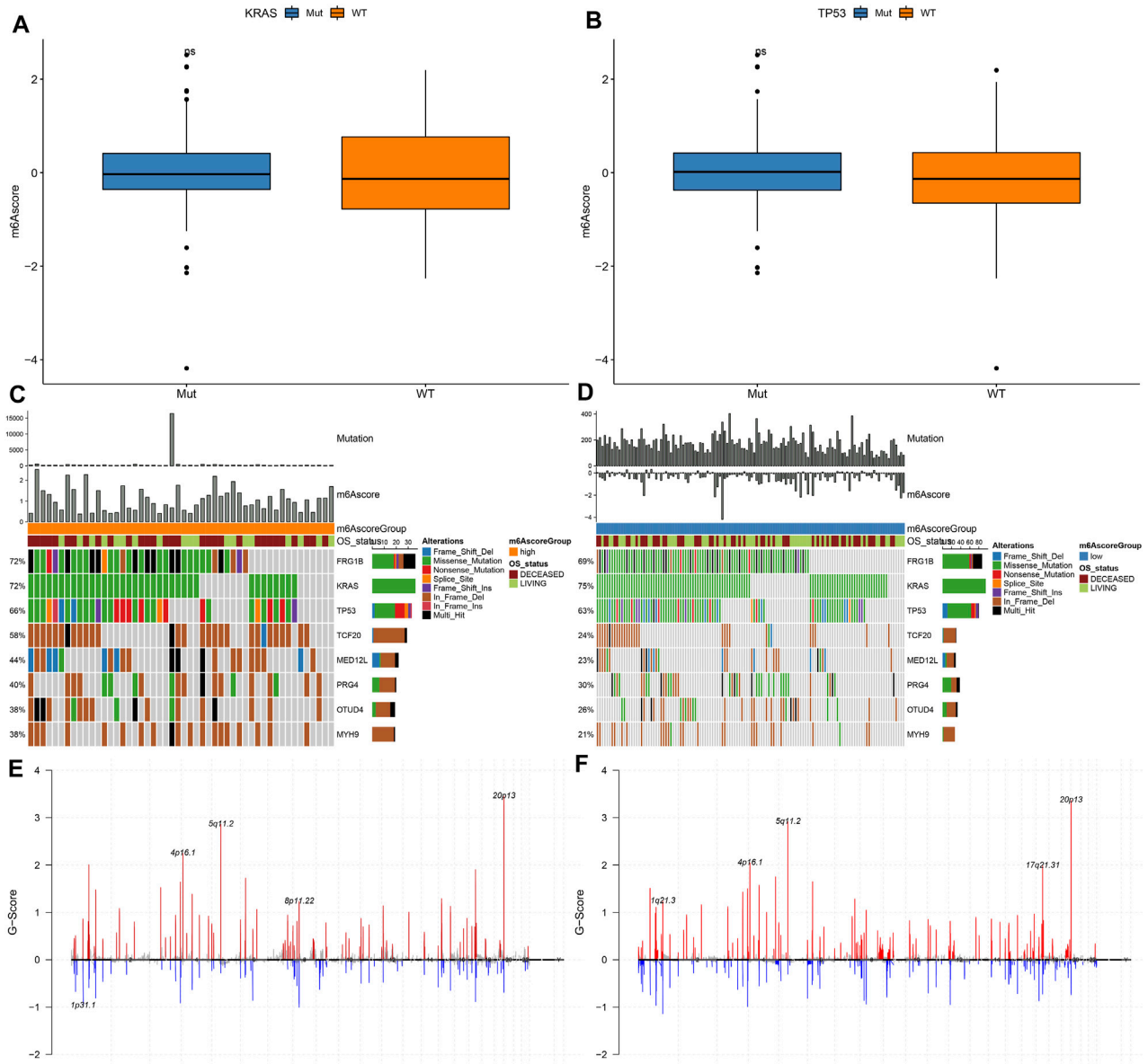

FIGURE 7 | Genetic mutations of samples with high and low m^{6}A scores. **(A)** Distribution of KRAS mutation in high and low m^{6}A score groups. **(B)** Distribution of TP53 mutation in high and low m^{6}A score groups. **(C,D)** The somatic mutation landscape of samples with high and low m^{6}A scores. **(E,F)** The CNV landscape of samples with high and low m^{6}A scores.

T cells, and type 2 T helper cells, demonstrating higher immunogenicity in m^{6}A cluster B. Consistently, previous studies have reported the interactions between m^{6}A and tumor microenvironment of pancreatic cancer. For instance, both arm-level gain and deletion of ALKBH5 is relation to decreased infiltration of CD8 + T cell in pancreatic adenocarcinoma (Tang et al., 2020b).

This study proposed m^{6}A score system for quantifying the m^{6}A modification pattern of individual pancreatic cancer by PCA algorithm. Lowered m^{6}A scores were detected in m^{6}A gene cluster A. Furthermore, we found that m^{6}A scores were not correlated to clinical characteristics including primary sites, sex, and age. Nevertheless, high m^{6}A scores were in relation to depressed OS duration, demonstrating that m^{6}A scores might be utilized for predicting pancreatic cancer prognoses. A previous study developed a six-m^{6}A-regulator-signature prognostic model that was markedly associated with OS as well as clinical features (pathologic M, N, clinical stages, and vital status) (Hou et al., 2020). To uncover the molecular mechanism behind m^{6}A scores, this study evaluated the enrichment scores of cancer-related pathways between high and low m^{6}A score groups. High m^{6}A scores were characterized by increased activation of EMT3, Wnt targets, and cell cycle regulators. YTHDF2 orchestrates EMT process in pancreatic cancer (Chen et al., 2017). ALKBH5

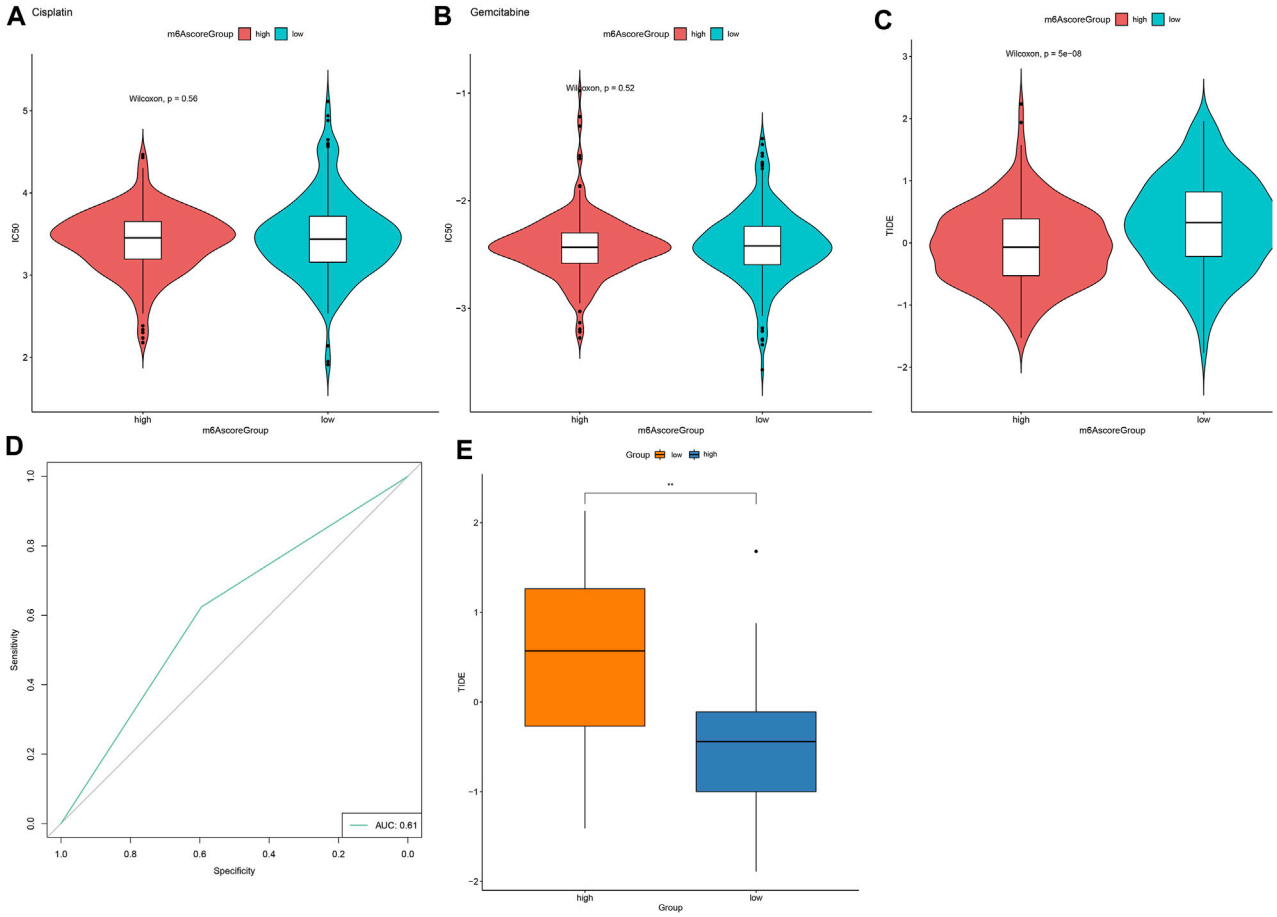

FIGURE 8 | m^{6}A score might be used for predicting the response to immunotherapy. **(A,B)** Violin plots for visualizing IC50 values of **(A)** cisplatin and **(B)** gemcitabine in high and low m^{6}A score groups. **(C)** Violin plots of TIDE scores in high and low m^{6}A score groups. Comparisons between groups were analyzed with Wilcoxon test. **(D)** ROC curves for assessing the response to immunotherapy based on m^{6}A scores. **(E)** Validation of TIDE scores in high and low m^{6}A score groups in the GSE79668 dataset. $^{**}p < 0.01$.

suppresses pancreatic cancer tumorigenesis through mediation of Wnt pathway (Tang et al., 2020a). Meanwhile, low m^{6}A scores were distinctly related to angiogenesis, cell cycle, DNA replication, nucleotide excision repair, homologous recombination, and mismatch repair. Here, both in high and low m^{6}A score groups, FRG1B, KRAS, TP53, TCF20, MED12L, PRG4, OTUD4, and MYH9 were the eight most frequently mutated genes. Missense mutation was the main type of mutation in pancreatic cancer. Genomic and transcriptomic research has uncovered key genetic mutations may drive pancreatic cancer initiation and progress, like KRAS driver mutation (beyond 90%) as well as frequently inactivated TP53 tumor suppressor (beyond 50%) (Peng et al., 2019). A previous study constructed a LASSO prognostic model based on the m^{6}A regulators and showed that, KRAS mutation status prominently differed between high- and low-risk subgroups in pancreatic cancer (Geng et al., 2020). In our study, no significant differences in KRAS and TP53 mutations were found in high and low m^{6}A score groups. Cisplatin and gemcitabine are standard chemotherapy protocols in pancreatic cancer (Liedtke et al., 2020). Nevertheless, chemo-resistance is the most common phenomenon in pancreatic cancer therapy (Herbst and Zheng, 2019). In previous research, up-regulating m^{6}A demethylase ALKBH5 may enhance the sensitivity to gemcitabine in pancreatic cancer (Tang et al., 2020a). Furthermore, pancreatic cancer cells with inhibition of m^{6}A writer METTL3 displays higher sensitivity to cisplatin and gemcitabine (Taketo et al., 2018). Above research emphasizes key roles of m^{6}A regulators in pancreatic cancer resistance. Nevertheless, no significant differences in sensitivity to cisplatin and gemcitabine were detected between high and low m^{6}A score groups.

ICB can produce long-lasting clinical effects. However, limited pancreatic cancer patients benefit from these therapies due to low immunogenicity as well as immunosuppressive tumor microenvironment (Macherla et al., 2018). Combining ICB with other modalities like vaccines, chemoradiotherapy, and target therapies possibly overcomes resistance and enhances immune response in pancreatic cancer. TIDE has been developed for predicting ICB response (Jiang et al., 2018). In previous research the efficacy of anti-PD-L1 therapy can be enhanced by m^{6}A-binding protein YTHDF1 inhibition (Han et al., 2019). Also, suppression of m^{6}A demethylase

FTO may enhance the responsiveness to anti-PD-1 blockade (Yang et al., 2019). Here, high m^{6}A score group displayed lower TIDE scores, indicating that these patients were more likely to respond to ICB therapies. AUC = 0.61 indicated that m^{6}A scores might be utilized for predicting immunotherapy response.

Taken together, this study offered new insights into prolonging pancreatic cancer patients' survival duration and enhancing the response to immunotherapy, thereby promoting personalized cancer immunotherapy.

CONCLUSION

Collectively, these data characterized two distinct m^{6}A methylation modification patterns and their associations with immune microenvironment. By comprehensively evaluating individualized m^{6}A modification patterns, we may fully understand immune microenvironment characteristics and develop more effective immunotherapeutic options.

DATA AVAILABILITY STATEMENT

The original contributions presented in the study are included in the article/**Supplementary Material**, further inquiries can be directed to the corresponding author.

AUTHOR CONTRIBUTIONS

Conception and design: KF, DT. Collection and assembly of data: DT, JM, CY, LG. Analysis and interpretation: KF, HQ. Article writing: JW, CY. Paper revision: KF.

SUPPLEMENTARY MATERIAL

The Supplementary Material for this article can be found online at: https://www.frontiersin.org/articles/10.3389/fgene.2021.702072/full#supplementary-material

REFERENCES

Bailey, P., Chang, D. K., Nones, K., Johns, A. L., Patch, A. M., Gingras, M. C., et al. (2016). Genomic analyses identify molecular subtypes of pancreatic cancer. *Nature* 531 (7592), 47–52. doi:10.1038/nature16965

Chen, J., Sun, Y., Xu, X., Wang, D., He, J., Zhou, H., et al. (2017). YTH domain family 2 orchestrates epithelial-mesenchymal transition/proliferation dichotomy in pancreatic cancer cells. *Cell Cycle* 16 (23), 2259–2271. doi:10.1080/15384101.2017.1380125

Colaprico, A., Silva, T. C., Olsen, C., Garofano, L., Cava, C., Garolini, D., et al. (2016). TCGAbiolinks: an R/Bioconductor package for integrative analysis of TCGA data. *Nucleic Acids Res.* 44 (8), e71. doi:10.1093/nar/gkv1507

Collisson, E. A., Bailey, P., Chang, D. K., and Biankin, A. V. (2019). Molecular subtypes of pancreatic cancer. *Nat. Rev. Gastroenterol. Hepatol.* 16 (4), 207–220. doi:10.1038/s41575-019-0109-y

Geng, Y., Guan, R., Hong, W., Huang, B., Liu, P., Guo, X., et al. (2020). Identification of m6A-related genes and m6A RNA methylation regulators in pancreatic cancer and their association with survival. *Ann. Transl Med.* 8 (6), 387. doi:10.21037/atm.2020.03.98

Guo, X., Li, K., Jiang, W., Hu, Y., Xiao, W., Huang, Y., et al. (2020). RNA demethylase ALKBH5 prevents pancreatic cancer progression by posttranscriptional activation of PER1 in an m6A-YTHDF2-dependent manner. *Mol. Cancer* 19 (1), 91. doi:10.1186/s12943-020-01158-w

Han, D., Liu, J., Chen, C., Dong, L., Liu, Y., Chang, R., et al. (2019). Anti-tumour immunity controlled through mRNA m6A methylation and YTHDF1 in dendritic cells. *Nature* 566 (7743), 270–274. doi:10.1038/s41586-019-0916-x

Hänzelmann, S., Castelo, R., and Guinney, J. (2013). GSVA: gene set variation analysis for microarray and RNA-seq data. *BMC Bioinformatics* 14, 7. doi:10.1186/1471-2105-14-7

He, L., Li, H., Wu, A., Peng, Y., Shu, G., and Yin, G. (2019). Functions of N6-methyladenosine and its role in cancer. *Mol. Cancer* 18 (1), 176. doi:10.1186/s12943-019-1109-9

Hegde, S., Krisnawan, V. E., Herzog, B. H., Zuo, C., Breden, M. A., Knolhoff, B. L., et al. (2020). Dendritic Cell Paucity Leads to Dysfunctional Immune Surveillance in Pancreatic Cancer. *Cancer Cell* 37 (3), 289–307. e289. doi:10.1016/j.ccell.2020.02.008

Herbst, B., and Zheng, L. (2019). Precision medicine in pancreatic cancer: treating every patient as an exception. *Lancet Gastroenterol. Hepatol.* 4 (10), 805–810. doi:10.1016/s2468-1253(19)30175-x

Ho, W. J., Jaffee, E. M., and Zheng, L. (2020). The tumour microenvironment in pancreatic cancer - clinical challenges and opportunities. *Nat. Rev. Clin. Oncol.* 17 (9), 527–540. doi:10.1038/s41571-020-0363-5

Hou, J., Wang, Z., Li, H., Zhang, H., and Luo, L. (2020). Gene Signature and Identification of Clinical Trait-Related m6 A Regulators in Pancreatic Cancer. *Front. Genet.* 11, 522. doi:10.3389/fgene.2020.00522

Jain, T., and Dudeja, V. (2021). The war against pancreatic cancer in 2020 - advances on all fronts. *Nat. Rev. Gastroenterol. Hepatol.* 18 (2), 99–100. doi:10.1038/s41575-020-00410-4

Jiang, P., Gu, S., Pan, D., Fu, J., Sahu, A., Hu, X., et al. (2018). Signatures of T cell dysfunction and exclusion predict cancer immunotherapy response. *Nat. Med.* 24 (10), 1550–1558. doi:10.1038/s41591-018-0136-1

Kirby, M. K., Ramaker, R. C., Gertz, J., Davis, N. S., Johnston, B. E., Oliver, P. G., et al. (2016). RNA sequencing of pancreatic adenocarcinoma tumors yields novel expression patterns associated with long-term survival and reveals a role for ANGPTL4. *Mol. Oncol.* 10 (8), 1169–1182. doi:10.1016/j.molonc.2016.05.004

Leek, J. T., Johnson, W. E., Parker, H. S., Jaffe, A. E., and Storey, J. D. (2012). The sva package for removing batch effects and other unwanted variation in high-throughput experiments. *Bioinformatics* 28 (6), 882–883. doi:10.1093/bioinformatics/bts034

Li, N., Kang, Y., Wang, L., Huff, S., Tang, R., Hui, H., et al. (2020). ALKBH5 regulates anti-PD-1 therapy response by modulating lactate and suppressive immune cell accumulation in tumor microenvironment. *Proc. Natl. Acad. Sci. USA* 117 (33), 20159–20170. doi:10.1073/pnas.1918986117

Liang, C., Shi, S., Qin, Y., Meng, Q., Hua, J., Hu, Q., et al. (2020). Localisation of PGK1 determines metabolic phenotype to balance metastasis and proliferation in patients with SMAD4-negative pancreatic cancer. *Gut.* 69 (5), 888–900. doi:10.1136/gutjnl-2018-317163

Liberzon, A., Birger, C., Thorvaldsdóttir, H., Ghandi, M., Mesirov, J. P., and Tamayo, P. (2015). The Molecular Signatures Database Hallmark Gene Set Collection. *Cel Syst.* 1 (6), 417–425. doi:10.1016/j.cels.2015.12.004

Liedtke, K.-R., Freund, E., Hermes, M., Oswald, S., Heidecke, C.-D., Partecke, L.-I., et al. (2020). Gas Plasma-Conditioned Ringer's Lactate Enhances the Cytotoxic Activity of Cisplatin and Gemcitabine in Pancreatic Cancer *In Vitro* and in Ovo. *Cancers* 12 (1), 123. doi:10.3390/cancers12010123

Ma, S., Chen, C., Ji, X., Liu, J., Zhou, Q., Wang, G., et al. (2019). The interplay between m6A RNA methylation and noncoding RNA in cancer. *J. Hematol. Oncol.* 12 (1), 121. doi:10.1186/s13045-019-0805-7

Macherla, S., Laks, S., Naqash, A., Bulumulle, A., Zervos, E., and Muzaffar, M. (2018). Emerging Role of Immune Checkpoint Blockade in Pancreatic Cancer. *Ijms* 19 (11), 3505. doi:10.3390/ijms19113505

Meng, Z., Yuan, Q., Zhao, J., Wang, B., Li, S., Offringa, R., et al. (2020). The m6A-Related mRNA Signature Predicts the Prognosis of Pancreatic Cancer Patients. *Mol. Ther. - Oncolytics* 17, 460–470. doi:10.1016/j.omto.2020.04.011

O'Reilly, E. M., Lee, J. W., Zalupski, M., Capanu, M., Park, J., Golan, T., et al. (2020). Randomized, Multicenter, Phase II Trial of Gemcitabine and Cisplatin

with or without Veliparib in Patients with Pancreas Adenocarcinoma and a Germline BRCA/PALB2 Mutation. *Jco* 38 (13), 1378–1388. doi:10.1200/jco.19.02931

Peng, J., Sun, B.-F., Chen, C.-Y., Zhou, J.-Y., Chen, Y.-S., Chen, H., et al. (2019). Single-cell RNA-seq highlights intra-tumoral heterogeneity and malignant progression in pancreatic ductal adenocarcinoma. *Cell Res.* 29 (9), 725–738. doi:10.1038/s41422-019-0195-y

Qin, C., Yang, G., Yang, J., Ren, B., Wang, H., Chen, G., et al. (2020). Metabolism of pancreatic cancer: paving the way to better anticancer strategies. *Mol. Cancer* 19 (1), 50. doi:10.1186/s12943-020-01169-7

Ritchie, M. E., Phipson, B., Wu, D., Hu, Y., Law, C. W., Shi, W., et al. (2015). limma powers differential expression analyses for RNA-sequencing and microarray studies. *Nucleic Acids Res.* 43 (7), e47. doi:10.1093/nar/gkv007

Taketo, K., Konno, M., Asai, A., Koseki, J., Toratani, M., Satoh, T., et al. (2018). The epitranscriptome m6A writer METTL3 promotes chemo- and radioresistance in pancreatic cancer cells. *Int. J. Oncol.* 52 (2), 621–629. doi:10.3892/ijo.2017.4219

Tang, B., Yang, Y., Kang, M., Wang, Y., Wang, Y., Bi, Y., et al. (2020a). m6A demethylase ALKBH5 inhibits pancreatic cancer tumorigenesis by decreasing WIF-1 RNA methylation and mediating Wnt signaling. *Mol. Cancer* 19 (1), 3. doi:10.1186/s12943-019-1128-6

Tang, R., Zhang, Y., Liang, C., Xu, J., Meng, Q., Hua, J., et al. (2020b). The role of m6A-related genes in the prognosis and immune microenvironment of pancreatic adenocarcinoma. *PeerJ* 8, e9602. doi:10.7717/peerj.9602

Torphy, R. J., Schulick, R. D., and Zhu, Y. (2020). Understanding the immune landscape and tumor microenvironment of pancreatic cancer to improve immunotherapy. *Mol. Carcinogenesis* 59 (7), 775–782. doi:10.1002/mc.23179

Wang, M., Liu, J., Zhao, Y., He, R., Xu, X., Guo, X., et al. (2020). Upregulation of METTL14 mediates the elevation of PERP mRNA N6 adenosine methylation promoting the growth and metastasis of pancreatic cancer. *Mol. Cancer* 19 (1), 130. doi:10.1186/s12943-020-01249-8

Wilkerson, M. D., and Hayes, D. N. (2010). ConsensusClusterPlus: a class discovery tool with confidence assessments and item tracking. *Bioinformatics* 26 (12), 1572–1573. doi:10.1093/bioinformatics/btq170

Xu, F., Zhang, Z., Yuan, M., Zhao, Y., Zhou, Y., Pei, H., et al. (2021). M6A Regulatory Genes Play an Important Role in the Prognosis, Progression and Immune Microenvironment of Pancreatic Adenocarcinoma. *Cancer Invest.* 39 (1), 39–54. doi:10.1080/07357907.2020.1834576

Yang, S., Wei, J., Cui, Y.-H., Park, G., Shah, P., Deng, Y., et al. (2019). m6A mRNA demethylase FTO regulates melanoma tumorigenicity and response to anti-PD-1 blockade. *Nat. Commun.* 10 (1), 2782. doi:10.1038/s41467-019-10669-0

Zhang, H., Shi, X., Huang, T., Zhao, X., Chen, W., Gu, N., et al. (2020). Dynamic landscape and evolution of m6A methylation in human. *Nucleic Acids Res.* 48 (11), 6251–6264. doi:10.1093/nar/gkaa347

Conflict of Interest: The authors declare that the research was conducted in the absence of any commercial or financial relationships that could be construed as a potential conflict of interest.

Publisher's Note: All claims expressed in this article are solely those of the authors and do not necessarily represent those of their affiliated organizations, or those of the publisher, the editors and the reviewers. Any product that may be evaluated in this article, or claim that may be made by its manufacturer, is not guaranteed or endorsed by the publisher.

frontiers in Genetics

REVIEW
published: 27 September 2021
doi: 10.3389/fgene.2021.742561

Emerging Advances in Combinatorial Treatments of Epigenetically Altered Pediatric High-Grade H3K27M Gliomas

Katarzyna B. Leszczynska[1]†, Chinchu Jayaprakash[1]†, Bozena Kaminska[1]† and Jakub Mieczkowski[1,2]*†*

[1] Laboratory of Molecular Neurobiology, Nencki Institute of Experimental Biology of the Polish Academy of Sciences, Warsaw, Poland, [2] 3P-Medicine Laboratory, Medical University of Gdańsk, Gdańsk, Poland

Somatic mutations in histone encoding genes result in gross alterations in the epigenetic landscape. Diffuse intrinsic pontine glioma (DIPG) is a pediatric high-grade glioma (pHGG) and one of the most challenging cancers to treat, with only 1% surviving for 5 years. Due to the location in the brainstem, DIPGs are difficult to resect and rapidly turn into a fatal disease. Over 80% of DIPGs confer mutations in genes coding for histone 3 variants (H3.3 or H3.1/H3.2), with lysine to methionine substitution at position 27 (H3K27M). This results in a global decrease in H3K27 trimethylation, increased H3K27 acetylation, and widespread oncogenic changes in gene expression. Epigenetic modifying drugs emerge as promising candidates to treat DIPG, with histone deacetylase (HDAC) inhibitors taking the lead in preclinical and clinical studies. However, some data show the evolving resistance of DIPGs to the most studied HDAC inhibitor panobinostat and highlight the need to further investigate its mechanism of action. A new forceful line of research explores the simultaneous use of multiple inhibitors that could target epigenetically induced changes in DIPG chromatin and enhance the anticancer response of single agents. In this review, we summarize the therapeutic approaches against H3K27M-expressing pHGGs focused on targeting epigenetic dysregulation and highlight promising combinatorial drug treatments. We assessed the effectiveness of the epigenetic drugs that are already in clinical trials in pHGGs. The constantly expanding understanding of the epigenetic vulnerabilities of H3K27M-expressing pHGGs provides new tumor-specific targets, opens new possibilities of therapy, and gives hope to find a cure for this deadly disease.

Keywords: pediatric high-grade gliomas, H3K27M, DIPG, combinatorial treatments, epigenetic therapy

OPEN ACCESS

Edited by:
Ata Abbas,
Case Western Reserve University, United States

Reviewed by:
Manabu Natsumeda,
Niigata University, Japan
Richard Alan Katz,
Fox Chase Cancer Center, United States
Narendra Singh,
Stowers Institute for Medical Research, United States

***Correspondence:**
Katarzyna B. Leszczynska
k.leszczynska@nencki.edu.pl
Jakub Mieczkowski
jakubm@gumed.edu.pl

†ORCID:
Katarzyna B. Leszczynska
orcid.org/0000-0002-3504-1553
Chinchu Jayaprakash
orcid.org/0000-0001-9967-0095
Bozena Kaminska
orcid.org/0000-0002-2642-4616
Jakub Mieczkowski
orcid.org/0000-0002-2091-012X

Specialty section:
This article was submitted to Epigenomics and Epigenetics, a section of the journal Frontiers in Genetics

Received: *16 July 2021*
Accepted: *17 August 2021*
Published: *27 September 2021*

Citation:
Leszczynska KB, Jayaprakash C, Kaminska B and Mieczkowski J (2021) Emerging Advances in Combinatorial Treatments of Epigenetically Altered Pediatric High-Grade H3K27M Gliomas. Front. Genet. 12:742561. doi: 10.3389/fgene.2021.742561

INTRODUCTION

Pediatric high-grade gliomas (pHGGs) are the prominent group of brain tumors that cause fatalities in childhood (Mendez et al., 2020). Diffuse midline gliomas (DMGs) that arise in midline structures of the brain (such as the brainstem, thalamus, or spinal cord) are the most malignant tumors among pHGGs, and diffuse intrinsic pontine glioma (DIPG) is the most lethal, with only 1% of

patients surviving 5 years post-diagnosis (Buczkowicz et al., 2014; Louis et al., 2016). Localization of DIPG to the pons (a major part of the brainstem, above the medulla and below the midbrain) presents a particular challenge for therapy, preventing resection, limiting treatment to radiation with adjuvant temozolomide, and offering only palliative care (Bartels et al., 2011; Jansen et al., 2012; Mendez et al., 2020). The stereotactic biopsies or postmortem tumor samples had been used to derive cell lines and patient-derived xenografts, which proved critical in advancing the drug screens and mechanistic research on the disease (Lin and Monje, 2017; Aziz-Bose and Monje, 2019). Despite recent advancements in understanding the genetic hallmarks of DIPG (Mackay et al., 2017; Filbin et al., 2018; Gröbner et al., 2018), further research into cellular responses to specific drug treatments and therapy resistance is necessary to improve the outcome of patients.

The typical molecular feature of pHGGs is the somatic heterozygous mutation in the *H3F3A* gene encoding the histone H3.3 resulting in the substitution of lysine to methionine at amino acid position 27 of the histone H3 variants (H3K27M), and less commonly in *HIST1H3B/C* and *HIST2H3C,* encoding histones H3.1 and H3.2, respectively (Khuong-Quang et al., 2012; Schwartzentruber et al., 2012; Wu et al., 2012). In the midline pHGGs, the H3K27M substitution occurs in 80% of the cases and is a driver event responsible for the tumor initiation and progression (Pathania et al., 2017; Harutyunyan et al., 2019; Larson et al., 2019; Silveira et al., 2019). It is still debatable whether DIPG starts already during embryonic development or postnatally in early childhood. Numerous experimental studies support the hypothesis that oligodendroglial progenitor-like cells (OPCs) are the cells of origin of DIPG (Monje et al., 2011; Funato et al., 2014; Pathania et al., 2017; Filbin et al., 2018; Nagaraja et al., 2019). In addition, super-enhancers in H3K27M pHGGs had been identified, which reflect the OPC cell of origin (Monje et al., 2011; Nagaraja et al., 2017). Some of the super-enhancers acting in DIPG include genes coding for Ephrins and Ephrin receptors. Receptor tyrosine kinases activated by binding to glycosylphosphatidylinositol (GPI)-linked and transmembrane ephrin ligands may play a role in the diffusive and invasive spread of DIPG through the brainstem (Nagaraja et al., 2017). However, a recent study using inducible pluripotent stem cells with the expression of H3.3-K27M targeted to the endogenous histone locus showed that H3.3-K27M drives tumorigenesis from neural stem cells but not glial progenitors (Haag et al., 2021).

The unique consequence of the H3K27M substitution in pHGGs is a global epigenetic dysregulation, including a loss of H3K27me3 (a repressive mark) and an increase in H3K27 acetylation (an activating mark) at the regulatory region of developmentally regulated genes. These global epigenetic changes occur despite the fact that the protein levels of the H3K27M mutant constitute only 3–17% of the total levels of all H3 histone proteins (Lewis et al., 2013). Since identifying the H3K27M mutation in pHGGs, extensive efforts have been made to characterize the properties of chromatin in these tumors, and druggable targets have started to emerge. In this review, we explicitly focus on the recent advances in epigenetic therapies against H3K27M-bearing pHGGs and especially on the potential of combinatorial therapies targeting chromatin via epigenetic pathways.

EPIGENETIC ALTERATIONS IN H3K27M pHGGs

Methylation of Lysine 27 in Histone H3

The drop in H3K27me3 in the H3K27M-expressing cells is very striking and consistent in multiple cellular models (Chan et al., 2013; Lewis et al., 2013; Krug et al., 2019; Silveira et al., 2019). The mechanism of the H3K27me3 loss, although still disputable, is mainly attributed to the inhibition of the *N*-methyltransferase enhancer of zeste homolog 2 (EZH2)—the catalytic subunit of PRC2 (polycomb repressive complexes 2). Deposition of the H3K27me3 mark by the PRC2 complex is critical in silencing the expression of specific genes, which, depending on the context, may include tumor suppressors or oncogenes (Chammas et al., 2020). Several studies showed that the H3K27M substitution has a dominant inhibitory effect on the PRC2 complex, which is being preferentially recruited to the H3K27M-containing nucleosomes and retained in an inactive form (Chan et al., 2013; Lewis et al., 2013; Justin et al., 2016; Fang et al., 2018; Diehl et al., 2019). Another study has shown that PRC2 is preferentially recruited to its strongest binding sites in H3K27M-expressing cells, which still retain partial H3K27me3 (Mohammad et al., 2017). However, other studies demonstrated temporary PRC2 recruitment to H3K27M-containing nucleosomes or even exclusion of PRC2 from the H3K27M nucleosomes (Piunti et al., 2017; Stafford et al., 2018). Piunti and colleagues showed that a residual activity of the PRC2 complex is retained outside of the heterotypic H3K27M-H3K27ac nucleosomes and is required for the proliferative potential of the H3K27M-bearing cells (Piunti et al., 2017). Stafford and colleagues, in turn, showed that the H3K27M protein needs to be expressed in great excess compared to the amount of the PRC2 complex in order to inhibit the catalytic activity of PRC2 (Stafford et al., 2018). Furthermore, while PRC2 is only temporarily recruited to H3K27M-containing chromatin, the inhibitory effect on PRC2 is retained even after its release from the chromatin (Stafford et al., 2018). Finally, recent studies by Harutyunyan and colleagues confirmed that PRC2 is indeed recruited to the chromatin in H3K27M pHGGs but is unable to spread the methylation mark from large unmethylated CpG islands (CGIs), which are its high affinity recruitment sites (Harutyunyan et al., 2019). Only a residual amount of H3K27me3 is retained at these CGIs. In addition, they showed that the H3K27me2 mark is deposited outside of CGIs in H3K27M cells and localizes to the areas normally marked by H3K27me3 in H3 wild-type cells (Harutyunyan et al., 2019, 2020).

Acetylation of Lysine 27 in Histone H3

In addition to decreasing H3K27me3, the H3K27M oncohistone leads to elevated levels of the acetylated H3K27, which is typically associated with active transcription (Wang et al., 2009; Lewis et al., 2013). Some studies showed that the histone H3.3K27M forms heterotypic nucleosomes with the wild-type H3.3, particularly with its acetylated form

(Piunti et al., 2017; Krug et al., 2019; Nagaraja et al., 2019). Furthermore, H3K27M-H3K27ac heterotypic nucleosomes recruit bromodomain-containing proteins (BRDs), which are known to recruit RNA Polymerase II (RNA Pol II) and therefore activate transcription (Jonkers and Lis, 2015). The pervasive acetylation of H3K27 in H3.3K27M-bearing cell lines localizes to repetitive elements (REs), including endogenous retroviral sequences (ERV), which are usually tightly controlled and silenced in the genome (Krug et al., 2019). This H3K27ac leads to increased expression of ERV elements and ultimately to so-called viral mimicry in H3K27M pHGGs (Pathania et al., 2017; Krug et al., 2019).

MOLECULAR AND PHENOTYPIC DIFFERENCES IN pHGGs EXPRESSING EITHER H3.1K27M OR H3.3K27M

Distinct characteristics of pHGG have been found, depending on whether H3K27M mutation occurs in H3.1 or H3.3 histone variants. The differences in the associated secondary mutations are also apparent, as H3.3K27M mainly co-occurs with mutations of *TP53* (coding for tumor suppressor protein 53) and amplification of *PDGFRA* (encoding platelet derived growth factor alpha). In contrast, H3.1K27M co-occurs with mutations in *ACVR1* (encoding the activin receptor type-1) and genes involved in the PI3K (phosphatidylinositol 3-kinase)-signaling pathway (Wu et al., 2012; Buczkowicz et al., 2014; Fontebasso et al., 2014; Taylor et al., 2014; Mackay et al., 2017). Moreover, distinct genome-wide distribution patterns of these oncohistones were found, with H3.3K27M incorporating into the nucleosomes at the active chromatin sites and gene bodies, while H3.1K27M localizing uniformly across the genome. These changes reflect the expression and the genome-wide distribution pattern of wild-type H3.3 and H3.1 variants, respectively (Nagaraja et al., 2019). Moreover, tumors with either H3.1K27M or H3.3K27M variants have distinct profiles of active enhancers and promoters, potentially influencing the treatment response. For example, H3.3K27M-expressing tumors exhibit increased activity of enhancers regulating genes of the noncanonical WNT (Wingless/Integrated) signaling and cytoskeletal remodeling. In contrast, enhancers of H3.1K27M-expressing tumors control genes implicated in the PI3K and p38 MAPK (mitogen activated protein kinases) signaling pathways (Nagaraja et al., 2019). In accordance with the hypothesis that H3K27M has an inhibitory effect on the PRC2 complex, a detailed study showed that these two mutated H3 variants disrupt different PRC2 targets (Nagaraja et al., 2019). Finally, DNA methylation profiles can also distinguish H3.1K27M and H3.3K27M histone variant-expressing cells (Sturm et al., 2012; Castel et al., 2015, 2018).

A SEARCH FOR SPECIFIC EPIGENETIC VULNERABILITIES OF H3K27M pHGGs

Targeting Modifiers of H3K27me3

A set of epigenetic alterations in H3K27M pHGGs created opportunities for therapeutic approaches (**Figure 1A**). One

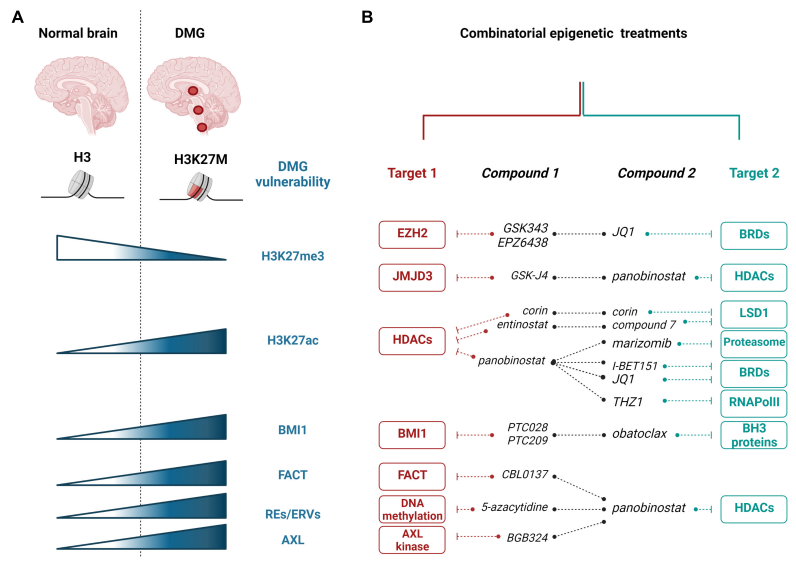

FIGURE 1 | Epigenetic targeting of H3K27M diffuse midline gliomas (DMGs). **(A)** Most of DMGs (localizing to the thalamus, brainstem, or spinal cord) are characterized by H3K27M substitution. The mutation leading to H3K27M is responsible for numerous changes in DMG cells, including the decrease in H3K27me3 and the increase in H3K27ac histone modifications, and increased expression of BMI1, FACT, and REs/ERVs. **(B)** Epigenetic vulnerabilities of H3K27M DMGs were targeted with epigenetic enzyme inhibitors and showed promising effects in preclinical studies using in vitro and in vivo models. Red and teal colors showed various targets that are inhibited with specific compounds in combinatorial treatments, as indicated. EZH2, enhancer of zeste homolog 2; JMJD3, Jumonji domain-containing 3; HDACs, histone deacetylases; BRDs, bromodomain containing proteins; LSD1, lysine-specific demethylase 1; RNAPolII, RNA Polymerase II; BH3, Bcl-2 Homology 3; BMI1, B cell-specific Moloney murine leukemia virus integration site 1; FACT, facilitates chromatin transcription complex; REs, repetitive elements; ERVs, endogenous retroviral sequences; AXL, AXL receptor tyrosine kinase. The figure was created with BioRender.com.

such strategy was to restore the H3K27me3 histone repressive mark. This strategy was achieved by selective inhibition of H3K27me3 demethylases (KDMs), namely KDM6 subfamily of Jumonji domain-containing 3 (JMJD3) K27 demethylases (Agger et al., 2007). Compound GSK-J4 specifically inhibited JMJD3, but not UTX (ubiquitously transcribed tetratricopeptide repeat on chromosome X, encoded by *KDM6A*), and decreased cell viability and clonogenic growth, while increasing the S-phase cell-cycle arrest and apoptosis (Hashizume et al., 2014). GSK-J4 was also potent in extending the survival of mice bearing H3K27M tumors. Importantly, the efficacy of GSK-J4 was more significant in mutant cells compared to H3 wild-type cells or the H3G34V-mutant cells. GSK-J4 treatment resulted in impaired DNA repair by homologous recombination and increased radiosensitivity of these cells (Katagi et al., 2019). At the moment, there are constrains of using GSK-J4 in clinical trials as it rapidly converts into an active drug GSK-J1 and has limited penetration into the brain.

While H3K27me3 levels are very low in H3K27M tumors, these marks are not entirely erased, and some loci in the genome retain this repressive mark (Chan et al., 2013). The residual methylation of the H3K27 residue is critical for DIPG survival and proliferation, as well as silencing of neural differentiation genes (Piunti et al., 2017). The PRC2 complex is required for the proliferative potential of H3K27M pHGGs, e.g., by silencing the expression of the tumor suppressor gene encoding $p16^{INK4A}$, through a remaining H3K27me3 mark at its promoter (Mohammad et al., 2017). Consequently, targeting EZH2, the methyltransferase subunit of the PRC2 complex, effectively decreased cell viability, proliferation, and prolonged survival of mice bearing H3K27M tumors (Mohammad et al., 2017).

Interfering With H3K27ac and Transcriptional Activity in H3K27M pHGGs

While H3K27M pHGGs have elevated levels of H3K27ac when compared to the tumors expressing the wild-type H3 variants, screening of various epigenetic modifying drugs showed that histone deacetylase (HDAC) inhibitors are among the most potent compounds decreasing the survival of pHGG cells (Grasso et al., 2015; Anastas et al., 2019). Several HDAC inhibitors were tested so far in pHGGs, including vorinostat, entinostat, and panobinostat (LBH589), with the latter showing the highest potency and being the most explored as a single agent or in combination with other drugs (see further sections) (Grasso et al., 2015; Nagaraja et al., 2017; Anastas et al., 2019; Krug et al., 2019; Lin et al., 2019; Ehteda et al., 2021; Vitanza et al., 2021). In addition, quisinostat and romidepsin emerged recently as potent HDAC inhibitors in treatment-naïve biopsy-derived DMG models (Vitanza et al., 2021). Overall, preclinical data showed that HDAC inhibitors potently kill DMG cells, reduce cell proliferation, and inhibit tumor growth *in vitro* and in animal models (Grasso et al., 2015; Anastas et al., 2019; Vitanza et al., 2021).

However, studies of panobinostat effects showed that despite a high potency of this drug at subnanomolar concentrations and an immediate impact on cell viability, the acquired resistance of H3K27M cells appears after the prolonged treatment (Grasso et al., 2015). Moreover, the systemic administration of panobinostat at different schedules and well-tolerated doses in mouse DIPG models and xenografts did not bring survival benefits compared to the controls (Hennika et al., 2017). Alternative compounds or combinations with other drugs might be needed to overcome treatment resistance. Moreover, a thorough investigation of the panobinostat action and the mechanism of cellular response is required. So far, it has been shown that, as expected, panobinostat increased histone acetylation. In addition, panobinostat partially restored the levels of H3K27me3 and normalized the pattern of gene expression affected by H3K27M (Grasso et al., 2015). The mechanism of the H3K27me3 restoration by HDAC inhibition is unclear. However, it was shown in a separate study that poly-acetylated H3 tails are able to "detoxify" a PRC2 complex by restoring its activity in H3K27M tumors (Brown et al., 2014). Moreover, the H3K27me3 increase in response to HDAC inhibition was observed in other tumor types not expressing H3K27M (Halsall et al., 2015). In the context of induced levels of H3K27ac at the REs and increased expression of ERVs in H3K27M pHGGs, the use of panobinostat increased histone acetylation at these sites and contributed to the so-called viral mimicry. Of note, mass spectrometry analysis showed that the increase in H3K27ac in response to panobinostat occurs mainly at H3.3 and not H3.1 or H3.2 histone variants (Krug et al., 2019).

Acetylation of the H3 N-tail, including H3K27ac, recruits bromodomain and extraterminal (BET) proteins, including BRD2 (Bromodomain Containing 2) or BRD4 (Bromodomain Containing 4), which are epigenetic readers of histone acetylation and, in turn, recruit cofactors for transcription initiation and ultimately trigger activation of RNA PolII-dependent transcription (Jonkers and Lis, 2015; Fujisawa and Filippakopoulos, 2017). Since H3K27ac is elevated in H3K27M tumors, targeting the BET proteins brings another intuitive strategy against H3K27M pHGGs. Piunti and colleagues showed that when an H3K27M oncohistone forms heterotypic nucleosomes with H3K27ac, these complexes recruit BRD2 and BRD4 to the chromatin (Piunti et al., 2017). Subsequently, targeting these cells with BET inhibitors JQ1 or I-BET151 significantly reduced cell viability and decreased overall H3K27ac levels. In addition, JQ1 and I-BET151 also potently inhibited tumor growth, decreased cell proliferation, and induced differentiation, as evidenced by increased expression of differentiation genes, including *TUBB3*, in mouse xenograft models. Interestingly, the use of JQ1 in xenografts *in vivo* was more efficient than using the GSK-J4 inhibitor against JMJD3 H3K27 demethylases (Piunti et al., 2017). However, it was not clarified whether JQ1 exhibited stronger toxicity in H3K27M-expressing cells when compared to H3 wild-type cells as did GSK-J4 (Hashizume et al., 2014). The potential of using JQ1 against DIPG tumors was also demonstrated by other studies, in parallel to targeting RNA PolII phosphorylation with the CDK7 (cyclin-dependent kinase 7) inhibitor, THZ1 (Taylor et al., 2015; Nagaraja et al., 2017).

Another study independently exposed a transcriptional activity as a vulnerability of DIPG tumors. Screening using RNAi library identified AF4/FMR2 Family Member 4 (AFF4), a scaffold protein in the super elongation complex (SEC), as a critical protein in maintaining the clonogenic potential, promoting self-renewal potential and stemness of DIPG tumors (Dahl et al., 2020). Depletion of AFF4 with shRNA induced the expression of prodifferentiation genes and reduced the self-renewal of DIPG cells. Subsequently, the authors used the CDK9 inhibitors atuveciclib and AZD4573, which interfere with the function of SEC by blocking the release of RNA Pol II from promoter-proximal pausing, which is normally mediated by RNA Pol II phosphorylation by CDK9 (Peterlin and Price, 2006; Zhou et al., 2012). Similarly to depletion of AFF4, CDK9 inhibitors induced the expression of pro-differentiation genes and reduced the self-renewal capacity of DIPG cells. In addition, atuveciclib and AZD4573 showed therapeutic benefits by delaying tumor growth and increasing mice survival in the orthotopic xenograft models of DMG (Dahl et al., 2020).

COMBINATORIAL EPIGENETIC TREATMENTS

Targeting HDACs and Histone Demethylases

While hopes regarding high *in vitro* potency of panobinostat in targeting H3K27M pHGGs were diminished by *in vivo* data showing a negligible survival effect at well-tolerable doses in animal tumor models, subsequent strategies evolved to combine the inhibition of HDACs with other epigenetic targets (**Figure 1B**; Grasso et al., 2015; Hennika et al., 2017). As a first attempt, a synergy in using panobinostat with GSK-J4 was shown. This treatment required much lower doses of each drug in combination than as single agents (Grasso et al., 2015). However, little is known about the exact molecular changes induced by this combinatorial treatment.

In another study, Anastas et al. (2019) searched for the drugs that would sensitize H3K27M-expressing cells to HDAC inhibitors. Cells were subjected to CRISPR KO screening with sgRNA library against 1,354 candidate genes related to chromatin regulation and treated with panobinostat for 3 weeks (Anastas et al., 2019). Among the top hits, *KDM1A,* encoding H3K4me1/2-specific demethylase lysine-specific demethylase 1 (LSD1), came out as a promising candidate (Anastas et al., 2019). Subsequently, the authors showed that simultaneous targeting of HDACs and LSD1 in H3K27M cells with entinostat and compound 7, respectively, synergistically decreased cell survival and proliferation. As an attractive alternative, the authors used a bifunctional single-molecule inhibitor, Corin, derived from compound 7 and entinostat, to inhibit both HDACs and LSD1 (Anastas et al., 2019). While the LSD1 inhibitor alone did not affect the cell viability of H3K27M cells, the use of Corin or a combination of entinostat with the LSD1 inhibitor compound 7 enhanced the sensitivity of these cells compared to the HDAC inhibitor alone. *In vivo,* Corin significantly reduced the xenograft growth when delivered intracranially as convection-enhanced delivery (CED). The rescue of H3K27ac and H3K27me3 was visible in the areas surrounding Corin injections but not in more distant tumor regions. Corin induced the differentiation of H3K27M cells and altered gene expression profiles differently than treatment with entinostat and compound 7 alone (Anastas et al., 2019). Interestingly, by performing gene set enrichment analysis on normal brains and DIPG tumor expression datasets, the authors found a strong analogy between the Corin-dependent gene expression signature and the one in a normal brain. This similarity emphasized the role of Corin in DIPG differentiation and reversing the gene expression pattern in tumor cells (Anastas et al., 2019).

Targeting HDACs and Transcription

Since the initial potency of panobinostat as a single agent was strong in DIPG preclinical studies, there was a need to find ways to overcome the resistance of cells to prolonged treatments with this drug (Grasso et al., 2015). Nagaraja et al. (2017) showed that targeting the transcriptional activity of DIPG cells through the CDK7 inhibitor THZ1 sensitized panobinostat-resistant DIPG cells. However, this effect was not achieved when panobinostat was combined with JQ1, a BET protein inhibitor. This might be explained by the fact that panobinostat and JQ1 induce similar transcriptional programs, while THZ1 treatment leads to a distinct transcriptional signature and thus inhibiting panobinostat-resistant cells with THZ1 has additional benefits (Nagaraja et al., 2017).

Targeting HDACs and DNA Methylation

Krug et al. (2019) showed that H3K27M pHGGs exhibit increased pervasive H3K27ac mark at REs, including ERVs, resulting in higher expression of these sequences. In healthy tissues, the expression of REs is tightly controlled and silenced in the genome via multiple epigenetic mechanisms, including DNA methylation or deposition of histone repressive marks (H3K9me3, H4K20me3, and H3K27me3) (Walsh et al., 1998; Bestor and Bourc'his, 2004). Hence, the authors speculated that demethylation of DNA with 5-azacytidine and additional increases in H3K27ac with panobinostat might increase the expression of REs even further and affect the viability of these cells (Krug et al., 2019). Indeed, the combination of panobinostat with 5-azacytidine significantly improved the survival of mice bearing H3K27M tumors when compared to either drug alone. The effect of 5-azacytidine alone or in combination with panobinostat was more substantial in H3K27M tumors when compared to the H3 wild-type group (Krug et al., 2019).

Targeting HDACs and FACT Complex

A recent study showed that subunits of the FACT (facilitates chromatin transcription) complex, namely structure-specific recognition protein 1 (SSRP1) and suppressor of Ty16 (SPT16), are overexpressed in DIPG tumors when compared to normal brain tissues and normal human astrocytes (Ehteda et al., 2021). The FACT complex works as a histone chaperone interacting with nucleosomes and is involved in DNA repair, DNA replication, and transcription (Hsieh et al., 2013; Prendergast et al., 2020).

Ehteda et al. (2021) showed that the SSRP1 subunit of FACT directly interacts with the H3.3K27M mutant histone. The FACT inhibitor, CBL0137, significantly decreased the survival of DIPG cells and impaired the growth of xenografts in mice as a single agent and synergized with panobinostat to cause these effects. In addition, CBL0137 increased trimethylation and acetylation of lysine 27 at H3, although the mechanism for this effect has not been explained (Ehteda et al., 2021). Moreover, the decrease in tumor sphere survival by CBL0137 was more pronounced in H3K27M-expressing DIPG spheres than in H3 wild-type human fibroblasts, normal human astrocytes, and H3K27 wild-type DIPG cells (Ehteda et al., 2021). Overall, the FACT complex emerged as a promising target specifically in H3K27M-expressing pHGGs.

Targeting HDACs and Proteasome

A high-throughput screen using a collection of approved drugs tested the efficiency of 9,195 drug–drug combinations in order to find agents that synergize in targeting pHGG cells (Lin et al., 2019). A synergy between panobinostat and a proteasome inhibitor, marizomib, in increasing cellular toxicity was found across the DIPG cell lines expressing either H3.1 or H3.3 K27M mutated histones as well as in patient-derived xenografts. However, an effect in decreasing cell survival and proliferation was equally strong in cells expressing either mutant or wild-type histone H3. The combination of panobinostat with marizomib induced profound transcriptional changes in pHGG cells, particularly a downregulation of cellular metabolism and respiration, as well as induction of unfolded protein response. The cytotoxic effect of the combined treatment was due to pushing cells into a metabolic catastrophe, which was then reversed by exogenously normalizing NAD^+ cellular levels (Lin et al., 2019).

Targeting HDACs and AXL

Ectopic expression of the H3K27M oncohistone in the murine embryonic hindbrain neural stem cells leads to the increased gene signature of epithelial to mesenchymal transition (EMT), which is also observed in DIPG tumors (Puget et al., 2012; Castel et al., 2015; Meel et al., 2020). An elevated expression of the AXL kinase, one of the initiators of the EMT, was identified in the DIPG biopsy samples and was correlated with the presence of H3K27M (Meel et al., 2020). This evidence provided a rationale for testing the AXL-specific inhibitor, BGB324, in DIPG cells. BGB324 significantly decreased cell viability at submicromolar concentrations. Moreover, inhibition of AXL with BGB324 or depletion with AXL-specific shRNA significantly impaired the invasion of neurospheres in the 3D matrigel invasion assay. AXL inhibition increased the expression of epithelial differentiation markers and downregulated the mesenchymal genes (Meel et al., 2020). Subsequently, AXL was tested in combination with panobinostat, as panobinostat alone was also shown to decrease the expression of mesenchymal genes (di Fazio et al., 2012; Rhodes et al., 2014; Grasso et al., 2015). The combination of BGB324 and panobinostat synergized in reducing cell viability in cells expressing H3K27M but not in cells with wild-type H3 histone variants. Importantly, this effect of treatment specificity to cells expressing the H3K27M oncohistone was not observed for panobinostat or BGB324 alone. The synergy between AXL and HDAC inhibition in antiproliferative effects in DIPG cells was also demonstrated with additional HDAC inhibitors and with shRNA against AXL, emphasizing the specificity of these drugs rather than potential off-target effects. Moreover, the combination of the AXL inhibitor and panobinostat synergized in decreasing cell migration and invasion, as well as in reversing the mesenchymal phenotype of DIPG cells, as shown by a decrease in the expression of genes such as *ZEB1*, *ZEB2, SNAI2, SOX2*, or *NES* and the induction of proneural pathways. While panobinostat alone sensitized DIPG cells to radiotherapy, this was enhanced by the addition of BGB324, as shown by neurosphere formation assay. Combined radiosensitization effect of panobinostat with BGB324 was justified by the most robust repression of DNA repair genes, including *FANCD2* and *RAD51*. In parallel to a decrease in DNA repair genes, an increase in γH2AX, a marker of DNA damage, was strongest in the combination treatments (Meel et al., 2020). Finally, it was demonstrated that BGB324 has a capacity of crossing the blood–brain barrier after oral administration. Moreover, when combined with panobinostat delivered through CED, BGB324 has a synergistic effect in delaying the tumor growth in mouse models of DIPG (Meel et al., 2020).

Targeting BET Bromodomains and PRC2

While single-agent targeting against either EZH2 or BET family of proteins in DIPG tumors proved to be efficient (Mohammad et al., 2017; Piunti et al., 2017), one study combined these two strategies by using the EZH2 inhibitor EPZ6438 and the JQ1 inhibitor against the BET proteins (Zhang et al., 2017). The authors used mouse primary neural stem cell (NSC) cultures, in which HA-PDGFB and either flag-H3.3K27M or flag-H3.3K27 wild-type transgenes were overexpressed. When injected into the mouse pons, H3.3 K27M NSCs formed larger tumors than those expressing wild-type histone H3. An even stronger effect of the combined JQ1 and EPZ6438 treatment in inhibiting tumor growth was observed compared to the single agents. The more substantial impact of this drug combination was explained by a decrease in H3K27me3 levels at the tumor suppressor gene $p16^{INK4A}$ (Zhang et al., 2017). Interestingly, another study showed a synergistic effect of combining the inhibition of EZH2 and HDACs with the induction of TRAIL-dependent cell death (by combining drugs such as EPZ6438, panobinostat, and ONC201/TIC10, respectively) (Zhang et al., 2021). While this approach showed promising results in inducing cell death *in vitro* in DIPG cells, it should be further verified in preclinical animal models.

Targeting BET Bromodomains and CBP

The BET bromodomain inhibitor JQ1 was tested in combination with a structural inhibitor of the acetyltransferase, CBP (CREB binding protein). ICG-001, the CBP inhibitor, prevents the interaction of CBP with other proteins, rather than interfering with its catalytic function (Wiese et al., 2020). Both inhibitors, when compared alone as single agents, had a potential in decreasing protumorigenic functions of DIPG cells, such as

reducing cellular survival, sphere formation, migration, invasion, or radioresistance. Interestingly, these drugs had opposing effects on the regulation of the majority of super-enhancers in DIPG cells when used separately: JQ1 inhibited and ICG-001 activated these regulatory sites. Moreover, JQ1 and ICG-001 alone inadvertently activated a set of super-enhancers, which was reversed when these drugs were used in combination (Wiese et al., 2020). Therefore, the cytotoxic and anti-self-renewing effects of these drugs when used in combination were very strong and give a rationale for further preclinical testing in animal models and potentially in clinical trials.

Targeting BMI1 and Anti-apoptotic Pathway

Another genetic screen searching for DIPG vulnerabilities found BMI1 (B cell-specific Moloney murine leukemia virus integration site 1), a component of the PRC1 complex, as a potential target in DIPG tumors (Balakrishnan et al., 2020). The PRC1 complex is a chromatin remodeler that monoubiquitinates lysine 119 at histone H2A (H2AK119Ub) (Barbour et al., 2020). Balakrishnan et al. (2020) found that BMI1 and H2AK119Ub histone mark are increased in H3K27M-expressing tumors compared to the normal pons. Increased expression of BMI1 was directly driven by the presence of H3K27M. Subsequently, inhibition of BMI1 with PTC209 or PTC028 inhibitors significantly inhibited the proliferation of tumor cells. A higher sensitivity was observed in cells expressing H3K27M mutation when compared to H3K27M-CRISPR-deleted cells (Kumar et al., 2017; Balakrishnan et al., 2020). Phenotypically, inhibition of BMI1 impaired stem cell renewal in DIPG cells by reversing the BMI1 and H2A-K119Ub-mediated repression of differentiation-related genes. In addition, BMI1 inhibition repressed DIPG cell proliferation and induced senescence concomitant with upregulated expression of p16 and p21 tumor suppressor genes. However, senescence induced by BMI1 inhibition led to an activation of the senescence-associated secretory phenotype (SASP), which increases the risk of a future recurrence of tumors. To overcome this hurdle, the authors combined the BMI1 inhibitor together with obatoclax, a BH3 mimetic, which binds to the anti-apoptotic BCL2 family of proteins and induces apoptosis in cells. Combined treatment with PTC028 and obatoclax had the strongest effect in decreasing tumor growth and improving mouse survival compared to single drugs. In summary, this study highlighted BMI1 as a therapeutic target that is specifically upregulated in the presence of H3K27M substitution. It provided a strong rationale to target the BMI1 chromatin remodeler together with the BH3 mimetic to inhibit the growth of H3K27M pHGGs and prevent SASP reprogramming (Balakrishnan et al., 2020).

CLINICAL TRIALS INCLUDING TARGETING EPIGENETIC MODIFIERS IN pHGGs

Multiple clinical trials including the use of drugs targeting the epigenetic landscape of pHGGs had been established to date (**Table 1**). HDAC inhibitors such as vorinostat and panobinostat have been clinically studied with favorable safety profiles in children. However, there have been concerns regarding the efficiency of panobinostat at crossing the blood–brain barrier (Rasmussen et al., 2015). A related clinical trial has used panobinostat in children with DIPG to study the side effects and the most effective dose in recurrent and progressing DIPG (NCT02717455). Another trial has used an HDAC/PI3K inhibitor fimepinostat in patients with DIPG, HGG, or medulloblastoma (NCT03893487). An ongoing clinical

TABLE 1 | A summary of past and present clinical trials in pHGGs, which include epigenetic treatments.

ID	Clinical trial	Epigenetic target	Compound
NCT02899715	Panobinostat in treating younger patients with progressive diffuse intrinsic pontine glioma	HDAC	Panobinostat
NCT02717455	Trial of panobinostat in children with diffuse intrinsic pontine glioma	HDAC	Panobinostat
NCT03566199	MTX110 by convection-enhanced delivery in treating participants with newly diagnosed diffuse intrinsic pontine glioma	HDAC	MTX110 (panobinostat nanoparticle formulation MTX110)
NCT01189266	Vorinostat and radiation therapy followed by maintenance therapy with vorinostat in treating younger patients with newly diagnosed diffuse intrinsic pontine glioma	HDAC	Vorinostat
NCT02420613	Vorinostat and temsirolimus with or without radiation therapy in treating younger patients with newly diagnosed or progressive diffuse intrinsic pontine glioma	HDAC and mTOR	Vorinostat, Temsirolimus
NCT00879437	Valproic acid and radiation followed by maintenance valproic acid and bevacizumab in children with high-grade gliomas or diffuse intrinsic pontine glioma	HDAC	Valproic acid
NCT03893487	Fimepinostat in treating brain tumors in children and young adults	HDAC and PI3K	Fimepinostat
NCT03605550	A Phase 1b study of PTC596 in children with newly diagnosed diffuse intrinsic pontine glioma and high-grade glioma	BMI1	PTC596
NCT02960230	H3.3K27M peptide vaccine with nivolumab for children with newly diagnosed DIPG and other gliomas	H3K27M epitope and PD-1	H3.3K27M Peptide, Nivolumab

trial has combined vorinostat and temsirolimus (an mTOR inhibitor), in experiment arms with and without radiotherapy (NCT02420613). Another clinical trial in DIPG includes a testing BMI1 inhibitor, PTC596 (NCT03605550). This trial is particularly promising, as a recent report showed antitumor effects with other BMI1 inhibitors, PTC209 or PTC028 (Balakrishnan et al., 2020). An ongoing Phase I/II clinical trial tries to establish the safety of a synthetic peptide vaccine specific for the H3.3K27M epitope in combination with poly-ICLC and the PD-1 inhibitor, Nivolumab, in newly diagnosed DIPG patients and other gliomas that are tested positive for H3.3K27M (NCT02960230).

The blood–brain barrier is a major challenge that needs to be addressed for any epigenetic drugs to achieve therapeutic efficacy in DIPG therapy. To circumvent this issue, CED technique is being explored as an alternative where the drugs are directly delivered to the tumor site with limited side effects (Souweidane et al., 2018). There are open clinical trials for the delivery of panobinostat with gadoteridol using CED in patients newly diagnosed with DIPG (NCT03566199). A lot of complex issues also surround the usage of CED in clinical trials. For example, targeted drugs such as tyrosine kinase inhibitors are promising agents; however, they are not soluble and currently do not have an IV/aqueous formulation to allow their delivery using CED. Along with this, there are also legal and logistical issues that hinder the scalability of complicated therapeutics such as CED (Wierzbicki et al., 2020).

SUMMARY AND FUTURE PERSPECTIVES

While radiotherapy is the current standard treatment regimen for H3K27M-positive pHGGs, the unique biology of these tumors opens avenues for promising epigenetic therapies. The hallmarks of these tumors, such as loss of H3K27me3, increased H3K27ac, or changes in the expression of chromatin modifiers, e.g., BMI1, invite further research into the efficacy and molecular response to these treatments. Inhibitors of H3K27me3 demethylases, DNA methylation, BMI1, or FACT show strong potency in targeting H3K27M-containing tumors when compared to pHGG cells expressing wild-type H3, suggesting potentially smaller systemic toxicity in patients. However, further research is needed to develop novel compounds with a similar function that will exhibit higher stability *in vivo* and cross the blood–brain barrier. Of the drugs summarized in this review, some have been shown to cross the blood–brain barrier after systemic administration at least in the preclinical animal models, including marizomib, BGB324, JQ1, THZ1, obatoclax, CBL0137, or Azacytidine (Korb et al., 2015; Lin et al., 2019; Balakrishnan et al., 2020; Butler et al., 2020; Meel et al., 2020; Ehteda et al., 2021). Panobinostat and Corin reached sufficient levels in the brain tumors when delivered via CED (Grasso et al., 2015; Singleton et al., 2018; Anastas et al., 2019; Meel et al., 2020). For the future perspective, the effects of promising combinatorial epigenetic treatments should be tested for their radiosensitizing capabilities to verify the rationale for including these combinations in the clinical trials with standard radiotherapy in pHGGs. For example, the radiosensitizing effects of panobinostat, BGB324, or GSK-J4 had been demonstrated (Katagi et al., 2019; Meel et al., 2020). However, similar tests on other combinatorial approaches in pHGGs would be informative for the potential future clinical trials. Recently, it was demonstrated that the radiosensitizing effect of GSK-J4 was further enhanced by combinatorial treatment with APR-246, an agent that targets p53 mutant proteins and leads to the accumulation of reactive oxygen species (Bykov et al., 2018; Nikolaev et al., 2020).

The promising efficacy of recent combinatorial epigenetic treatments in pHGGs invites novel drug combinations, some of which may include small molecule inhibitors against the cell surface receptors or druggable kinases, e.g., *PDGFR* and CDK4/6 (Hoeman et al., 2018). Another direction for combinatorial treatments explores mutations that coexist with the H3K27M substitution in pHGGs. As an example, mutations in the *PPM1D* gene were identified in approximately 9–23% of DIPG samples and mostly co-occur with the H3K27M oncohistone (Taylor et al., 2014; Wu et al., 2014; Zhang et al., 2014; El Ayoubi et al., 2017). *PPM1D* encodes a phosphatase responsible for dephosphorylation of multiple proteins involved in DNA damage response and DNA repair pathways (Deng et al., 2020). A recent study showed that the inhibitor of PPM1D, GSK2830371, sensitized DIPG cells with the background of *PPM1D* mutation toward PARP inhibition, emphasizing the DNA repair pathways as a vulnerability of these tumors (Wang et al., 2020).

It is important to note that while numerous studies have tried to determine the precise effects of tested epigenetic drugs, it is almost impossible to explore all the potential consequences of epigenetic inhibitors due to pleiotropic effects exerted by the targeted enzymes and induction of widespread global changes in the chromatin. The typical phenotype induced by many of the successful inhibitors included induction of differentiation of H3K27M glioma cells and reduction of the self-renewing potential, as observed for HDAC, HDAC/LSD1, BET bromodomain, CDK9, or BMI1 inhibitors (Nagaraja et al., 2017; Piunti et al., 2017; Anastas et al., 2019; Balakrishnan et al., 2020; Dahl et al., 2020; Meel et al., 2020). Broadly available next-generation sequencing techniques were key in determining the genome-wide changes in gene expression, chromatin accessibility, or localization of specific histone modifications, which gave a broad view on the global changes induced by tested epigenetic treatments. For example, identification of pervasive H3K27ac at the REs and ERVs in the H3K27M-expressing tumors exposed a specific vulnerability of these tumors that was further enhanced by the use of global inhibitors toward HDACs and DNA methylation (Krug et al., 2019).

Finally, little is known on the effects of epigenetic therapies on the tumor microenvironment of pediatric brain tumors, including the immune system. Latest advances in single-cell transcriptomics and epigenomics will be essential in providing new insights into the right selection of drugs and targets in the context of tumor immune responses. The common efforts

of scientists and neuro-oncologists will be critical in translating these promising preclinical data into clinical trials.

AUTHOR CONTRIBUTIONS

KL and JM conceived the hypothesis. KL and CJ did the literature search. KL, CJ, BK, and JM co-wrote the manuscript. All authors contributed to the article and approved the submitted version.

FUNDING

KL was supported by the 2019/33/B/NZ1/01556 grant from the National Science Center (Poland). CJ was supported by the 2017/27/B/NZ2/02827 grant from the National Science Center (Poland), awarded to JM. JM was supported by grants from the Foundation for Polish Science under the International Research Agendas Programme, cofinanced by the European Union under the European Regional Development Fund.

REFERENCES

Agger, K., Cloos, P. A. C., Christensen, J., Pasini, D., Rose, S., Rappsilber, J., et al. (2007). UTX and JMJD3 are histone H3K27 demethylases involved in HOX gene regulation and development. *Nature* 449, 731–734. doi: 10.1038/nature06145

Anastas, J. N., Zee, B. M., Kalin, J. H., Kim, M., Guo, R., Alexandrescu, S., et al. (2019). Re-programing chromatin with a bifunctional LSD1/HDAC inhibitor induces therapeutic differentiation in DIPG. *Cancer Cell* 36, 528–544.e10. doi: 10.1016/j.ccell.2019.09.005

Aziz-Bose, R., and Monje, M. (2019). Diffuse intrinsic pontine glioma: molecular landscape and emerging therapeutic targets. *Curr. Opin. Oncol.* 31, 522–530. doi: 10.1097/CCO.0000000000000577

Balakrishnan, I., Danis, E., Pierce, A., Madhavan, K., Wang, D., Dahl, N., et al. (2020). Senescence induced by BMI1 inhibition is a therapeutic vulnerability in H3K27M-Mutant DIPG. *Cell Rep.* 33:108286. doi: 10.1016/j.celrep.2020.108286

Barbour, H., Daou, S., Hendzel, M., and Affar, E. B. (2020). Polycomb group-mediated histone H2A monoubiquitination in epigenome regulation and nuclear processes. *Nat. Commun.* 11:5947. doi: 10.1038/s41467-020-19722-9

Bartels, U., Hawkins, C., Vézina, G., Kun, L., Souweidane, M., and Bouffet, E. (2011). Proceedings of the diffuse intrinsic pontine glioma (DIPG) toronto think tank: advancing basic and translational research and cooperation in DIPG. *J. Neuro-Oncol.* 105, 119–125. doi: 10.1007/s11060-011-0704-4

Bestor, T. H., and Bourc'his, D. (2004). Transposon silencing and imprint establishment in mammalian germ cells. *Cold Spring Harb. Symposia Quant. Biol.* 69, 381–387. doi: 10.1101/sqb.2004.69.381

Brown, Z. Z., Müller, M. M., Jain, S. U., Allis, C. D., Lewis, P. W., and Muir, T. W. (2014). Strategy for "Detoxification" of a cancer-derived histone mutant based on mapping its interaction with the methyltransferase PRC2. *J. Am. Chem. Soc.* 136, 13498–13501. doi: 10.1021/ja5060934

Buczkowicz, P., Bartels, U., Bouffet, E., Becher, O., and Hawkins, C. (2014). Histopathological spectrum of paediatric diffuse intrinsic pontine glioma: diagnostic and therapeutic implications. *Acta Neuropathol.* 128, 573–581. doi: 10.1007/s00401-014-1319-6

Butler, C., Sprowls, S., Szalai, G., Arsiwala, T., Saralkar, P., Straight, B., et al. (2020). Hypomethylating agent azacitidine is effective in treating brain metastasis triple-negative breast cancer through regulation of DNA methylation of keratin 18 gene. *Transl. Oncol.* 13:100775. doi: 10.1016/j.tranon.2020.100775

Bykov, V. J. N., Eriksson, S. E., Bianchi, J., and Wiman, K. G. (2018). Targeting mutant p53 for efficient cancer therapy. *Nat. Rev. Cancer* 18, 89–102. doi: 10.1038/nrc.2017.109

Castel, D., Philippe, C., Calmon, R., Le Dret, L., Truffaux, N., Boddaert, N., et al. (2015). Histone H3F3A and HIST1H3B K27M mutations define two subgroups of diffuse intrinsic pontine gliomas with different prognosis and phenotypes. *Acta Neuropathol.* 130, 815–827. doi: 10.1007/s00401-015-1478-0

Castel, D., Philippe, C., Kergrohen, T., Sill, M., Merlevede, J., Barret, E., et al. (2018). Transcriptomic and epigenetic profiling of "diffuse midline gliomas, H3 K27M-mutant" discriminate two subgroups based on the type of histone H3 mutated and not supratentorial or infratentorial location. *Acta Neuropathol. Commun.* 6:117. doi: 10.1186/s40478-018-0614-1

Chammas, P., Mocavini, I., and Di Croce, L. (2020). Engaging chromatin: PRC2 structure meets function. *Br. J. Cancer* 122, 315–328. doi: 10.1038/s41416-019-0615-2

Chan, K. M., Fang, D., Gan, H., Hashizume, R., Yu, C., Schroeder, M., et al. (2013). The histone H3.3K27M mutation in pediatric glioma reprograms H3K27 methylation and gene expression. *Genes Dev.* 27, 985–990. doi: 10.1101/gad.217778.113

Dahl, N. A., Danis, E., Balakrishnan, I., Wang, D., Pierce, A., Walker, F. M., et al. (2020). Super elongation complex as a targetable dependency in diffuse midline glioma. *Cell Rep.* 31:107485. doi: 10.1016/j.celrep.2020.03.049

Deng, W., Li, J., Dorrah, K., Jimenez-Tapia, D., Arriaga, B., Hao, Q., et al. (2020). The role of PPM1D in cancer and advances in studies of its inhibitors. *Biomed. Pharmacother.* 125:109956. doi: 10.1016/j.biopha.2020.109956

di Fazio, P., Montalbano, R., Quint, K., Alinger, B., Kemmerling, R., Kiesslich, T., et al. (2012). The pan-deacetylase inhibitor panobinostat modulates the expression of epithelial-mesenchymal transition markers in hepatocellular carcinoma models. *Oncol. Lett.* 5, 127–134. doi: 10.3892/ol.2012.951

Diehl, K. L., Ge, E. J., Weinberg, D. N., Jani, K. S., Allis, C. D., and Muir, T. W. (2019). PRC2 engages a bivalent H3K27M-H3K27me3 dinucleosome inhibitor. *Proc. Natl. Acad. Sci. U S A.* 116:201911775. doi: 10.1073/pnas.1911775116

Ehteda, A., Simon, S., Franshaw, L., Giorgi, F. M., Liu, J., Joshi, S., et al. (2021). Dual targeting of the epigenome via FACT complex and histone deacetylase is a potent treatment strategy for DIPG. *Cell Rep.* 35:108994. doi: 10.1016/j.celrep.2021.108994

El Ayoubi, R., Boisselier, B., and Rousseau, A. (2017). Molecular landscape of pediatric diffuse intrinsic pontine gliomas: about 22 cases. *J. Neuro-Oncol.* 134, 465–467. doi: 10.1007/s11060-017-2523-8

Fang, D., Gan, H., Cheng, L., Lee, J. H., Zhou, H., Sarkaria, J. N., et al. (2018). H3.3*K*27M mutant proteins reprogram epigenome by sequestering the PRC2 complex to poised enhancers. *eLife* 7:e36696. doi: 10.7554/eLife.36696

Filbin, M. G., Tirosh, I., Hovestadt, V., Shaw, M. L., Escalante, L. E., Mathewson, N. D., et al. (2018). Developmental and oncogenic programs in H3K27M gliomas dissected by single-cell RNA-seq. *Science* 360, 331–335. doi: 10.1126/science.aao4750

Fontebasso, A. M., Papillon-Cavanagh, S., Schwartzentruber, J., Nikbakht, H., Gerges, N., Fiset, P. O., et al. (2014). Recurrent somatic mutations in ACVR1 in pediatric midline high-grade astrocytoma. *Nat. Genet.* 46, 462–466. doi: 10.1038/ng.2950

Fujisawa, T., and Filippakopoulos, P. (2017). Functions of bromodomain-containing proteins and their roles in homeostasis and cancer. *Nat. Rev. Mol. Cell Biol.* 18, 246–262. doi: 10.1038/nrm.2016.143

Funato, K., Major, T., Lewis, P. W., Allis, C. D., and Tabar, V. (2014). Use of human embryonic stem cells to model pediatric gliomas with H3.3*K*27M histone mutation. *Science* 346, 1529–1533. doi: 10.1126/science.1253799

Grasso, C. S., Tang, Y., Truffaux, N., Berlow, N. E., Liu, L., Debily, M. A., et al. (2015). Functionally defined therapeutic targets in diffuse intrinsic pontine glioma. *Nat. Med.* 21, 555–559. doi: 10.1038/nm.3855

Gröbner, S. N., Worst, B. C., Weischenfeldt, J., Buchhalter, I., Kleinheinz, K., Rudneva, V. A., et al. (2018). The landscape of genomic alterations across childhood cancers. *Nature* 555, 321–327. doi: 10.1038/nature25480

Haag, D., Mack, N., Benites Goncalves, da Silva, P., Statz, B., Clark, J., et al. (2021). H3.3-K27M drives neural stem cell-specific gliomagenesis in a human iPSC-derived model. *Cancer Cell* 39, 407–422.e13. doi: 10.1016/j.ccell.2021.01.005

Halsall, J. A., Turan, N., Wiersma, M., and Turner, B. M. (2015). Cells adapt to the epigenomic disruption caused by histone deacetylase inhibitors through a coordinated, chromatin-mediated transcriptional response. *Epigenet. Chromatin* 8:29. doi: 10.1186/s13072-015-0021-9

Harutyunyan, A. S., Chen, H., Lu, T., Horth, C., Nikbakht, H., Krug, B., et al. (2020). H3K27M in gliomas causes a one-step decrease in H3K27 methylation and reduced spreading within the constraints of H3K36 methylation. *Cell Rep.* 33:108390. doi: 10.1016/j.celrep.2020.108390

Harutyunyan, A. S., Krug, B., Chen, H., Papillon-Cavanagh, S., Zeinieh, M., De Jay, N., et al. (2019). H3K27M induces defective chromatin spread of PRC2-mediated repressive H3K27me2/me3 and is essential for glioma tumorigenesis. *Nat. Commun.* 10:1262. doi: 10.1038/s41467-019-09140-x

Hashizume, R., Andor, N., Ihara, Y., Lerner, R., Gan, H., Chen, X., et al. (2014). Pharmacologic inhibition of histone demethylation as a therapy for pediatric brainstem glioma. *Nat. Med.* 20, 1394–1396. doi: 10.1038/nm.3716

Hennika, T., Hu, G., Olaciregui, N. G., Barton, K. L., Ehteda, A., Chitranjan, A., et al. (2017). Pre-clinical study of panobinostat in xenograft and genetically engineered murine diffuse intrinsic pontine glioma models. *PLoS One* 12:e0169485. doi: 10.1371/journal.pone.0169485

Hoeman, C., Shen, C., and Becher, O. J. (2018). CDK4/6 and PDGFRA signaling as therapeutic targets in diffuse intrinsic pontine glioma. *Front. Oncol.* 8:191. doi: 10.3389/fonc.2018.00191

Hsieh, F. K., Kulaeva, O. I., Patel, S. S., Dyer, P. N., Luger, K., Reinberg, D., et al. (2013). Histone chaperone FACT action during transcription through chromatin by RNA polymerase II. *Proc. Natl. Acad. Sci. U S A.* 110, 7654–7659. doi: 10.1073/pnas.1222198110

Jansen, M. H. A., van Vuurden, D. G., Vandertop, W. P., and Kaspers, G. J. L. (2012). Diffuse intrinsic pontine gliomas: a systematic update on clinical trials and biology. *Cancer Treatment Rev.* 38, 27–35. doi: 10.1016/j.ctrv.2011.06.007

Jonkers, I., and Lis, J. T. (2015). Getting up to speed with transcription elongation by RNA polymerase II. *Nat. Rev. Mol. Cell Biol.* 16, 167–177. doi: 10.1038/nrm3953

Justin, N., Zhang, Y., Tarricone, C., Martin, S. R., Chen, S., Underwood, E., et al. (2016). Structural basis of oncogenic histone H3K27M inhibition of human polycomb repressive complex 2. *Nat. Commun.* 7:11316. doi: 10.1038/ncomms11316

Katagi, H., Louis, N., Unruh, D., Sasaki, T., He, X., Zhang, A., et al. (2019). Radiosensitization by histone H3 demethylase inhibition in diffuse intrinsic pontine glioma. *Clin. Cancer Res.* 25, 5572–5583. doi: 10.1158/1078-0432.CCR-18-3890

Khuong-Quang, D. A., Buczkowicz, P., Rakopoulos, P., Liu, X. Y., Fontebasso, A. M., Bouffet, E., et al. (2012). K27M mutation in histone H3.3 defines clinically and biologically distinct subgroups of pediatric diffuse intrinsic pontine gliomas. *Acta Neuropathol.* 124, 439–447. doi: 10.1007/s00401-012-0998-0

Korb, E., Herre, M., Zucker-Scharff, I., Darnell, R. B., and Allis, C. D. (2015). BET protein Brd4 activates transcription in neurons and BET inhibitor Jq1 blocks memory in mice. *Nat. Neurosci.* 18, 1464–1473. doi: 10.1038/nn.4095

Krug, B., De Jay, N., Harutyunyan, A. S., Deshmukh, S., Marchione, D. M., Guilhamon, P., et al. (2019). Pervasive H3K27 acetylation leads to ERV expression and a therapeutic vulnerability in H3K27M gliomas. *Cancer Cell* 35, 782–797.e8. doi: 10.1016/j.ccell.2019.04.004

Kumar, S. S., Sengupta, S., Lee, K., Hura, N., Fuller, C., DeWire, M., et al. (2017). BMI-1 is a potential therapeutic target in diffuse intrinsic pontine glioma. *Oncotarget* 8, 62962–62975. doi: 10.18632/oncotarget.18002

Larson, J. D., Kasper, L. H., Paugh, B. S., Jin, H., Wu, G., Kwon, C. H., et al. (2019). Histone H3.3 K27M accelerates spontaneous brainstem glioma and drives restricted changes in bivalent gene expression. *Cancer Cell* 35, 140–155.e7. doi: 10.1016/j.ccell.2018.11.015

Lewis, P. W., Müller, M. M., Koletsky, M. S., Cordero, F., Lin, S., Banaszynski, L. A., et al. (2013). Inhibition of PRC2 activity by a gain-of-function H3 mutation found in pediatric glioblastoma. *Science* 340, 857–861. doi: 10.1126/science.1232245

Lin, G. L., and Monje, M. (2017). A protocol for rapid post-mortem cell culture of diffuse intrinsic pontine glioma (DIPG). *J. Vis. Exp.* 2017:55360. doi: 10.3791/55360

Lin, G. L., Wilson, K. M., Ceribelli, M., Stanton, B. Z., Woo, P. J., Kreimer, S., et al. (2019). Therapeutic strategies for diffuse midline glioma from high-throughput combination drug screening. *Sci. Transl. Med.* 11:eaaw0064. doi: 10.1126/scitranslmed.aaw0064

Louis, D. N., Perry, A., Reifenberger, G., von Deimling, A., Figarella-Branger, D., Cavenee, W. K., et al. (2016). The 2016 world health organization classification of tumors of the central nervous system: a summary. *Acta Neuropathol.* 131, 803–820. doi: 10.1007/s00401-016-1545-1

Mackay, A., Burford, A., Carvalho, D., Izquierdo, E., Fazal-Salom, J., Taylor, K. R., et al. (2017). Integrated molecular meta-analysis of 1,000 pediatric high-grade and diffuse intrinsic pontine glioma. *Cancer Cell* 32, 520–537.e5. doi: 10.1016/j.ccell.2017.08.017

Meel, M. H., de Gooijer, M. C., Metselaar, D. S., Sewing, C. P. A., Zwaan, K., Waranecki, P., et al. (2020). Combined therapy of AXL and HDAC inhibition reverses mesenchymal transition in diffuse intrinsic pontine glioma. *Clin. Cancer Res.* 26, 3319–3332. doi: 10.1158/1078-0432.CCR-19-3538

Mendez, F. M., Núñez, F. J., Garcia-Fabiani, M. B., Haase, S., Carney, S., Gauss, J. C., et al. (2020). Epigenetic reprogramming and chromatin accessibility in pediatric diffuse intrinsic pontine gliomas: a neural developmental disease. *Neuro Oncol.* 22, 195–206. doi: 10.1093/neuonc/noz218

Mohammad, F., Weissmann, S., Leblanc, B., Pandey, D. P., Højfeldt, J. W., Comet, I., et al. (2017). EZH2 is a potential therapeutic target for H3K27M-mutant pediatric gliomas. *Nat. Med.* 23, 483–492. doi: 10.1038/nm.4293

Monje, M., Mitra, S. S., Freret, M. E., Raveh, T. B., Kim, J., Masek, M., et al. (2011). Hedgehog-responsive candidate cell of origin for diffuse intrinsic pontine glioma. *Proc. Natl. Acad. Sci. U S A.* 108, 4453–4458. doi: 10.1073/pnas.1101657108

Nagaraja, S., Quezada, M. A., Gillespie, S. M., Arzt, M., Lennon, J. J., Woo, P. J., et al. (2019). Histone variant and cell context determine H3K27M reprogramming of the enhancer landscape and oncogenic state. *Mol. Cell* 76, 965–980.e12. doi: 10.1016/j.molcel.2019.08.030

Nagaraja, S., Vitanza, N. A., Woo, P. J., Taylor, K. R., Liu, F., Zhang, L., et al. (2017). Transcriptional dependencies in diffuse intrinsic pontine glioma. *Cancer Cell* 31, 635–652.e6. doi: 10.1016/j.ccell.2017.03.011

Nikolaev, A., Fiveash, J. B., and Yang, E. S. (2020). Combined targeting of mutant p53 and jumonji family histone demethylase augments therapeutic efficacy of radiation in H3K27M DIPG. *Int. J. Mol. Sci.* 21:490. doi: 10.3390/ijms21020490

Pathania, M., De Jay, N., Maestro, N., Harutyunyan, A. S., Nitarska, J., Pahlavan, P., et al. (2017). H3.3K27M cooperates with Trp53 loss and PDGFRA gain in mouse embryonic neural progenitor cells to induce invasive high-grade gliomas. *Cancer Cell* 32, 684–700.e9. doi: 10.1016/j.ccell.2017.09.014

Peterlin, B. M., and Price, D. H. (2006). Controlling the elongation phase of transcription with P-TEFb. *Mol. Cell* 23, 297–305. doi: 10.1016/j.molcel.2006.06.014

Piunti, A., Hashizume, R., Morgan, M. A., Bartom, E. T., Horbinski, C. M., Marshall, S. A., et al. (2017). Therapeutic targeting of polycomb and BET bromodomain proteins in diffuse intrinsic pontine gliomas. *Nat. Med.* 23, 493–500. doi: 10.1038/nm.4296

Prendergast, L., Hong, E., Safina, A., Poe, D., and Gurova, K. (2020). Histone chaperone FACT is essential to overcome replication stress in mammalian cells. *Oncogene* 39, 5124–5137. doi: 10.1038/s41388-020-1346-9

Puget, S., Philippe, C., Bax, D. A., Job, B., Varlet, P., Junier, M. P., et al. (2012). Mesenchymal transition and pdgfra amplification/mutation are key distinct oncogenic events in pediatric diffuse intrinsic pontine gliomas. *PLoS One* 7:e30313. doi: 10.1371/journal.pone.0030313

Rasmussen, T. A., Tolstrup, M., Møller, H. J., Brinkmann, C. R., Olesen, R., Erikstrup, C., et al. (2015). Activation of latent human immunodeficiency virus by the histone deacetylase inhibitor panobinostat: a pilot study to assess effects on the central nervous system. *Open Forum Infect Dis.* 2:ofv037. doi: 10.1093/ofid/ofv037

Rhodes, L. V., Tate, C. R., Segar, H. C., Burks, H. E., Phamduy, T. B., Hoang, V., et al. (2014). Suppression of triple-negative breast cancer metastasis by pan-DAC inhibitor panobinostat via inhibition of ZEB family of EMT master regulators. *Breast Cancer Res Treat.* 145, 593–604. doi: 10.1007/s10549-014-2979-6

Schwartzentruber, J., Korshunov, A., Liu, X. Y., Jones, D. T. W., Pfaff, E., Jacob, K., et al. (2012). Driver mutations in histone H3.3 and chromatin remodelling genes in paediatric glioblastoma. *Nature* 482, 226–231. doi: 10.1038/nature10833

Silveira, A. B., Kasper, L. H., Fan, Y., Jin, H., Wu, G., Shaw, T. I., et al. (2019). H3.3 K27M depletion increases differentiation and extends latency of diffuse intrinsic pontine glioma growth in vivo. *Acta Neuropathol.* 137, 637–655. doi: 10.1007/s00401-019-01975-4

Singleton, W. G. B., Bieneman, A. S., Woolley, M., Johnson, D., Lewis, O., Wyatt, M. J., et al. (2018). The distribution, clearance, and brainstem toxicity of panobinostat administered by convection-enhanced delivery. *J. Neurosurg. Pediatr.* 22, 288–296. doi: 10.3171/2018.2.PEDS17663

Souweidane, M. M., Kramer, K., Pandit-Taskar, N., Zhou, Z., Haque, S., Zanzonico, P., et al. (2018). Convection-enhanced delivery for diffuse intrinsic pontine glioma: a single-centre, dose-escalation, phase 1 trial. *Lancet Oncol.* 19, 1040–1050. doi: 10.1016/S1470-2045(18)30322-X

Stafford, J. M., Lee, C. H., Voigt, P., Descostes, N., Saldana-Meyer, R., Yu, J. R., et al. (2018). Multiple modes of PRC2 inhibition elicit global chromatin alterations in H3K27M pediatric glioma. *Sci. Adv.* 4:eaau593. doi: 10.1101/432781

Sturm, D., Witt, H., Hovestadt, V., Khuong-Quang, D. A., Jones, D. T. W., Konermann, C., et al. (2012). Hotspot mutations in H3F3A and IDH1 define distinct epigenetic and biological subgroups of glioblastoma. *Cancer Cell* 22, 425–437. doi: 10.1016/j.ccr.2012.08.024

Taylor, I. C., Hütt-Cabezas, M., Brandt, W. D., Kambhampati, M., Nazarian, J., Chang, H. T., et al. (2015). Disrupting NOTCH slows diffuse intrinsic pontine glioma growth, enhances radiation sensitivity, and shows combinatorial efficacy with bromodomain inhibition. *J. Neuropathol. Exp. Neurol.* 74, 778–790. doi: 10.1097/NEN.0000000000000216

Taylor, K. R., Mackay, A., Truffaux, N., Butterfield, Y. S., Morozova, O., Philippe, C., et al. (2014). Recurrent activating ACVR1 mutations in diffuse intrinsic pontine glioma. *Nat. Genet.* 46, 457–461. doi: 10.1038/ng.2925

Vitanza, N. A., Biery, M. C., Myers, C., Ferguson, E., Zheng, Y., Girard, E. J., et al. (2021). Optimal therapeutic targeting by HDAC inhibition in biopsy-derived treatment-naïve diffuse midline glioma models. *Neuro Oncol.* 23, 376–386. doi: 10.1093/neuonc/noaa249

Walsh, C. P., Chaillet, J. R., and Bestor, T. H. (1998). Transcription of IAP endogenous retroviruses is constrained by cytosine methylation [4]. *Nat. Genet.* 20, 116–117. doi: 10.1038/2413

Wang, Z., Xu, C., Diplas, B. H., Moure, C. J., Chen, C. P. J., Chen, L. H., et al. (2020). Targeting mutant PPM1D sensitizes diffuse intrinsic pontine glioma cells to the PARP inhibitor olaparib. *Mol. Cancer Res.* 18, 968–980. doi: 10.1158/1541-7786.MCR-19-0507

Wang, Z., Zang, C., Cui, K., Schones, D. E., Barski, A., Peng, W., et al. (2009). Genome-wide mapping of HATs and HDACs reveals distinct functions in active and inactive genes. *Cell* 138, 1019–1031. doi: 10.1016/j.cell.2009.06.049

Wierzbicki, K., Ravi, K., Franson, A., Bruzek, A., Cantor, E., Harris, M., et al. (2020). Targeting and therapeutic monitoring of H3K27M-Mutant glioma. *Curr. Oncol. Rep.* 22:19. doi: 10.1007/s11912-020-0877-0

Wiese, M., Hamdan, F. H., Kubiak, K., Diederichs, C., Gielen, G. H., Nussbaumer, G., et al. (2020). Combined treatment with CBP and BET inhibitors reverses inadvertent activation of detrimental super enhancer programs in DIPG cells. *Cell Death Dis.* 11:673. doi: 10.1038/s41419-020-02800-7

Wu, G., Broniscer, A., McEachron, T. A., Lu, C., Paugh, B. S., Becksfort, J., et al. (2012). Somatic histone H3 alterations in pediatric diffuse intrinsic pontine gliomas and non-brainstem glioblastomas. *Nat. Genet.* 44, 251–253. doi: 10.1038/ng.1102

Wu, G., Diaz, A. K., Paugh, B. S., Rankin, S. L., Ju, B., Li, Y., et al. (2014). The genomic landscape of diffuse intrinsic pontine glioma and pediatric non-brainstem high-grade glioma. *Nat. Genet.* 46, 444–450. doi: 10.1038/ng.2938

Zhang, L., Chen, L. H., Wan, H., Yang, R., Wang, Z., Feng, J., et al. (2014). Exome sequencing identifies somatic gain-of-function PPM1D mutations in brainstem gliomas. *Nat. Genet.* 46, 726–730. doi: 10.1038/ng.2995

Zhang, Y., Dong, W., Zhu, J., Wang, L., Wu, X., and Shan, H. (2017). Combination of EZH2 inhibitor and BET inhibitor for treatment of diffuse intrinsic pontine glioma. *Cell Biosci.* 7:56. doi: 10.1186/s13578-017-0184-0

Zhang, Y., Zhou, L., Safran, H., Borsuk, R., Lulla, R., Tapinos, N., et al. (2021). EZH2i EPZ-6438 and HDACi vorinostat synergize with ONC201/TIC10 to activate integrated stress response, DR5, reduce H3K27 methylation, ClpX and promote apoptosis of multiple tumor types including DIPG. *Neoplasia (United States)* 23, 792–810. doi: 10.1016/j.neo.2021.06.007

Zhou, Q., Li, T., and Price, D. H. (2012). RNA polymerase II elongation control. *Annu. Rev. Biochem.* 81, 119–143. doi: 10.1146/annurev-biochem-052610-095910

Conflict of Interest: The authors declare that the research was conducted in the absence of any commercial or financial relationships that could be construed as a potential conflict of interest.

Publisher's Note: All claims expressed in this article are solely those of the authors and do not necessarily represent those of their affiliated organizations, or those of the publisher, the editors and the reviewers. Any product that may be evaluated in this article, or claim that may be made by its manufacturer, is not guaranteed or endorsed by the publisher.

frontiers in Genetics

REVIEW
published: 01 October 2021
doi: 10.3389/fgene.2021.740794

CBX7 is Dualistic in Cancer Progression Based on its Function and Molecular Interactions

Jun Li[1†], Taohui Ouyang[2†], Meihua Li[2], Tao Hong[2], MHS Alriashy[3], Wei Meng[2†] and Na Zhang[4*†]*

[1]Department of the Second Clinical Medical College of Nanchang University, Jiangxi Province, China, [2]Department of Neurosurgery, the First Affiliated Hospital of Nanchang University, Jiangxi Province, China, [3]Department of Neurosurgery, Huashan Hospital of Fudan University, Shanghai, China, [4]Department of Neurology, the First Affiliated Hospital of Nanchang University, Jiangxi Province, China

Chromobox protein homolog 7 (CBX7) is a member of the Chromobox protein family and participates in the formation of the polycomb repressive complex 1(PRC1). In cells, CBX7 often acts as an epigenetic regulator to regulate gene expression. However, pathologically, abnormal expression of CBX7 can lead to an imbalance of gene expression, which is closely related to the occurrence and progression of cancers. In cancers, CBX7 plays a dual role; On the one hand, it contributes to cancer progression in some cancers by inhibiting oncosuppressor genes. On the other hand, it suppresses cancer progression by interacting with different molecules to regulate the synthesis of cell cycle-related proteins. In addition, CBX7 protein may interact with different RNAs (microRNAs, long noncoding RNAs, circular RNAs) in different cancer environments to participate in a variety of pathways, affecting the development of cancers. Furthermore, CBX7 is involved in cancer-related immune response and DNA repair. In conclusion, CBX7 expression is a key factor in the occurrence and progression of cancers.

Keywords: CBX7, cancer, molecular interaction, PRC1, RNAs

OPEN ACCESS

Edited by:
Rais Ahmad Ansari,
Nova Southeastern University,
United States

Reviewed by:
Luigi Aloia,
University College London,
United Kingdom
Nii Koney-Kwaku Koney,
University of Ghana, Ghana

****Correspondence:***
Wei Meng
601192795@qq.com
Na Zhang
hustzhangna@163.com

†These authors have contributed equally to this work

Specialty section:
This article was submitted to Epigenomics and Epigenetics, a section of the journal Frontiers in Genetics

Received: *22 July 2021*
Accepted: *17 September 2021*
Published: *01 October 2021*

Citation:
Li J, Ouyang T, Li M, Hong T, Alriashy MHS, Meng W and Zhang N (2021) CBX7 is Dualistic in Cancer Progression Based on its Function and Molecular Interactions. Front. Genet. 12:740794. doi: 10.3389/fgene.2021.740794

INTRODUCTION

CBX7 belongs to the Chromobox proteins family and participates in the formation of the polycomb repressive complex 1 (PRC1). The polycomb group (PcG) proteins are transcriptional inhibitors that regulate several important developmental and physiological processes in cells (Levine et al., 2002). PcG proteins are originally identified in *Drosophila* as epigenetic transcriptional repressors (Histones are modified to cause transcription inactivation) expressed by homologous genes (Hox). Nowadays, they have been found in various metazoans and are highly conserved in evolution (Wang et al., 2015). Two subunit complexes in PcG proteins play an important role in epigenetic control: one is the initial inhibitory complex (PRC2), with enhancer of zeste homolog 2 (EZH2), EED, and SUZ12 as the main components and the other is the maintenance inhibitory complex (PRC1), with B-lymphoma Mo-MLV insertion region 1 (BMI-1), Chromobox 7 (CBX7) and E3 ubiquitin ligase RING1A/B as the main components (Schuettengruber et al., 2007; Scott et al., 2007; Wu et al., 2009). Functionally, in the PRC2 complex, EZH2 performs methyltransferase activity on lysine 27 on histone H3(H3K27) and is involved in the mono-, di-, and tri-methylation of lysine 27 on histone H3 (H3K27me1/2/3), which is essential for inducing transcriptional inhibition and stable gene silencing (Satijn et al., 2001; Geng and Gao, 2020). Conversely, in the PRC1 complex, CBX7 can bind to the H3K27me3 with its

special domain (a highly conserved N-terminal chromodomain), thereby controlling the expression of multiple genes. In addition, the E3 ubiquitin ligase RING1A/B, a member of the PRC1 complex, is also recruited unto genes to promote histone H2A lysine 119 monoubiquitination (H2AK119ub1). These histone modifications induce chromatin compaction and aggregation, thereby inhibiting the transcriptional activity of target genes (Satijn et al., 2001; Ogawa et al., 2002; Gil et al., 2005; Wu et al., 2009; Kaito and Iwama, 2020). CBX7 inhibits genes expression at the transcriptional level in the nucleus.

Recent studies have shown that CBX7 not only regulates gene expression in the nucleus but also interacts with proteins involved in cell cycle regulation in the cytoplasm. The CBX7 protein can be divided into several subtypes, the classic ones being 36 KD protein CBX7 in the nucleus and 22KD protein CBX7 in the cytoplasm. Emerging evidence has shown that p22CBX7 rather than p36CBX7, inhibits cell proliferation, further demonstrating the complex mechanism of CBX7 regulating cell development (Cho et al., 2020). P22CBX7 in the cytoplasm may interact with some other proteins in the cytoplasm that play an important role in cell cycle progression to regulate cell proliferation, or that there is a reciprocal conversion that regulates cellular homeostasis in a complementary manner between CBX7 subtypes, thus forming negative feedback in CBX7 (Cho et al., 2020).

ABNORMAL EXPRESSION OF CBX7 IN CANCER PROGRESSION

Low Expression of CBX7 in Cancer Progression

Breast Cancer

Bioinformatic analysis of Chromobox proteins family has shown that the most significant difference between breast cancer and normal mammary tissue is the low mRNA expression of CBX7 (Li X. et al., 2020). One study of breast cancer implied that patients with low CBX7 had lower survival and were more likely to develop lymph node metastasis, P53 mutations, and the cancer further deteriorated, metastasized over time (Li X. et al., 2020). The mechanism for its carcinogenicity may be that CBX7 acts as a novel epigenetic regulator of the *Wnt*/β-catenin pathway in breast cancer to determine cancer progression (Li X. et al., 2020). In breast cancer, CBX7 increases Dickkopf-1 (DKK-1, a *Wnt* antagonist) gene transcription, thus indirectly affecting the *Wnt* signaling pathway (Bafico et al., 2001; Kim et al., 2015). For transcriptional activation of the DKK-1 gene, CBX7 can directly interact with p300 acetyltransferase and recruit p300/CREB binding protein (CBP) to the DKK-1 promoter, thereby inhibiting histone deacetylases (HDAC)-mediated histone deacetylation (Kim et al., 2015). In breast cancer, due to the lack of CBX7, the transcriptional activation complex p300/CBP dissociates from the promoter region of DKK-1 and restarts HDAC-mediated DKK-1 gene silencing. The decreased expression of *Wnt* antagonist DKK-1 can reactivate the *Wnt*/β-catenin/T-cell factor (TCF) pathway, leading to nuclear translocation of β-catenin and up-regulation of the expression of TCF target genes including *C-MYC* (Wang et al., 2008; Kim et al., 2015). Therefore, CBX7 plays a cancer-inhibiting role by guiding the synthesis of DKK-1 to attenuate the *Wnt* pathway in breast cancer cells. In addition, there is evidence that CBX7 also plays an important role in controlling glucose metabolism in breast cancer cells (Iqbal et al., 2021). mTORC1 signaling is a known determinant of cancer metabolism and frequently deregulated in breast cancer (Creighton, 2007; Mossmann et al., 2018). The increase of glycolysis induced by silencing CBX7 may imply that CBX7 regulates the mTORC1 pathway to control aerobic glycolysis in breast cancer (Iqbal et al., 2021). Both Chromobox 2 (CBX2) and CBX7 can be used as subunits of PRC1 to act as a reader to recognize H3K27m3, thus hindering the transcription of INK4a/ARF tumor suppressor genes (Jangal et al., 2019). Interestingly, CBX2, which is homologous to CBX7, has a high content in breast cancer (Liang et al., 2017). However, CBX7 content in breast cancer is often very low, indicating that CBX7 plays its other tumor suppressor role independently of PRC1. The reason why CBX7 is lost in breast cancer cells may be ascribed to lncRNA NEAT1 targeting CBX7 (Yan et al., 2020). It has been determined that the protein level of CBX7 is positively correlated with NEAT1 in breast cancer cells, proving that CBX7 is indeed a target gene regulated by NEAT1 (Yan et al., 2020). Moreover, miR-181b induced by high mobility group AT-hook 1 (HMGA1) interferes with CBX7 mRNA at the translation level to inhibit its expression, resulting in a lack of CBX7 in breast cancer (Mansueto et al., 2010). In these ways, CBX7 acts as an intermediate in breast cancer, creating a series of chain reactions.

Liver Cancer

The mRNA expression of CBX7 increases with liver development after birth and is maintained at a normal level to regulate the epigenome, transcriptome, and liver function (Lu et al., 2012). Accumulative evidence has shown that CBX7 content is significantly reduced in liver cancer tissues (Lu et al., 2012). In liver cancer, the expression of CBX7 mRNA is the highest in grade I tumors among grade classification of tumor. With the increase of tumor grade, the expression of CBX7 mRNA shows a downward trend (Ning et al., 2018). In addition, the decreased expression of CBX7 is significantly correlated with liver cirrhosis by the chi-square test (Zhu et al., 2019). In patients with hepatocellular carcinoma, the high expression of CBX7 is related to a better survival rate of patients (Ning et al., 2018). One of the proposed mechanisms for cancer suppression is that CBX7 exerts a cancer suppressor effect by inhibiting the expression of cyclin E (Forzati et al., 2012). CBX7 and HDAC2 combine to form a complex and are fixed on the promoter of CCNE1, thereby repressing its transcriptional activity. The study suggested that overexpression of CBX7 would interfere with the composition of PRC1. In addition, it was proven that CBX7 dose-dependently reduced the transcriptional activity of the CCNE1 promoter (Forzati et al., 2012). We postulate that CBX7 exerts special effects independently of PRC1. On the contrary, the HMGA1b protein is a competitor of this action. The antagonistic effect of CBX7 versus HMGA1b protein on the CCNE1 promoter could inhibit cell proliferation and migration (Fusco and Fedele, 2007;

Pallante et al., 2010; Forzati et al., 2012). For CBX7 itself, its expression may be regulated by non-coding RNA, such as miR-181 positively regulated by HMGA1. it may combine with the 3′-UTR of CBX7 mRNA to limit its translation (Forzati et al., 2014). Similarly, the mode of action of CBX7 in liver cancer is a continuous one-way pathway. CBX7 not only controls the synthesis of related proteins but also is restricted by other molecules.

Colonic Cancer

CBX7 is associated with multiple clinicopathologic parameters in colon cancer. Compared with normal colonic mucosa, CBX7 expression is reduced or absent in a large number of colon cancer specimens, and the absence of CBX7 expression is remarkably correlated with the poor prognosis of colon cancer patients (Pallante et al., 2010). The mRNA level of CBX7 in colon cancer samples is lower than that in normal colonic tissues, suggesting that the CBX7 expression is inhibited at the transcriptional level (Pallante et al., 2010). However, the mechanism by which it is suppressed at the transcriptional level remains unclear. Furthermore, CBX7 negatively regulates cyclin E which is involved in a G1-S phase transition. CBX7 is positively correlated with E-cadherin expression (Federico et al., 2009; Pallante et al., 2010). However, two components of the PRC1 which includes CBX7 and BMI-1 regulate the expression of E-cadherin differently. Studies had shown that BMI-1 significantly down-regulates the content of E-cadherin in colon cancer and promotes the epithelial-mesenchymal transition (EMT) process (Zhang et al., 2016). The different regulatory effects on the same protein between the two reveal that CBX7 may be independent of PRC1 composed of BMI-1 to achieve EMT inhibition. Not surprisingly, like CBX7 in breast cancer, abnormal activation of the *Wnt* signaling pathway is found in 90% of colon cancer, and one of the reasons may be the absence of secreted frizzled-related protein 4(sFRP4) (Liu et al., 2020). The sFRP4 could compete with *Wnt* proteins *via* binding their receptor (Frizzled) to act as an antagonist of the *Wnt* signaling pathway in colonic cancer (Liu et al., 2006; Liu et al., 2020). Interestingly, both DKK-1 and sFRP4 are antagonists of the *Wnt* signaling pathway, but the effect of CBX7 in regulating sFRP4 in colon cancer is quite different from the effect of regulating DKK-1 in breast cancer. CBX7 and other PcG proteins, such as EZH2 and Jumonji, AT rich interactive domain 2 (JARID2) are found to be enriched in the SFRP4 gene promoter region to regulate gene expression without DNA methylation (Liu et al., 2020). Perhaps it is the synergistic effect of CBX7, EZH2, and JARID2 on histone methylation modification that leads to epigenetic gene silencing (Walters et al., 2014; Pallante et al., 2015). Therefore, silencing the sFRP4 gene indirectly enhances the *Wnt* pathway, thereby promoting the development of cancer. The contradiction between the two roles of CBX7 in colon cancer further suggests that multiple CBX7 regulatory pathways may exist. In cancer progression, different cancer-promoting or anti-cancer pathways have gained corresponding advantages due to their expression intensity. It would be beneficial to further actively explore the pathways of CBX7 involvement.

Thyroid Cancer

It has been reported that the loss of CBX7 is associated with a highly malignant phenotype in thyroid cancer (Pallante et al., 2008). CBX7mRNA is high in most of follicular thyroid adenomas and rarely develops into cancer (Pallante et al., 2008; Monaco et al., 2014). However, a low level of CBX7 is shown in thyroid cancer. For example, Hurtle adenoma is a rare differentiated thyroid tumor with the highest incidence of metastasis, and as the tumor worsens, CBX7 gradually decreases at the transcriptional level and the tumor develops into Hurtle carcinoma (Cheung et al., 2000; Monaco et al., 2014). The decrease of CBX7 in thyroid cancer may be due to the negative regulation of tumor protein HMGA1 (Chiappetta et al., 1995). A loss of epithelial features and an acquisition of mesenchymal phenotypes are signs of tumor aggressiveness, which are often related to a lack of E-cadherin (Mansueto et al., 2010). It has been confirmed that CBX7 can actively regulate the expression of E-cadherin by interacting with HDAC2 and inhibiting its effect on the E-cadherin promoter (Federico et al., 2009). In addition, HDAC2 catalyzes the acetyl transfer of core histones and is generally considered to be a transcriptional repressor due to its ability to induce gene silencing (Federico et al., 2009; Mansueto et al., 2010). In thyroid cancer, H3k27me3 catalyzed by EZH2 is overexpressed (Tsai et al., 2019). However, CBX7, which has the recognition function of H3k27me3, did not follow its increasing trend to show high expression. This indicated that CBX7 did not act as a member of PRC1 to link up EZH2-mediated H3k27me3 to assist gene silencing. Instead, CBX7 can up-regulate the expression of FOS, FOSB, and EGR1, which are mostly involved in the physiological process of inhibiting cancer (Pallante et al., 2014). The exact molecular mechanism of promoting the expression of these genes is unclear. There is clear evidence that CBX7 is associated with osteopontin protein, which is encoded by the SPP1 gene (Sepe et al., 2015). Osteopontin is a well-known protein involved in cancer progression by promoting cell invasion and migration, leading to tumor metastasis (Rohde et al., 2007). On the one hand, CBX7 regulates cell migration by blocking HMGA1b and inhibiting SPP1 gene expression; on the other hand, CBX7 and HMGA1b limit SPP1 gene expression by regulating the activity of nuclear factor kB (NF-κB) (Sepe et al., 2015).

Glioma

In gliomas, unsurprisingly, CBX7 and HDAC2 jointly address the CCNE1 gene promoter induced G1/S phase arrest, which is similar to the effect of CBX7 in liver cancer, and CBX7 also enhances the expression of DKK-1 by binding to the DKK-1 promoter, which is similar to the effect of CBX7 in breast cancer (Mansueto et al., 2010; Kim et al., 2015; Bao et al., 2017; Yu et al., 2017). Not only that, there is a strong connection between CBX7 and the Hippo signaling pathway in gliomas (Nawaz et al., 2016). CBX7 inhibits YAP/TAZ, down-regulates CTGF (adverse prognostic product of tumor) with PRC2 as a member of PRC1, and reduces the phosphorylation level of c-Jun NH2-terminal kinase (JNK) (Nawaz et al., 2016). Among these, connective tissue growth factor (CTGF) plays an auxiliary role in gliomas by activating the ITGB1-TrkA-NF-kB pathway, which

can inhibit E-cadherin at the transcription level and enhance the invasion and migration of glioma cells (Edwards et al., 2011). Thus, CBX7 indirectly inhibits the decrease of E-cadherin, plays an important role in its quantity homeostasis. For CBX7 expression, the orphan nuclear receptor TLX (NR2E1, a transcription repressor) is related to the regulation of CBX7 expression (O'Loghlen et al., 2015b). The ectopic expression of NR2E1 binds to the CBX7 locus, activates CBX7 expression. In contrast, CBX7 binds to the NR2E1 locus as a member of the PRC1 and inhibits it as part of a regulatory feedback loop (O'Loghlen et al., 2015b). These also imply that different pathways can also influence each other to regulate cancer progression.

Pancreatic Cancer

In pancreatic cancer, the expression of CBX7 is lower than that of normal pancreatic tissues (Ni et al., 2017). Microarray and GO-pathway analysis predict that CBX7 promotes the activation of Phosphatase and tensin homolog (PTEN) and then inhibits the downstream phosphatidylinositol 3-phosphate kinase (PI3K)/AKT pathway (Ni et al., 2017). Interestingly, the mechanism of increasing PTEN transcription may be the same as the enhanced DKK-1 expression in breast cancer, where CBX7 recruits p300 independently of PRC1 to the promoter region to participate in epigenetic changes (Kim et al., 2015; Ni et al., 2017). It is well known that PTEN is a classic tumor suppressor (Ying et al., 2011). Once PTEN is abnormally expressed, it will lead to the activation of the PI3K/AKT signaling pathway, then target NF-kB and C-MYC transcription factors, which are conducive to the survival and development of cancers (Asano et al., 2004; Ying et al., 2011).

High Expression of CBX7 in Cancer Progression

Gastric Cancer

In gastric cancer, CBX7 is highly expressed, contrary to its low expression in all of the above-mentioned cancers. It has been proven that CBX7 acts as a carcinogen mainly by inducing the down-regulation of $p16^{INK4a}$/ARF, which is blocked by the BMI-1 protein (Guo et al., 2007; Zhang et al., 2010). Besides, accumulated evidence shows that CBX7 has a similar function to BMI-1 in gastric cancer, suggesting that CBX7 may participate and function in a way related to BMI-1 regulation (Guo et al., 2007; Ni et al., 2018). Although multivariate Cox proportional risk model analysis shows that CBX7 is not an independent prognostic factor for gastric cancer deterioration (Zhang et al., 2010), the carcinogenesis role of CBX7 should not be underestimated. In gastric cancer, CBX7 actively regulates the stem cell characteristics of gastric cancer cells through the AKT-NF-kB-miR-21 pathway (Ni et al., 2018). Therefore, CBX7 utilizes at least the two pathways mentioned above to play a cancer-promoting role in gastric cancer (Zhang et al., 2010; Ni et al., 2018). It is worth considering that miR-21 in the microRNA family is a downstream target of CBX7. However, in the presence of miR-421 inhibitors, the growth of gastric cancer cells is inhibited. Therefore, miR-421 may act as an upstream molecule to regulate the target CBX7, suggesting a deeper link between CBX7 and the microRNA family (Jiang et al., 2010; Ni et al., 2018).

Prostatic Cancer

In prostate cancer, CBX7 is also positively correlated to cancer progression (Bernard et al., 2005). Overexpression of CBX7 contributes to the down-regulation of the expression of the tumor suppressor gene *INK4a/ARF* (**Figure 1**) (Bernard et al., 2005). Generally, androgens are favorable factors for prostatic cancer development, but CBX7 plays an important role in maintaining prostate cancer cells growth by cooperating with C-MYC with androgen-independent transformation (Bernard et al., 2005). Recently, it has been reported that GOLPH3 can bind to the CBX7 protein in prostatic cancer to promote cell proliferation and inhibit cell apoptosis (Gong et al., 2020). More importantly, circGOLPH3, like most of circRNAs, has abundant microRNA binding sites (Gong et al., 2020). CircGOLPH3 may have a "sponge effect", absorbing microRNAs and reducing the number of microRNA bound to target mRNA, thus increasing the expression level of target protein such as CBX7 (Gong et al., 2020). While this clearly shows the interaction in RNAs to regulate CBX7, for the binding between GOLPH3 and CBX7, it is questionable whether circGOLPH3 can also directly regulate the activity of CBX7 protein in post-translational modification.

Lymphoma

Finally, CBX7 is also highly expressed in lymphomas. CBX7 promotes T-cell lymphoma, and when sensitized oncogenes are directed to B-cell loci, CBX7 also promotes aggressive B-cell lymphoma, with a presence and latency similar to that of BMI-1 (Scott et al., 2007). CBX7 may cause the occurrence of lymphoma by enhancing stem cell self-renewal or increasing the replication potential of cancer stem cells (Scott et al., 2007). Although CBX7 may affect the transcription of multiple genes, inhibiting *INK4a/ARF* seems to be more important for its carcinogenic potential (Scott et al., 2007). However, CBX7 does not regulate cancer progression alone, the long latency and incomplete penetrance observed after overexpression of CBX7 suggest that aberrant CBX7 expression is not sufficient for causing lymphoma. CBX7 usually cooperates with C-MYC in the formation of aggressive lymphomas during lymphocyte genesis (Scott et al., 2007). More commonly, CBX7 is co-expressed with ZBTB7 in human follicular lymphoma, increasing the possibility that these proteins collectively control *INK4a/ARF* expression (Maeda et al., 2005). It also should be noted that CBX7 often works with other proteins, such as B-cell lymphoma 2(BCL-2), to accelerate the progress of lymphoma (Ramaswamy et al., 2001; Scott et al., 2007). Therefore, CBX7 could work with different partner molecules to produce different effects (pro-cancer or anti-cancer). Determining the specific molecular mechanism of CBX7 is very interesting and deserves further study.

CBX7 INTERACTS WITH DIFFERENT RNAS IN DIFFERENT CANCER ENVIRONMENTS

Interaction of CBX7 With microRNAs

MicroRNAs have obvious tissue specificity and can interact with CBX7 to affect cancer progression (Correia de Sousa et al.,

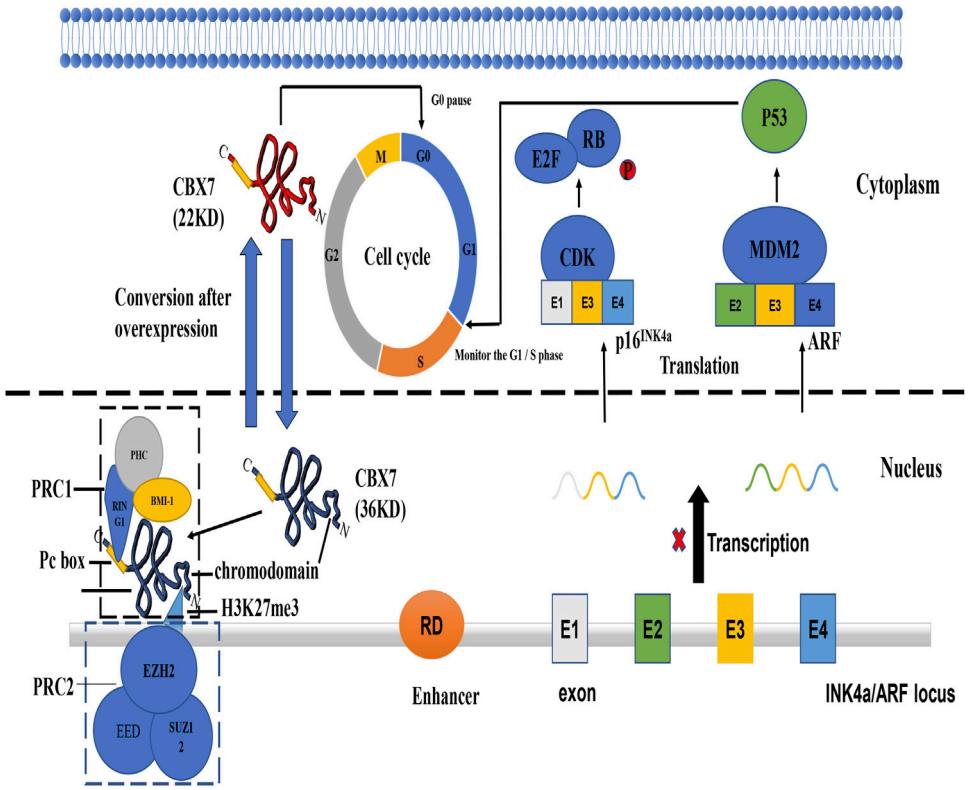

FIGURE 1 | The mechanism of tumor suppressor gene *INK4a/ARF* and functions of different CBX7 isoforms. (Kim and Sharpless, 2006) INK4a/ARF can express two co-exon products p16 and ARF. P16 ^{INK4a} can inhibit the phosphate of RB protein by interacting with cycle-dependent kinase. Inactivation of CDK4/6 promotes Rb/E2F1 association triggering G1/S transition. ARF can bind to Mouse Double Minute 2 protein (MMD2) protein to inactivate it, thereby releasing its inhibitory effect on p53 protein. P36CBX7 inhibits the expression of ARF in the nucleus to cause p53 protein abnormalities and make the cell cycle out of control at the G1/S regulatory point. P22CBX7 interacts with related proteins in the cytoplasm to keep the cell cycle in the G0 phase. Both have opposite effects on cell proliferation, showing the duality of CBX7.

2019). Many members of the microRNA family are involved in interference with CBX7 expression. For example, luciferase reporter assay has shown that miR-19 promotes the proliferation, migration of lung cancer cells by binding to the 3′-UTR of CBX7 mRNA and inhibits CBX7 expression at the translation level (Peng et al., 2018). Similarly, in lung adenocarcinomas, miR-181 overexpression promotes epithelial-mesenchymal transition (EMT) by directly targeting CBX7 (Pei et al., 2020). In addition, miR-375 plays a cancer-promoting role in prostate cancer by influencing the epigenetic regulation of transcriptional programs through its ability to directly target the polycomb complex member CBX7 (Pickl et al., 2016). Moreover, compared with CBX7+/+MEFs(mouse embryonic fibroblasts), CBX7−/−MEFs show a higher level of miR-181 in breast cancer while CBX7 ± MEFs express a moderate level, suggesting that CBX7 negatively regulates the expression of miR-181 (Pallante et al., 2015). Therefore, on the one hand, CBX7 can negatively regulate the expression of miR-181. On the other hand, since miR-181 binds to the mRNA 3′-UTR of CBX7, the expression of CBX7 is restricted, thus forming a synergistic cycle that promotes cancers (Pallante et al., 2015; Peng et al., 2018; Yan et al., 2020). MiR-155 is positively regulated by CBX7 in MEFs and colon carcinomas. Moreover, it has been determined that K-ras is a target of miR-155, the overexpression of miR-155 causes a sharp drop in K-ras mRNA and protein levels (Forzati et al., 2017). In glioma, the *in vitro* and *in vivo* functional assays results indicate that overexpression of miR-18a induced by miR-18a mimics may promote cell proliferation and migration of liver cancer cells by acting on CBX7 (Wu et al., 2017). On the contrary, miR-18a shows a cancer suppressor effect in primary ovarian tumors, due to the dual role of CBX7 as a bridge molecule in different cancers progression (Zhao et al., 2020). In addition, it has been reported that miR-9 can induce cell senescence without affecting the expression of CBX7, but the expression of CBX7 weakens its ability to induce senescence, which may be related to the regulation of senescence involved in p16^{INK4a} (O'Loghlen et al., 2015a).

Interaction of CBX7 With Long Noncoding RNAs

There are few studies on the regulatory relationship between long noncoding RNA lncRNA and CBX7. Some lncRNAs can directly or indirectly influence the role of CBX7 in cancer progression. In breast cancer, lncRNA NEAT1 is highly

TABLE 1 | CBX7 participates in various pathways and plays different physiological effects in different cancers.

Cancer types	Main pathway of participation	Effect	Result	References
Breast	Wnt pathway	Inhibit DKK-1 genomic protein deacetylation	Inhibit the self-renewal ability of breast cancer cells	Kim et al. (2015)
Liver	—	Bind to the CCNE1 promoter with HDAC2	Inhibit cell proliferation and migration	Forzati et al. (2012)
Colon	Wnt pathway	Combine sFRP4 promoter to methylate to silence genes	Promote cancer cell proliferation	Liu et al. (2020)
Pancreas	PI3K/AKT	Recruit P300 to promote the activation of PTEN	Induce apoptosis	Ni et al. (2017)
Thyroid	—	Regulate the expression of E-cadherin and osteopontin	Maintain epithelial characteristics and regulate cell migration	Federico et al. (2009); Sepe et al. (2015)
Glioma	Hippo pathway	Down-regulate the decrease in E-cadherin caused by CTGF	Prevent the invasion and migration of glioma cells	Nawaz et al. (2016)
Stomach	AKT—NF-kB—miR-21	Promote the activation of AKT and ERK	Actively regulate the stem cell characteristics of gastric cancer cells	Ni et al. (2018)
Prostate	INK4a/ARF	Epigenetic suppression of tumor suppressor gene	Maintain cell proliferation and growth	Bernard et al. (2005)
Lymph	INK4a/ARF	Epigenetic suppression of tumor suppressor gene	Enhance the replication potential of cancer stem cells	Scott et al. (2007)

expressed in breast cancer tissues and closely related to clinical stage, lymph node metastasis (Li et al., 2017; Yan et al., 2020). It has been reported that with the down-regulation of NEAT1, the expression of CBX7 protein in breast cancer cells is also significantly down-regulated ($p < 0.01$) (Yan et al., 2020). lncRNA NEAT1 is mainly located in the cytoplasm but also exists in the nucleus. It is speculated that lncRNA NEAT1 may play a role in regulating CBX7 expression in terms of chromatin status, DNA binding, or the fate of newly transcribed mRNA in the nucleus (Yan et al., 2020). lncRNA ANRIL can coordinate or reverse the "reader" function of CBX7 at the transcriptional level (Yap et al., 2010). The p16 gene and the gene transcribed into ANRIL are located on the same chromosome, and CBX7 chromodomain uses distinct regions and residues for binding H3K27me or lncRNA (Pasmant et al., 2007; Yap et al., 2010). Both PRC1 and PRC2 are retained at a repression site of a target gene through their association with the nascent ANRIL transcripts of Pol II, ANRIL/CBX7 binding could result in dissociation of PRC1 from H3K27me, leading to a reversal of transcriptional repression of the target gene (Yap et al., 2010). In addition, lncRNA SNHG7 can also indirectly influence the expression of CBX7 by regulating miR-181 in lung adenocarcinoma (Pei et al., 2020). It can be seen that the interaction between CBX7 and lncRNA family is not one-to-one, but a complex regulatory network between lncRNA and microRNA families.

Interaction of CBX7 With Circular RNAs

CircRNA has been proved to be an important molecule that can be used as a therapeutic target for tumors. However, studies on the relationship between circRNA and CBX7 are few and currently limited to prostate cancer (Chen et al., 2019; Gong et al., 2020). In the study of prostate cancer, it is found that CBX7 can specifically bind to circGOLPH3 based on the results of mass spectrometry, but the detailed mechanism of circRNA-CBX7 binding remains unclear (Gong et al., 2020). The answer to the direct and specific binding of GOLPH3 to CBX7 may be that the two directly bind to prevent CBX7 degradation. Moreover, in prostate cancer, circCSNK1G3 promotes cell growth by interacting with miR-181 involved in the regulation of CBX7 (Chen et al., 2019; Pei et al., 2020). Of note, circRNAs can bind, store, classify and isolate proteins to specific subcellular locations (Huang et al., 2020). Given that the above discussion in various cancers, CBX7 mainly functions as an epigenetic regulator in the nucleus. Therefore, it is possible to speculate whether CBX7 can be dispersed into different subcellular locations under the action of circular RNAs to show a confusing result, which is mistaken for the duality of CBX7. For example, CBX7 is highly expressed in cells, however, the amount of CBX7 in the nucleus is small and its regulatory role is not significant. The relationship between circRNA family and CBX7 may further uncover the complex mechanism of CBX7.

THE RELATIONSHIP BETWEEN THE PHYSIOLOGICAL FUNCTION OF CBX7 AND CANCER

CBX7 and the Immune Response

It has been reported that CBX7-deficient CD4+T cells express more FasL and display the FasL gene promoter demethylation after antigen-specific TCR activation (Li et al., 2014). It is

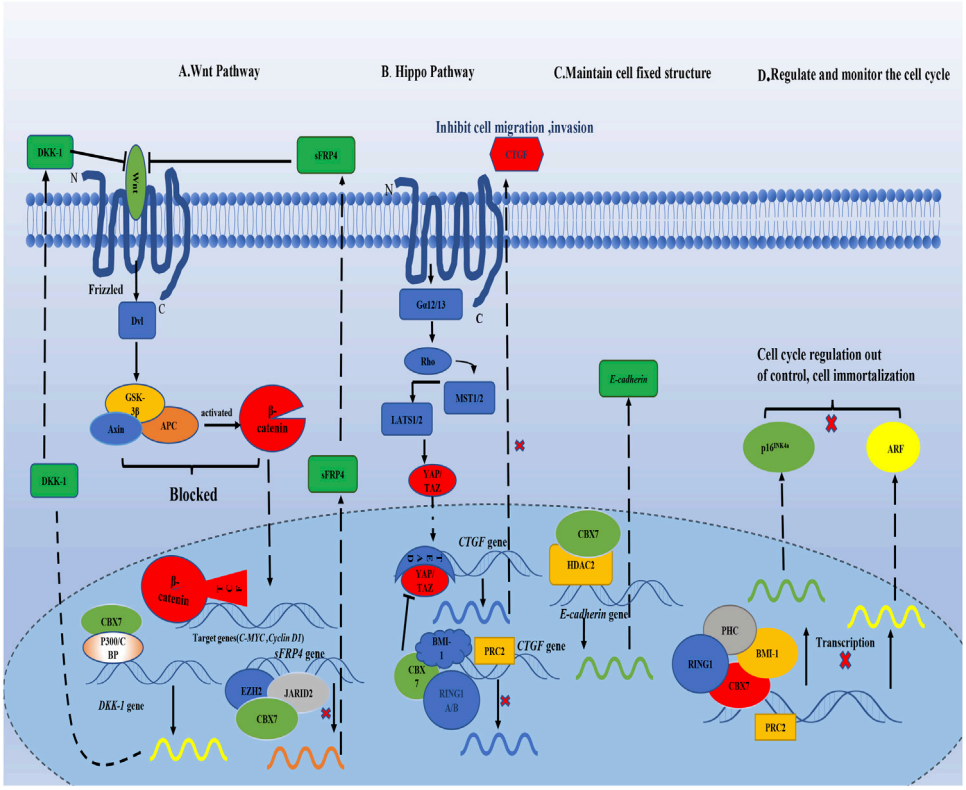

FIGURE 2 | CBX7 interacts with proteins in the nucleus, transcriptionally controls the synthesis of related proteins, and regulates different signaling pathways. **(A)** CBX7 enhances the expression of Wnt antagonist DKK-1 by interacting with other molecules in epigenetics, leading to the blockage of downstream signal transduction of Wnt pathway, and then the expression of C-MYC and Cyclin D are restricted to maintain normal cell proliferation. But CBX7 inhibits the expression of sFRP4, which is also a Wnt antagonist.**(B)** On the one hand, CBX7 directly inhibits CTGF expression epigenetically; on the other hand, CBX7 antagonizes YAP/TAZ to indirectly restrict CTGF expression, which inhibits cell invasion and migration. **(C)** CBX7 cooperates with HDAC2 to promote the synthesis of E-cadherin in transcription to maintain cell fixed structure. **(D)** CBX7 relies on PRC1, and cooperates with PRC2 to epigenetically inhibit the expression of INK4a/ARF, making cell proliferation out of control.

suggested that CBX7 can inhibit the expression of FasL in CD4+ T cells, resulting in significantly reduced demethylation of the FasL gene promoter. It is well known that the Fas-FasL association is a typical pathway that induces T cell apoptosis (Fisher et al., 1995). Therefore, CBX7 can inhibit activation-induced T cell apoptosis, indicating that it plays a role in the adaptive immune response. Interestingly, a small proportion of people infected with HIV remain asymptomatic and maintain a high CD4 + T cell count after years of seroconversion (Imami et al., 2013). A meta-analysis showed that the CBX7 gene is highly correlated with viral control (Ding et al., 2019). In addition, changes in somatic cell copy numbers of the CBX family inhibit the infiltration of immune cells in melanoma (Li D. et al., 2020). The analysis of immune infiltration for the CBX family showed that the expression of CBX7 is related to the abundance of these six immune cells (B cells, CD8+ T cells, CD4+ T cells, macrophages, neutrophils, and dendritic cells) (Li D. et al., 2020). Moreover, in prostate cancer, C-C motif chemokine ligand 2 (CCL2) is a main target of PRC1, and the H3K27me3 inhibitory marker that is bound with CBX7 is relatively low in the promoter region of the CCL2 gene, which leads to massive production of CCL2 (Su et al., 2019). The cytokine CCL2 not only promotes self-renewal by binding to C-C motif chemokine receptor 4 (CCR4) on prostate cancer cells but also recruits tumor-associated macrophages and Tregs in cancer metastasis sites by paracrine, thus creating a profound immunosuppression and angiogenesis microenvironment, confirming once again the importance of CBX7 in tumor immunity (Josefowicz et al., 2012; Su et al., 2019).

Immune cells infiltrating in the tumor microenvironment can regulate cancer progression, which is the current trend of cancer therapy (Quail and Joyce, 2013). CBX7 can play its duality in different cancer tissues, but it could be beneficial to the immune system of the human body. It would be interesting to assess whether CBX7 can be used as an intermediate molecule between cancers and immunity.

CBX7 and DNA Damage

It is well known that the source of cancers can be naturalized with proto-oncogene mutations and cancer suppressor gene deletions. The fundamental reason for cancer lies within the problems within DNA damage and repair (O'Connor, 2015). Recently, the contact between CBX7 and DNA damage repair has emerged in cancers. In melanoma, the downstream kinase targets of CBX7

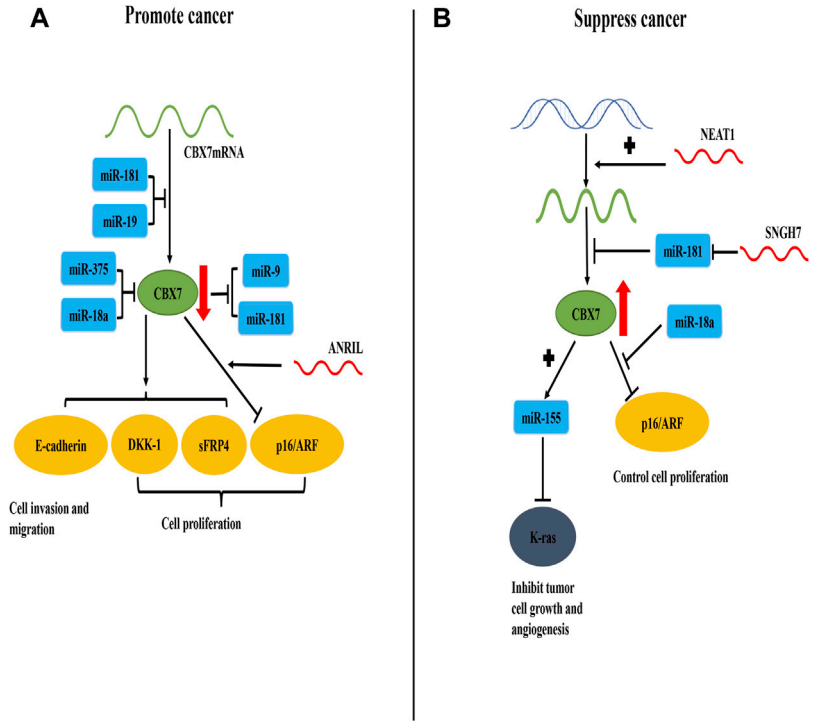

FIGURE 3 | CBX7 expression is regulated by RNA molecules and the interaction between CBX7 and RNA molecules promotes or inhibits cancer progression. **(A)** In terms of quantity, miR-181 and miR-19 combine with the 3′-UTR of CBX7 mRNA to inhibit its translation and reduce its content. In terms of function, miR-375 and miR-18a act on CBX7 protein to decrease its activity. Therefore, the expression of DKK-1, sFRP4 and E-cadherin mediated by CBX7 decreases, resulting in uncontrolled cell proliferation, cell migration and invasion. CBX7 can also strengthen the inhibition of INK4a/ARF expression under the action of ANRIL, leading to uncontrolled cell cycle regulation and cell proliferation. Meanwhile, CBX7 can also inhibit miR-9 and miR-181. **(B)** In terms of quantity, NEAT1 promotes the synthesis of CBX7 at the transcription level, and SNGH7 indirectly facilitates the synthesis of CBX7 protein by blocking miR-181 at the translation level. Therefore, high content of CBX7 protein can inhibit abnormal K-ras protein *via* miR-155, thereby controlling tumor cell growth and angiogenesis. Meanwhile, miR-18a can relieve the transcriptional inhibition of INK4a/ARF by CBX7, thereby restoring normal cell proliferation.

are Polo-like kinase 1(PLK1) and cyclin-dependent kinase 1(CDK1), which are related to genome stability. Therefore, CBX7 is indirectly involved in DNA damage repair (Li D. et al., 2020). Moreover, in melanoma studies, it has been shown that in the presence of CBX7 inhibitors, DNA damage repair is inhibited (Connelly et al., 2016). In addition, RING1, a member of the PRC1, has been shown to possess ubiquitin ligase activity toward histone H2A, suggesting that the recruitment of polycomb proteins may be responsible for the ubiquitination of histone H2A at DNA lesions. CBX7 is also a member of the PRC1. In other words, CBX7 may locate at DNA damage sites with the recruitment of PRC1 containing RING1 (Chou et al., 2010; Pei et al., 2020). All these suggest the importance of CBX7 in DNA damage repair.

DISCUSSION

Clinically, the expression of CBX7 in different cancers is inconsistent for cancer progression, showing double-sidedness. CBX7 is lowly expressed in cancers of the breast, pancreas, liver, thyroid, colon, and glioma, but highly expressed in cancers of the stomach, prostate, and lymph. We outline above that CBX7 may regulate cell proliferation, apoptosis, and metastasis through different targets in different tissues. Based on the circumstances regarding CBX7 in cancers, it may be bold to speculate that the double-sidedness of CBX7 in cancer progression is closely related to its regulatory pathways (**Table 1**). Limited by our understanding of various cancer pathways, we describe some of the regulatory pathways in which CBX7 participates in cancers.

In general, the current consensus on the carcinogenicity of CBX7 is that CBX7 inhibits the oncosuppressor gene *INK4a/ARF* (**Figure 1**). For its anti-cancer effect, CBX7 participates in different pathways according to the different tissue environments (**Table 1**). It mainly interacts with other molecules to epigenetically control the expression of related proteins, thereby regulating some cell signaling pathways to combat cancer manifestations (Such as proliferation, migration, invasion, etc. **Figure 2**). It needs to be pointed out that different RNA molecules have a complex relationship with CBX7, forming an intricate network between them, making the effect of CBX7 on cancer is not absolute (**Figure 3**).

CBX7 is involved in the reading recognition of H3K27me3 with its special structure and causes gene silencing, therefore

CBX7 may be used as a clinical cancer treatment target. Due to the high degree of homology in the CBX family, antagonists that specifically target the CBX7 reader protein binding to histone methylated lysine have not yet been discovered, but some antagonists have a higher selectivity for CBX7 than CBX2/6/8 (Simhadri et al., 2016). Small molecules such as suramin and Ms37452 can inhibit the binding of lysine methylated polypeptides to the CBX7 chromodomain, which can be used as a feasible cancer suppressor in some cancers with high CBX7 expression, such as prostate cancer (Ren et al., 2015). Furthermore, CBX7 can also increase the sensitivity of cancer cells to chemical drugs (Cacciola et al., 2015; Iqbal et al., 2021). For example, the sensitivity of lung carcinoma cells to irinotecan and the sensitivity of breast cancer cells to FDA-approved drugs. It is worth noting that when defining the function of inhibitory polycomb complexes and evaluating the anti-cancer drugs for CBX7, the overall expression pattern should be given priority, rather than the expression of a single complex member. Of course, the complete mechanism of CBX7 has not been clarified so far. As a subunit of the PcG proteins, CBX7 not only functions independently of PRC1 but also has the function of inhibiting gene expression together with PRC1 as a whole and PCR2 (Scott et al., 2007; Pallante et al., 2015). These phenomena deserve further investigation to elucidate their mechanisms and may provide evidence for the clinical prognostic value and therapeutic targets of cancer.

More importantly, in this review, we briefly illustrated the duality of the interaction between CBX7 and various RNAs in cancers (**Figure 3**). Similarly, other molecules that use CBX7 as an intermediate for physiological effects can also play a dual role in different cancer progression, such as miR-18a (Wu et al., 2017; Zhao et al., 2020). It is indisputable that the specificity of the environment in which the tissue cells are located affects the duality of CBX7. Additionally, the physical and chemical environment of the tissue may also greatly influence the expression of CBX7 (Chiu et al., 2020). It has been reported that under hypoxic conditions activated hypoxia-inducible factor-1α (HIF-1α) directly binds to the CBX7 gene promoter and activates the expression of CBX7, and hypoxia-induced overexpression of CBX7 stimulates the proliferation of nasopharyngeal carcinoma cells in the ischemic brain (Chiu et al., 2020).

CONCLUSION

The most important function of the CBX7 protein is to regulate gene expression by epigenetics. In some cases, it can control cell proliferation, cell apoptosis, and self-renewal. Besides, the cellular effects mediated by CBX7 are diverse in different cancer environments. Therefore, actively guiding the expression of CBX7 *in vivo* according to cancer types may be helpful in guiding the clinical progress of cancer treatment.

AUTHOR CONTRIBUTIONS

TO proposed ideas for this article and participated in revising the article. JL wrote, revised the paper, and made diagrams. ML, TH, AM, WM, and NZ reviewed and made significant revisions to the manuscript. All authors have read and approved the final manuscript.

FUNDING

The National Natural Science Foundation of China, grant no. 81760447 (TO); The National Natural Science Foundation of China, grant no. 81960247 (NZ); Project of Science and Technology Department of Jiangxi Province, grant no. S2019QNJJB1056 (NZ); Project of Science and Technology Department of Jiangxi Province, grant no.20202BABL206099 (WM); Jiangxi Provincial Education Department Project, grant no. GJJ180054 (TO); Jiangxi Provincial Education Department Project, grant no. GJJ180116 (NZ).

ACKNOWLEDGMENTS

We thank Emmy Graham for the language polish of this review and put forward suggestions.

REFERENCES

Asano, T., Yao, Y., Zhu, J., Li, D., Abbruzzese, J. L., and Reddy, S. A. G. (2004). The PI 3-kinase/Akt Signaling Pathway Is Activated Due to Aberrant Pten Expression and Targets Transcription Factors NF-Kb and C-Myc in Pancreatic Cancer Cells. *Oncogene* 23, 8571–8580. doi:10.1038/sj.onc.1207902

Bafico, A., Liu, G., Yaniv, A., Gazit, A., and Aaronson, S. A. (2001). Novel Mechanism of Wnt Signalling Inhibition Mediated by Dickkopf-1 Interaction with LRP6/Arrow. *Nat. Ce.l Biol.* 3, 683–686. doi:10.1038/35083081

Bao, Z., Xu, X., Liu, Y., Chao, H., Lin, C., Li, Z., et al. (2017). CBX7 Negatively Regulates Migration and Invasion in Glioma via Wnt/β-Catenin Pathway Inactivation. *Oncotarget* 8, 39048–39063. doi:10.18632/oncotarget.16587

Bernard, D., Martinez-Leal, J. F., Rizzo, S., Martinez, D., Hudson, D., Visakorpi, T., et al. (2005). CBX7 Controls the Growth of normal and Tumor-Derived Prostate Cells by Repressing the Ink4a/Arf Locus. *Oncogene* 24, 5543–5551. doi:10.1038/sj.onc.1208735

Cacciola, N. A., Sepe, R., Forzati, F., Federico, A., Pellecchia, S., Malapelle, U., et al. (2015). Restoration of CBX7 Expression Increases the Susceptibility of Human Lung Carcinoma Cells to Irinotecan Treatment. *Naunyn-Schmiedeberg's Arch. Pharmacol.* 388, 1179–1186. doi:10.1007/s00210-015-1153-y

Chen, S., Huang, V., Xu, X., Livingstone, J., Soares, F., Jeon, J., et al. (2019). Widespread and Functional RNA Circularization in Localized Prostate Cancer. *Cell* 176, 831–843.e822. doi:10.1016/j.cell.2019.01.025

Cheung, C. C., Ezzat, S., Ramyar, L., Freeman, J. L., and Asa, S. L. (2000). Molecular Basis of Hurthle Cell Papillary Thyroid Carcinoma1. *J. Clin. Endocrinol. Metab.* 85, 878–882. doi:10.1210/jcem.85.2.6404

Chiappetta, G., Bandiera, A., Berlingieri, M. T., Visconti, R., Manfioletti, G., Battista, S., et al. (1995). The Expression of the High Mobility Group HMGI (Y) Proteins Correlates with the Malignant Phenotype of Human Thyroid Neoplasias. *Oncogene* 10, 1307–1314.

Chiu, H. Y., Lee, H. T., Lee, K. H., Zhao, Y., Hsu, C. Y., and Shyu, W. C. (2020). Mechanisms of Ischaemic Neural Progenitor Proliferation: a Regulatory Role of the HIF-1α-CBX7 Pathway. *Neuropathol. Appl. Neurobiol.* 46, 391–405. doi:10.1111/nan.12585

Cho, K.-W., Andrade, M., Zhang, Y., and Yoon, Y.-S. (2020). Mammalian CBX7 Isoforms P36 and P22 Exhibit Differential Responses to Serum, Varying Functions for Proliferation, and Distinct Subcellular Localization. *Sci. Rep.* 10, 8061. doi:10.1038/s41598-020-64908-2

Chou, D. M., Adamson, B., Dephoure, N. E., Tan, X., Nottke, A. C., Hurov, K. E., et al. (2010). A Chromatin Localization Screen Reveals Poly (ADP Ribose)-Regulated Recruitment of the Repressive Polycomb and NuRD Complexes to Sites of DNA Damage. *Proc. Natl. Acad. Sci.* 107, 18475–18480. doi:10.1073/pnas.1012946107

Connelly, K. E., Martin, E. C., and Dykhuizen, E. C. (2016). CBX Chromodomain Inhibition Enhances Chemotherapy Response in Glioblastoma Multiforme. *Yale J. Biol. Med.* 89, 431–440.

Correia de Sousa, M., Gjorgjieva, M., Dolicka, D., Sobolewski, C., and Foti, M. (2019). Deciphering miRNAs' Action through miRNA Editing. *Ijms* 20, 6249. doi:10.3390/ijms20246249

Creighton, C. J. (2007). A Gene Transcription Signature of the Akt/mTOR Pathway in Clinical Breast Tumors. *Oncogene* 26, 4648–4655. doi:10.1038/sj.onc.1210245

Ding, J., Ma, L., Zhao, J., Xie, Y., Zhou, J., Li, X., et al. (2019). An Integrative Genomic Analysis of Transcriptional Profiles Identifies Characteristic Genes and Patterns in HIV-Infected Long-Term Non-Progressors and Elite Controllers. *J. Transl Med.* 17, 35. doi:10.1186/s12967-019-1777-7

Edwards, L. A., Woolard, K., Son, M. J., Li, A., Lee, J., Ene, C., et al. (2011). Effect of Brain- and Tumor-Derived Connective Tissue Growth Factor on Glioma Invasion. *J. Natl. Cancer Inst.* 103, 1162–1178. doi:10.1093/jnci/djr224

Federico, A., Pallante, P., Bianco, M., Ferraro, A., Esposito, F., Monti, M., et al. (2009). Chromobox Protein Homologue 7 Protein, with Decreased Expression in Human Carcinomas, Positively Regulates E-Cadherin Expression by Interacting with the Histone Deacetylase 2 Protein. *Cancer Res.* 69, 7079–7087. doi:10.1158/0008-5472.can-09-1542

Fisher, G. H., Rosenberg, F. J., Straus, S. E., Dale, J. K., Middelton, L. A., Lin, A. Y., et al. (1995). Dominant Interfering Fas Gene Mutations Impair Apoptosis in a Human Autoimmune Lymphoproliferative Syndrome. *Cell* 81, 935–946. doi:10.1016/0092-8674(95)90013-6

Forzati, F., De Martino, M., Esposito, F., Sepe, R., Pellecchia, S., Malapelle, U., et al. (2017). miR-155 Is Positively Regulated by CBX7 in Mouse Embryonic Fibroblasts and colon Carcinomas, and Targets the KRAS Oncogene. *BMC Cancer* 17, 170. doi:10.1186/s12885-017-3158-z

Forzati, F., Federico, A., Pallante, P., Abbate, A., Esposito, F., Malapelle, U., et al. (2012). CBX7 Is a Tumor Suppressor in Mice and Humans. *J. Clin. Invest.* 122, 612–623. doi:10.1172/jci58620

Forzati, F., Federico, A., Pallante, P., Colamaio, M., Esposito, F., Sepe, R., et al. (2014). CBX7 Gene Expression Plays a Negative Role in Adipocyte Cell Growth and Differentiation. *Biol. open* 3, 871–879. doi:10.1242/bio.20147872

Fusco, A., and Fedele, M. (2007). Roles of HMGA Proteins in Cancer. *Nat. Rev. Cancer* 7, 899–910. doi:10.1038/nrc2271

Geng, Z., and Gao, Z. (2020). Mammalian PRC1 Complexes: Compositional Complexity and Diverse Molecular Mechanisms. *Ijms* 21, 8594. doi:10.3390/ijms21228594

Gil, J., Bernard, D., and Peters, G. (2005). Role of Polycomb Group Proteins in Stem Cell Self-Renewal and Cancer. *DNA Cel. Biol.* 24, 117–125. doi:10.1089/dna.2005.24.117

Gong, L., Tang, Y., Jiang, L., Tang, W., and Luo, S. (2020). Regulation of circGOLPH3 and its Binding Protein CBX7 on the Proliferation and Apoptosis of Prostate Cancer Cells. *Biosci. Rep.* 40, BSR20200936. doi:10.1042/bsr20200936

Guo, W.-J., Zeng, M.-S., Yadav, A., Song, L.-B., Guo, B.-H., Band, V., et al. (2007). Mel-18 Acts as a Tumor Suppressor by Repressing Bmi-1 Expression and Down-Regulating Akt Activity in Breast Cancer Cells. *Cancer Res.* 67, 5083–5089. doi:10.1158/0008-5472.can-06-4368

Huang, A., Zheng, H., Wu, Z., Chen, M., and Huang, Y. (2020). Circular RNA-Protein Interactions: Functions, Mechanisms, and Identification. *Theranostics* 10, 3503–3517. doi:10.7150/thno.42174

Imami, N., Westrop, S. J., Grageda, N., and Herasimtschuk, A. A. (2013). Long-Term Non-Progression and Broad HIV-1-Specific Proliferative T-Cell Responses. *Front. Immunol.* 4, 58. doi:10.3389/fimmu.2013.00058

Iqbal, M. A., Siddiqui, S., Ur Rehman, A., Siddiqui, F. A., Singh, P., Kumar, B., et al. (2021). Multiomics Integrative Analysis Reveals Antagonistic Roles of CBX2 and CBX7 in Metabolic Reprogramming of Breast Cancer. *Mol. Oncol.* 15, 1450–1465. doi:10.1002/1878-0261.12894

Jangal, M., Lebeau, B., and Witcher, M. (2019). Beyond EZH2: Is the Polycomb Protein CBX2 an Emerging Target for Anti-cancer Therapy. *Expert Opin. Ther. Targets* 23, 565–578. doi:10.1080/14728222.2019.1627329

Jiang, Z., Guo, J., Xiao, B., Miao, Y., Huang, R., Li, D., et al. (2010). Increased Expression of miR-421 in Human Gastric Carcinoma and its Clinical Association. *J. Gastroenterol.* 45, 17–23. doi:10.1007/s00535-009-0135-6

Josefowicz, S. Z., Lu, L.-F., and Rudensky, A. Y. (2012). Regulatory T Cells: Mechanisms of Differentiation and Function. *Annu. Rev. Immunol.* 30, 531–564. doi:10.1146/annurev.immunol.25.022106.141623

Kaito, S., and Iwama, A. (2020). Pathogenic Impacts of Dysregulated Polycomb Repressive Complex Function in Hematological Malignancies. *Int. J. Mol. Sci.* 22, 74. doi:10.3390/ijms22010074

Kim, H. Y., Park, J. H., Won, H. Y., Lee, J. Y., and Kong, G. (2015). CBX7 Inhibits Breast Tumorigenicity through DKK-1-mediated Suppression of the Wnt/β-Catenin Pathway. *FASEB j.* 29, 300–313. doi:10.1096/fj.14-253997

Kim, W. Y., and Sharpless, N. E. (2006). The Regulation of INK4/ARF in Cancer and Aging. *Cell* 127, 265–275. doi:10.1016/j.cell.2006.10.003

Levine, S. S., Weiss, A., Erdjument-Bromage, H., Shao, Z., Tempst, P., and Kingston, R. E. (2002). The Core of the Polycomb Repressive Complex Is Compositionally and Functionally Conserved in Flies and Humans. *Mol. Cel. Biol.* 22, 6070–6078. doi:10.1128/mcb.22.17.6070-6078.2002

Li, D., Liu, Y., Hao, S., Chen, B., and Li, A. (2020a). Mining Database for the Clinical Significance and Prognostic Value of CBX Family in Skin Cutaneous Melanoma. *J. Clin. Lab. Anal.* 34, e23537. doi:10.1002/jcla.23537

Li, J., Li, Y., Cao, Y., Yuan, M., Gao, Z., Guo, X., et al. (2014). Polycomb Chromobox (Cbx) 7 Modulates Activation-Induced CD4+ T Cell Apoptosis. *Arch. Biochem. Biophys.* 564, 184–188. doi:10.1016/j.abb.2014.10.004

Li, X., Gou, J., Li, H., and Yang, X. (2020b). Bioinformatic Analysis of the Expression and Prognostic Value of Chromobox Family Proteins in Human Breast Cancer. *Sci. Rep.* 10, 17739. doi:10.1038/s41598-020-74792-5

Li, X., Wang, S., Li, Z., Long, X., Guo, Z., Zhang, G., et al. (2017). The lncRNA NEAT1 Facilitates Cell Growth and Invasion via the miR-211/HMGA2 axis in Breast Cancer. *Int. J. Biol. macromolecules* 105, 346–353. doi:10.1016/j.ijbiomac.2017.07.053

Liang, Y.-K., Lin, H.-Y., Chen, C.-F., and Zeng, D. (2017). Prognostic Values of Distinct CBX Family Members in Breast Cancer. *Oncotarget* 8, 92375–92387. doi:10.18632/oncotarget.21325

Liu, T.-H., Raval, A., Chen, S.-S., Matkovic, J. J., Byrd, J. C., and Plass, C. (2006). CpG Island Methylation and Expression of the Secreted Frizzled-Related Protein Gene Family in Chronic Lymphocytic Leukemia. *Cancer Res.* 66, 653–658. doi:10.1158/0008-5472.can-05-3712

Liu, Y., Yu, J., Xie, Y., Li, M., Wang, F., Zhang, J., et al. (2020). EZH2 Regulates sFRP4 Expression without Affecting the Methylation of sFRP4 Promoter DNA in Colorectal Cancer Cell Lines. *Exp. Ther. Med.* 20, 33. doi:10.3892/etm.2020.9160

Lu, H., Cui, J., Gunewardena, S., Yoo, B., Zhong, X.-B., and Klaassen, C. (2012). Hepatic Ontogeny and Tissue Distribution of mRNAs of Epigenetic Modifiers in Mice Using RNA-Sequencing. *Epigenetics* 7, 914–929. doi:10.4161/epi.21113

Maeda, T., Hobbs, R. M., Merghoub, T., Guernah, I., Zelent, A., Cordon-Cardo, C., et al. (2005). Role of the Proto-Oncogene Pokemon in Cellular Transformation and ARF Repression. *Nature* 433, 278–285. doi:10.1038/nature03203

Mansueto, G., Forzati, F., Ferraro, A., Pallante, P., Bianco, M., Esposito, F., et al. (2010). Identification of a New Pathway for Tumor Progression: MicroRNA-181b Up-Regulation and CBX7 Down-Regulation by HMGA1 Protein. *Genes & Cancer* 1, 210–224. doi:10.1177/1947601910366860

Monaco, M., Chiappetta, G., Aiello, C., Federico, A., Sepe, R., Russo, D., et al. (2014). CBX7 Expression in Oncocytic Thyroid Neoplastic Lesions (Hürthle Cell Adenomas and Carcinomas). *Eur. Thyroid J.* 3, 211–216. doi:10.1159/000367989

Mossmann, D., Park, S., and Hall, M. N. (2018). mTOR Signalling and Cellular Metabolism Are Mutual Determinants in Cancer. *Nat. Rev. Cancer* 18, 744–757. doi:10.1038/s41568-018-0074-8

Nawaz, Z., Patil, V., Arora, A., Hegde, A. S., Arivazhagan, A., Santosh, V., et al. (2016). Cbx7 Is Epigenetically Silenced in Glioblastoma and Inhibits Cell Migration by Targeting YAP/TAZ-Dependent Transcription. *Sci. Rep.* 6, 27753. doi:10.1038/srep27753

Ni, S.-J., Zhao, L.-Q., Wang, X.-F., Wu, Z.-H., Hua, R.-X., Wan, C.-H., et al. (2018). CBX7 Regulates Stem Cell-Like Properties of Gastric Cancer Cells via P16 and AKT-NF-Kb-miR-21 Pathways. *J. Hematol. Oncol.* 11, 17. doi:10.1186/s13045-018-0562-z

Ni, S., Wang, H., Zhu, X., Wan, C., Xu, J., Lu, C., et al. (2017). CBX7 Suppresses Cell Proliferation, Migration, and Invasion through the Inhibition of PTEN/Akt Signaling in Pancreatic Cancer. *Oncotarget* 8, 8010–8021. doi:10.18632/oncotarget.14037

Ning, G., Huang, Y.-L., Zhen, L.-M., Xu, W.-X., Jiao, Q., Yang, F.-J., et al. (2018). Transcriptional Expressions of Chromobox 1/2/3/6/8 as Independent Indicators for Survivals in Hepatocellular Carcinoma Patients. *Aging* 10, 3450–3473. doi:10.18632/aging.101658

O'Loghlen, A., Brookes, S., Martin, N., Rapisarda, V., Peters, G., and Gil, J. (2015a). CBX7 and miR-9 Are Part of an Autoregulatory Loop Controlling p16INK4a. *Aging cell* 14, 1113–1121. doi:10.1111/acel.12404

O'Loghlen, A., Martin, N., Krusche, B., Pemberton, H., Alonso, M. M., Chandler, H., et al. (2015b). The Nuclear Receptor NR2E1/TLX Controls Senescence. *Oncogene* 34, 4069–4077. doi:10.1038/onc.2014.335

O'Connor, M. J. (2015). Targeting the DNA Damage Response in Cancer. *Mol. Cel* 60, 547–560. doi:10.1016/j.molcel.2015.10.040

Ogawa, H., Ishiguro, K., Gaubatz, S., Livingston, D. M., and Nakatani, Y. (2002). A Complex with Chromatin Modifiers that Occupies E2F- and Myc-Responsive Genes in G0 Cells. *Science (New York, NY)* 296, 1132–1136. doi:10.1126/science.1069861

Pallante, P., Forzati, F., Federico, A., Arra, C., and Fusco, A. (2015). Polycomb Protein Family Member CBX7 Plays a Critical Role in Cancer Progression. *Am. J. Cancer Res.* 5, 1594–1601.

Pallante, P., Federico, A., Berlingieri, M. T., Bianco, M., Ferraro, A., Forzati, F., et al. (2008). Loss of the CBX7 Gene Expression Correlates with a Highly Malignant Phenotype in Thyroid Cancer. *Cancer Res.* 68, 6770–6778. doi:10.1158/0008-5472.can-08-0695

Pallante, P., Sepe, R., Federico, A., Forzati, F., Bianco, M., and Fusco, A. (2014). CBX7 Modulates the Expression of Genes Critical for Cancer Progression. *PLoS One* 9, e98295. doi:10.1371/journal.pone.0098295

Pallante, P., Terracciano, L., Carafa, V., Schneider, S., Zlobec, I., Lugli, A., et al. (2010). The Loss of the CBX7 Gene Expression Represents an Adverse Prognostic Marker for Survival of colon Carcinoma Patients. *Eur. J. Cancer* 46, 2304–2313. doi:10.1016/j.ejca.2010.05.011

Pasmant, E., Laurendeau, I., Héron, D., Vidaud, M., Vidaud, D., and Bièche, I. (2007). Characterization of a Germ-Line Deletion, Including the Entire INK4/ARF Locus, in a Melanoma-Neural System Tumor Family: Identification of ANRIL, an Antisense Noncoding RNA Whose Expression Coclusters with ARF. *Cancer Res.* 67, 3963–3969. doi:10.1158/0008-5472.can-06-2004

Pei, Y.-F., He, Y., Hu, L.-Z., Zhou, B., Xu, H.-Y., and Liu, X.-Q. (2020). The Crosstalk between lncRNA-SNHG7/miRNA-181/cbx7 Modulates Malignant Character in Lung Adenocarcinoma. *Am. J. Pathol.* 190, 1343–1354. doi:10.1016/j.ajpath.2020.02.011

Peng, X., Guan, L., and Gao, B. (2018). miRNA-19 Promotes Non-Small-Cell Lung Cancer Cell Proliferation via Inhibiting CBX7 Expression. *Onco Targets Ther.* 11, 8865–8874. doi:10.2147/ott.s181433

Pickl, J. M. A., Tichy, D., Kuryshev, V. Y., Tolstov, Y., Falkenstein, M., Schüler, J., et al. (2016). Ago-RIP-Seq Identifies Polycomb Repressive Complex I Member CBX7 as a Major Target of miR-375 in Prostate Cancer Progression. *Oncotarget* 7, 59589–59603. doi:10.18632/oncotarget.10729

Quail, D. F., and Joyce, J. A. (2013). Microenvironmental Regulation of Tumor Progression and Metastasis. *Nat. Med.* 19, 1423–1437. doi:10.1038/nm.3394

Ramaswamy, S., Tamayo, P., Rifkin, R., Mukherjee, S., Yeang, C.-H., Angelo, M., et al. (2001). Multiclass Cancer Diagnosis Using Tumor Gene Expression Signatures. *Proc. Natl. Acad. Sci.* 98, 15149–15154. doi:10.1073/pnas.211566398

Ren, C., Morohashi, K., Plotnikov, A. N., Jakoncic, J., Smith, S. G., Li, J., et al. (2015). Small-Molecule Modulators of Methyl-Lysine Binding for the CBX7 Chromodomain. *Chem. Biol.* 22, 161–168. doi:10.1016/j.chembiol.2014.11.021

Rohde, F., Rimkus, C., Friederichs, J., Rosenberg, R., Marthen, C., Doll, D., et al. (2007). Expression of Osteopontin, a Target Gene of De-regulated Wnt Signaling, Predicts Survival in colon Cancer. *Int. J. Cancer* 121, 1717–1723. doi:10.1002/ijc.22868

Satijn, D. P. E., Hamer, K. M., den Blaauwen, J., and Otte, A. P. (2001). The Polycomb Group Protein EED Interacts with YY1, and Both Proteins Induce Neural Tissue in Xenopus Embryos. *Mol. Cel. Biol.* 21, 1360–1369. doi:10.1128/mcb.21.4.1360-1369.2001

Schuettengruber, B., Chourrout, D., Vervoort, M., Leblanc, B., and Cavalli, G. (2007). Genome Regulation by Polycomb and Trithorax Proteins. *Cell* 128, 735–745. doi:10.1016/j.cell.2007.02.009

Scott, C. L., Gil, J., Hernando, E., Teruya-Feldstein, J., Narita, M., Martínez, D., et al. (2007). Role of the Chromobox Protein CBX7 in Lymphomagenesis. *Proc. Natl. Acad. Sci.* 104, 5389–5394. doi:10.1073/pnas.0608721104

Sepe, R., Formisano, U., Federico, A., Forzati, F., Bastos, A. U., D'Angelo, D., et al. (2015). CBX7 and HMGA1b Proteins Act in Opposite Way on the Regulation of the SPP1 Gene Expression. *Oncotarget* 6, 2680–2692. doi:10.18632/oncotarget.2777

Simhadri, C., Gignac, M. C., Anderson, C. J., Milosevich, N., Dheri, A., Prashar, N., et al. (2016). Structure-Activity Relationships of Cbx7 Inhibitors, Including Selectivity Studies against Other Cbx Proteins. *ACS Omega* 1, 541–551. doi:10.1021/acsomega.6b00120

Su, W., Han, H. H., Wang, Y., Zhang, B., Zhou, B., Cheng, Y., et al. (2019). The Polycomb Repressor Complex 1 Drives Double-Negative Prostate Cancer Metastasis by Coordinating Stemness and Immune Suppression. *Cancer Cell* 36, 139–155.e110. doi:10.1016/j.ccell.2019.06.009

Tsai, C.-C., Chien, M.-N., Chang, Y.-C., Lee, J.-J., Dai, S.-H., and Cheng, S.-P. (2019). Overexpression of Histone H3 Lysine 27 Trimethylation Is Associated with Aggressiveness and Dedifferentiation of Thyroid Cancer. *Endocr. Pathol.* 30, 305–311. doi:10.1007/s12022-019-09586-1

Walters, Z. S., Villarejo-Balcells, B., Olmos, D., Buist, T. W. S., Missiaglia, E., Allen, R., et al. (2014). JARID2 Is a Direct Target of the PAX3-FOXO1 Fusion Protein and Inhibits Myogenic Differentiation of Rhabdomyosarcoma Cells. *Oncogene* 33, 1148–1157. doi:10.1038/onc.2013.46

Wang, J., Wang, H., Li, Z., Wu, Q., Lathia, J. D., McLendon, R. E., et al. (2008). c-Myc Is Required for Maintenance of Glioma Cancer Stem Cells. *PLoS One* 3, e3769. doi:10.1371/journal.pone.0003769

Wang, W., Qin, J.-J., Voruganti, S., Nag, S., Zhou, J., and Zhang, R. (2015). Polycomb Group (PcG) Proteins and Human Cancers: Multifaceted Functions and Therapeutic Implications. *Med. Res. Rev.* 35, 1220–1267. doi:10.1002/med.21358

Wu, J. I., Lessard, J., and Crabtree, G. R. (2009). Understanding the Words of Chromatin Regulation. *Cell* 136, 200–206. doi:10.1016/j.cell.2009.01.009

Wu, W., Zhou, X., Yu, T., Bao, Z., Zhi, T., Jiang, K., et al. (2017). The Malignancy of miR-18a in Human Glioblastoma via Directly Targeting CBX7. *Am. J. Cancer Res.* 7, 64–76.

Yan, L., Zhang, Z., Yin, X., and Li, Y. (2020). lncRNA NEAT1 Facilitates Cell Proliferation, Invasion and Migration by Regulating CBX7 and RTCB in Breast Cancer. *Onco Targets Ther.* 13, 2449–2458. doi:10.2147/ott.s240769

Yap, K. L., Li, S., Muñoz-Cabello, A. M., Raguz, S., Zeng, L., Mujtaba, S., et al. (2010). Molecular Interplay of the Noncoding RNA ANRIL and Methylated Histone H3 Lysine 27 by Polycomb CBX7 in Transcriptional Silencing of INK4a. *Mol. Cel.* 38, 662–674. doi:10.1016/j.molcel.2010.03.021

Ying, H., Elpek, K. G., Vinjamoori, A., Zimmerman, S. M., Chu, G. C., Yan, H., et al. (2011). PTEN Is a Major Tumor Suppressor in Pancreatic Ductal Adenocarcinoma and Regulates an NF-Kb-Cytokine Network. *Cancer Discov.* 1, 158–169. doi:10.1158/2159-8290.cd-11-0031

Yu, T., Wu, Y., Hu, Q., Zhang, J., Nie, E., Wu, W., et al. (2017). CBX7 Is a Glioma Prognostic Marker and Induces G1/S Arrest via the Silencing of CCNE1. *Oncotarget* 8, 26637–26647. doi:10.18632/oncotarget.15789

Zhang, X.-W., Zhang, L., Qin, W., Yao, X.-H., Zheng, L.-Z., Liu, X., et al. (2010). Oncogenic Role of the Chromobox Protein CBX7 in Gastric Cancer. *J. Exp. Clin. Cancer Res.* 29, 114. doi:10.1186/1756-9966-29-114

Zhang, Z., Bu, X., Chen, H., Wang, Q., and Sha, W. (2016). Bmi-1 Promotes the Invasion and Migration of colon Cancer Stem Cells through the Downregulation of E-Cadherin. *Int. J. Mol. Med.* 38, 1199–1207. doi:10.3892/ijmm.2016.2730

Zhao, Y., Liu, X. L., Huang, J. H., Yin, A. J., and Zhang, H. (2020). MicroRNA-18a Suppresses Ovarian Carcinoma Progression by Targeting CBX7 and Regulating ERK/MAPK Signaling Pathway and Epithelial-To-Mesenchymal Transition. *Eur. Rev. Med. Pharmacol. Sci.* 24, 5292–5302. doi:10.26355/eurrev_202005_21311

Zhu, X., Qin, M., Li, C., Zeng, W., Bei, C., Tan, C., et al. (2019). Downregulated Expression of Chromobox Homolog 7 in Hepatocellular Carcinoma. *Genet. Test. Mol. Biomarkers* 23, 348–352. doi:10.1089/gtmb.2018.0293

Conflict of Interest: The authors declare that the research was conducted in the absence of any commercial or financial relationships that could be construed as a potential conflict of interest.

Publisher's Note: All claims expressed in this article are solely those of the authors and do not necessarily represent those of their affiliated organizations, or those of the publisher, the editors and the reviewers. Any product that may be evaluated in this article, or claim that may be made by its manufacturer, is not guaranteed or endorsed by the publisher.

frontiers in Cell and Developmental Biology

REVIEW
published: 07 October 2021
doi: 10.3389/fcell.2021.740303

The Role of MicroRNAs in Therapeutic Resistance of Malignant Primary Brain Tumors

Ilgiz Gareev[1†], Ozal Beylerli[1†], Yanchao Liang[2,3†], Huang Xiang[2,3], Chunyang Liu[2,3], Xun Xu[2,3], Chao Yuan[2,3], Aamir Ahmad[4] and Guang Yang[2,3*]*

[1] Central Research Laboratory, Bashkir State Medical University, Ufa, Russia, [2] Department of Neurosurgery, The First Affiliated Hospital of Harbin Medical University, Harbin, China, [3] Institute of Brain Science, Harbin Medical University, Harbin, China, [4] Interim Translational Research Institute, Academic Health System, Hamad Medical Corporation, Doha, Qatar

OPEN ACCESS

Edited by:
Ata Abbas,
Case Western Reserve University, United States

Reviewed by:
Mohd Wasim Nasser, University of Nebraska Medical Center, United States
Maria Braoudaki, University of Hertfordshire, United Kingdom

***Correspondence:**
Guang Yang
yangguang1227@163.com
Aamir Ahmad
aahmad9@hamad.qa

[†] *These authors have contributed equally to this work*

Specialty section:
This article was submitted to Epigenomics and Epigenetics, a section of the journal Frontiers in Cell and Developmental Biology

Received: *12 July 2021*
Accepted: *17 September 2021*
Published: *07 October 2021*

Citation:
Gareev I, Beylerli O, Liang Y, Xiang H, Liu C, Xu X, Yuan C, Ahmad A and Yang G (2021) The Role of MicroRNAs in Therapeutic Resistance of Malignant Primary Brain Tumors. Front. Cell Dev. Biol. 9:740303. doi: 10.3389/fcell.2021.740303

Brain tumors in children and adults are challenging tumors to treat. Malignant primary brain tumors (MPBTs) such as glioblastoma have very poor outcomes, emphasizing the need to better understand their pathogenesis. Developing novel strategies to slow down or even stop the growth of brain tumors remains one of the major clinical challenges. Modern treatment strategies for MPBTs are based on open surgery, chemotherapy, and radiation therapy. However, none of these treatments, alone or in combination, are considered effective in controlling tumor progression. MicroRNAs (miRNAs) are 18–22 nucleotide long endogenous non-coding RNAs that regulate gene expression at the post-transcriptional level by interacting with 3′-untranslated regions (3′-UTR) of mRNA-targets. It has been proven that miRNAs play a significant role in various biological processes, including the cell cycle, apoptosis, proliferation, differentiation, etc. Over the last decade, there has been an emergence of a large number of studies devoted to the role of miRNAs in the oncogenesis of brain tumors and the development of resistance to radio- and chemotherapy. Wherein, among the variety of molecules secreted by tumor cells into the external environment, extracellular vesicles (EVs) (exosomes and microvesicles) play a special role. Various elements were found in the EVs, including miRNAs, which can be transported as part of these EVs both between neighboring cells and between remotely located cells of different tissues using biological fluids. Some of these miRNAs in EVs can contribute to the development of resistance to radio- and chemotherapy in MPBTs, including multidrug resistance (MDR). This comprehensive review examines the role of miRNAs in the resistance of MPBTs (e.g., high-grade meningiomas, medulloblastoma (MB), pituitary adenomas (PAs) with aggressive behavior, and glioblastoma) to chemoradiotherapy and pharmacological treatment. It is believed that miRNAs are future therapeutic targets in MPBTs and such the role of miRNAs needs to be critically evaluated to focus on solving the problems of resistance to therapy this kind of human tumors.

Keywords: malignant primary brain tumors, miRNAs, resistance, therapy, oncogenesis, exosomes

INTRODUCTION

Malignant primary brain tumors (MPBTs) are one of the most difficult to treat types of tumors, resulting in significant morbidity and mortality in both children and adults. The most common MPBTs are glioblastomas, high-grade meningiomas, medulloblastoma (MB), and pituitary adenomas (PAs) with aggressive behavior, as aggressive prolactin PAs (Schiff and Alyahya, 2020; Thakkar et al., 2021). For example, for patients with glioblastoma or MB, the overall survival remains is poor, with conventional therapies such as radio- and chemotherapy only providing marginal benefits to patient survival. Therefore, new strategies are needed to overcome the barriers to successful treatment (Thakkar et al., 2021).

Over the past decades, significant progress has been achieved in the study of tumor biology, the study of the mechanisms of control of tumor metastasis, apoptosis, invasion, angiogenesis, and proliferation of tumor cells. These data were obtained by studying the cellular composition and microenvironment of tumors, various intracellular signaling pathways, and molecular processes of oncogenesis (Richardson et al., 2020). MicroRNAs (miRNAs) are 18–22 nucleotide endogenous non-coding RNAs that regulate gene expression at the post-transcriptional level by interacting with 3′-untranslated regions (3′-UTR) of mRNA-targets (Lu and Rothenberg, 2018; **Figure 1**). It is estimated that more than 60% of all human protein-coding genes are directly regulated by miRNAs (Ha and Kim, 2014; Dexheimer and Cochella, 2020). It has been proven that miRNAs are involved in various biological processes, including the cell cycle, apoptosis, cell proliferation, and differentiation (Rupaimoole and Slack, 2017; Saliminejad et al., 2019). In addition, miRNAs play a role in the oncogenesis of various human tumors, including brain tumors (Bertoli et al., 2015; Qadir and Faheem, 2017; Ali Syeda et al., 2020; Balachandran et al., 2020). Recently, most research has focused on the role of miRNAs in resistance to malignant human tumors therapy. In MPBTs, the role of miRNAs in radio- and chemotherapy resistance is an attractive area of research and is expected to lead to the development of novel treatment strategies. This review will focus on differential expression of miRNAs in MPBTs (e.g., high-grade meningiomas, MB, PAs with aggressive behavior, and glioblastoma) with their gene-targets and their potential role in resistance to radio- and chemotherapy, and to pharmacological treatment.

MICRORNAs DYSREGULATION IN MALIGNANT PRIMARY BRAIN TUMORS

MicroRNAs perform an important function in the complex mechanism of regulation of gene activity, since they determine the qualitative and quantitative composition of transcripts and proteins necessary for the development of individual tissues, organs and the whole organism. A growing body of evidence points to the importance of miRNAs deregulation in the initiation and progression of tumors, where they can act as oncogenic miRNAs (oncomiRs) or tumor-suppressor miRNAs, depending on the cellular function of their gene-targets (Liu et al., 2014). Moreover, the activation or suppression of specific miRNA families is the mechanism by which oncogenes such as epidermal growth factor receptor (*EGFR*) and *MET* or tumor suppressor genes such as phosphatase and tensin homolog deleted on chromosome 10 (*PTEN*), adenomatous polyposis coli (*APC*), and breast cancer type 1/2 (*BRCA1/2*) induce or inhibit oncogenesis (Zhang et al., 2007; Lee and Muller, 2010).

To date, a lot of evidence has been collected about the aberrant expression of miRNAs in various tumors, particular, malignant (Van Roosbroeck and Calin, 2017). It was shown that miRNAs control the expression of genes of regulatory pathways that play a key role in tumor development, control apoptosis and proliferation of tumor cells, tumor growth in response to DNA damage and repair, angiogenesis and response to hypoxia, the interaction of tumor cells with the microenvironment (Rupaimoole and Slack, 2017; Van Roosbroeck and Calin, 2017). A number of researchers isolate miRNAs directly related to individual processes in a tumor, or stages of development, of a disease (Vishnoi and Rani, 2017). Many miRNAs are involved in key signaling pathways associated with the regulation of the cell cycle and apoptosis. In one of the latest studies, Allahverdi et al. (2020) found that adipose-derived mesenchymal stem cells (AD-MSCs) delivering miR-4731 induces apoptosis and cell cycle arrest in the glioblastoma cell line. Another study provided evidence that miR-221-3p reduces MB cell proliferation by inducing apoptosis and G0/G1 arrest by suppressing eukaryotic translation initiation factor 5A-2 (*EIF5A2*) (Yang et al., 2019).

There is also a separate group of miRNAs associated with the metastatic activity of tumors – metastamiRs. Moreover, among such miRNAs, some promote (miR-9, miR-210, miR-21, miR-218, etc.) tumor metastasis, while others (miR-145, miR-7, miR-146-a, etc.), on the contrary, suppress it (Alsidawi et al., 2014; Lu et al., 2015; Lima et al., 2017; Ji et al., 2018; Maryam et al., 2021).

In recent years, thanks to advances in molecular oncology, it has been possible to decipher some of the mechanisms of oncogenesis and to determine the signs of a malignant phenotype, one of which is angiogenesis. Malignant tumors requires more oxygen and nutrients to grow (Viallard and Larrivée, 2017). The solution to this issue is to trigger the mechanism of angiogenesis in the tumor. Vascular endothelial growth factor (*VEGF*) is extremely important for the formation of an adequate functioning vascular system during embryogenesis and in the early postnatal period, but it also plays an important role in pathological angiogenesis. In many types of tumors, increased *VEGF* expression correlates with poor prognosis, including aggressive tumor growth, recurrence, metastasis, and decreased survival (Melincovici et al., 2018). In addition, *VEGF* expression correlates with a decrease in the density of the microvascular network in the malignant brain tumors, which in itself serves as an indicator of the prognosis of vascular rupture, followed by hemorrhage in the tumor bed (Apte et al., 2019). To date, a number of miRNAs have been identified that are highly expressed in endothelial cells (ECs) and/or are activated under hypoxic conditions. Among these miRNAs, it is worth noting miR-126, which is specifically expressed in the ECs and is a key regulator of the integrity of the vascular wall and angiogenesis in various tumors, including brain tumors (Fish et al., 2008).

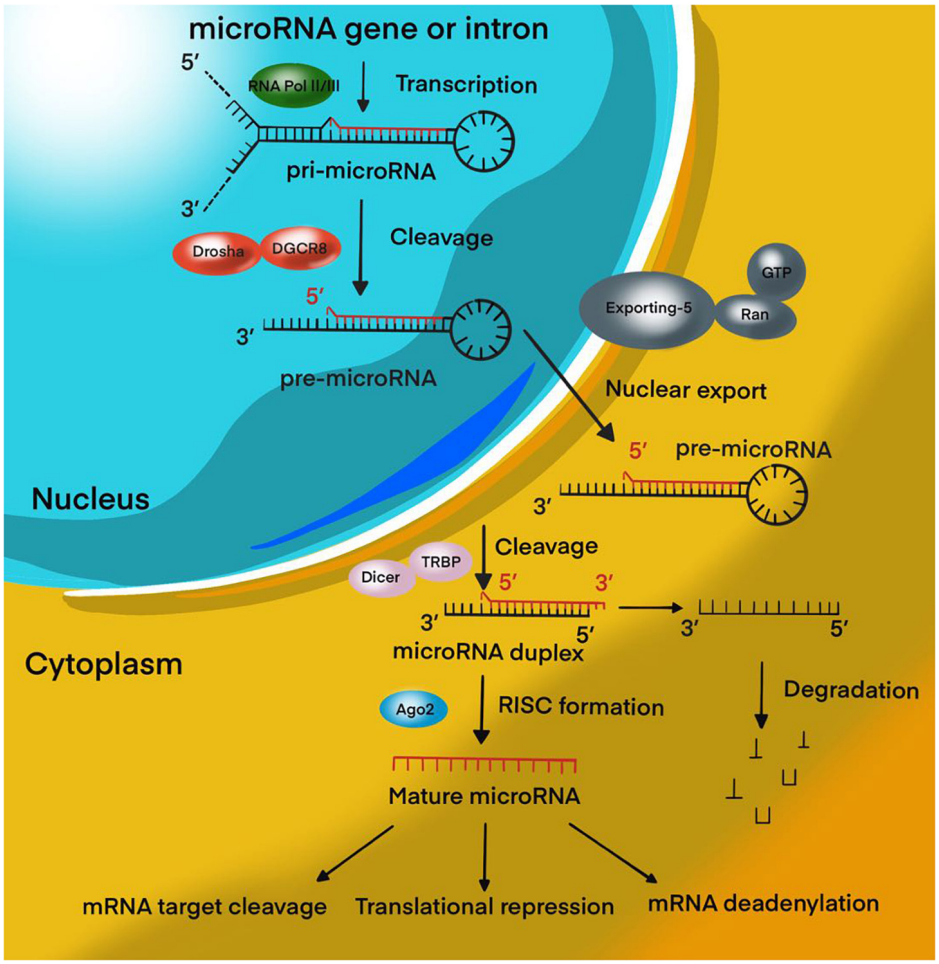

FIGURE 1 | MiRNA biogenesis pathway. Overview schematic representation of canonical miRNA biogenesis pathway.

Smits et al. (2012) showed there is significant low-expression of miR-125b in ECs co-cultured with U87 glioblastoma line cells. Moreover, the authors demonstrated that miRNA-125b inhibits angiogenic processes by directly regulating *Myc*-associated zinc finger protein (*MAZ*)/*VEGF* signaling pathway expression. It is known that, *MAZ*-binding sites are located in the promoter regions of angiogenic factor *VEGF*.

Xiao et al. (2016) demonstrated that miR-566 was overexpressed in glioblastoma *in vitro* and *in vivo*, and inhibition of miR-566 was able to suppress the invasion and migration of glioblastoma cells, and angiogenesis via the *VEGF*/Von Hippel–Lindau tumor suppressor (*VHL*) pathway. This suggests that miR-566 may function as an oncogene, and therefore, miR-566 may be considered a novel therapeutic target of glioblastoma (Xiao et al., 2016).

There is evidence that some miRNAs can participate in the processes of malignant transformation in benign brain tumors. Brain tumors of different histology are characterized by specific miRNAs expression profiles associated with the clinical and pathological properties of the tumor (Van Roosbroeck and Calin, 2017). For instance, miR-21 makes it possible to distinguish between the main histological types of meningioma, for which miR-21 expression showed a significant increase in World Health Organization (WHO) grade 2 and 3 lesions as compared to WHO grade 1 lesions (Katar et al., 2017).

Currently, there is an active search for new miRNAs and their target genes involved in other important processes associated with oncogenesis (and not only), for example, the control of the balance of self-renewal and differentiation of stem cells, epithelial-mesenchymal transition (EMT), regulation of the immune response, the relationship of the tumor with the microenvironment, etc.

It should also be borne in mind that the reason for the change in the expression of miRNA may be a violation of the expression of proteins involved in miRNA biogenesis. It is known that the loss or insufficient expression of Drosha, Dicer, and TRBP can lead to the development of a tumor process (Olejniczak et al., 2018). Several groups showed impaired expression of Drosha and Dicer in glioblastoma, pineoblastoma, and neuroblastoma, all of which correlated with a poor prognosis of survival (Lin et al., 2010; Mansouri et al., 2016; de Kock et al., 2020). Decreased expression of these proteins can be mediated by mutations or

epigenetic inactivation of their genes. In addition, mutations in Dicer can lead to impaired recognition of miRNA precursors and a change in the balance of strands. Argonaute 2 (Ago2) and GW proteins that act as direct partners of miRNAs are often susceptible to somatic mutations in glioblastoma, which are accompanied by a high level of instability of microsatellite tumor DNA (Li S. et al., 2014; Li Z. et al., 2019). Disruption of the transport of pre-miRNAs into the cytoplasm can also lead to a decrease in their expression. A mutation in the exportin-5 gene, leading to the synthesis of a truncated protein that is unable to recognize pre-miRNAs, causes a decrease in the level of mature miRNAs in a number of tumors (Wu et al., 2018).

A number of oncogenic proteins can directly interfere with miRNA biogenesis in tumors. Thus, wild and mutant forms of p53 are involved in the biogenesis of a number of miRNAs, primarily miR-34 (Zhang et al., 2019). It is known that mutant forms of p53 can inhibit Drosha activity and prevent the formation of pre-miRNA (Garibaldi et al., 2016). Transforming growth factor beta (*TGF*-β) affects the processing of miRNA through the binding of effector proteins to the microprocessor complex and pri-miRNA. YES-associated protein 1 (*YAP1*), one of the components of the Hippo pathway, regulates the activity of the microprocessor complex depending on the density of cells in culture (Ruan et al., 2016). Tumor suppressor protein *BRCA1* also stimulates the activity of the microprocessor complex (Lee and Muller, 2010). Under hypoxic conditions, activated *EGFR* can phosphorylate Ago2, inhibiting its interaction with Dicer and decreasing the level of activity of miRNA effector systems (Shen et al., 2013). In addition, the interaction of p53 with Ago2 leads to a change in the spectrum of miRNAs associated with it, leading to the formation of complexes carrying tumor suppressor miRNAs, for example, let-7 (Krell et al., 2016).

Thus, miRNAs are one of the key factors in the development of malignant forms of brain tumors, both as drivers of malignant transformation and as a victim of the deregulation of cellular regulatory systems. The close relationship of miRNAs with MPBTs has led to the fact that they are currently being actively studied (**Table 1**; Grunder et al., 2011; Kliese et al., 2013; Asuthkar et al., 2014; Wang et al., 2015; Wei et al., 2015; Yu et al., 2016; Zheng et al., 2017; Xu et al., 2018; Xue et al., 2019; Hou et al., 2020; Muñoz-Hidalgo et al., 2020; Negroni et al., 2020; Song et al., 2020), including with the aim of creating diagnostic and therapeutic systems designed to increase the effectiveness of treatment of this disease.

MICRORNAs IN RESISTANCE TO CHEMORADIOTHERAPY AND PHARMACOLOGICAL TREATMENT

Resistance to therapy of brain tumors is an important problem in modern neurosurgery. There are two main mechanisms for the emergence of radio- and chemotherapy resistance: (1) activation of specific signaling pathways responsible for the "neutralization" of the chemotherapy drug and ionizing radiation in the tumor cell. Such these signaling pathways include phosphoinositide 3-kinases/protein kinase B (*PI3K/AKT*) è mitogen-activated protein kinase (*MAPK*)/*ERK*; and 2) violation of the mechanism of cell death under the influence of chemotherapy and ionizing radiation (Cao et al., 2019; Kapoor et al., 2020). This mechanism includes the blocking of apoptosis with p53 mutations, overexpression of B-cell lymphoma 2 (*Bcl-2*), a decrease in the expression of cluster of differentiation 95 (CD95) (Kapoor et al., 2020). It is now known that miRNAs can control the regulation of target genes or signaling pathways involved in malignant tumor resistance to therapy, including MPBTs. Among these miRNAs, miR-21 is the most studied in glioblastoma. MiR-21 is one of the important miRNAs involved in glioblastoma oncogenesis. A large number of studies indicated that miR-21 could affect a variety of cellular and molecular pathways. It has been showing that deregulation of miR-21 could be associated with resistance to radio- and chemotherapy of glioblastoma (**Figure 2**; Lan et al., 2015; Masoudi et al., 2018; Buruiană et al., 2020). In this article, we will consider current knowledge about the role of miRNAs in the mechanisms of resistance to therapy in MPBTs. In addition, a summary of the role of some miRNAs in therapy resistance by targeting their gene targets is shown in **Table 2** (Pannuru et al., 2014; Dénes et al., 2015; Abdelfattah et al., 2018; Chen et al., 2018; Li J. et al., 2019; Bogner et al., 2020; Hu et al., 2020; Sun et al., 2020; Zhao C. et al., 2020; Cardoso et al., 2021) and **Table 3** (Lee et al., 2014; Li W. et al., 2014; Huynh et al., 2015; Wu et al., 2015; Yang F. et al., 2017; Zhang Q. et al., 2020).

Glioblastoma

Glioblastoma is the most aggressive primary brain tumor and usually has a poor prognosis. Thus, the median survival rate of patients with glioblastoma after surgical resection and standard radio- and chemotherapy is no more than 12–15 months, while the 2-year survival rate for this group of patients varies from 26 to 33% (Wirsching et al., 2016; Schiff and Alyahya, 2020). Angiogenesis is the most important pathophysiological mechanism for the growth and progression of glioblastoma due to the active development of the microvascular network. The accelerated development of the microvascular network in glioblastoma occurs due to the synthesis of a large number of growth factors by tumor cells, including the *VEGF* family, placental growth factor (*PLGF*), platelet-derived growth factor (*PDGF*), and fibroblast growth factor (*FGF*) (Le Rhun et al., 2019). It should be noted that the microvascular network of glioblastoma is characterized by a high degree of tortuosity, increased permeability, as well as an increased diameter of the vascular lumen, and a thickened basement membrane (Ahir et al., 2020). It is believed that these features of the microvascular network of glioblastoma increase the hypoxia of the tumor tissue, thereby reducing the effectiveness of the use of cytotoxic drugs. It is for this reason that the development and use of anti-angiogenic drugs seem to be one of the most promising methods of targeted treatment of glioblastoma patients. The effectiveness of the use of anti-angiogenic drugs in the treatment of glioblastoma has been clearly demonstrated in a number of clinical studies (Sousa et al., 2019; Schulte et al., 2020). However, the widespread use of anti-angiogenic drugs in clinical practice has led to the development of glioblastoma resistance to drugs of this group. The formation of drug resistance of glioblastoma to anti-angiogenic drugs is

TABLE 1 | The most relevant studies to study the role of miRNAs in the oncogenesis of malignant primary brain tumors (MPBTs).

Tumor type	miRNA	Gene-target	Biological function	Regulation	Phenotype	References
Glioblastoma	miR-191	*NDST1*	Promote tumor growth and cells migration	Up	OncomiR	Xue et al., 2019
Glioblastoma	miR-200c	*ZEB1*	Inhibit tumor growth and cells migration	Down	Tumor suppressor	Muñoz-Hidalgo et al., 2020
Glioblastoma	miR-449b-5p	*WNT2B/Wnt*/β-catenin	Inhibits tumor cells proliferation, invasion, and migration	Down	Tumor suppressor	Hou et al., 2020
Atypical and anaplastic meningiomas	miR-145	*COL5A1*	Inhibit motility and proliferation of tumor cells	Down	Tumor suppressor	Kliese et al., 2013
Anaplastic meningioma	miR-195	*FASN*	Inhibit proliferation, migration, and invasion	Down	Tumor suppressor	Song et al., 2020
Atypical and anaplastic meningiomas	miR-497∼195 cluster	*GATA-4*	Decreases tumor cell viability	Down	Tumor suppressor	Negroni et al., 2020
Atypical and anaplastic meningiomas	miR-224	*ERG2*	Promote tumor growth and reduce apoptosis of cells. Associated with poor prognosis	Up	OncomiR	Wang et al., 2015
MB	miR-21	*PDCD4*	Decrease the motility of tumor cells and reduce their migration	Up	OncomiR	Grunder et al., 2011
MB	miR-211	*PI3K/AKT* and *mTOR*	Inhibit growth, migration and invasion	Down	Tumor suppressor	Xu et al., 2018
MB	miR-494	*MMP-9* and *SDC1*	Reduce tumor growth and angiogenesis	Down	Tumor suppressor	Asuthkar et al., 2014
Invasive PA (NFA, GH, ACTH, PRL)	miR-106b	*PTEN-PI3K/AKT/MMP-9*	In tumor cells induces invasive properties	Up	OncomiR	Zheng et al., 2017
Invasive PA (NFA, GH, ACTH, PRL)	miR-26a	*PLAG1*	In tumor cells induces invasive properties. Associated with poor prognosis	Up	OncomiR	Yu et al., 2016
Pituitary carcinoma	miR-20a, miR-106b and miR-17-5p	*PTEN* and *TIMP2*	Activation of invasive properties and migration in a tumor cells. Carcinoma metastasis	Up	OncomiR	Wei et al., 2015

miR, microRNA; MB, medulloblastoma; PA, pituitary adenoma; miR, microRNA; NFA, non-functioning adenoma; GH, growth hormone-secreting adenoma; FSH, follicle-stimulating hormone adenoma; LH, luteinizing hormone-secreting adenoma; ACTH, adrenocorticotropic hormone-secreting adenoma; PRL, prolactin-secreting adenoma; NDST1, Bifunctional heparan sulfate N-deacetylase/N-sulfotransferase 1; ZEB1, E-box-binding homeobox 1; WNT2B, Wnt family member 2B; COL5A1, collagen type V alpha 1 chain; FASN, fatty acid synthase; GATA-4, GATA binding protein 4; Early growth response 2; MMP-9, matrix metallopeptidase 9; PDCD4, programmed cell death 4; AKT, protein kinase B; mTOR, mammalian target of rapamycin; SDC1, Syndecan 1; PTEN, tensin homolog deleted on chromosome 10; PI3K, phosphoinositide 3-kinases; PLAG1, pleomorphic adenoma gene 1; TIMP2, tissue inhibitor of metalloproteinases 2.

associated with molecular and cellular features of the behavior of tumor cells, including with the participation of certain miRNAs (Zeng et al., 2018b).

Autophagy is one of the main mechanisms of tumor resistance. It should be noted that autophagy is the main cellular defense mechanism in the development of hypoxic conditions, which does not require tissue and extracellular matrix remodeling (Kimmelman and White, 2017). As is already known, the use combination of anti-angiogenic therapy with radiotherapy leads to the development of tumor tissue hypoxia due to the disturbance of the angiogenesis process necessary for the growth and progression of the tumor (Le Rhun et al., 2019). It is generally accepted that the process of autophagy in tumor cells is aimed at the destruction of proteins and signaling molecules formed during hypoxic conditions, which leads to the preservation of intracellular structures and the leveling of the secondary effects of anti-angiogenic drugs. It is assumed that in glioblastoma, drug resistance to bevacizumab is associated with non-selective hypoxia-induced factor (*HIF*)-dependent autophagy-mediated through the activity of the protein-interacting protein 3 (*BNIP 3*) and hypoxia-inducible factor 1-alpha (*HIF1*-α) protein (Hu et al., 2012). It is known that *HIF-1*α can cause cell cycle arrest, initiating angiogenesis, and regulating cellular metabolism (Gabriely et al., 2017; Huang et al., 2019). Huang et al. identified that the expression of *HIF-1*α was increased in glioblastoma *in vitro* and *in vivo* under hypoxia (Cardoso et al., 2021). Moreover, the longer the duration of hypoxia, the higher was the expression of *HIF-1*α. However, the expression of miR-224-3p was decreased under hypoxia conditions in a time-dependent manner. Their data

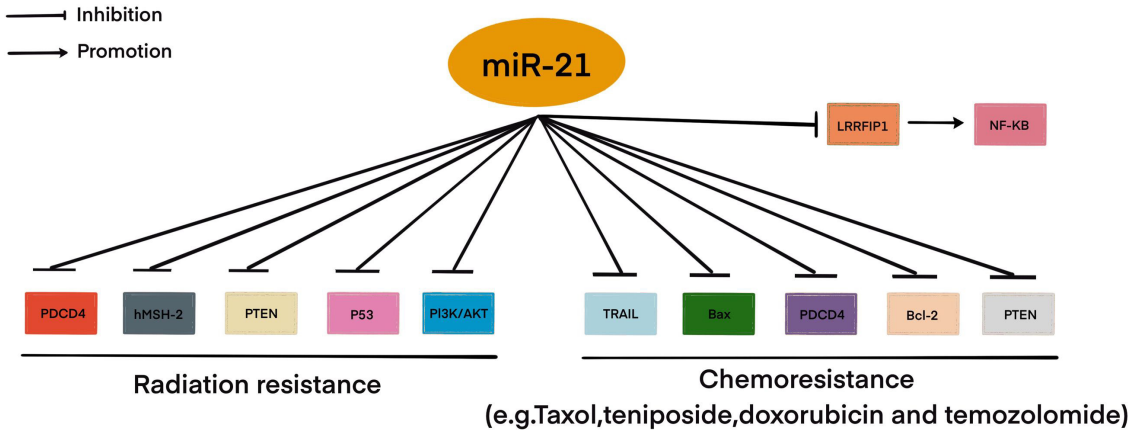

FIGURE 2 | MiR-21 involved in radio- and chemoresistance in glioblastoma. This figure shows through which signaling pathways miR-21 may be involved in resistance to therapy in glioblastoma.

TABLE 2 | MiRNAs involved in the regulation of chemotherapeutic and pharmacological drug treatment resistance in malignant primary brain tumors (MPBTs).

miRNA	Type of tumor	Type of drug	Drug	Gene-target	Mechanism	References
miR-128-3p	Glioblastoma	DNA-targeted drugs	TMZ	*c-Met/EMT* (*c-Met, PDGFRα, Notch1,* and *Slug*)	Reduces the proliferation, invasion, and migration	Zhao C. et al., 2020
miR-186	Glioblastoma	DNA-targeted drugs	Cisplatin	*YY1*	Inhibits the formation of the GIC phenotype	Li J. et al., 2019
miR-302a	Glioblastoma	Tyrosine kinase inhibitors	Cediranib	*PGK1*	Decrease glycolysis, cell growth, migration, and invasion	Cardoso et al., 2021
miR-let-7f-1	MB	DNA-targeted drugs	Cisplatin	*HMGB1*	Inhibit autophagy	Pannuru et al., 2014
miR-29c-3p	MB	DNA-targeted drugs	Cisplatin	*Bcl-2/Wnt2*	Increase apoptosis	Sun et al., 2020
miR-584-5p	MB	Tubulin inhibitors	Vincristine	*HDAC1/eIF4E3*	Cause cell cycle arrest, DNA damage, and spindle defects	Abdelfattah et al., 2018
miR-31	MB	DNA-targeted drugs	Ginsenoside Rh2	*Wnt/β-catenin*	Inhibit the proliferation and migration, and induce apoptosis	Chen et al., 2018
miR-197	Meningioma	DNA-targeted drugs	Quercetin	*Bcl-2/Bax*	Reduce tumor cell proliferation and increase apoptosis	Hu et al., 2020
miR-34a	Aggressive somatotropinoma	SSAs	Octreotide	*cAMP*	Antiproliferative effect	Bogner et al., 2020
miR-1299	Aggressive prolactinoma	DA	Bromocriptine	*FOXO1*	Promotes the synthesis and secretion of prolactin	Dénes et al., 2015

miR, MicroRNA; MB, medulloblastoma; SSAs, somatostatin analogs; DA, dopamine antagonist; TMZ, Temozolomide; EMT, epithelial-mesenchymal transition; PDGFRα, platelet-derived growth factor receptor A; YY1, Yin Yang 1; PGK1, phosphoglycerate kinase 1; HMGB1, high-mobility group protein B1; Bcl-2, B-cell lymphoma-2; Wnt2, wingless-type MMTV integration site family, member 2; HDAC1, histone deacetylase 1; IF4E3, eukaryotic translation initiation factor 4E type 3.

showed that the miR-224-3p mimic significantly suppressed the expression *HIF-1α* and inhibited cell mobility while increased chemosensitivity to Temozolomide (TMZ) of glioblastoma. In addition, the miR-224-3p mimic suppressed the expression of *VEGF* with an increased cell apoptosis rate. In another study, miR-203 could be a useful target for overcoming the radioresistance of glioblastoma by suppressing *HIF-1α* expression *in vitro* (Chang et al., 2016). However, further experiments are needed to understand the complex link between miR-203 and *HIF-1α* expression.

Medulloblastoma

Medulloblastoma is a malignant primary tumor of the posterior fossa (WHO grade 4), mainly manifested in children. MB arises in the posterior fossa, usually from the cerebellar vermis and in the roof of the fourth ventricle (Schiff and Alyahya, 2020).

TABLE 3 | Role miRNAs in regulating malignant primary brain tumors (MPBTs) radiosensitivity.

miRNA	Type of tumor	Gene-target	Regulation	Mechanism	Response	References
miR-221/222	Glioblastoma	*Akt*	Down	Inhibit tumor growth	Increase radiosensitive	Li W. et al., 2014
miR-181d	Glioblastoma	*NF-κB*	Up	Suppress tumor cell proliferation, colony formation and anchor-independent growth, as well as migration, invasion and tube formation	Increase radiosensitive	Yang F. et al., 2017
miR-124-3p	Glioblastoma	*mTOR, MAPK, TGFbeta*, and *PI3K-Akt*	Up	Inhibit tumor growth and promote apoptosis	Increase radiosensitive	Wu et al., 2015
miR-205	Glioblastoma	*GRP78, c-Myc,β-catenin* and *vimentin*	Up	Decreases tumor-sphere-formation and colony-forming abilities, inhibit migration and invasion	Increase radiosensitive	Huynh et al., 2015
miR142-3p	MB	*Sox2* and *ADCY9*	Down	Elevate the expression of miRNA decreases cancer stem-like characteristics and stemness	Increase radioresistance	Lee et al., 2014
miR-584-5p	MB	*HDAC1/eIF4E3*	Up	Cause cell cycle arrest, DNA damage, and spindle defects	Increase radiosensitive	Abdelfattah et al., 2018
miR-221/222	Meningioma	*PTEN*	Down	Inhibit tumor cell proliferation, invasive and colony formation, and promote apoptosis	Increase radiosensitive	Zhang Q. et al., 2020

miR, MicroRNA; MB, medulloblastoma; Akt, protein kinase B alpha; NF-κB, nuclear factor kappa-light-chain-enhancer of activated B cells; mTOR, mammalian target of rapamycin; MAPK, mitogen-activated protein kinase; TGF-beta, transforming growth factor beta; PI3K, phosphoinositide 3-kinases; GRP78, glucose regulatory protein 78; Sox2, SRY-Box transcription factor 2; ADCY9, adenylate cyclase 9; HDAC1, histone deacetylase 1; eIF4E3, eukaryotic translation initiation factor 4E family member 3; PTEN, phosphatase and tensin homolog deleted on chromosome 10.

MBs tend to metastasize along with the cerebrospinal fluid (CSF) pathways, which is detected in 35% of cases at the time of diagnosis. MBs are the most common malignant neoplasms of the brain in childhood and account for 15 to 30% of all primary CNS tumors in children, and about 70% of all cases are diagnosed in children under 15 years of age (Quinlan and Rizzolo, 2017). The age peak of diagnosis is between 3 and 5 years, and only 25% are patients between the ages of 20–44 (Millard and De Braganca, 2016; Quinlan and Rizzolo, 2017). Patients with MB have a poor outcome despite surgical, radio- and chemotherapy. However, the molecular mechanisms that confer sensitivity or resistance of MB to chemoradiation therapy are still unclear.

Recent evidence has implicated miRNAs in modulating chemo- and radiosensitivity in MBs (Joshi et al., 2019). It has been shown that in MB therapy there is a balance between cell cycle arrest and cell death (Kasuga et al., 2008). Melanoma-associated antigen-A (*MAGE-A*) family acts as a cell cycle regulatory protein and plays a key role in the oncogenesis and therapy resistance in MB. Kasuga et al. (2008) demonstrate that knockdown of *MAGE-A* increases apoptosis and sensitizes MB cells to chemotherapeutic agents such as cisplatin and etoposide. This finding supports the hypothesis that knockdown of *MAGE-A* genes increases the susceptibility of MB cells to cisplatin and etoposide, potentially by accumulating cells in the S phase. In contrast, Sheamal et al. showed that miR-34a directly targets the *MAGE-A* family (*MAGE-A2, MAGE-A3, MAGE-A6,* and *MAGE-A12*), disengaging p53 from *MAGE-A*–mediated repression (Weeraratne et al., 2011). Moreover, an important consequence of this is a positive feedback loop that sensitizes MB cells to cisplatin and etoposide via delayed G2/M progression and increased tumor cells apoptosis.

There is evidence that phosphatase and tensin homolog deleted on chromosome 10 (*PTEN*) dysfunction plays a crucial role in the development and progression MB. *PTEN* plays important roles in many cellular processes, including cell-cycle progression and apoptosis (Tolonen et al., 2020). Li et al. (2015) reported the upregulation of miR-106b in MB. In their study, the suppression of miR-106b inhibited cell proliferation, migration and invasion, and anchorage-independent growth, tumorsphere formation. In addition, downregulation of miR-106b suppressed the tumor growth by promoting G1 arrest and apoptosis. Besides, *PTEN* can be modulated by miR-106 family in various human cancers. For instance, miR-106b caused cell radio resistance in colorectal cancer via the *PTEN/PI3K/AKT* pathways (Zheng et al., 2015). MiR-106a induced cisplatin resistance via the *PTEN*/*AKT* pathway in gastric cancer cells (Fang et al., 2013). However, the role of miR-106b in therapy resistance of MB is still largely unknown. Nevertheless, this is an excellent opportunity to continue research on the role of miR-106b directly targeted *PTEN* in therapy resistance of MB.

Pituitary Adenomas With Aggressive Behavior

Among the tumors of the chiasmatic-sellar region, the most common are PAs, accounting for about 18% of all tumors of this localization. In the overwhelming majority of cases, these are benign neoplasms, characterized by slow growth rates and progression (Schiff and Alyahya, 2020). However, among them, there are PAs with aggressive behavior, which exhibits the properties of resistance to traditional treatment methods (Lake et al., 2020). Among PAs, the first place is occupied by tumors accompanied by the syndrome of hyperprolactinemia –

prolactinomas, as well as non-functioning (hormonally inactive) PAs, each approximately 40%. The next most frequent is somatotropinomas, about 13–15%, accompanied by symptoms of acromegaly. Gonadotropin-secreting PAs, ACTH-secreting PAs, GH-secreting PAs, mixed forms are less common. In the age range, PAs occupy a period from 30 to 50 years, which is the working age (Elsarrag et al., 2020; Lake et al., 2020). In connection with all of the above, PAs, their diagnosis, and especially, treatment are important medical and social problems.

The main methods of treatment for PAs are surgical removal of the tumor and pharmacological treatment and their combinations. Radio- and chemotherapy are used, as a rule, when it is impossible to perform a surgical intervention or when it is at high risk, and when the tumor is highly aggressive (Fleseriu and Popovic, 2020). Since there is no clear definition and availability of reliable prognostic markers, PAs with aggressive behavior are difficult to identify at initial presentation, and therefore the primary therapeutic approach is no different from other PAs depending on the type of tumor (Mete and Lopes, 2017). Resistance to drugs presenting as escalating hormone levels and/or tumor growth where can be an early indicator of aggressiveness. There are many studies examining changes in miRNA expression in PAs. Among them are studies on their role in drug resistance in various types of PAs (Ciato and Albani, 2020). However, there is no evidence base on their potential role in resistance to chemo- and radiotherapy in patients with PAs with aggressive behavior and pituitary carcinomas. It is possible to suggest from previous studies which miRNAs and through which signaling pathways can participate in the mechanisms of resistance to chemo- and radiotherapy. For instance, in a recent study, Wang Z. et al. (2019) successfully identified one key target gene, *EGFR*, and two crucial miRNAs, miR-489 and miR-520b, associated with aggressiveness of prolactinomas based on bioinformatics analysis. It is also known that *EGFR* is one of the most frequently altered oncogenes in tumors, which important role in therapy resistance and is often associated with a negative prognosis (Lee and Muller, 2010).

Prolactinoma is the most commonly seen secretory tumor of pituitary glands. More than 90% of prolactinomas are microprolactinomas (<1.0 cm), while the rest are macroprolactinomas (≥1.0 cm). Macroprolactinomas account for approximately half of all functioning pituitary macroadenomas (Huynh et al., 2021). Without a doubt, prolactinoma is an innocent tumor of its kind. Prolactinomas are more aggressive and are characterized by increased proliferative ability; they can turn into recurrent, invasive giant prolactinomas (Castinetti et al., 2021). Most patients with prolactinomas respond to standard doses of dopamine agonists (DA), while the rest of the patients remain resistant to therapy. In this case, the term is used – resistance to DA, the inability to achieve normalization of prolactin levels, and tumor reduction by 50%, while taking the maximum tolerated dosage of the drug (Giraldi and Ioachimescu, 2020). To overcome resistance, it is necessary to increase the dose of drugs, in this regard, the risk of developing side effects, such as liquorrhea, headaches, acute psychosis, etc., (Molitch, 2020; Vermeulen et al., 2020; Castinetti et al., 2021). Surgical intervention is indicated in case of intolerance or resistance to DA, or with a persistent increase in tumor size with the development of neuro-ophthalmic symptoms, or if there is a rapid loss of vision or cranial nerve paralysis due to intratumoral hemorrhage (Panigrahi et al., 2020). However, complete surgical removal of a giant tumor is rarely performed due to the technical complexity and the greater risk of side effects. Radio- and chemotherapy have a limited role in the treatment of giant prolactinomas; on the one hand, because of its dubious chemotherapy effectiveness and, on the other hand, because of the complications that appear during tumor irradiation (Iglesias et al., 2018). Therefore, a thorough and deeper understanding of the molecular mechanisms underlying drug resistance of PAs with aggressive behavior like aggressive prolactinomas are urgently needed to find potential new targets for improving therapeutic efficacy. For instance, Jian et al. (2019) demonstrated that miR-145-5p was greatly downregulated in bromocriptine-resistant prolactinoma cell lines and tissues *in vitro* and *in vivo*. In addition, transfer miR-145 mimic into tumor cells and revealed that overexpression of miR-145-5p increased sensitivity for bromocriptine markedly. In conclusion, identification of tumor protein, translationally controlled 1 (*TPT1*) as a direct target gene of miR-145-5p. In another study, miR-93-5p was related to fibrosis and was involved in the bromocriptine -resistance mechanisms in prolactinoma by regulating the transforming growth factor beta 1/mothers against decapentaplegic homolog 3 (*TGF-β1/Smad3*) signaling pathway (Hu et al., 2019). Interesting that previous studies showed that TGF-β1 promotes the synthesis and secretion of collagen fibers in fibroblasts and that the TGF-β1/Smad3 signaling pathway is involved in the drug-resistance mechanism of prolactinoma by increasing fibrosis through interactions with fibroblasts (Hu et al., 2018).

High-Grade Meningiomas

Meningiomas are common tumors of the CNS, originating from the meninges of the brain or spinal cord. Most meningiomas are benign tumors characterized by slow growth and are histologically WHO Grade 1 (Schiff and Alyahya, 2020). However, high-grade meningiomas [atypical (WHO Grade 2) and anaplastic (WHO Grade 3)] exhibit more aggressive biological behavior and are clinically associated with a high risk of recurrence and a less favorable prognosis (Maier et al., 2020). Atypical and anaplastic meningiomas account for about 30% of the total number of intracranial meningiomas (Maier et al., 2020). Atypical and anaplastic meningiomas are often accompanied by invasive growth into the surrounding anatomical structures, which is the main factor limiting the radical nature of the surgery and increasing the frequency of recurrence. The problem of diagnosis and treatment, including resistance to radio- and chemotherapy, of patients with high-grade meningiomas, is still far from its final solution, which cannot but affect the long-term results and the level of mortality and mortality (Zhao L. et al., 2020). A better understanding of the molecular mechanisms involved in meningioma oncogenesis may lead to the identification of new therapeutic targets responsible for therapeutic resistance. Numerous studies have identified multiple signaling pathways involved in the therapeutic resistance of

high-grade meningiomas and have suggested many important molecular targets for the development of new drugs for the treatment of high-grade meningiomas that are resistant to radio- and chemotherapy. In particular, growth factors, such as *PDGF*, epidermal growth factor (*EGF*) and their receptors, and cytokines, such as *TGF*-β, serve as major factors in high-grade meningiomas leading to therapeutic resistance (Birzu et al., 2020; Shao et al., 2020).

Unfortunately, studies on the role of miRNAs in the mechanisms of resistance to therapy in meningiomas are limited. For instance, microarray analysis, using the atypical meningioma tissue samples of 55 patients (43 from the radiosensitive and 12 from the radioresistant group), indicated that 14 miRNAs were significantly dysregulated in tumor tissue (Zhang X. et al., 2020). Among them 7 significantly upregulated miRNAs (miR-4286, miR-4695-5p, miR-6732-5p, miR-6855-5p, miR-7977, miR-6765-3p, miR-6787-5p) and 7 significantly downregulated miRNAs (miR-1275, miR-30c-1-3p, miR-4449, miR-4539, miR-4684-3p, miR-6129, miR-6891-5p) in patients resistant to radiotherapy. Furthermore, in order to investigate the signaling pathways affected by the differentially expressed 14 miRNAs between radiosensitive and radioresistant atypical meningioma, the authors used the DIANA-miRPath software and found three enriched pathways: two pathways were fatty acid biosynthesis and metabolism, and *TGF*-β signaling pathway. The role of *TGF*-β and these miRNAs in the oncogenesis, particularly radiosensitivity, of meningiomas remains to be established.

EXTRACELLULAR MICRORNAs IN TUMOR RESISTANCE

The main part of miRNAs is localized inside the cell. However, a certain proportion of miRNAs are present outside the cells and they are called extracellular or circulating miRNAs. A series of studies are devoted to the detection of extracellular miRNAs in various human fluids including whole blood, plasma/serum, saliva, urine, cerebrospinal fluid (Valihrach et al., 2020). In these biological fluids, the total concentration of miRNAs and their ratio varies considerably, which may be due to the peculiarities of the pathological or physiological status of the organism. The discovery of significant changes in the expression level of extracellular miRNAs in various diseases promoted the positioning of these molecules as promising non-invasive biomarkers (Sohel, 2020). MiRNAs can be secreted by the cell as part of extracellular vesicles (EVs) (exosomes and microvesicles) or apoptotic bodies; they can be found in the form of high-density lipoprotein (HDL) bound and mostly in the form of Argonaute2-containing ribonucleoprotein complexes (miRNA-Ago2) (**Figure 3**; Valihrach et al., 2020). Then, regardless of the forms, miRNAs pass from the extracellular space into the biological fluid (for example, the general blood flow).

Moreover, extracellular miRNAs, as exosomal miRNAs, play an important role in intracellular communication and the signaling system of cells. Over the past two decades, a broad evidence base has been obtained regarding the role of extracellular miRNAs in maintaining cellular homeostasis. Exosomes are a new form of intercellular communication (Pegtel and Gould, 2019). These are small membrane vesicles of endosomal origin with a diameter of 30 to 100 nm, which are secreted by various types of cells, normal or abnormal (Pegtel and Gould, 2019). Tumor cells play a particularly important role in the production of exosomes (Kalluri and LeBleu, 2020). In addition to miRNAs, exosomes contain a diverse set of molecules such as DNA, proteins, other non-coding RNAs, translation factors, metabolic enzymes, etc. There is evidence that exosomal miRNAs are actively involved in the oncogenesis of MPBTs, including resistance to therapy (Zhang and Yu, 2019). The presence of surface protein markers and adhesion molecules allows exosomes to bind to cells (including tumor cells) that exhibit the corresponding receptors, via micropinocytosis or endocytosis, to be transported into these cells. All this suggests that miRNAs carried by exosomes can enter recipient cells and regulate the expression of their target genes (**Figure 4**; Pegtel and Gould, 2019; Kalluri and LeBleu, 2020).

Glioblastoma

If we talk about the role of EVs in the formation of a resistant phenotype of tumor cells, then, of course, one of the most studied areas is the participation of exosomes in the development of multiple drug resistance (MDR) (Zhang and Yu, 2019). Further studies made it possible to significantly expand the list of biomolecules that are part of resistant tumor cell EVs and are capable of inducing MDR in recipient cells. This primarily refers to miRNAs that regulate the expression level of a number of genes. For instance, Munoz et al. demonstrated that anti-miR-9 delivered via exosomes from MSCs to the TMZ-resistant glioblastoma cells was able to reduce the endogenous upregulation of miR-9 in response to TMZ (Koritzinsky et al., 2017). Moreover, to determine whether multidrug resistance gene 1(*MDR1*) expression is miR-9 dependent for sensitivity to TMZ, the authors knocked down *MDR1* with short hairpin RNA (shRNA), and then examined whether this affects the sensitivity of glioblastoma cells to TMZ. The results indicated that anti-miR-9 increased active caspase by decreased the expression of *MDR1* and concomitantly caused enhanced glioblastoma cell death in response to TMZ treatment. At the same time, in the protocol using manumycin A, which prevented the release of vesicles, it was indicated that the transfer of anti-miR-9 occurs by vesicular transfer, particularly via exosomes.

It should be noted that not only miRNAs but also mRNAs could be transported by EVs. Therefore, exosomes secreted by glioblastoma cells are enriched in mRNA, which enzymes of DNA repair as methylation of the O(6)-Methylguanine-DNA methyltransferase (MGMT) promoter and alkylpurine–DNA–N-glycosylase (APNG), and the transfer of these mRNAs into recipient cells can significantly increase the level of chemoresistance (Shao et al., 2015).

While the participation of EVs in the formation of chemoresistance of tumor cells is not in doubt today, the role of EVs in the regulation of the response of cells to irradiation has been studied to a much lesser extent. Only a few studies are known in which the participation of EVs in the development of the tumor response to radiation has been demonstrated, and

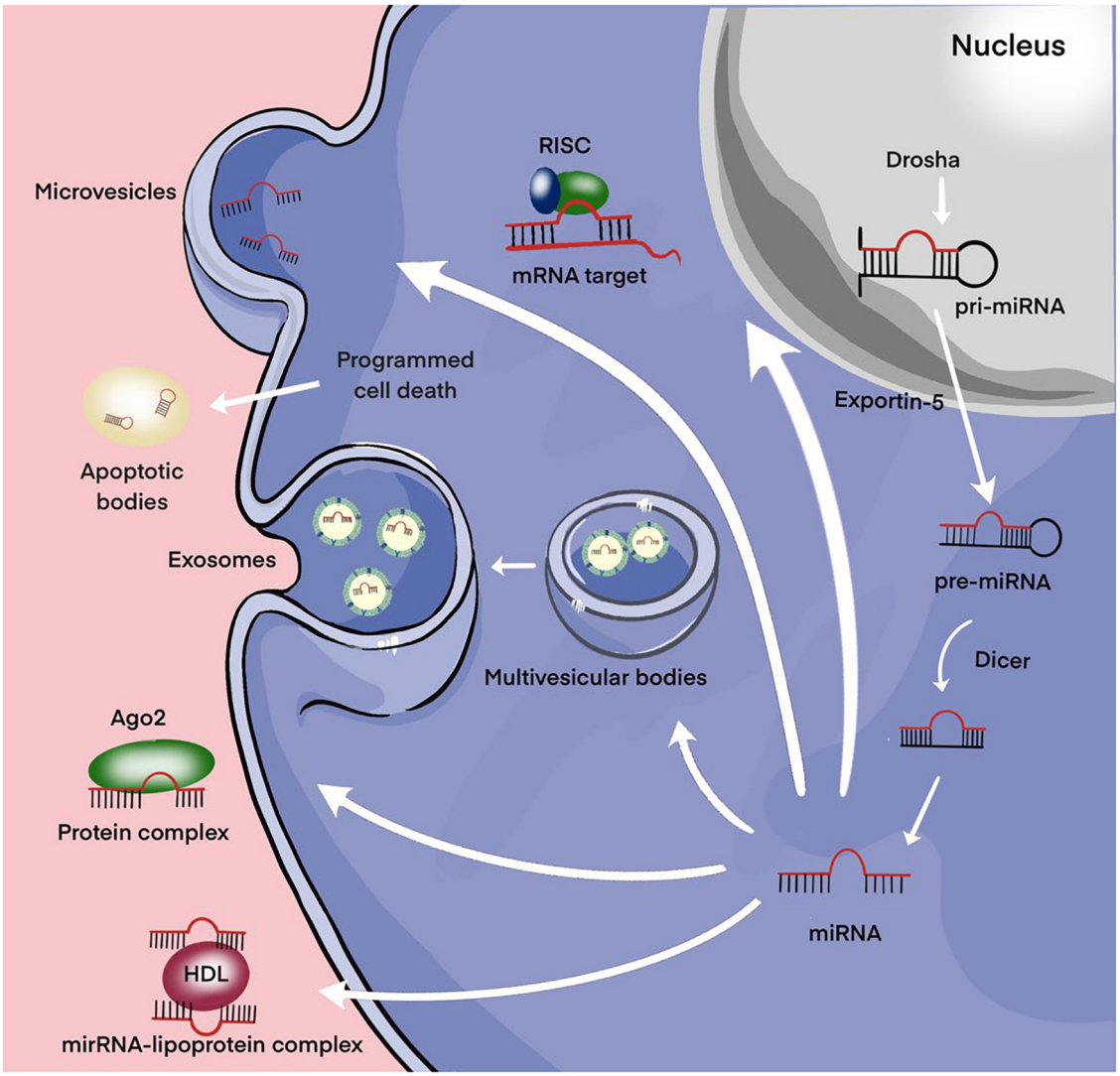

FIGURE 3 | Secretion of miRNAs into the extracellular environment. Primary microRNA (pri-miRNAs) are transcribed by RNA polymerase II and then processed by Drosha into precursor-miRNAs (pre-miRNAs). Exportin5 transfers these pre-miRNAs from the nucleus to the cytoplasm, where Dicer converts them into mature miRNAs. Mature miRNAs can be selectively incorporated into extracellular vesicles (EVs) (exosomes and microvesicles) or linked to the Argonaute 2 (Ago2) protein and released into the extracellular environment. Alternatively, they can be attached to high-density lipoprotein (HDL) or contained in apoptotic bodies and then released into the extracellular environment.

the results of these studies are rather contradictory. This is primarily due to the bystander effect, a well-known biological process, radio-induced changes transmitted from irradiated cells to non-irradiated ones (Li and Nabet, 2019). It is assumed that this effect is based on the transmission of induced or radiation-modified biometabolites (reactive oxygen species, cytokines, growth factors, nucleic acid fragments, etc.) non-irradiated cells either by paracrine pathway or through intercellular gap junctions (Ni et al., 2019). In recent years, studies have appeared in which, in on both normal and tumor cells, direct evidence has been obtained for the participation of EVs of irradiated cells in the induction of radiation changes (primarily, genetic instability, telomere contraction) in non-irradiated cells. At the same time, EVs of irradiated cells can also have protective properties, in particular, in experiments on glioblastoma cells, the ability of exosomes from irradiated cells has been described to promotes a migratory phenotype of non-irradiated cells, as the authors believe, as a result of the active accumulation of DNA repair enzymes in the exosomes of irradiated cells (Arscott et al., 2013).

Pituitary Adenomas With Aggressive Behavior

Hormone therapy is one of the most common types of treatment for hormone-dependent malignant neoplasms, primarily PAs with aggressive behavior. Hormone therapy is based on the principle of creating an artificial deficiency of hormones necessary for the growth of hormone-dependent tumors, which

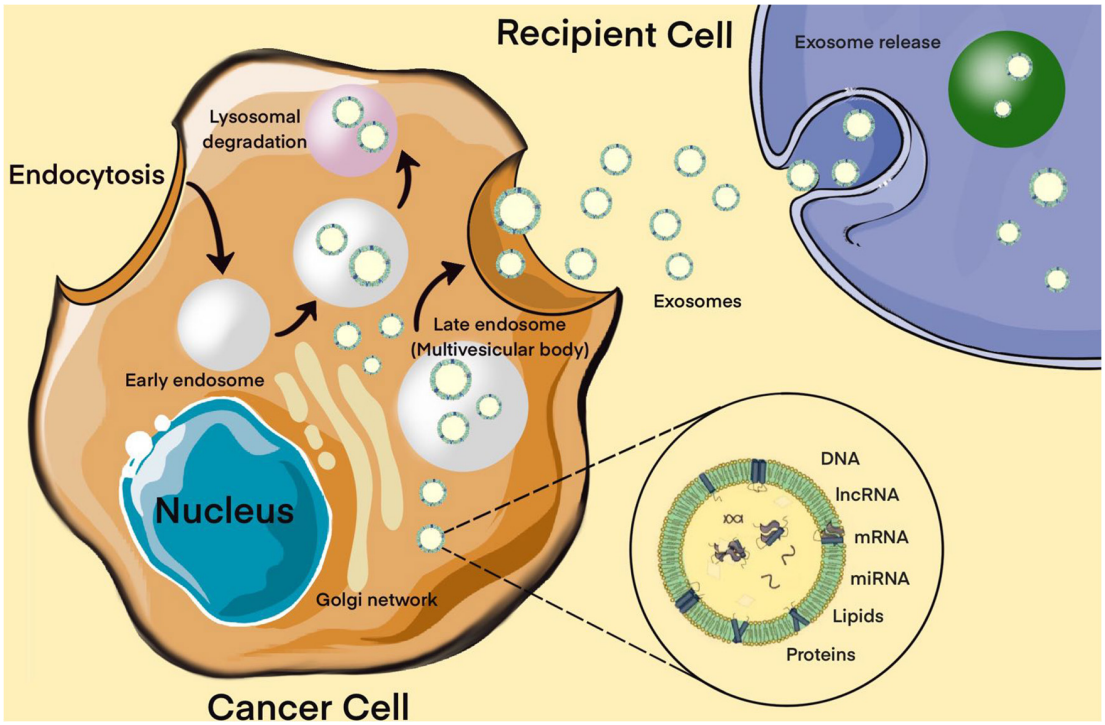

FIGURE 4 | Biogenesis of exosomes. The exosome membrane is formed as a result of the invagination of the early endosome into the membrane. Proteins, lipids, RNA, DNA enter the exosome from the cell cytoplasm. The fate of an endosome depends on the marking of its membrane with certain lipids: if it is labeled with lysobisphosphatidic acid, then its contents will be destroyed, and if ceramides, it will be pushed out of the cell. These processes are controlled by the GTPases of the Rab (G-protein) family, whose various members perform different functions: Rab5 directs the formation of the endosome, Rab7 organizes the degradation of the contents of the multivesicular body (late endosome) in the lysosome, and Rab11, Rab27, and Rab35 are necessary for the secretion of exosomes into the extracellular space. It has been shown that exosomes contain about 4,000 different proteins, more than 1,500 different miRNAs and mRNAs, as well as DNA. Bottom right – enlarged "generalized" exosome.

is achieved mainly in two ways: (1) by reducing the concentration of endogenous hormones and (2) by suppressing their synthesis or replacing hormones with their inactive analogs (Iglesias et al., 2020; van Bunderen and Olsson, 2021). Despite the unconditional effectiveness, the use of hormonal therapy is limited by the development of tumor resistance to hormones. The mechanism of hormonal resistance is well understood. Much less is known about the role of intercellular interactions in the development of hormonal resistance of tumors and, in particular, PAs. For instance, Zhao et al. (2021) demonstrated that 20 differentially expressed miRNAs were identified in human invasive and non-invasive PAs tissue, and rat PA cells, where among them, the expression level of miR-99a-3p and mir-149 was significantly reduced. Furthermore, it was shown that overexpression of miR-149 and miR-99a-3p inhibits the growth and metastasis of PA cells and the formation of EC tubes. Interestingly, delivery of miR-149 mimic and miR-99a-3p mimic via exosomes showed similar suppressive effects on cell viability, metastasis, tube formation ability, tumor growth *in vivo*, and expression of markers associated with angiogenesis as *VEGF*. In additional, the authors showed that *NOVA1*, denticleless E3 ubiquitin protein ligase homolog (*DTL*), and *RAB27B* were targeted by miR-99a-3p. It is known that this group of genes is directly promoted EMT in various human tumors (Aleksakhina et al., 2019). Finally, EMT has been shown to contribute to drug resistance in tumors (Du and Shim, 2016; Aleksakhina et al., 2019). Therefore, we can suggest that these miRNAs can be involved in the oncogenesis of PAs, and in particular, be responsible for drug resistance through intercellular communications. In another pilot study to discover that the expression levels of circulating miR-200a in plasma of patients with invasive PAs were significantly higher than that in plasma of patients with non-invasive PAs. Moreover, invasive PA patients with residual after surgery had lower expression levels of circulating miR-200a. Therefore, miR-200 was a potential influencing factor for invasiveness in PAs patients. However, further research is required for exploring the relationships between circulating miR-200a expression and tumor size, clinical characteristics, and molecular mechanism for packaging and secretion to biofluids of miR-200a (Beylerli et al., 2021).

High-Grade Meningiomas and Medulloblastoma

Aberrant expression of extracellular miRNA circulating in biofluids of certain brain tumor patients has recently been reported to be non-invasive biomarkers and potential regulators of the disease (Sohel, 2020; Valihrach et al., 2020). However, the existence and role of miRNAs in MB and malignant

meningioma extracellular environment are unknown. Therefore, better understanding of extracellular miRNA secretion and function in MB and malignant meningioma seems crucial for the development of novel insights for its regulation of oncogenesis including resistance to therapy. For instance, Choi et al. (2020) investigated whether secreted exosomal miR-135b and miR-135a function at the microenvironment level by possibly impacting the stemness of brain tumor spheroid-forming cells (BTSCs). The authors suggest that the inhibition of miR-135b or miR-135a can suppress the self-renewal capacity and expression of stem cell-related markers of BTSCs. In additional, they demonstrated that miR-135b, miR-135a targeted angiomotin-like2 (*AMOTL2*), and the expression of *AMOTL2* can be increased through miR-135b and miR-135a inhibition. This result might be a clue that exosomal miR-135b and miR-135a derived from BTSCs may be able to regulate the Hippo pathway via *AMOTL2*, which plays a significant role in chemoresistance (Mohajan et al., 2021; Zeng and Dong, 2021).

Negroni et al. (2020) using reverse transcriptase real-time quantitative polymerase chain reaction (qRT-PCR) assay demonstrated that exosomal miR-497 and miR-195 are downregulated in serum of patients with high-grade meningioma (WHO grade 2 and 3) compared to benign meningioma (WHO grade 1). However, receiver operating characteristic (ROC) curve analysis showed that exosomal miR-497 has better sensitivity and specificity than exosomal miR-195 in distinguishing between low-grade (WHO grade 1) and higher-grade (WHO grade 2 and 3) meningioma patients, where area under the curve (AUC) was 0.89 and 0.78, respectively. Furthermore, the authors demonstrated that the transcription factor GATA binding protein 4 (GATA-4) is overexpressed in malignant meningioma, which in turn regulates Cyclin D1, and it negatively regulates the miR-497 expression with an increase in cell viability *in vitro*. Importantly, that a cell cycle protein cyclin D1 is an established cancer-driving protein (Montalto and De Amicis, 2020). In recent years, studies have reported that the high expression of Cyclin D1 is involved in drug resistance processes such as chemo- and radiation treatment, and targeted therapy in various human tumors (Liu et al., 2020; Zuo et al., 2021). Therefore, the clinical values of exosomal miR-497 in the therapy resistance of high-grade meningioma must investigate in the future.

Discussion and Implications

The introduction of extracellular miRNAs into clinical practice is quite active. The search results of the clinical trial database clinicaltrials.gov for the keywords "extracellular," "vesicle,"

TABLE 4 | MiRNAs in extracellular vesicles (EVs) and their signaling pathways through which they may be responsible for glioblastoma therapeutic resistance.

miRNAs	Drug/radiation	Vehicle	Signaling pathways	Regulation	Effect	References
miR-151a	TMZ	Exosome	*XRCC4*	Up	Development of acquired resistance to TMZ	Zeng et al., 2018a
miR-301a	Ionizing radiation	Exosome	*Wnt/b-catenin/TCEAL7*	Up	Depresses radiation sensitivity	Yue et al., 2019
miR-221	TMZ	Exosome	*DNM3*	Down	Inhibit cell proliferation, migration, and TMZ resistance	Yang J. K. et al., 2017
miR-34a	TMZ	Exosome	*MYCN*	Up	Inhibit cell proliferation, migration, invasion and TMZ resistance	Wang B. et al., 2019
miR-124	TMZ	Exosome	*CDK6*	Up	Development of acquired resistance to TMZ and decreases the migration of tumor cells	Sharif et al., 2018
miR-603	Ionizing radiation	EV	*IGF1, IGF1R*, and *MGMT*	Up	Promotes the CSC state and up-regulated DNA repair to promote acquired resistance. Therapeutic platforms hold translational potential in the treatment of wtIDH/umMGMT glioblastoma	Ramakrishnan et al., 2020
miR-93 and miR-193	TMZ	Exosome	*Cyclin D1*	Up	Decreases cell cycling quiescence and contribute to TMZ resistance	Munoz et al., 2019
miR-1238	TMZ	Exosome	*CAV1/EGFR*	Down	Inhibit to TMZ resistance	Yin et al., 2019
miR-21-5p	Pacritinib + TMZ	Exosome	*STAT3/PDCD4*	Down	Inhibit to drug resistance	Chuang et al., 2019
miR-27a-3p, miR-22-3p and miR-221-3p	Ionizing radiation	EV	*CHD7*	Up	Promote PMT in GSCs. Inhibit radioresistance	Zhang Z. et al., 2020

XRCC4, X-ray repair cross-complementing protein 4; TCEAL7, transcription elongation factor A protein-like 7; DNM3, dynamin 3; CDK6, cyclin-dependent kinase 6; IGF1, insulin-like growth factor 1; IGF1R, insulin-like growth factor 1 receptor; MGMT, O(6)-Methylguanine-DNA methyltransferase; CAV1, caveolin 1; EGFR, epidermal growth factor receptor; STAT3, signal transducer and activator of transcription 3; PDCD4, programmed cell death protein 4; CHD7, chromodomain-helicase-DNA-binding protein 7; miR, microRNA; TMZ, Temozolomide; PMT, proneural-to-mesenchymal transition; GSCs, glioma stem cells.

"exosomes," "miRNA," and "tumor" contain more than 50 projects, some of which are in the recruitment phase. A number of projects have been launched to assess the effectiveness of tumor therapy. In previous studies, it was shown that metformin has cytotoxicity and decreases the viability of glioblastoma cells, a promising biguanide with pronounced antitumor activity (Al Hassan et al., 2018). Furthermore, Soraya et al. (2021) demonstrated that metformin significantly decreased the expression of miR-21, miR-155, and miR-182, indicating suppression of oncogenesis in glioblastoma cells. In addition, confirm metformin increased the exosome biogenesis and secretion in glioblastoma cells. Their result also showed that the expression level of Rab27a, Rab27b, and Rab11 upregulated in treated cells with metformin than that of control cells. In the author's opinion, the decreased expression levels of miR-21 and miR-182 may be responsible for Rab genes upregulation, which may correlate with increased exosomes secretion.

It turned out that not only exosomes of resistant cells, but also exosomes produced by cells of the tumor stroma can induce drug resistance in tumor cells. In experiments on head and neck cancer, it was found that exosomes produced by tumor-associated fibroblasts are able to induce cisplatin resistance in nearby tumor cells by transferring miR-196a and through targeting cyclin-dependent kinase inhibitor 1B (*CDKN1B*) and inhibitor of growth protein 5 (*ING5*) (Qin et al., 2019).

Another, no less important question is to what extent EVs can affect the initial level of tumor radiosensitivity and, given their protective properties, contribute to the spread of radioresistance to the brain tumors population. Research in this direction is just beginning, and we can expect that soon it will be possible to get answers to this and other questions concerning the role of EVs in the tumor response to radiation.

Thus, in recent years, extensive information has been accumulated on the correlations of miRNA profiles of EV s and the development of a resistant phenotype of tumor cells. Despite significant advances in research on the role of extracellular miRNAs in therapeutic resistance in MPBTs, studies besides glioblastoma with other tumors remains to be seen. In conclusion, the most common miRNAs in EVs that have been reported to be involved in glioblastoma therapeutic resistance are shown in **Table 4** (Zeng et al., 2018a).

CONCLUSION

The last decade has been accompanied by the emergence of a large number of studies devoted to the role of miRNAs in oncogenesis and the development of resistance to antitumor therapy. The discovery of EVs and, most importantly, their ability to transfer biological material as miRNAs from cell to cell has largely changed the understanding of the mechanism of tumor development and progression. First, this is the revealed ability of EVs to induce tumor transformation and/or induce a tumor-like phenotype in the cells of the surrounding tissue. Moreover, of course, one of the most significant achievements in this reign – the influence of EVs on the formation of a resistant phenotype of tumor cells. EVs can indeed provide the spread of resistance from resistant to sensitive cells through various mechanisms based on the transfer of specific regulatory molecules into cells including proteins, miRNAs, mRNA, etc. The induction of resistance to chemoradiotherapy and pharmacological treatment of MPBTs by miRNAs has been convincingly demonstrated in *in vitro* and *in vivo* experiments. However, there are a number of questions. And one of them in which To the extent that miRNAs are involved in the development of tumor resistance to antitumor therapy, can miRNAs actually participate in the development of resistance across the entire pool of tumor cells under *in vivo* conditions, and, most importantly, how important this process is in the development of acquired tumor resistance. Today these issues are being actively investigated, and, of course, their solution will make it possible to make significant progress in solving such an important problem in neurosurgery as the resistance of MPBTs to antitumor therapy.

AUTHOR CONTRIBUTIONS

IG: conceptualization, writing – original draft, and supervision. OB: writing – review and editing, investigation, project administration, and resources. AA: formal analysis, methodology, and original draft. YL, HX, CL, XX, and CY: data curation. GY: validation, visualization, and funding acquisition. All authors have read and agreed to the published version of the manuscript.

FUNDING

This work was supported by the National Natural Science Foundation of China (81971135); Natural Science Foundation of Heilongjiang (YQ2020H014); "Chunhui Plan" of Ministry of Education (HLJ2019009); Distinguished Young Foundations of the First Affiliated Hospital of Harbin Medical University (HYD2020JQ0014); and the reported study was funded by RFBR and NSFC, project number 21-515-53017.

REFERENCES

Abdelfattah, N., Rajamanickam, S., Panneerdoss, S., Timilsina, S., Yadav, P., Onyeagucha, B. C., et al. (2018). MiR-584-5p potentiates vincristine and radiation response by inducing spindle defects and DNA damage in medulloblastoma. *Nat. Commun.* 9:4541. doi: 10.1038/s41467-018-06808-8

Ahir, B. K., Engelhard, H. H., and Lakka, S. S. (2020). Tumor development and angiogenesis in adult brain tumor: glioblastoma. *Mol. Neurobiol.* 57, 2461–2478. doi: 10.1007/s12035-020-01892-8

Al Hassan, M., Fakhoury, I., El Masri, Z., Ghazale, N., Dennaoui, R., El Atat, O., et al. (2018). Metformin treatment inhibits motility and invasion of glioblastoma cancer cells. *Anal. Cell. Pathol. (Amst.)* 2018:5917470. doi: 10.1155/2018/5917470

Aleksakhina, S. N., Kashyap, A., and Imyanitov, E. N. (2019). Mechanisms of acquired tumor drug resistance. *Biochim. Biophys. Acta Rev. Cancer* 1872:188310. doi: 10.1016/j.bbcan.2019.188310

Ali Syeda, Z., Langden, S. S. S., Munkhzul, C., Lee, M., and Song, S. J. (2020). Regulatory mechanism of MicroRNA expression in cancer. *Int. J. Mol. Sci.* 21:1723. doi: 10.3390/ijms21051723

Allahverdi, A., Arefian, E., Soleimani, M., Ai, J., Nahanmoghaddam, N., Yousefi-Ahmadipour, A., et al. (2020). MicroRNA-4731-5p delivered by AD-mesenchymal stem cells induces cell cycle arrest and apoptosis in glioblastoma. *J. Cell. Physiol.* 235, 8167–8175. doi: 10.1002/jcp.29472

Alsidawi, S., Malek, E., and Driscoll, J. J. (2014). MicroRNAs in brain metastases: potential role as diagnostics and therapeutics. *Int. J. Mol. Sci.* 15, 10508–10526. doi: 10.3390/ijms150610508

Apte, R. S., Chen, D. S., and Ferrara, N. (2019). VEGF in signaling and disease: beyond discovery and development. *Cell* 176, 1248–1264. doi: 10.1016/j.cell.2019.01.021

Arscott, W. T., Tandle, A. T., Zhao, S., Shabason, J. E., Gordon, I. K., Schlaff, C. D., et al. (2013). Ionizing radiation and glioblastoma exosomes: implications in tumor biology and cell migration. *Transl. Oncol.* 6, 638–648. doi: 10.1593/tlo.13640

Asuthkar, S., Velpula, K. K., Nalla, A. K., Gogineni, V., Gondi, C., and Rao, J. S. (2014). Irradiation-induced angiogenesis is associated with an MMP-9-miR-494-syndecan-1 regulatory loop in medulloblastoma cells. *Oncogene* 33, 1922–1933. doi: 10.1038/onc.2013.151

Balachandran, A. A., Larcher, L. M., Chen, S., and Veedu, R. N. (2020). Therapeutically significant MicroRNAs in primary and metastatic brain malignancies. *Cancers (Basel)* 12:2534. doi: 10.3390/cancers12092534

Bertoli, G., Cava, C., and Castiglioni, I. (2015). MicroRNAs: new biomarkers for diagnosis, prognosis, therapy prediction and therapeutic tools for breast cancer. *Theranostics* 5, 1122–1143. doi: 10.7150/thno.11543

Beylerli, O., Khasanov, D., Gareev, I., Valitov, E., Sokhatskii, A., Wang, C., et al. (2021). Differential non-coding RNAs expression profiles of invasive and non-invasive pituitary adenomas. *Noncoding RNA Res.* 6, 115–122. doi: 10.1016/j.ncrna.2021.06.004

Birzu, C., Peyre, M., and Sahm, F. (2020). Molecular alterations in meningioma: prognostic and therapeutic perspectives. *Curr. Opin. Oncol.* 32, 613–622. doi: 10.1097/CCO.0000000000000687

Bogner, E. M., Daly, A. F., Gulde, S., Karhu, A., Irmler, M., Beckers, J., et al. (2020). miR-34a is upregulated in AIP-mutated somatotropinomas and promotes octreotide resistance. *Int. J. Cancer.* 147, 3523–3538. doi: 10.1002/ijc.33268

Buruiană, A., Florian, ŞI., Florian, A. I., Timiş, T. L., Mihu, C. M., Miclăuş, M., et al. (2020). The roles of miRNA in glioblastoma tumor cell communication: diplomatic and aggressive negotiations. *Int. J. Mol. Sci.* 21:1950. doi: 10.3390/ijms21061950

Cao, Z., Liao, Q., Su, M., Huang, K., Jin, J., and Cao, D. (2019). AKT and ERK dual inhibitors: the way forward? *Cancer Lett.* 459, 30–40. doi: 10.1016/j.canlet.2019.05.025

Cardoso, A. M., Morais, C. M., Rebelo, O., Tão, H., Barbosa, M., de Lima, M. C. P., et al. (2021). Downregulation of long non-protein coding RNA MVIH impairs glioblastoma cell proliferation and invasion through a miR-302a-dependent mechanism. *Hum. Mol. Genet.* 30, 46–64.

Castinetti, F., Albarel, F., Amodru, V., Cuny, T., Dufour, H., Graillon, T., et al. (2021). The risks of medical treatment of prolactinoma. *Ann. Endocrinol. (Paris)* 82, 15–19. doi: 10.1016/j.ando.2020.12.008

Chang, J. H., Hwang, Y. H., Lee, D. J., Kim, D. H., Park, J. M., Wu, H. G., et al. (2016). MicroRNA-203 modulates the radiosensitivity of human malignant glioma cells. *Int. J. Radiat. Oncol. Biol. Phys.* 94, 412–420. doi: 10.1016/j.ijrobp.2015.10.001

Chen, Y., Shang, H., Zhang, S., and Zhang, X. (2018). Ginsenoside Rh2 inhibits proliferation and migration of medulloblastoma Daoy by down-regulation of microRNA-31. *J. Cell. Biochem.* 119, 6527–6534. doi: 10.1002/jcb.26716

Choi, S. A., Koh, E. J., Kim, R. N., Byun, J. W., Phi, J. H., Yang, J., et al. (2020). Extracellular vesicle-associated miR-135b and -135a regulate stemness in Group 4 medulloblastoma cells by targeting angiomotin-like 2. *Cancer Cell Int.* 20:558. doi: 10.1186/s12935-020-01645-6

Chuang, H. Y., Su, Y. K., Liu, H. W., Chen, C. H., Chiu, S. C., Cho, D. Y., et al. (2019). Preclinical evidence of STAT3 inhibitor pacritinib overcoming temozolomide resistance via downregulating miR-21-Enriched exosomes from M2 glioblastoma-associated macrophages. *J. Clin. Med.* 8:959. doi: 10.3390/jcm8070959

Ciato, D., and Albani, A. (2020). Molecular mechanisms of glucocorticoid resistance in corticotropinomas: new developments and drug targets. *Front. Endocrinol. (Lausanne)* 11:21. doi: 10.3389/fendo.2020.00021

de Kock, L., Rivera, B., and Foulkes, W. D. (2020). Pineoblastoma is uniquely tolerant of mutually exclusive loss of DICER1, DROSHA or DGCR8. *Acta Neuropathol.* 139, 1115–1118. doi: 10.1007/s00401-020-02139-5

Dénes, J., Kasuki, L., Trivellin, G., Colli, L. M., Takiya, C. M., Stiles, C. E., et al. (2015). Regulation of aryl hydrocarbon receptor interacting protein (AIP) protein expression by MiR-34a in sporadic somatotropinomas. *PLoS One* 10:e0117107. doi: 10.1371/journal.pone.0117107

Dexheimer, P. J., and Cochella, L. (2020). MicroRNAs: from mechanism to organism. *Front. Cell Dev. Biol.* 8:409. doi: 10.3389/fcell.2020.00409

Du, B., and Shim, J. S. (2016). Targeting epithelial-mesenchymal transition (EMT) to overcome drug resistance in cancer. *Molecules* 21:965. doi: 10.3390/molecules21070965

Elsarrag, M., Patel, P. D., Chatrath, A., Taylor, D., and Jane, J. A. (2020). Genomic and molecular characterization of pituitary adenoma pathogenesis: review and translational opportunities. *Neurosurg. Focus* 48:E11. doi: 10.3171/2020.3.FOCUS20104

Fang, Y., Shen, H., Li, H., Cao, Y., Qin, R., Long, L., et al. (2013). miR-106a confers cisplatin resistance by regulating PTEN/Akt pathway in gastric cancer cells. *Acta Biochim. Biophys. Sin. (Shanghai)* 45, 963–972. doi: 10.1093/abbs/gmt106

Fish, J. E., Santoro, M. M., Morton, S. U., Yu, S., Yeh, R. F., Wythe, J. D., et al. (2008). miR-126 regulates angiogenic signaling and vascular integrity. *Dev. Cell* 15, 272–284. doi: 10.1016/j.devcel.2008.07.008

Fleseriu, M., and Popovic, V. (2020). The journey in diagnosis and treatment, from pituitary adenoma to aggressive pituitary tumors. *Rev. Endocr. Metab. Disord.* 21, 201–202. doi: 10.1007/s11154-020-09561-w

Gabriely, G., Wheeler, M. A., Takenaka, M. C., and Quintana, F. J. (2017). Role of AHR and HIF-1alpha in glioblastoma metabolism. *Trends Endocrinol. Metab.* 28, 428–436. doi: 10.1016/j.tem.2017.02.009

Garibaldi, F., Falcone, E., Trisciuoglio, D., Colombo, T., Lisek, K., Walerych, D., et al. (2016). Mutant p53 inhibits miRNA biogenesis by interfering with the microprocessor complex. *Oncogene* 35, 3760–3770. doi: 10.1038/onc.2016.51

Giraldi, E. A., and Ioachimescu, A. G. (2020). The role of dopamine agonists in pituitary adenomas. *Endocrinol. Metab. Clin. North Am.* 49, 453–474. doi: 10.1016/j.ecl.2020.05.006

Grunder, E., D'Ambrosio, R., Fiaschetti, G., Abela, L., Arcaro, A., Zuzak, T., et al. (2011). MicroRNA-21 suppression impedes medulloblastoma cell migration. *Eur. J. Cancer* 47, 2479–2490. doi: 10.1016/j.ejca.2011.06.041

Ha, M., and Kim, V. N. (2014). Regulation of microRNA biogenesis. *Nat. Rev. Mol. Cell Biol.* 15, 509–524. doi: 10.1038/nrm3838

Hou, W. Z., Chen, X. L., Qin, L. S., Xu, Z. J., Liao, G. M., Chen, D., et al. (2020). MiR-449b-5p inhibits human glioblastoma cell proliferation by inactivating WNT2B/Wnt/β-catenin signaling pathway. *Eur. Rev. Med. Pharmacol. Sci.* 24, 5549–5557. doi: 10.26355/eurrev_202005_21340

Hu, B., Mao, Z., Du, Q., Jiang, X., Wang, Z., Xiao, Z., et al. (2019). miR-93-5p targets Smad7 to regulate the transforming growth factor-β1/Smad3 pathway and mediate fibrosis in drug-resistant prolactinoma. *Brain Res. Bull.* 149, 21–31. doi: 10.1016/j.brainresbull.2019.03.013

Hu, B., Mao, Z., Jiang, X., He, D., Wang, Z., Wang, X., et al. (2018). Role of TGF-beta1/Smad3-mediated fibrosis in drug resistance mechanism of prolactinoma. *Brain Res.* 1698, 204–212. doi: 10.1016/j.brainres.2018.07.024

Hu, S. A., Cheng, J., Zhao, W. H., and Zhao, H. Y. (2020). Quercetin induces apoptosis in meningioma cells through the miR-197/IGFBP5 cascade. *Environ. Toxicol. Pharmacol.* 80:103439. doi: 10.1016/j.etap.2020.103439

Hu, Y. L., DeLay, M., Jahangiri, A., Molinaro, A. M., Rose, S. D., Carbonell, W. S., et al. (2012). Hypoxia-induced autophagy promotes tumor cell survival and adaptation to antiangiogenic treatment in glioblastoma. *Cancer Res.* 72, 1773–1783. doi: 10.1158/0008-5472.CAN-11-3831

Huang, S., Qi, P., Zhang, T., Li, F., and He, X. (2019). The HIF-1α/miR-224-3p/ATG5 axis affects cell mobility and chemosensitivity by regulating hypoxia-induced protective autophagy in glioblastoma and astrocytoma. *Oncol. Rep.* 41, 1759–1768. doi: 10.3892/or.2018.6929

Huynh, P. P., Ishii, L. E., and Ishii, M. (2021). Prolactinomas. *JAMA* 325:195. doi: 10.1001/jama.2020.3744

Huynh, T. T., Lin, C. M., Lee, W. H., Wu, A. T., Lin, Y. K., Lin, Y. F., et al. (2015). Pterostilbene suppressed irradiation-resistant glioma stem cells by modulating GRP78/miR-205 axis. *J. Nutr. Biochem.* 26, 466–475. doi: 10.1016/j.jnutbio.2014.11.015

Iglesias, P., Magallón, R., Mitjavila, M., Rodríguez Berrocal, V., Pian, H., and Díez, J. J. (2020). Multimodal therapy in aggressive pituitary tumors. *Endocrinol. Diabetes Nutr.* 67, 469–485. doi: 10.1016/j.endinu.2019.08.004

Iglesias, P., Rodríguez Berrocal, V., and Díez, J. J. (2018). Giant pituitary adenoma: histological types, clinical features and therapeutic approaches. *Endocrine* 61, 407–421. doi: 10.1007/s12020-018-1645-x

Ji, J., Rong, Y., Luo, C. L., Li, S., Jiang, X., Weng, H., et al. (2018). Up-Regulation of hsa-miR-210 promotes venous metastasis and predicts poor prognosis in hepatocellular carcinoma. *Front. Oncol.* 8:569. doi: 10.3389/fonc.2018.00569

Jian, M., Du, Q., Zhu, D., Mao, Z., Wang, X., Feng, Y., et al. (2019). Tumor suppressor miR-145-5p sensitizes prolactinoma to bromocriptine by downregulating TPT1. *J. Endocrinol. Invest.* 42, 639–652. doi: 10.1007/s40618-018-0963-4

Joshi, P., Katsushima, K., Zhou, R., Meoded, A., Stapleton, S., Jallo, G., et al. (2019). The therapeutic and diagnostic potential of regulatory noncoding RNAs in medulloblastoma. *Neurooncol. Adv.* 1:vdz023. doi: 10.1093/noajnl/vdz023

Kalluri, R., and LeBleu, V. S. (2020). The biology, function, and biomedical applications of exosomes. *Science* 367:eaau6977. doi: 10.1126/science.aau6977

Kapoor, I., Bodo, J., Hill, B. T., Hsi, E. D., and Almasan, A. (2020). Targeting BCL-2 in B-cell malignancies and overcoming therapeutic resistance. *Cell Death Dis.* 11:941. doi: 10.1038/s41419-020-03144-y

Kasuga, C., Nakahara, Y., Ueda, S., Hawkins, C., Taylor, M. D., Smith, C. A., et al. (2008). Expression of MAGE and GAGE genes in medulloblastoma and modulation of resistance to chemotherapy. Laboratory investigation. *J. Neurosurg. Pediatr.* 1, 305–313. doi: 10.3171/PED/2008/1/4/305

Katar, S., Baran, O., Evran, S., Cevik, S., Akkaya, E., Baran, G., et al. (2017). Expression of miRNA-21, miRNA-107, miRNA-137 and miRNA-29b in meningioma. *Clin. Neurol. Neurosurg.* 156, 66–70. doi: 10.1016/j.clineuro.2017.03.016

Kimmelman, A. C., and White, E. (2017). Autophagy and tumor metabolism. *Cell Metab.* 25, 1037–1043. doi: 10.1016/j.cmet.2017.04.004

Kliese, N., Gobrecht, P., Pachow, D., Andrae, N., Wilisch-Neumann, A., Kirches, E., et al. (2013). miRNA-145 is downregulated in atypical and anaplastic meningiomas and negatively regulates motility and proliferation of meningioma cells. *Oncogene* 32, 4712–4720. doi: 10.1038/onc.2012.468

Koritzinsky, E. H., Street, J. M., Star, R. A., and Yuen, P. S. (2017). Quantification of exosomes. *J. Cell. Physiol.* 232, 1587–1590. doi: 10.1002/jcp.25387

Krell, J., Stebbing, J., Carissimi, C., Dabrowska, A. F., de Giorgio, A., Frampton, A. E., et al. (2016). TP53 regulates miRNA association with AGO2 to remodel the miRNA-mRNA interaction network. *Genome Res.* 26, 331–341. doi: 10.1101/gr.191759.115

Lake, M. G., Krook, L. S., and Cruz, S. V. (2020). Pituitary adenomas: an overview. *Am. Fam. Physician* 88, 319–327. Rev Endocr Metab Disord. 21, 201–202.

Lan, F., Pan, Q., Yu, H., and Yue, X. (2015). Sulforaphane enhances temozolomide-induced apoptosis because of down-regulation of miR-21 via Wnt/beta-catenin signaling in glioblastoma. *J. Neurochem.* 134, 811–818. doi: 10.1111/jnc.13174

Le Rhun, E., Preusser, M., Roth, P., Reardon, D. A., van den Bent, M., Wen, P., et al. (2019). Molecular targeted therapy of glioblastoma. *Cancer Treat. Rev.* 80:101896. doi: 10.1016/j.ctrv.2019.101896

Lee, E. Y., and Muller, W. J. (2010). Oncogenes and tumor suppressor genes. *Cold Spring Harb. Perspect. Biol.* 2:a003236. doi: 10.1101/cshperspect.a003236

Lee, Y. Y., Yang, Y. P., Huang, M. C., Wang, M. L., Yen, S. H., Huang, P. I., et al. (2014). MicroRNA142-3p promotes tumor-initiating and radioresistant properties in malignant pediatric brain tumors. *Cell Transplant.* 23, 669–690. doi: 10.3727/096368914X678364

Li, I., and Nabet, B. Y. (2019). Exosomes in the tumor microenvironment as mediators of cancer therapy resistance. *Mol. Cancer* 18:32. doi: 10.1186/s12943-019-0975-5

Li, J., Song, J., and Guo, F. (2019). miR-186 reverses cisplatin resistance and inhibits the formation of the glioblastoma-initiating cell phenotype by degrading Yin Yang 1 in glioblastoma. *Int. J. Mol. Med.* 43, 517–524. doi: 10.3892/ijmm.2018.3940

Li, K. K., Xia, T., Ma, F. M., Zhang, R., Mao, Y., Wang, Y., et al. (2015). miR-106b is overexpressed in medulloblastomas and interacts directly with PTEN. *Neuropathol. Appl. Neurobiol.* 41, 145–164. doi: 10.1111/nan.12169

Li, S., Wang, L., Fu, B., Berman, M. A., Diallo, A., and Dorf, M. E. (2014). TRIM65 regulates microRNA activity by ubiquitination of TNRC6. *Proc. Natl. Acad. Sci. U.S.A.* 111, 6970–6975. doi: 10.1073/pnas.1322545111

Li, W., Guo, F., Wang, P., Hong, S., and Zhang, C. (2014). miR-221/222 confers radioresistance in glioblastoma cells through activating Akt independent of PTEN status. *Curr. Mol. Med.* 14, 185–195. doi: 10.2174/1566524013666131203103147

Li, Z., Hu, C., Zhen, Y., Pang, B., Yi, H., and Chen, X. (2019). Pristimerin inhibits glioma progression by targeting AGO2 and PTPN1 expression via miR-542-5p. *Biosci. Rep.* 39:BSR20182389. doi: 10.1042/BSR20182389

Lima, C. R., Gomes, C. C., and Santos, M. F. (2017). Role of microRNAs in endocrine cancer metastasis. *Mol. Cell. Endocrinol.* 456, 62–75. doi: 10.1016/j.mce.2017.03.015

Lin, R. J., Lin, Y. C., Chen, J., Kuo, H. H., Chen, Y. Y., Diccianni, M. B., et al. (2010). microRNA signature and expression of *Dicer* and *Drosha* can predict prognosis and delineate risk groups in neuroblastoma. *Cancer Res.* 70, 7841–7850. doi: 10.1158/0008-5472.CAN-10-0970

Liu, B., Chen, D., Chen, S., Saber, A., and Haisma, H. (2020). Transcriptional activation of cyclin D1 via HER2/HER3 contributes to EGFR-TKI resistance in lung cancer. *Biochem. Pharmacol.* 178:114095. doi: 10.1016/j.bcp.2020.114095

Liu, B., Li, J., and Cairns, M. J. (2014). Identifying miRNAs, targets and functions. *Brief. Bioinform.* 15, 1–19. doi: 10.1093/bib/bbs075

Lu, T. X., and Rothenberg, M. E. (2018). MicroRNA. *J. Allergy Clin. Immunol.* 141, 1202–1207. doi: 10.1016/j.jaci.2017.08.034

Lu, Y. F., Zhang, L., Waye, M. M., Fu, W. M., and Zhang, J. F. (2015). MiR-218 mediates tumorigenesis and metastasis: perspectives and implications. *Exp. Cell Res.* 334, 173–182. doi: 10.1016/j.yexcr.2015.03.027

Maier, A. D., Bartek, J. Jr., Eriksson, F., Ugleholdt, H., Juhler, M., Broholm, H., et al. (2020). Clinical and histopathological predictors of outcome in malignant meningioma. *Neurosurg. Rev.* 43, 643–653. doi: 10.1007/s10143-019-01093-5

Mansouri, S., Singh, S., Alamsahebpour, A., Burrell, K., Li, M., Karabork, M., et al. (2016). DICER governs characteristics of glioma stem cells and the resulting tumors in xenograft mouse models of glioblastoma. *Oncotarget* 7, 56431–56446. doi: 10.18632/oncotarget.10570

Maryam, M., Naemi, M., and Hasani, S. S. (2021). A comprehensive review on oncogenic miRNAs in breast cancer. *J. Genet.* 100:15.

Masoudi, M. S., Mehrabian, E., and Mirzaei, H. (2018). MiR-21: a key player in glioblastoma pathogenesis. *J. Cell. Biochem.* 119, 1285–1290. doi: 10.1002/jcb.26300

Melincovici, C. S., Boşca, A. B., Şuşman, S., Mărginean, M., Mihu, C., Istrate, M., et al. (2018). Vascular endothelial growth factor (VEGF) - key factor in normal and pathological angiogenesis. *Rom. J. Morphol. Embryol.* 59, 455–467.

Mete, O., and Lopes, M. B. (2017). Overview of the 2017 WHO classification of pituitary tumors. *Endocr. Pathol.* 28, 228–243. doi: 10.1007/s12022-017-9498-z

Millard, N. E., and De Braganca, K. C. (2016). Medulloblastoma. *J. Child Neurol.* 31, 1341–1353. doi: 10.1177/0883073815600866

Mohajan, S., Jaiswal, P. K., Vatanmakarian, M., Yousefi, H., Sankaralingam, S., Alahari, S. K., et al. (2021). Hippo pathway: regulation, deregulation and potential therapeutic targets in cancer. *Cancer Lett.* 507, 112–123. doi: 10.1016/j.canlet.2021.03.006

Molitch, M. E. (2020). Dopamine agonists and antipsychotics. *Eur. J. Endocrinol.* 183, C11–C13. doi: 10.1530/EJE-20-0607

Montalto, F. I., and De Amicis, F. (2020). Cyclin D1 in cancer: a molecular connection for cell cycle control, adhesion and invasion in tumor and stroma. *Cells* 9:2648. doi: 10.3390/cells9122648

Munoz, J. L., Walker, N. D., Mareedu, S., Pamarthi, S. H., Sinha, G., Greco, S. J., et al. (2019). Cycling quiescence in temozolomide resistant glioblastoma cells is partly explained by microRNA-93 and -193-mediated decrease of cyclin D. *Front. Pharmacol.* 10:134. doi: 10.3389/fphar.2019.00134

Muñoz-Hidalgo, L., San-Miguel, T., Megías, J., Serna, E., Calabuig-Fariñas, S., Monleón, D., et al. (2020). The status of EGFR modulates the effect of miRNA-200c on ZEB1 expression and cell migration in glioblastoma cells. *Int. J. Mol. Sci.* 22:368. doi: 10.3390/ijms22010368

Negroni, C., Hilton, D. A., Ercolano, E., Adams, C. L., Kurian, K. M., Baiz, D., et al. (2020). GATA-4, a potential novel therapeutic target for high-grade meningioma, regulates miR-497, a potential novel circulating biomarker for high-grade meningioma. *EBioMedicine* 59:102941. doi: 10.1016/j.ebiom.2020.102941

Ni, J., Bucci, J., Malouf, D., Knox, M., Graham, P., and Li, Y. (2019). Exosomes in cancer radioresistance. *Front. Oncol.* 6:869. doi: 10.3389/fonc.2019.00869

Olejniczak, M., Kotowska-Zimmer, A., and Krzyzosiak, W. (2018). Stress-induced changes in miRNA biogenesis and functioning. *Cell. Mol. Life Sci.* 75, 177–191. doi: 10.1007/s00018-017-2591-0

Panigrahi, M. K., Chandrasekhar, Y. B. V. K., and Vooturi, S. (2020). Current status of surgery in management of prolactinomas. *Neurol. India* 68(Suppl.), S39–S43. doi: 10.4103/0028-3886.287668

Pannuru, P., Dontula, R., Khan, A. A., Herbert, E., Ozer, H., Chetty, C., et al. (2014). miR-let-7f-1 regulates SPARC mediated cisplatin resistance in medulloblastoma cells. *Cell. Signal.* 26, 2193–2201. doi: 10.1016/j.cellsig.2014.06.014

Pegtel, D. M., and Gould, S. J. (2019). Exosomes. *Annu. Rev. Biochem.* 88, 487–514. doi: 10.1146/annurev-biochem-013118-111902

Qadir, M. I., and Faheem, A. (2017). miRNA: a diagnostic and therapeutic tool for pancreatic cancer. *Crit. Rev. Eukaryot. Gene Expr.* 27, 197–204. doi: 10.1615/CritRevEukaryotGeneExpr.2017019494

Qin, X., Guo, H., Wang, X., Zhu, X., Yan, M., Wang, X., et al. (2019). Exosomal miR-196a derived from cancer-associated fibroblasts confers cisplatin resistance in head and neck cancer through targeting CDKN1B and ING5. *Genome Biol.* 20:12. doi: 10.1186/s13059-018-1604-0

Quinlan, A., and Rizzolo, D. (2017). Understanding medulloblastoma. *JAAPA* 30, 30–36. doi: 10.1097/01.JAA.0000524717.71084.50

Ramakrishnan, V., Xu, B., Akers, J., Nguyen, T., Ma, J., Dhawan, S., et al. (2020). Radiation-induced extracellular vesicle (EV) release of miR-603 promotes IGF1-mediated stem cell state in glioblastomas. *EBioMedicine* 55:102736. doi: 10.1016/j.ebiom.2020.102736

Richardson, H. E., Cordero, J. B., and Grifoni, D. (2020). Basic and translational models of cooperative oncogenesis. *Int. J. Mol. Sci.* 21:5919. doi: 10.3390/ijms21165919

Ruan, T., He, X., Yu, J., and Hang, Z. (2016). MicroRNA-186 targets Yes-associated protein 1 to inhibit Hippo signaling and tumorigenesis in hepatocellular carcinoma. *Oncol. Lett.* 11, 2941–2945. doi: 10.3892/ol.2016.4312

Rupaimoole, R., and Slack, F. J. (2017). MicroRNA therapeutics: towards a new era for the management of cancer and other diseases. *Nat. Rev. Drug Discov.* 16, 203–222. doi: 10.1038/nrd.2016.246

Saliminejad, K., Khorram Khorshid, H. R., Soleymani Fard, S., and Ghaffari, S. H. (2019). An overview of microRNAs: biology, functions, therapeutics, and analysis methods. *J. Cell. Physiol.* 234, 5451–5465. doi: 10.1002/jcp.27486

Schiff, D., and Alyahya, M. (2020). Neurological and medical complications in brain tumor patients. *Curr. Neurol. Neurosci. Rep.* 20:33. doi: 10.1007/s11910-020-01054-2

Schulte, J. D., Aghi, M. K., and Taylor, J. W. (2020). Anti-angiogenic therapies in the management of glioblastoma. *Chin. Clin. Oncol.* 10:37. doi: 10.21037/cco.2020.03.06

Shao, H., Chung, J., Lee, K., Balaj, L., Min, C., Carter, B. S., et al. (2015). Chip-based analysis of exosomal mRNA mediating drug resistance in glioblastoma. *Nat. Commun.* 6:6999. doi: 10.1038/ncomms7999

Shao, Z., Liu, L., Zheng, Y., Tu, S., Pan, Y., Yan, S., et al. (2020). Molecular mechanism and approach in progression of meningioma. *Front. Oncol.* 10:538845. doi: 10.3389/fonc.2020.538845

Sharif, S., Ghahremani, M. H., and Soleimani, M. (2018). Delivery of exogenous miR-124 to glioblastoma multiform cells by Wharton's jelly mesenchymal stem cells decreases cell proliferation and migration, and confers chemosensitivity. *Stem Cell Rev. Rep.* 14, 236–246. doi: 10.1007/s12015-017-9788-3

Shen, J., Xia, W., Khotskaya, Y. B., Huo, L., Nakanishi, K., Lim, S. O., et al. (2013). EGFR modulates microRNA maturation in response to hypoxia through phosphorylation of AGO2. *Nature* 497, 383–387. doi: 10.1038/nature12080

Smits, M., Wurdinger, T., van het Hof, B., Drexhage, J. A., Geerts, D., Wesseling, P., et al. (2012). Myc-associated zinc finger protein (MAZ) is regulated by miR-125b and mediates VEGF-induced angiogenesis in glioblastoma. *FASEB J.* 26, 2639–2647. doi: 10.1096/fj.11-202820

Sohel, M. M. H. (2020). Circulating microRNAs as biomarkers in cancer diagnosis. *Life Sci.* 248:117473. doi: 10.1016/j.lfs.2020.117473

Song, L. R., Li, D., Weng, J. C., Li, C. B., Wang, L., Wu, Z., et al. (2020). MicroRNA-195 functions as a tumor suppressor by directly targeting fatty acid synthase in malignant meningioma. *World Neurosurg.* 136, e355–e364. doi: 10.1016/j.wneu.2019.12.182

Soraya, H., Sani, N. A., Jabbari, N., and Rezaie, J. (2021). Metformin increases exosome biogenesis and secretion in U87 MG human glioblastoma cells: a possible mechanism of therapeutic resistance. *Arch. Med. Res.* 52, 151–162. doi: 10.1016/j.arcmed.2020.10.007

Sousa, F., Dhaliwal, H. K., Gattacceca, F., Sarmento, B., and Amiji, M. M. (2019). Enhanced anti-angiogenic effects of bevacizumab in glioblastoma treatment upon intranasal administration in polymeric nanoparticles. *J. Control. Release.* 309, 37–47. doi: 10.1016/j.jconrel.2019.07.033

Sun, X. H., Fan, W. J., An, Z. J., and Sun, Y. (2020). Inhibition of long noncoding RNA CRNDE increases chemosensitivity of medulloblastoma cells by targeting miR-29c-3p. *Oncol. Res.* 28, 95–102. doi: 10.3727/096504019X15742472027401

Thakkar, J. P., Prabhu, V. C., Peters, K. B., and Lukas, R. V. (2021). What is new in neuro-oncology? *Neurol. Clin.* 39, 163–179. doi: 10.1016/j.ncl.2020.09.009

Tolonen, J. P., Hekkala, A., Kuismin, O., Tuominen, H., Suo-Palosaari, M., Tynninen, O., et al. (2020). Medulloblastoma, macrocephaly, and a pathogenic germline PTEN variant: cause or coincidence? *Mol. Genet. Genomic Med.* 8:e1302. doi: 10.1002/mgg3.1302

Valihrach, L., Androvic, P., and Kubista, M. (2020). Circulating miRNA analysis for cancer diagnostics and therapy. *Mol. Aspects Med.* 72:100825. doi: 10.1016/j.mam.2019.10.002

van Bunderen, C. C., and Olsson, D. S. (2021). Growth hormone deficiency and replacement therapy in adults: impact on survival. *Rev. Endocr. Metab. Disord.* 22, 125–133. doi: 10.1007/s11154-020-09599-w

Van Roosbroeck, K., and Calin, G. A. (2017). Cancer hallmarks and MicroRNAs: the therapeutic connection. *Adv. Cancer Res.* 135, 119–149. doi: 10.1016/bs.acr.2017.06.002

Vermeulen, E., D'Haens, J., Stadnik, T., Unuane, D., Barbe, K., Van Velthoven, V., et al. (2020). Predictors of dopamine agonist resistance in prolactinoma patients. *BMC Endocr. Disord.* 20:68. doi: 10.1186/s12902-020-0543-4

Viallard, C., and Larrivée, B. (2017). Tumor angiogenesis and vascular normalization: alternative therapeutic targets. *Angiogenesis* 20, 409–426. doi: 10.1007/s10456-017-9562-9

Vishnoi, A., and Rani, S. (2017). MiRNA biogenesis and regulation of diseases: an overview. *Methods Mol. Biol.* 1509, 1–10. doi: 10.1007/978-1-4939-6524-3_1

Wang, B., Wu, Z. H., Lou, P. Y., Chai, C., Han, S. Y., Ning, J. F., et al. (2019). Human bone marrow-derived mesenchymal stem cell-secreted exosomes overexpressing microRNA-34a ameliorate glioblastoma development via down-regulating MYCN. *Cell. Oncol. (Dordr.)* 42, 783–799. doi: 10.1007/s13402-019-00461-z

Wang, M., Deng, X., Ying, Q., Jin, T., Li, M., and Liang, C. (2015). MicroRNA-224 targets ERG2 and contributes to malignant progressions of meningioma. *Biochem. Biophys. Res. Commun.* 460, 354–361. doi: 10.1016/j.bbrc.2015.03.038

Wang, Z., Gao, L., Guo, X., Feng, C., Deng, K., Lian, W., et al. (2019). Identification of microRNAs associated with the aggressiveness of prolactin pituitary tumors using bioinformatic analysis. *Oncol. Rep.* 42, 533–548. doi: 10.3892/or.2019.7173

Weeraratne, S. D., Amani, V., Neiss, A., Teider, N., Scott, D. K., Pomeroy, S. L., et al. (2011). miR-34a confers chemosensitivity through modulation of MAGE-A and p53 in medulloblastoma. *Neuro Oncol.* 13, 165–175. doi: 10.1093/neuonc/noq179

Wei, Z., Zhou, C., Liu, M., Yao, Y., Sun, J., Xiao, J., et al. (2015). MicroRNA involvement in a metastatic non-functioning pituitary carcinoma. *Pituitary* 18, 710–721. doi: 10.1007/s11102-015-0648-3

Wirsching, H. G., Galanis, E., and Weller, M. (2016). Glioblastoma. *Handb. Clin. Neurol.* 134, 381–397. doi: 10.1016/B978-0-12-802997-8.00023-2

Wu, H. M., Wang, H. D., Tang, Y., Fan, Y. W., Hu, Y. B., Tohti, M., et al. (2015). Differential expression of microRNAs in postoperative radiotherapy sensitive and resistant patients with glioblastoma multiforme. *Tumour Biol.* 36, 4723–4730. doi: 10.1007/s13277-015-3121-z

Wu, K., He, J., Pu, W., and Peng, Y. (2018). The role of exportin-5 in MicroRNA biogenesis and cancer. *Genomics Proteomics Bioinformatics* 16, 120–126. doi: 10.1016/j.gpb.2017.09.004

Xiao, B., Zhou, X., Ye, M., Lv, S., Wu, M., Liao, C., et al. (2016). MicroRNA-566 modulates vascular endothelial growth factor by targeting Von Hippel-Landau

in human glioblastoma in vitro and in vivo. *Mol. Med. Rep.* 13, 379–385. doi: 10.3892/mmr.2015.4537

Xu, D., Chi, G., Zhao, C., and Li, D. (2018). Ligustrazine inhibits growth, migration and invasion of medulloblastoma daoy cells by up-regulation of miR-211. *Cell. Physiol. Biochem.* 49, 2012–2021. doi: 10.1159/000493712

Xue, J., Yang, M., Hua, L. H., and Wang, Z. P. (2019). MiRNA-191 functions as an oncogene in primary glioblastoma by directly targeting NDST1. *Eur. Rev. Med. Pharmacol. Sci.* 23, 6242–6249. doi: 10.26355/eurrev_201907_18443

Yang, F., Liu, X., Liu, Y., Liu, Y., Zhang, C., Wang, Z., et al. (2017). miR-181d/MALT1 regulatory axis attenuates mesenchymal phenotype through NF-kappaB pathways in glioblastoma. *Cancer Lett.* 396, 1–9. doi: 10.1016/j.canlet.2017.03.002

Yang, J. K., Yang, J. P., Tong, J., Jing, S. Y., Fan, B., Wang, F., et al. (2017). Exosomal miR-221 targets DNM3 to induce tumor progression and temozolomide resistance in glioma. *J. Neurooncol.* 131, 255–265. doi: 10.1007/s11060-016-2308-5

Yang, Y., Cui, H., and Wang, X. (2019). Downregulation of EIF5A2 by miR-221-3p inhibits cell proliferation, promotes cell cycle arrest and apoptosis in medulloblastoma cells. *Biosci. Biotechnol. Biochem.* 83, 400–408. doi: 10.1080/09168451.2018.1553604

Yin, J., Zeng, A., Zhang, Z., Shi, Z., Yan, W., and You, Y. (2019). Exosomal transfer of miR-1238 contributes to temozolomide-resistance in glioblastoma. *EBioMedicine* 42, 238–251. doi: 10.1016/j.ebiom.2019.03.016

Yu, C., Li, J., Sun, F., Cui, J., Fang, H., and Sui, G. (2016). Expression and clinical significance of miR-26a and pleomorphic adenoma gene 1 (PLAG1) in invasive pituitary adenoma. *Med. Sci. Monit.* 22, 5101–5108. doi: 10.12659/msm.898908

Yue, X., Lan, F., and Xia, T. (2019). Hypoxic glioma cell-secreted exosomal miR-301a activates Wnt/b-catenin signaling and promotes radiation resistance by targeting TCEAL7. *Mol. Ther.* 27, 1939–1949. doi: 10.1016/j.ymthe.2019.07.011

Zeng, A., Yin, J., Li, Y., Li, R., Wang, Z., Zhou, X., et al. (2018b). miR-129-5p targets Wnt5a to block PKC/ERK/NF-kappaB and JNK pathways in glioblastoma. *Cell Death Dis.* 9:394. doi: 10.1038/s41419-018-0343-1

Zeng, A., Wei, Z., Yan, W., Yin, J., Huang, X., Zhou, X., et al. (2018a). Exosomal transfer of miR-151a enhances chemosensitivity to temozolomide in drug-resistant glioblastoma. *Cancer Lett.* 436, 10–21. doi: 10.1016/j.canlet.2018.08.004

Zeng, R., and Dong, J. (2021). The hippo signaling pathway in drug resistance in cancer. *Cancers (Basel)* 13:318. doi: 10.3390/cancers13020318

Zhang, B., Pan, X., Cobb, G. P., and Anderson, T. A. (2007). microRNAs as oncogenes and tumor suppressors. *Dev. Biol.* 302, 1–12. doi: 10.1016/j.ydbio.2006.08.028

Zhang, L., and Yu, D. (2019). Exosomes in cancer development, metastasis, and immunity. *Biochim. Biophys. Acta Rev. Cancer* 1871, 455–468. doi: 10.1016/j.bbcan.2019.04.004

Zhang, L., Liao, Y., and Tang, L. (2019). MicroRNA-34 family: a potential tumor suppressor and therapeutic candidate in cancer. *J. Exp. Clin. Cancer Res.* 38:53. doi: 10.1186/s13046-019-1059-5

Zhang, Q., Song, L. R., Huo, X. L., Wang, L., Zhang, G. B., Hao, S. Y., et al. (2020). MicroRNA-221/222 inhibits the radiation-induced invasiveness and promotes the radiosensitivity of malignant meningioma cells. *Front. Oncol.* 10:1441. doi: 10.3389/fonc.2020.01441

Zhang, X., Zhang, G., Huang, H., Li, H., Lin, S., and Wang, Y. (2020). Differentially expressed MicroRNAs in radioresistant and radiosensitive atypical meningioma: a clinical study in Chinese patients. *Front. Oncol.* 10:501. doi: 10.3389/fonc.2020.00501

Zhang, Z., Xu, J., Chen, Z., Wang, H., Xue, H., Yang, C., et al. (2020). Transfer of microRNA via macrophage-derived extracellular vesicles promotes proneural-to-mesenchymal transition in glioma stem cells. *Cancer Immunol. Res.* 8, 966–981. doi: 10.1158/2326-6066.CIR-19-0759

Zhao, C., Guo, R., Guan, F., Ma, S., Li, M., Wu, J., et al. (2020). MicroRNA-128-3p enhances the chemosensitivity of temozolomide in glioblastoma by targeting c-Met and EMT. *Sci. Rep.* 10:9471. doi: 10.1038/s41598-020-65331-3

Zhao, L., Zhao, W., Hou, Y., Wen, C., Wang, J., Wu, P., et al. (2020). An overview of managements in meningiomas. *Front. Oncol.* 10:1523. doi: 10.3389/fonc.2020.01523

Zhao, P., Cheng, J., Li, B., Nie, D., Li, C., Gui, S., et al. (2021). Up-regulation of the expressions of MiR-149-5p and MiR-99a-3p in exosome inhibits the progress of pituitary adenomas. *Cell Biol. Toxicol.* 37, 633–651. doi: 10.1007/s10565-020-09570-0

Zheng, L., Zhang, Y., Liu, Y., Zhou, M., Lu, Y., Yuan, L., et al. (2015). MiR-106b induces cell radioresistance via the PTEN/PI3K/AKT pathways and p21 in colorectal cancer. *J. Transl. Med.* 13:252. doi: 10.1186/s12967-015-0592-z

Zheng, Z., Zhang, Y., Zhang, Z., Yang, Y., and Song, T. (2017). Effect of miR-106b on Invasiveness of Pituitary Adenoma via PTEN-PI3K/AKT. *Med. Sci. Monit.* 23, 1277–1285. doi: 10.12659/msm.900092

Zuo, Y., Zheng, W., Tang, Q., Liu, J., Wang, S., and Xin, C. (2021). miR-576-3p overexpression enhances cisplatin sensitivity of ovarian cancer cells by dysregulating PD-L1 and cyclin D1. *Mol. Med. Rep.* 23:81. doi: 10.3892/mmr.2020.11719

Conflict of Interest: The authors declare that the research was conducted in the absence of any commercial or financial relationships that could be construed as a potential conflict of interest.

Publisher's Note: All claims expressed in this article are solely those of the authors and do not necessarily represent those of their affiliated organizations, or those of the publisher, the editors and the reviewers. Any product that may be evaluated in this article, or claim that may be made by its manufacturer, is not guaranteed or endorsed by the publisher.

frontiers in Cell and Developmental Biology

ORIGINAL RESEARCH
published: 13 October 2021
doi: 10.3389/fcell.2021.758400

Targeted Inhibition of Fibroblast Growth Factor Receptor 1-GLI Through AZD4547 and GANT61 Modulates Breast Cancer Progression

Syeda Kiran Riaz[1,2,3†], Walizeb Khan[1†], Fen Wang[3], Tanwir Khaliq[2], Amber Malik[1], Eisha Tir Razia[1], Jahangir Sarwar Khan[4], Shafiul Haque[5,6], Anwar M. Hashem[7,8], Shadi S. Alkhayyat[9], Najiah Esam Azhar[10], Steve Harakeh[11,12], Mohammad Javed Ansari[13], Farhan Haq[1] and Muhammad Faraz Arshad Malik[1]**

[1] Department of Biosciences, COMSATS University, Islamabad, Pakistan, [2] Department of Molecular Biology and Biochemistry, Shaheed Zulfiqar Ali Bhutto Medical University, Islamabad, Pakistan, [3] College of Medicine, Texas A&M University, College Station, TX, United States, [4] Department of Surgery, Rawalpindi Medical University, Rawalpindi, Pakistan, [5] Research and Scientific Studies Unit, College of Nursing and Allied Health Sciences, Jazan University, Jazan, Saudi Arabia, [6] Faculty of Medicine, Bursa Uludağ University, Bursa, Turkey, [7] Vaccines and Immunotherapy Unit, King Fahd Medical Research Center, King Abdulaziz University, Jeddah, Saudi Arabia, [8] Department of Medical Microbiology and Parasitology, Faculty of Medicine, King Abdulaziz University, Jeddah, Saudi Arabia, [9] Faculty of Medicine, King Abdulaziz University, Jeddah, Saudi Arabia, [10] General Surgery, Department of Internal Medicine, King Abdullah Medical Complex, General Directorate of Health Affairs, Jeddah, Saudi Arabia, [11] Special Infectious Agents Unit, King Fahd Medical Research Center, King Abdulaziz University, Jeddah, Saudi Arabia, [12] Yousef Abdullatif Jameel Chair of Prophetic Medicine Application, Faculty of Medicine, King Abdulaziz University, Jeddah, Saudi Arabia, [13] Department of Botany, Hindu College (Moradabad), Mahatma Jyotiba Phule Rohilkhand University, Bareilly, India

OPEN ACCESS

Edited by:
Ata Abbas, Case Western Reserve University, United States

Reviewed by:
Atrayee Bhattacharya, Dana–Farber Cancer Institute, United States
Athina Myrto Chioni, Kingston University, United Kingdom

***Correspondence:**
Muhammad Faraz Arshad Malik
famalik@comsats.edu.pk
Farhan Haq
farhan.haq@comsats.edu.pk

† These authors have contributed equally to this work and share first authorship

Specialty section:
This article was submitted to Epigenomics and Epigenetics, a section of the journal Frontiers in Cell and Developmental Biology

Received: *13 August 2021*
Accepted: *07 September 2021*
Published: *13 October 2021*

Citation:
Riaz SK, Khan W, Wang F, Khaliq T, Malik A, Razia ET, Khan JS, Haque S, Hashem AM, Alkhayyat SS, Azhar NE, Harakeh S, Ansari MJ, Haq F and Malik MFA (2021) Targeted Inhibition of Fibroblast Growth Factor Receptor 1-GLI Through AZD4547 and GANT61 Modulates Breast Cancer Progression. Front. Cell Dev. Biol. 9:758400. doi: 10.3389/fcell.2021.758400

The underlying mechanism of fibroblast growth factor receptor 1 (FGFR1) mediated carcinogenesis is still not fully understood. For instance, FGFR1 upregulation leads to endocrine therapy resistance in breast cancer patients. The current study aimed to identify FGFR1-linked genes to devise improved therapeutic strategies. RNA-seq and microarray expression data of 1,425 breast cancer patients from two independent cohorts were downloaded for the analysis. Gene Set Enrichment Analysis (GSEA) was performed to identify differentially expressed pathways associated with FGFR1 expression. Validation was done using 150 fresh tumor biopsy samples of breast cancer patients. The clinical relevance of mRNA and protein expression of FGFR1 and its associated genes were also evaluated in mouse embryonic fibroblasts (MEFs) and breast cancer cell line (MDA-MB-231). Furthermore, MDA-MB-231 cell line was treated with AZD4547 and GANT61 to identify the probable role of FGFR1 and its associated genes on cells motility and invasion. According to GSEA results, SHH pathway genes were significantly upregulated in FGFR1 patients in both discovery cohorts of breast cancer. Statistical analyses using both discovery cohorts and 150 fresh biopsy samples revealed strong association of FGFR1 and GLI1, a member of SHH pathway. The

increase in the expression of these molecules was associated with poor prognosis, lymph node involvement, late stage, and metastasis. Combined exposures to AZD4547 (FGFR1 inhibitor) and GANT61 (GLI1 inhibitor) significantly reduced cell proliferation, cell motility, and invasion, suggesting molecular crosstalk in breast cancer progression and metastasis. A strong positive feedback mechanism between FGFR1–GLI1 axis was observed, which significantly increased cell proliferation and metastasis. Targeting FGFR1–GLI1 simultaneously will significantly improve the prognosis of breast cancer in patients.

Keywords: FGFR1, SHH pathway, GLI1, AZD4547, GANT61, breast cancer

INTRODUCTION

The fibroblast growth factor receptor (FGFR) signaling pathway plays an important role in a variety of biological processes including angiogenesis, cell growth, differentiation, and survival (Korc and Friesel, 2009; Wesche et al., 2011). The genetic aberrations in FGFs and FGFRs linked to tumor initiation and progression are extensively reported in many cancers (Parish et al., 2015). The development of Pan-FGFR(1–4) inhibitors including ASP5878 (NCT02038673), LY2874455 (NCT01212107), infigratinib (NCT02160041), erdafitinib (NCT02365597), and AZD4547 (NCT02038673) are under different phases of clinical trials (Raja et al., 2019). However, despite of the progress, substantial effort is required to thoroughly understand the underlying mechanism of FGFR-mediated carcinogenesis. FGFs are expressed in most tissue types and play vital roles by promoting mitosis in mesenchymal and epithelial transition. In humans, 23 different FGFs have been identified, out of which 18 ligands (FGF1–10 and 16–23) are mitogenic signaling molecules (Beenken and Mohammadi, 2009). These FGFs bind and activate FGFRs (1–4), highly conserved tyrosine kinase receptors, to modulate other signaling pathways (Kwabi-Addo et al., 2004; Babina and Turner, 2017), including PLCγ/DAG/PKC, PI3K/AKT, RAS/RAF, and MAPK (Dienstmann et al., 2014; Ornitz and Itoh, 2015). FGFs also bind to heparan sulfate glycosaminoglycans (HSGAGs), which enable the activation of FGF signaling through binding FGFRs in HSGAGs-dependent manner (Beenken and Mohammadi, 2009). A recent study showed that FGF upregulation also leads to activation of SHH pathway for the ventral patterning of spinal cord (Morales et al., 2016). Moreover, upregulated FGF-FGFRs are found in many cancers including breast, prostate, non-small cell lung, liver, and colorectal (Acevedo et al., 2009; Parish et al., 2015). The genetic aberrations in FGFR1 were first documented in breast cancer. Since then, strategies are underway to regulate FGFR1-modulated cancer initiation and progression (Adnane et al., 1991). However, recent studies showed that FGFR1 upregulation causes resistance to cyclin-dependent kinase (CDK) inhibitors in different breast cancer subtypes (Formisano et al., 2019). Another study demonstrated that FGFR1 upregulation also minimize effect of other potential inhibitors targeting PI3K, ER, and mTOR pathway (Drago et al., 2019). Studies are underway to identify FGFR1-linked gene set(s) to devise effective breast cancer treatment options. For instance, a recent study showed that MAP3K1 mutation may improve the prognosis of breast cancer patients with FGFR1 overexpression (Carene et al., 2020). The aim of the current study was to identify FGFR1-linked gene sets to devise effective breast cancer treatment options. For that purpose, a comprehensive and integrated strategy was devised to establish the clinical relevance of FGFR1 modulation in breast cancer. Initially, FGFR1-expression-dependent differentially expressed pathways were identified using RNA-seq and microarray expression data of 1,425 breast cancer patients. Next, expression and clinical validation were done in 150 fresh tumor biopsy samples of breast cancer patients. Furthermore, breast cancer cell line (MDA-MB-231) was used to investigate the probable association of FGFR1 with SHH and GLI1 in breast cancer progression. The current study provides new FGFR1-linked biomarkers, which suggest novel treatment options for improving the prognosis of breast cancer patients.

MATERIALS AND METHODS

Data Collection and Processing

The study design of the current study is described in **Supplementary Material ESM 1**. RNA-seq data of 1,098 breast cancer patients were downloaded from The Cancer Genome Atlas (TCGA) Database[1]. The mRNA expression levels of FGFR1 gene was estimated using z-score >2.0. The clinicopathological relevance of FGFR1 expression was assessed against multiple features including age, stage, grade, node stage, and metastasis. The details of clinical information are available in **Supplementary Material ESM 2**. Gene Set Enrichment Analysis (GSEA) based on FGFR1 expression was performed to identify new FGFR1-associated pathways in breast cancer (Subramanian et al., 2005). Clinicopathological association of those pathways in breast cancer was also evaluated. Additionally, another data (GSE20685) of 327 breast cancer patients were also downloaded to validate our findings in an independent cohort (**Supplementary Material ESM 3**). Similarly, clinical association of FGFR1 expression and FGFR1-associated pathways using GSEA was investigated. Common pathways identified between the two cohorts were selected for further analysis.

[1]https://portal.gdc.cancer.gov/projects/TCGA-BRCA

Validation Cohort

The present study was conducted after obtaining approval from institutional ethical review committees at our university and concerned hospital. Tumor biopsies (n = 150) along with matched control tissues were collected for validation of discovery cohort findings after receiving informed consents of participants. Clinicopathological information of these patients was collected through subsequent follow-up from pathology reports. Information regarding clinicopathological features of validation cohort is available in **Supplementary Material ESM 4**.

RNA Extraction and cDNA Synthesis

Total RNA was extracted from tumors and matched normal samples using TRIzol® (Invitrogen, Carlsbad, CA, United States). cDNA was generated using RevertAid First-Strand cDNA Synthesis Kit (Thermo Fisher Scientific, Carlsbad, CA, United States) as per manufacturer's instructions. Conventional PCR was performed with β-actin primers to confirm the cDNA synthesis. Amplified products were electrophoresed on 2% agarose gel and stained with ethidium bromide for further use.

Primer Designing and Quantitative Real-Time PCR

Primers for FGFR1 and GLI1 were designed using Integrated DNA Technology (IDT) software and synthesized for Macrogen, Korea (**Supplementary Material ESM 10**). Target specificity of these products was confirmed with NCBI Primer Blast to avoid non-specific binding. Quantitative real-time PCR (qRT-PCR) quantitative PCR (qPCR) was performed using VeriQuest SYBR Green qPCR Master Mix (Thermo Fisher Scientific, CA, United States). Expression of target gene was normalized using β-actin as an internal control. The reaction condition included an initial denaturation at 95°C for 15 min, followed by 40 cycles of denaturation at 95°C for 15 s and annealing at 53°C for 1 min in each cycle. Relative mRNA expression and fold change was evaluated using the $2^{-\Delta\Delta Ct}$ method.

Breast Cancer Cell Line Used in the Study

MDA-MB-231 was maintained as per American Type Culture Collection (ATCC). Expression of FGFR1, SHH, and GLI1 were assessed both at RNA and protein level. Similarly, the effect of these aforementioned molecules was evaluated on CRISPR/Cas9-mediated SHH knockout MDA-MB-231 cells (Riaz et al., 2019). Moreover, commercially available small interfering RNAs (siRNAs) targeting SHH (hs.Ri.SHH.13.1) and GLI1 (hs.Ri.GLI1.13.2) were purchased from IDT[2], and MDA-MB-231 cells were transfected with them for assessing the differential expression of FGFR1, SHH, and GLI1.

Exposure of GANT61 and AZD4547 Inhibitors Against SHH and GLI1

A stock of GANT61 (cat: G9048, Sigma) was dissolved in dimethyl sulfoxide (DMSO) maintaining a stock concentration of 1 mM. Briefly, 3×10^5 cells were seeded in six-well plates until confluency and treated with variable concentrations of GANT61. Similarly, AZD4547 (Selleckchem[3]) was added to the medium at a concentration of 100 nM. Both RNA and protein were quantified from treated and untreated wells for functional assays performed after 48 h of treatment with both inhibitors.

Protein Estimation Using Western Blot

Total protein content from respective cell lines were extracted and quantified using the Pierce BCA protein assay kit (23225, Thermo Fisher Scientific, United States). Extracted proteins were separated on 10% sodium dodecyl sulfate–polyacrylamide gel electrophoresis (SDS-PAGE), transferred to nitrocellulose membrane, and blocked by 5% non-fat milk at room temperature. Membranes were incubated with primary antibodies for FGFR1 (1:1,000), SHH (1:1,000), and GLI1 (1:1,000) (**Supplementary Material ESM 11**). After overnight incubation at 4°C, membranes were incubated with secondary antibodies at room temperature for 1 h (**Supplementary Material ESM 11**). Protein signals were visualized using ECL Prime Western Blotting Detection Reagent (GE Healthcare Japan) with β-actin as loading control.

Wound Healing Assay

Briefly, 3×10^5 cancer cells from respective cancer cell lines were seeded in six-well plates. The plate was left at 37°C incubation till it reaches confluent monolayer. Once attained, the medium was aspirated, and N-2-hydroxyethylpiperazine-N′-2-ethanesulfonic acid (HEPES) medium was introduced in each well. Wounding measurements were recorded using the previously mentioned protocol (Riaz et al., 2019).

Cell Invasion Assay

This assay was based on Boyden chamber using inserts (8 μm) placed in 24-well plate. These inserts were precoated with 50 μg/ml Matrigel (BD Biosciences, Berkshire, United Kingdom) prior to cell seeding. A total of 5×10^4 cancer cells were seeded in each insert placed in the respective wells. The plate was left at 37°C incubation for 24 h. After specified time duration, these inserts were fixed with methanol and stained with crystal violet. Cells were counted under light microscope at 40 × magnification as per protocol stated earlier (Malik et al., 2009).

Statistical Analysis

IBM SPSS 21 software (IBM Inc., Armonk, NY, United States) was used for all the statistical analyses. Data were represented as mean ± SD, and Wilcoxon signed-rank test was performed to evaluate difference between tumor and control. Mann–Whitney U test and Kruskal–Wallis ANOVA were applied to explore any probable association of these genes with

[2]https://sg.idtdna.com/pages

[3]https://www.selleckchem.com/products/azd4547.html

clinicopathological features. Furthermore, correlation between molecules was observed using Spearmen test. All *p*-values of 0.05 were considered statistically significant.

RESULTS

Expression Analysis of Fibroblast Growth Factor Receptor 1 Gene Expression (Discovery Cohorts)

Initially, in TCGA dataset of 1,098 patients, clinical relevance of FGFR1 expression with breast cancer patients was assessed. FGFR1 was significantly overexpressed in late tumor stage ($p = 0.05$) and node-positive patients ($p = 0.04$) (**Table 1**).

Fibroblast Growth Factor Receptor 1-Expression-Based Gene Set Enrichment Analysis

Next, GSEA was performed to identify common differentially expressed pathways in both breast cancer cohorts. A total of 20 pathways were found to be upregulated along with FGFR1 overexpression in TCGA dataset (**Supplementary Material ESM 5**). Similarly, a total of 14 pathways were found to be upregulated along with FGFR1

TABLE 1 | Clinicopathological analysis of *FGFR1* and *GLI1* in discovery cohort 1.

Variables	Total	Mean ± SD			
		FGFR1	***p*-value**	***GLI-1***	***p*-value**
Samples	1,091	6.69 ± 1.21	0.0001[c]	−0.11 ± 1.57	0.0001[c]
Stage-wise distribution					
Stage I/II	910	6.68 ± 1.21	–	−0.13 ± 1.56	0.0001[b]
Stage III/IV	177	6.73 ± 1.22		−0.001 ± 1.63	
Nodal Involvement					
N0 (none)	874	6.66 ± 1.24	0.002[b]	−0.12 ± 1.56	0.044[b]
Nodal metastasis	196	6.81 ± 1.04		−0.04 ± 1.62	
Metastasis involvement					
M0	907	6.66 ± 1.22	–	−0.17 ± 1.55	0.022
M1	22	6.77 ± 1.27		−0.96 ± 1.99	
Age group					
Above 50	760	6.69 ± 1.10	–	0.23 ± 1.54	0.0001[a]
Below 50	329	6.73 ± 1.25		−0.26 ± 1.57	

[a] *Mann–Whitney test.*
[b] *Kruskal–Wallis test.*
[c] *Wilcoxon signed-rank test.*

TABLE 2 | Clinicopathological analysis of *FGFR1* and *GLI1* expression in *in vitro* cohort.

Variables	Total	Mean ± SD			
		FGFR1	***p*-value**	***GLI-1***	***p*-value**
Tumor	150	18.6 ± 26	0.0001[a]	20.5 ± 28.96	0.0001[a]
Control	150	1 ± 1.41	–	1 ± 1.95	–
Grade-wise distribution					
Grade I	14	22.71 ± 34.69	–	9.27 ± 11.55	0.05[b]
Grade II	90	15.65 ± 19.3		20.11 ± 29.76	
Grade III	46	23.12 ± 33.41		24.74 ± 30.48	
Stage-wise distribution					
Stage I/II	111	16.12 ± 21.31	0.004[b]	17.29 ± 24.22	0.011[b]
Stage III/IV	39	25.65 ± 35.69		29.71 ± 38.38	
Nodal involvement					
N0 (none)	48	16.86 ± 23.49	–	20.06 ± 32.80	–
Nodal metastasis	102	19.42 ± 27.23		20.73 ± 27.14	
Metastasis involvement					
M0	145	17.97 ± 26	0.040[b]	19.67 ± 28.88	0.006[b]
M1	5	36.66 ± 22.39		45.17 ± 20.9	

[a] *Wilcoxon Signed-ranks test.*
[b] *Mann–Whitney test.*

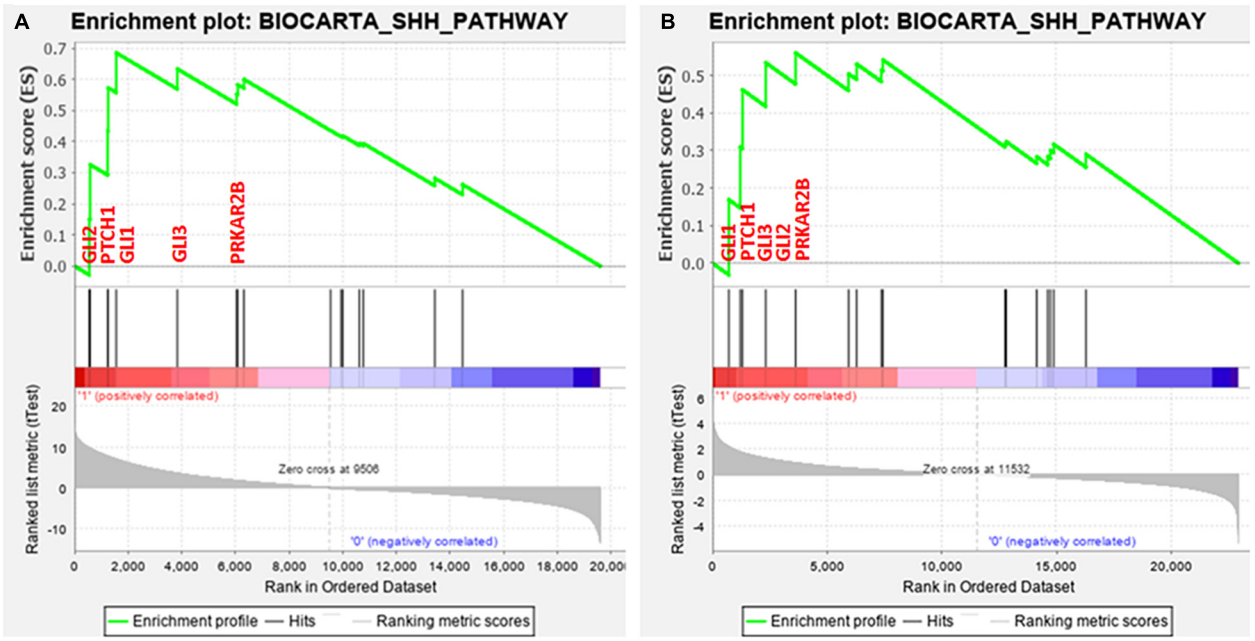

FIGURE 1 | Enrichment plot: BIOCARTA_SHH_PATHWAY of both datasets. **(A)** TCGA and **(B)** GSE20685 that shows profile of the running ES score and positions of gene set members on the rank ordered list.

overexpression in the GEO20685 cohort (**Supplementary Material ESM 6**). Out of all pathways, three pathways including ALK, SHH, and PRION were common in both datasets (**Supplementary Material ESM 7**). Since SHH pathway dysregulation is reported as an early event in several breast cancer studies, we selected SHH pathway to evaluate the association of FGFR1 and SHH pathway in modulating breast carcinogenesis.

Clinicopathological Relevance of SHH Pathway Genes

Interestingly, 5 out of 16 SHH pathway genes showed core enrichment in FGFR1-expressed breast cancer patients using leading-edge subset method (**Figure 1** and **Supplementary Material ESM 8**). Of note, all GLI family genes including GLI1, GLI2, and GLI3 were significantly associated with FGFR1 in both datasets. Therefore, to further establish the link of FGFR1 overexpression with GLI genes, clinicopathological association of genes including FGFR1, GLI1, GLI2, and GLI3 were evaluated (**Supplementary Material ESM 9**). According to the results, GLI1 gene was the most frequently associated gene with the poor prognostic features of breast cancer patients including late stage ($p = 0.0001$), node positive ($p = 0.044$), and metastasis ($p = 0.022$) (**Table 1** and **Supplementary Material ESM 9**). Similarly, in the second dataset of 327 breast cancer patients, GLI1 overexpression was the only gene in the SHH pathway that showed significant associations with late stage ($p = 0.047$). Therefore, based on all the expression and statistical analyses in discovery cohorts, we further established the potential prognostic association of GLI1 and FGFR1 genes using normal and tumor pairs of 150 breast cancer patients.

In vitro Validation of Fibroblast Growth Factor Receptor 1 and GLI1 Association in 150 Breast Cancer Patients

The demographics and clinical characteristics of the cohort exhibited that the mean age of breast-cancer-affected patients included in the study was 45 years, ranging from 23 to 75 years. According to Wilcoxon test, both FGFR1 ($p = 0.0001$) and GLI1 ($p = 0.0001$) were significantly overexpressed in tumor samples compared to their respective controls. Interestingly, FGFR1 and GLI1 expression showed strong positive correlation (Spearman's correlation = 0.513, $p = 0.0001$). Of note, consistent with discovery cohort findings, overexpression of GL1 and FGFR1 genes was significantly associated with high grade ($p = 0.05$), late stage ($p = 0.011$, $p = 0.004$), and metastasis ($p = 0.006$, $p = 0.04$), respectively (**Table 2**). These findings suggest strong biological and prognostic relevance of GLI1 and FGFR1 expression in modulating subtypes of breast cancer progression.

Effect of GANT61 and AZD4547 Treatment on Fibroblast Growth Factor Receptor 1-GLI1 Expression in MDA-MB231

Next, the effect of GANT61 (GLI1 inhibitor) and AZD4547 (FGFR1 inhibitor) on both GLI1 and FGFR1 was studied in MDA-MB-231 cell line. To perform the analysis, multiple genes including SHH, AKT, and MAPK were also selected to compare the effect. According to the results, a significant decrease in the expression of GLI1, SHH, and FGFR1 was observed after treatment with GANT61 at 24 and 48 h. MAPK expression was

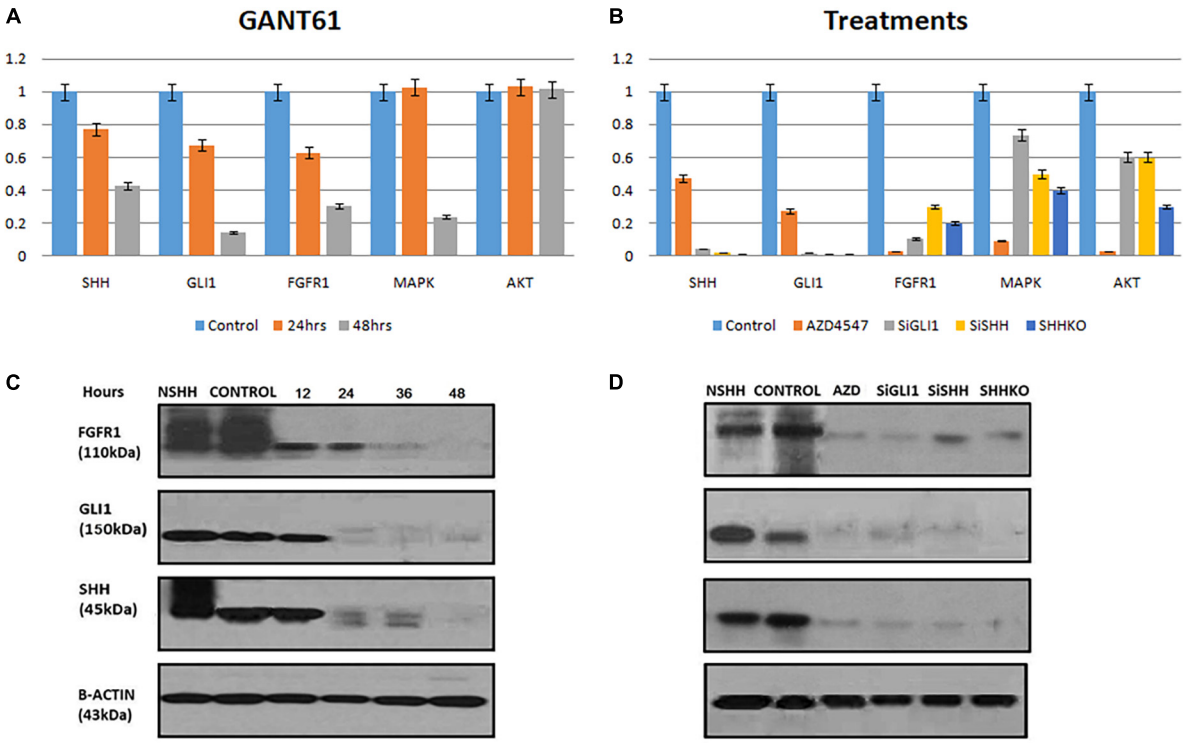

FIGURE 2 | Synergistic effect of FGFR1 and Hedgehog signaling in breast cancer cells. **(A)** MDA-MB-231 cells were treated with 10 μM GANT61, and samples were collected after 24 and 48 h of treatment. Significant decrease in mRNA expression of FGFR1 was observed after treatment with GANT61 at 24 and 48 h both, while expression of MAPK was reduced after 48 h of treatment. No effect of GANT61 treatment was observed on transcription of AKT in MDA-MB-231 cells. **(B)** Effect of FGFR1 inhibitor [AZD4547 (0.2 nM)], GLI1 knockdown (SiGLI1), SHH knockdown (SiSHH), and SHH knockout (SHHKO) on SHH, GLI1, FGFR1, MAPK, and AKT at transcriptional level. Cells were collected after 48 h of treatment or gene silencing. Western blot showing decrease in expression of FGFR1, GLI1, and SHH upon treatment with **(C)** GANT61 (10 μM) administered until 48 h with a 12-h interval and **(D)** AZD4547 (0.2 nM), SiGLI1, SiSHH, and CRISPR/Cas9-mediated SHH knockout in MDA-MB-231 breast cancer cells. Cells were collected 48 h after treatment AZD4547, SiGLI1, and SiSHH. SHH ligand (NSHH) was also added to MDA-MB-231 cells to observe effect of pathway induction. B-Actin was used as internal control.

reduced after 48 h of treatment. However, no change in the expression of AKT gene was observed (**Figure 2A**). Interestingly, a significant downregulation of FGFR1 expression was observed compared to other genes when cells were treated with AZD4547, GLI1 knockdown (SiGLI1), SHH knockdown (SiSHH), and SHH knockout (SHHKO), suggesting a crosstalk between SHH pathway and FGFR1 activation (**Figure 2B**).

Synergistic Effect of Fibroblast Growth Factor Receptor 1 and Hedgehog Signaling

Next, using Western blot analysis, the impact of GANT61, AZD4547, SiGLI1, and SiSHH was assessed in MDA-MB-231 cells on SHH, GLI1, and FGFR1 expression. First, GANT61 treatment was administered until 48 h with 12-h intervals. A significant decrease in protein expression was observed after 12 h for all three genes including SHH, GLI1, and FGFR1 (**Figure 2C**). In addition, AZD4547, SiGLI1, SiSHH, and CRISPR/Cas9-mediated SHH knockout in MDA-MB-231 breast cancer cells was also assessed (**Figure 2D**). Consistently, a similar pattern of decrease in protein expression was observed for SHH, GLI1, and FGFR1, suggesting the synergistic role of FGFR1 and SHH pathway. Furthermore, we also evaluated the effect of SHH and GLI1 expression in mouse embryonic fibroblasts (MEFs) with MEFFGFR WT and MEFFGFR1 KO cells. Significant downregulation of SHH and GLI1 was observed in the FGFR1 knockout mouse MEFs, further indicating crosstalks between FGFR–SHH pathways (**Figure 3**).

Combined Treatment of GANT61 and AZD4547 Reduces Cell Motility and Invasion

Furthermore, the effect of FGFR1–SHH pathway signaling on the motility of breast cancer cells was evaluated using wound-healing assay. MDA-MB-231 cells were treated with AZD4547 only, GANT61 only, and AZD + GANT61 combined (**Figure 4**). Breast cancer cell migration was evaluated after 48 h of treatment. Of note, invasion and migration of MDA-MB-231 decreased significantly upon AZD + GANT61 treatment compared to AZD4547 or GANT61 treatment alone. Therefore, the data suggest that targeting FGFR1–GLI1 simultaneously significantly reduce cell invasion and metastasis.

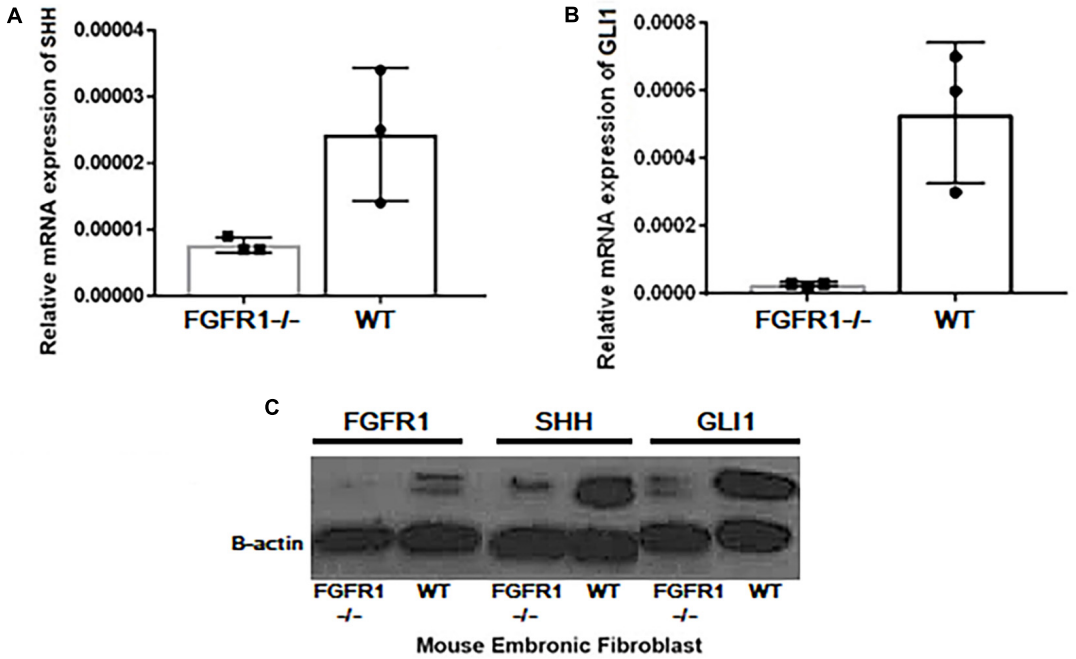

FIGURE 3 | Expressional variation of SHH and GLI1 at transcript level in MEF^{WT} and $MEF^{FGFR1KO(-/-)}$. Significant downregulation of **(A)** SHH and **(B)** GLI1 at mRNA and **(C)** protein level was observed in the FGFR1 knockout (–/–) and wild-type (WT) mouse embryonic fibroblast cells (MEFs) showing crosstalks between both pathways.

DISCUSSION

Fibroblast Growth Factor Receptor 1 DNA amplification is the most frequently reported FGF-pathway alteration in breast cancer (Sobhani et al., 2020). *FGFR1* is a known poor prognostic marker also associated with poor survival in breast cancer patients (Wu et al., 2018). Herein, we reported a different mechanism by which coexpression of *FGFR1* and *GLI1* genes leads to breast cancer invasion and metastasis. We also demonstrated that simultaneous targeting of FGFR1 and GLI1 using GANT61 and AZD4547 inhibitors significantly decreases breast cancer invasion and metastasis, suggesting new approaches for clinical studies. The dysregulation of Hedgehog signaling, including GLI1 upregulation, is frequently reported in young breast cancer patients with shorter overall survival (Riaz et al., 2018). Of note, FGFR–Hedgehog pathway crosstalk showed variable prognostic roles in different cancers. For instance, in non-small cell lung cancer, FGFR1–GLI1 axis promotes lung carcinogenesis (Ji et al., 2016). On the contrary, preclinical study in medulloblastoma showed antagonistic role between FGFR1 and GLI1 expression, suggesting tissue-specific role of these pathways (Neve et al., 2019). However, crosstalk between FGFR and Hedgehog signaling is not elucidated in breast cancer. Here, using large-scale transcriptomic data of 1,425 breast cancer patients, we demonstrated that FGFR/SHH pathway crosstalk leads to poor prognosis of breast cancer patients. Particularly, FGFR1 and GLI1 showed strong correlation with late stage, node, and metastasis in luminal subtypes of breast cancer patients.

These observations were further validated using qPCR method in 150 paired tumor-normal cases. The results showed strong correlation ($p < 0.5$) between FGFR1 and GLI1 and significant association with late stage, high grade, and metastasis, further emphasizing on the FGFR1–GLI1 nexus in breast carcinogenesis. Next, the prognostic impact of FGFR1–GLI1 axis inhibition was evaluated. Cyclin-dependent kinase 6 (CDK6) inhibitors are the most widely used treatment options in breast cancer patients (Parish et al., 2015). However, it has been observed that FGFR1 upregulation causes resistance to CDK inhibitors in subtypes of breast cancer patients, suggesting alternate treatment strategies (Formisano et al., 2019). Recently, it has been demonstrated that treatment with multiple inhibitors may improve the prognosis and increase the survival of breast cancer patients (Slamon et al., 2020). For that purpose, the efficacy of AZD4547, a selective inhibitor of FGFR1, and GANT61, a GLI1 inhibitor, was evaluated in FGFR1–GLI1-overexpressed MDA-MB-231 cell line. Interestingly, the results showed coexpression of FGFR1 and GLI1, suggesting molecular crosstalk between both genes (**Figure 1**). Moreover, inhibiting either FGFR1 or GLI using AZD4547 or GANT61, respectively, also decreases expression of both genes (**Figure 2**). Furthermore, combined inhibition of FGFR1–GLI1 with AZD + GANT61 inhibitors drastically decreased the migratory and invasive abilities of breast cancer cells, suggesting a novel mechanism to treat breast cancer patients. In conclusion, a comprehensive and integrated strategy was devised to find new therapeutic options for the treatment of breast cancer. Clinical analyses of whole transcriptomic data and multiple *in vitro* functional assays strongly suggested that

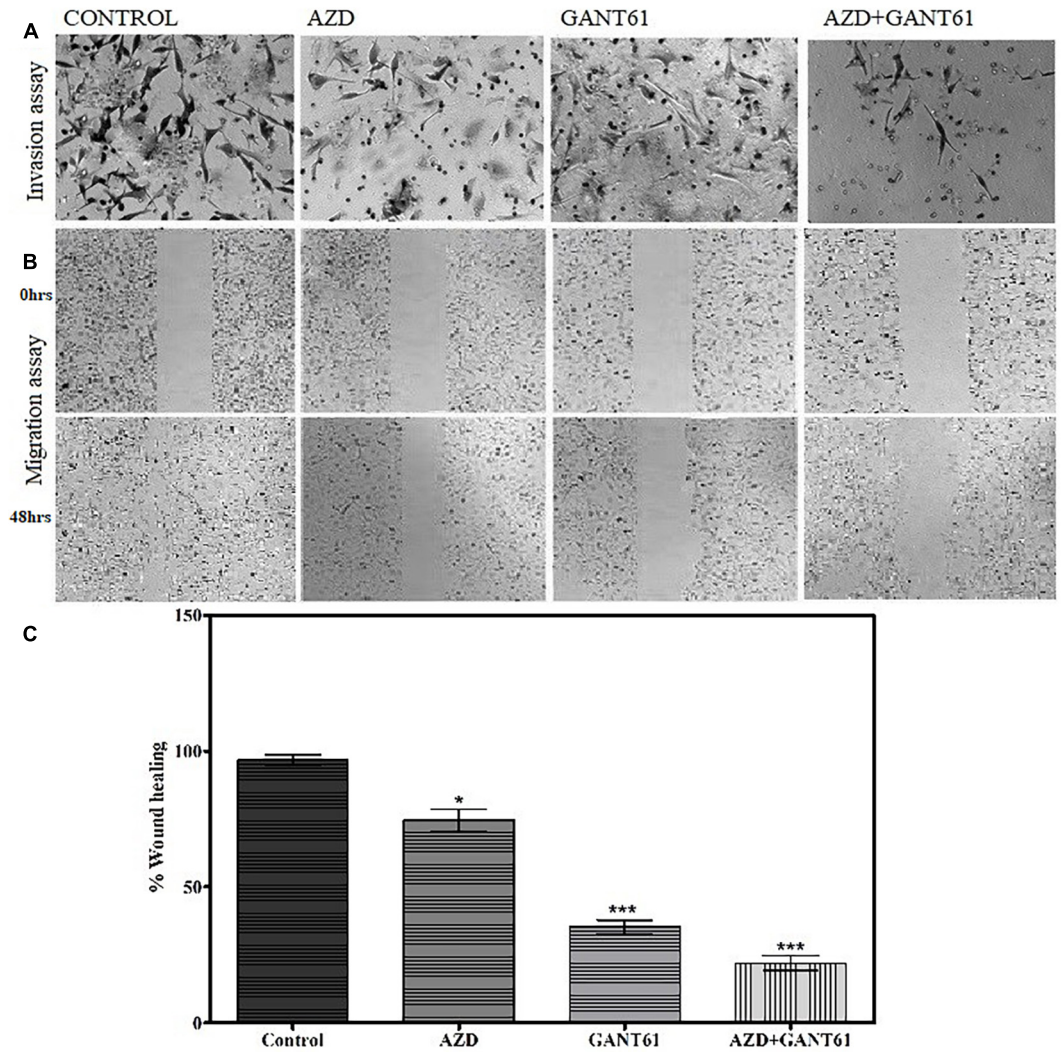

FIGURE 4 | Decrease in migratory and invasive abilities of breast cancer cells was observed upon inhibition of FGFR1-GLI1 using *in vitro* models. **(A)** Invasion and **(B)** migration assay was performed in control cells, AZD4547 (0.2 nM)-treated cells, GANT61 (10 μM)-treated cells, and AZD + GANT61 combined treatment in MDA-MB-231 cells (scale bar, 50 μm). **(C)** Histogram showing overall difference in migration of cells after 48 h of AZD4547, GANT61, or combined treatment. Invasion and migration of MDA-MB-231 decreased significantly upon AZD + GANT61 treatment (ANOVA with Dunnett's *post hoc* test, $^{*}p < 0.05$, $^{***}p < 0.0001$). All results are representative of three independent experiments.

targeting FGFR1–GLI1 crosstalk can significantly improve the prognosis of breast cancer. Interestingly, FGFR1 and GLI1 also activate many downstream oncogenic genes, which lead to cancer cell migration, proliferation, and survival (Luca et al., 2017; Riaz et al., 2018). Hence, our study provided a novel hotspot target site as plausible therapeutic option for breast cancer treatment.

DATA AVAILABILITY STATEMENT

The original contributions presented in the study are included in the article/**Supplementary Material**, further inquiries can be directed to the corresponding authors.

ETHICS STATEMENT

The studies involving human participants were reviewed and approved by the ERB Shaheed Zulfiqar Ali Bhutto. The patients/participants provided their written informed consent to participate in this study. The animal study was reviewed and approved by the Ethics Review Board of the Texas A&M University.

AUTHOR CONTRIBUTIONS

SKR, WK, FW, AM, TK, ER, JK, ShH, AH, SA, NA, StH, FH, and MFM: conceptualization, visualization, and writing—original

draft. SKR, WK, FW, TK, AM, ER, and JK: data curation. SKR, WK, FW, TK, AM, ER, JK, FH, and MFM: formal analysis, methodology, and validation. FW, FH, and MFM: funding acquisition. SKR, ER, TK, JK, ShH, AH, SA, NA, StH, FH, and MFM: investigation. ShH, AH, SA, NA, StH, FH, and MFM: project administration. ShH, AH, StH, FH, and MFM: resources and supervision. FH and MFM: software. ShH, AH, StH, FH, and MFM: writing—review and editing. All authors contributed to the article and approved the submitted version.

FUNDING

The study was partially funded by the COMSATS University Islamabad, Pakistan, Texas A&M Health Science Centre, United States, and Higher Education Commission, Pakistan (Grant ID 2603/SRGP).

ACKNOWLEDGMENTS

We thank all the participants included in the study.

SUPPLEMENTARY MATERIAL

The Supplementary Material for this article can be found online at: https://www.frontiersin.org/articles/10.3389/fcell.2021.758400/full#supplementary-material

REFERENCES

Acevedo, V. D., Ittmann, M., and Spencer, D. M. (2009). Paths of FGFR-driven tumorigenesis. *Cell Cycle* 8, 580–588. doi: 10.4161/cc.8.4.7657

Adnane, J., Gaudray, P., Dionne, C. A., Crumley, G., Jaye, M., Schlessinger, J., et al. (1991). BEK and FLG, two receptors to members of the FGF family, are amplified in subsets of human breast cancers. *Oncogene* 6, 659–663.

Babina, I. S., and Turner, N. C. (2017). Advances and challenges in targeting FGFR signalling in cancer. *Nat. Rev. Cancer* 17, 318–332. doi: 10.1038/nrc.2017.8

Beenken, A., and Mohammadi, M. (2009). The FGF family: biology, pathophysiology and therapy. *Nat. Rev. Drug Discov.* 8, 235–253. doi: 10.1038/nrd2792

Carene, D., Tran-Dien, A., Lemonnier, J., Dalenc, F., Levy, C., Pierga, J.-Y., et al. (2020). Association between FGFR1 copy numbers, MAP3K1 mutations, and survival in axillary node-positive, hormone receptor-positive, and HER2-negative early breast cancer in the PACS04 and METABRIC studies. *Breast. Cancer Res. Treat.* 179, 387–401. doi: 10.1007/s10549-019-05462-y

Dienstmann, R., Rodon, J., Prat, A., Perez-Garcia, J., Adamo, B., Felip, E., et al. (2014). Genomic aberrations in the FGFR pathway: opportunities for targeted therapies in solid tumors. *Ann. Oncol.* 25, 552–563. doi: 10.1093/annonc/mdt419

Drago, J. Z., Formisano, L., Juric, D., Niemierko, A., Servetto, A., Wander, S. A., et al. (2019). FGFR1 amplification mediates endocrine resistance but retains torc sensitivity in metastatic hormone Receptor-Positive (HR+) Breast Cancer. *Clin. Cancer Res.* 25, 6443–6451. doi: 10.1158/1078-0432.CCR-19-0138

Formisano, L., Lu, Y., Servetto, A., Hanker, A. B., Jansen, V. M., Bauer, J. A., et al. (2019). Aberrant FGFR signaling mediates resistance to CDK4/6 inhibitors in ER+ breast cancer. *Nat. Commun.* 10:1373. doi: 10.1038/s41467-019-09068-2

Ji, W., Yu, Y., Li, Z., Wang, G., Li, F., Xia, W., et al. (2016). FGFR1 promotes the stem cell-like phenotype of FGFR1-amplified non-small cell lung cancer cells through the Hedgehog pathway. *Oncotarget* 7, 15118–15134.

Korc, M., and Friesel, R. (2009). The role of fibroblast growth factors in tumor growth. *Curr. Cancer Drug. Targets* 9, 639–651. doi: 10.2174/156800909789057006

Kwabi-Addo, B., Ozen, M., and Ittmann, M. (2004). The role of fibroblast growth factors and their receptors in prostate cancer. *Endocr. Relat. Cancer* 11, 709–724. doi: 10.1677/erc.1.00535

Luca, A. D., Frezzetti, D., Gallo, M., and Normanno, N. (2017). FGFR-targeted therapeutics for the treatment of breast cancer. *Expert Opin. Invest. Drugs* 26, 303–311. doi: 10.1080/13543784.2017.1287173

Malik, F. A., Sanders, A. J., Kayani, M. A., and Jiang, W. G. (2009). Effect of expressional alteration of KAI1 on Breast cancer cell growth, adhesion, migration and invasion. *Cancer Genomics Proteomics* 6, 205–213.

Morales, A. V., Espeso-Gil, S., Ocaña, I., Nieto-Lopez, F., Calleja, E., Bovolenta, P., et al. (2016). FGF signaling enhances a sonic hedgehog negative feedback loop at the initiation of spinal cord ventral patterning. *Dev. Neurobiol.* 76, 956–971. doi: 10.1002/dneu.22368

Neve, A., Migliavacca, J., Capdeville, C., Schönholzer, M. T., Gries, A., Ma, M., et al. (2019). Crosstalk between SHH and FGFR signaling pathways controls tissue invasion in medulloblastoma. *Cancers* 11:1985. doi: 10.3390/cancers11121985

Ornitz, D. M., and Itoh, N. (2015). The fibroblast growth factor signaling pathway. *WIREs Dev. Biol.* 4, 215–266. doi: 10.1002/wdev.176

Parish, A., Schwaederle, M., Daniels, G., Piccioni, D., Fanta, P., Schwab, R., et al. (2015). Fibroblast growth factor family aberrations in cancers: clinical and molecular characteristics. *Cell Cycle* 14, 2121–2128. doi: 10.1080/15384101.2015.1041691

Raja, A., Park, I., Haq, F., and Ahn, S.-M. (2019). FGF19–FGFR4 signaling in hepatocellular carcinoma. *Cells* 8:536. doi: 10.3390/cells8060536

Riaz, S. K., Ke, Y., Wang, F., Kayani, M. A., and Malik, M. F. A. (2019). Influence of SHH/GLI1 axis on EMT mediated migration and invasion of breast cancer cells. *Sci. Rep.* 9:6620. doi: 10.1038/s41598-019-43093-x

Riaz, S. K., Khan, J. S., Shah, S. T. A., Wang, F., Ye, L., Jiang, W. G., et al. (2018). Involvement of hedgehog pathway in early onset, aggressive molecular subtypes and metastatic potential of breast cancer. *Cell Commun. Signal.* 16:3. doi: 10.1186/s12964-017-0213-y

Slamon, D. J., Neven, P., Chia, S., Fasching, P. A., De Laurentiis, M., Im, S.-A., et al. (2020). Overall survival with ribociclib plus fulvestrant in advanced Breast Cancer. *N. Engl. J. Med.* 382, 514–524. doi: 10.1056/NEJMoa1911149

Sobhani, N., Fan, C., O Flores-Villanueva, P., Generali, D., and Li, Y. (2020). The fibroblast growth factor receptors in Breast Cancer: from oncogenesis to better treatments. *IJMS* 21:2011. doi: 10.3390/ijms21062011

Subramanian, A., Tamayo, P., Mootha, V. K., Mukherjee, S., Ebert, B. L., Gillette, M. A., et al. (2005). Gene set enrichment analysis: a knowledge-based approach for interpreting genome-wide expression profiles. *Proc. Natl. Acad. Sci. U.S.A.* 102, 15545–15550. doi: 10.1073/pnas.0506580102

Wesche, J., Haglund, K., and Haugsten, E. M. (2011). Fibroblast growth factors and their receptors in cancer. *Biochem. J.* 437, 199–213. doi: 10.1042/BJ20101603

Wu, J., Wang, Y., Liu, J., Chen, Q., Pang, D., and Jiang, Y. (2018). Effects of FGFR1 gene polymorphisms on the risk of Breast Cancer and FGFR1 protein expression. *Cell. Physiol. Biochem.* 47, 2569–2578. doi: 10.1159/000491653

Conflict of Interest: The authors declare that the research was conducted in the absence of any commercial or financial relationships that could be construed as a potential conflict of interest.

Publisher's Note: All claims expressed in this article are solely those of the authors and do not necessarily represent those of their affiliated organizations, or those of the publisher, the editors and the reviewers. Any product that may be evaluated in this article, or claim that may be made by its manufacturer, is not guaranteed or endorsed by the publisher.

frontiers in Genetics

REVIEW
published: 22 October 2021
doi: 10.3389/fgene.2021.742802

A Review on the Therapeutic Role of TKIs in Case of CML in Combination With Epigenetic Drugs

*Mohd Amir and Saleem Javed**

Department of Biochemistry, Faculty of Life Sciences, Aligarh Muslim University, Aligarh, India

Chronic myeloid leukemia is a malignancy of bone marrow that affects white blood cells. There is strong evidence that disease progression, treatment responses, and overall clinical outcomes of CML patients are influenced by the accumulation of other genetic and epigenetic abnormalities, rather than only the BCR/ABL1 oncoprotein. Both genetic and epigenetic factors influence the efficacy of CML treatment strategies. Targeted medicines known as tyrosine-kinase inhibitors have dramatically improved long-term survival rates in CML patients during the previous 2 decades. When compared to earlier chemotherapy treatments, these drugs have revolutionized CML treatment and allowed most people to live longer lives. Although epigenetic inhibitors' activity is disrupted in many cancers, including CML, but when combined with TKI, they may offer potential therapeutic strategies for the treatment of CML cells. The epigenetics of tyrosine kinase inhibitors and resistance to them is being studied, with a particular focus on imatinib, which is used to treat CML. In addition, the use of epigenetic drugs in conjunction with TKIs has been discussed. Resistance to TKIs is still a problem in curing the disease, necessitating the development of new therapies. This study focused on epigenetic pathways involved in CML pathogenesis and tumor cell resistance to TKIs, both of which contribute to leukemic clone breakout and proliferation.

Keywords: chronic myeloid leukemia, tyrosine kinase inhibitors, imatinib, epigenetic, DNMT inhibitors, HDAC inhibitors, TKI resistance

OPEN ACCESS

Edited by:
Rais Ahmad Ansari,
Nova Southeastern University,
United States

Reviewed by:
Ahmet Emre Eskazan,
Istanbul University-Cerrahpasa,
Turkey
Koji Sasaki,
University of Texas MD Anderson
Cancer Center, United States

****Correspondence:***
Saleem Javed
saleemjaved70@gmail.com

Specialty section:
This article was submitted to Epigenomics and Epigenetics, a section of the journal Frontiers in Genetics

Received: *16 July 2021*
Accepted: *30 September 2021*
Published: *22 October 2021*

Citation:
Amir M and Javed S (2021) A Review on the Therapeutic Role of TKIs in Case of CML in Combination With Epigenetic Drugs. Front. Genet. 12:742802. doi: 10.3389/fgene.2021.742802

CHRONIC MYELOID LEUKEMIA

The malignancy of white blood cells in chronic myeloid leukemia (CML), often referred to as chronic myelogenous leukemia. CML is a clonal myeloproliferative disease that affects over 15% of adults and the average age for the outbreak of this disease is 57 years (Hochhaus et al., 2020; Jabbour and Kantarjian, 2020). CML is more prevalent in men than in women (ratio 1.4:1), accounting for 15–25% of all juvenile leukemias and 14% of all leukemias in the countries lying towards the west. The Philadelphia chromosome (Ph), which occurs between chromosomes 9 and 22, is the characteristic feature of CML and has been regarded to be the first malignancy related to genetic abnormalities. This translocation results in the formation of the BCR-ABL1 hybrid gene, which expresses a constitutively active oncokinase protein. The ABL kinase domain that spans around 300 amino acids, has a bilobed conformation with a C-terminal and an N-terminal lobe, with ATP binding in a cleft flanked by these lobes. Because of the flexibility of C-terminal loop, which contains a "DFG"-motif (Asp381-Phe382-Gly383), the kinase can be in an active (open) or inactive (closed) conformation (Reddy and Aggarwal, 2012; Balabanov et al., 2014). CML is classified into

three phases namely chronic phase (CP), accelerated phase (AP) and blast crisis (BC). The presence of one of the various hematological (like persistent thrombocytopenia) or provisional (like hematological resistance to the drug) criteria for responding to tyrosine kinase inhibitor (TKI) defines AP phase, as per WHO criteria (Arber et al., 2016).

TARGETED THERAPY FOR CML USING TYROSINE KINASE INHIBITORS

Current Use of TKIs for CML Treatment

TKIs are small molecules that are used to treat a wide range of malignancies, including leukemia and solid tumors (Amir et al., 2020). TKIs have been developed as a targeted treatment for BCR-ABL1 kinase activity suppression (Cilloni and Saglio, 2012). TKI therapy for CML patients has resulted in a substantial improvement in disease outcomes and a near-normal lifespan. CML is a well-studied TK-dependent alteration model disease. As a consequence of fundamental and clinical research in clinical practice, TKIs are currently the benchmark in the treatment of CML patients and an effective example of targeted therapy (Balabanov et al., 2014). Imatinib, for example, is one of the first TKIs to be certified for the treatment of CML and is presently used as a first-line treatment, while nilotinib and dasatinib are the next discoveries (Özgür Yurttaş and Eşkazan, 2020).

The first generation TKI binds to an inactive form of BCR-ABL conformation, while second generation TKIs show binding affinity for both the active and inactive forms. The TKIs of second generation (dasatinib, nilotinib, bosutinib) are approximately 1,000 times more sensitive than imatinib in terms of efficacy against BCR-ABL resistant mutations (Kantarjian et al., 2010; Saglio et al., 2010). The binding of imatinib with BCR-ABL kinase in its ATP-binding pocket is hampered by T315I mutation, which is the result of a substitution of isoleucine for threonine at position 315 of the amino acid chain. Approximately 12 percent of adult patients with BCR-ABL leukemia have seen this mutation, and is more common in people with severe conditions. However, dasatinib and nilotinib against T315I are not effective (Soverini et al., 2006; Soverini et al., 2007).

The Survival Rate and Long Term Response in CML Patients in the Era of TKI Therapy

The survival has improved significantly to the point the survival in patients with CML is approaching that of the normal population with access to TKI therapy. Patients with newly diagnosed CML-CP had an OS rate that is only marginally lower than the normal population when treated with TKIs. Patients who obtained CCyR or better, on the other hand, have an OS rate that is comparable to the general population. This highlights the need of ensuring the best possible care for CML patients of all ages to maximize the benefits of these life-changing treatments (Sasaki et al., 2015). The long-term response of patients treated with different TKI therapies and their outcomes were examined by Jain et al. using Kaplan-Meier method. Patients treated with imatinib 800, dasatinib, or nilotinib had better long-term responses and outcomes than those treated with imatinib 400. Transformation to AP and BC phases, as well as mortality from CML, are now uncommon with current TKI therapy methods when well managed. However, discontinuation of treatment was more prevalent in imatinib patients than in TKIs of the second generation (Jain et al., 2015).

In the era of TKIs, CML-CP patients who lived for a certain number of years had good clinical results. Patients may, however, quit medication for some reason throughout time, affecting OS. It's worth noting that the good conditional long-term outcomes predicted are based on rigorous ongoing monitoring of patients for CML and other comorbidities, as well as side events related to TKI usage, as done in clinical studies. It is not reasonable to believe that this may be generalized to situations where patients are treated less strictly (Sasaki et al., 2016). A clinical study showed that patients with the best long-term ELN responses have the best long-term results, and patients who received imatinib 800, dasatinib, or nilotinib have a greater chance of attaining optimum response at various periods (Jain et al., 2016).

According to Issa et al. during TKI therapy, if non-Y CCA/Ph$^-$ (clonal chromosomal abnormalities in Philadelphia chromosome-negative) is detected, physicians should be alerted to the possibility of poor survival outcomes, which may need careful monitoring. For most indices of response and long-term survival, patients with CCA/Ph$^-$ exhibited a trend toward inferiority. Early response assessment, such as BCR-ABL, was found to have a substantial predictive influence on the multivariate analysis. Patients with CCA/Ph$^-$ were less likely to get this reaction (74 vs. 81%). For individuals with monosomy 7, the emergence of nondeletion Y CCA/Ph$^-$ following therapy with different TKI is linked to reduced FFS, EFS, TFS, and OS, as well as a low but substantial chance of developing MDS or AML (Issa et al., 2017; Sasaki et al., 2018).

CML Patients Receiving TKIs and COVID-19

COVID-19 patients have been compared to an age, sex, and condition matched control group to determine the therapeutic effects of TKIs on their outcome (Başcı et al., 2020). Neither CP CML nor BCR-ABL TKIs induces clinically significant immune suppression, and there is no evidence that CP CML patients are at greater risk of complications by SARS-CoV-2 than the normal community. The clinical diagnosis of COVID-19 is not worse in TKI-treated CML patients than it is in the non-TKI-treated individuals. TKIs should be studied in wide-scale prospective and randomized studies to see if they improve COVID-19 outcomes (Başcı et al., 2020).

The clinical parameters of various TKI drugs used to treat CML are shown in **Table 1** (Gleevec, 2008; Sprycel, 2010; Iclusig, 2016; Bosulif, 2017; Tasigna, 2017).

Adverse Events Associated With TKI Therapy

Imatinib is generally well absorbed, with far fewer complications than traditional drug treatment. The percentage of individuals

TABLE 1 | Clinical parameters of different TKIs approved by FDA to treat CML.

Parameters		Imatinib	Dasatinib	Nilotinib	Bosutinib	Ponatinib
Generation		**first**	**second**	**second**	**second**	**third**
FDA approval		2001	2006	2007	2012	2012
Molecular formula		$C_{29}H_{31}N_7O$	C22H26ClN7O2S	C28H22F3N7O	C26H29Cl2N5O3	C29H27F3N6O
Dosage	CP	400 mg OD	100 mg OD	300 mg BD	500 mg OD	45 mg OD
	AP/BC	600 mg OD	140 mg OD	400 mg BD		
Plasma bound		95%	96%	98%	94%	99%
Metabolism		They are primarily metabolized by CYP3A4				
T_{max} (hours)		2–4	0.5–6	3	3–6	6
$T_{1/2}$ (hours)		18	3–5	17	22–27	22
Elimination		The major route of drug elimination is through feces and a small amount of urine				
CYP3A4 inducers		When coadministered, drug exposure (AUC and Cmax values) gets decreased				
CYP3A4 inhibitors		When coadministered, drug exposure (AUC and Cmax values) gets increased				
Sensitivity for T315I mutation[a]		>6,400	>200	>2,000	1,890	11
Potency against BCR-ABL		1-fold	325-folds	30-folds	100-folds	400-folds
T315I Resistant		Yes	Yes	Yes	Yes	No

[a]*Sensitivity of BCR-ABL T315I mutation against TKIs (IC_{50} in nM),* in vitro *(Balabanov et al., 2014).*

with CML in CP that had neutropenia and thrombocytopenia of grade 3/4, is approximately 13 and 7%, respectively. In children, 27 percent of patients had neutropenia, 5 percent had thrombocytopenia, and 2.5 percent had anemia, all of grade 3 or 4. By temporarily halting imatinib, the cytopenia is usually fairly controllable. Gastrointestinal disorders like diarrhea, nausea, and vomiting are examples of nonhematologic toxicity. Bone pain, edema, rashes, myalgia and elevated levels of ALT and AST, etc., are the further side effects (Millot et al., 2011).

CHALLENGES AND RESISTANCE TO TKI TREATMENT IN CML

Although TKIs are found to be one of the effective targeted chemotherapy for treatment of individuals with CML. But every drug has some toxic responses against the body mechanism or metabolism that has to be overcome either by drug dose modifications or, in some cases, by permanently discontinuing the drug. Similar challenges and actions that have to be taken under treatment of CML using TKI are depicted in **Table 2** (Gleevec, 2008; Sprycel, 2010; Iclusig, 2016; Bosulif, 2017; Tasigna, 2017).

Even with more effective second-and third-generation TKIs, many CML individuals have developed primary (5–10%) or secondary (20–30%) intolerance and thus become resistant to TKI therapy. Secondary resistance is most commonly caused by acquired Abl-kinase domain (Abl-KD) alterations, which can be noticed in roughly 60% of instances; nevertheless, the most of primary resistance pathways are still unknown (Bower et al., 2016; Russo et al., 2020). The 6-year review of the IRIS study revealed that imatinib therapy is ineffective in around one-third of patients because of 1° or 2° resistance. Approximately 40–90 percent of individuals who are resistant to imatinib have BCR-ABL mutation, based on the cancer stage and detection equipment's sensitivity. T315I is an especially important mutation as it is quite prevalent (15–20%) and causes tolerance to almost all TKIs currently used in clinical practice, except ponatinib. It is found in ABL kinase domain's ATP-binding region and provides one of imatinib's six binding sites. This binding site is destroyed when threonine is replaced by isoleucine, as well as a structural impediment that prevents imatinib, nilotinib, dasatinib, and bosutinib from reaching it (Hughes et al., 2014). Imatinib resistance can be caused by either primary or secondary causes. Pharmacokinetic changes, such as anomalies in transport or drug efflux, may cause primary resistance. Because of BCR-ABL mutations or the involvement of salvage mechanisms, patients are more prone to develop secondary or acquired resistance. The T315I mutation is the most dreaded mutation since it is resistant to all the TKIs that have been approved by FDA for this disease. Several drugs, such as ponatinib, are being tested in clinical studies to block kinase activity linked to T315I (O'Hare et al., 2009). According to prior studies, TKI can restore the levels of specific miRNAs, and this mechanism can mediate the effects of TKIs on CML cells (Bugler et al., 2019).

CML is divided into three stages, referred to as CP, AP, and BP. With the introduction of TKIs and the subsequent success of TKI cessation, a fourth-phase, treatment-free remission (TFR-CML), has developed. In the absence of CML-directed treatment, this phase begins after TKI therapy is stopped and is defined by sustained remission with undetectable (or very low detectable) illness by the most sensitive technique of testing. This phase differs from CP since there is no additional molecular, cytogenetic, or hematological development. A clinical study revealed that patients were treated with TKIs for 11 years, and MMR and MR4.5 were maintained for 10 and 5.5 years, respectively, until therapy was discontinued. As a result, the rapid transition to BP CML was not preceded by CP development, and this sudden transformation had been reported in fewer than 1% of the CML individuals

TABLE 2 | The adverse conditions and dose modifications of TKIs during CML treatment.

TKIs	TKI drug response		Action to be taken
Imatinib	CP CML	ANC <1.0 × 10^9/L and/or Platelets <50 × 10^9/L	Withhold until ANC ≥1.5 × 10^9/L and platelets ≥75 × 10^9/L; then resume at a lower dose
	AP/ BC CML	ANC <0.5 × 10^9/L and/or Platelets <10 × 10^9/L	Withhold until ANC ≥1 × 10^9/L and platelets ≥20 × 10^9/L; then resume at a lower dose
Dasatinib	CP CML	ANC <0.5 × 10^9/L and/or Platelets <50 × 10^9/L	Withhold until ANC ≥1.0 × 10^9/L and platelets ≥50 × 10^9/L; then resume at a lower dose. Permanently discontinue if AE persists
	AP/ BC CML	ANC <0.5 × 10^9/L and/or Platelets <10 × 10^9/L	Withhold until ANC ≥1 × 10^9/L and platelets ≥20 × 10^9/L; then resume at a lower dose
Nilotinib	ANC <1.0 × 10^9/Land/or Platelets <50 × 10^9/L		Withhold until ANC ≥1.0 × 10^9/L and platelets ≥50 × 10^9/L; then resume at a lower dose
	ECG with QTC >480 msec		Withhold until QTC <450 msec, then resume with the initial dose
	Increased serum lipase/amylase, bilirubin, hepatic transaminases ≥ Grade 3 and other hepatic impairment		Withhold until AE disappears then resume with a lower dose. Slowly escalates to initial dose if tolerable
Bosutinib	ANC <1.0 × 10^9/L and/or Platelets <50 × 10^9/L		Withhold until ANC ≥1.5 × 10^9/L and platelets ≥75 × 10^9/L; then resume at a lower dose
Ponatinib	ANC <1.0 × 10^9/L and/or Platelets <50 × 10^9/L		Withhold until ANC ≥1.5 × 10^9/L and platelets ≥75 × 10^9/L; then resume at a lower dose
	Elevated AST/ALT (Grade ≥2), Elevated serum lipase (Grade 3/4), Grade 3 pancreatitis		Withhold until AE disappears then resume at a lower dose. Permanently discontinue if AE persists
	Elevated AST/ALT (Grade ≥2) concurrent with Elevated Bilirubin and ALP (Grade ≥1), Grade 4 pancreatitis		Permanently discontinue

undergoing imatinib therapy. Cellular immunity, in the form of natural killer cells and cytotoxic T lymphocytes, may have a role in TFR-CML, according to one theory. This rapid blastic change might be the outcome of a lack of immune monitoring or a disease breakout (Alfayez et al., 2019). But it might also be related to some genetic and epigenetic abnormalities that require further clinical research for validation.

Clinical study data show that epigenetic medication treatment can produce objective responses in CML patients, even in later stages and amid imatinib resistance. Though, these reactions are rarely long-lasting, necessitating the pursuit of alternative recovery methods. Not only are many TKI options available (e.g., Imatinib, nilotinib, dasatinib, ponatinib, and bosutinib), but novel agents (e.g., ABL001) are being investigated, and for individuals with chronic or non-responsive illness, allogeneic transplantation remains a surgical option.

Given below are the possible reasons/mechanisms for TKI resistance (Balabanov et al., 2014).

1. BCR-ABL Dependent
   i. Overexpression of BCR-ABL kinases as a result of amplification leads to a TKI-resistant scenario.
   ii. Mutations in BCR-ABL resist TKI binding as a result of conformational change in ABL.
2. BCR-ABL Independent
   i. Initiation of other compensatory intracellular signaling pathways (like LYN, HCK), due to which, despite successful suppression of the primary oncogenic driver kinase, cells continue to proliferate and thus results in TKI resistance.
   ii. The overexpression of efflux transporters, like ABCB1 (MRD-1, for which imatinib acts as a substrate), results in a decrease of TKI levels in cells.
   iii. The downregulation of influx transporters, like OCT1 (in the case of imatinib), also results in reduced efficacy of TKI and finally leads to TKI resistance.

An Epigenetic Mechanism of Imatinib Resistance Associated With HOXA4 Gene Promotor

The inhibition of the HOXA4 protein may interfere with the normal growth and proliferation of myeloid progenitors. Imatinib resistance in CML patients may be caused by an epigenetic mechanism in the BCR-ABL-independent pathway. The hypermethylation of HOXA4 gene appears to be inhibiting the clinical response to IM, and as a result, is acting as a significant inhibitor of normal leukemogenesis. Inhibition of this process might be a superior treatment option, necessitating hypomethylating drugs in CML patients with this epigenetic resistance mechanism. As a result, apart from BCR-ABL gene mutation analyses, the hypermethylation profile of the HOXA4 gene might be used as an epigenetic biomarker in CML patients for predicting reaction to imatinib treatment (Elias et al., 2013).

According to recent research, the long noncoding RNA (lncRNA) HOTAIR (HOX transcript antisense RNA) is involved in the development of both solid tumors like breast cancer and NSCLC, as well as hematopoietic malignancies like AML. The epigenetic regulatory mechanisms of HOTAIR in advanced CML, on the other hand, remain unknown. Li et al. suggested that demethylation drugs may provide a novel remedy for CML-BC, as HOTAIR is a possible therapeutic target (Li and Luo, 2018).

Second Malignancies Incidence in CML Patients

In the age of TKIs, the incidence of second malignancies in CML patients has increased. Sasaki et al. (2019), reported data of newly diagnosed CML patients in 2001–2014, and it was found that 5.6% of the cancer patients had more than one malignancy after the CML diagnosis. The most prevalent sites of second cancers were the male genital system, digestive system and respiratory

system. CML-CP had a slightly higher relative incidence of total second malignancies than the general population, with a modest rise in the AER (Sasaki et al., 2019).

The Epigenetic Mutation Associated With Cardiovascular Events in CML Patients

There have been reports of cardiovascular or arteriothrombotic adverse events (CV- or AT-AEs) in CML patients receiving TKI therapy. The second or third-generation TKIs, such as ponatinib, significantly increase the risk of CV-AEs (excluding hypertension) and AT-AEs in CML patients (Jain et al., 2019). Myelopoeisis epigenetic regulation is controlled by the *TET2* gene, which codes for the protein TET2 methylcytosine dioxygenase. Through the oxidation of methyl-cytosine, TET proteins play a role in DNA alteration, also in normal and malignant growth. A DNA epigenetic modification termed as hydroxymethylation is catalyzed by Tet2. As a result, it had been postulated that Tet2 regulated gene expression in macrophages exposed to excessive cholesterol. As a result, somatic mutations in hematopoietic cells have a role in the onset of atherosclerosis in humans. It was suggested that clonal hematopoiesis might be a controllable risk factor, either by using cholesterol-lowering medicines or targeting certain inflammatory processes (Jaiswal et al., 2017).

Role of Cytogenetic Abnormalities in Prognosis

Patients with severe CML are more likely to have additional cytogenetic abnormalities (ACAs) in addition to the Philadelphia chromosome. Long-term survival may be improved by combining TKI treatment with systemic chemotherapy. No matter what the blast count is, the existence of CBF translocations determines whether or not a patient has AML, because CBF rearrangements are seldom diagnosed as ACAs. In individuals with CML, CBF rearrangements as ACAs might be regarded as high-risk characteristics (Morita et al., 2021a).

EPIGENETIC EMERGING THERAPIES FOR CML IN COMBINATION WITH TKIS: EFFICACY AND CHALLENGES

There is significant evidence that the accumulation of various genetic and epigenetic abnormalities, in addition to the BCR/ABL1 oncoprotein, influences disease progression, treatment response, and overall clinical prognosis in CML patients. The development of a variety of illnesses has been related to DNA hydroxymethylation. Disease development, drug reaction, and clinical outcome of different diseases are all influenced by the DNA hydroxymethylation of gene promoters (Jelinek et al., 2011). The previous results of the clinical studies suggest that in CML patients undergoing imatinib treatment, hydroxymethylation of gene promoters of cell cycle regulators and autophagy genes may be a significant predictor of tumor growth, identifies inefficient imatinib responders, and indicates a relatively poor treatment outcome. As a result, the findings encouraged the use of demethylating agents in conjunction with TKI treatment to improve clinical consequences (Jelinek et al., 2011). The previous studies linking hypermethylation of SOCS1 gene to downregulation of expression suggested that the lack of negative cytokine signaling caused by SOCS1 protein epigenetic suppression might contribute to CML development. Small molecules with two src homology domains make up SOCS proteins. As a result, SOCS1 expression may be a new and valuable marker for CML therapeutic follow-up, as well as a new therapeutic strategy for developing successful CML target therapies (Liu et al., 2003).

Over the last 20 years, the invention of TKIs to counteract the BCR-ABL protein's constitutive tyrosine kinase function has greatly increased disease control and clinical outcomes. However, most patients are not healed, and designing treatment strategies that target epigenetic pathways is a potential way of increasing cure rates. During the formation and growth of CML, various epigenetic pathways are changed or reprogrammed, leading to changes in histone modifications, DNA methylation, and transcriptional dysregulation (Bugler et al., 2019). Consequently, with the advent of TKIs as the primary mode of therapy, the occurrence of CML has risen, rendering it a manageable, chronic condition. Although TKI therapy has revolutionized CML treatment, 25–30 percent of patients with CP-CML have failed TKI treatment, half had mutations in the BCR–ABL1 kinase domain and 50 percent of patients are unknown for the failure of this therapy (Rohrbacher and Hasford, 2009; Baccarani et al., 2013). Potentially harmful somatic mutations of epigenetic modifiers are common in CP-CML at the time of diagnosis, and when combined with other factors associated, they can be useful predictive indicators to identify the best TKI for every patient (Nteliopoulos et al., 2019). The chemotherapy resistance during treatment might occur at any stage, and thus the emergence of drug resistance remains a major issue.

Combination Therapy Using TKI With Other Drugs/Inhibitors: An Epigenetic Reprogramming

In 1983, after the discovery of the first cancer-epigenetic reprogramming relations, emerging evidence indicates that genetic and epigenetic changes cause cancers and that some of them occurring before profound leukemia commences preleukemia (Feinberg et al., 2006; Feinberg and Vogelstein, 1983). The BCR-ABL1 mutation induces epigenetic reprogramming, which is important in CML, as well as converting HSCs to LSCs. Polycomb-group (PcG) proteins are one kind of epigenetic regulator that is believed to be disrupted in CML LSC (Di Carlo et al., 2019). There are two complexes in PcG proteins, namely PRC1 and PRC2 (Polycomb Repressive Complex). Given the number of studies that PRC2 plays a role in cancer (including solid tumors and multiple myeloma), it's no surprise that a variety of therapeutics targeting this complex have appeared and are under clinical studies of Phase I and II (Fioravanti et al., 2018; Gulati et al., 2018). In comparison to

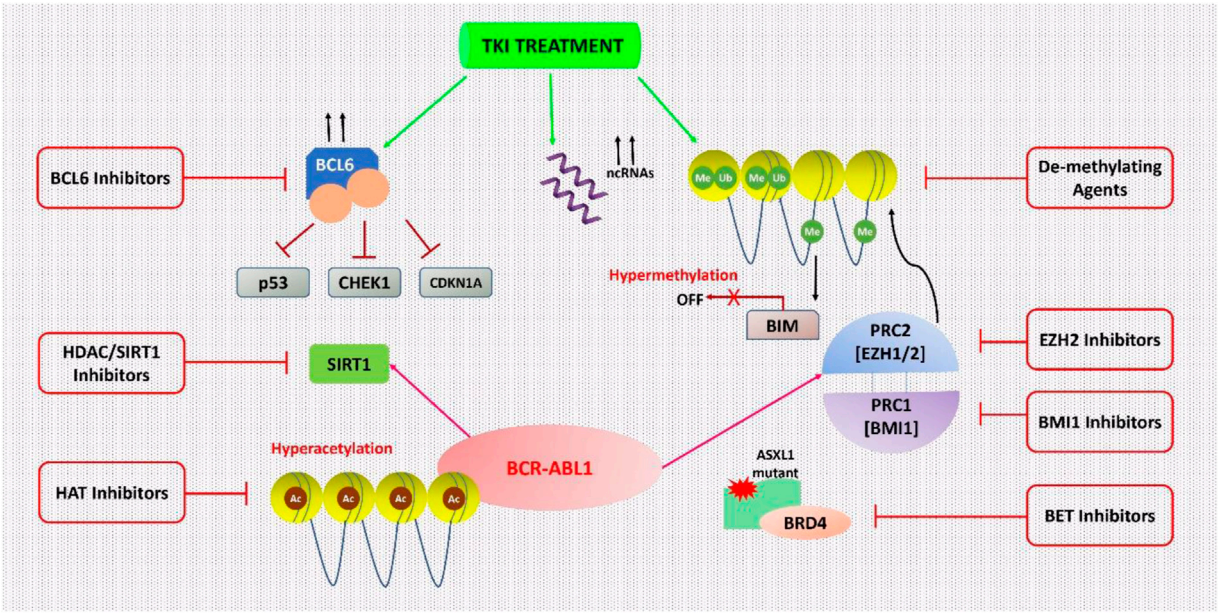

FIGURE 1 | Epigenetic processes in CML cells are being targeted. CML cells are epigenetically reprogrammed via several mechanisms. This dysregulation can occur only in the presence of TKI therapy in various cases. With this understanding, many epigenetic treatments were suggested to inhibit these mechanisms and to result in the complete destruction of CML cells especially in combination with TKI therapy.

TKI therapy alone, Scott et al. demonstrated significant targeting of CML stem cells using the EZH2 (a core component of PRC2) inhibitor Tazemetostat in conjunction with TKI. As a result, combined therapy may be a new clinical option for CML treatment, as shown in **Figure 1** (Scott et al., 2016).

Sirtuin 1 (SIRT1) is a NAD-dependent HDAC that acts on the nonhistone target p53 in $CD34^+$ CML cells and has been associated with leukemogenesis and the persistence of CML LSCs. After imatinib therapy, SIRT1 expression significantly decreased but not completely depleted in CML cell lines, paving the way for effective SIRT1 inhibition. The treatment with the SIRT1 inhibitor (e.g., Selisistat or EX-527) via activation of p53 signaling, improved the effect of TKI treatment (Chen and Bhatia, 2013; Li et al., 2012; Yuan et al., 2012). SIRT1's function is one of the most prevalent causes of treatment resistance in several malignancies, including CML (S et al., 2021).

BCL6 is a transcription factor that can epigenetically control a variety of its targets by altering the accessibility of chromatin at promoter and enhancer sites. It is often mutated in lymphoma cells (Hatzi et al., 2013). BCL6 expression is modest in TKI-naive CML cells, but it is substantially increased in CML cell lines and primary CD34+ cells after TKI therapy, although its function in CML is unknown (Hurtz et al., 2011). In Ph+ ALL patients, the BCL6 peptide inhibitor, RI-BPI was coupled with imatinib to avoid TKI resistance and to enhance imatinib's efficacy (Duy et al., 2011). In $CD34^+38^-$ CML LSCs, the use of RI-BPI increased the effectiveness of imatinib treatment, and decreased the ability to form CML cell colony, thus eliminated $CD34^+38^-$ LSCs by enhancing programmed cell death. Other BCL6 small molecule inhibitors, such as FX1, significantly reduced CML $CD34^+$ cells' colony-forming ability, in combination with TKI (Madapura et al., 2017).

It had been suggested by San José-Eneriz et al. (2009), that the concomitant use of imatinib and a de-methylating drug such as 5-aza-2′-deoxycytidine (Decitabine) might result in better outcomes in individuals with reduced expression of the pro-apoptotic BCL-2-interacting mediator (BIM). This downregulation is epigenetically mediated by BIM methylation in most CML individuals and has a negative impact on health (San José-Eneriz et al., 2009). TKI-resistant leukemic stem cells (LSCs) are still a big problem in CML, and finding ways to get rid of them is a major unsatisfied clinical need. Scott et al. (2016) showed that for the existence of LSC, EZH2 and H3K27me3 reprogramming is essential, nevertheless, it also makes LSCs vulnerable to the mutual effects of EZH2 inhibitor and TKI. That becomes a novel strategy for more efficiently targeting LSCs in TKI receiving patients (Scott et al., 2016).

Concomitant Use of TKI and DNMT Inhibitor (a Class of Epigenetic Drugs)

DNMT inhibitors are cytosine analogs that bind to DNA and inactivate genes, inhibiting the methyltransferase enzyme reversibly. Azacytidine and decitabine are DNMT inhibitors that had been approved by the FDA for the treatment of myelodysplastic syndrome (MDS). Low doses of these inhibitors are effective, but high doses are lethal (Yang et al., 2006). Decitabine is a cytosine derivative that is used as an intravenous antineoplastic agent in the treatment of MDS. It receives FDA approval in 2006 for the treatment of MDS and was also approved by the EU for the treatment of AML. The strategy

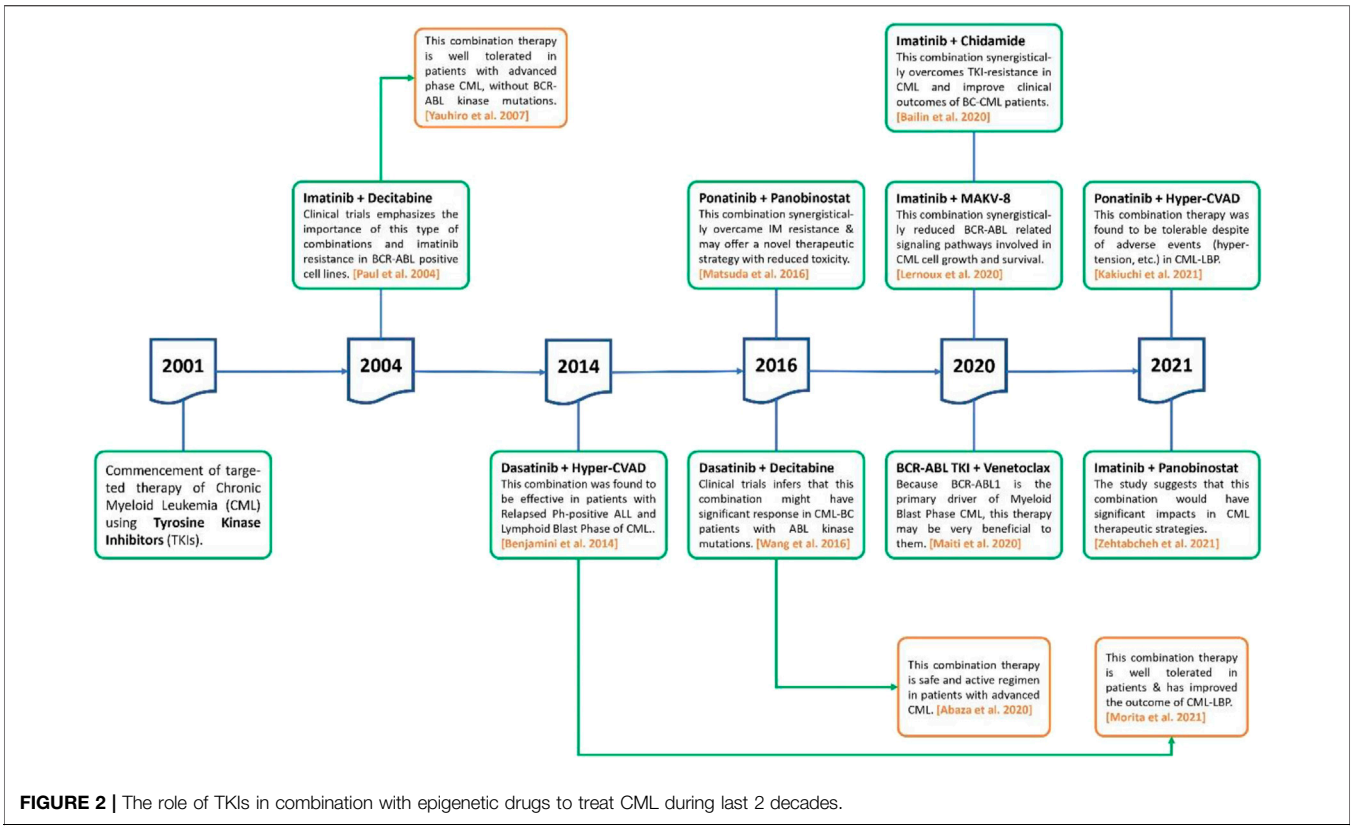

FIGURE 2 | The role of TKIs in combination with epigenetic drugs to treat CML during last 2 decades.

of concomitant use of TKIs with epigenetic drugs for CML therapy was initiated after the approval of the first tinib drug (imatinib) in 2001 (**Figure 2**).

Imatinib Plus Decitabine

In CML patients with AP or BC phase, a Phase II trial of low-dose decitabine in conjunction with an active metabolite of imatinib (i.e., imatinib mesylate, IM) was performed. Imatinib 600 mg OD and decitabine 15 mg/m^2 intravenously (5 days a week) were given to patients for 2 weeks. The major and modest cytogenetic responses were reported which includes: 32% patients with complete and 4% patients had moderate hematologic responses, while 7% patients had hematological development. The individuals who lack BCR-ABL kinase mutations had a greater hematologic response rate (53%) than those with mutations (14%). The median hematologic response lasted 18 weeks. The most common side effect was myelosuppression, which resulted in neutropenic fever in 32% of individuals. So, in AP CML without BCR-ABL kinase mutations, it was concluded that decitabine with imatinib in combination treatment, is well tolerated and effective (Oki et al., 2007).

In recent years, the reprogramming of mitochondrial metabolism has been identified as a hallmark of cancer, including CML, and could be used for medicinal purposes. The impacts of various drugs on mitochondrial activity in the CML cell line K562 were explored, and it was shown that decitabine in combination with 5-aminoimidazole-4-carboxamide ribotide (AICAR) might efficiently boost ATP content and mitochondrial biogenesis. Furthermore, it has been shown that AICAR-decitabine therapy increased the sensitivity of the K562 cells for imatinib. Based on these findings, it is clear that TKIs coupled with mitochondrial modulation may give treatment strategies for CML treatment (Zhu et al., 2020).

Dasatinib Plus Decitabine

Treatment for AP CML still lacks, as single-agent TKIs exhibit weak and short-lived action. A phase I/II study was undertaken in patients with advanced CML to see if the concomitant use of dasatinib and decitabine was safe and effective. Two distinct dosing regimens were tested with a beginning decitabine dose of either 10 or 20 mg/m^2 OD for 10 days with dasatinib 100 mg OD. Decitabine 10 or 20 mg/m^2 OD for 10 days, with dasatinib 140 mg OD, was the target dosage. There was no dose-limiting toxicity identified with either regimen at the initial dosages. In 93% of individuals, treatment-emergent hematological adverse effects of grade 3 were observed. Meanwhile, 48% of patients had a major hematopoietic response, whereas 22% had a weak hematologic reaction, with 44% of them having a large cytogenetic reaction and 33% having a significant biomolecular response. Decitabine with dasatinib is a safe, innovative, and effective treatment for advanced CML, with a life expectancy among patients that looks to be higher than with either agent alone (Abaza et al., 2020).

TABLE 3 | This data has been extracted from Matsuda et al. (2016). For 72 h, cells were exposed to the same concentration of ponatinib, panobinostat, or their combination, before being tested using XTT assay.

Drug/s	CML cell lines (IC_{50} values in μM)			
	K562	K562/IM-R1	Ba/F3	Ba/F3/T315I
Ponatinib	2	3	5	30
Panobinostat	50	51	40	47
Combination	0.7	1.3	3.7	10

Venetoclax Plus BCR-ABL TKIs

As a BCL2 inhibitor, venetoclax is authorized for use in aged or "unsuitable" individuals with newly diagnosed AML, together with low-dose cytarabine or HMA. Venetoclax has demonstrated preclinical efficacy against TKI-resistant CML cells and synergy with BCR-ABL TKI in eliminating leukemic stem cells in advanced CML In CML-MBP, dasatinib is effective as a single treatment; however, the venetoclax-TKI combination may be more effective than dasatinib alone. Ponatinib has shown promising results in advanced Ph+ leukemias and relapsed/refractory pre-B ALL whether used alone or in conjunction with nonchemotherapeutic treatments. Ponatinib synergizes with venetoclax in Ph+ ALL samples by inducing LYN-mediated pro-apoptotic BIM, reducing anti-apoptotic MCL1, and perhaps removing venetoclax resistance. The combination of venetoclax and ponatinib in this patient population is therefore supported by clinical trials. Thus, treatment of advanced Ph+ myeloid leukemias with venetoclax and TKI-based combination regimens is a viable option. Because BCR-ABL1 is the primary factor of CML-MBP, this combination could be very beneficial to them (Maiti et al., 2020).

Crawford et al. (2009) observed that a rise in proteasome proteolytic activity is linked to BCR/ABL genetic and epigenetic alterations, and inhibiting the proteasome might cause extremely higher cell apoptosis in BCR/ABL positive cells than in BCR/ABL negative cells. The combined inhibition of HDACs and the proteasome leads to a significant decrease in both efficacy and metabolism of CML-derived BCR/ABL-expressing K562 cells than either drug alone, indicating that treatment with concomitant use of HDAC and proteasome inhibitors could be a successful approach in CML therapy. According to Jagannath et al. (2010) in relapsed/refractory multiple myeloma patients, the clinical therapy with the combined use of HDAC and proteasome inhibitors showed promising anticancer activity (Jagannath et al., 2010).

Concomitant Use of TKI and IC/HMA in Myeloid BP-CML Patients

It has been demonstrated that TKI + IC/HMA (intensive chemotherapy/hypomethylating agent) therapy provides greater response rates, reduced recurrence risk, and superior 5-years EFS/OS than TKI alone, suggesting that rather than TKI alone, the combination therapy with IC or HMA + TKI (especially received decitabine) should be taken into account for the appropriate frontline therapy for such patients. Long-term survival rates were similar between IC + TKI and HMA + TKI, with a long-term survival rate of around 30% and improved outcomes for patients who were able to undergo ASCT (allogeneic stem cell transplant). However, while being less intensive than an IC method, the combination of HMA and second/third generation TKI is extremely successful (Saxena et al., 2021). As a result of their poor prognosis, patients with CML-BP require novel treatment options (Jain et al., 2017). It was found that the use of hyper-CVAD (cyclophosphamide, vincristine sulfate, doxorubicin hydrochloride/adriamycin, and dexamethasone) with dasatinib therapy, the outcome of CML-lymphoid BP has improved, and the survival rate is equivalent to that of Ph+ ALL. Using new TKIs and targeted agents, further improvements may be made in the future (Morita et al., 2021b).

Concomitant Use of TKI and HDAC Inhibitor (a Class of Epigenetic Drugs)

HDAC inhibitors are chemical compounds that inhibit histone deacetylases. They have a long tradition of use as mood stabilizers and anti-epileptics in psychology and neurology. They've recently been studied as potential cancer, viral, and infectious disease therapies (Miller et al., 2003; Blanchard and Chipoy, 2005; Mwakwari et al., 2010; Patil et al., 2010). HDAC inhibitors are derived from natural and synthetic compounds of varying target specificity and actions. HDAC inhibitors are divided into four categories: hydroxamic acids (or hydroxamates), cyclic tetrapeptides, benzamides and short-chain fatty acids. Due to the concept that BCR/ABL signaling and epigenetic changes might act as two major reasons for disease and tolerance, the combined effects of BCR/ABL inhibition utilizing imatinib with panobinostat (a multi-HDAC inhibitor) in K562 cells were studied (Housman et al., 2014). In CML-derived K562 cells, the combination of panobinostat with imatinib showed synergistic antineoplastic responses and improved therapeutic effectiveness, as predicted (Zehtabcheh et al., 2021).

TABLE 4 | The combination therapy for CML using TKIs with epigenetic drugs.

S.No.	TKIs	Epigenetic drug	Response
1	Imatinib	Decitabine	Well tolerated and effective
2	Dasatinib	Decitabine	Safe, innovative and effective
3	Imatinib/Dasatinib/Nilotinib/Ponatinib	Venetoclax	Beneficient and effective
4	Imatinib/Dasatinib/Nilotinib/Ponatinib	IC/HMA, Hyper-CVAD	Extremely successful and improved survival rate
5	Imatinib	MAKV-8	BCR-ABL expression and phosphorylation inhibited
6	Imatinib	Panobinostat	Synergistic antileukemic effects
7	Ponatinib	Panobinostat	Significantly greater inhibitory growth impact on all cell lines
8	Imatinib	Chidamide	Induce synergetic fatality

Imatinib Plus MAKV-8

MAKV-8 has been first reported for its IC_{50} of 2 pM, *in vitro*, against HDAC3 and HDAC6 and its anti-proliferative effect for pancreatic tumor cells, which was analogous to SAHA. It comprises the 6-methylene linker and a CAP group containing arylisoxazole. The chemical MAKV-8 is a potent pan-HDAC inhibitor *in vitro* and also in several cell lines of CML. In addition, in imatinib-sensitive/resistant BCR-ABL-positive CML cells, MAKV-8 in combination with imatinib displayed substantial anti-tumor properties, while healthy cell types exposed to this co-therapy showed relatively minimal impact. BCR-ABL expression and phosphorylation, as well as downstream targets expression important in CML growth and survival, were all inhibited by MAKV-8-imatinib combination (Lernoux et al., 2020).

Imatinib Plus Panobinostat

Investigation of the combined effects of BCR/ABL inhibition with Imatinib and the multi-HDAC inhibitor panobinostat was performed in K562 cells The combination of panobinostat with imatinib was reported to have synergistic antileukemic effects and increased treatment effectiveness in K562 cells generated from CML patients (Zehtabcheh et al., 2021).

Ponatinib Plus Panobinostat

The concomitant use of panobinostat with ponatinib to treat IM resistance which was caused by either gene amplification or T315I mutation in BCR-ABL was found to be effective. This synergetic impact could just be because of the kinase activity suppression of ABL accompanied by BCR-ABL protein degradation. The concomitant use of these drugs could lead to a novel treatment approach with outstanding anti-CML efficacy and few side effects. The XTT test was used to assess the growth inhibitory effects of IM, panobinostat, and ponatinib alone or in combination on K562 cells, K562/IM-R1 cells, Ba/F3 cells, and Ba/F3/T315I cells. K562/IM-R1 cells 12 times, while Ba/F3/T315I cells were shown to be 13 times more IM-resistant than parental counterparts in this experiment. Importantly, as compared to either drug alone, the panobinostat and ponatinib combination demonstrated a significantly greater inhibitory growth impact on all cell lines (**Table 3**) (Matsuda et al., 2016).

Imatinib Plus Chidamide

Chidamide is a new selective HDAC inhibitor that has demonstrated its efficacy to treat hematological cancers. Chidamide reduced the development of the CML cell, causing apoptosis and arrest of the cell cycle when used alone. Furthermore, in the CML cell line KBM5, as well as IM-resistant CML cells KBM5 bearing T315I mutations, chidamide in conjunction with imatinib induced synergistic fatality, with a significant decrease in kinase activity of BCR-ABL and expression of acetyl-histone H3. In IM-resistant cells, the combined therapy significantly reduced the fundamental activity of β-catenin signaling and eliminated the mesenchymal stromal cells (MSCs) shielding effects on CML cells. As a result, this combination therapy is likely to be a feasible way to treat TKI-resistant CML and improve treatment strategies with BC-CML (**Table 4**) (He et al., 2020).

CONCLUSION AND FUTURE PROSPECTS

Today, one of the finest examples of effective targeted therapy in CML is that the survival rate of CML patients treated with TKIs seems to be relatively close to the healthy individuals. Since the development of first and second-line TKIs, substantial progress in CML therapy has been accomplished. Despite the TKI treatment's excellent efficacy, some patients developed resistance owing to BCR-ABL kinase domain alterations, resulting in therapeutic failure. The development of CML and its resistance to treatments are both influenced by abnormal epigenetic control of key genes. Because epigenetic alterations may be controlled, novel medications that target distinct epigenetic pathways, such as demethylating agents and HDAC inhibitors, have been evaluated for CML treatment, particularly in individuals who have developed imatinib resistance. Finally, recent advances in biotechnology and bioinformatics have created new potential techniques for *de novo* epigenetic factor characterization and greater knowledge of epigenetic pathways, which can further develop tailored CML therapies in the future.

AUTHOR CONTRIBUTIONS

MA prepared the manuscript and SJ reviewed and edited the manuscript.

ACKNOWLEDGMENTS

MA is thankful to UGC for providing fellowship.

REFERENCES

Abaza, Y., Kantarjian, H., Alwash, Y., Borthakur, G., Champlin, R., Kadia, T., et al. (2020). Phase I/II Study of Dasatinib in Combination with Decitabine in Patients with Accelerated or Blast Phase Chronic Myeloid Leukemia. *Am. J. Hematol.* 95 (11), 1288–1295. doi:10.1002/ajh.25939

Alfayez, M., Richard-Carpentier, G., Jabbour, E., Vishnu, P., Naqvi, K., Sasaki, K., et al. (2019). Sudden Blastic Transformation in Treatment-free Remission Chronic Myeloid Leukaemia. *Br. J. Haematol.* 187 (4), 543–545. doi:10.1111/bjh.16245

Amir, M., Qureshi, M. A., and Javed, S. (2020). Biomolecular Interactions and Binding Dynamics of Tyrosine Kinase Inhibitor Erdafitinib, with Human Serum Albumin. *J. Biomol. Struct. Dyn.* 39 (11), 3934–3947. doi:10.1080/07391102.2020.1772880

Arber, D. A., Orazi, A., Hasserjian, R., Thiele, J., Borowitz, M. J., Le Beau, M. M., et al. (2016). The 2016 Revision to the World Health Organization Classification of Myeloid Neoplasms and Acute Leukemia. *Blood* 127 (20), 2391–2405. doi:10.1182/blood-2016-03-643544

Baccarani, M., Deininger, M. W., Rosti, G., Hochhaus, A., Soverini, S., Apperley, J. F., et al. (2013). European LeukemiaNet Recommendations for the Management of Chronic Myeloid Leukemia: 2013. *Blood* 122 (6), 872–884. doi:10.1182/blood-2013-05-501569

Balabanov, S., Braig, M., and Brümmendorf, T. H. (2014). Current Aspects in Resistance against Tyrosine Kinase Inhibitors in Chronic Myelogenous Leukemia. *Drug Discov. Today Tech.* 11 (1), 89–99. doi:10.1016/j.ddtec.2014.03.003

Başcı, S., Ata, N., Altuntaş, F., Yiğenoğlu, T. N., Dal, M. S., Korkmaz, S., et al. (2020). Outcome of COVID-19 in Patients with Chronic Myeloid Leukemia Receiving Tyrosine Kinase Inhibitors. *J. Oncol. Pharm. Pract.* 26 (7), 1676–1682. doi:10.1177/1078155220953198

Blanchard, F., and Chipoy, C. (2005). Histone Deacetylase Inhibitors: New Drugs for the Treatment of Inflammatory Diseases?. *Drug Discov. Today* 10 (3), 197–204. doi:10.1016/S1359-6446(04)03309-4

Bosulif (2017). Bosutinib. US FDA, 1–17. Available at: https://www.accessdata.fda.gov/drugsatfda_docs/label/2017/203341s009lbl.pdf (Accessed September 10, 2021).

Bower, H., Björkholm, M., Dickman, P. W., Höglund, M., Lambert, P. C., and Andersson, T. M.-L. (2016). Life Expectancy of Patients with Chronic Myeloid Leukemia Approaches the Life Expectancy of the General Population. *Jco* 34 (24), 2851–2857. doi:10.1200/JCO.2015.66.2866

Bugler, J., Kinstrie, R., Scott, M. T., and Vetrie, D. (2019). Epigenetic Reprogramming and Emerging Epigenetic Therapies in CML. *Front. Cel Dev. Biol.* 7 (July), 1–14. doi:10.3389/fcell.2019.00136

Chen, W., and Bhatia, R. (2013). Roles of SIRT1 in Leukemogenesis. *Curr. Opin. Hematol.* 20 (Issue 4), 308308–313313. doi:10.1097/MOH.0b013e328360ab64

Cilloni, D., and Saglio, G. (2012). Molecular Pathways: BCR-ABL. *Clin. Cancer Res.* 18 (Issue 4), 930–937. doi:10.1158/1078-0432.CCR-10-1613

Crawford, L. J., Windrum, P., Magill, L., Melo, J. V., McCallum, L., McMullin, M. F., et al. (2009). Proteasome Proteolytic Profile is Linked to Bcr-Abl Expression. *Exp. Hematol.* 37, 357–366. doi:10.1016/j.exphem.2008.11.004

Di Carlo, V., Mocavini, I., and Di Croce, L. (2019). Polycomb Complexes in normal and Malignant Hematopoiesis, Rockefeller University Press. *J. Cel Biol.* 218 (Issue 1), 55–69. doi:10.1083/jcb.201808028

Duy, C., Hurtz, C., Shojaee, S., Cerchietti, L., Geng, H., Swaminathan, S., et al. (2011). BCL6 Enables Ph+ Acute Lymphoblastic Leukaemia Cells to Survive BCR-ABL1 Kinase Inhibition. *Nature* 473 (7347), 384–388. doi:10.1038/nature09883

Elias, M. H., Baba, A. A., Husin, A., Sulong, S., Hassan, R., Sim, G. A., et al. (2013). HOXA4Gene Promoter Hypermethylation as an Epigenetic Mechanism Mediating Resistance to Imatinib Mesylate in Chronic Myeloid Leukemia Patients. *Biomed. Res. Int.* 2013, 1–7. doi:10.1155/2013/129715

Feinberg, A. P., Ohlsson, R., and Henikoff, S. (2006). The Epigenetic Progenitor Origin of Human Cancer. *Nat. Rev. Genet.* 7 (Issue 1), 21–33. doi:10.1038/nrg1748

Feinberg, A. P., and Vogelstein, B. (1983). Hypomethylation Distinguishes Genes of Some Human Cancers from Their normal Counterparts. *Nature* 301 (5895), 89–92. doi:10.1038/301089a0

Fioravanti, R., Stazi, G., Zwergel, C., Valente, S., and Mai, A. (2018). Six Years (2012-2018) of Researches on Catalytic EZH2 Inhibitors: The Boom of the 2-Pyridone Compounds, John Wiley and Sons Inc. *Chem. Rec.* 18 (Issue 12), 1818–1832. doi:10.1002/tcr.201800091

Gleevec (2008). Gleevec (Imatinib Mesylate) FDA US. Available at: https://www.accessdata.fda.gov/drugsatfda_docs/label/2008/021588s024lbl.pdf (Accessed September 10, 2021).

Gulati, N., Béguelin, W., and Giulino-Roth, L. (2018). Enhancer of Zeste Homolog 2 (EZH2) Inhibitors, Taylor and Francis Ltd. *Leuk. Lymphoma.* 59 (7), 1574–1585. doi:10.1080/10428194.2018.1430795

Hatzi, K., Jiang, Y., Huang, C., Garrett-Bakelman, F., Gearhart, M. D., Giannopoulou, E. G., et al. (2013). A Hybrid Mechanism of Action for BCL6 in B Cells Defined by Formation of Functionally Distinct Complexes at Enhancers and Promoters. *Cel Rep.* 4 (3), 578–588. doi:10.1016/j.celrep.2013.06.016

He, B., Wang, Q., Liu, X., Lu, Z., Han, J., Pan, C., et al. (2020). A Novel HDAC Inhibitor Chidamide Combined with Imatinib Synergistically Targets Tyrosine Kinase Inhibitor Resistant Chronic Myeloid Leukemia Cells. *Biomed. Pharmacother.* 129, 110390. doi:10.1016/j.biopha.2020.110390

Hochhaus, A., Baccarani, M., Silver, R. T., Schiffer, C., Apperley, J. F., Cervantes, F., et al. (2020). European LeukemiaNet 2020 Recommendations for Treating Chronic Myeloid Leukemia, Springer Nature. *Leukemia* 34 (4), 966–984. doi:10.1038/s41375-020-0776-2

Housman, G., Byler, S., Heerboth, S., Lapinska, K., Longacre, M., Snyder, N., et al. (2014). Drug Resistance in Cancer: An Overview. *CancersMDPI AG* 6 (3), 1769–1792. doi:10.3390/cancers6031769

Hughes, T. P., Saglio, G., Kantarjian, H. M., Guilhot, F., Niederwieser, D., Rosti, G., et al. (2014). Early Molecular Response Predicts Outcomes in Patients with Chronic Myeloid Leukemia in Chronic Phase Treated with Frontline Nilotinib or Imatinib. *Blood* 123 (9), 1353–1360. doi:10.1182/blood-2013-06-510396

Hurtz, C., Hatzi, K., Cerchietti, L., Braig, M., Park, E., Kim, Y.-m., et al. (2011). BCL6-mediated Repression of P53 Is Critical for Leukemia Stem Cell Survival in Chronic Myeloid Leukemia. *J. Exp. Med.* 208 (11), 2163–2174. doi:10.1084/jem.20110304

Iclusig (2016). Ponatinib. FDA US, 3, 2016 . Available at: https://www.accessdata.fda.gov/drugsatfda_docs/label/2012/203469lbl.pdf (Accessed September 10, 2021).

Issa, G. C., Kantarjian, H. M., Gonzalez, G. N., Borthakur, G., Tang, G., Wierda, W., et al. (2017). Clonal Chromosomal Abnormalities Appearing in Philadelphia Chromosome-Negative Metaphases during CML Treatment. *Blood* 130 (19), 2084–2091. doi:10.1182/blood-2017-07-792143

Jabbour, E., and Kantarjian, H. (2020). Chronic Myeloid Leukemia: 2020 Update on Diagnosis, Therapy and Monitoring. *Am. J. Hematol.* 95 (6), 691–709. doi:10.1002/ajh.25792

Jagannath, S., Dimopoulos, M. A., and Lonial, S. (2010). Combined Proteasome and Histone Deacetylase Inhibition: A Promising Synergy for Patients with Relapsed/refractory Multiple Myeloma. *Leuk. Res.* 34 (Issue 9), 1111–1118. doi:10.1016/j.leukres.2010.04.001

Jain, P., Kantarjian, H., Alattar, M. L., Jabbour, E., Sasaki, K., Gonzalez, G. N., et al. (2015). Analysis of Long Term Responses and Their Impact on Outcomes in Patients with Chronic Phase CML Treated with Four Different TKI Modalities – Analysis of 5 Prospective Clinical Trials. *Lancet Haematol.* 2 (3), 118–128. doi:10.1016/S2352-3026(15)00021-6

Jain, P., Kantarjian, H., Boddu, P. C., Nogueras-González, G. M., Verstovsek, S., Garcia-Manero, G., et al. (2019). Analysis of Cardiovascular and Arteriothrombotic Adverse Events in Chronic-phase CML Patients after Frontline TKIs. *Blood Adv.* 3 (6), 851–861. doi:10.1182/bloodadvances.2018025874

Jain, P., Kantarjian, H. M., Ghorab, A., Sasaki, K., Jabbour, E. J., Nogueras Gonzalez, G., et al. (2017). Prognostic Factors and Survival Outcomes in Patients with Chronic Myeloid Leukemia in Blast Phase in the Tyrosine Kinase Inhibitor Era: Cohort Study of 477 Patients. *Cancer* 123 (22), 4391–4402. doi:10.1002/cncr.30864

Jain, P., Kantarjian, H., Sasaki, K., Jabbour, E., Dasarathula, J., Nogueras Gonzalez, G., et al. (2016). Analysis of 2013 European LeukaemiaNet (ELN) Responses in Chronic Phase CML across Four Frontline TKI Modalities and Impact on Clinical Outcomes. *Br. J. Haematol.* 173 (1), 114–126. doi:10.1111/bjh.13936

Jaiswal, S., Natarajan, P., Silver, A. J., Gibson, C. J., Bick, A. G., Shvartz, E., et al. (2017). Clonal Hematopoiesis and Risk of Atherosclerotic Cardiovascular Disease. *N. Engl. J. Med.* 377 (2), 111–121. doi:10.1056/nejmoa1701719

Jelinek, J., Gharibyan, V., Estecio, M. R., Kondo, K., He, R., Chung, W., et al. (2011). Aberrant DNA Methylation is Associated with Disease Progression, Resistance to Imatinib and Shortened Survival in Chronic Myelogenous Leukemia. *PLoS One* 6 (7), 22110. doi:10.1371/journal.pone.0022110

Kantarjian, H., Shah, N. P., Hochhaus, A., Cortes, J., Shah, S., Ayala, M., et al. (2010). Dasatinib versus Imatinib in Newly Diagnosed Chronic-phase Chronic Myeloid Leukemia. *N. Engl. J. Med.* 362 (24), 2260–2270. doi:10.1056/NEJMoa1002315

Lernoux, M., Schnekenburger, M., Losson, H., Vermeulen, K., Hahn, H., Gérard, D., et al. (2020). Novel HDAC Inhibitor MAKV-8 and Imatinib Synergistically Kill Chronic Myeloid Leukemia Cells via Inhibition of BCR-ABL/MYC-signaling: Effect on Imatinib Resistance and Stem Cells. *Clin. Epigenet.* 12 (1), 1–26. doi:10.1186/s13148-020-00839-z

Li, L., Wang, L., Li, L., Wang, Z., Ho, Y., McDonald, T., et al. (2012). Activation of P53 by SIRT1 Inhibition Enhances Elimination of CML Leukemia Stem Cells in Combination with Imatinib. *Cancer Cell.* 21 (2), 266–281. doi:10.1016/j.ccr.2011.12.020

Li, Z., and Luo, J. (2018). Epigenetic Regulation of HOTAIR in Advanced Chronic Myeloid Leukemia. *Cmar* 10, 5349–5362. doi:10.2147/CMAR.S166859

Liu, T.-C., Lin, S.-F., Chang, J.-G., Yang, M.-Y., Hung, S.-Y., and Chang, C.-S. (2003). Epigenetic Alteration of theSOCS1gene in Chronic Myeloid Leukaemia. *Br. J. Haematol.* 123 (4), 654–661. doi:10.1046/j.1365-2141.2003.04660.x

Madapura, H. S., Nagy, N., Ujvari, D., Kallas, T., Kröhnke, M. C. L., Amu, S., et al. (2017). Interferon γ Is a STAT1-dependent Direct Inducer of BCL6 Expression in Imatinib-Treated Chronic Myeloid Leukemia Cells. *Oncogene* 36 (32), 4619–4628. doi:10.1038/onc.2017.85

Maiti, A., Franquiz, M. J., Ravandi, F., Cortes, J. E., Jabbour, E. J., Sasaki, K., et al. (2020). Venetoclax and BCR-ABL Tyrosine Kinase Inhibitor Combinations: Outcome in Patients with Philadelphia Chromosome-Positive Advanced Myeloid Leukemias. *Acta Haematol.* 143 (6), 567–573. doi:10.1159/000506346

Matsuda, Y., Yamauchi, T., Hosono, N., Uzui, K., Negoro, E., Morinaga, K., et al. (2016). Combination of Panobinostat with Ponatinib Synergistically Overcomes Imatinib-resistant CML Cells. *Cancer Sci.* 107 (7), 1029–1038. doi:10.1111/cas.12965

Miller, T. A., Witter, D. J., and Belvedere, S. (2003). Histone Deacetylase Inhibitors. *J. Med. Chem.* 46 (24), 5097–5116. doi:10.1021/jm0303094

Millot, F., Baruchel, A., Guilhot, J., Petit, A., Leblanc, T., Bertrand, Y., et al. (2011). Imatinib Is Effective in Children with Previously Untreated Chronic Myelogenous Leukemia in Early Chronic Phase: Results of the French National Phase IV Trial. *Jco* 29 (20), 2827–2832. doi:10.1200/JCO.2010.32.7114

Morita, K., Jabbour, E., Ravandi, F., Borthakur, G., Khoury, J. D., Hu, S., et al. (2021a). Clinical Outcomes of Patients with Chronic Myeloid Leukemia with Concurrent Core Binding Factor Rearrangement and Philadelphia Chromosome. *Clin. Lymphoma Myeloma Leuk.* 21 (5), 338–344. doi:10.1016/j.clml.2020.12.025

Morita, K., Kantarjian, H. M., Sasaki, K., Issa, G. C., Jain, N., Konopleva, M., et al. (2021b). Outcome of Patients with Chronic Myeloid Leukemia in Lymphoid Blastic Phase and Philadelphia Chromosome-Positive Acute Lymphoblastic Leukemia Treated with hyper-CVAD and Dasatinib. *Cancer* 127 (15), 2641–2647. doi:10.1002/cncr.33539

Mwakwari, S. C., Patil, V., Guerrant, W., and Oyelere, A. K. (2010). Macrocyclic Histone Deacetylase Inhibitors. *Curr. Top. Med. Chem.* 10 (14), 1423–1440. doi:10.2174/156802610792232079

Nteliopoulos, G., Bazeos, A., Claudiani, S., Gerrard, G., Curry, E., Szydlo, R., et al. (2019). Somatic Variants in Epigenetic Modifiers Can Predict Failure of Response to Imatinib but Not to Second-Generation Tyrosine Kinase Inhibitors. *Haematologica* 104 (12), 2400–2409. doi:10.3324/haematol.2018.200220

O'Hare, T., Shakespeare, W. C., Zhu, X., Eide, C. A., Rivera, V. M., Wang, F., et al. (2009). AP24534, a Pan-BCR-ABL Inhibitor for Chronic Myeloid Leukemia, Potently Inhibits the T315I Mutant and Overcomes Mutation-Based Resistance. *Cancer Cell.* 16 (5), 401–412. doi:10.1016/j.ccr.2009.09.028

Oki, Y., Kantarjian, H. M., Gharibyan, V., Jones, D., O'Brien, S., Verstovsek, S., et al. (2007). Phase II Study of Low-Dose Decitabine in Combination with Imatinib Mesylate in Patients with Accelerated or Myeloid Blastic Phase of Chronic Myelogenous Leukemia. *Cancer* 109 (5), 899–906. doi:10.1002/cncr.22470

Özgür Yurttaş, N., and Eşkazan, A. E. (2020). Novel Therapeutic Approaches in Chronic Myeloid Leukemia. *Leuk. Res.* 91, 106337. doi:10.1016/J.LEUKRES.2020.106337

Patil, V., Guerrant, W., Chen, P. C., Gryder, B., Benicewicz, D. B., Khan, S. I., et al. (2010). Antimalarial and Antileishmanial Activities of Histone Deacetylase Inhibitors with Triazole-Linked Cap Group. *Bioorg. Med. Chem.* 18 (1), 415–425. doi:10.1016/j.bmc.2009.10.042

Reddy, E. P., and Aggarwal, A. K. (2012). The Ins and Outs of Bcr-Abl Inhibition. *Genes. Cancer* 3 (5–6), 447–454. doi:10.1177/1947601912462126

Rohrbacher, M., and Hasford, J. (2009). Epidemiology of Chronic Myeloid Leukaemia (CML). *Best Pract. Res. Clin. Haematol.* 22 (3), 295–302. doi:10.1016/j.beha.2009.07.007

Russo, D., Garcia-Gutierrez, J. V., Soverini, S., and Baccarani, M. (2020). Chronic Myeloid Leukemia Prognosis and Therapy: Criticisms and Perspectives. *Jcm* 9 (6), 1709. doi:10.3390/jcm9061709

Saglio, G., Kim, D.-W., Issaragrisil, S., le Coutre, P., Etienne, G., Lobo, C., et al. (2010). Nilotinib versus Imatinib for Newly Diagnosed Chronic Myeloid Leukemia. *New Engl. J. Med.* 362 (24), 2251–2259. doi:10.1056/nejmoa0912614

San José-Eneriz, E., Agirre, X., Jiménez-Velasco, A., Cordeu, L., Martín, V., Arqueros, V., et al. (2009). Epigenetic Down-Regulation of BIM Expression Is Associated with Reduced Optimal Responses to Imatinib Treatment in Chronic Myeloid Leukaemia. *Eur. J. Cancer.* 45 (10), 1877–1889. doi:10.1016/j.ejca.2009.04.005

Sasaki, K., Kantarjian, H. M., Jain, P., Jabbour, E. J., Ravandi, F., Konopleva, M., et al. (2016). Conditional Survival in Patients with Chronic Myeloid Leukemia in Chronic Phase in the Era of Tyrosine Kinase Inhibitors. *Cancer* 122 (2), 238–248. doi:10.1002/cncr.29745

Sasaki, K., Kantarjian, H. M., O'Brien, S., Ravandi, F., Konopleva, M., Borthakur, G., et al. (2019). Incidence of Second Malignancies in Patients with Chronic Myeloid Leukemia in the Era of Tyrosine Kinase Inhibitors. *Int. J. Hematol.* 109 (5), 545–552. doi:10.1007/s12185-019-02620-2

Sasaki, K., Kantarjian, H., O'Brien, S., Ravandi, F., Konopleva, M., Borthakur, G., et al. (2018). Prediction for Sustained Deep Molecular Response of BCR-ABL1 Levels in Patients with Chronic Myeloid Leukemia in Chronic Phase. *Cancer* 124 (6), 1160–1168. doi:10.1002/cncr.31187

Sasaki, K., Strom, S. S., O'brien, S., Jabbour, E., Ravandi, F., Konopleva, M., et al. (2015). Prospective Analysis: Relative Survival in Patients with Chronic Myeloid Leukemia in Chronic Phase in the Era of Tyrosine Kinase Inhibitors. *Lancet Haematol.* 2 (5), 186–193. doi:10.1016/S2352-3026(15)00048-4

Saxena, K., Jabbour, E., Issa, G., Sasaki, K., Ravandi, F., Maiti, A., et al. (2021). Impact of Frontline Treatment Approach on Outcomes of Myeloid Blast Phase CML. *J. Hematol. Oncol.* 14 (1), 1–10. doi:10.1186/s13045-021-01106-1

Scott, M. T., Korfi, K., Saffrey, P., Hopcroft, L. E. M., Kinstrie, R., Pellicano, F., et al. (2016). Epigenetic Reprogramming Sensitizes CML Stem Cells to Combined EZH2 and Tyrosine Kinase Inhibition. *Cancer Discov.* 6 (11), 1248–1257. doi:10.1158/2159-8290.CD-16-0263

Soverini, S., Colarossi, S., Gnani, A., Rosti, G., Castagnetti, F., Poerio, A., et al. (2006). Contribution of ABL Kinase Domain Mutations to Imatinib Resistance in Different Subsets of Philadelphia-positive Patients: By the GIMEMA Working Party on Chronic Myeloid Leukemia. *Clin. Cancer Res.* 12 (24), 7374–7379. doi:10.1158/1078-0432.CCR-06-1516

Soverini, S., Iacobucci, I., Baccarani, M., and Martinelli, G. (2007). Targeted Therapy and the T315I Mutation in Philadelphia-positive Leukemias. *Haematologica* 92 (4), 437–439. doi:10.3324/haematol.11248

Sprycel (2010). Dasatinib. FDA US, 1–37. Available at: http://www.accessdata.fda.gov/drugsatfda_docs/label/2010/021986s7s8lbl.pdf (Accessed September 10, 2021).

Tasigna (2017). Nilotinib. *US FDA*. Available at: https://www.accessdata.fda.gov/drugsatfda_docs/label/2010/022068s004s005lbl.pdf (Accessed September 10, 2021).

Yang, A. S., Doshi, K. D., Choi, S. W., Mason, J. B., Mannari, R. K., Gharybian, V., et al. (2006). DNA Methylation Changes After 5-aza-2′-deoxycytidine Therapy in Patients with Leukemia. *Cancer Res.* 66 (10), 5495–5503. doi:10.1158/0008-5472.CAN-05-2385

Yuan, H., Wang, Z., Li, L., Zhang, H., Modi, H., Horne, D., et al. (2012). Activation of Stress Response Gene SIRT1 by BCR-ABL Promotes Leukemogenesis. *Blood* 119 (8), 1904–1914. doi:10.1182/blood-2011-06-361691

Zehtabcheh, S., Yousefi, A.-M., Salari, S., Safa, M., Momeny, M., Ghaffari, S. H., et al. (2021). Abrogation of Histone Deacetylases (HDACs) Decreases Survival of Chronic Myeloid Leukemia Cells: New Insight into Attenuating Effects of the PI3K/c-Myc axis on Panobinostat Cytotoxicity. *Cel Biol. Int.* 45 (5), 1111–1121. doi:10.1002/CBIN.11557

Zhu, X.-Y., Liu, W., Liang, H.-T., Tang, L., Zou, P., You, Y., et al. (2020). AICAR and Decitabine Enhance the Sensitivity of K562 Cells to Imatinib by Promoting Mitochondrial Activity. *Curr. Med. Sci.* 40 (5), 2020. doi:10.1007/s11596-020-2266-1

Conflict of Interest: The authors declare that the research was conducted in the absence of any commercial or financial relationships that could be construed as a potential conflict of interest.

Publisher's Note: All claims expressed in this article are solely those of the authors and do not necessarily represent those of their affiliated organizations, or those of the publisher, the editors and the reviewers. Any product that may be evaluated in this article, or claim that may be made by its manufacturer, is not guaranteed or endorsed by the publisher.

GLOSSARY

ACAs Additional cytogenetic abnormalities

AE Adverse effects

AER Absolute excess risk

ALL Acute lymphoblastic leukemia

ALT Alanine transaminase

AML Acute myeloid leukemia

ANC Absolute neutrophil count

AP Accelerated phase

ASCT Allogeneic stem cell transplant

AST Aspartate aminotransferase

AUC Area under the curve that represents the total drug exposure across time

BC Blast crisis

BCR Breakpoint cluster region

BD Bis in die (two times daily)

BP Blast Phase

CBF Core binding factor

CCyR Complete cytogenetic response

CHR Complete hematologic remission

Cmax Maximum serum concentration that a drug achieves after administration

CML Chronic myeloid leukemia

COVID-19 Coronavirus Disease 2019

CP Chronic phase

DNMT DNA methylation

EFS Event-free survival

ELN European LeukemiaNet

EMR Major molecular remission

FDA Food and drug administration

FFS Failure-free survival

HDAC Histone deacetylase

HMA Hypomethylating agent

HOTAIR HOX transcript antisense RNA

IC Intensive chemotherapy

IC_{50} Half maximal inhibitory concentration

LSC Leukemic stem cell

MDS Myelodysplastic Syndrome

OD Omne in die (once a day)

OS Overall survival

PcG Polycomb-group

PCyR Partial cytogenetic response

PRC Polycomb repressive complex

QTc QT corrected for heart rate

SAHA Suberoylanilide hydroxamic acid

SARS CoV-2 Severe acute respiratory syndrome coronavirus 2

SIRT Sirtuin

SOCS Suppressor of cytokine signaling

$T_{1/2}$ Elimination half-life of a drug

TFS Transformation-free survival

TKI Tyrosine kinase inhibitor

T_{max} Time at which the Cmax is observed

WHO World Health Organization

frontiers in Cell and Developmental Biology

ORIGINAL RESEARCH
published: 28 October 2021
doi: 10.3389/fcell.2021.759813

Targeted Bisulfite Sequencing Reveals DNA Methylation Changes in Zinc Finger Family Genes Associated With KRAS Mutated Colorectal Cancer

Weilin Pu[1,2,3†], Fei Qian[4†], Jing Liu[2], Keke Shao[5], Feng Xiao[6], Qin Jin[7], Qingmei Liu[8], Shuai Jiang[2], Rui Zhang[2], Jun Zhang[9], Shicheng Guo[10], Jianfeng Zhang[11], Yanyun Ma[3,12], Shaoqing Ju[1]* and Weifeng Ding[1]**

[1] Department of Laboratory Medicine, Affiliated Hospital of Nantong University, Nantong, China, [2] State Key Laboratory of Genetic Engineering, Collaborative Innovation Center for Genetics and Development, School of Life Sciences, Fudan University, Shanghai, China, [3] Human Phenome Institute, Fudan University, Shanghai, China, [4] Department of Gastrointestinal Surgery, Affiliated Hospital of Nantong University, Nantong, China, [5] Department of Laboratory Medicine, The First People's Hospital of Yancheng City, Yancheng, China, [6] Department of Pathology, The Third People's Hospital of Nantong City, Nantong, China, [7] Department of Pathology, Affiliated Hospital of Nantong University, Nantong, China, [8] Department of Dermatology, Huashan Hospital, Fudan University, Shanghai, China, [9] Department of Gastroenterology, Huashan Hospital, Fudan University, Shanghai, China, [10] Center for Precision Medicine Research, Marshfield Clinic Research Institute, Marshfield, WI, United States, [11] Department of Gastroenterology, Affiliated Hospital of Nantong University, Nantong, China, [12] Six Industrial Research Institute, Fudan University, Shanghai, China

Background: Colorectal cancer (CRC) is a leading cause of cancer death, and early diagnosis of CRC could significantly reduce its mortality rate. Previous studies suggest that the DNA methylation status of zinc finger genes (ZFGs) could be of potential in CRC early diagnosis. However, the comprehensive evaluation of ZFGs in CRC is still lacking.

Methods: We first collected 1,426 public samples on genome-wide DNA methylation, including 1,104 cases of CRC tumors, 54 adenomas, and 268 para-tumors. Next, the most differentially methylated ZFGs were identified and validated in two replication cohorts comprising 218 CRC patients. Finally, we compared the prediction capabilities between the ZFGs and the SEPT9 in all CRC patients and the KRAS + and KRAS- subgroup.

Results: Five candidate ZFGs were selected: *ESR1*, *ZNF132*, *ZNF229*, *ZNF542*, and *ZNF677*. In particular, *ESR1* [area under the curve (AUC) = 0.91] and *ZNF132* (AUC = 0.93) showed equivalent or better diagnostic capability for CRC than *SEPT9* (AUC = 0.91) in the validation dataset, suggesting that these two ZFGs might be of potential for CRC diagnosis in the future. Furthermore, we performed subgroup analysis and found a significantly higher diagnostic capability in KRAS + (AUC ranged from 0.97 to 1) than that in KRAS- patients (AUC ranged from 0.74 to 0.86) for all these

OPEN ACCESS

Edited by:
Ata Abbas,
Case Western Reserve University,
United States

Reviewed by:
Matteo Pellegrini,
University of California, Los Angeles,
United States
Sabiha Khatoon,
Texas Tech University Health Sciences Center, United States

***Correspondence:**
Weifeng Ding
dwf@ntu.edu.cn
Yanyun Ma
mayymail@163.com
Shaoqing Ju
jsq814@hotmail.com

† These authors have contributed equally to this work

Specialty section:
This article was submitted to Epigenomics and Epigenetics, a section of the journal Frontiers in Cell and Developmental Biology

Received: *17 August 2021*
Accepted: *11 October 2021*
Published: *28 October 2021*

Citation:
Pu W, Qian F, Liu J, Shao K, Xiao F, Jin Q, Liu Q, Jiang S, Zhang R, Zhang J, Guo S, Zhang J, Ma Y, Ju S and Ding W (2021) Targeted Bisulfite Sequencing Reveals DNA Methylation Changes in Zinc Finger Family Genes Associated With KRAS Mutated Colorectal Cancer. Front. Cell Dev. Biol. 9:759813. doi: 10.3389/fcell.2021.759813

five ZFGs, suggesting that these ZFGs could be ideal diagnostic markers for KRAS mutated CRC patients.

Conclusion: The methylation profiles of the candidate ZFGs could be potential biomarkers for the early diagnosis of CRC, especially for patients carrying KRAS mutations.

Keywords: colorectal cancer, DNA methylation, zinc finger family, KRAS, diagnosis

INTRODUCTION

Colorectal cancer (CRC) is the second most common cause of cancer in the United States and accounts for 10% of cancer incidences and 9.4% of cancer deaths worldwide in 2020 (Siegel et al., 2020; Sung et al., 2021). Previous studies have found that the accumulations of both genetic and epigenetic alterations lead to CRC carcinogenesis. The 5-year survival rate of CRC ranges from 90% in its early stages (when it is localized and regional), but it decreases significantly to about 14% when detected at a distant stage, highlighting the importance of early detection methods (Siegel et al., 2020).

Recently, the application of screening modalities, including colonoscopy and image-based detection, significantly decreased the mortality of CRC (Siegel et al., 2017). However, these screening methods are not widely used across populations due to abdominal pain, discomfort, and other contraindications. Thus, the development of non-invasive and precise diagnostic methods for CRC is needed.

DNA methylation is a crucial epigenetic modification in the human genome and plays vital roles in embryonic development, transcription regulation (He et al., 2011; Jiang et al., 2018), and genomic imprinting (Schubeler, 2015). Moreover, the dynamic changes of DNA methylation in different tissues and disease courses make it a promising tool to develop the tissue-of-origin test (Guo et al., 2017a) and disease prediction (Guo et al., 2015), especially for cancers (Koch et al., 2018) and immune diseases (Guo et al., 2017b; Ding et al., 2018). Till now, A series of DNA methylation-based biomarkers have been found in CRC, including *SEPT9* (Barault et al., 2018; Freitas et al., 2018; Wills et al., 2018; Sun et al., 2019). However, the performance of *SEPT9* is not as good as that of the stool DNA test (Ahlquist et al., 2012; Church et al., 2014; Song et al., 2017). Therefore, identifying better DNA-methylation-based biomarkers with high accuracy would be beneficial in liquid biopsy in CRC.

Zinc finger proteins (ZFPs) are a prominent component of transcriptional factors in eukaryotes. The ZFP family can be divided into eight categories according to their distinct motifs: Cys2His2 (C2H2)-like, Gag knuckle, Treble clef, Zinc ribbon, Zn2/Cys6, TAZ2 domain-like, zinc-binding loops, and metallothionein (Jen and Wang, 2016). The C2H2-type zinc finger motifs form the largest class. Currently, growing bodies of evidence suggest that ZFPs could contribute to tumor progression or suppress it *via* transcriptional regulation. The DNA methylation alterations of multiple ZFPs have been recognized as promising biomarkers for tumor diagnosis, prognosis, and drug response due to their vital roles in cancers. However, a comprehensive and systemic assessment of the DNA methylation profiles of zinc finger genes (ZFGs) in CRC is lacking.

In this study, we exhaustively searched and combined public microarray datasets on high-throughput DNA methylation for the first time, including 1,104 CRC tumors, 54 adenomas, and 268 para-tumors. We identified seven candidate zinc finger genes using comprehensive filtering procedures, and five of them were successfully validated in 104 CRC Han Chinese patients, especially in the CRC tumors carrying the KRAS mutation. To confirm the findings, we recruited another 114 CRC patients of Han Chinese descent and yielded consistent results. In particular, two of these ZFGs, *ESR1,* and *ZNF132*, showed a significantly higher diagnostic capability than *SEPT9*, suggesting that they might be promising biomarkers for CRC diagnosis, especially for KRAS mutated patients.

RESULTS

Five Zinc Finger Genes Were Identified as Candidate Colorectal Cancer Diagnostic Biomarkers

To identify robust DNA methylation-based biomarkers, we searched the public datasets for the DNA methylation status in CRC cases and collected 1,104 CRC tumors, 268 para-tumor samples, and 54 adenomas for further analysis (See section "Materials and Methods," **Supplementary Table 1**). We also obtained the complete list of genes belonging to the ZFP family (**Supplementary Table 2**). Based on the feature selection procedures described in the section "Materials and Methods," we finally identified five candidate genes: *ESR1*, *ZNF132*, *ZNF229*, *ZNF542,* and *ZNF677* (**Figure 1**).

These five genes were significantly hypermethylated in both CRC and adenoma tissues compared to the para-tumors (**Supplementary Figure 1**). Consistently, the expression levels of these genes were also significantly down-regulated in CRC tumors compared to para-tumors in the TCGA dataset (**Figure 2**). To characterize the abilities of these biomarkers quantitatively in the combined discovery dataset, we constructed a univariate logistic regression model for each gene and obtained robust discrimination between CRC tumors and para-tumor

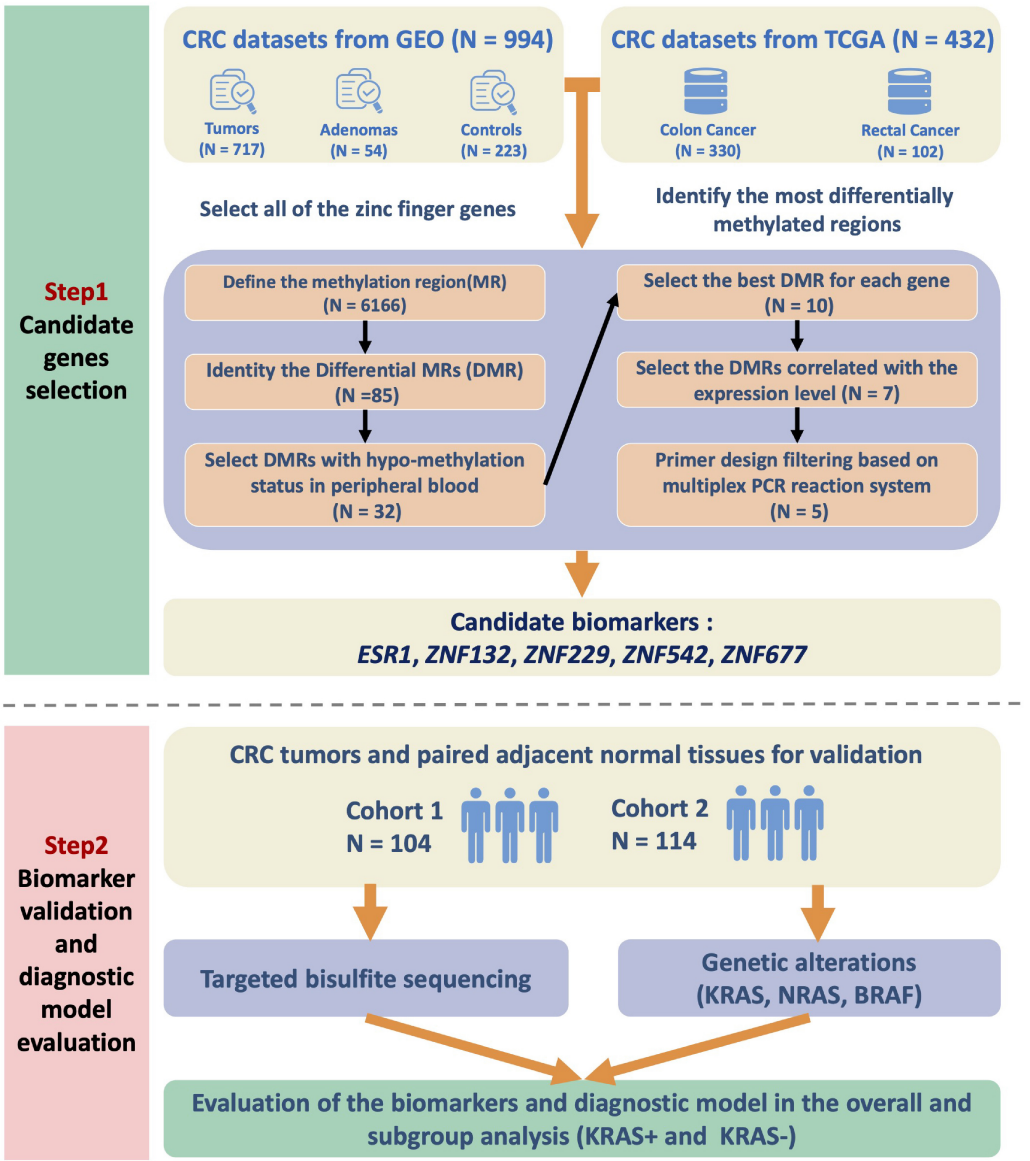

FIGURE 1 | Flow chart of the study design. We first integrated the high-throughput DNA methylation microarray datasets from GEO and TCGA databases and examined the methylation profiles of all the zinc finger genes. To identify the most significantly differentially methylated genes in CRC, we first defined the methylation region and selected the differentially methylated regions (DMRs). The methylation status of the candidate DMRs in the whole blood, peripheral blood mononuclear cells and peripheral blood leukocytes were also utilized for biomarker filtering. The correlations between the methylation and expression level of the candidates were also calculated for further filtering. Finally, the candidate zinc finger genes-based biomarkers were validated in two independent CRC cohorts of the Han Chinese population. In addition, the KRAS mutation status of the patients was also detected and assessed for subgroup analysis.

tissues (sensitivity = 0.82–0.90, specificity = 0.88–0.97, AUC = 0.93–0.97).

Targeted Bisulfite Sequencing in the Han Chinese Population Confirmed the Efficacy of the Candidate Zinc Finger Genes-Based Biomarkers

To further verify these DNA methylation-based biomarkers, we recruited 104 CRC patients of the Han Chinese population. The characteristics of these CRC patients (replication cohort 1) are shown in **Table 1**. The CRC tumors and their matched para-tumors were obtained for targeted bisulfite sequencing. The methylation profiles of the candidates and the known biomarker (*SEPT9*) were examined using targeted bisulfite sequencing (See section "Materials and Methods"). The bisulfite conversion rate (C to T) was high (>99%) in both tumors and para-tumors, and no significant difference in the read mapping rate was found between groups (**Supplementary Figure 2**). After quality control, 187 samples were retained

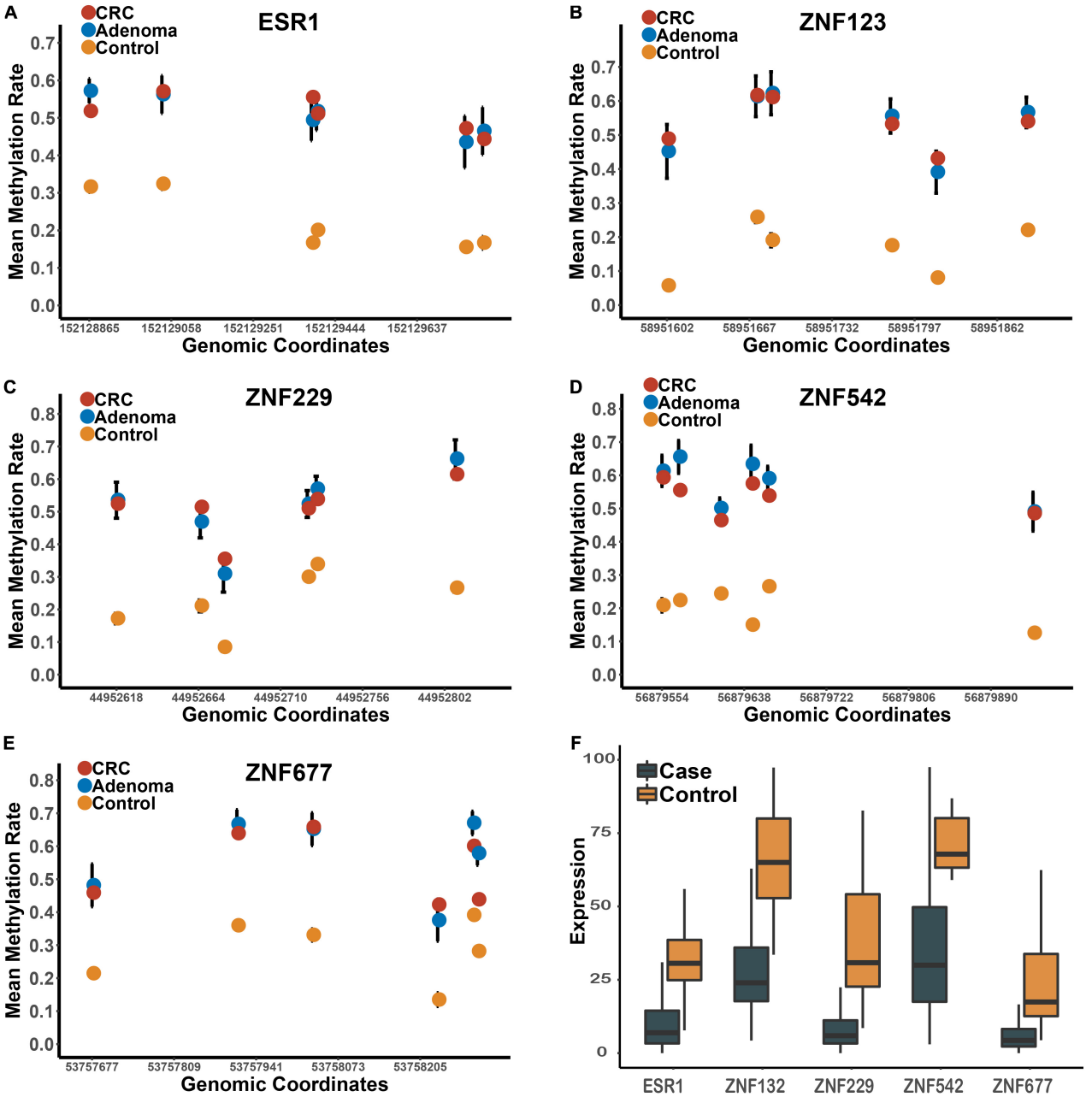

FIGURE 2 | The methylation and expression profiles of the candidate biomarkers in the discovery datasets. Panels **(A–E)** represents the methylation profiles of the five candidates in the tumors, adenomas and para-tumors in the integrated dataset. Panel **(F)** represents the expression profiles of these five candidate zinc finger genes between CRC tumor and para-tumors in TCGA.

for further analysis, including 98 CRC tumors and 89 para-tumors.

Based on the methylation profiles of these five ZFGs, we performed principal component analysis (PCA) and found a significant distinction between CRC tumors and para-tumors (**Supplementary Figure 3**). A differential methylation analysis was also conducted for these candidates, and we found that all candidate genes were significantly hypermethylated in CRC tumors (**Figure 3** and **Supplementary Figure 4**). Furthermore, we performed a univariate logistic regression analysis without adjusting for covariates, and created the receiver operating characteristic (ROC) curve to reveal the diagnostic ability of each candidate gene. As shown in **Supplementary Table 3**, the area under the curve (AUCs) of these candidates ranged from 0.85 to 0.93. In particular, we found that the diagnostic capability of *ZNF132* (AUC = 0.91) and *ESR1* (AUC = 0.93) was equal to or better than that of *SEPT9* (AUC = 0.91), indicating that these ZFGs might have great potential for CRC diagnosis.

The Diagnostic Abilities of the Candidates Were Significantly Affected by the KRAS Mutation Status of Colorectal Cancer Patients

In addition to the overall differential methylation analysis, we also evaluated the effects of age, gender, tumor stage, location of the tumor (colon or rectum), and the mutation status (KRAS + vs. KRAS-) of the CRC samples (**Supplementary Tables 4–8**). No significant differences were found in the diagnostic capability between CRC patients in the young/old, male/female, early/late stage, and colon/rectum subgroups (**Supplementary Table 9**, see section "Materials and Methods"). However, the diagnostic capability for CRC patients carrying the KRAS mutation (KRAS +) was significantly better than that for KRAS- samples (**Supplementary Tables 8, 9**). In the KRAS + group, the sensitivity of each gene ranged from 0.86 to 0.98, the specificity range was 0.89 to 1.00, and the AUC range was 0.97 to 1.00, which is significantly higher than the sensitivity (0.52 to 0.82), specificity (0.80 to 0.98) and AUC (0.74 to 0.86) in the KRAS- group (**Supplementary Table 8**). Moreover, the hierarchical clustering analysis revealed that all CRC tumors misclassified into the control group were KRAS- samples (**Figure 4**). In addition, we further examined if other factors may be associated with these misclassified CRC tumors (n = 17). However, none of the age, gender, tumor stage, and tumor locations showed significant differences in our study's overall CRC tumors. Furthermore, we examined the diagnostic abilities of the ZFGs in the KRAS + and KRAS- subgroup from the TCGA dataset for verification. Consistently, the diagnostic capability of the ZFGs in the KRAS + subgroup (AUC = 0.96–1) was significantly higher than in the KRAS- subgroup (AUC = 0.93–0.97), suggesting the significant methylation changes between KRAS + and KRAS- subgroup (**Supplementary Table 10**).

TABLE 1 | Characteristics of the CRC patients included in this study.

Characteristics	Patient distribution	Patient distribution
	Cohort 1 (*N* = 104)	Cohort 2 (*N* = 114)
Age	66 (IQR = 62 to 74)	68 (IQR = 60 to 75)
Gender		
Male	71	75
Female	33	39
Subtype[a]		
Colon	55	68
Rectum	49	45
UICC Stage[b]		
I	18	28
II	35	38
III	40	38
IV	11	9
Tumor invasion depth[c]		
T1	5	7
T2	21	22
T3	70	69
T4	6	15
Tx	2	1
Lymph node involvement[c]		
N0	57	72
N1	29	25
N2	11	15
N3	5	2
Nx	2	
Distant metastasis[c]		
M0	93	105
M1	11	9
KRAS mutation[d]		
Positive	50	52
Negative	52	62

[a] *The tumors were classified into colon or rectum based on the location of the tumor.*
[b] *The UICC stage was determined after surgical intervention and histological examination of the specimen.*
[c] *TNM Stages were assessed by the seventh edition of the TNM classification criteria.*
[d] *The KRAS mutation status was examined using the FastTarget next-generation sequencing method.*

An Independent Replication Cohort Validated the Association Between KRAS Mutation and Diagnostic Capabilities of the Zinc Finger Genes

Due to the limited sample size in replication cohort 1, we recruited another sample group (replication cohort 2), including 114 CRC tumors and matched para-tumors from patients of Han Chinese descent (**Table 1**) for further validation. The methylation profiles of these ZFGs were measured in replication cohort 2 (**Supplementary Figures 5, 6**). Consistently, we found that *ESR1* (AUC = 0.90) and *ZNF132* (AUC = 0.94) still showed the best diagnostic capability for CRC (**Supplementary Table 11**).

Furthermore, the significant differences of methylation profiles between the KRAS + and KRAS- subgroups were also validated (**Supplementary Figure 7**). In the KRAS + subgroup, the sensitivity (0.90 to 1.00), specificity (0.91 to 0.98), and the AUC (0.92 to 1.00) of each gene was significantly higher than that in the KRAS- subgroup (sensitivity: 0.58 to 0.85, specificity: 0.78 to 0.96, AUC: 0.71 to 0.88) (**Supplementary Table 12**). Similarly, the CRC tumors misclassified as the para-tumors were in the KRAS- subgroup, confirming that the KRAS + CRC samples were more epigenetically homogeneous than the KRAS- CRC samples (**Figure 5**).

The Diagnostic Abilities of Zinc Finger Genes Could Achieve Superior Performance Than That of *SEPT9* for Colorectal Cancer Diagnosis Using All Replication Samples

To further identify the robust diagnostic biomarker for CRC diagnosis, we combined the datasets from replication cohort 1 and replication cohort 2. As shown in **Figure 6**, *ZNF132* had the highest diagnostic capability (sensitivity = 0.83, specificity = 0.97, AUC = 0.93) than other genes, including

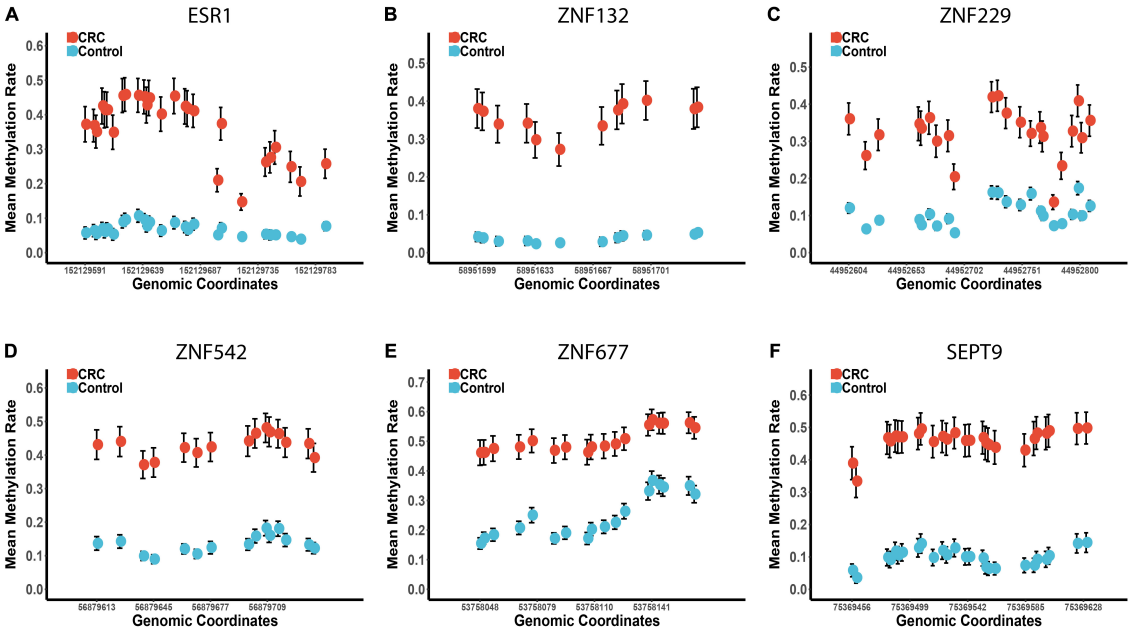

FIGURE 3 | The methylation profiles of the five zinc finger genes and SEPT9 in the replication cohort 1. Panels **(A–F)** represents the mean methylation status of the CpG sites in regions covering *ESR1*, *ZNF132*, *ZNF229*, *ZNF542*, *ZNF677,* and *SEPT9*, respectively. The x-axis represents the genomic positions of the CpG sites in the targeted regions. The y-axis represents the mean methylation percentage in the CRC tumor tissues and paired normal tissues for each CpG site. The error bar of each CpG site represents the confidence interval of the methylation percentage.

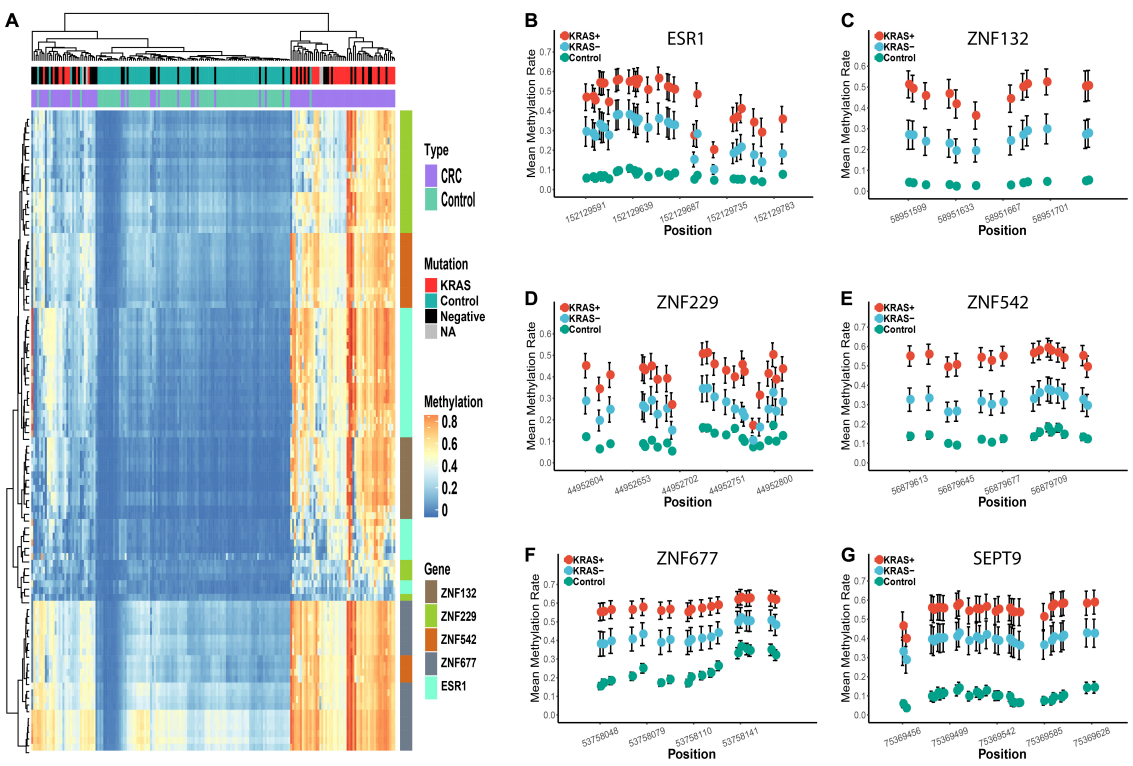

FIGURE 4 | Differential methylation profiles of these candidate biomarkers in KRAS + and KRAS- subgroup in replication cohort 1. Panel **(A)** represents the heatmap of the methylation levels of these five candidate genes. The tumor and para-tumors tissues were differently colored. The KRAS mutation status of the CRC tumors is also differently colored. Panels **(B–G)** represents the methylation profiles of the five zinc finger genes and SEPT9. The mean methylation percentage of each CpG site is shown for KRAS +, KRAS- and control groups.

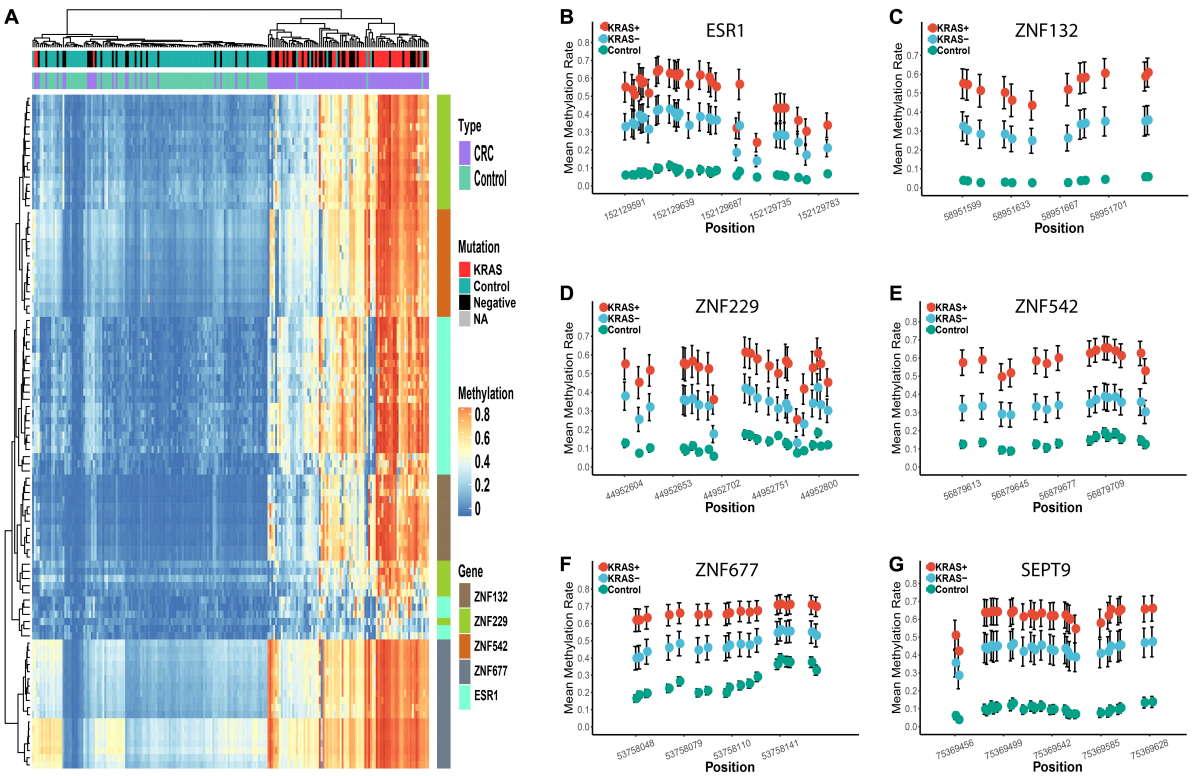

FIGURE 5 | Differential methylation profiles of these candidate biomarkers in KRAS + and KRAS- subgroup in replication cohort 2. Panel **(A)** represents the heatmap of the methylation levels of these five candidate genes. The tumor and para-tumors were differently colored. The KRAS mutation status of the CRC tumors is also differently colored. Panels **(B–G)** represents the methylation profiles of the five zinc finger genes and SEPT9. The mean methylation percentage of each CpG site is shown for KRAS +, KRAS- and control groups.

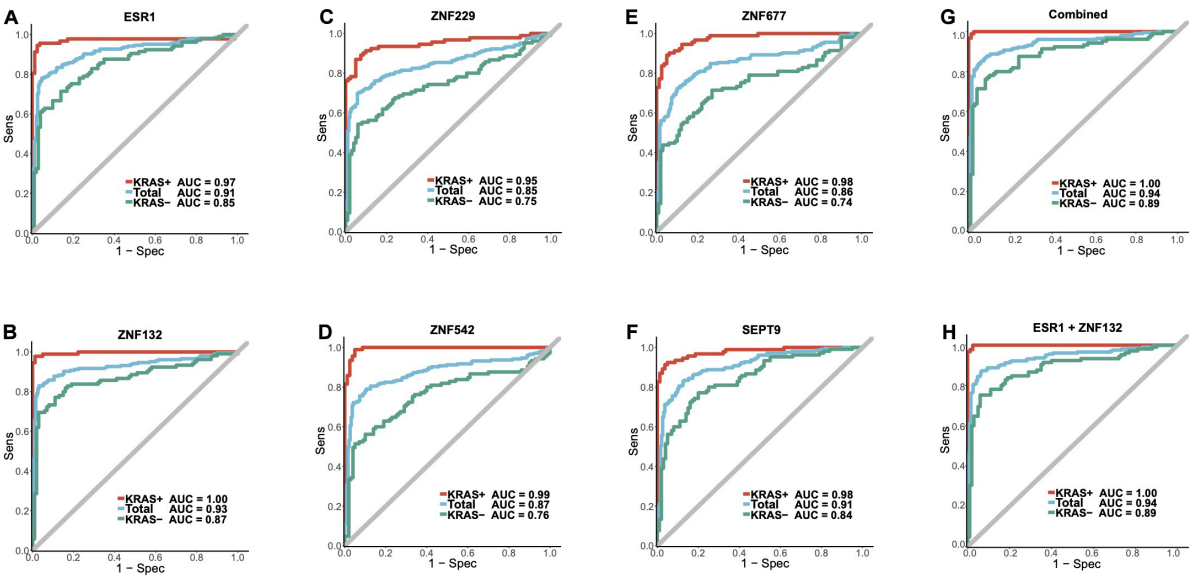

FIGURE 6 | The diagnostic abilities for the candidate biomarkers and ZFGx model in the combined replication cohort. Panels **(A–F)** represents the diagnostic ability of *ESR1*, *ZNF132*, *ZNF229*, *ZNF542*, *ZNF677*, *SEPT9* individually. Panel **(G)** represents the ROC curve of the diagnostic model using all five candidate zinc finger genes (*ESR1*, *ZNF132*, *ZNF229*, *ZNF542*, *ZNF677*). Panel **(H)** represents the ROC curve of the ZFGx model using only *ESR1* and *ZNF132* as variables. The diagnostic ability of each model for the overall samples, KRAS + and KRAS- subgroups are shown.

TABLE 2 | The mean methylation status of the five genomic regions in the KRAS + and KRAS- samples of replication cohort 1 and cohort 2.

	Genomic Region[a]	Gene[b]	McaM[c]	McoM[c]	*P* value[d]	FDR	OR	95% CI[e]	Sens[f]	Spec[f]	AUC[f]
KRAS +	6:152129591-152129791	*ESR1*	0.49	0.06	8.00×10^{-27}	9.60×10^{-27}	11.00	7.53–15.60	0.96	0.98	0.97
	19:58951599-58951728	*ZNF132*	0.51	0.03	2.10×10^{-29}	1.20×10^{-28}	29.00	17.6–47.90	0.98	0.99	1.00
	19:44952604-44952808	*ZNF229*	0.47	0.11	1.70×10^{-24}	1.70×10^{-24}	10.20	7.19–14.00	0.90	0.93	0.95
	19:56879613-56879735	*ZNF542*	0.57	0.13	4.00×10^{-29}	1.20×10^{-28}	14.30	9.60–21.50	0.99	0.95	0.99
	19:53758048-53758164	*ZNF677*	0.63	0.25	3.40×10^{-27}	5.10×10^{-27}	10.90	7.64–15.30	0.90	0.95	0.98
	17:75369456-75369630	*SEPT-9*	0.58	0.08	2.40×10^{-27}	4.70×10^{-27}	7.85	5.55–11.00	0.91	0.96	0.98
KRAS-	6:152129591-152129791	*ESR1*	0.31	0.08	2.60×10^{-18}	7.90×10^{-18}	4.63	3.21–6.39	0.75	0.83	0.85
	19:58951599-58951728	*ZNF132*	0.28	0.04	1.30×10^{-19}	7.70×10^{-19}	6.10	4.09–8.73	0.70	0.97	0.87
	19:44952604-44952808	*ZNF229*	0.29	0.12	6.90×10^{-10}	8.20×10^{-10}	3.30	2.20–4.60	0.54	0.94	0.75
	19:56879613-56879735	*ZNF542*	0.33	0.15	1.50×10^{-10}	2.30×10^{-10}	2.78	1.87–3.84	0.50	0.96	0.76
	19:53758048-53758164	*ZNF677*	0.46	0.27	1.80×10^{-09}	1.80×10^{-09}	2.38	1.62–3.25	0.71	0.73	0.74
	17:75369456-75369630	*SEPT-9*	0.41	0.11	2.30×10^{-17}	4.70×10^{-17}	2.94	2.11–3.92	0.77	0.80	0.84
Total	6:152129591-152129791	*ESR1*	0.39	0.07	1.20×10^{-45}	3.50×10^{-45}	6.06	4.81–7.52	0.78	0.95	0.91
	19:58951599-58951728	*ZNF132*	0.39	0.04	6.30×10^{-49}	3.80×10^{-48}	8.67	6.60–11.20	0.83	0.97	0.93
	19:44952604-44952808	*ZNF229*	0.37	0.11	3.50×10^{-33}	3.50×10^{-33}	5.04	3.99–6.24	0.70	0.94	0.85
	19:56879613-56879735	*ZNF542*	0.44	0.14	1.00×10^{-37}	1.50×10^{-37}	4.42	3.56–5.39	0.79	0.90	0.87
	19:53758048-53758164	*ZNF677*	0.54	0.26	1.60×10^{-34}	1.90×10^{-34}	3.85	3.11–4.67	0.73	0.90	0.86
	17:75369456-75369630	*SEPT-9*	0.49	0.10	5.50×10^{-45}	1.10×10^{-45}	4.02	3.27–4.02	0.83	0.87	0.91

[a] *Genomic region represents the genomic coverage of the reads with targeted bisulfite sequencing, and the genomic coordinates shown here is based on the hg19 version of the genome.*

[b] *The gene name of the genomic region.*

[c] *McaM represents the mean methylation percentage of the cases in each region, which consisting of several CpG sites, while the McoM represents the mean methylation percentage of the controls in each region.*

[d] *P value is calculated through the wilcoxon rank-sum test following with FDR (false discovery rate) adjustment for multiple corrections.*

[e] *OR and 95% CI were conducted through logistic regression.*

[e] *Sens, sensitivity; while Spec, specificity; AUC, area under curve.*

[f] *The sensitivity, specificity, and the AUC were calculated through a logistic regression prediction model without adjustment for gender, age and smoking status and alcohol status.*

SEPT9 (sensitivity = 0.83, specificity = 0.87, AUC = 0.91). In addition, *ESR1* also achieved comparable diagnostic capability (sensitivity = 0.78, specificity = 0.97, AUC = 0.91) to *SETP9* (**Table 2**), suggesting that these two genes have great potential in the liquid biopsy of CRC. Simultaneously, we assessed the diagnostic abilities of these ZFGs in the KRAS + subgroups and KRAS- group using all samples. Concordantly, all candidate biomarkers achieved better performance (AUC $\geq$ 0.95) in the KRAS + group than that in the KRAS- group, further indicating that KRAS- CRC patients are more epigenetically homogeneous.

To further improve the robustness of the diagnostic abilities of these ZFGs, we performed multiple machine-learning algorithms following the fivefold cross-validation method, which split the dataset into training and validation dataset randomly to obtain an unbiased estimation (see section "Materials and Methods," **Supplementary Table 13**). As shown in **Supplementary Table 13**, the random forest (RF) model achieved the best accuracy (accuracy = 0.89) in the test dataset. In the KRAS + subgroup, the Naïve Bayes algorithm performed best on the test dataset (sensitivity = 0.99, specificity = 0.97, accuracy = 0.98), while the Neural Network model had the best performance in the KRAS- subgroup (sensitivity = 0.75, specificity = 0.89, accuracy = 0.82). Therefore, we suggested that the diagnostic abilities of these ZFGs are reliable for CRC diagnosis in test dataset.

DISCUSSION

To our knowledge, few studies have extensively explored the methylation alterations of ZFGs in CRC. Herein, we integrated datasets from TCGA and GEO databases to identify robust and statistically powerful biomarkers. In total, we identified five hyper-methylated ZFGs as candidate biomarkers and validated them using Han Chinese CRC patients. Two ZFGs, *ZNF132,* and *ESR1,* were recognized as promising diagnostic biomarkers for CRC. Moreover, we found significantly higher diagnostic abilities of these ZFGs in the KRAS + group than the KRAS- group, suggesting the significant association between somatic mutations and DNA methylation alterations. Our results highlighted the importance of combining genetic mutations and epigenetic alterations for CRC diagnosis in further studies.

The interaction between genetic mutations and epigenetic alterations in the tumorigenesis of CRC has been reported previously. Gazin et al. (2007) performed a genome-wide RNA interference (RNAi) screening of K-ras-transformed NIH 3T3 cells and identified 28 genes that are required for Ras-mediated epigenetic silencing of the pro-apoptotic Fas gene. It was suggested that Ras-mediated epigenetic silencing could lead to CRC oncogenesis through the epigenetic inactivation of key genes. Nagasaka et al. also found that both *KRAS* and *BRAF* mutation could contribute to the global hypermethylation

phenotype of CIMP genes in colon cancer. Furthermore, Serra et al. (2014) revealed that *KRAS* mutation could result in the hypermethylation and transcriptional silencing of CIMP genes through *ZNF304*, indicating the importance of ZFPs in the carcinogenesis of CRC. In our study, the methylation profiles of the five ZFGs were significantly associated with the *KRAS* mutation status, suggesting that *KRAS* mutation may alter the downstream pathways through the epigenetic regulation of these ZFGs and required further verification.

Among the five ZFGs, *ZNF132* was identified as the most promising biomarker for CRC diagnosis in our analysis. *ZNF132* is located at 19q13.4 and belongs to the C2H2 ZFP family (Tommerup and Vissing, 1995). Previous studies have identified the DNA methylation alterations of *ZNF132* in breast cancer, esophageal squamous cell carcinoma (ESCC), oropharyngeal squamous cell carcinoma, and prostate cancer (Lleras et al., 2011; Abildgaard et al., 2012; Stefansson et al., 2015; Jiang et al., 2018). It is reported that *ZNF132* hypermethylation could reduce the Sp1 transcript factor activity and decrease the growth, migration, invasion, and tumorigenicity capabilities of cells in a nude mouse model of ESCC (Jiang et al., 2018). Our study identified the hypermethylation and down-regulation of *ZNF132* in CRC, especially in KRAS-mutated samples, suggesting its biological implications in CRC tumorigenesis.

ESR1 (estrogen receptor alpha 1) has been recognized as a tumor-suppressor gene and an estrogen receptor gene. It encodes the main mediator of estrogen effects in breast epithelial cells and has also been shown to be activated by epidermal growth factor (EGF). The hyper-methylation status of *ESR1* has been reported previously in lung adenocarcinoma, breast cancer, prostate cancer, squamous cell cervical cancer, and CRC (Li et al., 2004; Lin et al., 2009; Kim et al., 2010; Elliott et al., 2013; Kirn et al., 2014; Martinez-Galan et al., 2014). *ESR1* hypermethylation is also correlated with poor prognosis and drug response in breast cancer (Ramos et al., 2010; Mastoraki et al., 2018). Additionally, the *ESR1* promoter hypermethylation has been associated with KRAS mutation, which is consistent with our results (Horii et al., 2009).

ZNF229 is a protein-coding gene, and few studies have suggested the hypermethylation status of *ZNF229* in cancer diagnosis. The biological functions and their role in CRC tumorigenesis should be explored further. *ZNF542* may involve in the epigenetic regulation of puberty through transcriptional repression (Lomniczi et al., 2015). Moreover, a CpG site located at *ZNF542* has been found to be a promising biomarker for ESCC (Pu et al., 2017). A pan-cancer study revealed that *ZNF542* was significantly hypermethylated in 10 kinds of cancers (Gevaert et al., 2015). *ZNF677* is located at chromosomal region 19q13 and was found to regulate the putative tumor cell growth suppressor in non-small cell lung cancers through hypermethylation (Heller et al., 2015). In addition, *ZNF677* is frequently down-regulated by promoter methylation in primary papillary thyroid cancers (PTC), and the decreased expression of *ZNF677* is significantly correlated with poor survival (Li et al., 2018).

Currently, most CRC patients are still diagnosed at later stages, especially in developing countries, and there is an urgent need for better diagnostic biomarkers. DNA methylation alterations may occur before mRNA and protein changes and could thus be ideal for early diagnosis. *SEPT9* has been approved as a DNA methylation-based diagnostic biomarker for CRC. The first release of the cfDNA *SEPT9* DNA methylation assay achieved considerable sensitivity (72%) and specificity (86%) in CRC detection using plasma (deVos et al., 2009). Since then, an updated version of the assay (Epi proColon 2.0) has shown better sensitivities (68–95%) and specificities (80–99%) in CRC diagnosis (Payne, 2010). However, the significant heterogeneity of CRC makes it challenging to use a single DNA methylation-based biomarker to diagnose CRC accurately. Therefore, the present study showed that *ZNF132* and *ESR1* have comparable or even better diagnostic capability than *SEPT9*, suggesting that the panel integrating *ZNF132, ESR1, and SEPT9* may better serve as a robust non-invasive diagnostic tool for CRC. In addition, the diagnostic ability of our model and the *SEPT9* model were both significantly affected by the KRAS mutation status in patients, and none of them achieved satisfactory sensitivities and specificities in the diagnosis of KRAS- CRC patients, suggesting that the mutation landscape of the patients should be taken into account to diagnose CRC accurately.

We acknowledge that our study has several limitations. First, our study's sample size and patient diversity are limited, and studies with larger sample size and diverse populations are required to identify better CRC diagnostic markers. Second, we identified the candidate ZFGs by analyzing public DNA methylation datasets using Illumina HumanMethylation 450K microarray, which only covered a small proportion of the genome while a large amount of the genome remains undetected. Further studies using whole-genome bisulfite sequencing may be required to identify better DNA methylation-based biomarkers for CRC. Finally, our study only detected the methylation profiles of these ZFGs in tumor or para-tumor tissues, while the efficacy of these ZFGs for CRC non-invasive diagnosis using plasma or stool is elusive. We will try to validate the diagnostic abilities of these ZFGs in our future studies.

MATERIALS AND METHODS

Integration of Public Datasets and Biomarker Discovery

Public high-throughput DNA methylation microarray datasets (Illumina HumanMethylation 450K) were searched exhaustively from TCGA and GEO databases. Two datasets from TCGA and nine datasets from GEO were included, yielding a total of 1,104 CRC tumor samples, 268 control samples, and 54 adenoma samples (**Supplementary Table 1**). The comprehensive list of genes in the zinc finger family (n = 1,594) was obtained from HGNC (**Supplementary Table 2**).

As shown in a previous study, the methylation linkage equilibrium decreased significantly when the block was longer than 1,000 bp (Guo et al., 2017a). Therefore, we defined the methylation region (MR) to have at least 6 CpG sites with less than 1,000 bp. We then arranged all the CpG sites in the high-throughput microarray according to their genomic coordinates and applied the sliding window method to identify

all MRs. In total, we identified 6,166 MRs and performed differential methylation analyses (**Supplementary Table 14**). The 85 DMRs (McaM > 0.50, MadM > 0.50 and McoM < 0.30) were found for further analysis. To correct the noise from DNA originating from mixed-in peripheral blood, we suggested that the methylation rate of the DMRs need to be extremely low in the peripheral blood. Thus, we integrated the public high-throughput microarray datasets of the whole blood (WB, $n = 1438$), peripheral blood mononuclear cells (PBMC, $n = 111$), and peripheral blood leukocytes (PBL, $n = 529$) as references for DMR identification (**Supplementary Table 15**). The 32 DMRs were retained due to their low methylation rates in WB, PBMC, or PBL (mean methylation rate < 0.10).

Several DMRs were located at the same gene, and we selected the DMR with the most significant differences between CRC and control tissues for each gene ($N = 10$). To obtain the DMRs that may regulate the expression of neighboring genes, we further selected the DMRs with transcription factor binding sites (TFBSs) that correlate significantly with the expression of neighboring genes (**Supplementary Tables 16, 17**). In total, seven out of the ten candidate DMRs were selected for validation. However, due to the difficulties in the primer design due to CG percent, PolyT, and the number of SNPs, two candidate DMRs were removed (*SALL1* and *ZSCAN23*). Finally, we obtained the top five candidate DMRs for further validation (*ESR1*, *ZNF132*, *ZNF229*, *ZNF542,* and *ZNF677*).

Patients, Samples, and DNA

Colorectal cancer patients in both replication cohort 1 and cohort 2 were recruited from the Affiliated Hospital of Nantong University between 2016 and 2018. The earlier recruited samples ($N = 104$) were included in replication cohort 1, while the others belonged to replication cohort 2. The recruited patients with available CRC tumors and matched para-tumors (the corresponding adjacent normal tissue at least 5 cm distant from the tumor tissue) were selected in this study. The patients recruited had not been treated with any neoadjuvant therapy before. Tumors were classified according to TNM (Tumor Node Metastasis)/UICC (Union for International Cancer Control) criteria following the histopathological examination. At least two professional pathologists evaluated all tumor samples carefully. All procedures performed in this study were in accordance with the ethical standards of the institutional research committee, as well as the 1964 Declaration of Helsinki and its later amendments. The study was approved by the institutional review boards of the Affiliated Hospital of Nantong University. Written informed consent was obtained from each participant of the study. All tumors and para-tumors were immediately frozen at −80°C after surgical resection.

Targeted Bisulfite Sequencing Assay and Detection of *KRAS*, *NRAS*, and *BRAF* Mutation Status

DNA extraction was performed using the AIIperp DNA/RNA Mini Kit (Qiagen, Duesseldorf, Germany) according to the manufacturer's protocols. The EpiTect Fast DNA Bisulfite Kit (Qiagen, Duesseldorf, Germany) was further used for bisulfite conversion. After carefully evaluating CG percent, PolyT, and the occurrence of SNPs in the targeted regions of the candidate DMRs, we designed primers to detect them in a panel for NGS sequencing (**Supplementary Table 18**). The PCR amplicons were then diluted and amplified using these primers, and the products (170–270 bp) were further separated and purified by QIAquick Gel Extraction kit (Qiagen, Duesseldorf, Germany). Finally, the sequencing libraries from different samples were pooled together and sequenced using the Illumina Hiseq 2000 platform according to the manufacturer's protocols.

The BSseeker2 was applied for read mapping and methylation calling. After that, we removed the samples with a bisulfite conversion rate < 98%. The methylation level of each CpG site for each sample has been provided in **Supplementary Tables 19,20**. The average coverage and missing rate for each CpG site were calculated and utilized for quality control (average coverage > 20X, missing rate < 20%). In addition, the sample whose missing rate > 30% were also filtered out. FastTarget next-generation sequencing was used to detect tumor DNA for the mutations in codons 12, 13, 59, 61, 117, and 146 of the *KRAS* and *NRAS* genes, as well as the mutation in codon 600 of the *BRAF* gene (Liao et al., 2019).

Statistical Analysis and Machine Learning Methods

The Wilcoxon rank-sum test was performed in the discovery stage to identify the differential methylation sites and regions between CRC tumors, adenomas, and para-tumors. Moreover, the differential methylation status (odds ratios) between tumors and para-tumors of the DMRs were calculated with logistic regression. Benjamini-Hochburg correction was utilized for multiple test correction.

To identify the factors that may affect the diagnostic abilities of these ZFGs in CRC, we first split the dataset based on these covariates, including young (age ≤ median age) vs. old (age > median age), male vs. female, early (Stage I/II) vs. late (Stage III/IV), colon vs. rectum and KRAS + vs. KRAS- subgroups. Second, we performed the univariate logistic regression model using each gene in these subgroups separately. The cut-off value was determined as the value which maximized the sum of both sensitivity and specificity of the model. After that, the predicted sample type for each sample was obtained, and was used to calculate the number of accurate predictions (true positive + true negative) and inaccurate predictions (false positive + false negative) of the logistic model. Finally, we utilized the Fisher exact test to explore if there are significant differences between the prediction outcomes between these subgroups.

To further give an unbiased estimation of the diagnostic ability of these ZFGs, we performed fivefold cross-validation of our dataset using the logistic regression (Package stats), support vector machine (SVM, Package e1071), random forest (Package randomForest), Naïve Bayes (Package e1071), neural network (Package nnet), linear discriminant analysis (LDA, Package mda),

mixture discriminant analysis (MDA, Package mda), flexible discriminant analysis (FDA, Package mda), gradient boosting machine (Package gbm), catboost (Package catboost), and XGBoost (Package xgboost) methods. We randomly selected 80% of our samples as the training dataset, and the remaining 20% of samples were used as the test dataset. After that, we optimized these machine learning methods using the training dataset and validate these optimized models in the test dataset. We repeated these procedures 1,000 times, and obtained the sensitivities, specificities and accuracies for both training and test datasets. The averaged sensitivities, specificities and accuracies for both training and test datasets were calculated and shown in **Supplementary Table 13**. All statistical analyses were conducted using R (v3.4.3).

DATA AVAILABILITY STATEMENT

Datasets related to this article can be found at Zenodo (doi: 10.5281/zenodo.5214274) and in **Supplementary Tables 19, 20**. The analysis steps, functions, and parameters used are described in detail in section "Materials and Methods". The custom R scripts used to analyze data and generate figures are available at a GitHub repository: https://github.com/puweilin/CRC_MethylationAnalysis.git.

ETHICS STATEMENT

The studies involving human participants were reviewed and approved by the institutional review boards of the Affiliated Hospital of Nantong University. The patients/participants provided their written informed consent to participate in this study.

AUTHOR CONTRIBUTIONS

WD, WP, SG, YM, and SJ contributed to the conception and design of the study. WD, FQ, KS, FX, QJ, SJ, RZ, JZ, JFZ, and SQJ collected the samples of the study. FQ, WD, and SQJ performed the experiments of this study. WP, WD, FQ, JL, YM, and SJ performed the statistical analysis. WP and WD wrote the first draft of the manuscript. SJ, YM, and SG revised the manuscript. All authors contributed to manuscript revision, read, and approved the submitted version.

FUNDING

This study was supported by the National Natural Science Foundation of China (81974313 and 82003360), Postdoctoral Science Foundation of China (2018M641919 and 2019M651930), the Natural Science Foundation of Jiangsu Commission of Health (M2020065), the Natural Science Foundation of Higher Education of Jiangsu Province (20KJB320001), and Nantong People's Livelihood Science and Technology Plan (MS12018032 and JC2019066).

SUPPLEMENTARY MATERIAL

The Supplementary Material for this article can be found online at: https://www.frontiersin.org/articles/10.3389/fcell.2021.759813/full#supplementary-material

Supplementary Figure 1 | The Mean methylation rate of the candidate zinc finger genes in the CRC tumors, adenomas and control tissues. The y-axis represents the mean methylation percentage in the CRC tumor tissues and paired normal tissues for each CpG site. The error bar of each CpG site represents the confidence interval of the methylation percentage.

Supplementary Figure 2 | Bisulfite conversion rate and mapping rate between CRC tumors and para-tumors. Panels **(A,B)** represent the bisulfite conversion rate and the reads mapping rate of the samples in replication cohort 1, respectively.

Supplementary Figure 3 | Principal Component Analysis of the methylation profiles of the samples in replication cohort 1. All of the CpG sites were preprocessed and simplified into the two-variable space through principal component analysis. The green and red dots represented the CRC tumors and paired controls in replication cohort 1.

Supplementary Figure 4 | Boxplot of the methylation rate of the KRAS +, KRAS- and control samples in replication cohort 1. The mean methylation rate of all the CpG sites in each candidate gene of each sample was depicted as one dot in the boxplot.

Supplementary Figure 5 | Bisulfite conversion rate and mapping rate between CRC tumors and para-tumors. Panels **(A,B)** represent the bisulfite conversion rate and the reads mapping rate of the samples in replication cohort 2, respectively.

Supplementary Figure 6 | Principal Component Analysis of the methylation profiles of the samples in replication cohort 1. All of the CpG sites were preprocessed and simplified into the two-variable space through principal component analysis. The green and red dots represented the CRC tumors and paired controls in replication cohort 2.

Supplementary Figure 7 | Boxplot of the methylation rate of the KRAS +, KRAS- and control samples in replication cohort 2. The mean methylation rate of all the CpG sites in each candidate gene of each sample was depicted as one dot in the boxplot.

REFERENCES

Abildgaard, M. O., Borre, M., Mortensen, M. M., Ulhoi, B. P., Torring, N., Wild, P., et al. (2012). Downregulation of zinc finger protein 132 in prostate cancer is associated with aberrant promoter hypermethylation and poor prognosis. *Int. J. Cancer* 130, 885–895. doi: 10.1002/ijc.26097

Ahlquist, D. A., Taylor, W. R., Mahoney, D. W., Zou, H., Domanico, M., Thibodeau, S. N., et al. (2012). The stool DNA test is more accurate than the plasma septin 9 test in detecting colorectal neoplasia. *Clin. Gastroenterol. Hepatol.* 10, 272–277. doi: 10.1016/j.cgh.2011.10.008

Barault, L., Amatu, A., Siravegna, G., Ponzetti, A., Moran, S., Cassingena, A., et al. (2018). Discovery of methylated circulating DNA biomarkers for comprehensive non-invasive monitoring of treatment response in metastatic colorectal cancer. *Gut* 67, 1995–2005. doi: 10.1136/gutjnl-2016-313372

Church, T. R., Wandell, M., Lofton-Day, C., Mongin, S. J., Burger, M., Payne, S. R., et al. (2014). Prospective evaluation of methylated SEPT9 in plasma for detection of asymptomatic colorectal cancer. *Gut* 63, 317–325. doi: 10.1136/gutjnl-2012-304149

deVos, T., Tetzner, R., Model, F., Weiss, G., Schuster, M., Distler, J., et al. (2009). Circulating methylated SEPT9 DNA in plasma is a biomarker for

colorectal cancer. *Clin. Chem.* 55, 1337–1346. doi: 10.1373/clinchem.2008.115808

Ding, W., Pu, W., Wang, L., Jiang, S., Zhou, X., Tu, W., et al. (2018). Genome-wide DNA methylation analysis in systemic sclerosis reveals hypomethylation of IFN-Associated Genes in CD4(+) and CD8(+) T Cells. *J. Invest. Dermatol.* 138, 1069–1077. doi: 10.1016/j.jid.2017.12.003

Elliott, G. O., Johnson, I. T., Scarll, J., Dainty, J., Williams, E. A., Garg, D., et al. (2013). Quantitative profiling of CpG island methylation in human stool for colorectal cancer detection. *Int. J. Colorectal. Dis.* 28, 35–42. doi: 10.1007/s00384-012-1532-5

Freitas, M., Ferreira, F., Carvalho, S., Silva, F., Lopes, P., Antunes, L., et al. (2018). A novel DNA methylation panel accurately detects colorectal cancer independently of molecular pathway. *J. Transl. Med.* 16:45. doi: 10.1186/s12967-018-1415-9

Gazin, C., Wajapeyee, N., Gobeil, S., Virbasius, C. M., and Green, M. R. (2007). An elaborate pathway required for Ras-mediated epigenetic silencing. *Nature* 449, 1073–1077. doi: 10.1038/nature06251

Gevaert, O., Tibshirani, R., and Plevritis, S. K. (2015). Pancancer analysis of DNA methylation-driven genes using MethylMix. *Genome Biol.* 16:17. doi: 10.1186/s13059-014-0579-8

Guo, S., Diep, D., Plongthongkum, N., Fung, H. L., Zhang, K., and Zhang, K. (2017a). Identification of methylation haplotype blocks aids in deconvolution of heterogeneous tissue samples and tumor tissue-of-origin mapping from plasma DNA. *Nat. Genet.* 49, 635–642. doi: 10.1038/ng.3805

Guo, S., Zhu, Q., Jiang, T., Wang, R., Shen, Y., Zhu, X., et al. (2017b). Genome-wide DNA methylation patterns in CD4+ T cells from Chinese Han patients with rheumatoid arthritis. *Mod. Rheumatol.* 27, 441–447. doi: 10.1080/14397595.2016.1218595

Guo, S., Yan, F., Xu, J., Bao, Y., Zhu, J., Wang, X., et al. (2015). Identification and validation of the methylation biomarkers of non-small cell lung cancer (NSCLC). *Clin. Epigenetics* 7:3. doi: 10.1186/s13148-014-0035-3

He, Y., Cui, Y., Wang, W., Gu, J., Guo, S., Ma, K., et al. (2011). Hypomethylation of the hsa-miR-191 locus causes high expression of hsa-mir-191 and promotes the epithelial-to-mesenchymal transition in hepatocellular carcinoma. *Neoplasia* 13, 841–853. doi: 10.1593/neo.11698

Heller, G., Altenberger, C., Schmid, B., Marhold, M., Tomasich, E., Ziegler, B., et al. (2015). DNA methylation transcriptionally regulates the putative tumor cell growth suppressor ZNF677 in non-small cell lung cancers. *Oncotarget* 6, 394–408. doi: 10.18632/oncotarget.2697

Horii, J., Hiraoka, S., Kato, J., Saito, S., Harada, K., Fujita, H., et al. (2009). Methylation of estrogen receptor 1 in colorectal adenomas is not age-dependent, but is correlated with K-ras mutation. *Cancer Sci.* 100, 1005–1011. doi: 10.1111/j.1349-7006.2009.01140.x

Jen, J., and Wang, Y. C. (2016). Zinc finger proteins in cancer progression. *J. Biomed. Sci.* 23:53. doi: 10.1186/s12929-016-0269-9

Jiang, D., He, Z., Wang, C., Zhou, Y., Li, F., Pu, W., et al. (2018). Epigenetic silencing of ZNF132 mediated by methylation-sensitive Sp1 binding promotes cancer progression in esophageal squamous cell carcinoma. *Cell Death Dis.* 10:1. doi: 10.1038/s41419-018-1236-z

Kim, M. S., Lee, J., and Sidransky, D. (2010). DNA methylation markers in colorectal cancer. *Cancer Metastasis Rev.* 29, 181–206. doi: 10.1007/s10555-010-9207-6

Kirn, V., Zaharieva, I., Heublein, S., Thangarajah, F., Friese, K., Mayr, D., et al. (2014). ESR1 promoter methylation in squamous cell cervical cancer. *Anticancer Res.* 34, 723–727.

Koch, A., Joosten, S. C., Feng, Z., de Ruijter, T. C., Draht, M. X., Melotte, V., et al. (2018). Analysis of DNA methylation in cancer: location revisited (vol 15, pg 459, 2018). *Nat. Rev. Clin. Oncol.* 15, 467–467. doi: 10.1038/s41571-018-0028-9

Li, L. C., Shiina, H., Deguchi, M., Zhao, H., Okino, S. T., Kane, C. J., et al. (2004). Age-dependent methylation of ESR1 gene in prostate cancer. *Biochem. Biophys. Res. Commun.* 321, 455–461. doi: 10.1016/j.bbrc.2004.06.164

Li, Y., Yang, Q., Guan, H., Shi, B., Ji, M., and Hou, P. (2018). ZNF677 suppresses Akt phosphorylation and tumorigenesis in thyroid cancer. *Cancer Res.* 78, 5216–5228. doi: 10.1158/0008-5472.CAN-18-0003

Liao, X., Zhang, T., Li, B., Hu, S., Liu, J., Deng, J., et al. (2019). Rare RNF213 variants and the risk of intracranial artery stenosis/occlusion disease in Chinese population: a case-control study. *BMC Med. Genet.* 20:55. doi: 10.1186/s12881-019-0788-9

Lin, Q., Geng, J., Ma, K., Yu, J., Sun, J., Shen, Z., et al. (2009). RASSF1A, APC, ESR1, ABCB1 and HOXC9, but not p16INK4A, DAPK1, PTEN and MT1G genes were frequently methylated in the stage I non-small cell lung cancer in China. *J. Cancer Res. Clin. Oncol.* 135, 1675–1684. doi: 10.1007/s00432-009-0614-4

Lleras, R. A., Adrien, L. R., Smith, R. V., Brown, B., Jivraj, N., Keller, C., et al. (2011). Hypermethylation of a cluster of Kruppel-type zinc finger protein genes on chromosome 19q13 in oropharyngeal squamous cell carcinoma. *Am. J. Pathol.* 178, 1965–1974. doi: 10.1016/j.ajpath.2011.01.049

Lomniczi, A., Wright, H., Castellano, J. M., Matagne, V., Toro, C. A., Ramaswamy, S., et al. (2015). Epigenetic regulation of puberty via Zinc finger protein-mediated transcriptional repression. *Nat. Commun.* 6:10195. doi: 10.1038/ncomms10195

Martinez-Galan, J., Torres-Torres, B., Nunez, M. I., Lopez-Penalver, J., Del Moral, R., Ruiz De Almodovar, J. M., et al. (2014). ESR1 gene promoter region methylation in free circulating DNA and its correlation with estrogen receptor protein expression in tumor tissue in breast cancer patients. *BMC Cancer* 14:59. doi: 10.1186/1471-2407-14-59

Mastoraki, S., Strati, A., Tzanikou, E., Chimonidou, M., Politaki, E., Voutsina, A., et al. (2018). ESR1 Methylation: A liquid biopsy-based epigenetic assay for the follow-up of patients with metastatic breast cancer receiving endocrine treatment. *Clin. Cancer Res.* 24, 1500–1510. doi: 10.1158/1078-0432.CCR-17-1181

Payne, S. R. (2010). From discovery to the clinic: the novel DNA methylation biomarker (m)SEPT9 for the detection of colorectal cancer in blood. *Epigenomics* 2, 575–585. doi: 10.2217/epi.10.35

Pu, W., Wang, C., Chen, S., Zhao, D., Zhou, Y., Ma, Y., et al. (2017). Targeted bisulfite sequencing identified a panel of DNA methylation-based biomarkers for esophageal squamous cell carcinoma (ESCC). *Clin. Epigenetics* 9:129. doi: 10.1186/s13148-017-0430-7

Ramos, E. A., Camargo, A. A., Braun, K., Slowik, R., Cavalli, I. J., Ribeiro, E. M., et al. (2010). Simultaneous CXCL12 and ESR1 CpG island hypermethylation correlates with poor prognosis in sporadic breast cancer. *BMC Cancer* 10:23. doi: 10.1186/1471-2407-10-23

Schubeler, D. (2015). Function and information content of DNA methylation. *Nature* 517, 321–326. doi: 10.1038/nature14192

Serra, R. W., Fang, M., Park, S. M., Hutchinson, L., and Green, M. R. (2014). A KRAS-directed transcriptional silencing pathway that mediates the CpG island methylator phenotype. *Elife* 3:e02313. doi: 10.7554/eLife.02313

Siegel, R. L., Miller, K. D., Fedewa, S. A., Ahnen, D. J., Meester, R. G. S., Barzi, A., et al. (2017). Colorectal cancer statistics, 2017. *CA Cancer J. Clin.* 67, 177–193. doi: 10.3322/caac.21395

Siegel, R. L., Miller, K. D., Goding Sauer, A., Fedewa, S. A., Butterly, L. F., Anderson, J. C., et al. (2020). Colorectal cancer statistics, 2020. *CA Cancer J. Clin.* 70, 145–164. doi: 10.3322/caac.21601

Song, L., Jia, J., Peng, X., Xiao, W., and Li, Y. (2017). The performance of the SEPT9 gene methylation assay and a comparison with other CRC screening tests: A meta-analysis. *Sci. Rep.* 7:3032. doi: 10.1038/s41598-017-03321-8

Stefansson, O. A., Moran, S., Gomez, A., Sayols, S., Arribas-Jorba, C., Sandoval, J., et al. (2015). A DNA methylation-based definition of biologically distinct breast cancer subtypes. *Mol. Oncol.* 9, 555–568. doi: 10.1016/j.molonc.2014.10.012

Sun, J., Fei, F., Zhang, M., Li, Y., Zhang, X., Zhu, S., et al. (2019). The role of (m)SEPT9 in screening, diagnosis, and recurrence monitoring of colorectal cancer. *BMC Cancer* 19:450. doi: 10.1186/s12885-019-5663-8

Sung, H., Ferlay, J., Siegel, R. L., Laversanne, M., Soerjomataram, I., Jemal, A., et al. (2021). Global cancer statistics 2020: GLOBOCAN estimates of incidence and mortality worldwide for 36 cancers in 185 countries. *CA Cancer J. Clin.* 71, 209–249. doi: 10.3322/caac.21660

Tommerup, N., and Vissing, H. (1995). Isolation and fine mapping of 16 novel human zinc finger-encoding cDNAs identify putative candidate genes for developmental and malignant disorders. *Genomics* 27, 259–264. doi: 10.1006/geno.1995.1040

Wills, B., Gorse, E., and Lee, V. (2018). Role of liquid biopsies in colorectal cancer. *Curr. Probl. Cancer* 42, 593–600. doi: 10.1016/j.currproblcancer.2018.08.004

Conflict of Interest: The authors declare that the research was conducted in the absence of any commercial or financial relationships that could be construed as a potential conflict of interest.

Publisher's Note: All claims expressed in this article are solely those of the authors and do not necessarily represent those of their affiliated organizations, or those of the publisher, the editors and the reviewers. Any product that may be evaluated in this article, or claim that may be made by its manufacturer, is not guaranteed or endorsed by the publisher.

frontiers in Genetics

ORIGINAL RESEARCH
published: 01 November 2021
doi: 10.3389/fgene.2021.760744

Low APOA-1 Expression in Hepatocellular Carcinoma Patients Is Associated With DNA Methylation and Poor Overall Survival

Yingyun Guo[1†], Binglu Huang[1†], Ruixue Li[2], Jiao Li[1], Shan Tian[3], Cheng Peng[3] and Weiguo Dong[1]**

[1]Department of Gastroenterology, Renmin Hospital of Wuhan University, Wuhan, China, [2]Department of Gastroenterology, Macheng Renmin Hospital, Macheng, Huanggang, China, [3]Department of Infectious, Union Hospital, Tongji Medical College, Huazhong University of Science and Technology, Wuhan, China

OPEN ACCESS

Edited by:
Rais Ahmad Ansari, Nova Southeastern University, United States

Reviewed by:
Emily Fink, Lerner Research Institute, United States
Megan Beetch, University of Minnesota Medical School, United States

***Correspondence:**
Weiguo Dong
Ddongweiguo@163.com
Cheng Peng
questionpc2005@163.com

[†]These authors have contributed equally to this work

Specialty section:
This article was submitted to Cancer Genetics and Oncogenomics, a section of the journal Frontiers in Genetics

Received: *18 August 2021*
Accepted: *04 October 2021*
Published: *01 November 2021*

Citation:
Guo Y, Huang B, Li R, Li J, Tian S, Peng C and Dong W (2021) Low APOA-1 Expression in Hepatocellular Carcinoma Patients Is Associated With DNA Methylation and Poor Overall Survival. Front. Genet. 12:760744. doi: 10.3389/fgene.2021.760744

Background: Hepatocellular carcinoma (HCC) is the most frequent fatal malignancy, and it has a poor prognosis. Apolipoprotein 1 (APOA-1), the main protein component of high-density lipoproteins, is involved in numerous biological processes. Thus, this study was performed to detect the clinical significance of APOA-1 mRNA, APOA-1 expression, and APOA-1DNA methylation in patients with HCC.

Methods: Data mining was performed using clinical and survival data from the Cancer Genome Atlas (TCGA) and Oncomine databases. The serum concentration of APOA-1 was measured in 316 patients with HCC and 100 healthy individuals at Renmin Hospital of Wuhan University, and the intact clinical information was reviewed and determined using univariate and multivariate Cox hazard models.

Results: Bioinformatic analysis revealed that APOA-1 mRNA was present at lower levels in the serum of patients with HCC than in that of healthy individuals, and there was a strong negative correlation between levels of APOA-1 mRNA and APOA-1 DNA methylation. High expression of APOA-1 transcription correlated with better overall survival ($p = 0.003$), and APOA-1 hypermethylation correlated with progress-free survival ($p = 0.045$) in HCC sufferers. Next, the clinical data analysis demonstrated that APOA-1 protein levels in the serum were significantly lower in patients with HCC than in healthy controls. Furthermore, the expression of APOA-1 was significantly associated with some significant clinical indexes, and elevated APOA-1 expression was significantly associated with favorable (OS; HR:1.693, 95% CI: 1.194–2.401, $p = 0.003$) and better progression-free survival (PFS; HR = 1.33, 95% CI = 1.194–2.401, $p = 0.045$). Finally,

Abbreviations: APOA-1, Apolipoprotein A1; AFP, α-fetoprotein; BCLC, Barcelona Clinic Liver Cancer; BP, biological process; BC, bladder cancer; CEA, carcinoembryonic antigen; CA199, Carbohydrate antigen199; CA125, Carbohydrate antigen125; CHO, cholesterol; HDL-C, high-density lipoprotein; HCC, hepatocellular carcinoma; HBV, Hepatitis B virus; OMAPK, mitogen-activated protein kinase; NAFLD, non-alcoholic fatty liver disease; OS, Overall survival; PDAC, pancreatic ductal adenocarcinoma; PFS,Progree-free survival; ROC, receiver operating characteristics; RCT, cholesterol transport regulator; ROS, reactive oxygen species; TSGs, tumor suppressor gene.

enrichment analysis suggested that co-expressed genes of APOA-1 were involved in lipoprotein metabolism and FOXA2/3 transcription factor networks.

Conclusion: APOA-1 mRNA expression is negatively regulated by DNA methylation in HCC. Low expression of APOA-1 might be a potential risk biomarker to predict survival in patients with HCC.

Keywords: apolipoprotein A1 (APOA-1), hepatocellular carcinoma (HCC), DNA-methylation, prognosis, bioinformatic analysis

INTRODUCTION

Hepatocellular carcinoma (HCC) is the largest primary liver cancer subtype (80–90%) and one of the most common clinical malignancies (Villanueva, 2019). It has the third-highest cancer mortality rate among all malignant tumors and has limited therapeutic options (Sharma, 2020). In the past few decades, although the diagnostic methods and treatment schedules of HCC have progressed, the long-term survival of patients has not significantly improved owing to delayed diagnosis, easy metastasis, and common relapse (Tellapuri et al., 2018; Pinto Marques et al., 2020). Therefore, the search for a novel and reliable biomarker for predicting the prognosis of patients with HCC is of great importance.

Recent studies have pointed out that abnormal lipid metabolism plays an important role in tumor progression (Cine et al., 2014; Guo et al., 2019). Apolipoprotein A1 (APOA-1) is the main protein component of high-density lipoproteins; it has been reported to be involved in numerous biological processes, inhibiting the formation of tumor blood vessels and inducing tumor immune microenvironment to prevent malignant tumor development (Borgquist et al., 2016). In this regard, Gao et al. suggested that APOA-1 may be used as a potential therapeutic target for cancer treatment (Gao et al., 2011; Zamanian-Daryoush et al., 2013).

With the development of high-throughput sequencing technology, epigenetic regulation has become a research focus in recent years. One of the epigenetic regulators, DNA methylation, may disrupt the regulation of specific promoters in cancer and play a vital role in tumorigenesis (Skvortsova et al., 2019). Additionally, aberrant DNA methylation has been perceived as a biomarker of HCC (Cancer Genome Atlas Research Network et al., 2017; C.; Zhang et al., 2016). Long et al.(Long et al., 2019) established a diagnostic, prognostic, and recurrence model for distinguishing HCC, including two DNA methylation-driven genes. Hence, identification of the correlation between mRNA expression and DNA methylation will provide crucial insights into the molecular mechanisms of HCC and may offer novel research directions for individualized treatment of patients with HCC.

Several studies have explored the association between APOA-1 and survival, but the available data on APOA-1 in HCC are limited. For example, MA et al. (Ma et al., 2016) found that the concentration of serum APOA-1 is associated with tumor-free survival and overall survival (OS) in HCC after curative resection. However, no study has specifically investigated the correlation between APOA-1 transcription and APOA-1 DNA methylation. Hence, whether APOA-1 DNA methylation can affect the prognosis of patients with HCC is currently unknown. Thus, in this study based on data mining, we first attempted to investigate the association between the differential expression of APOA-1 transcription between HCC specimens and correspondingly normal tissues across all available datasets. We then also explored the prognostic role of APOA-1 mRNA and APOA-1 DNA methylation in patients with HCC in a public database. Finally, we retrospectively collected clinicopathological data of 316 patients with HCC undergoing surgical treatment and 100 healthy controls from the Renmin Hospital of Wuhan University; this data was used to explore the importance of serum APOA-1 protein in evaluating the prognosis of patients with HCC to provide new indicators for the diagnosis and prognostic assessment of HCC.

MATERIALS AND METHODS

Bioinformatics Analysis in Public Databases

To evaluate the level of APOA-1 expression across all human cancers, we examined the transcription level of APOA-1 from the Oncomine database (Tian et al., 2020) (https://www.oncomine.org/resource/login.html). Expression profiles of APOA-1 mRNA in different cancer types were further verified using the Tumor IMune Estimation Resource (TIMER) (T. Li et al., 2017). To further explore the correlation between APOA-1 mRNA expression, APOA-1 DNA methylation and OS/PFS, the corresponding clinical information of 365 patients with HCC was examined by data mining in TCGA (up to September 1, 2020) using the UCSC Xena Browser (https://xenabrowser.net) (Liang et al., 2020) (T. Liang et al., 2020). Besides, the GSE54503 microarray dataset, in current research were acquired from the Gene Expression Omnibus (GEO) database (Y. Li et al., 2018), including gene DNA-methylation profiles (66 HCC samples and 66 nontumor samples) to detect the APOA-1 DNA methylation statues in HCC tumor tissues and normal sample.

We utilized the Co-expression module from Cbioportal website (http://www.cbioportal.org/) to identify the most correlated gens with APOA-1, and we also adopted STRING (https://www.string-db.org/) to search for the Protein-Protein Interaction (PPI) network of APOA-1 in HCC. FunRich software (Benito-Martin and Peinado, 2015) was employed to take functional enrichment analysis and investigate the mechanisms related to APOA-1 expression in HCC tissues.

We considered that the differences were statistically significant in p-value < 0.05 and false discovery rate <25%.

In this analysis, the median value of APOA-1 transcription in TCGA was used to divided HCC patients into low and high APOA-1 groups. Similarly, the median value of APOA-1 DNA methylation in TCGA was set to divided HCC patients into hypomethylation and hypomethylation groups. All data were analyzed according to relevant regulations and guidelines.

Collection of Serum APOA-1 Protein of Patients with HCC and Healthy Control Individuals.

The intact clinicopathological parameters of 316 patients with HCC and 100 healthy individuals from Renmin Hospital of Wuhan University from January 2015 to January 2017 were retrospectively collected and reviewed. The criteria used to recruit patients with HCC were: 1) patients without radiotherapy, chemotherapy, or targeted therapy before enrollment; 2) patients diagnosed with HCC after histological examination; 3) patient complete clinical data available; 4) patient informed consent provided.

Individuals were excluded from the study based on 1) patients combined with other malignancies; 2) patients with metabolic diseases (history of diabetes, dyslipidemia, hyperuricemia, Non-alcoholic fatty liver disease and related Lipid modifying drug use); and 3) patients with missing information. In addition, all healthy individuals were recruited from the Health Examination Center; all had received complete health checks, and none of them had a history of malignant tumors. The study was approved by the Ethics Committee of Renmin Hospital of Wuhan University, Hubei Province (No. WDRY2019-K104). All participants provided written informed consent after the study protocol was fully explained, and this study was performed in accordance with the Helsinki Declaration.

Follow-Up

Survival analysis started from the day of surgery and consisted of the survival time. The patients were approached by telephone and outpatient follow-up. To record the survival status of the patients, follow-ups were conducted every 3 months within half a year after the operation and then every 6 months. OS was defined as the time from diagnosis to death due to any reason or the last follow-up. Progression-free survival (PFS) was calculated as the interval between the first diagnosis and the date of recurrence. The last follow-up date was December 31, 2019.

Statistical Analysis

Statistical analyses were performed using SPSS version 21.0 (IBM Corporation) and GraphPad Prism 5 (San Diego, CA) software. The experimental values for continuous variables are expressed as the mean ± standard error of the mean. The chi-squared test, Fisher's exact probability test, and Student's t-test were used to determine the significance of the differences in the data between groups. Receiver operating characteristic (ROC) analysis was used to assess the diagnostic value of APOA-1 mRNA in differentiating HCC tissues from normal tissues. Survival analyses were performed using Kaplan–Meier curves and the log-rank test. Univariate and multivariate Cox regression proportional hazards analyses were used to assess significant prognostic factors among the clinicopathological features. All p-values were determined from two-tailed tests. Differences with a p-value < 0.05 were considered to be statistically significant.

RESULTS

APOA-1 Expression in HCC and Normal Tissues

The differential expression of APOA-1 in various types of tumors and normal individuals was explored using the Oncmine database. APOA-1 was lowly expressed in HCC, lung cancer, esophageal cancer, and sarcoma and highly expressed in breast, kidney, and ovarian cancers (**Figure 1A**). Moreover, this differential expression of APOA-1 was also verified with data from the TIMER database (**Figure 1B**). The results revealed that the expression of APOA-1 is varied with different types of cancer.

The expression of APOA-1 in HCC was further analyzed in specific datasets. Next, we used related HCC datasets from the Oncomine and GEO databases to explore APOA-1 transcription in HCC and corresponding normal tissues. As shown in **Figure 2**, APOA-1 mRNA levels were significantly downregulated in HCC tissues than in normal tissues. Significant differences were observed (p < 0.001) in the Chen liver (**Figure 2A**), Roessier liver 2 (**Figure2B**), TCGA-LIHC (**Figure 2C**), GSE14520 (**Figure 2D**), GSE63898 (**Figure 2E**), and GSE6764 (**Figure 2F**) HCC datasets.

We then used ROC curves to determine the ability of circulating APOA-1 protein to discriminate between individuals with and without HCC. The result indicated that circulating APOA-1 protein was a good discriminator with good diagnostic efficiency (**Figures 3A–F**). Serum APOA-1 protein showed the highest diagnostic potential to discriminate HCC tissues from normal tissues in the GSE14520 dataset, as reflected by an area under the curve (AUC) of 0.902 (**Figure 3D**).

APOA-1 mRNA Transcription Is Negatively Regulated by DNA Methylation

A comparable heatmap (**Figure 4A**) was generated using the UCSC Xena website, which included APOA-1 mRNA expression and APOA-1 DNA methylation in the TCGA-LIHC dataset. The results demonstrated that the expression levels of APOA-1 were significantly related to DNA methylation. As illustrated in **Figure 4**, APOA-1 mRNA expression was significantly negatively regulated by DNA methylation (Spearman, r = −0.679, p < 0.0001). In addition, the association between APOA-1 mRNA expression and APOA-1 DNA methylation levels of specific CpG sites was also studied using Spearman correlation analysis (**Supplementary Table S1**). Both the heatmap and the regression analysis showed that APOA-1 mRNA expression was negatively correlated with the 15 CpG sites of APOA-1 DNA methylation (**Figure 5**). Additionally, we also mined a HCC dataset related to DNA methylation (GSE54503). As illustrated in **Supplementary Figure S1A**, we

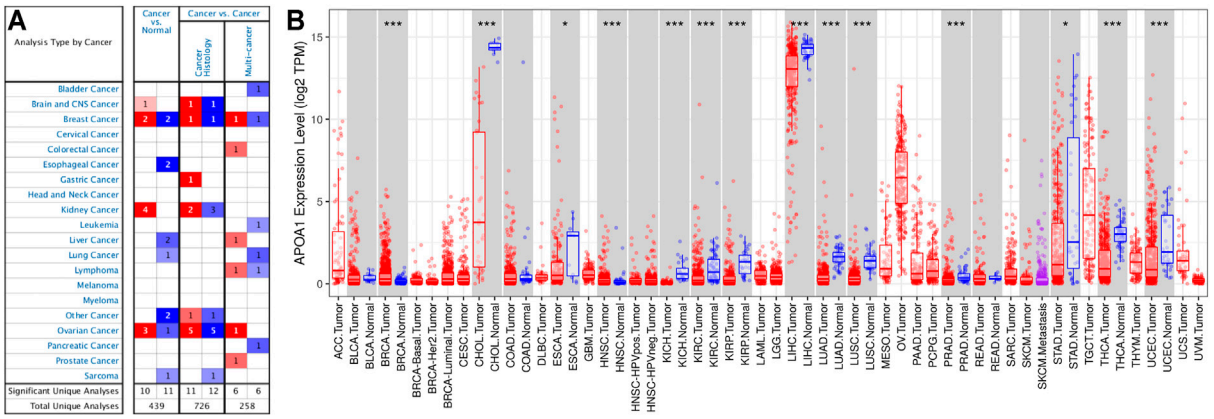

FIGURE 1 | Expression of APOA-1 in human cancers. **(A)** Disease summary for APOA-1. Red: high expression, blue: low expression. The threshold was set as follows: *p*-value < 0.05, fold change: 2, gene rank: 10%; **(B)** Bar plot of APOA-1 expression profile in various cancers and normal specimens. All data were derived from the Oncomine database and the Tumor IMune Estimation Resource (TIMER).

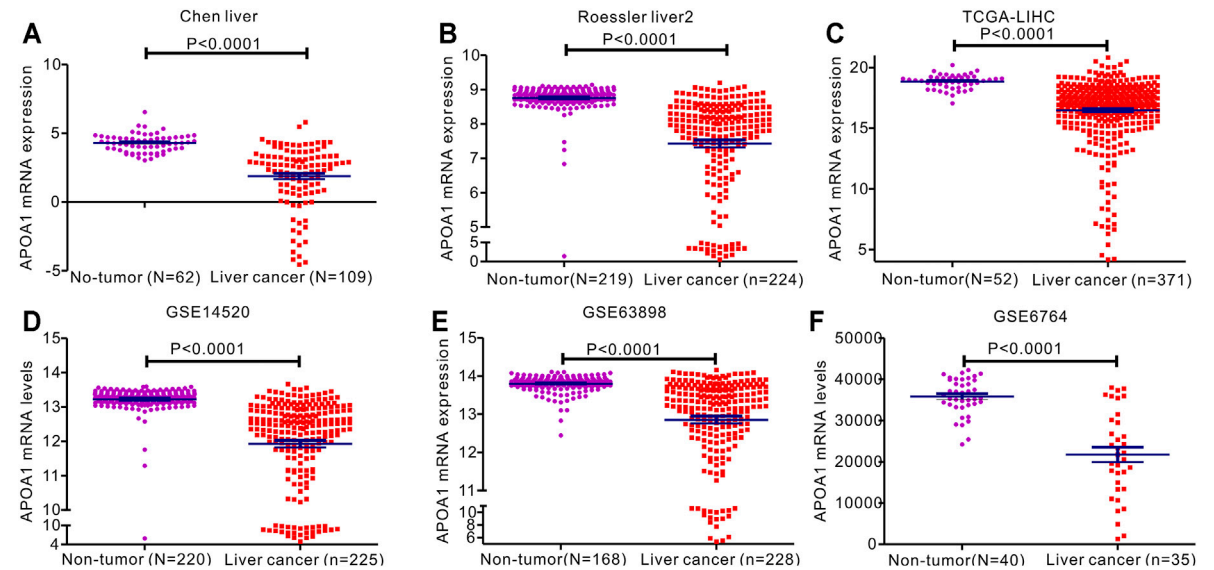

FIGURE 2 | Expression of APOA-1mRNA expression in patients with HCC. Levels of serum APOA-1 are higher in healthy controls than in patients with HCC. Differential expression of APOA-1 in **(A)** Chen liver; **(B)** Roessler liver 2; **(C)** TCGA-LIHC; **(D)** GSE14520; **(E)** GSE63898; and **(F)** GSE6764.

found that average methylation levels of APOA-1 were significantly higher in healthy individuals than in patients with HCC from TCGA dataset ($p < 0.005$). We then analyzed the GSE54503 database, and the results show average methylation levels of APOA-1 were also significantly higher in healthy individuals than in patients with HCC (**Supplementary Figure S1B,C**).

Prognostic Value of APOA-1 mRNA and DNA Methylation in Patients With HCC in TCGA Database

The associations between APOA-1 mRNA expression and clinical parameters among the 365 patients with HCC were statistically analyzed. As demonstrated in **Supplementary Table S2**, high APOA-1 mRNA levels were significantly correlated with advanced race ($p = 0.010$), α-fetoprotein (AFP) ($p < 0.001$), BMI ($p = 0.033$), and methylation status ($p < 0.001$), whereas no correlations were observed with age ($p = 0.238$), gender ($p = 0.316$), G stage ($p = 0.110$), or M stage ($p = 0.841$). The Kaplan–Meier curves were then used to explore the prognostic value of APOA-1 mRNA in the 365 patients with HCC. As illustrated in **Figure 6**, high APOA-1 mRNA expression was significantly associated with good OS ($p = 0.003$, **Figure 6A**). However, PFS showed no correlation with the level of APOA-1 mRNA expression ($p = 0.18$, **Figure 6B**). Kaplan-Meier survival analysis was used to descriptively show the association between

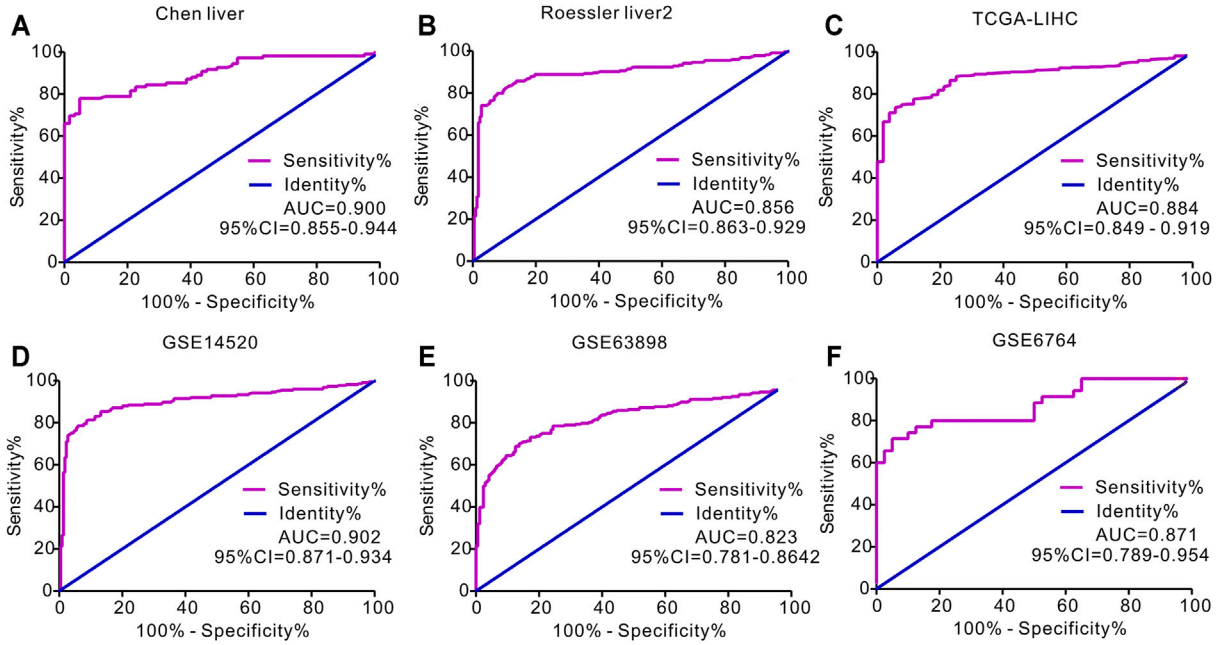

FIGURE 3 | Receiver operating characteristics (ROC) curve for APOA-1 mRNA expression in predicting HCC. ROC curve of APOA-1 in **(A)** Chen liver, **(B)** Roessler liver 2, **(C)** TCGA-LIHC, **(D)** GSE14520, **(E)** GSE63898, and **(F)** GSE6764.

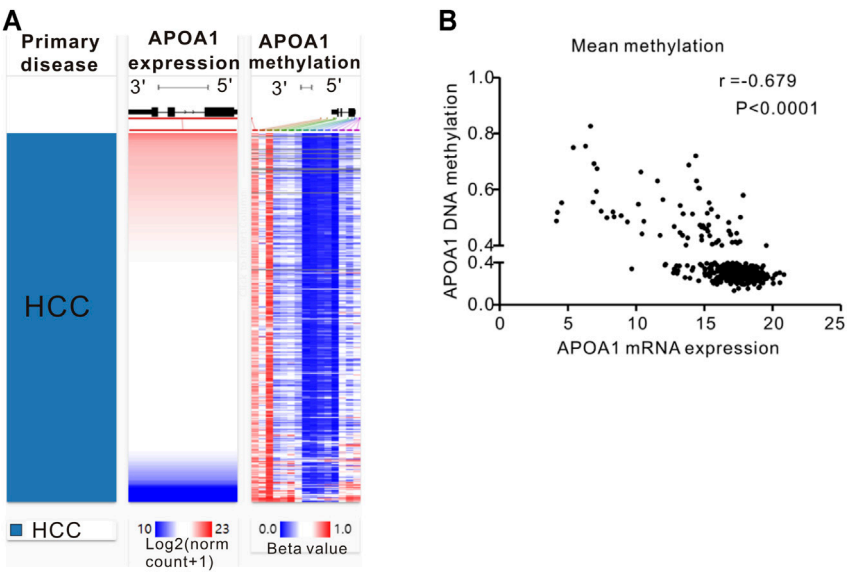

FIGURE 4 | The epigenetic mechanism underlying aberrant expression of APOA-1 in HCC revealed by bioinformatic analysis. **(A)** Heatmap of the association between expression of APOA-1 mRNA and the methylation of APOA-1 DNA CpG sites; **(B)** a negative correlation is observed between APOA-1 mRNA and APOA-1 DNA methylation.

APOA-1 mRNA and OS based on the GSE14520 dataset as validation. The results also indicate that the low APOA-1 group patients have a worse prognosis (**Supplementary Figure S2**).

Additionally, based on the 365 cases of HCC with corporate clinical information and APOA-1 methylation data, the chi-squared test or Fisher's exact test was used to assess the correlations between APOA-1 DNA methylation and clinical features. As shown in **Supplementary Table S2**, the APOA-1 DNA methylation status was influenced by race (p = 0.034), BMI ($p < 0.001$), and APOA-1 mRNA expression levels ($p < 0.001$). As exhibited in the Kaplan–Meier curves, the OS showed no correlation with low or high APOA-1 DNA

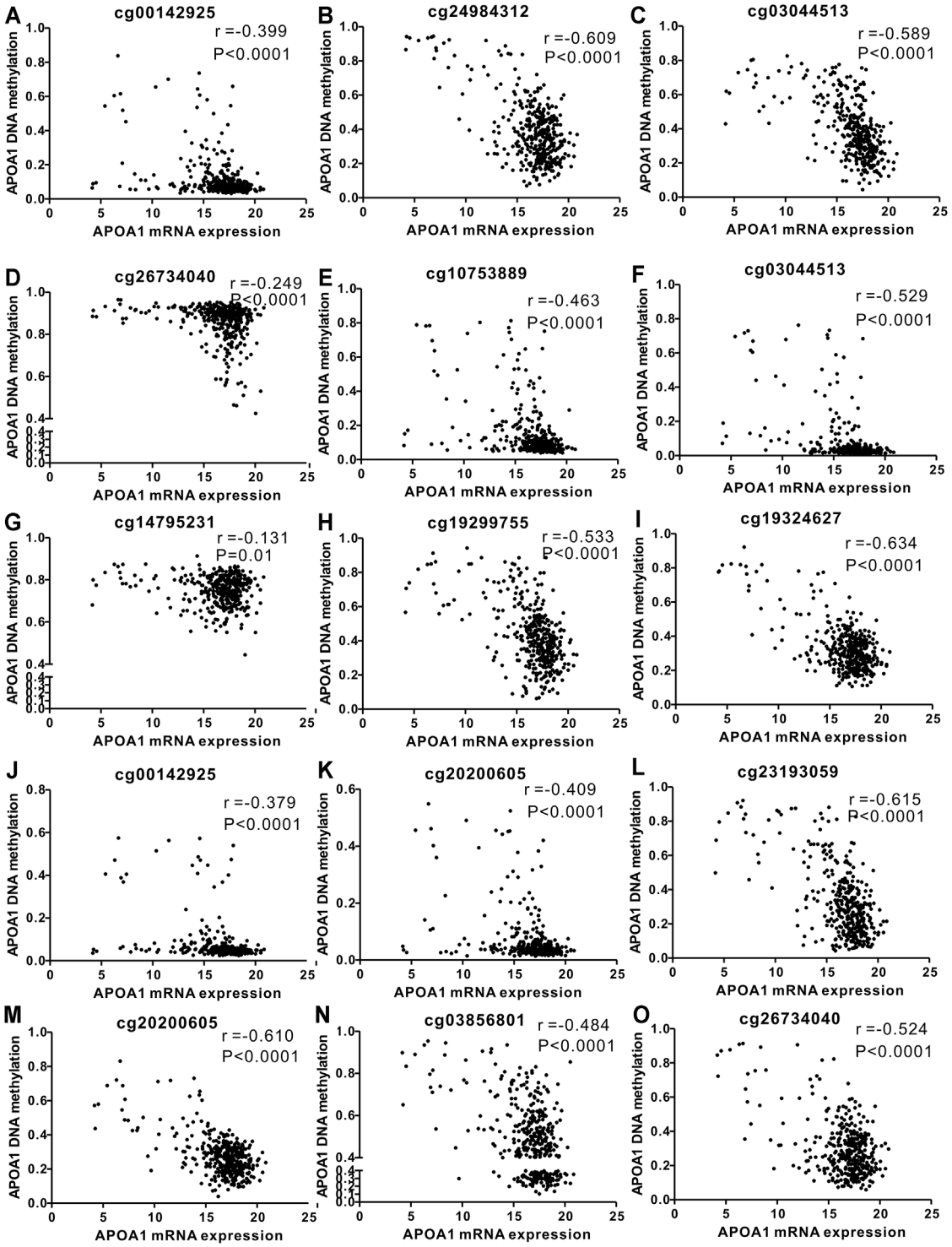

FIGURE 5 | Correlation analysis of the relationship between APOA-1 mRNA expression and methylation of APOA-1 DNA CpG sites in TCGA dataset. **(A)** cg00142925; **(B)** cg24984312; **(C)** cg03044513; **(D)** cg26734040; **(E)** cg10753889; **(F)** cg03044513; **(G)** cg14795231; **(H)** cg19299755; **(I)** cg19324627; **(J)** cg00142925; **(K)** cg20200605; **(L)** cg23193059; **(M)** cg20200605; **(N)** cg03856801; and **(O)** cg26734040.

methylation (p = 0.77, **Figure 6C**), while APOA-1 DNA hypermethylation was significantly associated with favorable PFS (p = 0.045, **Figure 6D**).

Multivariate Cox regression analyses were performed to identify independent risk factors for the prognosis of patients with HCC. **Table 1** demonstrates that the serum level of APOA-1

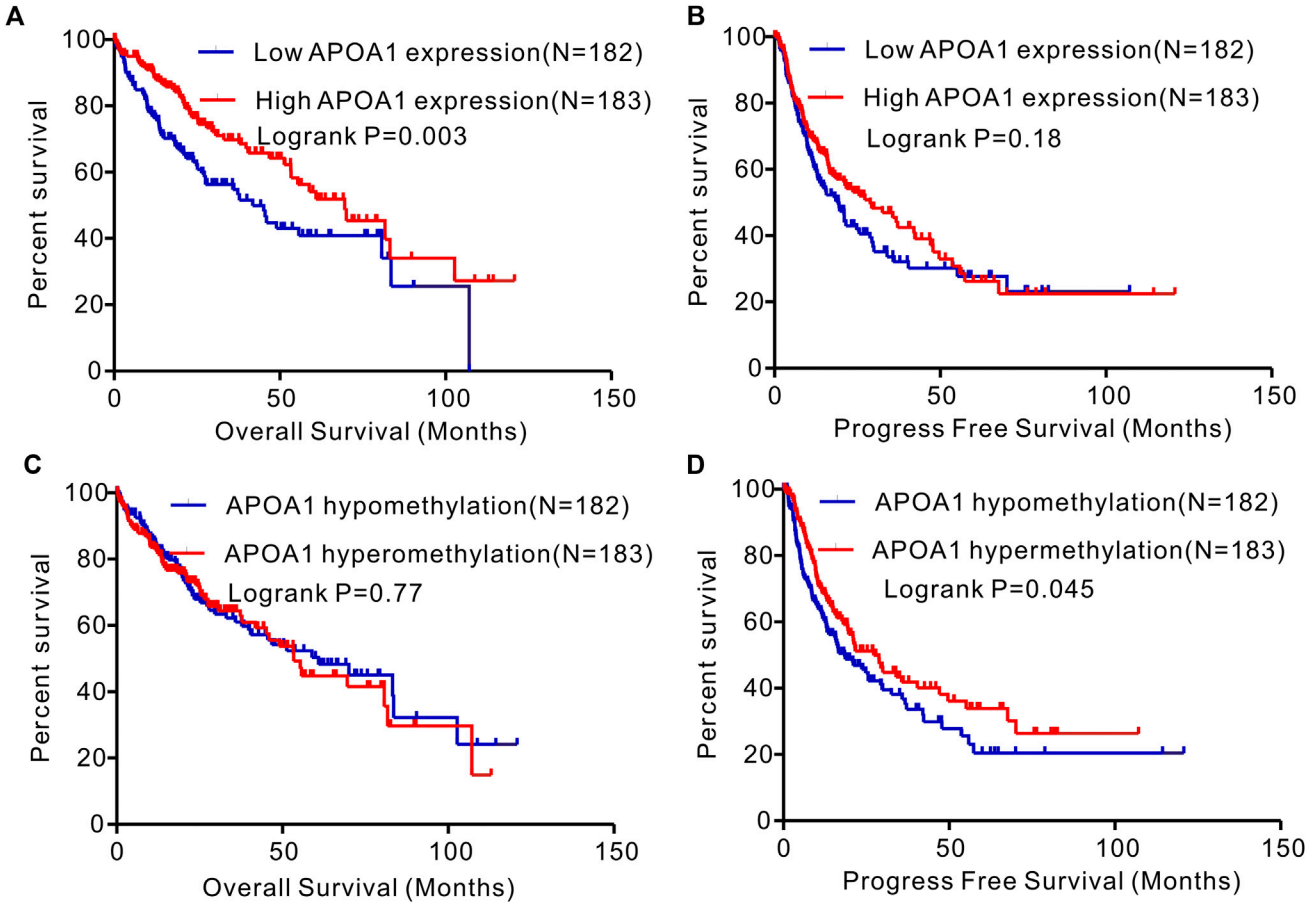

FIGURE 6 | Kaplan–Meier curves of OS and PFS in patients with HCC in the TCGA database. **(A)** High expression APOA-1 is associated with better OS in patients with HCC; **(B)** but not associated with PFS. **(C)**APOA-1 hypermethylation is not correlated with OS in patients with HCC; **(D)** but correlated with favorable PFS.

was an independent prognostic factor for OS among patients with HCC (HR = 0.594, 95% CI = 0.419–0.842, $p = 0.007$). T stage (HR = 22.649,95% CI = 1.605–3.022, $p < 0.001$) and TNM staging (HR = 2.222, 95% CI = 1.603–3.081, $p < 0.001$) were independent prognostic factors for PFS among patients with HCC.

Correlation Between Serum APOA-1 Protein and Clinical Features

As shown in **Figure 7A**, serum APOA-1 levels of healthy individuals was significantly higher than that in patients with HCC (1.46 ± 0.21 vs. 1.20 ± 0.21 g/L, $p < 0.001$). Next, ROC analysis was used to evaluate the measurement accuracy of serum APOA-1 in differentiating patients with HCC from healthy controls. The AUC of serum APOA-1 for identifying patients with HCC from healthy controls was 0.714, the cutoff value of APOA-1 was 1.18 ug/mL, and the sensitivity and specificity were 50.5 and 81.3%, respectively (**Figure 7B**).

Furthermore, the correlation between serum APOA-1 protein levels and clinical features has been detected and summarized in **Table 2**. Specifically, serum APOA-1 levels were significantly correlated with differences in hs-CRP ($p = 0.003$), HBsAg ($p < 0.001$), tumor number ($p < 0.001$), Child-Pugh score ($p = 0.027$), and BCLC stage ($p = 0.041$). However, no statistical significance was observed with age ($p = 0.580$), gender ($p = 0.359$), or AFP ($p = 0.732$).

APOA-1 Was an Independent Prognostic Marker for HCC

We further performed survival analysis to explore the correlation between serum APOA-1 levels and survival outcomes in the 316 of patients with HCC. Kaplan–Meier survival curves were constructed to determine the prognostic significance of circulating APOA-1 protein levels in HCC. High serum APOA-1 protein levels were significantly associated with good OS ($p = 0.021$, **Figure 7C**) and PFS ($p = 0.023$, **Figure 7D**).

Intact clinical information was included in the univariate and multivariate analyses to detect the association between serum APOA-1 protein levels and HCC patient prognosis. Multivariate analyses were performed to identify the factors that were identified in the univariate analyses. As shown in **Table 3**, hs-CRP (HR = 1.698, 95% CI = 1.010–2.853, $p = 0.046$), BCLC stage (HR = 1.285, 95% CI = 1.132–1.770, $p = 0.023$), and APOA-1

TABLE 1 | Multivariate Cox regression analyses of independent prognostic factors for overall survival and Progression-free survival in patients with HCC from TCGA cohort.

Variables		OS		PFS	
		HR (95% CI)	P	HR (95% CI)	P
Age	≤55	1.173 (0.807–1.706)	0.403		
	>55			0.968 (0.709–1.32)	0.836
G stage	G1+G2				
	G3+G4	1.114 (0.776–1.599)	0.559	1.166 (0.859–1.582)	0.325
M stage	M0				
	M1+Mx	1.176 (1.211–2.519)	**0.003**	1.258 (0.912–1.734)	0.162
N stage	N0				
	N1+Nx	1.519 (1.052–2.193)	**0.026**	1.222 (0.889–1.681)	0.216
T stage	T1+T2				
	T3+T4	2.483 (1.746–3.531)	<**0.001**	22.649 (1.605–3.022)	<**0.001**
Race	White				
	Asia	0.911 (0.395–2.100)	0.828	0.77 (0.566–1.048)	0.097
	Black or African American	0.673 (0.286–1.583)	0.364	0.583 (0.256–1.33)	0.200
	American Indian or Alaska Native				
Radiation Therapy	No				
	Yes	0.929 (0.295–2.926)	0.900	1.557 (0.688–3.524)	0.288
Sex	female				
	male	0.805 (0.565–1.148)	0.232	0.939 (0.688–1.283)	0.694
AFP ng/mL	≤400				
	>400	0.787 (0.495–1.252)	0.312	0.956 (0.647–1.413)	0.823
BMI	<18.5	1.296 (0.793–2.119)	0.301	1.227 (0.788–1.909)	0.365
	18.5–24	0.799 (0.544–1.174)	0.253		
	>24			0.903 (0.654–1.246)	0.533
APOA-1	≤17.12				
	>17.12	0.594 (0.419–0.842)	**0.003**	0.818 (0.609–1.098)	0.181
APOA-1 methylation	≤0.3147				
	>0.3147	1.053 (0.745–1.488)	0.769	0.752 (0.559–1.011)	0.059
TNM staging	I + II				
	III + IV	2.373 (1.639–3.435)	<**0.001**	2.222 (1.603–3.081)	<**0.001**

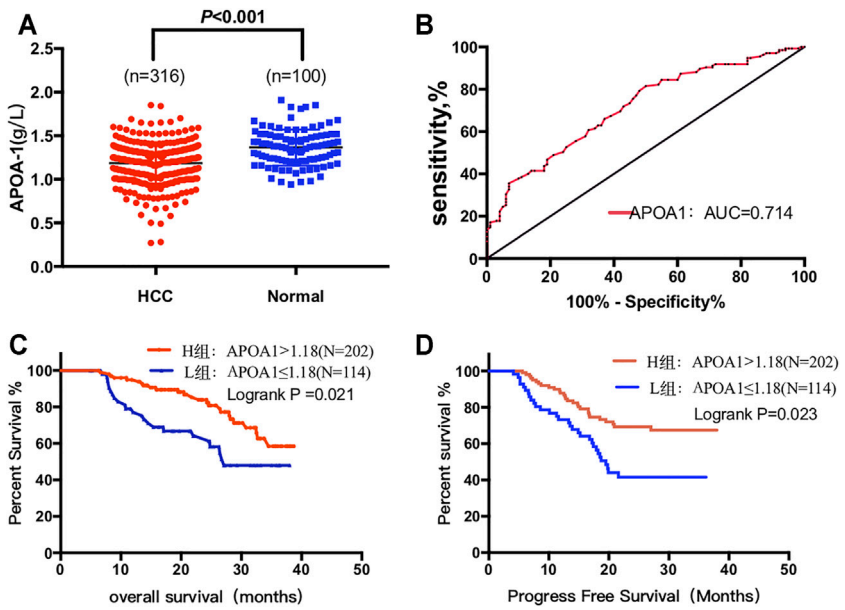

FIGURE 7 | Circulating serum APOA-1 protein in patients with HCC. **(A)** serum APOA-1 protein is higher in healthy controls than in HCC; **(B)** AUC for APOA-1. High expression APOA-1 is associated with better **(C)** OS and **(D)** PFS in 316 patients with HCC.

TABLE 2 | Correlation between serum APOA-1 levels and clinicopathologic characteristics of 316 patients with HCC.

Clinical characteristics		Low APOA-1 (≤1.18, N = 114)	High APOA-1 (>1.18, N = 202)	P
Age(years)	≤50	34 (29.8%)	52 (25.7%)	0.580
	>50	80 (70.2%)	150 (74.3%)	
Gender	Male	100 (87.7%)	166 (82.2%)	0.359
AFP, ng/mL	≤400	72 (63.2%)	122 (60.4%)	0.732
	>400	42 (36.8%)	80 (39.6%)	
ALT, U/L	≤75	98 (86.0%)	180 (89.1%)	0.560
	>75	16 (14.0%)	22 (10.9%)	
Fn, mg/L	≤280	102 (89.5%)	170 (84.2%)	0.354
	>280	12 (10.5%)	32 (15.8%)	
hs-CRP, mg/L	≤10	42 (36.8%)	109 (54.0%)	**0.003**
	>10	72 (63.2%)	93 (46.0%)	
APOB	≤0.84	66 (57.9%)	98 (48.5%)	0.257
	>0.84	48 (42.1%)	104 (51.5%)	
NLR	≤4.2	78 (68.4%)	154 (76.2%)	0.466
	>4.2	36 (31.6%)	48 (23.8%)	
HBsAg	Negative	30 (26.3%)	152 (75.2%)	**<0.001**
	Positive	84 (73.7%)	50 (24.8%)	
Liver cirrhosis	No	54 (47.4%)	92 (45.5%)	0.755
	Yes	60 (52.6%)	110 (54.5%)	
Tumor size,cm	≤5	50 (43.9%)	96 (47.5%)	0.632
	>5	64 (56.1%)	106 (52.5%)	
No.of tumors	Single	62 (54.4%)	166 (82.2%)	**<0.001**
	Multiple	52 (45.6%)	36 (17.8%)	
Satellite lesion	No	84 (73.7%)	172 (85.1%)	0.078
	Yes	30 (26.3%)	30 (14.9%)	
Vascular invasion	No	62 (54.4%)	130 (64.4%)	0.218
	Yes	52 (45.6%)	72 (35.6%)	
Tumor differentiation	Well	32 (28.1%)	66 (32.7%)	0.315
	Moderately	54 (47.4%)	106 (52.5%)	
	Poorly	28 (24.6%)	30 (14.9%)	
Child-Pugh score	A	76 (66.7%)	166 (82.2%)	**0.027**
	B	38 (33.3%)	36 (17.8%)	
BCLC stage	0 + A	72 (63.2%)	158 (78.2%)	**0.041**
	B + C	42 (36.8%)	44 (21.8%)	

(HR = 0.831, 95% CI = 0.482–0.940, $p < 0.001$) were identified as significant independent predictors of OS in patients with HCC. Besides, hs-CRP (HR = 1.632, 95% CI = 1.353–2.782, $p = 0.018$), NLR (HR = 2.546, 95% CI = 1.415–4.579, $p = 0.002$), tumor size (HR = 1.828, 95% CI = 1.059–3.156, $p = 0.030$), tumor differentiation (HR = 1.605, 95% CI = 1.059–2.433, $p = 0.026$) and APOA-1 (HR = 0.682, 95% CI = 0.390–0.912, $p < 0.001$) were independent prognostic indicators of PFS (**Table 4**).

Enrichment Analysis of Genes Co-expressed With APOA-1

To further clarify the potential role of APOA-1 in HCC, we first selected genes that were co-expressed with APOA-1 in LIHC dataset. We then used STRING database to investigate the PPI network of APOA1 in HCC by setting p-value < 0.05 and false discovery rate <25% as threshold, and we found that APOA1 is the hub gene in HCC (**Figure 8A**). Finally, we applied enrichment analysis using FunRich software, implicating that co-expressed genes were significantly enriched in lipoprotein metabolism and FOXA2 and FOXA3 transcription factor networks (**Figure 8B**).

DISCUSSION

As one of the leading causes of cancer-related deaths, HCC is a significant public health burden (Sartoris et al., 2021). Therefore, it is of great importance to detect indicators for optimizing early diagnosis and improving the prognosis of HCC (Mustafa et al., 2013). In our study, according to the univariate and multivariate analysis results, the clinical value of traditional HCC diagnosis and prognostic indicators such as tumor size/number (Yim et al., 2016; Tzartzeva and Singal, 2018), degree of differentiation, and inflammatory factors (CRP, NLR) (Greten and Grivennikov, 2019; Huang et al., 2019; Chan et al., 2020; Rogovskii, 2020) have been verified. Moreover, public gene expression and DNA methylation data are easily available, presenting a valuable opportunity to study diseases at the gene level (Yang et al., 2020). Hence, we found that the lipid metabolism biomarker APOA-1 is closely related to the prognosis of patients with HCC. To our knowledge, this is the first study to combine data mining and clinicopathological variables to explore the relationships between APOA-1 mRNA/DNA-methylation/protein expression levels and prognosis.

TABLE 3 | Univariate and multivariate cox hazards analysis for Overall survival in 316 patients with HCC.

Variables	Univariate analysis		Multivariate analysis	
	HR (95% CI)	P	HR (95%CI)	P
Gender Male vs. Female	0.783 (0.436–1.409)	0.415		
Age(years) ≤50 vs.>50	1.036 (0.650–1.653)	0.881		
AFP, ng/mL ≤400 vs.>400	1.551 (1.110–2.164)	**0.008**	0.961 (0.469–1.970)	0.961
ALT, U/L ≤75 vs.>75	1.203 (0.681–2.132)	0.545		
Fn ≤280 vs.>280	1.591 (0.851–2.975)	0.146		
hs-CRP ≤10 vs.>10	1.699 (1.173–2.242)	**0.023**	1.698 (1.010–2.853)	**0.046**
APOB ≤0.84 vs.>0.84	1.358 (0.852–2.165)	0.199		
NLR ≤4.2 vs.>4.2	1.571 (1.272–2.049)	**0.008**	0.567 (0.297–1.079)	0.567
HBsAg Negative vs. Positive	1.346 (0.832–2.177)	0.226		
Tumor size(cm) ≤5 vs.>5	1.921 (1.559–2.461)	**<0.001**	0.811 (0.482–1.366)	0.431
Tumor number single vs. Multiple	1.563 (1.243–2.568)	**<0.001**	1.254 (0.605–2.599)	0.542
Satellite lesion No vs. Yes	1.681 (1.482–2.413)	**0.002**	1.283 (0.922–1.763)	0.140
Vascular invasion No vs.Yes	1.553 (0.814–2.903)	0.129		
Tumor differentiation Well vs. Moderately vs. Poorly	1.112 (1.799–1.547)	**0.043**	1.011 (0.711–1.437)	0.952
Child-Pugh score A vs. B	1.791 (1.070–2.998)	**0.027**	1.592 (0.805–3.150)	0.181
BCLC stage 0+A vs. B + C	1.306 (1.020–1.672)	**0.034**	1.285 (1.132–1.770)	**0.023**
APOA-1 ≤1.18 vs.>1.18	0.732 (0.452–0.985)	**0.004**	0.831 (0.482–0.940)	**<0.001**

In our study, we identified a potential tumor suppressor gene (TSG; APOA-1), which is commonly suppressed by DNA CpG methylation in HCC. Our study elucidated that both APOA-1 mRNA and DNA methylation are innovative prognostic biomarkers in patients with HCC using comprehensive database analysis. Furthermore, we analyzed the differential expression of APOA-1 at the protein level and found that serum APOA-1 protein levels were much lower in patients with HCC than in healthy control groups, which further indicated that APOA-1 might be a tumor suppressor protein in HCC. Taken together, our findings strongly suggest that APOA-1 is a critical tumor suppressor and APOA-1 hypomethylation could serve as an independent prognostic factor in HCC.

Recent studies have reported that abnormal lipid metabolism is closely correlated with the development of malignant tumors (Estirado et al., 2018). These results demonstrate that abnormal lipid metabolism increases the risk of colorectal cancer (X. Zhang et al., 2014), ovarian cancer (D. Zhang et al., 2020), breast cancer (Kumar et al., 2015), and other cancers. Jiang et al. (Jiang et al., 2016) found that low levels of high-density lipoprotein cholesterol (HDL-C) and cholesterol (CHO) are preoperative risk factors for PFS and OS in patients with HCC. The reduction in CHO levels was associated with a reduction in OS ($p = 0.003$) and a reduction in PFS ($p = 0.012$). These results clarify that abnormal lipid metabolism is involved in the progression of HCC. Currently, only two studies (Ma et al., 2016; M.; Mao et al., 2018) have investigated the prognostic role of APOA-1 mRNA in patients with HCC. These studies have ascertained that the low APOA-1 expression group has a higher risk of recurrence and a poor survival outcome which is consistent with the results of our study.

DNA methylation, one of the most common epigenetic processes, can alter gene expression without changing the DNA sequence (Skvortsova et al., 2019). CpG sites can accumulate in CpG islands, and the CpG islands in gene promoter regions are generally unmethylated under normal conditions. However, the amount of methylation in a CpG island can change because of gene regulation processes in the pathologic process (Greenberg and Bourc'his, 2019; Grosser and Metzler, 2020). In some types of malignant tumors, DNA hypermethylation in the promoter region can induce

TABLE 4 | Univariate and multivariate cox hazards analysis for Progression-free survival in 316 patients with HCC.

Variables	Univariate analysis		Multivariate analysis	
	HR (95% CI)	P	HR (95%CI)	P
Gender Male vs. Female	0.705 (0.365–1.361)	0.298		
Age(years) ≤50 vs.>50	0.775(0.458–1.312)	0.343		
AFP, ng/mL ≤400 vs.>400	1.502(1.312–1.163)	**0.015**	1.355 (0.621–2.955)	0.446
ALT, U/L ≤75 vs.>75	1.156 (0.729–1.836)	0.545		
Fn ≤280 vs.>280	1.064 (0.522–2.169)	0.865		
hs-CRP ≤10 vs.>10	1.974 (1.152–3.384)	**0.013**	1.632 (1.353–2.782)	**0.018**
APOB ≤0.84 vs.>0.84	1.052 (0.626–1.769)	0.849		
NLR ≤4.2 vs.>4.2	3.250 (1.912–5.522)	**<0.001**	2.546 (1.415–4.579)	**0.002**
HBsAg Negative vs. Positive	1.179 (0.692–2.008)	0.544		
Tumor size(cm) ≤5 vs.>5	1.911 (1.121–3.259)	**0.017**	1.828 (1.059–3.156)	**0.030**
Tumor number Single vs. Multiple	0.553 (0.221–1.385)	0.206		
Satellite lesion No vs. Yes	0.552 (0.220–1.383)	0.205		
Vascular invasion No vs.Yes	0.774 (0.485–1.142)	0.189		
Tumor differentiation Well vs. Moderately vs. Poorly	1.704 (1.172–2.479)	**0.005**	1.605 (1.059–2.433)	**0.026**
Child-Pugh score A vs. B	2.041 (1.191–3.500)	**0.009**	1.185 (0.574–2.446)	0.646
BCLC stage 0+A vs. B + C	1.635 (1.260–2.122)	**<0.001**	1.217 (0.845–1.754)	0.291
APOA-1 ≤1.18 vs.>1.18	0.547 (0.323–0.926)	**0.004**	0.682 (0.390–0.912)	**<0.001**

deregulated silencing of some TSGs (Jones, 2012). Previous studies have demonstrated that APOA-1 gene expression is related to DNA methylation. Wang et al. (Wang et al., 2016) revealed that APOA-1 mRNA expression was downregulated by hypermethylation of CpG islands for hepatitis B virus (HBV) infection, which may contribute to the development of cirrhosis, liver failure, and HCC. Unlike previous studies, our study revealed that APOA-1 DNA methylation levels in HCC tissues were lower than those in non-tumor tissues. This may be due to the complexity of the regulatory mechanism of mRNA expression. Thus, further research is needed to clarify this point. Furthermore, Kaplan–Meier survival curves demonstrated that the PFS time of patients with HCC with APOA-1 DNA hypermethylation was significantly longer than that of patients with APOA-1 DNA hypomethylation. Our study suggests that APOA-1 DNA hypermethylation may serve as a unique prognostic indicator for patients with HCC.

Additionally, APOA-1 protein, as a member of the apolipoprotein A1/A4/E family encoded by the APOA-1 gene, plays a vital role in the formation of lipoprotein complexes of low-density and high-density lipoproteins (Chyu and Shah, 2015). From this perspective, APOA-1 has been implicated in the progression and recurrence of many metabolic and cardiovascular diseases (Dufresne et al., 2019; C.; Li et al., 2019). Nonetheless, some investigators have increasingly turned their attention to the interaction between serum APOA-1 protein and cancer. Kim et al. (Kim et al., 2020) collected blood samples from 180 patients with pancreatic ductal adenocarcinoma (PDAC) and 573 healthy controls to determine whether APOA-1 is a new biomarker for early diagnosis of PDAC. Peng et al. (Peng et al., 2019) found that high-grade bladder cancer (BC) patients have significantly higher APOA-1 levels than do low-grade BC patients, indicating that circulating APOA-1 protein may be a novel biomarker for BC diagnosis and prognosis monitoring. In our study, we specifically observed that the expression of APOA-1 protein was significantly associated with hs-CRP, HBsAg, tumor number, Child-Pugh score, and BCLC stage. In addition, our results demonstrated that low APOA-1 levels were strongly correlated with inferior OS and PFS.

The exact mechanism of action of APOA-1 in tumorigenesis is unclear. Recent studies have reported that APOA-1 may be implicated in the involvement of tumor microenvironment, tumor growth, immune cells, and tumor cell proliferation

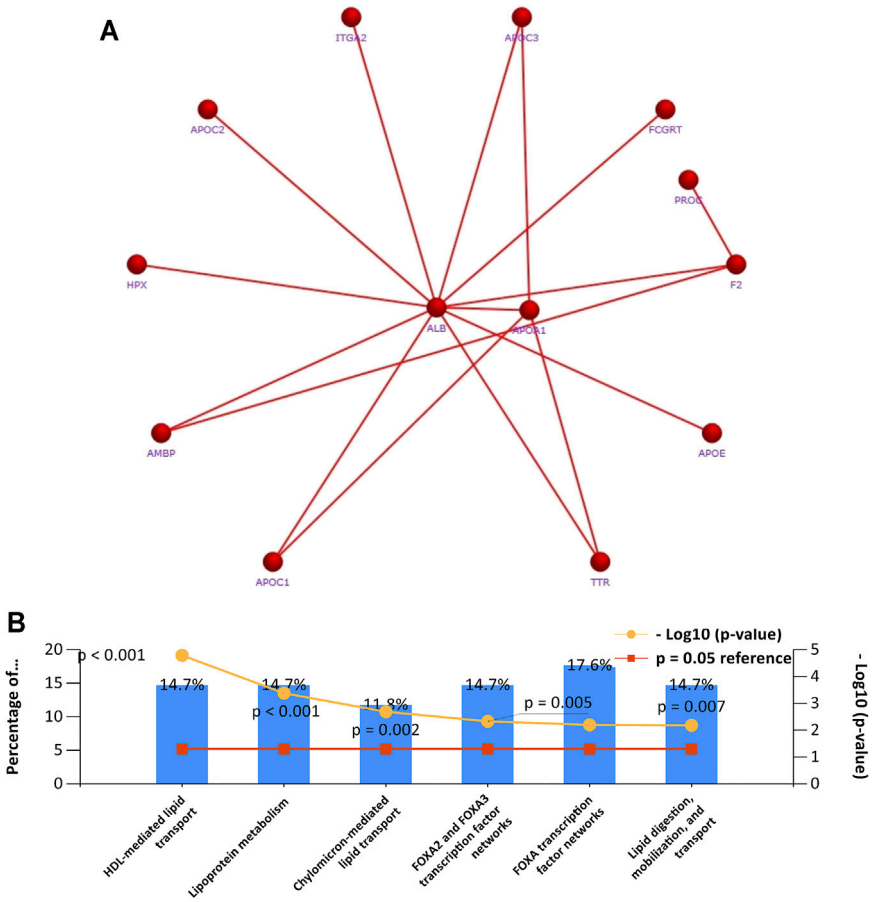

FIGURE 8 | Gene set enrichment analysis of PCR-array. **(A)** The network of APOA-1 and its co-expressed genes in various cells; **(B)** gene set enrichment analysis of biological processes.

(M. Mao et al., 2018). Moreover, Cristina et al. (Aguirre-Portoles et al., 2018) observed that APOA1 can reverse the malignant phenotypes displayed by cells overexpressing a cholesterol transport regulator (RCT). Thus, intracellular cholesterol metabolism and APOA-1 emerge as new relevant players in CRC progression to metastasis by modulating intracellular cholesterol metabolism. Mao et al. (J. Mao et al., 2014) demonstrated that APOA-1 overexpression is associated with the inhibition of COX-2 expression in hepatocytes. Besides, APOA-1 overexpression can reduce steatosis by decreasing reactive oxygen species (ROS) levels and suppressing COX-2-induced inflammation in hepatocytes. In addition, Fessler et al. found that APOA-1 can affect the response of immune cells to tumors by regulating the cholesterol content in membrane lipid rafts (Fessler and Parks, 2011). It can also inhibit the proliferation of tumor cells by promoting cell cycle arrest and promote apoptosis by regulating the mitogen-activated protein kinase pathway (Ma et al., 2016). At the genetic level, some studies (W. C. Liang et al., 2018; Liu et al., 2018) have shown that the Forkhead transcription family member FOXA2 plays a critical role in HCC progression and metastasis, which is consistent with our gene enrichment analysis results. This may be related to the mechanism of APOA-1 in tumorigenesis. Although further validation is required before the intact mechanism is clarified, the clinical use of APOA-1 has potential implications.

However, there were several limitations to our study. First, some recognized factors, such as tumor size, AFP, and vascular invasion, are not independent risk factors for OS and PFS in patients with HCC. This might be due to the relatively short follow-up time and the limitations of the small cohort size. It should be noted that most patients with HCC in China have been infected with HBV. However, abnormal levels of lipid metabolism variables may be associated with non-alcoholic fatty liver disease. Hence, a large-cohort, multi-center, long-term, and etiology-clear study including patients from different backgrounds is warranted in the future.

CONCLUSION

Our study demonstrated that the expression of APOA-1 protein is significantly downregulated in HCC than in

healthy individuals. APOA-1 DNA methylation, mRNA expression, and protein expression may act as vital predictors of the prognosis of patients with HCC undergoing surgical resection. APOA-1 hypermethylation is an independent protective factor for improved survival in patients with HCC. Additionally, further studies should aim to clarify the molecular mechanism that may facilitate the identification of new drug targets for HCC.

DATA AVAILABILITY STATEMENT

The datasets presented in this study can be found in online repositories. The names of the repository/repositories and accession number(s) can be found in the article/ **Supplementary Material**.

ETHICS STATEMENT

The studies involving human participants were reviewed and approved by the Ethics Committee of Renmin Hospital of Wuhan University in the Hubei Province (No. WDRY2019-K104). The patients/participants provided their written informed consent to participate in the study.

AUTHOR CONTRIBUTIONS

Study conception and design: YG and ST. Data collection: YG. Statistical analysis: ST, BH, and YG. Manuscript draft: YG, RL, and ST. Manuscript review and editing: CP, WD, and JL.

FUNDING

This work was supported by a special scientific research project for the cultivation of scientific and technological talents of Wuhan fourth hospital-Macheng Renmin Hospital (N0. KY-Y-202012).

ACKNOWLEDGMENTS

The authors thank the participating patients for the source of clinical blood samples.

SUPPLEMENTARY MATERIAL

The Supplementary Material for this article can be found online at: https://www.frontiersin.org/articles/10.3389/fgene.2021.760744/full#supplementary-material

REFERENCES

Aguirre-Portolés, C., Feliu, J., Reglero, G., and Ramírez de Molina, A. (2018). ABCA1 Overexpression Worsens Colorectal Cancer Prognosis by Facilitating Tumour Growth and Caveolin-1-dependent Invasiveness, and These Effects Can Be Ameliorated Using the BET Inhibitor Apabetalone. *Mol. Oncol.* 12 (10), 1735–1752. doi:10.1002/1878-0261.12367

Benito-Martin, A., and Peinado, H. (2015). FunRich Proteomics Software Analysis, Let the Fun Begin!. *Proteomics* 15 (15), 2555–2556. doi:10.1002/pmic.201500260

Borgquist, S., Butt, T., Almgren, P., Shiffman, D., Stocks, T., Orho-Melander, M., et al. (2016). Apolipoproteins, Lipids and Risk of Cancer. *Int. J. Cancer* 138 (11), 2648–2656. doi:10.1002/ijc.30013

Cancer Genome Atlas Research Network; Electronic address w. b. e.; Cancer Genome Atlas Research Network. (2017). Comprehensive and Integrative Genomic Characterization of Hepatocellular Carcinoma. *Cell* 169 (7), 1327–1341.23. doi:10.1016/j.cell.2017.05.046

Chan, S. L., Wong, L.-L., Chan, K.-C. A., Chow, C., Tong, J. H.-M., Yip, T. C.-F., et al. (2020). Development of a Novel Inflammation-Based Index for Hepatocellular Carcinoma. *Liver Cancer* 9 (2), 167–181. doi:10.1159/000504252

Chyu, K.-Y., and Shah, P. K. (2015). HDL/ApoA-1 Infusion and ApoA-1 Gene Therapy in Atherosclerosis. *Front. Pharmacol.* 6, 187. doi:10.3389/fphar.2015.00187

Cine, N., Baykal, A. T., Sunnetci, D., Canturk, Z., Serhatli, M., and Savli, H. (2014). Identification of ApoA1, HPX and POTEE Genes by Omic Analysis in Breast Cancer. *Oncol. Rep.* 32 (3), 1078–1086. doi:10.3892/or.2014.3277

Dufresne, J., Bowden, P., Thavarajah, T., Florentinus-Mefailoski, A., Chen, Z. Z., Tucholska, M., et al. (2019). The Plasma Peptides of Breast versus Ovarian Cancer. *Clin. Proteom.* 16, 43. doi:10.1186/s12014-019-9262-0

Estirado, C., Ceccato, A., Guerrero, M., Huerta, A., Cilloniz, C., Vilaró, O., et al. (2018). Microorganisms Resistant to Conventional Antimicrobials in Acute Exacerbations of Chronic Obstructive Pulmonary Disease. *Respir. Res.* 19 (1), 119. doi:10.1186/s12931-018-0820-1

Fessler, M. B., and Parks, J. S. (2011). Intracellular Lipid Flux and Membrane Microdomains as Organizing Principles in Inflammatory Cell Signaling.*J Immunol.* 187 (4), 1529–1535. doi:10.4049/jimmunol.1100253

Gao, F., Vasquez, S. X., Su, F., Roberts, S., Shah, N., Grijalva, V., et al. (2011). L-5F, an Apolipoprotein A-I Mimetic, Inhibits Tumor Angiogenesis by Suppressing VEGF/basic FGF Signaling Pathways. *Integr. Biol.* 3 (4), 479–489. doi:10.1039/c0ib00147c

Greenberg, M. V. C., and Bourc'his, D. (2019). The Diverse Roles of DNA Methylation in Mammalian Development and Disease. *Nat. Rev. Mol. Cel Biol.* 20 (10), 590–607. doi:10.1038/s41580-019-0159-6

Greten, F. R., and Grivennikov, S. I. (2019). Inflammation and Cancer: Triggers, Mechanisms, and Consequences. *Immunity* 51 (1), 27–41. doi:10.1016/j.immuni.2019.06.025

Grosser, K., and Metzler, D. (2020). Modeling Methylation Dynamics with Simultaneous Changes in CpG Islands. *BMC Bioinf.* 21 (1), 115. doi:10.1186/s12859-020-3438-5

Guo, G., Wang, Y., Zhou, Y., Quan, Q., Zhang, Y., Wang, H., et al. (2019). Immune Cell Concentrations Among the Primary Tumor Microenvironment in Colorectal Cancer Patients Predicted by Clinicopathologic Characteristics and Blood Indexes. *J. Immunother. Cancer* 7 (1), 179. doi:10.1186/s40425-019-0656-3

Huang, P.-Y., Wang, C.-C., Lin, C.-C., Lu, S.-N., Wang, J.-H., Hung, C.-H., et al. (2019). Predictive Effects of Inflammatory Scores in Patients with BCLC 0-A Hepatocellular Carcinoma after Hepatectomy. *Jcm* 8 (10), 1676. doi:10.3390/jcm8101676

Jiang, S.-S., Weng, D.-S., Jiang, L., Zhang, Y.-J., Pan, K., Pan, Q.-Z., et al. (2016). The Clinical Significance of Preoperative Serum Cholesterol and High-Density Lipoprotein-Cholesterol Levels in Hepatocellular Carcinoma. *J. Cancer* 7 (6), 626–632. doi:10.7150/jca.13837

Jones, P. A. (2012). Functions of DNA Methylation: Islands, Start Sites, Gene Bodies and beyond. *Nat. Rev. Genet.* 13 (7), 484–492. doi:10.1038/nrg3230

Kim, H., Kang, K. N., Shin, Y. S., Byun, Y., Han, Y., Kwon, W., et al. (2020). Biomarker Panel for the Diagnosis of Pancreatic Ductal Adenocarcinoma. *Cancers* 12 (6), 1443. doi:10.3390/cancers12061443

Kumar, V., Singh, A., Sidhu, D. S., and Panag, K. M. (2015). A Comparitive Study to Evaluate the Role of Serum Lipid Levels in Aetiology of Carcinoma Breast. *J. Clin. Diagn. Res.* 9 (2), PC01–03. doi:10.7860/JCDR/2015/12273.5563

Li, T., Fan, J., Wang, B., Traugh, N., Chen, Q., Liu, J. S., et al. (2017). TIMER: A Web Server for Comprehensive Analysis of Tumor-Infiltrating Immune Cells. *Cancer Res.* 77 (21), e108–e110. doi:10.1158/0008-5472.CAN-17-0307

Li, Y., Gu, J., Xu, F., Zhu, Q., Ge, D., and Lu, C. (2018). Transcriptomic and Functional Network Features of Lung Squamous Cell Carcinoma through Integrative Analysis of GEO and TCGA Data. *Sci. Rep.* 8 (1), 15834. doi:10.1038/s41598-018-34160-w

Li, C., Zhou, Y., Liu, J., Su, X., Qin, H., Huang, S., et al. (2019). Potential Markers from Serum-Purified Exosomes for Detecting Oral Squamous Cell Carcinoma Metastasis. *Cancer Epidemiol. Biomark. Prev.* 28 (10), 1668–1681. doi:10.1158/1055-9965.EPI-18-1122

Liang, W.-C., Ren, J.-L., Wong, C.-W., Chan, S.-O., Waye, M. M.-Y., Fu, W.-M., et al. (2018). LncRNA-NEF Antagonized Epithelial to Mesenchymal Transition and Cancer Metastasis via Cis-Regulating FOXA2 and Inactivating Wnt/β-Catenin Signaling. *Oncogene* 37 (11), 1445–1456. doi:10.1038/s41388-017-0041-y

Liang, T., Sang, S., Shao, Q., Chen, C., Deng, Z., Wang, T., et al. (2020). Abnormal Expression and Prognostic Significance of EPB41L1 in Kidney Renal clear Cell Carcinoma Based on Data Mining. *Cancer Cel Int.* 20, 356. doi:10.1186/s12935-020-01449-8

Liu, J., Yu, Z., Xiao, Y., Meng, Q., Wang, Y., and Chang, W. (2018). Coordination of FOXA2 and SIRT6 Suppresses the Hepatocellular Carcinoma Progression through ZEB2 Inhibition. *Cancer Manag. Res.* 10, 391–402. doi:10.2147/CMAR.S150552

Long, J., Chen, P., Lin, J., Bai, Y., Yang, X., Bian, J., et al. (2019). DNA Methylation-Driven Genes for Constructing Diagnostic, Prognostic, and Recurrence Models for Hepatocellular Carcinoma. *Theranostics* 9 (24), 7251–7267. doi:10.7150/thno.31155

Ma, X.-L., Gao, X.-H., Gong, Z.-J., Wu, J., Tian, L., Zhang, C.-Y., et al. (2016). Apolipoprotein A1: a Novel Serum Biomarker for Predicting the Prognosis of Hepatocellular Carcinoma after Curative Resection. *Oncotarget* 7 (43), 70654–70668. doi:10.18632/oncotarget.12203

Mao, J., Liu, W., and Wang, Y. (2014). Apolipoprotein A-I Expression Suppresses COX-2 Expression by Reducing Reactive Oxygen Species in Hepatocytes. *Biochem. Biophys. Res. Commun.* 454 (3), 359–363. doi:10.1016/j.bbrc.2014.10.094

Mao, M., Wang, X., Sheng, H., Liu, Y., Zhang, L., Dai, S., et al. (2018). A Novel Score Based on Serum Apolipoprotein A-1 and C-Reactive Protein Is a Prognostic Biomarker in Hepatocellular Carcinoma Patients. *BMC Cancer* 18 (1), 1178. doi:10.1186/s12885-018-5028-8

Mustafa, M. G., Petersen, J. R., Ju, H., Cicalese, L., Snyder, N., Haidacher, S. J., et al. (2013). Biomarker Discovery for Early Detection of Hepatocellular Carcinoma in Hepatitis C-Infected Patients. *Mol. Cell Proteomics* 12 (12), 3640–3652. doi:10.1074/mcp.M113.031252

Peng, C., Hua, M.-Y., Li, N.-S., Hsu, Y.-P., Chen, Y.-T., Chuang, C.-K., et al. (2019). A Colorimetric Immunosensor Based on Self-Linkable Dual-Nanozyme for Ultrasensitive Bladder Cancer Diagnosis and Prognosis Monitoring. *Biosens. Bioelectron.* 126, 581–589. doi:10.1016/j.bios.2018.11.022

Pinto Marques, H., Gomes da Silva, S., De Martin, E., Agopian, V. G., and Martins, P. N. (2020). Emerging Biomarkers in HCC Patients: Current Status. *Int. J. Surg.* 82, 70–76. doi:10.1016/j.ijsu.2020.04.043

Rogovskii, V. (2020). Modulation of Inflammation-Induced Tolerance in Cancer. *Front. Immunol.* 11, 1180. doi:10.3389/fimmu.2020.01180

Sartoris, R., Gregory, J., Dioguardi Burgio, M., Ronot, M., and Vilgrain, V. (2021). HCC Advances in Diagnosis and Prognosis: Digital and Imaging. *Liver Int.* 41 (Suppl. 1), 73–77. doi:10.1111/liv.14865

Sharma, R. (2020). Descriptive Epidemiology of Incidence and Mortality of Primary Liver Cancer in 185 Countries: Evidence from GLOBOCAN 2018. *Jpn. J. Clin. Oncol.* 50, 1370–1379. doi:10.1093/jjco/hyaa130

Skvortsova, K., Stirzaker, C., and Taberlay, P. (2019). The DNA Methylation Landscape in Cancer. *Essays Biochem.* 63 (6), 797–811. doi:10.1042/EBC20190037

Tellapuri, S., Sutphin, P. D., Beg, M. S., Singal, A. G., and Kalva, S. P. (2018). Staging Systems of Hepatocellular Carcinoma: A Review. *Indian J. Gastroenterol.* 37 (6), 481–491. doi:10.1007/s12664-018-0915-0

Tian, Z., He, W., Tang, J., Liao, X., Yang, Q., Wu, Y., et al. (2020). Identification of Important Modules and Biomarkers in Breast Cancer Based on WGCNA. *Onco. Targets Ther.* 13, 6805–6817. doi:10.2147/OTT.S258439

Tzartzeva, K., and Singal, A. G. (2018). Testing for AFP in Combination with Ultrasound Improves Early Liver Cancer Detection. *Expert Rev. Gastroenterol. Hepatol.* 12 (10), 947–949. doi:10.1080/17474124.2018.1512855

Villanueva, A. (2019). Hepatocellular Carcinoma. *N. Engl. J. Med.* 380 (15), 1450–1462. doi:10.1056/NEJMra1713263

Wang, Y., Hao, J., Liu, X., Wang, H., Zeng, X., Yang, J., et al. (2016). The Mechanism of Apoliprotein A1 Down-Regulated by Hepatitis B Virus. *Lipids Health Dis.* 15, 64. doi:10.1186/s12944-016-0232-5

Yang, J., Li, Y., Liu, Q., Li, L., Feng, A., Wang, T., et al. (2020). Brief Introduction of Medical Database and Data Mining Technology in Big Data Era. *J. Evid. Based Med.* 13 (1), 57–69. doi:10.1111/jebm.12373

Yim, W.-w., Kwan, S. W., and Yetisgen, M. (2016). Tumor Reference Resolution and Characteristic Extraction in Radiology Reports for Liver Cancer Stage Prediction. *J. Biomed. Inform.* 64, 179–191. doi:10.1016/j.jbi.2016.10.005

Zamanian-Daryoush, M., Lindner, D., Tallant, T. C., Wang, Z., Buffa, J., Klipfell, E., et al. (2013). The Cardioprotective Protein Apolipoprotein A1 Promotes Potent Anti-tumorigenic Effects. *J. Biol. Chem.* 288 (29), 21237–21252. doi:10.1074/jbc.M113.468967

Zhang, X., Zhao, X. W., Liu, D. B., Han, C. Z., Du, L. L., Jing, J. X., et al. (2014). Lipid Levels in Serum and Cancerous Tissues of Colorectal Cancer Patients. *World J. Gastroenterol.* 20 (26), 8646–8652. doi:10.3748/wjg.v20.i26.8646

Zhang, C., Li, J., Huang, T., Duan, S., Dai, D., Jiang, D., et al. (2016). Meta-analysis of DNA Methylation Biomarkers in Hepatocellular Carcinoma. *Oncotarget* 7 (49), 81255–81267. doi:10.18632/oncotarget.13221

Zhang, D., Xi, Y., and Feng, Y. (2020). Ovarian Cancer Risk in Relation to Blood Lipid Levels and Hyperlipidemia: a Systematic Review and Meta-Analysis of Observational Epidemiologic Studies. *Eur. J. Cancer Prev.* 30, 161–170. doi:10.1097/CEJ.0000000000000597

Conflict of Interest: The authors declare that the research was conducted in the absence of any commercial or financial relationships that could be construed as a potential conflict of interest.

Publisher's Note: All claims expressed in this article are solely those of the authors and do not necessarily represent those of their affiliated organizations, or those of the publisher, the editors and the reviewers. Any product that may be evaluated in this article, or claim that may be made by its manufacturer, is not guaranteed or endorsed by the publisher.

frontiers in Genetics

REVIEW
published: 09 November 2021
doi: 10.3389/fgene.2021.758733

Role of Flavonoids as Epigenetic Modulators in Cancer Prevention and Therapy

*Nishat Fatima[1], Syed Shabihe Raza Baqri[2], Atrayee Bhattacharya[3], Nii Koney-Kwaku Koney[4], Kazim Husain[5], Ata Abbas[6,7] and Rais A. Ansari[8]**

[1]Department of Chemistry, Shia Postgraduate College, Lucknow, India, [2]Department of Zoology, Shia Postgraduate College, Lucknow, India, [3]Department of Medical Oncology, Dana-Farber Cancer Institute, Harvard Medical School, Boston, MA, United States, [4]Department of Anatomy, University of Ghana Medical School, College of Health Sciences, University of Ghana, Accra, Ghana, [5]Department of Molecular Medicine, University of South Florida, Tampa, FL, United States, [6]Division of Hematology and Oncology, Department of Medicine, Case Western Reserve University, Cleveland, OH, United States, [7]Case Comprehensive Cancer Center, Case Western Reserve University School of Medicine, Cleveland, OH, United States, [8]Department of Pharmaceutical Sciences, Nova Southeastern University, Fort Lauderdale, FL, United States

Epigenetic regulation involves reversible changes in histones and DNA modifications that can be inherited without any changes in the DNA sequence. Dysregulation of normal epigenetic processes can lead to aberrant gene expression as observed in many diseases, notably cancer. Recent insights into the mechanisms of DNA methylation, histone modifications, and non-coding RNAs involved in altered gene expression profiles of tumor cells have caused a paradigm shift in the diagnostic and therapeutic approaches towards cancer. There has been a surge in search for compounds that could modulate the altered epigenetic landscape of tumor cells, and to exploit their therapeutic potential against cancers. Flavonoids are naturally occurring phenol compounds which are abundantly found among phytochemicals and have potentials to modulate epigenetic processes. Knowledge of the precise flavonoid-mediated epigenetic alterations is needed for the development of epigenetics drugs and combinatorial therapeutic approaches against cancers. This review is aimed to comprehensively explore the epigenetic modulations of flavonoids and their anti-tumor activities.

Keywords: cancer, flavonoids, epigenetics, DNA methylation, histone modifications, non-coding RNAs

OPEN ACCESS

Edited by:
Kai Tang,
Purdue University, United States

Reviewed by:
Nabab Khan,
University of North Dakota, United States
Yao Xu,
Wuhan University of Science and Technology, China

****Correspondence:***
Rais A. Ansari
ra557@nova.edu

Specialty section:
This article was submitted to Epigenomics and Epigenetics, a section of the journal Frontiers in Genetics

Received: *14 August 2021*
Accepted: *26 October 2021*
Published: *09 November 2021*

Citation:
Fatima N, Baqri SSR, Bhattacharya A, Koney NK-K Husain K, Abbas A and Ansari RA (2021) Role of Flavonoids as Epigenetic Modulators in Cancer Prevention and Therapy. Front. Genet. 12:758733. doi: 10.3389/fgene.2021.758733

INTRODUCTION

Epigenetics can be defined as the study of heritable changes in gene expression without involving any changes in the DNA sequence (Weinhold, 2006). Epigenetic changes are established during early differentiation of cells and stably inherited through multiple cell divisions resulting in distinct cellular phenotypes without any changes in the underlying DNA sequence (Cheedipudi et al., 2014). The process of epigenetic regulation of gene expression involves chromatin remodeling mediated by events like DNA methylation, histone modifications and effects of non-coding RNAs as shown in **Figure 1**. These epigenetic changes are essential for normal development of cells, but their deregulation can lead to certain disease states including cancer (Egger et al., 2004).

There is a consensus among biologists that cancer can be considered as a genetic inevitability. DNA mutations accumulate in the cells as we age. The mutations can be either spontaneous due to

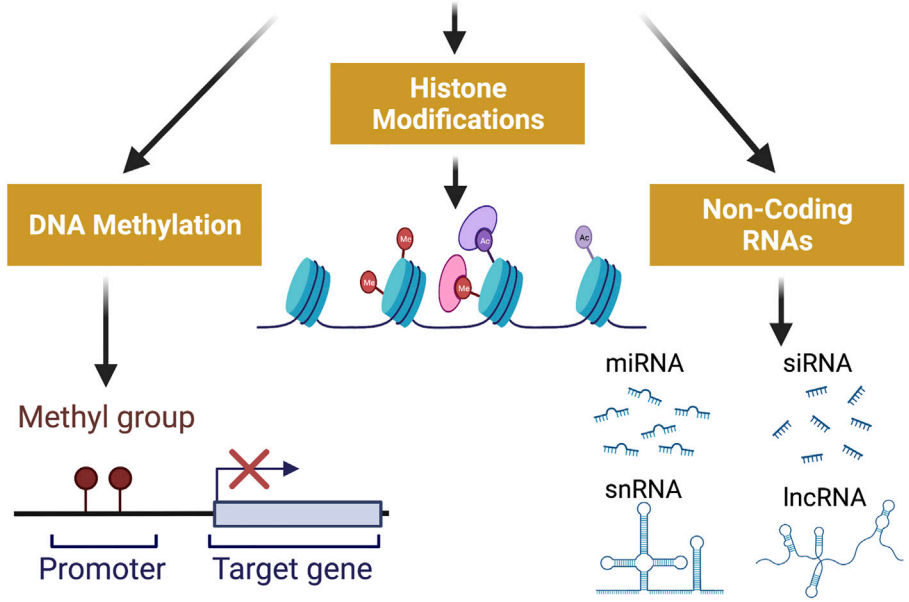

FIGURE 1 | Epigenetic Mechanisms involved in gene expression: DNA methylation, Histone Modifications and Non-Coding RNAs constitute the three mechanisms involved in epigenetic regulation of gene expression. Methylation of DNA occurs at gene promoters and hypermethylation represses gene expression. Histone modifications include acetylation and methylation of histones which can either activate or repress gene expression. Non-coding RNAs which consist of short chain non-coding RNAs (<200 nt) and long non-coding RNAs (>200 nt) also play a significant role in regulation of gene expression. (Created with BioRender.com). Ac, acetylated histone; Me, methylated histone; miRNA, micro RNA; siRNA, small interfering RNA; snRNA, small nuclear RNA; lncRNA, long non-coding RNA.

errors of DNA replication or may be caused by physical or chemical mutagens. Hence, 90–95% of cancers involve mutations due to environmental or lifestyle factors and in the remaining 10% of cases, the genetic cause of cancer is hereditary (Anand et al., 2008). Interestingly, many of the gene defects in cancers are not due to changes in sequences but are a result of epigenetic changes that affect the expression profile of these genes (Taby and Issa, 2010; Cavalli and Heard, 2019). Recent advances in the field of epigenetics have highlighted global epigenetic abnormalities in cancer cells which can occur during the early stages of tumor development. Due to their reversible nature and early occurrence in the process of malignant transformation of normal cells, epigenetic modifications can serve as novel drug targets for the treatment of cancer (Dawson and Kouzarides, 2012; Bennett and Licht, 2018).

Even though, in 2020, the global estimate of new cancer cases was 19.3 million which resulted in almost 10 million deaths, cancer related deaths have been declining since 1991 leading to a decrease of 31% in 2018 (Siegel et al., 2021). This improvement in patient's survival rate is a result of advancement in cancer treatments. Cancer treatments usually involve chemotherapeutic agents, radiotherapy, and immunotherapy, and these treatments have shown a lot of promise (Yu et al., 2019). Epigenetic modulators (e.g., histone deacetylases inhibitors) have been used to treat aberrant epigenetic modifications in cancer along with some novel approaches such as chimeric antigen receptor-engineered T cells (CAR-T cells) which have proven very efficient in treating malignancies of B-cells (Wang et al., 2020b). However, most of the cancer therapies including immunotherapy are associated with numerous side effects (Lacouture and Sibaud, 2018).

Thus, considering the adverse effects of radiation and chemotherapeutic agents on patients, there is an increased quest for alternative therapies without extreme side effects. Phytochemicals fit best in this criterion and are hence explored for their anticancer properties. Anticarcinogenic factors in plant-based foods are known to inhibit cancer by a variety of mechanisms ranging from antioxidant effects to immunomodulatory properties. Interestingly, it has been reported that phytochemicals can modulate epigenetic processes through DNA methyltransferases (DNMTs) and histone deacetylases (HDACs) (Shukla et al., 2014). Flavonoids which constitute an important class of phytochemicals are implicated in modulation of gene expression patterns underlying cancer (Busch et al., 2015). In this review we first discuss the role of epigenetic aberrations in cancer and then present an overview of the usefulness of flavonoids as epigenetic modulators having chemotherapeutic and chemo-preventive properties.

Cancer Epigenetics

In eukaryotic cells, DNA is wrapped around a core of histone proteins to form nucleosomes which may wrap over themselves to adopt a condensed state temporarily or permanently. The degree to which a gene is expressed in each cell is controlled by a range of gene regulatory mechanisms, most of which interfere

with chromatin condensation. The condensation of chromatin involves a compact packing of nucleosomes which renders the genes hetero-chromatinzed and hence inactive. On the contrary, decondensation of chromatin opens the nucleosomes and increased expression of genes. The transformation of normal cells into cancer cells involves epigenetic alterations and in most cases is preceded by genetic mutations (Brower, 2011). Amongst the key mechanisms involved in epigenetic regulation are DNA modifications (e.g., methylation), histone modifications (e.g., deacetylation, phosphorylation, and ubiquitination, etc.), nucleosome positioning, and non-coding RNAs (e.g., miRNA, siRNA, lncRNA, etc.) (**Figure 1**). These mechanisms have a significant impact on cellular homeostasis (Zhang et al., 2020).

DNA Methylation

The methylation or hydroxymethylation of DNA is an important epigenetic mechanism of gene regulation in cells (Gao and Das, 2014) and DNA methylation patterns contribute in establishing epigenetic memory (Bird, 2002). The methylation of DNA is usually negatively correlated with gene expression, but it also depends on the location of methylated bases in relation to coding regions of the genes being regulated (Blake et al., 2020). Cytosine methylation most commonly occurs at CpG sites which are widely distributed through the genome (Jones, 2012). The specific regions of CpG sites are designated as CpG islands when they have a length of more than 200 bp, a GC content of more than 55% and a >60% observed-to-expected CpG ratio (Takai and Jones, 2002). CpG islands are particularly abundant at promoter region of the gene, and are present in around 70% of human promoters (Deaton and Bird, 2011). When CpG sites are present in the promoter or enhancer regions of genes their methylation represses gene expression whereas it induces transcriptional activity if the CpG sites are present in the coding regions of genes (Greenberg and Bourc'his, 2019). The pattern of CpG methylation in cancer cells is different to that of normal cells (Esteller, 2007). In normal cells, whereas the CpG islands preceding promoters are unmethylated allowing active transcription while other CpG sites in the genome remain methylated. In cancer cells, the CpG dinucleotides have up to 50% less methylation than normal cells and CpG islands are also generally hypomethylated (Herman and Baylin, 2003). In general, promoters of tumor suppressor genes become hypermethylated thereby inhibiting their expression while those of oncogenes get hypomethylated and activated in cancer. Genes involved in DNA repair, cell cycle, migration and apoptosis are dysregulated due to aberrant DNA methylation in cancer cells (Cheung et al., 2009). This process of *de novo* DNA methylation is carried out by DNMTs and include three isoenzymes: DNMT1, DNMT3a and DNMT3b.

Histone Modifications

Histones are positively charged proteins that play a role in condensing and packaging the DNA into chromatin inside the nucleus. Open chromatin structure (euchromatin) is associated with transcriptional activation and closed chromatin structure (heterochromatin) is associated with repression of transcription. Histone modifications especially acetylation, phosphorylation, and methylation regulate structural changes in the chromatin influencing gene expression (Karlic et al., 2010; Bannister and Kouzarides, 2011).

Histone acetylation is defined as the addition of an acetyl group to lysine residues present at the histone tail by histone acetyl transferases (HATs). This modification weakens the DNA-histone interaction eventually leading to decondensation of chromatin and increased gene expression. On the contrary, HDACs constitute an important class of enzymes and are responsible for deacetylation of *e*-amino groups of lysine residues leading to condensation of chromatin and decreased gene expression. (Milazzo et al., 2020). The pattern of histone acetylation has been found to be remarkably different between normal and cancerous cells (Di Cerbo and Schneider, 2013). Histone H4 exhibits a decrease in monoacetylation of Lys20 and trimethylation of Lys16 in malignant cells (Fraga et al., 2005). Besides, decreased acetylation of histones H3 and H4 has also been observed in cancer progression (Audia and Campbell, 2016).

Histone methylation is another epigenetic modification that plays a role in regulating gene expression in cancer. These modifications are catalyzed by Histone Methyltransferases (HMTs) and Histone Demethylases (HDMs) of the specific amino acids in histones. Cancer specific gene transcription profiles are often related to the regulation of histone methylation (Varier and Timmers, 2011). For instance, there is a cancer-associated decrease in trimethylation on Lysine 4 of histone H3 (H3K4me3) along with a simultaneous increase of monomethylation on Lysine 9 of histone H3 that affects gene expression (Richon et al., 2000).

Phosphorylation is another histone posttranslational modification mediated by cell-cycle related kinases (Rossetto et al., 2014). The phosphorylation of serine at the C-terminus of a DNA double-strand break marker H2A histone family member X (H2AX), eventually contributes to genomic instability leading to cancer (Bonner et al., 2008).

Non-Coding RNAs

The next important epigenetic mechanism controlling cell function involves non-coding RNAs which are being shown to regulate gene expression to a great extent (Kurokawa et al., 2014; Statello et al., 2020). Small non-coding RNAs composed of 18–25 nucleotides are called MicroRNAs (miRNAs) which usually interacts with the 3' region of the mRNA affecting mRNA stability and translation. One miRNA can regulate the expression of several genes or multiple miRNAs can affect the expression of the same gene (Mohr and Mott, 2015). Transcriptional activity of up to 60% of mammalian protein coding genes has been found to be controlled by miRNAs (Friedman et al., 2009). Several miRNAs have been associated with the regulation of oncogenes and tumor suppressor genes thereby having a role in cancer (Peng and Croce, 2016). The most common cancer associated miRNAs (onco-miRNAs) that are promising candidates for cancer treatment are let-7, miR-15, and miR-16 (Esquela-Kerscher and Slack, 2006). Also, miR-125b1 has been shown to act as a tumor suppressor as its decrease is associated with ovarian and prostate cancers (Soto-Reyes et al., 2012). The roles of micro RNAs in cancer progression are

contributing to a great bulk of emerging knowledge about cancer (Ali Syeda et al., 2020). Events like genetic alterations, promoter hypermethylation, or other epigenetic modifications regulate the expression of miRNAs and promotes cellular transformation and cancer progression (Baer et al., 2013; Liu et al., 2013; Cammaerts et al., 2015).

Long non-coding RNAs (lncRNAs) are polyadenylated RNAs with a length of more than 200 nucleotides that can bind to DNA, RNA, and proteins. Epigenetic modulation is the most common method of lncRNAs based regulation of gene expression and is often associated with gene repression. Studies have reported that lncRNAs can function as oncogenes or tumor suppressors through a wide range of activities, including interaction with Polycomb Repressive Compex (PRC) regulating transcript stability, processing and translation; interaction with miRNAs, gene enhancers and repressors; and interaction with transcription factors affecting transcript production and transport (Marín-Béjar et al., 2013; Vance and Ponting, 2014; Marchese et al., 2017; Zhang et al., 2019b; Hou et al., 2019). LncRNAs like MALAT1 and HOTAIR which are associated with metastasis are over expressed in cancer and MEG3 and PTENP1 which inhibit cell proliferation and migration are downregulated in cancer (Huarte, 2015).

Flavonoids as Epigenetic Modulators

Flavonoids belong to an important class of natural low-molecular-weight polyphenolic compounds having basic benzo-γ-pyrone structure (Panche et al., 2016). These plant secondary metabolites are widely found in various vegetables, fruits, cereal, nuts and specially in certain beverages (tea, coffee). Flavonoids are linked with a wide spectrum of health-promoting goods and are an important constituent in a range of pharmaceutical, nutraceutical, cosmetic and medicinal applications. Flavonoids have several subgroups based on their chemical structures, which comprise flavan-3-ols, flavonols, flavones, flavanones, isoflavones, and anthocyanidins (Kumar and Pandey, 2013). Furthermore, flavonoids possess a wide array of beneficial pharmacological activities including antiviral, hepatoprotective, antibacterial, analgesic, cytostatic, antiallergic, anti-oestrogenic, oestrogenic and apoptotic (Kumar and Pandey, 2013). These assorted pharmacological activities of flavonoids have been accredited to several molecular mechanisms including direct and indirect antioxidant task, modulation of the activities of phase I and II detoxification enzymes, inhibition of protein kinases, modulation of gene transcription, consequence on cell cycle and epigenetic mechanisms (Pietta, 2000; Woo et al., 2005; Kumar and Pandey, 2013; Miron et al., 2017; Jucá et al., 2018; Khan et al., 2021). There are recent reports indicating that flavonoids may reinstate the standard epigenetic marks which are changed during carcinogenesis (Carlos-Reyes et al., 2019; Jiang et al., 2021; Khan et al., 2021). Generally, these photochemical agents block the progress of tumors by targeting key signaling transducers resulting in the reinstatement of tumor suppressor genes, and blocking of oncogenes expression. These alterations and resulting anti-tumor activities often come from epigenetic modulatory activities of flavonoids by altering epigenetic enzymes such as DNMTs, HDACs and HATs (Pandey et al., 2012; Abbas et al., 2013; Abbas et al., 2016; Jiang et al., 2021; Khan et al., 2021). It was also documented that flavonoids are proficient in modulating of miRNA and lncRNA expression that is changed during ailments (Izzo et al., 2020).

Despite the lifesaving role of chemotherapeutic agents in treating cancer, a disadvantage of these drugs is their potential cytotoxic effects on normal cells. Thus, there is a need for better substitutes without undesirable side-effects. In this regard, flavonoids show promising results as many of the anticarcinogenic flavonoids have relatively less toxicity towards normal cells (Galati and O'Brien, 2004); however, more in-depth toxicity studies are needed to evaluate their safety and side-effects. It is also documented that on normal cells they may act as pro-oxidants that generate free radicals, mutagens and act as inhibitors of key enzymes involved in hormone metabolism when consumed at higher doses (Skibola and Smith, 2000). Nonetheless, flavonoids having epigenetic modifying potential can be an attractive choice for potential cancer therapies, including combinatorial therapy (**Figure 2**; **Table 1**).

Cancer Prevention and Therapy by Epigenetically Active Flavonoids

Flavan-3-Ols/ Flavanols/ Catechins

Epigallocatechin gallate (EGCG) is a powerful polyphenolic, chemo-preventive compound isolated from green tea belongs to the catechin class of flavonoids (Singh et al., 2011). The other components of green tea consist of epigallocatechin, epicatechin-3-gallate and epicatechin. There are numerous *in vitro*, *in vivo*, and clinical studies that showed potential anti-proliferative, anti-angiogenic, pro-apoptotic and anti-invasive properties of EGCG (Singh et al., 2011). There are significant literatures demonstrating the impact of green tea components in involved in epigenetic modulations in cancer (Henning et al., 2013; Giudice et al., 2018; Jiang et al., 2021). Fang *et al.*, first time revealed that EGCG act as inhibitor of DNA hypermethylation of CpG islands by acting on DNMT (Fang et al., 2003). Another study has shown the profound effects of EGCG on human prostate cancer cells (Paschka et al., 1998). Green tea causes an accumulation of acetylated histone H3 in total cellular chromatin resulting in epigenetically reactivation of p21/waf1 and Bax in prostate cancer cells that leads to cell cycle arrest and apoptosis (Thakur et al., 2012).

Lee *et al.*, examined the regulation of androgen receptor acetylation by measuring histone acetyltransferase activity in androgen-dependent prostate cancer cells treated with green tea catechins (epicatechin, epigallocatechin and epigallocatechin-3-gallate). These catechins induce prostate cancer cell death, suppressed agonist-dependent androgen receptor (AR) activation and AR-regulated gene transcription (Lee et al., 2012). Another report showed that the combinatorial exposures of clofarabine and EGCG or genistein synergistically inhibited the growth of breast cancer cells (MCF7 and MDA-MB-231 cells) and induces apoptosis followed by *RARB* hypomethylation with consequent manifold increase in *RARB*, *CDKN1A,* and *PTEN* transcript levels. This combination

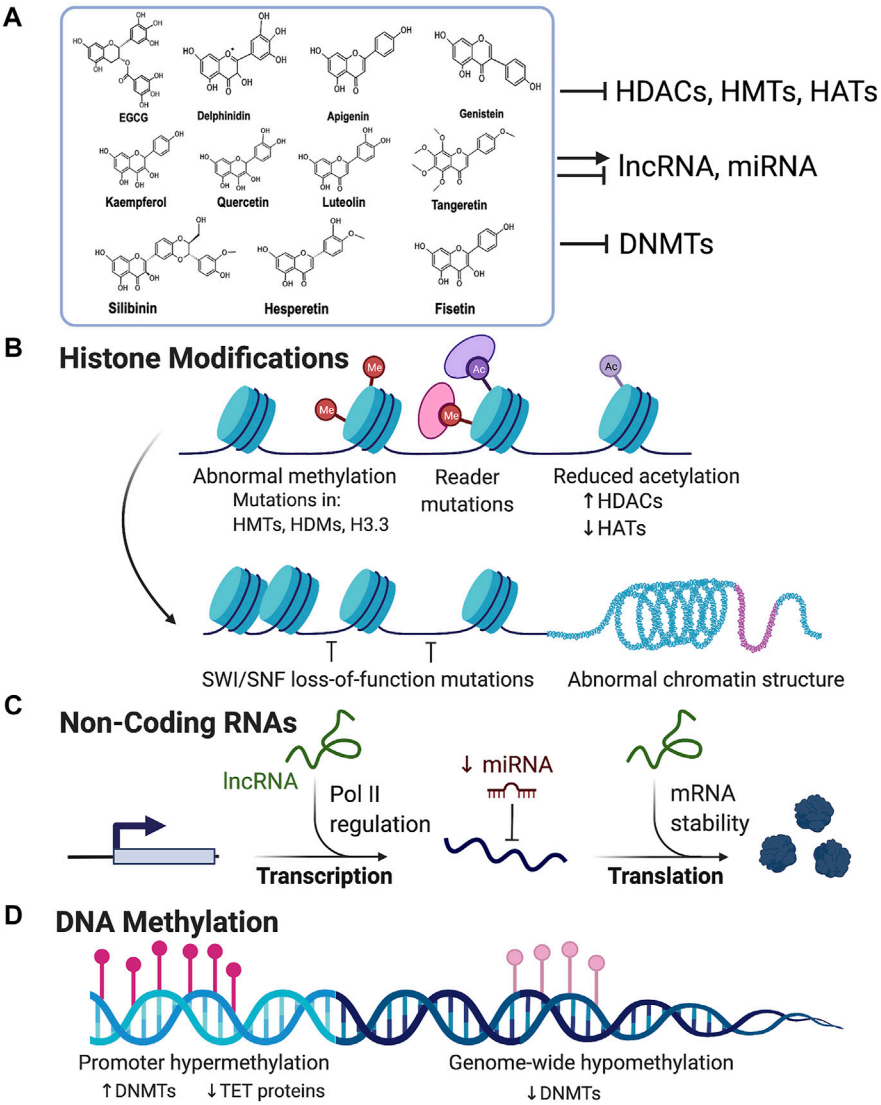

FIGURE 2 | Flavonoids as epigenetic modulators in cancer: **(A)** Flavonoids are polyhydroxy compounds found in various plants and generally consist of two phenyl rings and a heterocyclic ring. Flavonoids are reported to exhibit inhibitory activity for HDACs, HMTs, HATs, and DNMTs. They can also either inhibit or activate miRNA and lncRNA. **(B)** Illustration showing various mechanisms of histone modifications associated with carcinogenesis. Flavonoids can block the aberrant expression of HMTs, HATs, and HDACs, and activate tumor suppressor genes and block the expression of oncogenes. **(C)** Flavonoids can either activate or repress non-coding RNAs which regulates chromatin structure and aberrant gene expression in cancer. **(D)** Promoter hypermethylation and genome-wide hypomethylation are associated with cancer. Flavonoids can inhibit DNA Methyl Transferases (DNMTs) and thus prevent hypermethylation of gene promoters like tumor suppressor genes thereby reactivating their expression. (Created with BioRender.com).

promotes apoptosis and reactivates DNA methylation-silenced tumor suppressor genes in human breast cancer cells with unusual invasive prospective (Lubecka et al., 2018).

EGCG alters the expression of various tumor-suppressor genes by inhibiting DNA methyltransferases and histone deacetylases in human cervical cancer HeLa cells (Khan et al., 2015). Moreover, time-dependent exposure to EGCG resulted in reactivation of well-known tumor-suppressor genes (TSGs) in these cells due to marked transformations in the methylation of the promoter area of these genes (Khan et al., 2015). Recently Ciesielski et al., 2020 studied the impact of EGCG on the histone posttranslational modifications machinery along with chromatin remodeling in human endothelial cells (HMEC-1 and HUVECs origin). Results showed that EGCG increases methylation of both active (H3K4me3) and repressive (H3K9me3) chromatin marks and histone acetylation (H3K9/14ac, H3ac). These results indicated the broad epigenetic potential of EGCG concerning expression and action of epigenome modulators including HDAC5, and HDAC7, CREBP, KMT2A, p300 and LSD1 (Ciesielski et al., 2020).

Another study reported the anticancer mechanism of EGCG *via* synchronized transcriptional modification of numerous

TABLE 1 | Epigenetic modulations by some potent flavonoids (↑ increase, ↓ decrease).

Phytochemical	Dose	Epigenic modulation	Gene targets	Cancer type	Cancer cell line	Biological approach	Biological effect	References
EGCG (Flavanol)	0–100 μM	↓ DNMT	*SCUBE2*, vimentin	Breast cancer	MCF-7 and MDA-MB-231	*in vitro*	↓ Cell viability, ↓ Cell migration ↓ Invasion	Sheng et al. (2019)
	5–50 M	↓ DNMT	p16, *RARB*, *MGMT*, *hMLH1*	Esophageal, prostate and colon cancer	KYSE 510, PC3, HT-29, KYSE 150	*in vitro/ in silico*	↑ Apoptosis	Fang et al. (2003)
		↓ DNMT ↓ HDAC	*GAS1*, *TIMP4*, *ICAM1,* and *WISP2*	Non-small-cell lung cancer	NSCLC, A549/DDP	*in vitro/in vivo*	↓ Cell proliferation ↑ Apoptosis	Zhang et al. (2015)
	0.5% in diet	↓ DNMT1	*Cdh13*, *Prdm2*, and *Runx3*	Lung cancer	-	*in vivo*	p-AKT, and γ-H2AX inductions	Jin et al. (2015)
	20 μM	↓ HDAC	*MMP-2/MMP-9, EZH2,* and *TIMP*-3	Prostate cancer	DUPRO and LNCaP cells	*in vitro/ clinical trial*	↓ Cell invasion and migration	Deb et al. (2019)
	5–20 μM	↓ HDAC1, 2, 3 and 8	p53	Prostate cancer	LNCaP	*in vitro*	↑ Apoptosis Cell cycle arrest	Thakur et al. (2012)
	50 μM	↓ HAT	p300	Prostate cancer	LNCaP, PC3	*in vitro*	↑ Apoptosis	Lee et al. (2012)
	1–10 μg/ml	↓ DNMT	*GSTP1*, *S100P*	Prostate cancer	LNCaP	*in vitro*	↑ Apoptosis growth arrest	Pandey et al. (2010)
	0.2–400 μM	↓ mRNA	*Ccna2*, *Ccnb1*, *Ccnd1*, *Ccne1*, *E2f1*, *Dr5*, *p21*, *Cd24*, *Cd133*, *Abcg2*, *Eed*, *Ezh2*, and *Suz12*	Biliary tract cancer	CCSW-1, EGI-1, GBC, MzChA-1, MzChA-2, TFK-1, BDC and SkChA-1	*in vitro*	↑ Apoptosis ↓Cell viability Cell cycle arrest ↑ caspase activity	Mayr et al. (2015)
	25 μM	↓ DNMT ↓ HDAC	*RARβ*, *CDH1*, *DAPK1*	Cervical cancer	HeLa	*in vitro/in silico*	↑ Apoptosis	Khan et al. (2015)
	-	↓ DNMT1, ↓ HDAC1, ↓ HDAC2	p27, *CAF*, C/*EBPα*, C/*EBPε, EZH2*, *SUZ12*, and *EED*	Promyelocytic leukemia	-	*in vitro*	↑ Apoptosis Cell cycle arrest	Borutinskaitė et al. (2018)
		↓ HDAC	p53, p21	Lung cancer	PC-9	*in vitro*	↑ Apoptosis	Oya et al. (2017)
Quercetin (Flavonol)	20 μM/L	hnRNPA1	-	Pancreatic, thyroid cancer	CD18, K1 and 8505c, MDA-T85	*in vitro/in vivo*	↑ Apoptosis, ↓Cell proliferation	Pham et al. (2019)
	20–60 μM	↓DNMT1 ↓HDAC1	NF-κB p65, $p16^{INK4α}$	Esophageal cancer	9,706	*in vitro*	↑Apoptosis	Zheng et al. (2014)
	50 μM/L	↓HDAC1 ↓DNMT1 and ↓DNMT3a ↑mRNA	*DAPK1*, *BCL2L11*, *BAX*, *APAF1*, *BNIP3*, and *BNIP3L*	Leukemia	HL60 and U937	*in vitro/in vivo*	Cell cycle arrest ↑ Apoptosis ↑ Bax Activity ↑caspase Activity	Alvarez et al. (2018)
Kaempferol (Flavonol)	1.25–5 μM	↓DNMT1	*DACT2*	Colorectal Cancer	HCT116, HT29, and YB5	*in vitro/in vivo/in silico*	↑ Apoptosis ↓Proliferation ↓Migration Wnt/β-catenin pathway	Lu et al. (2018)
	50–200 μM	↓HDAC2, 4, 7 or 8	-	Hepatoma and colon cancer	HepG2, Hep3B HCT-116	*in vitro/in silico*	↑ Apoptosis ↓ cell proliferation	Berger et al. (2013)
	50 μM	↓HDAC	p62 and *ATG5*	Gastric cancer	AGS, SNU-216, NCI-N87, SNU-638, and MKN-74	*in vitro*	↑Autophagy ↑Cell death ↓ Cell viability ↑caspase Activity AMPKα/ULK1 and mTOR/p70S6K pathways	Kim et al. (2018)

(Continued on following page)

TABLE 1 | (*Continued*) Epigenetic modulations by some potent flavonoids (↑ increase, ↓ decrease).

Phytochemical	Dose	Epigenic modulation	Gene targets	Cancer type	Cancer cell line	Biological approach	Biological effect	References
Fisetin (Flavonol)	0–400 μM 160-mg/kg	histone demethylation	*RFXAP* and *KDM4A*	Pancreatic adenocarcinoma	BxPC-3, MiaPACA-2, PANC-1, and HPC-Y5	*in vitro/in vivo*	↑ Apoptosis ↓ Cell proliferation DNA damage Cell cycle arrest	Ding et al. (2020)
Apigenin (Flavone)	20–40 μM	↓ HDAC1 and HDAC3 ↑bax, ↓ bcl2	p21	Prostate cancer	PC-3 and 22Rv1	*in vitro/in vivo*	↑ Apoptosis Cell cycle arrest	Pandey et al. (2012)
	-	↓HDAC Induce histone acetylation	*CDK1* and p21	Breast cancer	MDA-MB-231	*in vitro/in vivo*	↓Cell proliferation Cell cycle arrest	Tseng et al. (2017)
Luteolin (Flavone)	0–30 μM	↓ AKT/mTOR-inducing H3K27Ac and H3K56Ac	*MMP9*	Breast cancer	Triple-negative breast cancer cells	*in vitro*	↓Cell proliferation, ↓Metastasis	Wu et al. (2021)
	-	↓ DNMT	*UHRF1* and p16	Colorectal cancer	-	*in vitro*	↑Cytotoxicity, Cell cycle perturbation	Krifa et al. (2014)
Tangeretin derivative (Flavone)	14.6 μM	↓ DNMT 3B and HDACs 1, 2, and 4/5/9	p21	Prostate cancer	LNCaP	*in vitro*	↑ Apoptosis, upregulated Bad and Bax, downregulated Bcl-2, and activated caspase-3 and PARP	Wei et al. (2019)
Hesperetin (Flavanone)	-	↓histone H3K79 methylation,	*DOT1L*	Gastric cancer	-	*in vitro/in vivo*	↓Cell migration and ↓Invasion	Wang et al. (2021a)
Silibinin (Flavanone)	25–75 μg/ml	↑DNMT, ↓HDACs1-2 ↑H3K27me3	*EZH2*	Prostate cancer	DU145 and PC3	*in vitro*	↑ Apoptosis	Anestopoulos et al. (2016)
Genistein (Isoflavone)	40 μM	DNA hypermethylation	*BRCA1*, *GSTP1*, *EPHB2,* and *BRCA2*	Prostate cancer	DU-145 and PC-3	*in vitro*	↓ Cancer cell growth	Adjakly et al. (2011)
	25–50 μM	↓ DNMT ↑HAT Histone modifications	*BTG3*	Prostate cancer	LNCaP, PC-3	*in vitro*	↑ Apoptosis	Majid et al. (2010)
	2–20 μM/L	↓ DNMT	*RARB*, p16, and *MGMT*	Esophageal cancer	KYSE 510	*in vitro*	↓ Cancer cell growth	Fang et al. (2005)
	75 μM/L	↓ DNMT	*WNT5a*	Colon cancer	DLD-1, SW480, and SW1116	*in vitro*	↓ Cell proliferation	Wang and Chen, (2010)
Delphinidin (Anthocyanidin)	10–100 μM	↓ DNMT1, ↓ DNMT3a, ↓ I/II HDACs).	*Hmox1*, *Nqo1,* and Sod1	Skin cancer	JB6 P+	*in vitro*	↑Apoptosis ↓Colony formation	Kuo et al. (2019)
	50–150 mM	↓ HDAC3	p53	Prostate cancer	LNCaP	*in vitro*	↑Apoptosis ↑ Caspase-3,7,8 activity	Jeong et al. (2016)

molecular targets through different signaling pathways in Hela cells (Kedhari Sundaram et al., 2020). In this study, transcriptional modulation of several epigenetic modifiers including histone modifiers and DNA methyltransferases (DNMT1, DNMT3A, DNMT3B, AURKA, AURKB, AURKC, PRMT6, PRMT7, KDM4A, KDM5C, HDAC5, HDAC6, HDAC7, HDAC11 and UBE2B) were observed. Downregulation of key signaling moieties of PI3K, Wnt and MAPK pathways, metastasis regulators, cell cycle regulators and pro-inflammatory moieties including CCNB1, CCNB2, TERT, PIK3C2B, PIK3CA, IL6, MMP2, MMP7 and MAPK8 were also detected (Kedhari Sundaram et al., 2020).

Kang et al., demonstrated that EGCG may hamper efficiently IR-induced injury to mouse normal hepatic cells (AML-12), and

improve noticeably the radio-sensitivity of mouse hepatoma cells H22 to ^{60}Coγ. They also revealed that EGCG played the key task of radio-sensitization on H22 cells because it activates the miR-34a/Sirt1/p53 signaling pathway (Kang et al., 2019). Deb *et al.*, reported that treatment of human prostate cancer cell lines (DUPro and LNCaP) with green tea polyphenols (GTPs) and their major constituent, epigallocatechin-3-gallate (EGCG) induced TIMP3 expression by epigenetic mechanisms (Deb et al., 2019). Furthermore, a clinical study on patients undergoing prostatectomy consuming EGCG showed an increase in plasma TIMP3 levels (Deb et al., 2019).

Dietary flavonoids have potential to modulate non-coding RNAs, including miRNAs in cancer (Ahmed et al., 2020; Yang et al., 2020; Singh et al., 2021). In a recent *in vivo* study by Kang et al., revealed that oral administration of EGCG suppresses miR483–3p induced metastasis of hepatocellular carcinoma (Kang et al., 2021). EGCG modulate non-coding RNAs and inhibit tumor growth by targeting LINC00511/miR-29b/KDM2A axis in gastric cancer (Zhao et al., 2020). EGCG-capped gold nanoparticle significantly increased expression of tumor suppressor let-7a and miR-34a miRNAs (Mostafa et al., 2020).

Flavonols

Flavonols (3-hydroxylavones) are most prevalent flavonoids in food. Quercetin, myricetin, kaempferol and fisetin are the most common plant flavonols found in many vegetables and fruits, e.g., onions, apples, strawberries etc. The defensive impacts of quercetin on human health are facilitated by multidimensional, pleiotropic action still from an epigenetic perspective (Russo and Ungaro, 2019).

Quercetin modulates the expression of various chromatin modifiers and declines the activity of HDACs, DNMTs and HMTs in a dose-dependent manner in human cervical cancer (HeLa) cells (Kedhari Sundaram et al., 2019). It also downregulated global DNA methylation concentrations in a dose- and time-dependent manner and tested tumor suppressor genes showed steep dose-dependent decrease in promoter methylation with the restoration of their expression. Quercetin along with BET inhibitors promoted apoptosis and decreases the cell proliferation and sphere-forming ability by pancreatic cancer cells. It was also evidenced that quercetin also mediates some anti-tumor effects with the help of hnRNPA1 which is a nuclear protein well-known to monitor mRNA export and mRNA translation of anti-apoptotic proteins (Pham et al., 2019). Quercetin also induced let-7c which decreased pancreatic tumor growth by posttranscriptional activation of Numbl and indirect inhibition of Notch (Nwaeburu et al., 2016); Zheng et al. (2014) reported that nanoliposomal quercetin combined with butyrate modulated aberrant epigenetic alteration in Eca9706 cells *via* epigenetic-NF-κB signaling. In this study reverse expressions of global DNMT1, HDAC1, NF-κB p65 and Cyclin D1 were down-regulated, although expressions of p16INK4α and caspase-3 were up-regulated. Furthermore, quercetin modulate miR-1-3p/TAGLN2 (Wang et al., 2021b), miR-197/IGFBP5 (Hu et al., 2020), miR-16–5p/WEE1 (Wang et al., 2020a), miR-22/WNT1/β-catenin (Zhang et al., 2019a), miR-16/HOXA10 (Zhao et al., 2019), TP53/miR-15/miR-16 (Ahmed Youness et al., 2018) axes as well as miR15a/16 (Ramos et al., 2021), miR-200b-3p (Nwaeburu et al., 2017), miR-145 (Zhou et al., 2015), and miR-146a (Tao et al., 2015) in various cancers.

Kaempferol (3,4′,5,7-tetrahydroxyflavone) is a potential HDAC inhibitor and an anti-cancer agent against many types of cancers (Imran et al., 2019). Berger *et al.*, reported first time that kaempferol has a distinctive epigenetic activity by inhibition of HDACs (Berger et al., 2013). The *in-silico* docking analysis fits kaempferol into binding pocket of HDAC2, 4, 7 or 8 and *in vitro* profiling of all conserved human HDACs of class I, II and IV demonstrated that it inhibited all tested HDACs. Furthermore, kaempferol stimulates hyperacetylation of histone H3 in HepG2 and Hep3B (hepatoma cancer cell lines) as well as on HCT-116 (colon cancer cell line) (Berger et al., 2013). Kaempferol induces autophagic cell death *via* IRE1-JNK-CHOP signaling and inhibiting HDAC/G9a axis in gastric cancer cells (Kim et al., 2018). In lung cancer A549 cell, kaempferol induces miR-340 expression (Han et al., 2018) which is known to induce apoptosis and inhibit cell proliferation in NSCLC (Fernandez et al., 2014).

Flavonol, fisetin is also a powerful anticancer agent, used to inhibit different stages of cancer cells, induce apoptosis, inhibit cell growth, prevent cell cycle progression, cause PARP cleavage, and modulate the expressions of Bcl-2 family proteins in various cancer cell lines (Imran et al., 2020). It also suppresses the activation of the ROS/ PKCα/ p38 MAPK and ERK1/2 signaling pathways, down-regulates the level of the oncoprotein securin and lowers the NF-κB activation (Pal et al., 2016). Recently, Ding *et al.*, revealed that fisetin inhibits proliferation of pancreatic adenocarcinoma by inducing DNA damage *via* RFXAP/KDM4A-dependent histone H3K36 demethylation (Ding et al., 2020).

Flavones

Flavones are a group of flavonoids that contain the backbone of 2-phenylchromen-4-one (2-phenyl-1-benzopyran-4-one) having diverse pharmacological properties and are commonly found in herbs such as celery, parsley and in almost all edible cereal species. Apigenin, luteolin, tangeretin, chrysin, Tricin, baicalein, rhoifolin and 6-hydroxyflavone are some common flavones (Barreca et al., 2020).

Pandey et al. (2012) reported first time that apigenin inhibits class I HDACs, particularly HDAC1 and HDAC3, alters chromatin to induce growth arrest and apoptosis in human prostate cancer cells. Apigenin inhibited MDA-MB-231 breast cancer cell proliferation and tumor growth by induction of G2/M arrest and histone H3 acetylation-mediated p21 expression (Tseng et al., 2017). Apigenin enhances miR-16 (Chen et al., 2016) and miRNA215–5p (Cheng et al., 2021) expression to inhibits glioma and colon cancer growth respectively, as well as chemo-sensitize doxorubicin-resistant liver cancer cells by targeting miR-520b/ATG7 axis (Gao et al., 2018).

Recently Wu et al. (2021) discovered that luteolin inhibited the proliferation and metastasis of androgen receptor-positive triple-negative breast cancer cell by epigenetic regulation of MMP9 expression through a reduction in the levels of

AKT/mTOR-inducing H3K56Ac and H3K27Ac. Earlier it was also revealed that luteolin suppresses the metastasis of triple-negative breast cancer, downregulates the *ß*-catenin expression for reversing epithelial-to-mesenchymal transition (Lin et al., 2017). In colorectal cancer cells Luteolin induces apoptosis by the downregulations of UHRF1, calpain, and DNMT1 expressions. This research further suggests that calpain might be involved in the epigenetic code inheritance by regulating the epigenetic integrator UHRF1(Krifa et al., 2014). In human prostate cancer (PC-3) cells, Luteolin and gefitinib regulate cell cycle pathway genes (*CCNA2*, *CCNE2*, *CDC25A*, *CDKN1B*, and *PLK*-1) through a mutual mechanism involving EGFR-associated tyrosine kinase (Markaverich et al., 2010). Authors suggested that these phytochemicals likely modulate the epigenetic control of gene expression as previously shown by their group that luteolin interacts with type II binding sites on histone H4 (Shoulars et al., 2010). Recently, Farooqi et al. and Mishan et al. have systematically reviewed the potent ability of luteolin to modulate miRNA expression in various cancers (Farooqi et al., 2020; Mishan et al., 2021). A derivative of tangeretin prevents the progress of human prostate cancer cells by epigenetically restoring p21 gene expression and inhibits cancer stem-like cell proliferation (Wei et al., 2019).

Baicalein (5,6,7-trihydroxyflavone) suppresses cancer cell proliferation, cell cycle arrest and induces apoptosis in human prostate, breast, T24 bladder and myeloma cancer cells (Gao et al., 2016). Lai *et al.*, studied the epigenetic role of baicalin hydrate in nasopharyngeal carcinoma (NPC) and identified that it inhibits NPC cell growth both *in vivo* and *in vitro*. Furthermore, instead of DNA methylation, baicalin hydrate increased of m6A RNA methylation and promoted Suv39H1 gene splicing. (Lai et al., 2018). It is also documented that baicalin improves the developmental proficiency of *in vitro* cultured mouse embryos through reticence of cellular apoptosis and HSP70 expression and enhancement of DNA methylation (Qi et al., 2016). Several recent studies have shown that baicalein modulate the expression of miR-183 (Lei et al., 2021), miR-139–3p and miR-196b-5p (Ma et al., 2021), and miR-25 (Örenlil Yaylagül and Ülger, 2020) in various cancers.

Flavanones

Flavanones are aromatic, colourless ketones mainly present in citrus fruits (Barreca et al., 2017). Hesperetin, isosakuranetin, naringin, naringenin, isosakuranetin and eriodictyol and their particular glycosides are some main flavanones (Khan et al., 2013). Hesperetin is a common citrus flavanone that endorses DOT1L degradation and decreases histone H3K79 methylation to prevent gastric cancer metastasis, showing its epigenetic effect (Wang et al., 2021a). Natural flavonolignan, silibinin is the most effective phytochemical of silymarin. It is active both alone and in combination with other chemotherapeutic and epigenetic agents, substantially inhibit the growth of different cancer cells. It synergizes with DNA methyltransferase and histone deacetylase inhibitors in upregulating e-cadherin expression, also inhibits the invasion and migration of human non-small cell lung cancer cells. These results are highly substantial since failure of E-cadherin and metastatic dispersed of the illness *via* epithelial-to-mesenchymal transition is associated with poor prognosis and high mortalities in this type of cancer cells (Mateen et al., 2013). In human prostate cancer (DU145 and PC3) cells, silibinin reduces gene expression levels of EZH2 accompanied by an increase in H3K27me3 levels (Anestopoulos et al., 2016). Such responses were dependent on decreased expression levels of phosphorylated EZH2 (ser21) and phosphorylated Akt (ser473). Moreover, it also exerted other epigenetic impacts involving, decrease histone deacetylases 1–2 (HDACs1-2) expression levels while it increases total DNA methyltransferase (DNMT) activity, proving that it induces epigenetic alterations in human prostate cancer cells. (Anestopoulos et al., 2016). Hossainzadeh et al. reported that silibinin encapsulated in polymersome nanoparticles supress the expression of oncogenic miRNAs miR-125b and miR-182 (Hossainzadeh et al., 2019).

Naringenin (4,5,7 trihydroxyflavanone) is an aglycone form of naringin found in citrus fruits. When it combined with suberoylanilide hydroxamic acid (HDAC inhibitor), synergistically improved transamidation activity and suberoylanilide hydroxamic acid induced cytotoxicity in neuroblastoma cells which showed no cytotoxicity on normal non-malignant cells (Ling et al., 2012). This suggest that naringenin possesses effective histone deacetylase inhibitory activity; however, more comprehensive studies are needed understand its epigenetic potential.

Isoflavones

Isoflavones are naturally occurring isoflavonoids, mainly found in legumes, soy beans, and soy foods. They have several potent pharmacological activities like anti-inflammatory, antioxidant, antimicrobial, and anticancer (Panche et al., 2016). It is also well evidential that they exert estrogenic and/or antiestrogenic impacts. Isoflavones are considered as chemoprotective in nature and used in various type of alternative therapies for a broad range of hormonal ailments including several types of cancers, osteoporosis, menopausal problems and cardiovascular diseases (Taku et al., 2011; Vitale et al., 2012; Qin et al., 2013; Sathyapalan et al., 2018; Nakai et al., 2020). There are conflicting reports that isoflavones disrupt endocrine function; however, it appears the most common harmful effect is mild and appears at the gastrointestinal level (Křížová et al., 2019; Gómez-Zorita et al., 2020). Some common examples of isoflavones are Daidzein, Genistein, Genistin and Glycitein.

Among all isoflavones, genistein is the most potent and biologically active phytochemical, demonstrating different *in vivo* and *in vitro* anticancer and anti-proliferative effects on numerous types of human cancers (Spagnuolo et al., 2015). Prostate cell lines (DU-145 and PC-3) when treated with soy phytoestrogens, genistein and daidzein, cause decrease in DNA methylation at *EPHB2*, *BRCA1* and *GSTP1* promoters (Adjakly et al., 2011). Karsli-Ceppioglu *et al.*, reported that phytoestrogens (genistein and daidzein) modulate genome-wide DNA methylation status in prostate cancer. They found that methylation profiles of 58 genes have been modified by genistein and daidzein treatments in prostate cancer DU-145

and LNCaP cell lines (Karsli-Ceppioglu et al., 2015). Notably, the methylation frequencies of the *hTERT*, *MAD1L1*, *KDM4B* and *TRAF7* genes were remarkably altered by genistein treatment. Genistein regulates miRNAs expression in pan cancer (Javed et al., 2021). In head and neck cancer, genistein activate miR-34a/RTCB axis that results in ROS-associated apoptosis, decrease in stemness properties, and inhibition of EMT (Hsieh et al., 2020). Recently, Imai-Sumida *et al.*, reported that genistein suppress kidney cancer by repressing HOTAIR/chromatin remodeling pathways (Imai-Sumida et al., 2020). Conversely, Allred *et al.*, reported that dietary genistin as well as genistein can stimulates estrogen-dependent breast cancer cell growth *in vivo* (Allred et al., 2001). These conflicting reports compel a need for in-depth mechanistic studies to understand the biological effects of these dietary compounds, including their epigenetic modifying potentials, cytotoxicity, and anticancer properties.

Anthocyanidins

Anthocyanidins are the sugar-free counterparts of anthocyanins and are highly important water-soluble pigments found in plants. Among all anthocyanidins, delphinidin is the most potent and abundant flavonoid found in pigmented fruits (especially blueberry) and vegetables (Khoo et al., 2017).

Kuo *et al.*, reported that delphinidin epigenetically re-activates Nrf2-ARE pathway and prevents neoplastic transformation of mouse skin JB6 P+ cells (Kuo et al., 2019). The Nrf2-ARE pathway activation was associated with demethylation of 15 CpG sites in the mouse Nrf2 promoter region between nucleotide -1,226 and -863 from the transcription start site. The decreased CpG methylation proportion in the Nrf2 promoter region was consistent with detected declines in the protein expression of DNA methyltransferases 1 (DNMT1), DNMT3a, and class I/II histone deacetylases (HDACs) (Kuo et al., 2019). Jeong *et al.*, identified the epigenetic modulators that mediate the apoptotic effect of delphinidin (major anthocyanidin compound) in human prostate cancer cells (Jeong et al., 2016). They treated these cancer cells with delphinidin and observed an increase in caspase-3, -7, and -8 activity along with an increased histone deacetylase activity. Amongst all class I HDACs, the activity of HDAC3 was exclusively prevented by delphinidin. Moreover, the apoptosis induced by delphinidin was reliant on caspase-mediated cleavage of HDAC3, resulting in the stabilization and acetylation of p53. They also observed that this anthocyanidin effectively upregulated pro-apoptotic genes that are definitely regulated by p53 and also downregulated numerous anti-apoptotic genes (Jeong et al., 2016). Delphinidin targets HOTAIR/miR-34a axis to suppress the breast carcinogenesis (Han et al., 2019) and inhibits colorectal cancer metastasis by inducing miR-204–3p expression (Huang et al., 2019).

CONCLUSION

The existing literatures on cancer pathobiology has established that genetics and epigenetics play a central role in cancer initiation and progression. The reversible nature of epigenetic changes can be exploit for a better therapeutic intervention. Epigenetic modifiers such as DNMTs, HATs, HMTs, HDACs, and others can be modulated or inhibited by naturally occurring substances such as phytochemicals (**Figure 2**). In this review, several flavonoids (e.g., flavones, flavanones, flavonols) were described along with their epigenetic modulation, therapeutic, and chemo-preventive potentials in cancer (**Table 1**). Various plant-based drugs, including vinca alkaloids (e.g., vinblastine and vincristine), taxanes (e.g., paclitaxel and docetaxel), camptothecins, and others are routinely used for cancer treatment. There are numerous phytochemicals, including flavonoids with potent anticancer activity are in various preclinical and clinical trial stages. However, there are some limitations, including their low water solubility, poor bioavailability, rapid uptake by normal cells, poor therapeutic index and adverse effects on liver. Developing novel strategies such as nanocarriers can overcome these drawbacks.

The emerging role of phytochemicals in cancer therapy and prevention is enormous. Their potential to rectify epigenetic alterations of cancer cells add substantial armaments in fight against cancer. Combinatorial therapies using plant-based epigenetic modifiers with existing chemo and targeted therapies can help manage the disease better and reduce the side effects. However, an extensive research is needed into identification and characterization of anticarcinogenic phytochemicals and their respective mechanisms of actions. Given the fast pace of technological developments, this seems to be a promising pursuit in our battle against cancer.

AUTHOR CONTRIBUTIONS

NF and SSRB wrote the initial manuscript draft; AB, NK-KK, and KH helped finalizing the figures, provided inputs in epigenetic components of the manuscript; and AA and RAA conceptualized, supervised, and finalized the draft.

REFERENCES

Abbas, A., Hall, J. A., Patterson, W. L., 3rd, Ho, E., Hsu, A., Al-Mulla, F., et al. (2016). Sulforaphane Modulates Telomerase Activity via Epigenetic Regulation in Prostate Cancer Cell Lines. *Biochem. Cel Biol.* 94, 71–81. doi:10.1139/bcb-2015-0038

Abbas, A., Patterson, W., 3rd, and Georgel, P. T. (2013). The Epigenetic Potentials of Dietary Polyphenols in Prostate Cancer Management. *Biochem. Cel Biol.* 91, 361–368. doi:10.1139/bcb-2012-0044

Adjakly, M., Bosviel, R., Rabiau, N., Boiteux, J.-P., Bignon, Y.-J., Guy, L., et al. (2011). DNA Methylation and Soy Phytoestrogens: Quantitative Study in DU-145 and PC-3 Human Prostate Cancer Cell Lines. *Epigenomics* 3, 795–803. doi:10.2217/epi.11.103

Ahmed, F., Ijaz, B., Ahmad, Z., Farooq, N., Sarwar, M. B., and Husnain, T. (2020). Modification of miRNA Expression through Plant Extracts and Compounds against Breast Cancer: Mechanism and Translational Significance. *Phytomedicine* 68, 153168. doi:10.1016/j.phymed.2020.153168

Ahmed Youness, R., Amr Assal, R., Mohamed Ezzat, S., Zakaria Gad, M., and Abdel Motaal, A. (2018). A Methoxylated Quercetin Glycoside Harnesses HCC Tumor Progression in a TP53/miR-15/miR-16 Dependent Manner. *Nat. Product. Res.* 34, 1475–1480. doi:10.1080/14786419.2018.1509326

Ali Syeda, Z., Langden, S. S. S., Munkhzul, C., Lee, M., and Song, S. J. (2020). Regulatory Mechanism of MicroRNA Expression in Cancer. *Int. J. Mol. Sci.* 21, 1723. doi:10.3390/ijms21051723

Allred, C. D., Ju, Y. H., Allred, K. F., Chang, J., and Helferich, W. G. (2001). Dietary Genistin Stimulates Growth of Estrogen-dependent Breast Cancer Tumors Similar to that Observed with Genistein. *Carcinogenesis* 22, 1667–1673. doi:10.1093/carcin/22.10.1667

Alvarez, M. C., Maso, V., Torello, C. O., Ferro, K. P., and Saad, S. T. O. (2018). The Polyphenol Quercetin Induces Cell Death in Leukemia by Targeting Epigenetic Regulators of Pro-apoptotic Genes. *Clin. Epigenet* 10, 139. doi:10.1186/s13148-018-0563-3

Anand, P., Kunnumakara, A. B., Sundaram, C., Harikumar, K. B., Tharakan, S. T., Lai, O. S., et al. (2008). Cancer Is a Preventable Disease that Requires Major Lifestyle Changes. *Pharm. Res.* 25, 2097–2116. doi:10.1007/s11095-008-9661-9

Anestopoulos, I., Sfakianos, A. P., Franco, R., Chlichlia, K., Panayiotidis, M. I., Kroll, D. J., et al. (2016). A Novel Role of Silibinin as a Putative Epigenetic Modulator in Human Prostate Carcinoma. *Molecules* 22. doi:10.3390/molecules22010062

Audia, J. E., and Campbell, R. M. (2016). Histone Modifications and Cancer. *Cold Spring Harb Perspect. Biol.* 8, a019521. doi:10.1101/cshperspect.a019521

Baer, C., Claus, R., and Plass, C. (2013). Genome-Wide Epigenetic Regulation of miRNAs in Cancer. *Cancer Res.* 73, 473–477. doi:10.1158/0008-5472.can-12-3731

Bannister, A. J., and Kouzarides, T. (2011). Regulation of Chromatin by Histone Modifications. *Cell Res* 21, 381–395. doi:10.1038/cr.2011.22

Barreca, D., Gattuso, G., Bellocco, E., Calderaro, A., Trombetta, D., Smeriglio, A., et al. (2017). Flavanones: Citrus Phytochemical with Health-Promoting Properties. *BioFactors* 43, 495–506. doi:10.1002/biof.1363

Barreca, D., Mandalari, G., Calderaro, A., Smeriglio, A., Trombetta, D., Felice, M. R., et al. (2020). Citrus Flavones: An Update on Sources, Biological Functions, and Health Promoting Properties. *Plants (Basel)* 9. doi:10.3390/plants9030288

Bennett, R. L., and Licht, J. D. (2018). Targeting Epigenetics in Cancer. *Annu. Rev. Pharmacol. Toxicol.* 58, 187–207. doi:10.1146/annurev-pharmtox-010716-105106

Berger, A., Venturelli, S., Kallnischkies, M., Böcker, A., Busch, C., Weiland, T., et al. (2013). Kaempferol, a New Nutrition-Derived Pan-Inhibitor of Human Histone Deacetylases. *J. Nutr. Biochem.* 24, 977–985. doi:10.1016/j.jnutbio.2012.07.001

Bird, A. (2002). DNA Methylation Patterns and Epigenetic Memory. *Genes Dev.* 16, 6–21. doi:10.1101/gad.947102

Blake, L. E., Roux, J., Hernando-Herraez, I., Banovich, N. E., Perez, R. G., Hsiao, C. J., et al. (2020). A Comparison of Gene Expression and DNA Methylation Patterns across Tissues and Species. *Genome Res.* 30, 250–262. doi:10.1101/gr.254904.119

Bonner, W. M., Redon, C. E., Dickey, J. S., Nakamura, A. J., Sedelnikova, O. A., Solier, S., et al. (2008). γH2AX and Cancer. *Nat. Rev. Cancer* 8, 957–967. doi:10.1038/nrc2523

Borutinskaitė, V., Virkšaitė, A., Gudelytė, G., and Navakauskienė, R. (2018). Green tea Polyphenol EGCG Causes Anti-cancerous Epigenetic Modulations in Acute Promyelocytic Leukemia Cells. *Leuk. Lymphoma* 59, 469–478. doi:10.1080/10428194.2017.1339881

Brower, V. (2011). Epigenetics: Unravelling the Cancer Code. *Nature* 471, S12–S13. doi:10.1038/471s12a

Busch, C., Burkard, M., Leischner, C., Lauer, U. M., Frank, J., and Venturelli, S. (2015). Epigenetic Activities of Flavonoids in the Prevention and Treatment of Cancer. *Clin. Epigenet* 7, 64. doi:10.1186/s13148-015-0095-z

Cammaerts, S., Strazisar, M., De Rijk, P., and Del Favero, J. (2015). Genetic Variants in microRNA Genes: Impact on microRNA Expression, Function, and Disease. *Front. Genet.* 6, 186. doi:10.3389/fgene.2015.00186

Carlos-Reyes, Á., López-González, J. S., Meneses-Flores, M., Gallardo-Rincón, D., Ruíz-García, E., Marchat, L. A., et al. (2019). Dietary Compounds as Epigenetic Modulating Agents in Cancer. *Front. Genet.* 10, 79. doi:10.3389/fgene.2019.00079

Cavalli, G., and Heard, E. (2019). Advances in Epigenetics Link Genetics to the Environment and Disease. *Nature* 571, 489–499. doi:10.1038/s41586-019-1411-0

Cheedipudi, S., Genolet, O., and Dobreva, G. (2014). Epigenetic Inheritance of Cell Fates during Embryonic Development. *Front. Genet.* 5, 19. doi:10.3389/fgene.2014.00019

Chen, X.-J., Wu, M.-Y., Li, D.-H., and You, J. (2016). Apigenin Inhibits Glioma Cell Growth through Promoting microRNA-16 and Suppression of BCL-2 and Nuclear Factor-Kb/mmp-9. *Mol. Med. Rep.* 14, 2352–2358. doi:10.3892/mmr.2016.5460

Cheng, Y., Han, X., Mo, F., Zeng, H., Zhao, Y., Wang, H., et al. (2021). Apigenin Inhibits the Growth of Colorectal Cancer through Down-Regulation of E2F1/3 by miRNA-215-5p. *Phytomedicine* 89, 153603. doi:10.1016/j.phymed.2021.153603

Cheung, H.-H., Lee, T.-L., Rennert, O. M., and Chan, W.-Y. (2009). DNA Methylation of Cancer Genome. *Birth Defect Res. C* 87, 335–350. doi:10.1002/bdrc.20163

Ciesielski, O., Biesiekierska, M., and Balcerczyk, A. (2020). Epigallocatechin-3-gallate (EGCG) Alters Histone Acetylation and Methylation and Impacts Chromatin Architecture Profile in Human Endothelial Cells. *Molecules* 25, 2326. doi:10.3390/molecules25102326

Dawson, M. A., and Kouzarides, T. (2012). Cancer Epigenetics: From Mechanism to Therapy. *Cell* 150, 12–27. doi:10.1016/j.cell.2012.06.013

Deaton, A. M., and Bird, A. (2011). CpG Islands and the Regulation of Transcription. *Genes Dev.* 25, 1010–1022. doi:10.1101/gad.2037511

Deb, G., Shankar, E., Thakur, V. S., Ponsky, L. E., Bodner, D. R., Fu, P., et al. (2019). Green tea-induced Epigenetic Reactivation of Tissue Inhibitor of Matrix Metalloproteinase-3 Suppresses Prostate Cancer Progression through Histone-Modifying Enzymes. *Mol. Carcinog* 58, 1194–1207. doi:10.1002/mc.23003

Di Cerbo, V., and Schneider, R. (2013). Cancers with Wrong HATs: the Impact of Acetylation. *Brief. Funct. Genomics* 12, 231–243. doi:10.1093/bfgp/els065

Ding, G., Xu, X., Li, D., Chen, Y., Wang, W., Ping, D., et al. (2020). Fisetin Inhibits Proliferation of Pancreatic Adenocarcinoma by Inducing DNA Damage via RFXAP/KDM4A-dependent Histone H3K36 Demethylation. *Cell Death Dis* 11, 893. doi:10.1038/s41419-020-03019-2

Egger, G., Liang, G., Aparicio, A., and Jones, P. A. (2004). Epigenetics in Human Disease and Prospects for Epigenetic Therapy. *Nature* 429, 457–463. doi:10.1038/nature02625

Esquela-Kerscher, A., and Slack, F. J. (2006). Oncomirs - microRNAs with a Role in Cancer. *Nat. Rev. Cancer* 6, 259–269. doi:10.1038/nrc1840

Esteller, M. (2007). Cancer Epigenomics: DNA Methylomes and Histone-Modification Maps. *Nat. Rev. Genet.* 8, 286–298. doi:10.1038/nrg2005

Fang, M. Z., Wang, Y., Ai, N., Hou, Z., Sun, Y., Lu, H., et al. (2003). Tea Polyphenol (-)-Epigallocatechin-3-Gallate Inhibits DNA Methyltransferase and Reactivates Methylation-Silenced Genes in Cancer Cell Lines. *Cancer Res.* 63, 7563–7570.

Fang, M. Z., Chen, D., Sun, Y., Jin, Z., Christman, J. K., and Yang, C. S. (2005). Reversal of Hypermethylation and Reactivation ofp16INK4a, RARβ, andMGMTGenes by Genistein and Other Isoflavones from Soy. *Clin. Cancer Res.* 11, 7033–7041. doi:10.1158/1078-0432.ccr-05-0406

Farooqi, A. A., Butt, G., El-Zahaby, S. A., Attar, R., Sabitaliyevich, U. Y., Jovic, J. J., et al. (2020). Luteolin Mediated Targeting of Protein Network and microRNAs in Different Cancers: Focus on JAK-STAT, NOTCH, mTOR and TRAIL-Mediated Signaling Pathways. *Pharmacol. Res.* 160, 105188. doi:10.1016/j.phrs.2020.105188

Fernandez, S., Risolino, M., Mandia, N., Talotta, F., Soini, Y., Incoronato, M., et al. (2014). miR-340 Inhibits Tumor Cell Proliferation and Induces Apoptosis by Targeting Multiple Negative Regulators of P27 in Non-small Cell Lung Cancer. *Oncogene* 34, 3240–3250. doi:10.1038/onc.2014.267

Fraga, M. F., Ballestar, E., Villar-Garea, A., Boix-Chornet, M., Espada, J., Schotta, G., et al. (2005). Loss of Acetylation at Lys16 and Trimethylation at Lys20 of Histone H4 Is a Common Hallmark of Human Cancer. *Nat. Genet.* 37, 391–400. doi:10.1038/ng1531

Friedman, R. C., Farh, K. K., Burge, C. B., and Bartel, D. P. (2009). Most Mammalian mRNAs Are Conserved Targets of microRNAs. *Genome Res.* 19, 92–105. doi:10.1101/gr.082701.108

Galati, G., and O'brien, P. J. (2004). Potential Toxicity of Flavonoids and Other Dietary Phenolics: Significance for Their Chemopreventive and Anticancer Properties. *Free Radic. Biol. Med.* 37, 287–303. doi:10.1016/j.freeradbiomed.2004.04.034

Gao, A.-M., Zhang, X.-Y., Hu, J.-N., and Ke, Z.-P. (2018). Apigenin Sensitizes Hepatocellular Carcinoma Cells to Doxorubic through Regulating miR-520b/ATG7 axis. *Chemico-Biological Interactions* 280, 45–50. doi:10.1016/j.cbi.2017.11.020

Gao, F., and Das, S. K. (2014). Epigenetic Regulations through DNA Methylation and Hydroxymethylation: Clues for Early Pregnancy in Decidualization. *Biomol. Concepts* 5, 95–107. doi:10.1515/bmc-2013-0036

Gao, Y., Snyder, S. A., Smith, J. N., and Chen, Y. C. (2016). Anticancer Properties of Baicalein: a Review. *Med. Chem. Res.* 25, 1515–1523. doi:10.1007/s00044-016-1607-x

Giudice, A., Montella, M., Boccellino, M., Crispo, A., D'arena, G., Bimonte, S., et al. (2018). Epigenetic Changes Induced by Green Tea Catechins a Re Associated with Prostate Cancer. *Curr. Mol. Med.* 17, 405–420. doi:10.2174/1566524018666171219101937

Gómez-Zorita, S., González-Arceo, M., Fernández-Quintela, A., Eseberri, I., Trepiana, J., and Portillo, M. P. (2020). Scientific Evidence Supporting the Beneficial Effects of Isoflavones on Human Health. *Nutrients* 12, 3853. doi:10.3390/nu12123853

Greenberg, M. V. C., and Bourc'his, D. (2019). The Diverse Roles of DNA Methylation in Mammalian Development and Disease. *Nat. Rev. Mol. Cel Biol* 20, 590–607. doi:10.1038/s41580-019-0159-6

Han, B., Peng, X., Cheng, D., Zhu, Y., Du, J., Li, J., et al. (2019). Delphinidin Suppresses Breast Carcinogenesis through the HOTAIR/micro RNA -34a axis. *Cancer Sci.* 110, 3089–3097. doi:10.1111/cas.14133

Han, X., Liu, C.-F., Gao, N., Zhao, J., and Xu, J. (2018). Kaempferol Suppresses Proliferation but Increases Apoptosis and Autophagy by Up-Regulating microRNA-340 in Human Lung Cancer Cells. *Biomed. Pharmacother.* 108, 809–816. doi:10.1016/j.biopha.2018.09.087

Henning, S. M., Wang, P., Carpenter, C. L., and Heber, D. (2013). Epigenetic Effects of green tea Polyphenols in Cancer. *Epigenomics* 5, 729–741. doi:10.2217/epi.13.57

Herman, J. G., and Baylin, S. B. (2003). Gene Silencing in Cancer in Association with Promoter Hypermethylation. *N. Engl. J. Med.* 349, 2042–2054. doi:10.1056/nejmra023075

Hossainzadeh, S., Ranji, N., Naderi Sohi, A., and Najafi, F. (2019). Silibinin Encapsulation in Polymersome: A Promising Anticancer Nanoparticle for Inducing Apoptosis and Decreasing the Expression Level of miR-125b/miR-182 in Human Breast Cancer Cells. *J. Cel Physiol* 234, 22285–22298. doi:10.1002/jcp.28795

Hou, Y., Zhang, R., and Sun, X. (2019). Enhancer LncRNAs Influence Chromatin Interactions in Different Ways. *Front. Genet.* 10, 936. doi:10.3389/fgene.2019.00936

Hsieh, P. L., Liao, Y. W., Hsieh, C. W., Chen, P. N., and Yu, C. C. (2020). Soy Isoflavone Genistein Impedes Cancer Stemness and Mesenchymal Transition in Head and Neck Cancer through Activating miR-34a/RTCB Axis. *Nutrients* 12, 1924. doi:10.3390/nu12071924

Hu, S. A., Cheng, J., Zhao, W. H., and Zhao, H. Y. (2020). Quercetin Induces Apoptosis in Meningioma Cells through the miR-197/IGFBP5 cascade. *Environ. Toxicol. Pharmacol.* 80, 103439. doi:10.1016/j.etap.2020.103439

Huang, C. C., Hung, C. H., Hung, T. W., Lin, Y. C., Wang, C. J., and Kao, S. H. (2019). Dietary Delphinidin Inhibits Human Colorectal Cancer Metastasis Associating with Upregulation of miR-204-3p and Suppression of the Integrin/FAK axis. *Sci. Rep.* 9, 18954. doi:10.1038/s41598-019-55505-z

Huarte, M. (2015). The Emerging Role of lncRNAs in Cancer. *Nat. Med.* 21, 1253–1261. doi:10.1038/nm.3981

Imai-Sumida, M., Dasgupta, P., Kulkarni, P., Shiina, M., Hashimoto, Y., Shahryari, V., et al. (2020). Genistein Represses HOTAIR/Chromatin Remodeling Pathways to Suppress Kidney Cancer. *Cell Physiol Biochem* 54, 53–70. doi:10.33594/000000205

Imran, M., Salehi, B., Sharifi-Rad, J., Aslam Gondal, T., Saeed, F., Imran, A., et al. (2019). Kaempferol: A Key Emphasis to its Anticancer Potential. *Molecules* 24. doi:10.3390/molecules24122277

Imran, M., Saeed, F., Gilani, S. A., Shariati, M. A., Imran, A., Afzaal, M., et al. (2020). Fisetin: An Anticancer Perspective. *Food Sci. Nutr.* 9, 3–16. doi:10.1002/fsn3.1872

Izzo, S., Naponelli, V., and Bettuzzi, S. (2020). Flavonoids as Epigenetic Modulators for Prostate Cancer Prevention. *Nutrients* 12, 1010. doi:10.3390/nu12041010

Javed, Z., Khan, K., Herrera-Bravo, J., Naeem, S., Iqbal, M. J., Sadia, H., et al. (2021). Genistein as a Regulator of Signaling Pathways and microRNAs in Different Types of Cancers. *Cancer Cel Int* 21, 388. doi:10.1186/s12935-021-02091-8

Jeong, M.-H., Ko, H., Jeon, H., Sung, G.-J., Park, S.-Y., Jun, W. J., et al. (2016). Delphinidin Induces Apoptosis via Cleaved HDAC3-Mediated P53 Acetylation and Oligomerization in Prostate Cancer Cells. *Oncotarget* 7, 56767–56780. doi:10.18632/oncotarget.10790

Jiang, W., Xia, T., Liu, C., Li, J., Zhang, W., and Sun, C. (2021). Remodeling the Epigenetic Landscape of Cancer-Application Potential of Flavonoids in the Prevention and Treatment of Cancer. *Front. Oncol.* 11, 705903. doi:10.3389/fonc.2021.705903

Jin, H., Chen, J. X., Wang, H., Lu, G., Liu, A., Li, G., et al. (2015). NNK-induced DNA Methyltransferase 1 in Lung Tumorigenesis in A/J Mice and Inhibitory Effects of (−)-Epigallocatechin-3-Gallate. *Nutr. Cancer* 67, 167–176. doi:10.1080/01635581.2015.976314

Jones, P. A. (2012). Functions of DNA Methylation: Islands, Start Sites, Gene Bodies and beyond. *Nat. Rev. Genet.* 13, 484–492. doi:10.1038/nrg3230

Jucá, M. M., Cysne Filho, F. M. S., De Almeida, J. C., Mesquita, D. D. S., Barriga, J. R. D. M., Dias, K. C. F., et al. (2018). Flavonoids: Biological Activities and Therapeutic Potential. *Nat. Product. Res.* 34, 692–705. doi:10.1080/14786419.2018.1493588

Kang, Q., Zhang, X., Cao, N., Chen, C., Yi, J., Hao, L., et al. (2019). EGCG Enhances Cancer Cells Sensitivity under 60Coγ Radiation Based on miR-34a/Sirt1/p53. *Food Chem. Toxicol.* 133, 110807. doi:10.1016/j.fct.2019.110807

Kang, Q., Tong, Y., Gowd, V., Wang, M., Chen, F., and Cheng, K.-W. (2021). Oral Administration of EGCG Solution Equivalent to Daily Achievable Dosages of Regular tea Drinkers Effectively Suppresses miR483-3p Induced Metastasis of Hepatocellular Carcinoma Cells in Mice. *Food Funct.* 12, 3381–3392. doi:10.1039/d1fo00664a

Karlic, R., Chung, H.-R., Lasserre, J., Vlahovicek, K., and Vingron, M. (2010). Histone Modification Levels Are Predictive for Gene Expression. *Proc. Natl. Acad. Sci.* 107, 2926–2931. doi:10.1073/pnas.0909344107

Karsli-Ceppioglu, S., Ngollo, M., Adjakly, M., Dagdemir, A., Judes, G., Lebert, A., et al. (2015). Genome-wide DNA Methylation Modified by Soy Phytoestrogens: Role for Epigenetic Therapeutics in Prostate Cancer? *OMICS: A J. Integr. Biol.* 19, 209–219. doi:10.1089/omi.2014.0142

Kedhari Sundaram, M., Haque, S., Somvanshi, P., Bhardwaj, T., and Hussain, A. (2020). Epigallocatechin Gallate Inhibits HeLa Cells by Modulation of Epigenetics and Signaling Pathways. *3 Biotech.* 10, 484. doi:10.1007/s13205-020-02473-1

Kedhari Sundaram, M., Hussain, A., Haque, S., Raina, R., and Afroze, N. (2019). Quercetin Modifies 5′CpG Promoter Methylation and Reactivates Various Tumor Suppressor Genes by Modulating Epigenetic marks in Human Cervical Cancer Cells. *J. Cel Biochem* 120, 18357–18369. doi:10.1002/jcb.29147

Khan, H., Belwal, T., Efferth, T., Farooqi, A. A., Sanches-Silva, A., Vacca, R. A., et al. (2021). Targeting Epigenetics in Cancer: Therapeutic Potential of Flavonoids. *Crit. Rev. Food Sci. Nutr.* 61, 1616–1639. doi:10.1080/10408398.2020.1763910

Khan, M. A., Hussain, A., Sundaram, M. K., Alalami, U., Gunasekera, D., Ramesh, L., et al. (2015). (−)-Epigallocatechin-3-gallate Reverses the Expression of Various Tumor-Suppressor Genes by Inhibiting DNA Methyltransferases and Histone Deacetylases in Human Cervical Cancer Cells. *Oncol. Rep.* 33, 1976–1984. doi:10.3892/or.2015.3802

Khan, M., Zill, E. H., and Dangles, O. (2013). A Comprehensive Review on Flavanones, the Major Citrus Polyphenols. *J. Food Compost. Anal.* 33, 85-104. doi:10.1016/j.jfca.2013.11.004

Khoo, H. E., Azlan, A., Tang, S. T., and Lim, S. M. (2017). Anthocyanidins and Anthocyanins: Colored Pigments as Food, Pharmaceutical Ingredients, and the Potential Health Benefits. *Food Nutr. Res.* 61, 1361779. doi:10.1080/16546628.2017.1361779

Kim, T. W., Lee, S. Y., Kim, M., Cheon, C., and Ko, S.-G. (2018). Kaempferol Induces Autophagic Cell Death via IRE1-JNK-CHOP Pathway and Inhibition of G9a in Gastric Cancer Cells. *Cel Death Dis* 9, 875. doi:10.1038/s41419-018-0930-1

Krifa, M., Leloup, L., Ghedira, K., Mousli, M., and Chekir-Ghedira, L. (2014). Luteolin Induces Apoptosis in BE Colorectal Cancer Cells by Downregulating Calpain, UHRF1, and DNMT1 Expressions. *Nutr. Cancer* 66, 1220–1227. doi:10.1080/01635581.2014.951729

Křížová, L., Dadáková, K., Kašparovská, J., and Kašparovský, T. (2019). Isoflavones. *Molecules* 24, 1076. doi:10.3390/molecules24061076

Kumar, S., and Pandey, A. K. (2013). Chemistry and Biological Activities of Flavonoids: an Overview. *Sci.Wor.J.* 2013, 162750. doi:10.1155/2013/162750

Kuo, H.-C. D., Wu, R., Li, S., Yang, A. Y., and Kong, A.-N. (2019). Anthocyanin Delphinidin Prevents Neoplastic Transformation of Mouse Skin JB6 P+ Cells:

Epigenetic Re-activation of Nrf2-ARE Pathway. *Aaps j* 21, 83. doi:10.1208/s12248-019-0355-5

Kurokawa, R., Rosenfeld, M. G., and Glass, C. K. (2014). Transcriptional Regulation through Noncoding RNAs and Epigenetic Modifications. *RNA Biol.* 6, 233–236. doi:10.4161/rna.6.3.8329

Lacouture, M., and Sibaud, V. (2018). Toxic Side Effects of Targeted Therapies and Immunotherapies Affecting the Skin, Oral Mucosa, Hair, and Nails. *Am. J. Clin. Dermatol.* 19, 31–39. doi:10.1007/s40257-018-0384-3

Lai, W., Jia, J., Yan, B., Jiang, Y., Shi, Y., Chen, L., et al. (2018). Baicalin Hydrate Inhibits Cancer Progression in Nasopharyngeal Carcinoma by Affecting Genome Instability and Splicing. *Oncotarget* 9, 901–914. doi:10.18632/oncotarget.22868

Lee, Y. H., Kwak, J., Choi, H. K., Choi, K. C., Kim, S., Lee, J., et al. (2012). EGCG Suppresses Prostate Cancer Cell Growth Modulating Acetylation of Androgen Receptor by Anti-histone Acetyltransferase Activity. *Int. J. Mol. Med.* 30, 69–74. doi:10.3892/ijmm.2012.966

Lei, H., Shi, J., Teng, Y., Song, C., Zou, L., Ye, F., et al. (2021). Baicalein Modulates the Radiosensitivity of Cervical Cancer Cells *In Vitro* via miR-183 and the JAK2/STAT3 Signaling Pathway. *Adv. Clin. Exp. Med.* 30, 727–736. doi:10.17219/acem/135478

Lin, D., Kuang, G., Wan, J., Zhang, X., Li, H., Gong, X., et al. (2017). Luteolin Suppresses the Metastasis of Triple-Negative Breast Cancer by Reversing Epithelial-To-Mesenchymal Transition via Downregulation of β-catenin Expression. *Oncol. Rep.* 37, 895–902. doi:10.3892/or.2016.5311

Ling, D., Marshall, G. M., Liu, P. Y., Xu, N., Nelson, C. A., Iismaa, S. E., et al. (2012). Enhancing the Anticancer Effect of the Histone Deacetylase Inhibitor by Activating Transglutaminase. *Eur. J. Cancer* 48, 3278–3287. doi:10.1016/j.ejca.2012.02.067

Liu, X., Chen, X., Yu, X., Tao, Y., Bode, A. M., Dong, Z., et al. (2013). Regulation of microRNAs by Epigenetics and Their Interplay Involved in Cancer. *J. Exp. Clin. Cancer Res.* 32, 96. doi:10.1186/1756-9966-32-96

Lu, L., Wang, Y., Ou, R., Feng, Q., Ji, L., Zheng, H., et al. (2018). DACT2 Epigenetic Stimulator Exerts Dual Efficacy for Colorectal Cancer Prevention and Treatment. *Pharmacol. Res.* 129, 318–328. doi:10.1016/j.phrs.2017.11.032

Lubecka, K., Kaufman-Szymczyk, A., Cebula-Obrzut, B., Smolewski, P., Szemraj, J., and Fabianowska-Majewska, K. (2018). Novel Clofarabine-Based Combinations with Polyphenols Epigenetically Reactivate Retinoic Acid Receptor Beta, Inhibit Cell Growth, and Induce Apoptosis of Breast Cancer Cells. *Int. J. Mol. Sci.* 19, 3970. doi:10.3390/ijms19123970

Ma, D., Chen, S., Wang, H., Wei, J., Wu, H., Gao, H., et al. (2021). Baicalein Induces Apoptosis of Pancreatic Cancer Cells by Regulating the Expression of miR-139-3p and miR-196b-5p. *Front. Oncol.* 11, 653061. doi:10.3389/fonc.2021.653061

Majid, S., Dar, A. A., Shahryari, V., Hirata, H., Ahmad, A., Saini, S., et al. (2010). Genistein Reverses Hypermethylation and Induces Active Histone Modifications in Tumor Suppressor Gene B-Cell Translocation Gene 3 in Prostate Cancer. *Cancer* 116, 66–76. doi:10.1002/cncr.24662

Marchese, F. P., Raimondi, I., and Huarte, M. (2017). The Multidimensional Mechanisms of Long Noncoding RNA Function. *Genome Biol.* 18, 206. doi:10.1186/s13059-017-1348-2

Marín-Béjar, O., Marchese, F. P., Athie, A., Sánchez, Y., González, J., Segura, V., et al. (2013). Pint lincRNA Connects the P53 Pathway with Epigenetic Silencing by the Polycomb Repressive Complex 2. *Genome Biol.* 14, R104. doi:10.1186/gb-2013-14-9-r104

Markaverich, B. M., Vijjeswarapu, M., Shoulars, K., and Rodriguez, M. (2010). Luteolin and Gefitinib Regulation of EGF Signaling Pathway and Cell Cycle Pathway Genes in PC-3 Human Prostate Cancer Cells. *J. Steroid Biochem. Mol. Biol.* 122, 219–231. doi:10.1016/j.jsbmb.2010.06.006

Mateen, S., Raina, K., Agarwal, C., Chan, D., and Agarwal, R. (2013). Silibinin Synergizes with Histone Deacetylase and DNA Methyltransferase Inhibitors in Upregulating E-Cadherin Expression Together with Inhibition of Migration and Invasion of Human Non-small Cell Lung Cancer Cells. *J. Pharmacol. Exp. Ther.* 345, 206–214. doi:10.1124/jpet.113.203471

Mayr, C., Wagner, A., Neureiter, D., Pichler, M., Jakab, M., Illig, R., et al. (2015). The green tea Catechin Epigallocatechin Gallate Induces Cell Cycle Arrest and Shows Potential Synergism with Cisplatin in Biliary Tract Cancer Cells. *BMC Complement. Altern. Med.* 15, 194. doi:10.1186/s12906-015-0721-5

Milazzo, G., Mercatelli, D., Di Muzio, G., Triboli, L., De Rosa, P., Perini, G., et al. (2020). Histone Deacetylases (HDACs): Evolution, Specificity, Role in Transcriptional Complexes, and Pharmacological Actionability. *Genes* 11, 556. doi:10.3390/genes11050556

Miron, A., Aprotosoaie, A. C., Trifan, A., and Xiao, J. (2017). Flavonoids as Modulators of Metabolic Enzymes and Drug Transporters. *Ann. N.Y. Acad. Sci.* 1398, 152–167. doi:10.1111/nyas.13384

Mishan, M. A., Khazeei Tabari, M. A., Mahrooz, A., and Bagheri, A. (2021). Role of microRNAs in the Anticancer Effects of the Flavonoid Luteolin: a Systematic Review. *Eur. J. Cancer Prev.* 30, 413–421. doi:10.1097/cej.0000000000000645

Mohr, A., and Mott, J. (2015). Overview of MicroRNA Biology. *Semin. Liver Dis.* 35, 003–011. doi:10.1055/s-0034-1397344

Mostafa, S. M., Gamal-Eldeen, A. M., Maksoud, N. A. E., and Fahmi, A. A. (2020). Epigallocatechin Gallate-Capped Gold Nanoparticles Enhanced the Tumor Suppressors Let-7a and miR-34a in Hepatocellular Carcinoma Cells. *Acad. Bras Cienc* 92, e20200574. doi:10.1590/0001-3765202020200574

Nakai, S., Fujita, M., and Kamei, Y. (2020). Health Promotion Effects of Soy Isoflavones. *J. Nutr. Sci. Vitaminol* 66, 502–507. doi:10.3177/jnsv.66.502

Nwaeburu, C. C., Abukiwan, A., Zhao, Z., and Herr, I. (2017). Quercetin-induced miR-200b-3p Regulates the Mode of Self-Renewing Divisions in Pancreatic Cancer. *Mol. Cancer* 16, 23. doi:10.1186/s12943-017-0589-8

Nwaeburu, C. C., Bauer, N., Zhao, Z., Abukiwan, A., Gladkich, J., Benner, A., et al. (2016). Up-regulation of microRNA Let-7c by Quercetin Inhibits Pancreatic Cancer Progression by Activation of Numbl. *Oncotarget* 7, 58367–58380. doi:10.18632/oncotarget.11122

Örenlil Yaylagül, E., and Ülger, C. (2020). The Effect of Baicalein on Wnt/β-Catenin Pathway and miR-25 Expression in Saos-2 Osteosarcoma Cell Line. *Turkish J. Med. Sci.* 50, 1168–1179. doi:10.3906/sag-2001-161

Oya, Y., Mondal, A., Rawangkan, A., Umsumarng, S., Iida, K., Watanabe, T., et al. (2017). Down-regulation of Histone Deacetylase 4, −5 and −6 as a Mechanism of Synergistic Enhancement of Apoptosis in Human Lung Cancer Cells Treated with the Combination of a Synthetic Retinoid, Am80 and green tea Catechin. *J. Nutr. Biochem.* 42, 7–16. doi:10.1016/j.jnutbio.2016.12.015

Pal, H. C., Pearlman, R. L., and Afaq, F. (2016). Fisetin and its Role in Chronic Diseases. *Adv. Exp. Med. Biol.* 928, 213–244. doi:10.1007/978-3-319-41334-1_10

Panche, A. N., Diwan, A. D., and Chandra, S. R. (2016). Flavonoids: an Overview. *J. Nutr. Sci.* 5, e47. doi:10.1017/jns.2016.41

Pandey, M., Shukla, S., and Gupta, S. (2010). Promoter Demethylation and Chromatin Remodeling by green tea Polyphenols Leads to Re-expression of GSTP1 in Human Prostate Cancer Cells. *Int. J. Cancer* 126, 2520–2533. doi:10.1002/ijc.24988

Pandey, M., Kaur, P., Shukla, S., Abbas, A., Fu, P., and Gupta, S. (2012). Plant Flavone Apigenin Inhibits HDAC and Remodels Chromatin to Induce Growth Arrest and Apoptosis in Human Prostate Cancer Cells: *In Vitro* and *In Vivo* Study. *Mol. Carcinog.* 51, 952–962. doi:10.1002/mc.20866

Paschka, A. G., Butler, R., and Young, C. Y.-F. (1998). Induction of Apoptosis in Prostate Cancer Cell Lines by the green tea Component, (−)-Epigallocatechin-3-Gallate. *Cancer Lett.* 130, 1–7. doi:10.1016/s0304-3835(98)00084-6

Peng, Y., and Croce, C. M. (2016). The Role of MicroRNAs in Human Cancer. *Signal. Transduct Target. Ther.* 1, 15004. doi:10.1038/sigtrans.2015.4

Pham, T. N. D., Stempel, S., Shields, M. A., Spaulding, C., Kumar, K., Bentrem, D. J., et al. (2019). Quercetin Enhances the Anti-tumor Effects of BET Inhibitors by Suppressing hnRNPA1. *Int. J. Mol. Sci.* 20, 4293. doi:10.3390/ijms20174293

Pietta, P.-G. (2000). Flavonoids as Antioxidants. *J. Nat. Prod.* 63, 1035–1042. doi:10.1021/np9904509

Qi, X., Li, H., Cong, X., Wang, X., Jiang, Z., Cao, R., et al. (2016). Baicalin Increases Developmental Competence of Mouse Embryos *In Vitro* by Inhibiting Cellular Apoptosis and Modulating HSP70 and DNMT Expression. *J. Reprod. Dev.* 62, 561–569. doi:10.1262/jrd.2016-047

Qin, Y., Niu, K., Zeng, Y., Liu, P., Yi, L., Zhang, T., et al. (2013). Isoflavones for Hypercholesterolaemia in Adults. *Cochrane Database Syst. Rev.* 6, CD009518. doi:10.1002/14651858.cd009518.pub2

Ramos, Y. a. L., Souza, O. F., Novo, M. C. T., Guimarães, C. F. C., and Popi, A. F. (2021). Quercetin Shortened Survival of Radio-Resistant B-1 Cells *In Vitro* and *In Vivo* by Restoring miR15a/16 Expression. *Oncotarget* 12, 355–365. doi:10.18632/oncotarget.27883

Richon, V. M., Sandhoff, T. W., Rifkind, R. A., and Marks, P. A. (2000). Histone Deacetylase Inhibitor Selectively Induces p21WAF1 Expression

and Gene-Associated Histone Acetylation. *Proc. Natl. Acad. Sci.* 97, 10014–10019. doi:10.1073/pnas.180316197

Rossetto, D., Avvakumov, N., and Côté, J. (2014). Histone Phosphorylation. *Epigenetics* 7, 1098–1108. doi:10.4161/epi.21975

Russo, G. L., and Ungaro, P. (2019). "Epigenetic Mechanisms of Quercetin and Other Flavonoids in Cancer Therapy and Prevention," in *Epigenetics of Cancer Prevention*,(Amsterdam: Elsevier Inc)187–202. doi:10.1016/b978-0-12-812494-9.00009-3

Sathyapalan, T., Aye, M., Rigby, A. S., Thatcher, N. J., Dargham, S. R., Kilpatrick, E. S., et al. (2018). Soy Isoflavones Improve Cardiovascular Disease Risk Markers in Women during the Early Menopause. *Nutr. Metab. Cardiovasc. Dis.* 28, 691–697. doi:10.1016/j.numecd.2018.03.007

Sheng, J., Shi, W., Guo, H., Long, W., Wang, Y., Qi, J., et al. (2019). The Inhibitory Effect of (-)-Epigallocatechin-3-Gallate on Breast Cancer Progression via Reducing SCUBE2 Methylation and DNMT Activity. *Molecules* 24, 2899. doi:10.3390/molecules24162899

Shoulars, K., Rodriguez, M. A., Thompson, T., and Markaverich, B. M. (2010). Regulation of Cell Cycle and RNA Transcription Genes Identified by Microarray Analysis of PC-3 Human Prostate Cancer Cells Treated with Luteolin. *J. Steroid Biochem. Mol. Biol.* 118, 41–50. doi:10.1016/j.jsbmb.2009.09.016

Shukla, S., Meeran, S. M., and Katiyar, S. K. (2014). Epigenetic Regulation by Selected Dietary Phytochemicals in Cancer Chemoprevention. *Cancer Lett.* 355, 9–17. doi:10.1016/j.canlet.2014.09.017

Siegel, R. L., Miller, K. D., Fuchs, H. E., and Jemal, A. (2021). Cancer Statistics, 2021. *CA A. Cancer J. Clin.* 71, 7–33. doi:10.3322/caac.21654

Singh, B. N., Shankar, S., and Srivastava, R. K. (2011). Green tea Catechin, Epigallocatechin-3-Gallate (EGCG): Mechanisms, Perspectives and Clinical Applications. *Biochem. Pharmacol.* 82, 1807–1821. doi:10.1016/j.bcp.2011.07.093

Singh, S., Raza, W., Parveen, S., Meena, A., and Luqman, S. (2021). Flavonoid Display Ability to Target microRNAs in Cancer Pathogenesis. *Biochem. Pharmacol.* 189, 114409. doi:10.1016/j.bcp.2021.114409

Skibola, C. F., and Smith, M. T. (2000). Potential Health Impacts of Excessive Flavonoid Intake. *Free Radic. Biol. Med.* 29, 375–383. doi:10.1016/s0891-5849(00)00304-x

Soto-Reyes, E., González-Barrios, R., Cisneros-Soberanis, F., Herrera-Goepfert, R., Pérez, V., Cantú, D., et al. (2012). Disruption of CTCF at the miR-125b1 Locus in Gynecological Cancers. *BMC Cancer* 12, 40. doi:10.1186/1471-2407-12-40

Spagnuolo, C., Russo, G. L., Orhan, I. E., Habtemariam, S., Daglia, M., Sureda, A., et al. (2015). Genistein and Cancer: Current Status, Challenges, and Future Directions. *Adv. Nutr.* 6, 408–419. doi:10.3945/an.114.008052

Statello, L., Guo, C.-J., Chen, L.-L., and Huarte, M. (2020). Gene Regulation by Long Non-coding RNAs and its Biological Functions. *Nat. Rev. Mol. Cel Biol* 22, 96–118. doi:10.1038/s41580-020-00315-9

Taby, R., and Issa, J.-P. J. (2010). Cancer Epigenetics. *CA: A Cancer J. Clinicians* 60, 376–392. doi:10.3322/caac.20085

Takai, D., and Jones, P. A. (2002). Comprehensive Analysis of CpG Islands in Human Chromosomes 21 and 22. *Pnas* 99, 3740–3745. doi:10.1073/pnas.052410099

Taku, K., Melby, M. K., Nishi, N., Omori, T., and Kurzer, M. S. (2011). Soy Isoflavones for Osteoporosis: An Evidence-Based Approach. *Maturitas* 70, 333–338. doi:10.1016/j.maturitas.2011.09.001

Tao, S.-F., He, H.-F., and Chen, Q. (2015). Quercetin Inhibits Proliferation and Invasion Acts by Up-Regulating miR-146a in Human Breast Cancer Cells. *Mol. Cel Biochem* 402, 93–100. doi:10.1007/s11010-014-2317-7

Thakur, V. S., Gupta, K., and Gupta, S. (2012). Green tea Polyphenols Increase P53 Transcriptional Activity and Acetylation by Suppressing Class I Histone Deacetylases. *Int. J. Oncol.* 41, 353–361. doi:10.3892/ijo.2012.1449

Tseng, T.-H., Chien, M.-H., Lin, W.-L., Wen, Y.-C., Chow, J.-M., Chen, C.-K., et al. (2017). Inhibition of MDA-MB-231 Breast Cancer Cell Proliferation and Tumor Growth by Apigenin through Induction of G2/M Arrest and Histone H3 Acetylation-Mediated p21WAF1/CIP1expression. *Environ. Toxicol.* 32, 434–444. doi:10.1002/tox.22247

Vance, K. W., and Ponting, C. P. (2014). Transcriptional Regulatory Functions of Nuclear Long Noncoding RNAs. *Trends Genet.* 30, 348–355. doi:10.1016/j.tig.2014.06.001

Varier, R. A., and Timmers, H. T. M. (2011). Histone Lysine Methylation and Demethylation Pathways in Cancer. *Biochim. Biophys. Acta (Bba) - Rev. Cancer* 1815, 75–89. doi:10.1016/j.bbcan.2010.10.002

Vitale, D. C., Piazza, C., Melilli, B., Drago, F., and Salomone, S. (2012). Isoflavones: Estrogenic Activity, Biological Effect and Bioavailability. *Eur. J. Drug Metab. Pharmacokinet.* 38, 15–25. doi:10.1007/s13318-012-0112-y

Wang, Q., Chen, Y., Lu, H., Wang, H., Feng, H., Xu, J., et al. (2020a). Quercetin Radiosensitizes Non-small Cell Lung Cancer Cells through the Regulation of miR-16-5p/WEE1 axis. *IUBMB Life* 72, 1012–1022. doi:10.1002/iub.2242

Wang, S.-w., Sheng, H., Zheng, F., and Zhang, F. (2021a). Hesperetin Promotes DOT1L Degradation and Reduces Histone H3K79 Methylation to Inhibit Gastric Cancer Metastasis. *Phytomedicine* 84, 153499. doi:10.1016/j.phymed.2021.153499

Wang, X., Waschke, B. C., Woolaver, R. A., Chen, S. M. Y., Chen, Z., and Wang, J. H. (2020b). HDAC Inhibitors Overcome Immunotherapy Resistance in B-Cell Lymphoma. *Protein Cell* 11, 472–482. doi:10.1007/s13238-020-00694-x

Wang, Y., Chen, X., Li, J., and Xia, C. (2021b). Quercetin Antagonizes Esophagus Cancer by Modulating miR-1-3p/TAGLN2 Pathway-dependent Growth and Metastasis. *Nutr. Cancer*, 1–10. doi:10.1080/01635581.2021.1972125

Wang, Z., and Chen, H. (2010). Genistein Increases Gene Expression by Demethylation of WNT5a Promoter in colon Cancer Cell Line SW1116. *Anticancer Res.* 30, 4537–4545.

Wei, G.-J., Chao, Y.-H., Tung, Y.-C., Wu, T.-Y., and Su, Z.-Y. (2019). A Tangeretin Derivative Inhibits the Growth of Human Prostate Cancer LNCaP Cells by Epigenetically Restoring P21 Gene Expression and Inhibiting Cancer Stem-like Cell Proliferation. *Aaps j* 21, 86. doi:10.1208/s12248-019-0345-7

Weinhold, B. (2006). Epigenetics: the Science of Change. *Environ. Health Perspect.* 114, A160–A167. doi:10.1289/ehp.114-a160

Woo, H.-H., Jeong, B. R., and Hawes, M. C. (2005). Flavonoids: from Cell Cycle Regulation to Biotechnology. *Biotechnol. Lett.* 27, 365–374. doi:10.1007/s10529-005-1521-7

Wu, H.-T., Lin, J., Liu, Y.-E., Chen, H.-F., Hsu, K.-W., Lin, S.-H., et al. (2021). Luteolin Suppresses Androgen Receptor-Positive Triple-Negative Breast Cancer Cell Proliferation and Metastasis by Epigenetic Regulation of MMP9 Expression via the AKT/mTOR Signaling Pathway. *Phytomedicine* 81, 153437. doi:10.1016/j.phymed.2020.153437

Yang, L., Zhang, W., Chopra, S., Kaur, D., Wang, H., Li, M., et al. (2020). The Epigenetic Modification of Epigallocatechin Gallate (EGCG) on Cancer. *Cdt* 21, 1099–1104. doi:10.2174/1389450121666200504080112

Yu, W.-D., Sun, G., Li, J., Xu, J., and Wang, X. (2019). Mechanisms and Therapeutic Potentials of Cancer Immunotherapy in Combination with Radiotherapy And/or Chemotherapy. *Cancer Lett.* 452, 66–70. doi:10.1016/j.canlet.2019.02.048

Zhang, C., Hao, Y., Sun, Y., and Liu, P. (2019a). Quercetin Suppresses the Tumorigenesis of Oral Squamous Cell Carcinoma by Regulating microRNA-22/wnt1/β-Catenin axis. *J. Pharmacol. Sci.* 140, 128–136. doi:10.1016/j.jphs.2019.03.005

Zhang, L., Lu, Q., and Chang, C. (2020). Epigenetics in Health and Disease. *Adv. Exp. Med. Biol.* 1253, 3–55. doi:10.1007/978-981-15-3449-2_1

Zhang, X., Wang, W., Zhu, W., Dong, J., Cheng, Y., Yin, Z., et al. (2019b). Mechanisms and Functions of Long Non-coding RNAs at Multiple Regulatory Levels. *Int. J. Mol. Sci.* 20, 5573. doi:10.3390/ijms20225573

Zhang, Y., Wang, X., Han, L., Zhou, Y., and Sun, S. (2015). Green tea Polyphenol EGCG Reverse Cisplatin Resistance of A549/DDP Cell Line through Candidate Genes Demethylation. *Biomed. Pharmacother.* 69, 285–290. doi:10.1016/j.biopha.2014.12.016

Zhao, J., Fang, Z., Zha, Z., Sun, Q., Wang, H., Sun, M., et al. (2019). Quercetin Inhibits Cell Viability, Migration and Invasion by Regulating miR-16/HOXA10 axis in Oral Cancer. *Eur. J. Pharmacol.* 847, 11–18. doi:10.1016/j.ejphar.2019.01.006

Zhao, Y., Chen, X., Jiang, J., Wan, X., Wang, Y., and Xu, P. (2020). Epigallocatechin Gallate Reverses Gastric Cancer by Regulating the Long Noncoding RNA LINC00511/miR-29b/KDM2A axis. *Biochim. Biophys. Acta (Bba) - Mol. Basis Dis.* doi:10.1016/j.bbadis.2020.165856

Zheng, N.-G., Wang, J.-L., Yang, S.-L., and Wu, J.-L. (2014). Aberrant Epigenetic Alteration in Eca9706 Cells Modulated by Nanoliposomal Quercetin Combined with Butyrate Mediated via Epigenetic-NF-Kb Signaling. *Asian Pac. J. Cancer Prev.* 15, 4539–4543. doi:10.7314/apjcp.2014.15.11.4539

Zhou, J., Gong, J., Ding, C., and Chen, G. (2015). Quercetin Induces the Apoptosis of Human Ovarian Carcinoma Cells by Upregulating the Expression of microRNA-145. *Mol. Med. Rep.* 12, 3127–3131. doi:10.3892/mmr.2015.3679

Conflict of Interest: The authors declare that the research was conducted in the absence of any commercial or financial relationships that could be construed as a potential conflict of interest.

Publisher's Note: All claims expressed in this article are solely those of the authors and do not necessarily represent those of their affiliated organizations, or those of the publisher, the editors and the reviewers. Any product that may be evaluated in this article, orclaim that may be made by its manufacturer, is not guaranteed or endorsed by the publisher.

GLOSSARY

ABCG2 ATP-binding cassette G2
AKT Ak strain transforming
AMPK 5' adenosine monophosphate-activated protein kinase
APAF1 Apoptotic protease activating factor 1
AR Androgen receptor
ARE Antioxidant responsive element
ATG5 /7 Autophagy related 5 /7
AURKA /B /C Aurora kinase A /B /C
BAX BCL2 associated X
BCL-2 B-cell lymphoma 2
BCL2L11 Bcl-2-like protein 11
BDC Bile duct cancer
BET Bromodomain and extraterminal
BNIP3 BCL2 and adenovirus E1B 19-kDa-interacting protein 3
BNIP3L BCL2 and adenovirus E1B 19-kDa-interacting protein 3-like
BRCA1 /2 Breast cancer gene 1 /2
BTG3 B-cell translocation gene 3
C/EBPα CCAAT enhancer-binding protein alpha
CAF Chromatin assembly factor
CCNA2 /B1 /B2 / D1 /E1 /E2 Cyclin A2 /B1 /B2 /D1 /E1 /E2
CD Cluster of differentiation
CDC25A Cell division cycle 25 A
CDH1 /13 Cadherin 1 /13
CDK1 Cyclin-dependent kinase 1
CDKN1A /1B Cyclin dependent kinase inhibitor 1A /1B
CHOP C/EBP homologous protein
CREB cAMP-response element binding protein
DACT2 Disheveled-associated antagonist of β-catenin homolog 2
DAPK1 Death-associated protein kinase 1
DOT1L DOT1-like histone H3K79 methyltransferase
DR5 Death receptor 5
E2F1 E2F transcription factor 1
EED Embryonic ectoderm development
EGFR Epidermal growth factor receptor
EMT epithelial-mesenchymal transition
EPHB2 EPH receptor B2
ERK Extracellular signal-regulated protein kinase
EZH2 Enhancer of zeste homolog 2
GAS1 Growth arrest specific 1
GBC Gall bladder carcinoma
GSTP1 Glutathione S-transferase pi 1
hMLH1 Human mutL homolog 1
HMOX1 Heme oxygenase 1
hnRNPA1 Heterogeneous nuclear ribonucleoprotein A1
HOTAIR HOX transcript antisense RNA
HOXA10 Homeobox A10
HSP70 Heat shock proteins 70 kda;
hTERT Human telomerase reverse transcriptase
ICAM1 Intercellular adhesion molecule 1
IGFBP5 Insulin like growth factor binding protein 5
IL Interleukin
IRE1 Inositol-requiring enzyme1
JNK c-Jun N-terminal kinase
KDM4A /4B /5C Lysine (K)-specific demethylase 4A /4B /5C
KMT2A Lysine (K)-specific methyltransferase 2A
Let -7 Lethal-7
LSD1 Lysine-specific demethylase 1
m6A N^6-methyl-adenosine
MAD1L1 MAD1 mitotic arrest deficient 1-like 1
MALAT1 Metastasis associated lung adenocarcinoma transcript 1
MAPK Mitogen-activated protein kinase
MEG3 Maternally expressed gene 3
MGMT O6-methylguanine-DNA methyltransferase
MMP Matrix metallopeptidase
mTOR Mammalian target of rapamycin
NF-κB Nuclear factor kappa B
NQO1 NAD(P)H quinone dehydrogenase 1
NRF2 Nuclear factor erythroid 2-related factor 2
NSCLC Non-small cell lung cancer
NUMBL NUMB Like Endocytic Adaptor Protein
p70S6K Ribosomal protein S6 kinase beta-1
PARP Poly (ADP-ribose) polymerase
PI3K Phosphoinositide 3-kinases
PIK3C2B Phosphatidylinositol-4-phosphate 3-kinase catalytic subunit type 2 beta
PIK3CA Phosphatidylinositol-4,5-bisphosphate 3-kinase catalytic subunit alpha
PKCα Protein kinase C alpha
PLK-1 Polo-like kinase 1
PRC Polycomb repressive complex
PRDM2 PR domain zinc finger protein 2
PRMT6 /7 Protein arginine N-methyltransferase 6 /7
PTEN Phosphatase and tensin homolog
PTENP1 PTEN pseudogene 1
RARB Retinoic acid receptor beta
RFXAP Regulatory factor X associated protein

ROS Reactive oxygen species
RTCB RNA 2',3'-cyclic phosphate and 5'-OH ligase
RUNX3 Runt-related transcription factor 3
S100P S100 calcium binding protein P
SCUBE2 Signal peptide-CUB-EGF domain-containing protein 2
SOD1 Superoxide dismutase 1
SUV39H1 Suppressor of variegation 3-9 homolog 1
SUZ12 Suppressor of zeste homolog 12
TAGLN2 Transgelin 2
TIMP3 Tissue inhibitor of metalloproteinase 3
TRAF7 TNF receptor associated factor 7
UBE2B Ubiquitin conjugating enzyme E2 B
UHRF1 Ubiquitin like with PHD and ring finger domains 1
ULK1 Unc-51 like autophagy activating kinase
WEE1 WEE1 G2 Checkpoint Kinase
WISP2 WNT1-inducible-signaling pathway protein 2
WNT Wingless/Integrated
WNT5a Wnt family member 5A
γ-H2AX Gamma H2A histone family member X

frontiers in Genetics

ORIGINAL RESEARCH
published: 25 November 2021
doi: 10.3389/fgene.2021.767590

CircARVCF Contributes to Cisplatin Resistance in Gastric Cancer by Altering miR-1205 and FGFR1

Ruirui Zhang[1], Huanyu Zhao[1], Hongmei Yuan[2], Jian Wu[1], Haiyan Liu[1], Suan Sun[1], Zhengwei Zhang[1] and Jiayang Wang[3]**

[1]Department of Pathology, Huai'an First People's Hospital, Nanjing Medical University, Huaian, China, [2]Department of Pathology, Huai'an Huaiyin Hospital, Huaian, China, [3]Department of Rodio Chemotherapy, Huai'an First People's Hospital, Nanjing Medical University, Huaian, China

OPEN ACCESS

Edited by:
Ata Abbas,
Case Western Reserve University, United States

Reviewed by:
Atrayee Bhattacharya,
Dana–Farber Cancer Institute, United States
Zhigang Bai,
Beijing Friendship Hospital, China

***Correspondence:**
Jian Wu
wu776jian@163.com
Jiayang Wang
wang2020jiayang@163.com

Specialty section:
This article was submitted to Cancer Genetics and Oncogenomics, a section of the journal Frontiers in Genetics

Received: *31 August 2021*
Accepted: *01 November 2021*
Published: *25 November 2021*

Citation:
Zhang R, Zhao H, Yuan H, Wu J, Liu H, Sun S, Zhang Z and Wang J (2021) CircARVCF Contributes to Cisplatin Resistance in Gastric Cancer by Altering miR-1205 and FGFR1. Front. Genet. 12:767590. doi: 10.3389/fgene.2021.767590

Background: Chemoresistance is a major barrier to the treatment of human cancers. Circular RNAs (circRNAs) are implicated in drug resistance in cancers, including gastric cancer (GC). In this study, we aimed to explore the functions of circRNA Armadillo Repeat gene deleted in Velo-Cardio-Facial syndrome (circARVCF) in cisplatin (DDP) resistance in GC.

Methods: The expression of circARVCF, microRNA-1205 (miR-1205) and fibroblast growth factor receptor 1 (FGFR1) was detected by quantitative real-time polymerase chain reaction (qRT-PCR), western blot assay or immunohistochemistry (IHC) assay. Cell Counting Kit-8 (CCK-8) assay and colony formation assay were performed to evaluate DDP resistance and cell colony formation ability. Transwell assay was conducted to assess cell migration and invasion. Flow cytometry analysis was done to analyze cell apoptosis. Dual-luciferase reporter assay and RNA immunoprecipitation (RIP) assay were manipulated to analyze the relationships of circARVCF, miR-1205 and FGFR1. Murine xenograft model was constructed to explore DDP resistance *in vivo*.

Results: CircARVCF level was increased in DDP-resistant GC tissues and cells. CircARVCF silencing inhibited DDP resistance, colony formation and metastasis and induced apoptosis in DDP-resistant GC cells. CircARVCF directly interacted with miR-1205 and miR-1205 inhibition reversed circARVCF silencing-mediated effect on DDP resistance in DDP-resistant GC cells. FGFR1 served as the target gene of miR-1205. MiR-1205 overexpression restrained the resistance of DDP-resistant GC cells to DDP, but FGFR1 elevation abated the effect. In addition, circARVCF knockdown repressed DDP resistance *in vivo*.

Conclusion: CircARVCF enhanced DDP resistance in GC by elevating FGFR1 through sponging miR-1205.

Keywords: GC, DDP, resistance, circARVCF, miR-1205, FGFR1

HIGHLIGHTS

1. CircARVCF is upregulated in DDP-resistant GC tissues and cells.
2. CircARVCF knockdown suppresses DDP resistance in DDP-resistant GC cells.
3. CircARVCF directly interacts with miR-1205 to regulate FGFR1 expression.
4. CircARVCF promotes DDP resistance in DDP-resistant GC cells by miR-1205/FGFR1 axis.
5. CircARVCF enhances DDP resistance of GC *in vivo*.

INTRODUCTION

Gastric cancer (GC) is a worldwide life-threatening malignant tumor with strong a ability of metastasis and proliferation (Guggenheim and Shah, 2013; Bray et al., 2018). The patients are often diagnosed at the late stage for lacking specific symptoms and diagnostic indicators in early GC, and then lead to poor prognosis (Song et al., 2017). Surgery and adjuvant chemotherapy are the major treatment methods for GC, although molecular targeted therapy has been developed. Cisplatin (DDP) is the main first-line drug for GC treatment (Wang et al., 2019a). However, drug resistance impedes the effectiveness of chemotherapy (Galluzzi et al., 2012; Marin et al., 2016). Based on the above reasons, studying the mechanism of chemoresistance is necessary for improving the survival of GC.

Circular RNAs (circRNAs) are newly discovered non-coding RNAs (ncRNAs) that are distinguished by signal-stranded closed loop (Chen and Yang, 2015). CircRNAs are dysregulated and play vital roles in the biological and pathological processes in human cancers (Wang et al., 2017). Moreover, circRNAs can act as the competitive endogenous sponge for microRNAs (miRNAs), which then directly targeted related mRNAs to alter gene expression (Zhong et al., 2018). CircRNAs are linked to the development of chemoresistance in GC (Cui et al., 2020). For instance, circ_0000144 restrained oxaliplatin (OXA) resistance of GC *via* altering miR-502-5p and ADAM9 (Gao et al., 2021). CircFN1 promoted the malignancy and DDP resistance of GC *via* decoying miR-182-5p (Huang et al., 2020). CircARVCF (hsa_circ_0092330) was formed by the exons of ARVCF gene and was found to be upregulated in GC (Ouyang et al., 2019). However, the functions of circARVCF in the carcinogenesis and drug resistance of GC are unclear.

The involvement of miRNAs in tumor progression and chemoresistance is widely characterized (Taheri et al., 2021). For example, miR-149 facilitated 5-FU resistance in GC through binding to TREM2 (Wang et al., 2020a). MiR-127-5p impeded the resistance of GC to Apatinib (Yu et al., 2021). MiR-1205 functioned as a tumor inhibitor in diverse cancers, such as colorectal cancer (Han et al., 2021), glioma (Wang et al., 2021), ovarian cancer (Wang et al., 2020b) as well as GC (Lin et al., 2020). Even so, it remains unclear whether miR-1205 is related to the drug resistance of GC. Moreover, fibroblast growth factor receptor 1 (FGFR1) was found to contain miR-1205 binding sites, but their relationship is still unknown.

TABLE 1 | Primers sequences used for qRT-PCR.

Name		Primers for PCR (5′-3′)
CircARVCF	Forward	TGAGGACTCCCTGTTCCTTTG
	Reverse	TTGGTATGAGGCTGTGACCG
ARVCF	Forward	CTATTGTCACATCCGAAGATGGC
	Reverse	CGTACTGTCCGAGTGGTCAC
miR-1205	Forward	ACACTCCAGCTGGGTCTGCAGGGTTTGC
	Reverse	TGGTGTCGTGGAGTCG
FGFR1	Forward	CCCGTAGCTCCATATTGGACA
	Reverse	TTTGCCATTTTTCAACCAGCG
β-actin	Forward	ATCAAGATCATTGCTCCTCCTGAG
	Reverse	CTGCTTGCTGATCCACATCTG
U6	Forward	CTCGCTTCGGCAGCACA
	Reverse	AACGCTTCACGAATTTGCGT

In this paper, we elucidated the functions and relationships of circARVCF, miR-1205, and FGFR1 in regulating the chemoresistance of GC, attempting to find a novel target to relieve chemoresistance in GC.

MATERIALS AND METHODS

Tissue Collection

The GC and matched adjacent non-tumor tissues were collected from 37 GC patients (20 males and 17 females, aged 25–71) at Huai'an First People's hospital. The enrolled patients received DDP-based chemotherapy before this surgery. According to the resistance of GC patients to DDP (Bagrodia et al., 2016), the patients were divided into two groups: chemoresistant group (n = 20; tumor relapse during DDP-based chemotherapy) and chemosensitive group (n = 17; no tumor recurrence during DDP-based therapy). All patients provided the written informed consents. The research granted approval by the Ethics Committee of Huai'an First People's Hospital.

Cell Culture

Human normal gastric mucosa cells (GES-1) and GC cells (N87, HGC-27, MKN-45, and AGS) were acquired from Procell (Wuhan, China). All cells were cultured in RPMI1640 (Procell) added with 1% penicillin/streptomycin (Procell) and 10% FBS (Procell) at 37°C and 5% CO_2.

The DDP-resistant GC cells (MKN-45/DDP and AGS/DDP) were generated by continuous gradient exposing MKN-45 and AGS cells to increasing doses of DDP (Sigma-Aldrich, St. Louis, MO, United States) from 0.03 μg/ml until the cells acquired resistance to 1 μg/ml (0.05, 0.1, 0.15, 0.2, 0.3, 0.4, 0.5, 0.6 0.7, 0.8, 0.9, 1 μg/ml) for about 12 months. The DDP-resistant cells were cultured in cisplatin (1 μM)-contained RPMI1640 (Procell) and cultured in cisplatin-free RPMI1640 (Procell) for 1 week before further use.

Quantitative Real-Time Polymerase Chain Reaction

RNA isolation was manipulated with RNAiso Plus (Takara, Dalian, China). Then M-MLV Reverse Transcriptase reagent

(Promega, Madison, WI, United States) or All-in-One™ miRNA Detection reagent (GeneCopoeia, FulenGen, China) was employed on total RNA for the synthesis of cDNAs. Afterward, SYBR Green qPCR mix (Takara) was used for the reaction on an ABI 7500 Real-Time PCR system (Applied Biosystems, Foster City, CA, United States). The expression was computed by the $2^{-\Delta\Delta Ct}$ way. β-actin and U6 served as the internal controls. The primers were listed in **Table 1**.

Cell Counting Kit-8 Assay

To determine DDP resistance, MKN-45/DDP and AGS/DDP cells (1×10^4 cells/well) were cultured in 96-well plates. On the next day, the cells were treated with varying doses of DDP (0.01, 0.1, 1, 10, and 100 μM) for 48 h. 10 μL CCK-8 (Sigma-Aldrich) was then supplemented into the well and incubated for 4 h. Finally, the absorption at 450 nm was examined by a microplate reader and the 50% inhibitory concentration (IC_{50}) of DDP was analyzed.

Actinomycin D and RNase R Treatment

For the cyclization analysis of circARVCF, MKN-45/DDP, and AGS/DDP cells were interacted with Actinomycin D (Sigma-Aldrich) for indicated times. Total RNA was managed with RNase R (3 U/μg; Epicenter, Madison, WI, United States) at 37°C for 20 min. Afterward, the levels of circARVCF and ARVCF were detected via qRT-PCR.

Cell Transfection

Specific small interfering RNAs targeting circARVCF (si-circARVCF#1, si-circARVCF#2, and si-circARVCF#3) and scramble control si-NC, miR-1205 mimics (miR-1205), inhibitors (in-miR-1205) and related controls miR-NC and in-miR-NC, FGFR1 overexpression vector (FGFR1) and empty control pcDNA, short hairpin RNA targeting circARVCF (sh-circARVCF) and sh-NC were synthesized by GeneCopoeia (Guangzhou, China). Then MKN-45/DDP and AGS/DDP cells were seeded into 24-well plates and transfected with the oligonucleotides or vectors through Lipofectamine 3,000 (Invitrogen, Carlsbad, CA, United States) according to the manufacturers' instructions.

Colony Formation Assay

MKN-45/DDP and AGS/DDP cells (300 cells/well) were planted into 6-well plates and maintained for 2 weeks. The medium was changed every 3 days. The colonies were fixed with 4% paraformaldehyde (Sigma-Aldrich) and then dyed with 0.1% crystal violet solution (Sigma-Aldrich). After that, the colonies were calculated.

Transwell Assay

By using the transwell insert chambers (Corning, Corning, NY, United States) with or without Matrigel (Corning) coverage, cell invasion and migration were assessed. In short, MKN-45/DDP and AGS/DDP cells (1×10^4) were resuspended in 200 μL serum-free medium was added into the top chamber. The 600 μL complete medium was filled into the lower chamber. Following 24 h of incubation, the migrated or invaded cells were fixed with 4% paraformaldehyde (Sigma-Aldrich) anddyed with 0.1% crystal violet (Sigma-Aldrich). Next, the number of migrated or invaded cells was counted via a microscope (100×; Olympus, Tokyo, Japan) through the five random areas.

Flow Cytometry Analysis

After indicated transfection, MKN-45/DDP and AGS/DDP cells were resuspended in binding buffer and double-dyed with Annexin V-fluorescein isothiocyanate (FITC) and propidium iodide (PI) for 15 min without light based on the instructions of the Apoptosis Detection Kit (Beyotime, Shanghai, China). The apoptotic cells were detected using flow cytometry.

Western Blot Assay

After being extracted from tissues and cells with RIPA buffer (Beyotime), the proteins (20 μg) were separated through 10% SDS-PAGE electrophoresis. Then the proteins were transferred onto PVDF membranes, followed by blockage in 5% skim milk for 2 h. Subsequently, the membranes were maintained overnight with primary antibodies at 4°C and corresponding secondary antibody (bs-0293G-HRP; 1:10,000; Bioss, Beijing, China) for 2 h at room temperature. The protein blots were subjected to ECL kit (Beyotime) for visualization. The signal intensity of the proteins was determined by ImageJ software. The antibodies included multidrug resistance protein 1 (MRP1; bs-24241R; 1:2000; Bioss), p-glycoprotein (MDR1; bs-0563R; 1:2000; Bioss), B-cell lymphoma-2 (Bcl-2; bs-20351R; 1:2000; Bioss), BCL2-Associated X (Bax; bs-28034R; 1:2000; Bioss), FGFR1 (bs-0230R; 1:2000; Bioss) and β-actin (bs-0061R; 1:10,000; Bioss).

Dual-Luciferase Reporter Assay

CircARVCF-wide type (WT), circARVCF-mutant (MUT), -FGFR1 3′UTR WT and FGFR1 3′UTR MUT were designed by cloning the fragments of WT circARVCF, WT FGFR1 3′UTR, as well as related mutant (lacking miR-1205 binding sites) into pGL3 vector (Promega). Then the designed vectors and miR-NC/miR-1205 were introduced into MKN-45/DDP and AGS/DDP cells. The luciferase signal was analyzing utilizing Dual-Luciferase Reporter Assay kit (Promega) after 48 h. Renilla luciferase activity was normalized to firefly luciferase activity.

RNA Immunoprecipitation Analysis

The Magna RIP™ reagent (Millipore, Bedford, MA, United States) was used for this analysis. In brief, MKN-45/DDP and AGS/DDP cells were lysed in RIP buffer and then cell lysates were incubated with Anti-AGO2 or Anti-IgG coupled with magnetic beads. Then the immunoprecipitated RNA was extracted and qRT-PCR was used for circARVCF and miR-1205 levels.

Murine Xenograft Model

Beijing Vital River Laboratory Animal Technology Co., Ltd. (Beijing, China) provided the male BALB/c nude mice (5-week-old). Lentivirus vectors embracing harboring sh-NC or sh-circARVCF were constructed. Then AGS/DDP cells (1×10^7) with Lenti-sh-NC or Lenti-sh-circARVCF transfection

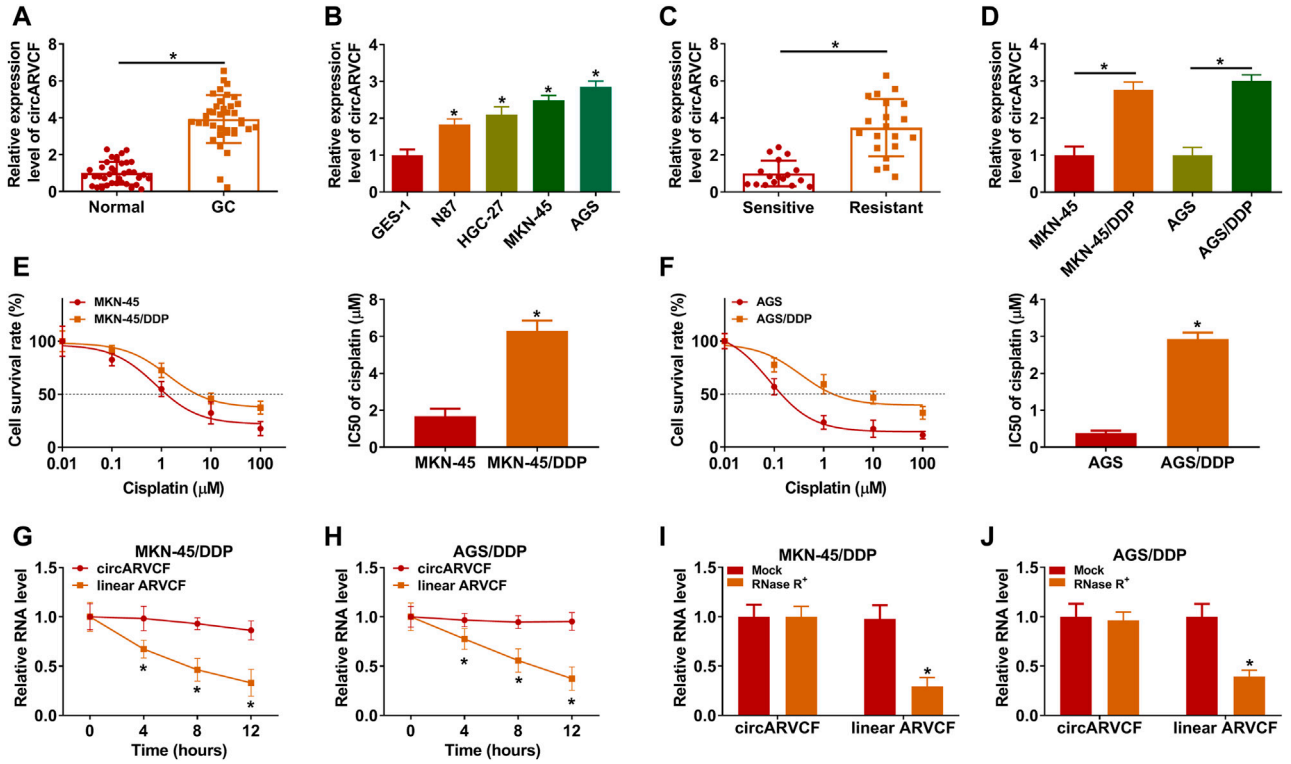

FIGURE 1 | CircARVCF was overexpressed in DDP-resistant GC tissues and cells. **(A)** CircARVCF expression in GC tissues and normal tissues was detected *via* qRT-PCR. **(B)** CircARVCF expression in GES-1, N87, HGC-27, MKN-45, and AGS cells was detected by qRT-PCR. **(C)** CircARVCF expression in DDP-resistant GC tissues and DDP-sensitive GC tissues was detected by qRT-PCR. **(D)** CircARVCF expression in MKN-45, MKN-45/DDP, AGS, and AGS/DDP cells was detected by qRT-PCR. **(E,F)** IC50 of cisplatin in MKN-45, MKN-45/DDP, AGS, and AGS/DDP cells was assessed by CCK-8 assay. **(G,H)** The levels of circARVCF and ARVCF in MKN-45/DDP and AGS/DDP cells treated with Actinomycin D were examined by qRT-PCR. **(I,J)** Total RNA in MKN-45/DDP and AGS/DDP cells was treated with RNase R and then circARVCF and linear ARVCF levels were detected by qRT-PCR. $^*p < 0.05$.

were subcutaneously injected into the flank of the mice. After 7 days, the mice were intraperitoneally administrated with 6 mg/kg of DDP (Sigma-Aldrich) or PBS every 3 days (Zhi et al., 2015). The xenograft tumors were monitored every 7 days and tumor volume (0.5 × length × width^2) was calculated. After 28 days, the mice were euthanized and tumors were weighed and preserved at −80°C for further use. This animal experiment was permitted by the Ethics Committee of Animal Research of Huai'an First People's Hospital.

Immunohistochemistry Assay

The xenograft tumors were sectioned at 5 μm, fixed with 4% formalin (Sigma-Aldrich) and embedded with paraffin (Sigma-Aldrich). Next, the slides were incubated with anti-FGFR1 (bs-0230R; Bioss) overnight and secondary antibody (bs-0293G-HRP) for 1 h. After that, the signal was developed with DAB solution and counterstained with hematoxylin (Sigma-Aldrich) as previously described (Wang et al., 2019b).

Statistical Analysis

Data analysis was conducted using GraphPad Prism 7. The experiments were repeated three times. The data were exhibited as mean ± SD. Differences were compared through Student's *t*-test or one-way ANOVA. It was defined as significant when $p < 0.05$.

RESULTS

CircARVCF Was Upregulated in DDP-Resistant GC Tissues and Cells

As exhibited in **Figures 1A,B**, circARVCF was overexpressed in GC tissues and cell lines compared to normal tissues and cell lines. To explore the functions of circARVCF in the chemoresistance of GC, the expression of circARVCF in DDP-resistant GC tissues and cells was detected by qRT-PCR. The results showed that circARVCF was upregulated in DDP-resistant GC tissues compared to DDP-sensitive GC tissues (**Figure 1C**). Compared to MKN-45 and AGS cells, circARVCF was increased in MKN-45/DDP and AGS/DDP cells (**Figure 1D**). CCK-8 assay showed that the cisplatin resistance of MKN-45/DDP and AGS/DDP cells was enhanced for the elevation of IC50 of cisplatin (**Figures 1E,F**). Moreover, Actinomycin D assay indicated that circARVCF possessed a longer half-life than linear ARVCF after Actinomycin D exposure (**Figures 1G,H**). RNase R assay indicated that

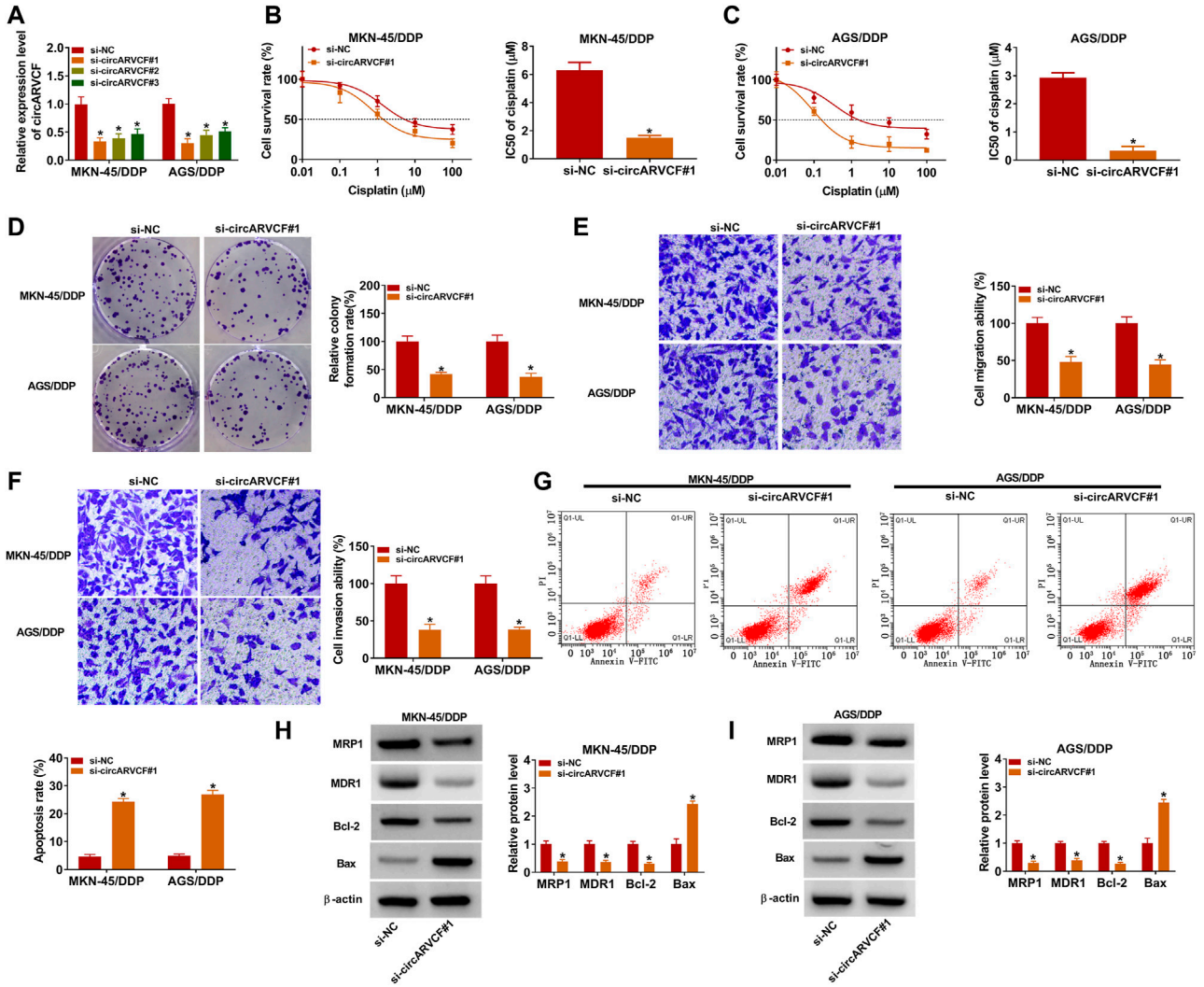

FIGURE 2 | CircARVCF knockdown suppressed DDP resistance in DDP-resistant GC cells. **(A)** The expression of circARVCF in MKN-45/DDP and AGS/DDP cells transfected with si-circARVCF#1, si-circARVCF#2, si-circARVCF#3, or si-NC was detected by qRT-PCR. **(B–I)** MKN-45/DDP and AGS/DDP cells were transfected with si-NC or si-circARVCF#1. **(B,C)** IC50 of cisplatin in MKN-45/DDP and AGS/DDP cells was examined with CCK-8 assay. **(D)** The colony formation of MKN-45/DDP and AGS/DDP cells was evaluated by colony formation assay. **(E,F)** The migration and invasion of MKN-45/DDP and AGS/DDP cells were tested by transwell assay. **(G)** The apoptosis of MKN-45/DDP and AGS/DDP cells was analyzed by flow cytometry analysis. **(H,I)** The protein levels of MRP1, MDR1, Bcl-2 and Bax in MKN-45/DDP and AGS/DDP cells were measured *via* western blot assay. *$p < 0.05$.

circARVCF was resistant to RNase R digestion, while linear ARVCF was digested by RNase R (**Figures 1I,J**).

CircARVCF Knockdown Repressed the Resistance of DDP-Resistant GC Cells to DDP

To explore the exact roles of circARVCF in DDP resistance in GC, si-circARVCF#1, si-circARVCF#2, or si-circARVCF#3 was transfected into MKN-45/DDP and AGS/DDP cells to silence circARVCF expression. As presented in **Figure 2A**, the transfection of si-circARVCF#1, si-circARVCF#2, or si-circARVCF#3 markedly reduced circARVCF expression in MKN-45/DDP and AGS/DDP cells compared to si-NC transfected cells. Then CCK-8 assay showed that circARVCF knockdown suppressed DDP resistance in MKN-45/DDP and AGS/DDP cells compared to si-NC control groups (**Figures 2B,C**). Colony formation assay showed that circARVCF silencing suppressed the colony formation capacity of MKN-45/DDP and AGS/DDP cells compared to si-NC control groups (**Figure 2D**). The results of transwell assay indicated that circARVCF knockdown repressed the migration and invasion of MKN-45/DDP and AGS/DDP cells in comparison with si-NC control groups (**Figures 2E,F**). Flow cytometry analysis exhibited that circARVCF deficiency led to a marked promotion in the apoptosis of MKN-45/DDP and AGS/DDP cells (**Figure 2G**). In addition, our results showed that circARVCF interference decreased the levels of drug resistance-related genes (MRP1

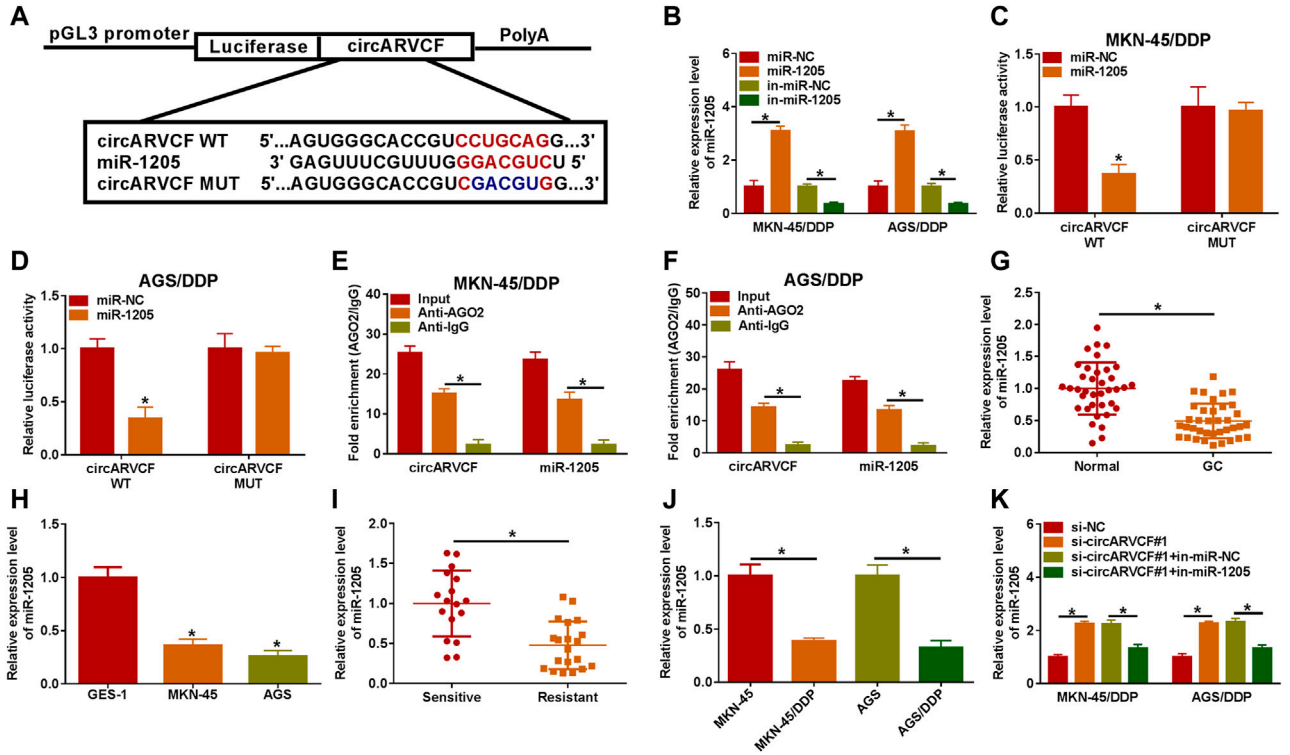

FIGURE 3 | MiR-1205 was the target of circARVCF. **(A)** The complementary sequences between circARVCF and miR-1205. **(B)** The expression of miR-1205 in MKN-45/DDP and AGS/DDP cells transfected with miR-NC, miR-1205, in-miR-NC or in-miR-1205 was detected by qRT-PCR. **(C–F)** The interaction between miR-1205 and circARVCF was demonstrated by dual-luciferase reporter assay and RIP assay. **(G,H)** The expression of miR-1205 in GC tissues, normal tissues, GC cells and normal cells was detected by qRT-PCR. **(I,J)** The expression of miR-1205 in DDP-resistant GC tissues and cells was examined with qRT-PCR. **(K)** The expression of miR-1205 in MKN-45/DDP and AGS/DDP cells with si-NC, si-circARVCF#1, si-circARVCF#1+in-miR-NC, or si-circARVCF#1+in-miR-1205 was detected by qRT-PCR. $^*p < 0.05$.

and MDR1) and anti-apoptotic protein Bcl-2 and increased pro-apoptotic protein Bax in MKN-45/DDP and AGS/DDP cells (**Figures 2H,I**). Collectively, circARVCF promoted DDP resistance in DDP-resistant GC cells.

CircARVCF Directly Targeted miR-1205 to Regulate miR-1205 Expression

It was widely documented that circRNAs can act as the sponge for miRNAs (Zhong et al., 2018). Thus, we further explored the underlying mechanism of circARVCF in the chemoresistance of GC through searching circinteractome (https://circinteractome.nia.nih.gov/api/v2/mirnasearch?circular_rna_query=hsa_circ_0092330&mirna_query=&submit=miRNA+Target+Search) and found that miR-1205 was the target of circARVCF (**Figure 3A**). MiR-1205 mimic transfection apparently increased miR-1205 expression and miR-1205 inhibitor (in-miR-1205) transfection markedly reduced miR-1205 expression in MKN-45/DDP and AGS/DDP cells (**Figure 3B**). Then dual-luciferase reporter assay and RIP assay were performed to analyze the relationship between circARVCF and miR-1206. The results showed that miR-1205 overexpression restrained the luciferase activity of circARVCF WT in MKN-45/DDP and AGS/DDP cells, but had no effect on circARVCF MUT luciferase activity (**Figures 3C,D**). RIP assay showed that circARVCF and miR-1205 enrichment was increased by Anti-AGO2 RIP compared to Anti-IgG and Input control groups (**Figures 3E,F**). As expected, miR-1205 was lowly expressed in GC tissues and cells compared to normal tissues and cells (**Figures 3G,H**). Furthermore, miR-1205 was downregulated in DDP-resistant GC tissues and cells in comparison with DDP-sensitive GC tissues and cells (**Figures 3I,J**). In addition, it was found that circARVCF knockdown significantly increased miR-1205 expression in MKN-45/DDP and AGS/DDP cells, while in-miR-1205 transfection reversed the effect (**Figure 3K**). To summarize, circARVCF directly targeted miR-1205 to regulate miR-1205 expression.

CircARVCF Knockdown Inhibited DDP Resistance in DDP-Resistant GC Cells by Targeting miR-1205

Thereafter, whether circARVCF could regulate DDP resistance by targeting miR-1205 was clarified by transfecting MKN-45/DDP and AGS/DDP cells with si-NC, si-circARVCF#1, si-circARVCF#1+in-miR-NC, or si-circARVCF#1+in-miR-1205. CCK-8 assay showed that the inhibitory effect of circARVCF knockdown on the resistance of MKN-45/DDP and AGS/DDP cells to DDP was recovered by miR-1205 inhibition (**Figures**

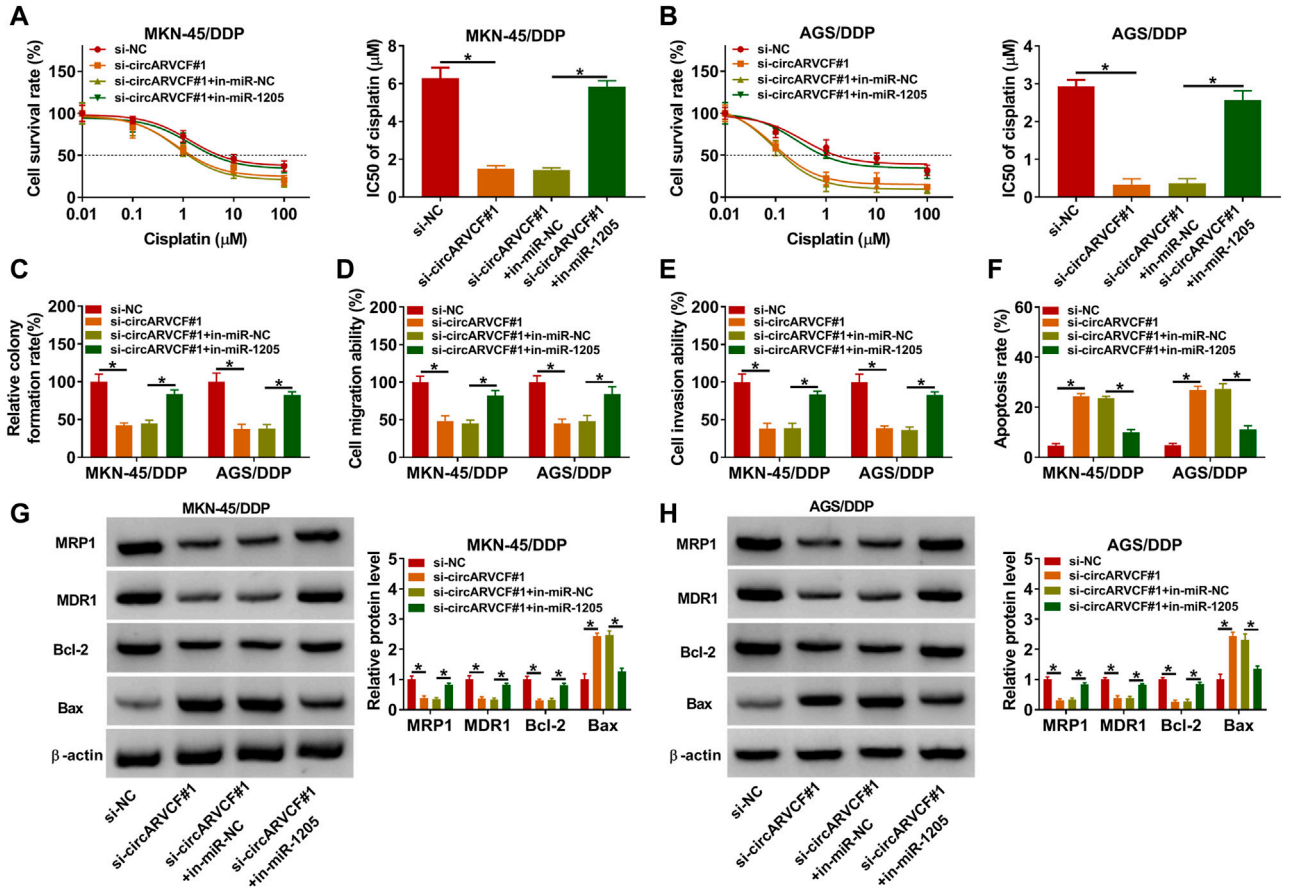

FIGURE 4 | Inhibition of miR-1205 reversed the effects of circARVCF knockdown on DDP resistance, cell colony formation, migration, invasion, and apoptosis in DDP-resistant GC cells. MKN-45/DDP and AGS/DDP cells were transfected with si-NC, si-circARVCF#1, si-circARVCF#1+in-miR-NC, or si-circARVCF#1+in-miR-1205. **(A,B)** IC50 of cisplatin was estimated by CCK-8 assay. **(C)** The colony formation of MKN-45/DDP and AGS/DDP cells was examined with colony formation assay. **(D,E)** The migration and invasion of MKN-45/DDP and AGS/DDP cells were assessed by transwell assay. **(F)** The apoptosis of MKN-45/DDP and AGS/DDP cells was analyzed by flow cytometry analysis. **(G,H)** The protein levels of MRP1, MDR1, Bcl-2 and Bax in MKN-45/DDP and AGS/DDP cells were measured *via* western blot assay. $^*p < 0.05$.

4A,B). Colony formation assay showed that circARVCF silencing repressed MKN-45/DDP and AGS/DDP cell colony formation ability, while miR-1205 inhibition reversed the effect (**Figure 4C**). As illustrated by transwell assay, circARVCF deficiency hampered MKN-45/DDP and AGS/DDP cells to migrate and invade, whereas these impacts were weakened by reducing miR-1205 (**Figures 4D,E**). Flow cytometry analysis indicated that circARVCF silencing facilitated the apoptosis of MKN-45/DDP and AGS/DDP cells, with miR-1205 inhibition abated the impact (**Figure 4F**). In addition, circARVCF silencing reduced the levels of MRP1, MDR1 and Bcl-2 and elevated the level of Bax in MKN-45/DDP and AGS/DDP cells, while miR-1205 downregulation reversed the effects (**Figures 4G,H**). These findings suggested that circARVCF inhibited DDP resistance in DDP-resistant GC cells by binding to miR-1205.

FGFR1 Was the Target Gene of miR-1205

Subsequently, the potential target genes of miR-1205 wwere analyzed by Targetscan (http://www.targetscan.org/cgi-bin/targetscan/vert_71/view_gene.cgi?rs=ENST00000397091.5&taxid=9606&members=miR-1205&showcnc=1&shownc=1&shownc_nc=1&showncf1=1&showncf2=1&subset=1). As a result, FGFR1 was found to contain the binding sites of miR-1205 (**Figure 5A**). Then dual-luciferase reporter assay further demonstrated the interaction between miR-1205 and FGFR1 for the luciferase activity of FGFR1 3′UTR WT in MKN-45/DDP and AGS/DDP cells was inhibited after miR-1205 overexpression (**Figures 5B,C**). Indeed, the mRNA and protein levels of FGFR1 were upregulated in GC tissues compared to adjacent normal tissues (**Figures 5D,E**). Compared to GES-1 cells, FGFR1 protein level was increased in MKN-45 and AGS cells (**Figure 5F**). Moreover, FGFR1 mRNA and protein levels were increased in DDP-resistant GC tissues compared to DDP-sensitive GC tissues (**Figures 5G,H**). The protein level of FGFR1 was higher in MKN-45/DDP and AGS/DDP cells than MKN-45 and AGS cells (**Figure 5I**). Besides, miR-1205 overexpression reduced FGFR1 protein level in MKN-45/DDP and AGS/DDP cells, while the effect

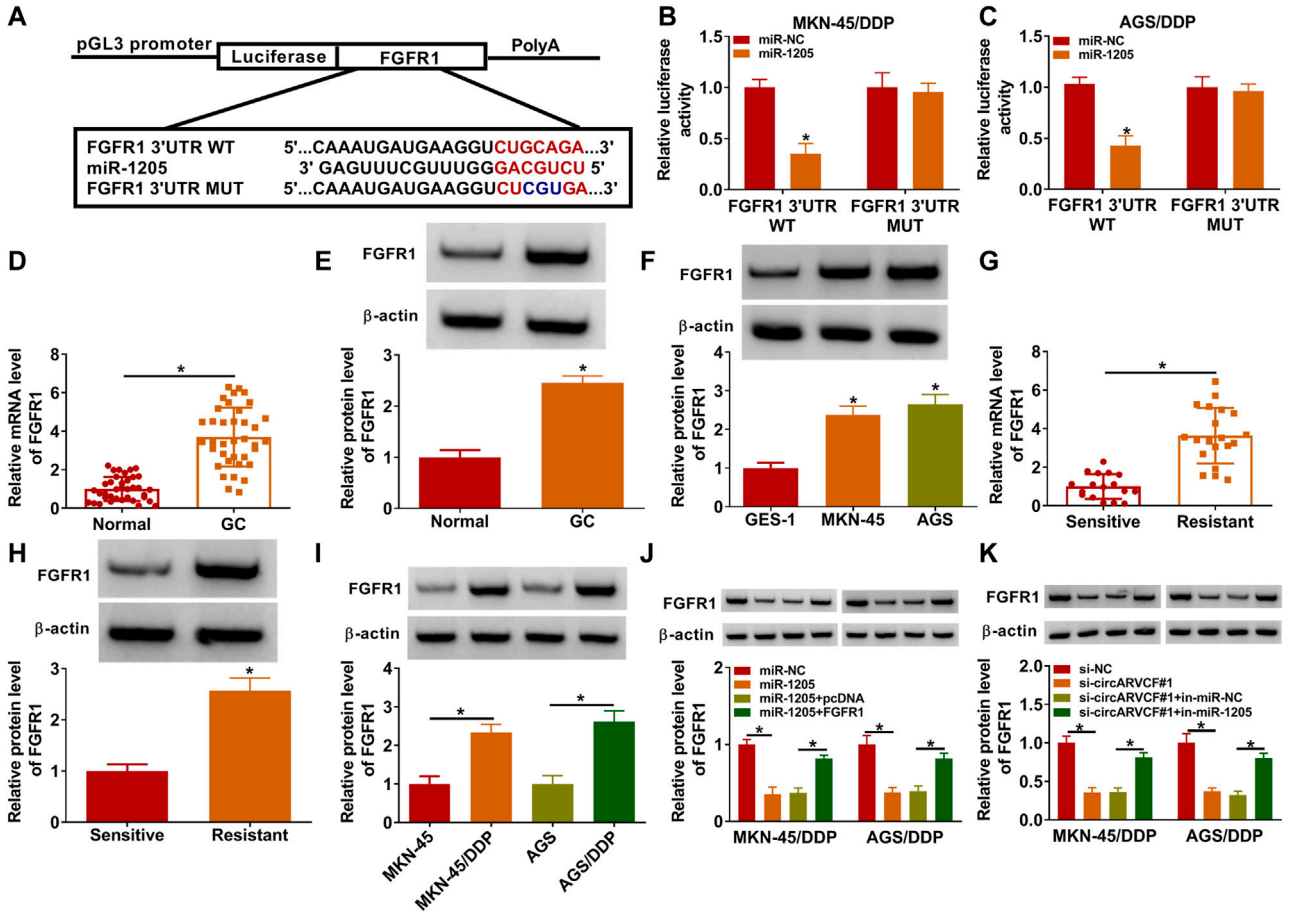

FIGURE 5 | CircARVCF regulated FGFR1 expression by targeting miR-1205. **(A)** The complementary sequences between FGFR1 and miR-1205 were exhibited. **(B,C)** The relationship between FGFR1 and miR-1205 was analyzed by dual-luciferase reporter assay. **(D,E)** The mRNA and protein levels of FGFR1 in GC tissues and normal tissues were measured by qRT-PCR or western blot assay. **(F)** The protein level of FGFR1 in GES-1, MKN-45 and AGS cells was measured via western blot assay. **(G,H)** The mRNA and protein levels of FGFR1 in DDP-resistant and DDP-sensitive GC tissues were quantified by qRT-PCR or western blot. **(I)** The protein level of FGFR1 in MKN-45, MKN-45/DDP, AGS and AGS/DDP cells was measured via western blot assay. **(J)** The protein level of FGFR1 in MKN-45/DDP and AGS/DDP cells transfected with miR-NC, miR-1205, miR-1205 + pcDNA or miR-1205 + FGFR1 was measured via western blot assay. **(K)** The protein level of FGFR1 in MKN-45/DDP and AGS/DDP cells transfected with si-NC, si-circARVCF#1, si-circARVCF#1+in-miR-NC or si-circARVCF#1+in-miE-1205 was measured through western blot assay. *$p < 0.05$.

was rescued by elevating FGFR1 (**Figure 5J**). Remarkably, circARVCF interference decreased the protein level of FGFR1 in MKN-45/DDP and AGS/DDP cells, whereas miR-1205 inhibition restored the impact (**Figure 5K**). Taken together, circARVCF directly targeted miR-1205 to positively regulate FGFR1 expression.

MiR-1205 Overexpression Suppressed DDP Resistance in DDP-Resistant GC Cells *via* Regulating FGFR1 Expression

To explore whether miR-1205 could regulate the resistance of DDP-resistant GC cells to DDP, MKN-45/DDP, and AGS/DDP cells were introduced with miR-NC, miR-1205, miR-1205 + pcDNA or miR-1205 + FGFR1. As indicated by CCK-8 assay, miR-1205 overexpression inhibited DDP resistance in MKN-45/DDP and AGS/DDP cells, while FGFR1 elevation ameliorated the effect (**Figures 6A,B**). The results of colony formation assay, transwell assay and flow cytometry analysis exhibited that miR-1205 overexpression restrained cell colony formation, migration and invasion and promoted apoptosis in MKN-45/DDP and AGS/DDP cells, while these impacts were abrogated by increasing FGFR1 expression (**Figures 6C–F**). Additionally, miR-1205 overexpression reduced MRP1, MDR1 and Bcl-2 levels and elevated Bax level in MKN-45/DDP and AGS/DDP cells, with FGFR1 enhancement ameliorated the effects (**Figures 6G,H**). To sum up, miR-1205 overexpression inhibited the resistance of DDP-resistant GC cells to DDP through interacting with FGFR1.

CircARVCF Knockdown Suppressed DDP Resistance *in Vivo*

Finally, the role of circARVCF in DDP resistance *in vivo* was investigated. Our results showed that circARVCF knockdown

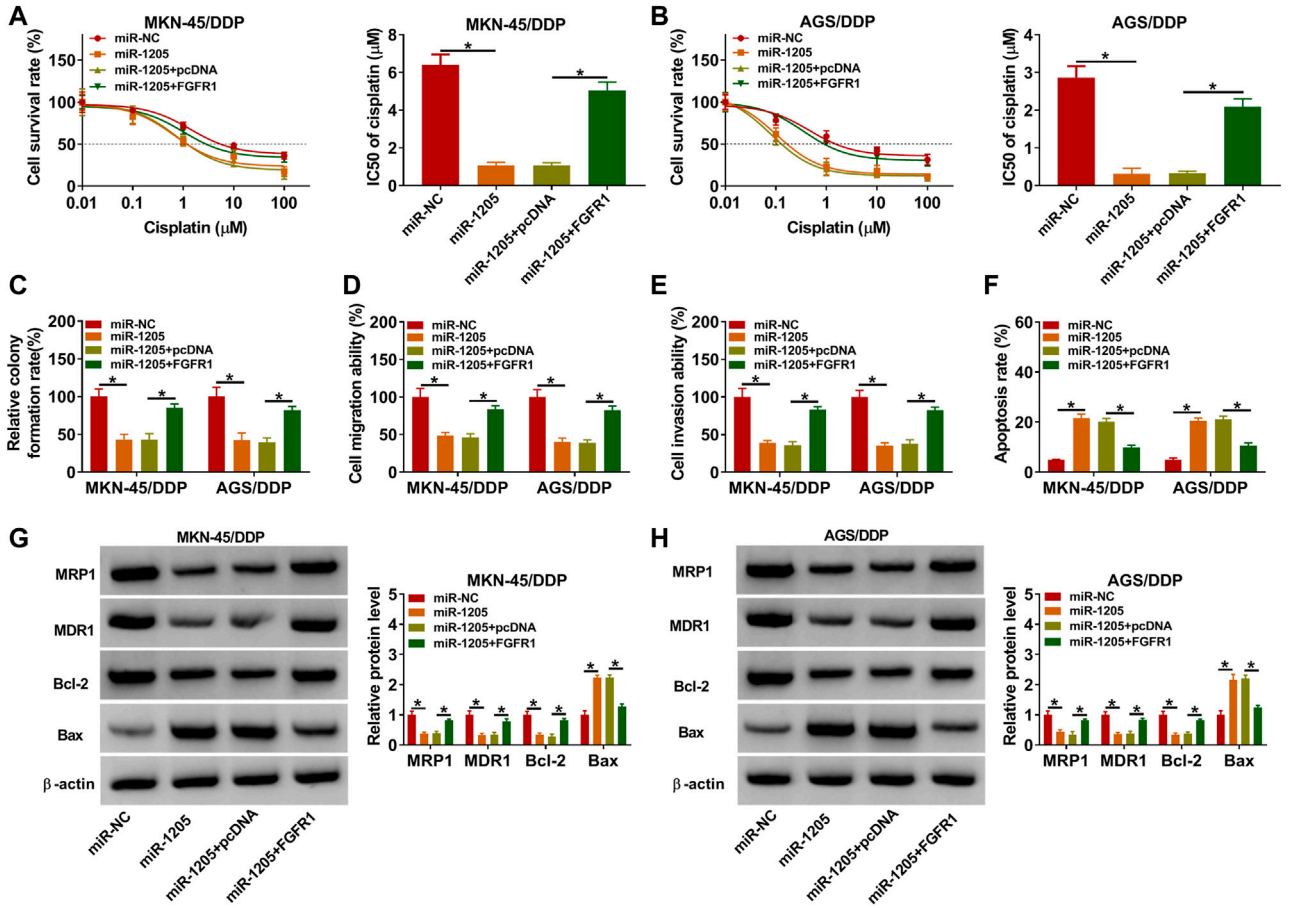

FIGURE 6 | MiR-1205 regulated the DDP resistance and malignant behaviors of DDP-resistant GC cells by targeting FGFR1. MKN-45/DDP and AGS/DDP cells were transfected with miR-NC, miR-1205, miR-1205 + pcDNA or miR-1205 + FGFR1. **(A,B)** DDP resistance was analyzed by CCK-8 assay. **(C–F)** The colony formation, migration, invasion and apoptosis of MKN-45/DDP and AGS/DDP cells were evaluated by colony formation assay, transwell assay and flow cytometry analysis, respectively. **(G,H)** The protein levels of MRP1, MDR1, Bcl-2 and Bax in MKN-45/DDP and AGS/DDP cells were measured via western blot assay. *$p < 0.05$.

and DDP treatment repressed tumor growth (including tumor volume and tumor weight) (**Figures 7A,B**). As determined by qRT-PCR, western blot assay and IHC assay, the levels of circARVCF and FGFR1 were decreased and the level of miR-1205 was increased in the tumors in sh-circARVCF + PBS and sh-circARVCF + DDP groups compared to sh-NC + PBS and sh-NC + DDP groups (**Figures 7C–F**). These results suggested the suppressive role of circARVCF knockdown on DDP resistance in GC *in vivo*.

DISCUSSION

Chemoresistance is the main obstacle in the process of human cancer therapy (Marin et al., 2016). CircRNAs have been disclosed to play vital roles in tumor advancement and therapeutic resistance (Wei et al., 2020). Even so, there are still large amounts of circRNAs that have not been identified. In this study, the functions of circARVCF in DDP resistance were clarified. As a result, circARVCF inhibited the sensitivity of GC to DDP through a new regulatory axis of circARVCF/miR-1205/FGFR1.

Currently, the involvement of circRNAs and miRNAs in regulating GC chemoresistance has been reported. For example, Zhong *et al.* declared that circ_0032821 facilitated OXA resistance and malignant cell behaviors in GC partially *via* influencing miR-515-5p/SOX9 axis (Zhong et al., 2021). Zhang *et al.* demonstrated the suppressive role of circ_0026359/miR-1200/POLD4 axis in DDP sensitivity of GC (Zhang et al., 2020). Circ-PVT1 enhanced the resistance of GC cells to paclitaxel by increasing ZEB1 *via* sponging miR-124-3p (Liu et al., 2019). Circ_0110805 aggravated the cisplatin resistance of GC by sponging miR-299-3p and elevating ENDOPDI (Yang et al., 2020a). CircAKT3/miR-198/PIK3RI played a promotional effect on cisplatin resistance of GC (Huang et al., 2019). These reports all indicated that chemoresistance could be modulated by circRNAs. In the present study, circARVCF was increased in DDP-resistant GC tissues and cells. Next, we performed experiments to explore the functions of circARVCF in DDP resistance of GC. It was found

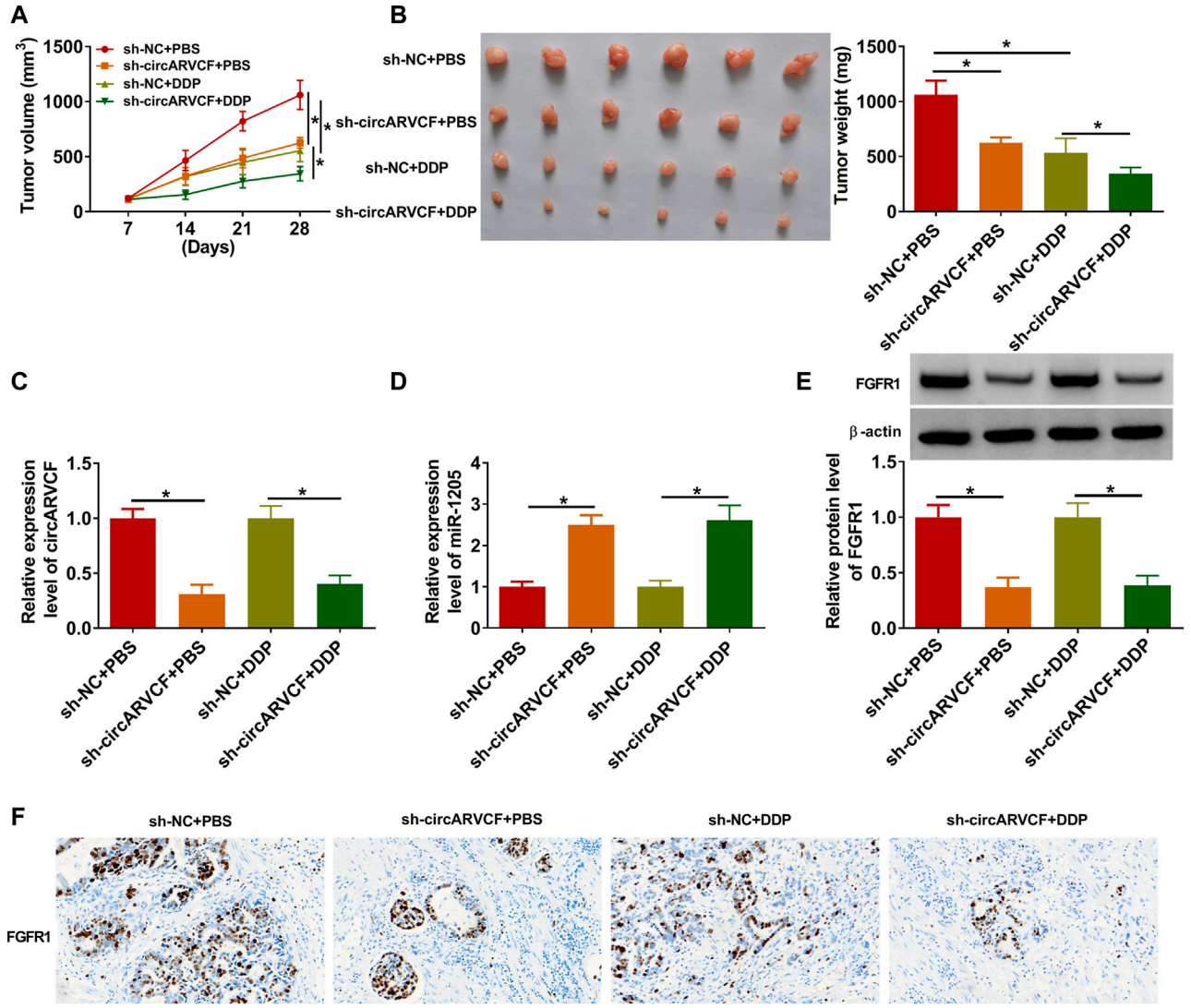

FIGURE 7 | CircARVCF enhanced DDP resistance in GC *in vivo*. **(A,B)** Tumor volume and tumor weight were examined. **(C,D)** The levels of circARVCF and miR-1205 in the tumors were examined by qRT-PCR. **(E,F)** The level of FGFR1 in the tumors was examined by western blot assay and IHC assay. *$p < 0.05$.

that circARVCF silencing inhibited IC50 of DDP, cell colony formation and metastasis and triggered apoptosis in DDP-resistant GC cells. Moreover, the *in vivo* experiments demonstrated the promotional effect of circARVCF knockdown on DDP sensitivity *in vivo*. These findings suggested that circARVCF boosted the resistance of GC to DDP.

CircRNAs can be involved in the chemoresistance of cancers by binding to miRNAs and then alter miRNA target gene expression (Hansen et al., 2013). Herein, circARVCF could interact with miR-1205, which then targeted FGFR1 to alter FGFR1 expression. MiR-1205 has been reported to repress the metastasis and proliferation of GC cells *via* circCYFIP2/miR-1205/E2F1 pathway (Lin et al., 2020). Moreover, miR-1205 was associated with sorafenib resistance in hepatocellular carcinoma by interacting with circFN1 and E2F1 (Yang et al., 2020b). Nonetheless, we firstly explored the functions of miR-1205 in DDP sensitivity of GC. It was found that miR-1205 was reduced in DDP-resistant GC. Inhibition of miR-1205 restored circARVCF knockdown-mediated inhibitory influence on DDP sensitivity of chemo-resistant GC cells. Overexpression of miR-1205 enhanced DDP sensitivity and restrained malignant cell phenotypes in DDP-resistant GC cells.

FGFR1 can be activated to influence the proliferation, survival, migration and differentiation of tumor cells (Neal et al., 1985; Guo et al., 2017). FGFR1 could serve as the target for diverse miRNAs, such as miR-198 (Gu et al., 2019), miR-497 (Xie et al., 2018), and miR-133b (Wen et al., 2013). However, FGFR1 was verified to be the target gene of miR-1205 for the first time. Moreover, FGFR1 participated in the regulation of chemosensitivity in several cancers (Hong et al., 2020; Kong et al., 2020). In the research, FGFR1 could combine with miR-

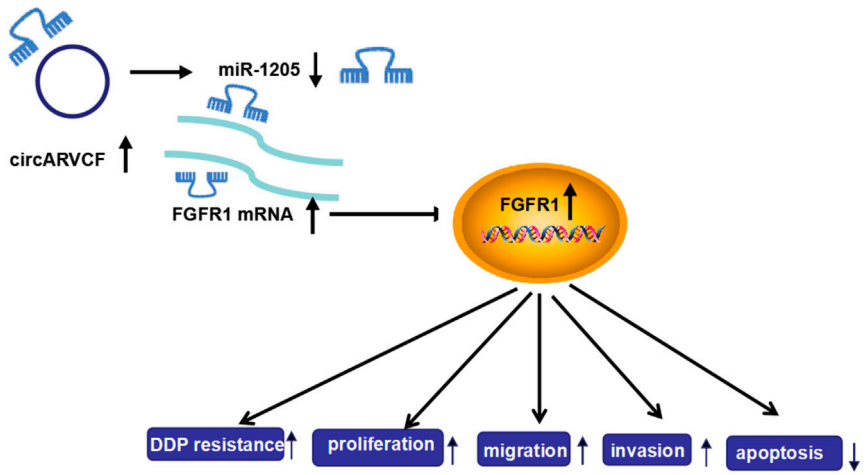

FIGURE 8 | The frame diagram of circARVCF/miR-1205/FGFR1 axis in regulating DDP resistance and cell progression in GC.

1205 to alter DDP resistance in GC. In addtion, FGFR1 has been reported to regulate the biologocal processess, including wound repair, tissue regeneration, inflammation and angiogenesis, which are implcated in cancer progression and drug resistance (Liang et al., 2021; Yang et al., 2021). However, whether circARVCF/miR-1205/FGFR1 axis is involved in these biological processes to regulate DDP resistance is still unclear.

Taken together, circARVCF contributed to DDP resistance and promoted tumor cell proliferation, migration, and invasion in GC by regulating miR-1205 and FGFR1 expression (**Figure 8**). This study deepened our understanding of the progression of chemoresistance and provided a novel insight to resist drug resistance in GC.

DATA AVAILABILITY STATEMENT

The original contributions presented in the study are included in the article/**Supplementary Material**, further inquiries can be directed to the corresponding authors.

ETHICS STATEMENT

The studies involving human participants were reviewed and approved by the Huai'an First People's Hospital. The patients/participants provided their written informed consent to participate in this study.

AUTHOR CONTRIBUTIONS

All authors have been involved in the management of the patient and in the conception of the manuscript. RZ and JW have been involved in the drafting of the manuscript or its critical revision for important intellectual content. All authors have read and approved the final manuscript.

SUPPLEMENTARY MATERIAL

The Supplementary Material for this article can be found online at: https://www.frontiersin.org/articles/10.3389/fgene.2021.767590/full#supplementary-material

REFERENCES

Bagrodia, A., Lee, B. H., Lee, W., Cha, E. K., Sfakianos, J. P., Iyer, G., et al. (2016). Genetic Determinants of Cisplatin Resistance in Patients with Advanced Germ Cell Tumors. *J. Clin. Oncol.* 34 (33), 4000–4007. doi:10.1200/jco.2016.68.7798

Bray, F., Ferlay, J., Soerjomataram, I., Siegel, R. L., Torre, L. A., and Jemal, A. (2018). Global Cancer Statistics 2018: GLOBOCAN Estimates of Incidence and Mortality Worldwide for 36 Cancers in 185 Countries. *CA Cancer J. Clin.* 68 (6), 394–424. doi:10.3322/caac.21492

Chen, L.-L., and Yang, L. (2015). Regulation of circRNA Biogenesis. *RNA Biol.* 12 (4), 381–388. doi:10.1080/15476286.2015.1020271

Cui, C., Yang, J., Li, X., Liu, D., Fu, L., and Wang, X. (2020). Functions and Mechanisms of Circular RNAs in Cancer Radiotherapy and Chemotherapy Resistance. *Mol. Cancer* 19 (1), 58. doi:10.1186/s12943-020-01180-y

Galluzzi, L., Senovilla, L., Vitale, I., Michels, J., Martins, I., Kepp, O., et al. (2012). Molecular Mechanisms of Cisplatin Resistance. *Oncogene* 31 (15), 1869–1883. doi:10.1038/onc.2011.384

Gao, H., Xu, J., Qiao, F., and Xue, L. (2021). Depletion of Hsa_circ_0000144 Suppresses Oxaliplatin Resistance of Gastric Cancer Cells by Regulating miR-502-5p/ADAM9 Axis. *Onco. Targets Ther.* 14, 2773–2787. doi:10.2147/ott.s281238

Gu, J., Li, X., Li, H., Jin, Z., and Jin, J. (2019). MicroRNA-198 Inhibits Proliferation and Induces Apoptosis by Directly Suppressing FGFR1 in Gastric Cancer. *Biosci. Rep.* 39 (6), BSR20181258. doi:10.1042/BSR20181258

Guggenheim, D. E., and Shah, M. A. (2013). Gastric Cancer Epidemiology and Risk Factors. *J. Surg. Oncol.* 107 (3), 230–236. doi:10.1002/jso.23262

Guo, Q., Sun, Y., Yu, S., Bai, H., Zhao, J., Zhuo, M., et al. (2017). Programmed Cell Death-Ligand 1 (PD-L1) Expression and Fibroblast Growth Factor Receptor 1

(FGFR1) Amplification in Stage III/IV Lung Squamous Cell Carcinoma (SQC). *Thorac. Cancer* 8 (2), 73–79. doi:10.1111/1759-7714.12399

Han, B., Wang, X., and Yin, X. (2021). Knockdown of circRAD23B Exerts Antitumor Response in Colorectal Cancer via the Regulation of miR-1205/TRIM44 axis. *Dig. Dis. Sci.* doi:10.1007/s10620-021-06859-w

Hansen, T. B., Jensen, T. I., Clausen, B. H., Bramsen, J. B., Finsen, B., Damgaard, C. K., et al. (2013). Natural RNA Circles Function as Efficient microRNA Sponges. *Nature* 495 (7441), 384–388. doi:10.1038/nature11993

Hong, S., Yan, Z., Song, Y., Bi, M., and Li, S. (2020). LncRNA AGAP2-AS1 Augments Cell Viability and Mobility, and Confers Gemcitabine Resistance by Inhibiting miR-497 in Colorectal Cancer. *Aging* 12 (6), 5183–5194. doi:10.18632/aging.102940

Huang, X., Li, Z., Zhang, Q., Wang, W., Li, B., Wang, L., et al. (2019). Circular RNA AKT3 Upregulates PIK3R1 to Enhance Cisplatin Resistance in Gastric Cancer via miR-198 Suppression. *Mol. Cancer* 18 (1), 71. doi:10.1186/s12943-019-0969-3

Huang, X. X., Zhang, Q., Hu, H., Jin, Y., Zeng, A. L., Xia, Y. B., et al. (2020). A Novel Circular RNA circFN1 Enhances Cisplatin Resistance in Gastric Cancer via Sponging miR-182-5p. *J. Cel Biochem.* 122. doi:10.1002/jcb.29641

Kong, S., Cao, Y., Li, X., Li, Z., Xin, Y., and Meng, Y. (2020). MiR-3116 Sensitizes Glioma Cells to Temozolomide by Targeting FGFR1 and Regulating the FGFR1/PI3K/AKT Pathway. *J. Cel Mol. Med.* 24 (8), 4677–4686. doi:10.1111/jcmm.15133

Liang, Q., Wang, J., Zhao, L., Hou, J., Hu, Y., and Shi, J. (2021). Recent Advances of Dual FGFR Inhibitors as a Novel Therapy for Cancer. *Eur. J. Med. Chem.* 214, 113205. doi:10.1016/j.ejmech.2021.113205

Lin, J., Liao, S., Li, E., Liu, Z., Zheng, R., Wu, X., et al. (2020). circCYFIP2 Acts as a Sponge of miR-1205 and Affects the Expression of its Target Gene E2F1 to Regulate Gastric Cancer Metastasis. *Mol. Ther. Nucleic Acids* 21, 121–132. doi:10.1016/j.omtn.2020.05.007

Liu, Y. Y., Zhang, L. Y., and Du, W. Z. (2019). Circular RNA Circ-PVT1 Contributes to Paclitaxel Resistance of Gastric Cancer Cells through the Regulation of ZEB1 Expression by Sponging miR-124-3p. *Biosci. Rep.* 39 (12), BSR20193045. doi:10.1042/BSR20193045

Marin, J. J. G., Al-Abdulla, R., Lozano, E., Briz, O., Bujanda, L., M. Banales, J., et al. (2016). Mechanisms of Resistance to Chemotherapy in Gastric Cancer. *Acamc* 16 (3), 318–334. doi:10.2174/1871520615666150803125121

Neal, D., Bennett, M., Hall, R., Marsh, C., Abel, P., Sainsbury, J. R. C., et al. (1985). Epidermal-growth-factor Receptors in Human Bladder Cancer: Comparison of Invasive and Superficial Tumours. *Lancet* 325 (8425), 366–368. doi:10.1016/s0140-6736(85)91386-8

Ouyang, Y., Li, Y., Huang, Y., Li, X., Zhu, Y., Long, Y., et al. (2019). CircRNA circPDSS1 Promotes the Gastric Cancer Progression by Sponging miR-186-5p and Modulating NEK2. *J. Cel Physiol.* 234 (7), 10458–10469. doi:10.1002/jcp.27714

Song, Z., Wu, Y., Yang, J., Yang, D., and Fang, X. (2017). Progress in the Treatment of Advanced Gastric Cancer. *Tumour Biol.* 39 (7), 1010428317714626. doi:10.1177/1010428317714626

Taheri, M., Shoorei, H., Tondro Anamag, F., Ghafouri-Fard, S., and Dinger, M. E. (2021). LncRNAs and miRNAs Participate in Determination of Sensitivity of Cancer Cells to Cisplatin. *Exp. Mol. Pathol.*, 104602. doi:10.1016/j.yexmp.2021.104602

Wang, Y., Mo, Y., Gong, Z., Yang, X., Yang, M., Zhang, S., et al. (2017). Circular RNAs in Human Cancer. *Mol. Cancer* 16 (1), 25. doi:10.1186/s12943-017-0598-7

Wang, G., Yang, B., Fu, Z., Wang, X., and Zhang, Z. (2019). Efficacy and Safety of Oxaliplatin-Based Regimen versus Cisplatin-Based Regimen in the Treatment of Gastric Cancer: a Meta-Analysis of Randomized Controlled Trials. *Int. J. Clin. Oncol.* 24 (6), 614–623. doi:10.1007/s10147-019-01425-x

Wang, L., Shang, X., and Feng, Q. (2019). LncRNA TATDN1 Contributes to the Cisplatin Resistance of Non-small Cell Lung Cancer through TATDN1/miR-451/TRIM66 axis. *Cancer Biol. Ther.* 20 (3), 261–271. doi:10.1080/15384047.2018.1529091

Wang, X.-y., Zhou, Y.-c., Wang, Y., Liu, Y.-y., Wang, Y.-x., Chen, D.-d., et al. (2020). miR-149 Contributes to Resistance of 5-FU in Gastric Cancer via Targeting TREM2 and Regulating β-catenin Pathway. *Biochem. Biophys. Res. Commun.* 532 (3), 329–335. doi:10.1016/j.bbrc.2020.05.135

Wang, G., Zhang, H., and Li, P. (2020). Upregulation of hsa_circRNA_102958 Indicates Poor Prognosis and Promotes Ovarian Cancer Progression through miR-1205/SH2D3A Axis. *Cmar* 12, 4045–4053. doi:10.2147/cmar.s248560

Wang, J., Li, T., and Wang, B. (2021). Circ-UBAP2 Functions as Sponges of miR-1205 and miR-382 to Promote Glioma Progression by Modulating STC1 Expression. *Cancer Med.* 10 (5), 1815–1828. doi:10.1002/cam4.3759

Wei, L., Sun, J., Zhang, N., Zheng, Y., Wang, X., Lv, L., et al. (2020). Noncoding RNAs in Gastric Cancer: Implications for Drug Resistance. *Mol. Cancer* 19 (1), 62. doi:10.1186/s12943-020-01185-7

Wen, D., Li, S., Ji, F., Cao, H., Jiang, W., Zhu, J., et al. (2013). miR-133b Acts as a Tumor Suppressor and Negatively Regulates FGFR1 in Gastric Cancer. *Tumor Biol.* 34 (2), 793–803. doi:10.1007/s13277-012-0609-7

Xie, G., Ke, Q., Ji, Y. Z., Wang, A. Q., Jing, M., and Zou, L. L. (2018). FGFR1 Is an Independent Prognostic Factor and Can Be Regulated by miR-497 in Gastric Cancer Progression. *Braz. J. Med. Biol. Res.* 52 (1), e7816. doi:10.1590/1414-431X20187816

Yang, X., Zhang, Q., and Guan, B. (2020). Circ_0110805 Knockdown Enhances Cisplatin Sensitivity and Inhibits Gastric Cancer Progression by miR-299-3p/ENDOPDI Axis. *Onco. Targets Ther.* 13, 11445–11457. doi:10.2147/ott.s279563

Yang, C., Dong, Z., Hong, H., Dai, B., Song, F., Geng, L., et al. (2020). circFN1 Mediates Sorafenib Resistance of Hepatocellular Carcinoma Cells by Sponging miR-1205 and Regulating E2F1 Expression. *Mol. Ther. Nucleic Acids* 22, 421–433. doi:10.1016/j.omtn.2020.08.039

Yang, L., Zhou, F., Zheng, D., Wang, D., Li, X., Zhao, C., et al. (2021). FGF/FGFR Signaling: From Lung Development to Respiratory Diseases. *Cytokine Growth Factor. Rev.* doi:10.1016/j.cytogfr.2021.09.002

Yu, J., Zhang, X., Ma, Y., Li, Z., Tao, R., Chen, W., et al. (2021). MiR-129-5p Restrains Apatinib Resistance in Human Gastric Cancer Cells via Downregulating HOXC10. *Cancer Biother. Radiopharm.* 36 (1), 95–105. doi:10.1089/cbr.2019.3107

Zhang, Z., Yu, X., Zhou, B., Zhang, J., and Chang, J. (2020). Circular RNA Circ_0026359 Enhances Cisplatin Resistance in Gastric Cancer via Targeting miR-1200/POLD4 Pathway. *Biomed. Res. Int.* 2020, 5103272. doi:10.1155/2020/5103272

Zhi, X., Tao, J., Xiang, G., Cao, H., Liu, Z., Yang, K., et al. (2015). APRIL Induces Cisplatin Resistance in Gastric Cancer Cells via Activation of the NF-κB Pathway. *Cell Physiol. Biochem.* 35 (2), 571–585. doi:10.1159/000369720

Zhong, Y., Du, Y., Yang, X., Mo, Y., Fan, C., Xiong, F., et al. (2018). Circular RNAs Function as ceRNAs to Regulate and Control Human Cancer Progression. *Mol. Cancer* 17 (1), 79. doi:10.1186/s12943-018-0827-8

Zhong, Y., Wang, D., Ding, Y., Tian, G., and Jiang, B. (2021). Circular RNA Circ_0032821 Contributes to Oxaliplatin (OXA) Resistance of Gastric Cancer Cells by Regulating SOX9 via miR-515-5p. *Biotechnol. Lett.* 43 (2), 339–351. doi:10.1007/s10529-020-03036-3

Conflict of Interest: The authors declare that the research was conducted in the absence of any commercial or financial relationships that could be construed as a potential conflict of interest.

Publisher's Note: All claims expressed in this article are solely those of the authors and do not necessarily represent those of their affiliated organizations, or those of the publisher, the editors and the reviewers. Any product that may be evaluated in this article, or claim that may be made by its manufacturer, is not guaranteed or endorsed by the publisher.

frontiers in Genetics

ORIGINAL RESEARCH
published: 12 January 2022
doi: 10.3389/fgene.2021.768130

Chrysin Modulates Aberrant Epigenetic Variations and Hampers Migratory Behavior of Human Cervical (HeLa) Cells

Ritu Raina[1], Abdulmajeed G. Almutary[2], Sali Abubaker Bagabir[3], Nazia Afroze[1], Sharmila Fagoonee[4], Shafiul Haque[5,6] and Arif Hussain[1]**

[1]School of Life Sciences, Manipal Academy of Higher Education, Dubai, United Arab Emirates, [2]Department of Medical Biotechnology, College of Applied Medical Sciences, Qassim University, Saudi Arabia, [3]Department of Medical Laboratory Technology, Faculty of Applied Medical Sciences, Jazan University, Jazan, Saudi Arabia, [4]Molecular Biotechnology Center, Institute of Biostructure and Bioimaging (CNR), Turin, Italy, [5]Research and Scientific Studies Unit, College of Nursing and Allied Health Sciences, Jazan University, Jazan, Saudi Arabia, [6]Bursa Uludağ University Faculty of Medicine, Görükle Campus, Bursa, Turkey

OPEN ACCESS

Edited by:
Ata Abbas,
Case Western Reserve University, United States

Reviewed by:
Lubna Wasim,
All India Institute of Medical Sciences, India
Sabiha Khatoon,
Texas Tech University Health Sciences Center, United States

***Correspondence:**
Arif Hussain
dr.arifhussain@yahoo.co.in
Abdulmajeed G. Almutary
abdulmajeed.almutary@qu.edu.sa

Specialty section:
This article was submitted to Cancer Genetics and Oncogenomics, a section of the journal Frontiers in Genetics

Received: *31 August 2021*
Accepted: *06 December 2021*
Published: *12 January 2022*

Citation:
Raina R, Almutary AG, Bagabir SA, Afroze N, Fagoonee S, Haque S and Hussain A (2022) Chrysin Modulates Aberrant Epigenetic Variations and Hampers Migratory Behavior of Human Cervical (HeLa) Cells. Front. Genet. 12:768130. doi: 10.3389/fgene.2021.768130

Purpose: Plant-derived phytochemicals have shown epigenetic modulatory effect in different types of cancer by reversing the pattern of DNA methylation and chromatin modulation, thereby restoring the function of silenced tumor-suppressor genes. In the present study, attempts have been made to explore chrysin-mediated epigenetic alterations in HeLa cells.

Methods: Colony formation and migration assays followed by methylation-specific PCR for examining the methylation status of CpG promoters of various tumor-suppressor genes (TSGs) and the expression of these TSGs at the transcript and protein levels were performed. Furthermore, global DNA methylation; biochemical activities of DNA methyltransferases (DNMTs), histone methyl transferases (HMTs), histone deacetylases (HDACs), and histone acetyl transferases (HATs) along with the expression analysis of chromatin-modifying enzymes; and H3 and H4 histone modification marks analyses were performed after chrysin treatment.

Results: The experimental analyses revealed that chrysin treatment encourages cytostatic behavior as well as inhibits the migration capacity of HeLa cells in a time- and dose-dependent manner. Chrysin reduces the methylation of various tumor-suppressor genes, leading to their reactivation at mRNA and protein levels. The expression levels of various chromatin-modifying enzymes *viz* DNMTs, HMTs, HDACs, and HATS were found to be decreased, and H3 and H4 histone modification marks were modulated too. Also, reduced global DNA methylation was observed following the treatment of chrysin.

Conclusion: This study concludes that chrysin can be used as a potential epigenetic modifier for cancer treatment and warrants for further experimental validation.

Keywords: phytochemicals, epigenetic modification, DNA methylation, epigenome, chrysin

INTRODUCTION

Regular cell functions are modifiable by different epigenetic modifications, and these alterations play a crucial role during cellular growth and development (Rahman et al., 2016; Shankar et al., 2016). The epigenetic modifications occur by the way of regulatory mechanisms involving histone modifications, DNA methylation, microRNAs, and chromatin remodeling that modulates gene expression and disturbs cellular machinery and homeostasis in cancer cells (Huang et al., 2011; Ong et al., 2011; You and Jones, 2012; Ho et al., 2013; Aggarwal et al., 2015; Busch et al., 2015; Shankar et al., 2016). DNA methylation at CpG residues of the promoters of tumor suppressor genes (TSGs) causes repression of tumor-suppressor genes (Hatzimichael and Crook, 2013; Shankar et al., 2016), which is considered as a key regulatory mechanism of gene silencing and is correlated with the overexpression of DNA methyltransferases (DNMTs) (Kogan et al., 2017; Li and Wang, 2017; Piyathilake et al., 2017). Similarly, the modification of histone proteins by epigenetic enzymes, that is, HDAC (histone deacetylase), HMT (histone methyltransferase), HATs (histone acetyltransferase), and phosphorylases, leads to the repression or activation of gene activity. The equilibrium between the erasers and the writers of histone modifications is crucial for normal expression of genes, and their dysregulation may lead to cancer development (Sharma et al., 2009).

Methylation of histones at H3 and H4 lysine residues is catalyzed by histone methyl transferases (HMTs) (Ho et al., 2013; Shankar et al., 2016). Methylation marks at H3K79, H3K36, and H3K4 are supposed to be active marks, whereas H4K20, H3K27, and H3K9 methylation marks are related with transcriptional suppression (Sharma et al., 2009; Ho et al., 2013; Shankar et al., 2016). In the past, aberrant expression of both HMTs and HDMs has been reported in cancer (McLaughlin–Drubin et al., 2011; Busch et al., 2015). Histone acetylation is another important histone modification state, and hyper-acetylation leads to the stimulation of suppressed genes. Aberrant expression of HDAC has been found in cancer and is linked with gene repression and tumorigenesis (Sharma et al., 2009; Kogan et al., 2017; Andrijauskaite et al., 2019). Likewise, aberrant expressions of HATs and HDACs as well as HMTs and HDMs have been reported in various types of cancer in the past (Lin et al., 2009; Chen et al., 2017).

In the recent times, epigenetic-based cancer treatment is gaining more interest due to its reversible nature. Several FDA-approved drugs, for example, azacytidine and decitabine (DNMT inhibitors), and vorinostat and romidepsin (HDAC inhibitors), have shown promising results in solid malignancies and myelodysplastic syndrome (Herranz and Esteller, 2007a; Ong et al., 2011; Hatzimichael and Crook, 2013; Ho et al., 2013; Guo et al., 2015; Shankar et al., 2016). The combinational cancer treatment strategy in which both HDAC inhibitors and DNMT inhibitors are being used together has proven to be more effective (Herranz and Esteller, 2007a; Herranz and Esteller, 2007b; Ho et al., 2013; Shankar et al., 2016). However, low specificity and high systemic toxicity have limited their use (Paredes-Gonzalez et al., 2014). Hence, plant-derived chemopreventive agents are the main focus of scientific scope. Earlier studies have reported that dietary agents like EGCG, quercetin, genistein, curcumin, resveratrol, luteolin, and apigenin modulate the activity of DNMT and HDAC, and can lead to re-expression of silenced TSGs (Kai et al., 2010; Kim and Kim, 2013; Aggarwal et al., 2015; Guo et al., 2015; Mocanu et al., 2015; Chang and Yu, 2016a; Kanwal et al., 2016; Loh et al., 2019; Yan et al., 2020; Ganai et al., 2021a).

Chrysin (5-dihydroxyflavone), a flavone found in honey, bee propolis, and blue passion flower (*Passiflora caerulea*) extract, has gained importance as an antioxidant, antiviral, and anticancer compound (Pal-Bhadra et al., 2012; Yang et al., 2014; Kanwal et al., 2016). It induces cell cycle arrest, inhibits cell adhesion and tumor cell–induced angiogenesis, and induces apoptosis in various types of cancer, and also downregulates pathways including AKT (Khoo et al., 2010; Kasala et al., 2015; Ryu et al., 2017; Lim et al., 2018). Earlier, antiproliferative and apoptosis-inducing effects of chrysin on HeLa cells (Raina et al., 2021) have been observed. However, the role and mechanistic action of chrysin in the modulation of epigenome is not fully explored, except scanty reports wherein the role of chrysin in the modulation of epigenetic enzymes has been studied. Chrysin was found to decrease the expression of HDAC two and HDAC eight, and increase the expression of H4acK16, H3acK14, and H4acK12. It decreases H3me2K9 in (melanoma cell) A375 cells and restores the transcriptional activity of the tumor-suppressor gene $p21^{WAFI}$. Chrysin is capable enough to modify DNMT and HMT expressions in prostate cancer cells, and behaves as an epigenetic modifier (Pal-Bhadra et al., 2012; Kanwal et al., 2016; Ganai et al., 2021b). The precise mechanism of modulation of epigenome is not well explored and documented. Keeping the abovesaid facts in view, this study was performed to evaluate the significance of chrysin treatment on cell migration, DNA methylation, and histone modifications in human cervical cancer (HeLa) cells.

MATERIALS AND METHODS

Maintenance of Cervical Cancer (HeLa) Cells and Drug Dilution

Human cervical cancer (HeLa) cells were used as an *in vitro* cancer model during this study. HeLa cells were maintained in complete Dulbecco's modified Eagle medium (DMEM; Sigma-Aldrich; Merck, KGaA) containing 10% FBS (Sigma-Aldrich; Merck KGaA) and penicillin (100U/mL) (Sigma-Aldrich; Merck KGaA), and incubated at 37 °C with 5% CO_2.

Chrysin (powdered, mol wt. 254.241 g/mol) was procured from Sigma-Aldrich (Merck, KGaA), and stock solution was prepared with DMSO (78.67 mM) using DMSO (stock solution). Furthermore, sub-stock (1 mM) and concentrations (5, 10, and 15 μM) of chrysin were prepared using the complete media as a diluent.

Colony-Forming Assay

The colony-forming assay was performed following the protocol used by Crowley et al. (2016) and Sundaram et al. (2019), with

minor modifications (Crowley et al., 2016; Kedhari Sundaram et al., 2019a). Briefly, ~2.5 × 10^5 (Ho et al., 2013) cells were dispensed in six-well plates and incubated overnight followed by the treatment with increasing doses of chrysin (5, 10, and 15 μM) for 48 h. DMSO control (i.e., solvent control) and treated cells were collected after 48 h and plated at approximately 500 cells/well, and allowed to grow. The medium was changed time to time as per the requirement. After 14 days, the colonies formed were fixed by using absolute CH_3OH and stained with crystal violet. Olympus inverted microscope (Labomed, United States) was used to obtain the images of the colonies formed. ImageJ software program was used to count the colonies in treated and DMSO control wells.

Scratch-Wound Assay

The scratch-aound assay was performed to examine the inhibitory effect of chrysin on cell migration (Yang et al., 2014; Kedhari Sundaram et al., 2019a). Approximately 2 × 10^5 (Ho et al., 2013) cells were plated in a six-well plate and incubated at 37°C overnight. On the next day, a "wound" or a "cell-free" line was created on a confluent monolayer of the cells by scratching the monolayer with a pipette tip. The cells were incubated in the presence of different chrysin dilutions (10 and 15 μM) and "healing" of wounds, which ensues through cell migration, and growth toward the cell-free zone was monitored on a regular basis. An inverted microscope was used for capturing the wound images in each well prior and after 24–48 h of the treatment.

Trans-Well Chamber Assay

The invasion assay was performed to evaluate the migratory and invasive capability of chrysin-treated HeLa cells and DMSO control using the Boyden chamber (Yang et al., 2014). Briefly, 5.0 × 10^3 (Aggarwal et al., 2015) cells/well were seeded on the upper side of the insert in separate inserts, and below it in the well of a 24-well plate, the medium with FBS was kept. After 48 h, absolute methanol was used to fix the cells, and 0.1% crystal violet was used for staining purposes. The cells present inside of the chamber were cleared using an ear bud. The assessment of complete migration was performed under the microscope, and any of the five fields were scanned (five fields per filter). The images were captured for each treatment and control using ×200 magnification with an inverted microscope (Olympus Corporation). ImageJ program was used for counting the colonies. The experiment was repeated three times, and mean ± SD was used to plot the graphs considering p-value ≤0.05.

DNMT Activity Assay

Nuclear extracts from the untreated HeLa cells were prepared using the EpiQuik™ Nuclear Extraction Kit (Catalog No. OP-0002, Epigentek, United States) following the manufacturer's protocol. The EpiQuik DNMT Activity Assay Kit (Catalog No. #P-3009, Epigentek, USA) was used to check the effect of chrysin on the DNMT activity. Briefly, chrysin (@ conc. 5, 10 and 15 μM) was added to the untreated nuclear extract, buffer, and Adomet (methyl group donor) to the cytosine-rich DNA substrate–coated assay plate and incubated for 1.5 h at 37 °C. It was followed by incubation with capture and detection antibody. After signal development, the absorbance was read on an ELISA reader at 450 nm. DNMT activity inhibition was calculated by comparing with DMSO controls. The experiment was repeated three times, and the mean ± SD was used to plot the graph. The statistical significance level was calculated using one-way ANOVA, and the p-value was maintained at ≤ 0.05.

HDAC Activity Assay

The EpiQuik HDAC Activity Assay Kit (Catalog Number P-4002, Epigentek, United States) was used for evaluating the effect of chrysin on the HDAC activity. The acetylated histone substrate–coated assay plate was prepared by adding 50 μL of the biotinylated HDAC substrate diluted in wash buffer to all wells. The assay plate was incubated at room temperature for 45 min and washed with wash buffer. HDAC assay buffer was dispensed to the wells in chrysin (5, 10, and 15 μM) treated and untreated nuclear extract placed. The plate was kept at 37°C for an hour followed by incubation with capture and detection antibody. Developing solution was used to develop the signal, stop solution stopped the reaction, and OD was read at 450 nm. The percentage inhibition of the HDAC activity against chrysin treatment was calculated by comparing with DMSO control. The experiment was repeated three times, and mean ± SD was used to plot a graph. One-way ANOVA was used to check the statistical significance at the p-value ≤ 0.05.

HMT H3K9 Activity Assay

The assay was done by using the EpiQuik HMT H3K9 Activity Assay Kit (Catalog No. P-3003, Epigentek, USA) following the protocol given by the manufacturer. Briefly, to the histone three lysine substrate–coated assay plate, chrysin (@ conc. of 5, 10, and 15 μM) was added in separate wells, with untreated nuclear extract, buffer biotinylated substrate, and Adomet (methyl group donor), and incubated at 37 °C for 1.5 h. Following this step, capture antibody and detection antibody were added to the wells, and incubated at room temp for 30 min. Finally, a color was developed, and absorbance was measured using an ELISA reader at 450 nm. The percentage inhibition was calculated by comparing with DMSO control. The experiment was repeated three times, and the mean ± SD was calculated to plot a graph. One-way ANOVA was used for checking the statistical significance, and the p-value was maintained as ≤ 0.05.

HAT Activity

The assay was done using the EpiQuik™ HAT Activity Assay Kit (Catalog No. P-4003 Epigenetek, United States) following the manufacturer's protocol. Briefly, the nuclear extract and the substrate for HAT were incubated for 1 h followed by washing with the wash buffer. An inhibitor was added in the test samples, and signals were captured and detected by the capture and detection antibody, respectively. After color development, the plate was read at 450 nm using the ELISA plate reader. HAT activity and percentage inhibition were calculated by comparing with DMSO control samples. A graph was plotted by taking the mean of three experiments ± SD. One-way ANOVA was used to check the statistical significance at fixed p-value ≤ 0.05.

Global DNA Methylation Assay

DNA isolation was done by using GenElute Mammalian Genomic DNA Miniprep Kit (Catalog No. G1N70, Sigma-Aldrich, Merck, KGaA) following the manufacturer's protocol. About 1.5×10^6 cells were treated with chrysin (@ conc. 5, 10, and 15 μM for 48 h) and DMSO control. DNA was isolated from chrysin treated and the DMSO control samples, and its quality was checked by gel electrophoresis using 1% agarose gel (Catalog No. A9539, Sigma-Aldrich, Merck, KGaA) in 0.5XTBE buffer with ethidium bromide. The quantitation of DNA samples was completed by spectrophotometry using NanoDrop 2000 (Thermo Scientific™, USA) and stored at-80°C.

MethylFlash™ Methylated DNA Quantification Kit (Catalog No. P-1034, Epigentek, USA) was used to analyze the methylated DNA in treated cells (@ chrysin conc. 5, 10, and 15 μm for 48 h) and DMSO controls. The kit was used for the detection of methylated DNA using antibodies against 5-mC (cytosine) that can be analyzed calorimetrically. Optical density was measured using the ELISA reader at 450 nm wavelength. As established, the extent of methylation on the gene is directly related to the optical density. The levels of methylation were calculated in comparison with the DMSO control. The experiment was performed three times at a significance level of p-value ≤0.05.

Methylation-Specific PCR (MSRE–PCR)

CpG island DNA methylation quantification was conducted for estimating the percentage of methylated DNA in the total DNA content of HeLa cells by using the EpiTect Methyl II PCR System (Catalog No. 335452, Qiagen, United States). The method employed calculates the methylation of promoter regions in the input DNA after cleavage with methylation-dependent restriction enzymes and methylation-sensitive restriction enzymes that digest methylated and unmethylated DNA, respectively. Following restriction digestion, the cleaved DNA from each reaction was computed by using it as a template for Human Tumor Suppressor Genes EpiTect Methyl II Signature PCR Array (Qiagen, United States) real-time PCR in an assay plate with primers that border the promoter region of the anticipated genes. The relative amounts of unmethylated and methylated DNA were calculated by comparing the amounts of each reaction with that of a control (no enzymes added) reaction using the $^{\Delta\Delta}$CT method. The gene panel (with predesigned primers) consisted of tumor-suppressor genes comprising *TP73*, *MGMT*, *APC*, *CDKN2A*, *BRCA1*, *PTEN*, *CDH1*, *DAPK1*, *CDH13*, *SOC51*, *RARB*, *ESR1*, *FHIT*, *RASSF1*, *WIF1*, *GSTP1*, *RUNX3*, *MLH1*, *NEUROG1*, *VHL*, *PDLIM4*, and *TIMP3*.

The amount of DNA left after the restriction digestion was calculated by using qPCR array results. This was used for constructing the methylation profile of each gene with the $^{\Delta\Delta}$CT method. The methylation and unmethylation fraction of the promoter of tested tumor-suppressor genes in chrysin-treated and untreated HeLa cells was estimated as per the protocol available with the kit. The levels of methylation were presented in the form of a graph. Statistical significance was calculated by taking the mean of three experiments by one-way ANOVA using the SPSS program with p-value ≤ 0.05.

qRT-PCR–Based Expression Analysis of Tumor-Suppressor, Migration, and Inflammation-Related Genes

The RNA from chrysin-treated (conc. 10 and 15 μM for 48 h) and DMSO control HeLa cells were extracted by using the GenElute Mammalian Genomic Total RNA Kit (Catalog No. RTN70 Sigma-Aldrich, Merck KGaA) and further quantified with the help of NanoDrop. The RNA (2 μg was used as a template) was then subjected to cDNA synthesis by using Applied Biosystems™ High-Capacity cDNA Reverse Transcription Kit (Catalog No. 4368814, ABI-Thermo Fisher, United States). This kit supports random primers' scheme for initiating the synthesis of cDNA. The expression of genes related to various pathways of migration, inflammation, and TSGs was analyzed with the help of TaqMan-based custom array (4391524 and 4369514 master mix). The PCR array was run on QuantStudio3 and analyzed with the $^{\Delta\Delta}C_T$ method using the DataAssist™ program (Thermo Fisher, United States). GAPDH (housekeeping gene) was used for normalizing the data. Relative expression was calculated in comparison with the DMSO control. The statistical significance was calculated by maintaining p-value <0.05.

Protein Expression by Proteome Profiler Array

The expression analysis of TSGs, migration, and inflammation-related proteins was performed by the Proteome Profiler Array (Catalog No. ARY026, R&D, USA). The relative expression levels of 84 oncogenes were investigated with the help of this array. Briefly, 1.5×10^6 HeLa cells were plated in 25 cm^2 flasks, and four such flasks were treated with 10 and 15 μM of chrysin for 48 h. The treated and DMSO control cells were collected and suspended in lysis buffer 17 (1 ml per 10^7 cells) containing 10 μg/ml each of aprotinin (Catalog No. A6279; Sigma, USA), Leupeptin (Catalog No. 1167/25, Tocris, USA), and pepstatin (Catalog No. 1190/10, Tocris, United States) and shaken gently at 2–8°C for 30 min. The lysate produced was quantitated by the Pierce BCA Assay Kit (Catalog No. 23225; Thermo-Fisher Scientific, United States) following the manufacturer's protocol. For this assay, 400 μg of a protein in 250 μL volume of the diluted cell lysate treated with chrysin (10 and 15 μM for 48 h) and the DMSO control was used for each membrane. The signal produced was then quantified by the chemiluminescent detector gel-doc system (Bio-Rad Laboratories, United States). The expression of proteins was analyzed by the intensity of proteins in the blot using Image Lab software (version 6.1). The fold change after normalization with the reference spot was calculated by comparing the treated (chrysin) values with the DMSO control values (mean of three experiments ±SD at p-value ≤ 0.05).

Expression Analysis of Epigenetic Enzymes Involved in Chromatin Modification

Chromatin-modifying enzymes like writers—DNA and histone methyl transferases, histone acetyl transferases, and erasers like

histone deacetylases and histone demethylases—help in dynamically sustaining cell metabolism and controlling processes such as cell growth propagation and gene expression by recognition of specific "marks" on histone proteins and DNA (Kouzarides, 2007). RNA was extracted from the DMSO control and chrysin-treated HeLa cells (10 and 15 μM for 48 h). RT^2 Profiler™ PCR Array Human Epigenetic Chromatin Modification Enzymes (Catalog No. PAHS-085Z, Qiagen, United States) were used to check the expression of genes responsible for the modulation of DNA and histones including DNA methyl transferases, histone methyl transferases, histone acetyl transferases, and demethylases. RNA at a concentration of 1 μg was used to synthesize cDNA, and it was diluted to 1,350 μL with nuclease-free water and an equal amount of RT2 SYBR® Green qPCR Master mix (Catalog No. 330504; Qiagen, United States) was added to this. From this mixture, 25 μL was poured into each well of the array plate having predefined primers, and the plate was run on ABI Quant Studio 3. The normalization was performed using GAPDH housekeeping gene and the fold change was calculated by comparing the chrysin-treated samples with the DMSO control. The statistical significance was calculated at p-value ≤ 0.5.

H3 and H4 Histone Modification Marks

In order to understand the role of chrysin as an epigenetic modifier, the Histone Extraction kit (Catalog No. ab113476, Abcam, Cambridge, UK), and Histone H3 and H4 Modification Multiplex Assay kits (Catalog Nos. ab185910 and ab185914) were procured from Abcam, Cambridge, UK. Following the extraction of histone using the Histone Extraction Kit, ~100 ng of histone protein was used per well, and the protocol given by the manufacturer was followed. OD was measured at 405 nm, and graphs were plotted for reflecting the effect of chrysin compared to the DMSO control. The experiments were performed in triplicates, one-way ANOVA was used to determine the significance of the experiments, and p-value was maintained at ≤0.05.

Statistical Analysis

Statistical analysis was performed by SPSS program (version 21). The data were examined by using one-way ANOVA followed by Tukey's HSD *post hoc* analysis. All experiments were performed in triplicate. The results are expressed as the mean ± SD of three distinct experimentations. The statistical significance was set at p-value ≤0.05.

RESULTS

Chrysin-Inhibited Colony Formation and Migration of HeLa Cells

The colony-forming assay was performed to understand the long-term effect of chrysin on the growth and division of HeLa cells. After calculating the survival factor (SF), it was observed that the DMSO control had plating efficiency (PE) of 95%, whereas the survival factor for 5 and 10 μM of chrysin showed only 120 and 30 colonies, respectively. At 15 μM chrysin conc., very few colonies were formed. Hence, it can be inferred that chrysin restrained the capability of cells to form colonies. These results suggest that chrysin is not only capable of causing cell death but also leads to cytostatic state (**Figure 1A** and **Figure 1B**).

Likewise, chrysin decreased the migration capacity of HeLa cells as demonstrated by scratch-wound and invasion assay using trans-well. Chrysin increased the wound width by 8 and 14% at 10 μM conc. treatment for 24 and 48 h and 17 and 25% at 15 μM conc. treatment for 24 and 48 h, respectively, whereas in DMSO control cells, there was almost complete wound closure after 48 h (**Figure 2A** and **Figure 2B**). This was further corroborated by significant decrease in the number of migrating cells after chrysin treatment using the trans-well assay. Only 15 and 2.5% migration at 10 and 15 μM chrysin treatment for 48 h was observed, respectively, in comparison with the DMSO control cells (**Figure 2C** and **Figure 2D**).

Chrysin Reexpresses Tumor-Suppressor Genes (TSGs) and Downregulates Genes Related to Migration and Inflammation

qPCR was done to understand the effect of decreased methylation of various tumor-suppressor genes following the treatment of chrysin. It was observed that chrysin treatment increased the expression of various TSGs (such as *TIMP3*, *TIMP4*, *RARB*, *RASIF1*, *TP53*, *PTEN*, *CDH1*, and *SOCS1*) and reduced the expression of genes responsible for metastasis (*viz. MMP 2*, *MMP 9*, *MMP 14*, *SNAIL1*, *SMAD3*, *SMAD4*, and *MTA1*, *2*) and the genes involved in the inflammatory process (*viz. IL2*, *IL1A*, *IL6*, and *CxCL8*). Chrysin treatment also decreased the expression of oncogenes like *FOS*, *JUN*, *MYC*, *ESR1*, and *TWIST1* (**Figure 3A** and **Table 1**). Relative quantification (RQ) derived from the $2^{-\Delta\Delta Ct}$ method specifies the fold change in gene expression against the DMSO control after normalization with the selected endogenous gene (GAPDH). The upregulation is documented at RQ ≥ 1.5 and downregulation at RQ ≤ 0.5.

Chrysin Modulates the Protein Expression of Genes Involved in Migration, Inflammation, and Tumor Suppression

Proteome profiler–based quantitation of proteins that are involved in proliferation and migration and other cellular events revealed chrysin-supported modulation was consistent with mRNA expression. The treatment of HeLa cells with 10 and 15 μM of chrysin resulted in the downregulation of the expression of various proteins related to migration *viz* MMP2, MMP9, and MMP3, mesothelin, MUC1, leptin, and M_CSF; inflammatory proteins like CCL8/MCP-2, CCL7/MCP-3, IL-18 BPa, CXCL8/IL-8, and IL-2 Rα; and oncogenes like HER1, 2, 3, and 4, and ICAM-1/CD54. Proteins related to cell proliferation, growth, and apoptosis like BCL-X, HIF-1α, HNF-3β, and HO-1/HMOX1 were also downregulated, that is, related to tumor progression,

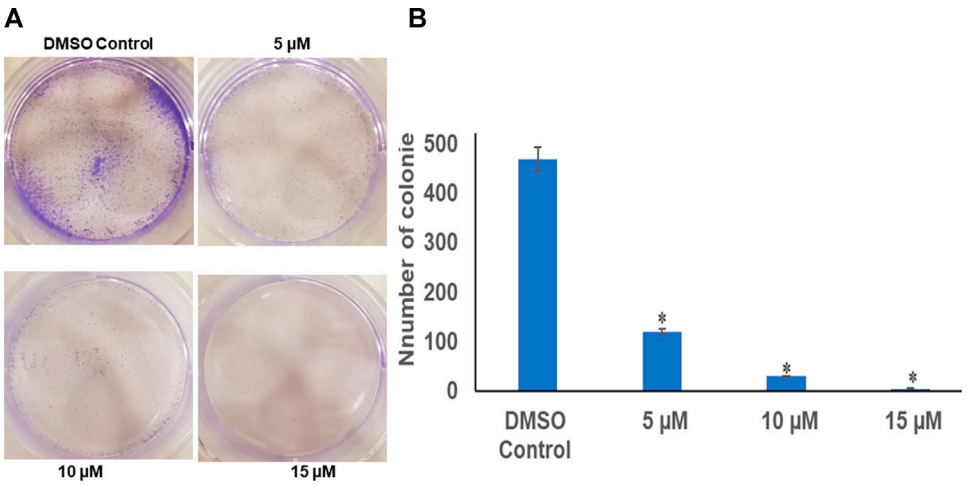

FIGURE 1 | (A) Chrysin inhibits colony formation in a dose-dependent manner with almost no colonies at 15 μM chrysin treatment for 48 h. **(B)** Graphical representation of inhibition of colony formation.

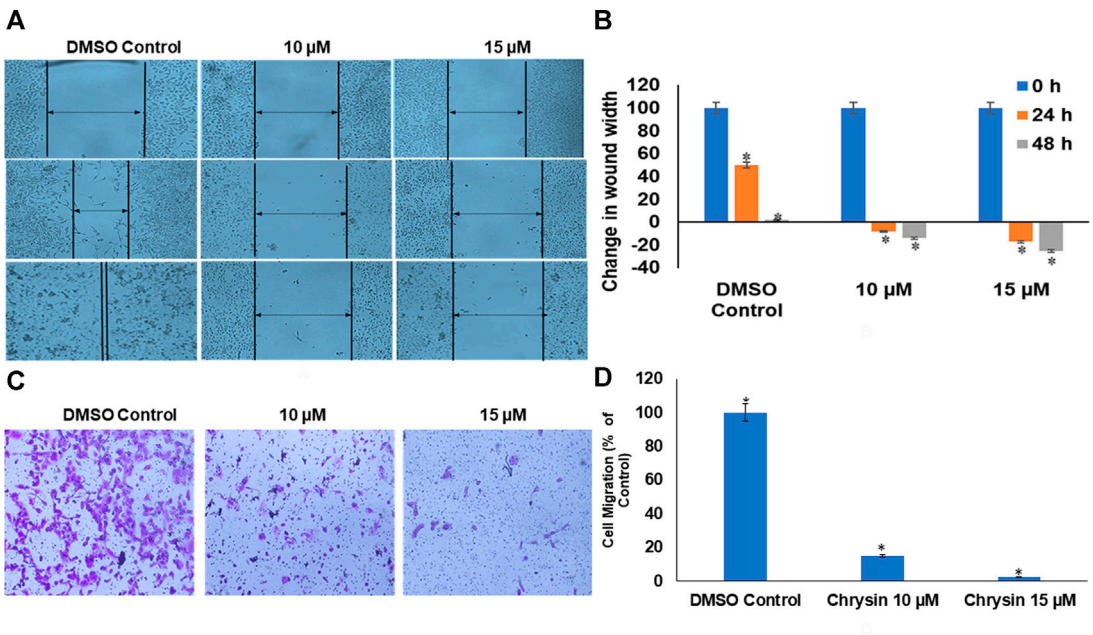

FIGURE 2 | (A) Chrysin treatment prevented migration of HeLa cells, as compared to the DMSO control wells, the chrysin treatment showed increase in wound width after 10–15 μM treatment. **(B)** Graphical representation of increase in wound width after chrysin treatment at 10–15 μM concentrations for 24–48 h. **(C)** The chrysin-treated HeLa cells depicted significant decrease in cell migration using trans-well inserts. **(D)** Graphical representation of inhibition of cell migration by chrysin.

whereas upregulation of E-cadherin (CDH1) was observed after chrysin treatment (**Figure 3B**, **Figure 3C** and **Table 2**). Fold changes in protein expression were calculated by comparing the treated cells with those of the DMSO control. The upregulation was fixed at ≥1.5 fold and downregulation at ≤0.5 fold.

Chrysin Inhibits DNMT Activity in HeLa Cells

Chrysin inhibited DNMT activity in HeLa cells in a dose-dependent manner. The incubation of the nuclear extract with 5, 10, and 15 μM of chrysin resulted in the inhibition of DNMT activity by 35, 54, and 61%, respectively, compared to the DMSO control (**Figure 4A**).

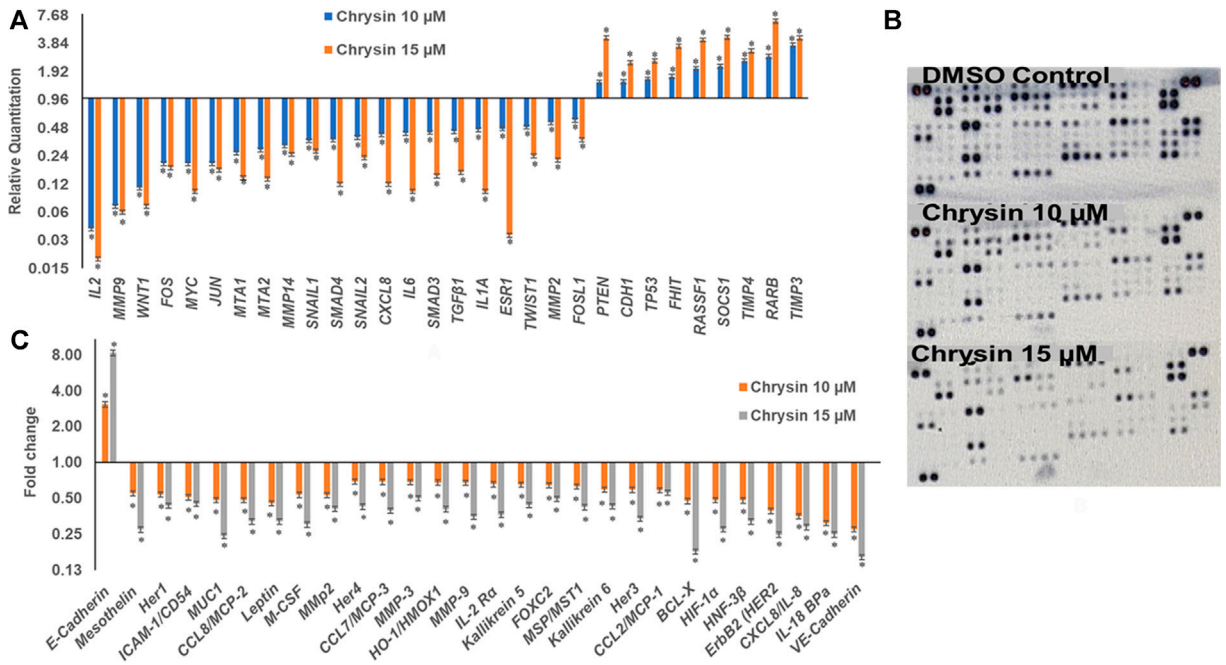

FIGURE 3 | (A) Chrysin modulated the expression of various TSGs and migration related genes in a dose-dependent manner. The TSGs were reactivated, whereas inflammatory- and migration-related genes were downregulated. **(B)** The nitrocellulose membranes depicting the expression of different proteins. **(C)** Chrysin treatment modulates the proteins related to migration and inflammation in a dose-dependent manner.

Chrysin Inhibits HDAC Activity

Nuclear extracts were incubated with increasing concentrations (5, 10, and 15 μM) of chrysin; it was found that it inhibited the activity of HDACs by 30, 36, and 42% in a dose-dependent response compared with the DMSO control (**Figure 4B**).

Chrysin Decreases HAT Activity in a Dose-Dependent Manner

Histone acetyl transferases cause acetylation at N-terminal tails of histone proteins. The incubation of nuclear extract with varying concentrations of chrysin (5, 10, and 15 μM) showed decline in HAT activity in the treated cells compared to the DMSO control. A decrease of 22, 34, and 52% was observed at 5, 10, and 15 μM conc. of chrysin treatment, respectively (**Figure 4C**).

Chrysin Reduces HMT H3K9 Enzyme

HMT H3K9 can add methyl groups at histone three and lysine 9. All the methylation marks—mono, di, and trimethylation—are repressive marks. The incubation of HeLa cell nuclear extracts with 5, 10, and 15 μM conc. of chrysin reduced the activity of the enzyme by 25, 38, and 45%, respectively (**Figure 4D**).

Chrysin Modifies the Expression of Chromatin-Modifying Genes

RT (Rahman et al., 2016) Profiler™ PCR Array Human Epigenetic Chromatin Modification Enzymes (Catalog No. PAHS-085Z; Qiagen, USA) were used to check the expression of various chromatin-modifying enzymes following the treatment of chrysin (@ conc. 10 and 15 μM) for 48 h compared to the DMSO control. Chrysin treatment down-regulated the expression of DNA methyltransferases like *DNMT1*, *3A*, and *3B* significantly. *HDAC1*, *2*, *3*, *4*, and *11* also showed a steep decline after the above-stated chrysin treatment. Remarkably, downregulation of *WHSC1*, *AURKA*, *AURKB*, and *AURKX*. *EHM2*, *PRMT8*, and *HAT1* were also observed after 10 and 15 μM of chrysin treatment. However, enhanced expression of *SETD2*, *ESC O 2*, and *CIITA* was found after the same chrysin treatment (RQ in **Figure 5A** and **Table 3**).

Chrysin Modulates H3 and H4 Histone Marks

Chrysin modulated the expression of methylation, acetylation, and phosphorylation H3 and H4 marks. H3K9me1, H3K9me2, H3K9me3, H3K27me1, H3K27me2, H3K27me3, H3K36me1, H3K36me3, H3K79me1, H3K79me2, and H3K79me3 marks were reduced after the treatment of HeLa cells with 15 μM of chrysin for 48 h; similarly, H3 acetylation marks were diminished after treatment with 15 μM of chrysin (**Figure 5B**). The expression of H3K9ac, H3K18ac, H3K14ac, and H3K56ac was reduced after chrysin treatment. Likewise, the acetylation marks at H4 were also modulated against chrysin treatment including H4K5ac, H4K8ac, H4K12ac, and H4K16ac. H4 methylation marks, like H4K20me1, H4K20me2, and H4K20me3, showed decreased expression after chrysin

TABLE 1 | Relative expression of TSGs and genes related to migration and metastasis. The values are taken as mean of three experiments ±SD ($p \leq 0.05$).

Genes	Gene ensemble no.	Gene information	RQ chrysin 10 μM	RQ chrysin 15 μM
IL2	Hs00174114_m1	Interleukin 2	0.04	0.02
MMP9	Hs00234579_m1	Matrix metallopeptidase 9	0.07	0.06
WNT1	Hs00180529_m1	Wnt family member 1	0.11	0.07
FOS	Hs00170630_m1	Fos proto-oncogene	0.20	0.18
MYC	Hs99999003_m1	Myelocytomatosis viral oncogene homolog	0.20	0.10
JUN	Hs99999141_s1	Jun proto-oncogene	0.20	0.17
MTA1	Hs00183042_m1	Metastasis associated 1	0.26	0.14
MTA2	Hs00191018_m1	metastasis associated 2	0.28	0.14
MMP14	Hs01037009_g1	matrix metallopeptidase 14	0.31	0.25
SNAIL1	Hs00195591_m1	Snail family transcriptional repressor1	0.35	0.27
SMAD4	Hs00232068_m1	SMAD family member 4	0.36	0.12
SNAIL2	Hs00161904_m1	Snail family transcriptional repressor2	0.38	0.23
CXCL8	Hs99999034_m1	C-X-C motif chemokine ligand 8	0.41	0.12
IL6	Hs00174131_m1	Interleukin 6	0.42	0.10
SMAD3	Hs00969210_m1	SMAD family member 3	0.43	0.15
TGFβ1	Hs00998133_m1	Transforming growth factor beta 1	0.44	0.16
IL1A	Hs00174092_m1	Interleukin 1 alpha	0.46	0.10
ESR1	Hs01046816_m1	Estrogen receptor 1 metastasis associated 2	0.47	0.03
TWIST1	Hs00361186_m1	Twist family bHLH transcription factor 1	0.49	0.24
MMP2	Hs00234422_m1	Matrix metallopeptidase 2	0.55	0.22
FOSL1	Hs04187685_m1	1FOS-like 1	0.58	0.36
PTEN	Hs01920652_s1	Phosphatase and tensin homolog	1.48	4.41
CDH1	Hs00170423_m1	Cadherin 1	1.50	2.40
TP53	Hs01034249_m1	Tumor protein p53	1.60	2.50
FHIT	Hs00896860_m1	Fragile histidine triad	1.70	3.60
RASSF1	Hs00945255_g1	Ras association domain family member 1	2.08	4.20
SOCS1	Hs00705164_s1	Suppressor of cytokine signaling 1	2.20	4.50
TIMP4	Hs00162784_m1	TIMP metallopeptidase inhibitor 4	2.50	3.20
RARB	Hs00977140_m1	Retinoic acid receptor beta	2.80	6.70
TIMP3	Hs00165949_m1	TIMP metallopeptidase inhibitor 3	3.70	4.40

treatment (**Figure 5C**). Phosphorylation marks of H3ser28p, H4ser10 p, H4R3m2a, and H4Rm2s were also decreasingly expressed after 15 μM chrysin treatment of HeLa cells for 48 h (**Figure 5B and 5C**).

Chrysin Diminishes Global DNA Methylation of HeLa Cells

An obvious decrease in global methylation was observed after 48 h treatment of 5, 10, and 15 μM of chrysin against HeLa cells. Global DNA methylation was studied by comparing with the DMSO control. This was reduced to 61, 44, and 30% against 5, 10, and 15 μM chrysin treatment of HeLa cells, respectively (**Figure 6A**).

Chrysin Reduces Methylation of the Promoter Region of Various Tumor-Suppressor Genes

Methylation-sensitive restriction enzyme PCR revealed that chrysin decreased the promoter methylation of crucial tumor-suppressor genes of HeLa cells. These TSGs included *APC*, *BRCA1*, *CDH1*, *PTEN*, *GSTP1*, *FHIT*, *DAPK1*, *CDH13*, *CDKN2A*, *MGMT*, *MLH1*, *RARB*, *RASSF1*, *SOCS1*, *VHL*, *WIFI*, and *TIMP3*. The methylation percentage of the abovesaid genes decreased significantly as *APC* (8%, 3%), *BRCA1* (18%, 2%), *CDH1* (55%, 43%), *CDH13* (39%, 3%), *CDKN2A* (14%, 4%), *DAPK1* (17%, 11%), *FHIT* (5%, 3%), *GSTP1* (7%, 3%), *MGMT* (14%, 4%) *MLH1* (22%, 15%), *PTEN* (14%, 11%), *RARB* (22%, 11%), *RASSF1* (19%, 15%), *SOCS1* (73%, 56%), *TIMP3* (13%, 3%), *VHL* (15%, 12%), and *WIFI* (82%, 61%) at 10 and 15 μM chrysin, respectively, compared to the DMSO control, wherein the methylation percentage was much higher (**Figure 6B** and **Table 4**).

DISCUSSION

Epigenetic alterations are commonly associated with carcinogenesis and metastasis (Wang et al., 2018a). Cancer metastasis is the major cause of treatment failure and mortality in women detected with cervical cancer. This suggests that the inhibition of metastasis serves a pivotal role in survival improvement, and hence can be exploited as a potential target for cancer treatment and prevention (Chatterjee et al., 2018). Additionally, epigenetic alteration in key metastatic genes is one of the reasons of metastasis (Chatterjee et al., 2018). The modifiable nature of epigenetics makes the epigenetic regulation an attractive target for cancer prevention and treatment (Busch et al., 2015; Kanwal et al., 2015).

TABLE 2 | Expression of proteins involved in migration and inflammation. The values are taken as mean of three experiments ±SD ($p \leq 0.05$).

Oncogene proteins	Fold change chrysin 10 μM	Fold change chrysin 15 μM
E-cadherin	3.07	8.27
Mesothelin	0.55	0.27
Her1	0.54	0.43
ICAM-1/CD54	0.51	0.45
MUC1	0.48	0.24
CCL8/MCP-2	0.48	0.32
Leptin	0.46	0.32
M-CSF	0.53	0.30
MMp2	0.53	0.41
Her4	0.69	0.43
CCL7/MCP-3	0.69	0.39
MMP-3	0.69	0.50
HO-1/HMOX1	0.68	0.41
MMP-9	0.67	0.35
IL-2 Rα	0.66	0.36
Kallikrein 5	0.65	0.44
FOXC2	0.65	0.50
MSP/MST1	0.63	0.42
Kallikrein 6	0.59	0.43
Her3	0.59	0.34
CCL2/MCP-1	0.59	0.56
BCL-X	0.48	0.18
HIF-1α	0.48	0.28
HNF-3β	0.48	0.32
ErbB2 (HER2)	0.39	0.25
CXCL8/IL-8	0.35	0.29
IL-18 BPa	0.31	0.25
VE-cadherin	0.28	0.16

Currently available synthetic drugs direct at crucial epigenetic signature enzymes, for example, HDACs and DNMTs. Nevertheless, these synthetic drugs have shown many adverse side effects (Ho et al., 2013; Heerboth et al., 2014); therefore, it is crucial to probe the natural agents which are derived from plants that can regulate all cell processes including epigenetic mechanisms and can potentially reverse malignancy-associated epigenetic patterns (Shankar et al., 2016).

Earlier, studies on flavonoids targeting various types of cancer have demonstrated their anticancer effect by modulation of various molecular pathways involved in migration and epigenetics (Pal-Bhadra et al., 2012; Kanwal et al., 2016; Liskova et al., 2020). Considering the anticancer potential of plant flavonoids in view, the present study was carried out to explore the antiproliferative, antimigratory, and modulatory effects of chrysin on DNA methylation and histone modification on human cervical cancer (HeLa) cells. Previously, it was reported from the lab that chrysin inhibits the proliferation of HeLa cells in a dose- and time-dependent manner, induces apoptosis, and modulates various signaling pathways (Raina et al., 2021).

In the present study, 5 and 10 μM chrysin-treated HeLa cells showed reduced colony formation as 120 and 30 colonies were formed, respectively, after 48 h, whereas at 15 μM chrysin, there was no noticeable colony formation (**Figure 1A** and **1B**). To understand chrysin-mediated antimigratory effects, the scratch-wound assay that depicted significant inhibition of cell migration was carried out. Chrysin treatment of HeLa cells

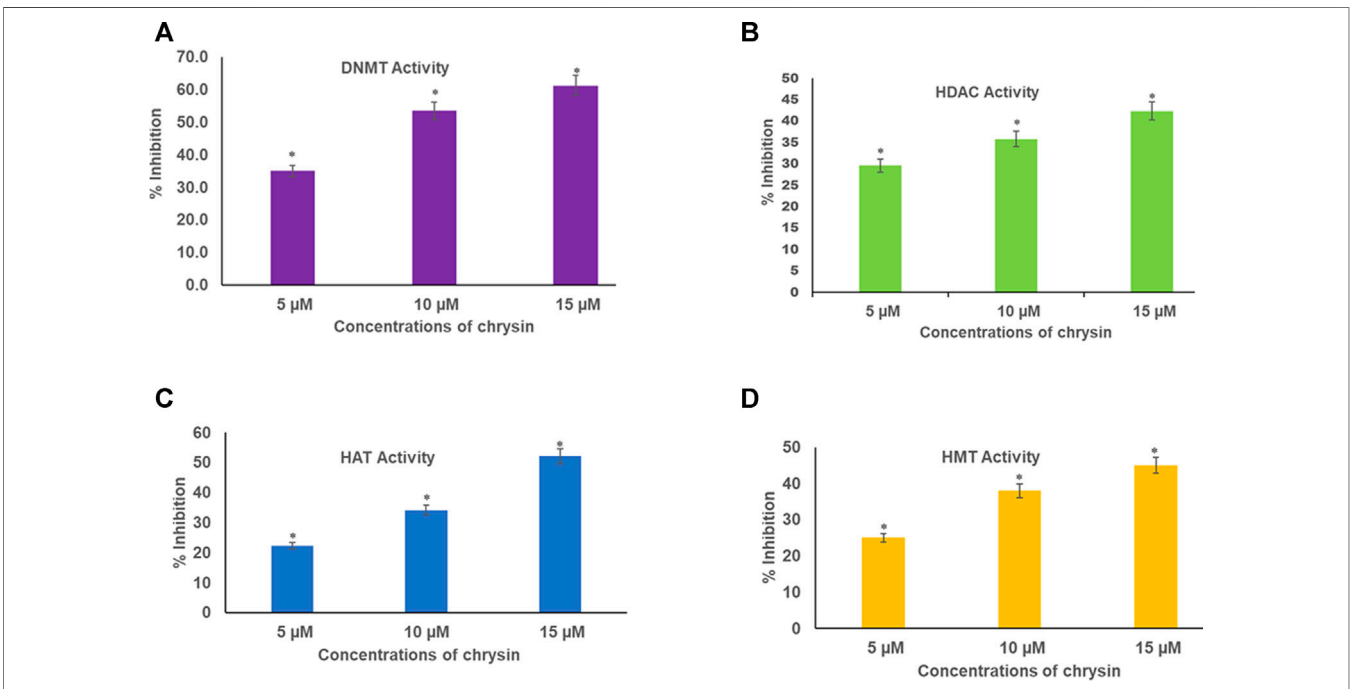

FIGURE 4 | (A) Chrysin decreased DNMT activity in HeLa cells irrespective of their location on the genome in a concentration-dependent manner. **(B)** Chrysin inhibited HDAC activity in HeLa cells in a concentration-dependent manner. The activity decreased with increase in the dose of chrysin **(C)** Chrysin decreased the activity of HAT in a dose-dependent manner. As the concentration of chrysin increased, the inhibition percentage increased. **(D)** Chrysin decreased HMT H3K9 enzyme activity in HeLa cells, irrespective of their location on the genome in a concentration-dependent way.

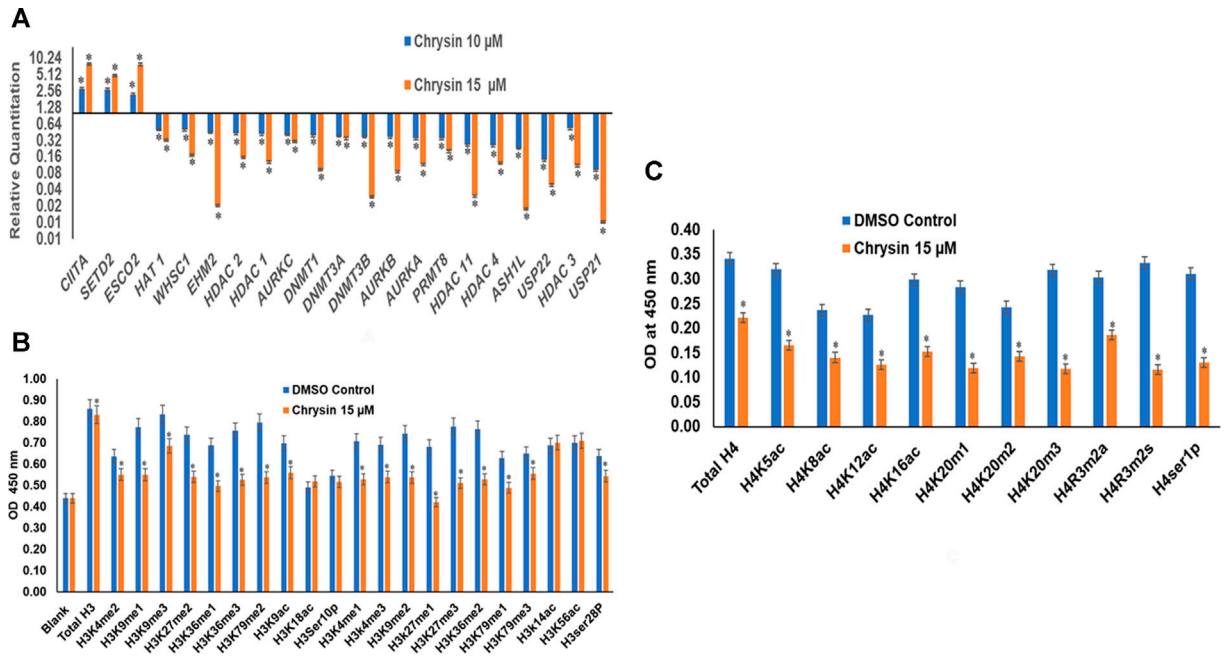

FIGURE 5 | (A) Treatment of HeLa cells with chrysin at 10 and 15 μM for 48 h modulated the expression of epigenetic enzymes (HDACs, DNMTs, HATs, HMTs *etc*.) in a dose-dependent manner. **(B)** Chrysin modulates the H3 acetylation and methylation histone marks at 15–48 h. **(C)** H4 histone marks modulated by chrysin as compared to the DMSO controls.

TABLE 3 | RQ values of chromatin-modifying enzymes after chrysin treatment. The values are taken as mean of three experiments ±SD ($p \leq 0.05$).

Gene information	Genes	RQ chrysin 10 μM	RQ chrysin 15 μM
Class II major histocompatibility complex transactivator	CIITA	2.80	7.90
SET domain containing	SETD2	2.70	4.90
Establishment of sister chromatid cohesion N-acetyltransferase 2	ESCO2	2.20	7.80
Histone deacetylase IV	HAT 1	0.50	0.32
Wolf–Hirschhorn syndrome candidate 1 gene	WHSC1	0.49	0.17
A member of NF2/ERM/4.1 superfamily	EHM2	0.44	0.02
Histone deacetylase 2	HDAC 2	0.42	0.15
Histone deacetylase 1	HDAC 1	0.41	0.13
Aurora kinase C	AURKC	0.40	0.30
DNA methyl transferase 1	DNMT1	0.39	0.09
DNA methyl transferase 3A	DNMT3A	0.38	0.34
DNA methyl transferase 3B	DNMT3B	0.37	0.03
Aurora kinase B	AURKB	0.36	0.08
Aurora kinase A	AURKA	0.34	0.11
Protein Arginine methyltransferase 8	PRMT8	0.34	0.20
Histone deacetylase 11	HDAC 11	0.26	0.03
Histone deacetylase 4	HDAC 4	0.25	0.12
A SH1-like histone lysine methyltransferase	ASH1L	0.23	0.02
Ubiquitin-specific peptidase 22	USP22	0.14	0.05
Histone deacetylase 3	HDAC 3	0.52	0.11
Ubiquitin-specific peptidase 21	USP21	0.09	0.01

at a conc. of 10 and 15 μM showed wound width increment by 8 and 17%, respectively, after 24 h incubation, whereas the wound width was increased by 14 and 25% after 48 h compared to the DMSO control, where complete wound closure was found after 48 h (**Figure 2A** and **2B**). The trans-well assay also depicted the inhibition of migration at varying concentrations of chrysin (**Figure 2C** and **Figure 2D**). Hence, it can be inferred that chrysin at 10 and 15 μM at 48 h is a strong inhibitor of migration. Earlier studies from various research groups have also reported that chrysin bears antiproliferative

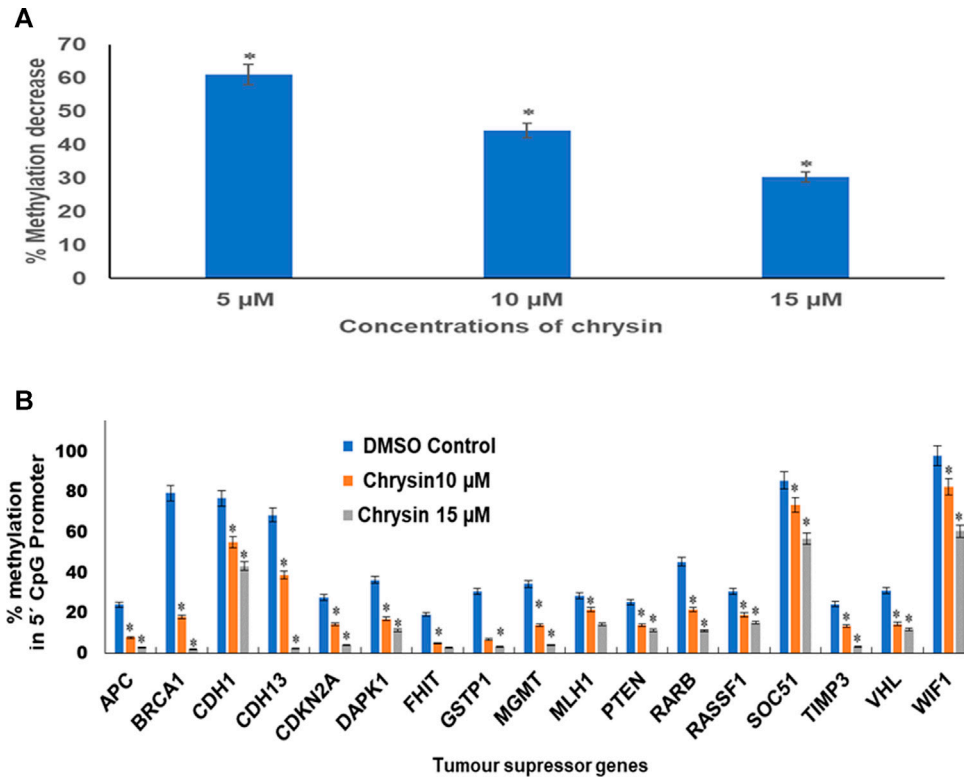

FIGURE 6 | (A) Chrysin treatment at 5, 10, and 15 μM–48 h decreased the global DNA methylation in a dose-dependent manner. **(B)** Chrysin treatment of HeLa cells at 10 and 15 μM for 48 h demonstrated profound decrease in percent methylation in 5′ CpG promoter regions of TSGs as compared to the DMSO controls in a dose-dependent manner.

TABLE 4 | Percentage of CpG promoter methylation after chrysin treatment as compared to untreated control. The values are taken as mean of three experiments ±SD ($p \leq 0.05$).

Target name	Gene name	Untreated control	Chrysin 10 μM	Chrysin 15 μM
APC	Adenomatous polyposis 1	24.20	7.88	2.72
BRCA1	Breast cancer gene 1	79.49	18.12	2.11
CDH1	E-cadherin	76.91	55.01	43.25
CDH13	H-cadherin	68.56	38.89	2.60
CDKN2A	Cyclin-dependent inhibitor 2A	27.74	14.43	4.19
DAPK1	Death-associated protein kinase 1	36.49	17.06	11.46
FHIT	Fragile histidine triad protein	19.35	5.04	2.94
GSTP1	Glutathione S-transferase Pi 1	30.80	6.88	3.11
MGMT	O-6-Methylguanine-dna methyltransferase	34.38	13.99	4.29
MLH1	MutI homolog 1	28.49	21.88	14.50
PTEN	Phosphatase and tensin homolog	25.43	14.11	11.30
RARB	Retinoic acid receptor beta	45.47	21.88	11.22
RASSF1	Ras association domain family member 1	30.71	19.24	15.27
SOC51	Suppressor of cytokine signaling 1	85.82	73.50	56.97
TIMP3	Metalloproteinase inhibitor 3	24.44	13.49	3.32
VHL	Von Hippel–Lindau tumor suppressor	31.10	14.59	11.78
WIF1	Wnt inhibitory factor 1	98.14	82.56	60.68

and cytostatic effects and inhibits migration and invasion in various cancer cell lines (Kasala et al., 2015; Wang et al., 2018b).

Matrix metalloproteinases are important proteolytic enzymes involved in the cancer cell invasion process. Epithelial mesenchymal transition (EMT) increases cell migration, and

the transforming growth factor pathway has an important role to play in epithelial mesenchymal transition; it induces EMT either by transforming growth factor-β (TGF-β)/SMAD pathway or *via* the non-SMAD pathway by activating the AKT/PI3K pathway, thus triggering migration (Wu et al., 2021; Xue et al., 2012). The downregulation of TGF-β/SMAD mediates reduction in the expression of MMPS and TWIST1 (Wu et al., 2021; Xue et al., 2012; Baruah et al., 2016). Cadherins are a class of type-1 transmembrane proteins that maintain the adhesion between cells, their loss lead to invasion and metastasis, and snails are their inhibitors. *MTA1* and *MTA2* are metastasis promoters, and their reduction leads to the inhibition of metastasis (Wu et al., 2021; Xue et al., 2012; Baruah et al., 2016). In the study, chrysin-mediated inhibition of migration was found to be well correlated with the downregulation of metalloproteases *MMP 9*, *MMP 2*, and *MMP 14* and their co-operators like *SMAD3*, *SMAD4*, *SNAIL1*, *SNAIL2*, *MTA1*, and *MTA2*, and upregulation of their inhibitors like *TIMP3*, *TIMP4*, and *CDH1*, hence endorsing the inhibitory effect of chrysin on migration. In addition, the downregulation of genes related to inflammation like *IL2*, *IL1A*, and *IL6* and oncogenes like *Fos*, *Jun*, *Myc*, *WNT1*, and *FOSL1* (**Figure 3A** and **Table 1**) was observed. Inflammation subsequent to viral infection is a power tool that accelerates cancer progression; hence, downregulation of inflammatory proteins aids in cancer prevention and treatment (Deivendran et al., 2014).

In the study, gene expression studies at mRNA levels were found to be consistent with their protein level expression, and various genes involved in inflammation and migration such as *HER1*, *HER2*, *Her3*, and *Her4*, and *MMPs* like *MMP 9*, *MMP 2*, *MMP 3*, *FOXC2*, *IL-2 Rα*, *IL-18 BPa*, *CXCL8/IL-8*, *CCL2/MCP-1*, *CL8/MCP-2*, *CCL7/MCP-3*, Mesothelin, *ICAM-1/CD54*, *MUC1*, Leptin, *M-CSF*, *H O-1/HMOX1*, *Kallikrein 5*, *MSP/MST1*, *Kallikrein 6*, *HIF-1α*, and *HNF-3β* were significantly downregulated against chrysin treatment, while upregulation of E-cadherins was observed at different chrysin concentrations (**Figure 3B**, **3C** and **Table 2**). Our current findings are in line with the available reports wherein *in vitro/in vivo* models have shown that chrysin inhibits tumor metastasis by decreasing the expression of *MMP9* and *MMP2* as well as *COX-2* and *i-NOS*, and modulates the *PI3K/AKT* signaling pathway (Yang et al., 2014; Xia et al., 2015; Koosha et al., 2016; Zam and Khadour, 2017).

Furthermore, epigenetic modulations induced by chrysin were also analyzed in this study. Epigenetic modifications including aberrant DNA methylation and histone modifications interactions are crucial for controlling the operational activities of the genome by changing the chromatin structure, thereby leading to silencing of various tumor-suppressor genes (Guo et al., 2015; Chistiakov et al., 2017). DNMTs catalyze the transfer of the acetyl group onto 5′cytosine at promoter CpG island of TSGs. Hypermethylation of CpG islands in the promoter region of TSGs leads to silencing of these genes (Ali Khan et al., 2015). DNMTs are found to be upregulated in cervical cancer cells, and their expression levels are correlated to disease progression (Piyathilake et al., 2017; Charostad et al., 2019). The analysis of biochemical activity of DNMTs after chrysin treatment was performed, and it was observed that chrysin decreased the biochemical activity of DNMTs in a dose-dependent manner, and it was reduced by 35, 53.5, and 61.2% at 5, 10, and 15 μM chrysin treatment, respectively (**Figure 4A**).

Furthermore, the downregulation of DNMT activity against chrysin treatment was verified by downregulation of *DNMT1*, *DNMT3A*, and *DNMT3B* in a dose-dependent manner at transcript levels (**Figure 5A** and **Table 3**). Various flavonoids have attracted attention because of their chemopreventive and antitumor effects including chrysin, luteolin, and apigenin, and are known to inhibit DNMTs and histone methyl transferases (Busch et al., 2015; Kanwal et al., 2016). The decrease in DNMT expression after chrysin treatment was well correlated with the decrease in global DNA methylation (**Figure 6A**) and modulation pattern of CpG promoter methylation of TSGs (*APC*, *BRCA1*, *FHIT*, *CDH1*, *CDH13*, *MGMT*, *MLH1*, *GSTP1*, *TIMP3*, *RARB*, *RASSIF1*, *SOCS1*, *PTEN*, *VHL*, and *WIFI*) (**Figure 6B**) after chrysin treatment of 10 and 15 μM for 48 h. This study revealed that chrysin treatment downregulated global DNA methylation levels by decreasing to 61, 44, and 30% at 5, 10, and 15 μM chrysin treatment, respectively, for 48 h compared to DMSO controls (**Figure 6A**). Hypermethylation of TSGs leads to silencing of these genes and has been found to be well correlated with the overexpression of various DNMTs in cervical cancer (Guo et al., 2015; Jiménez–wences et al., 2014). Interestingly, this is the very first time it has been reported that chrysin treatment significantly decreases the methylation levels at the promoter region of several TSGs *viz APC*, *CDH1*, *CDH13*, *BRCA1*, *CDKN2A*, *DAPK1*, *FHIT*, *GSTP1*, *MGMT*, *MLH1*, *PTEN*, *RARB*, *RASSF1*, *SOCS1*, *TIMP3*, and *WIFI* (**Figure 6B** and **Table 4**), which are found to be hypermethylated in many cancers and have critical roles to play in various cellular processes (Mukherjee et al., 2015). Hypermethylation of *PTEN* and *RASSIF1* is a common feature in cervical cancers. *PTEN* has an important role in cell migration and proliferation, and inhibits migration by being the antagonist of MMPs (Salimi Sartakhti et al., 2017), whereas reduced RASSIF1 quenches cell death by the receptor mode. VHL is important for stabilization of HIF1 and HIF2, and methylation of other TSGs like RARB and FHIT leads to uncontrolled proliferation; GSTP1 is involved in detoxification of harmful compounds, and MGMT is important for DNA repair (Mukherjee et al., 2015). A reduction of CpG methylation at the abovementioned gene loci can be correlated to reactivation of these genes at the transcription level; chrysin treatment upregulated the expression of *PTEN*, *CDH1*, *TP53*, *FHIT*, *RASSIFI*, *SOCS1*, *RARB*, *TIMP3*, and *TIMP4* (**Figure 3A**) in our study. Several polyphenols including chrysin and luteolin have shown modulation of methylation, and thus reactivation of the silenced TSGs (Aggarwal et al., 2015; Ali Khan et al., 2015; Busch et al., 2015; Kanwal et al., 2016; Carlos-Reyes et al., 2019).

Apart from DNA modification, histone modifications like histone acetylation and histone methylation influence the expression of various genes that have an important role in cancer cell proliferation and migration (Chakravarthy et al., 2005; Dueñas–González et al., 2005; Soto et al., 2017). HDACs deacetylate histone and non-histone proteins such as TP53, rendering them non-functional (Chakrabarti et al., 2015). Overexpression of HDAC1, HDAC2, HDAC3, and HDAC6 has been reported in different cancers (Kogan et al., 2017; Lin et al., 2009; Huang et al., 2005; Zhang et al., 2016; Ahn and Yoon, 2017). HDAC overexpression together with DNA methylation and other histone

modifications silences tumor-suppressor genes (Rose and Klose, 2014; Jenuwein and Allis, 2001). In our study, chrysin was found to decrease the expression of various HDACs (1, 2, 3, 11, and 4), HAT1, EHM2, AURKA, AURKB, PRMT 8, ASH1l, USP21, and USP22 at the transcript level, and increased the expression of ESCO2 and CIITA in a dose-dependent manner (RQs are given in **Table 3** and **Figure 5A**). Chrysin treatment decreased the HDAC activity in a dose-dependent manner; HDAC activity decreased by 30, 36, and 42% after 5, 10, and 15 μM chrysin treatment, respectively (**Figure 4B**). This was further endorsed by decrease in the expression at the transcript level of HDACs 1, 2, 3, 4, and 11 in a significant manner at 10 and 15 μM chrysin treatment for 48 h (**Figure 5A**). HAT1 is upregulated in cervical cancer and is responsible for the induction of colony formation (Kedhari Sundaram et al., 2019b). Chrysin downregulated the activity of HAT by 22, 34, and 52% at 5, 10, and 15 μM chrysin, respectively (**Figure 4C**). It also reduced the expression of HAT in a dose-dependent manner at the transcript level with RQ of 0.31 at 15 μM (**Figure 5A**) and thus correlated with complete inhibition of colony formation. Similar results were reported by other researchers who observed inhibition of HDAC two and eight and upregulation of H3acK14, H4acK12, and H4acK16, and decrease in H3me2K9 methylation in different cell lines (Pal-Bhadra et al., 2012; Sun et al., 2012).

CIITA and ESCO2 were up-regulated after chrysin treatment (**Figure 5A**). CIITA positively regulates the expression of class II major histocompatibility complex and is often found to be methylated in cancer cells (Ramia et al., 2019). ESCO2 histone acetyltransferase curbs MMP2 and also encourages apoptosis in cancer cells (Guo et al., 2018). Trimethylation of lysine 9 and 27 of histone 3 (H3K9 and H3K27) at the promoter region is related to reduced TSG expression (Trievel, 2004; Daniel et al., 2005; Lachner et al., 2001). These marks are found to be overactive in cervical cancer (Chen et al., 2017). Remarkably, in the current study, chrysin downregulated all mono, di, and trimethylation marks at H3K9 (**Figure 5B**), and this was further verified by the assessment of H3K9 methyltransferase activity after incubation of HeLa cells with chrysin. Also, it was found that H3K9 HMT activity was significantly reduced by 25, 38, and 45% against 5, 10, and 15 μM chrysin treatment (**Figure 4D**). Moreover, chrysin also downregulated EHM2 expression (**Figure 5A**), which is responsible for methylation of H3K9. All the methylation marks at H3K27, H3K36, H3K79, and H3K4 were downregulated after chrysin treatment (**Figure 5B**). H3K4 mono and demethylation are related to transcription activation (Chang and Yu, 2016b). H4 acetylation marks such as H4K5, H4K8, H4K12, and H4k16 were also reduced by chrysin (**Figure 5C**). This is in line with the previously published report on a flavone luteolin, wherein it blocks the acetylation of histone H4 and controls the activity of c-FOS, p21, and other genes related to cell cycle control (Izzo et al., 2020). Thus, it can be suggested that chrysin is a potent inhibitor of DNA methyl transferases and histone methyltransferases, and thus modulates the methylation of TSGs.

The overexpression of any one of the EMT inducers such as Twist TGF-β1 or Snail upregulates FOXC2 expression and can lead to the initiation of EMT (Mani et al., 2007). In fact, a significant cadherin switch from E-cadherin to N-cadherin is expressed in cancer progression (Kouzarides, 2007). VE-cadherin, another cadherin, mediates cell-to-cell bonding by holding the catenin in between, which in turn connects the actin cytoskeleton of the cells. Both E cadherin and VE-cadherin are down-regulated in cancer progression (Ramis-Conde et al., 2009). It was observed that chrysin (10 and 15 μM for 48 h) decreased the expression of *SNAIL*, *TWIST* (**Figure 3A**), and FOXC2 (**Figure 3B** and **3C**), and increased the expression of E cadherin (**Figure 3B**). The suppressor of cytokine signaling 1 (SOCS1) is a tumor-suppressor gene and suppresses cytokine signaling and destroys the HPV E7 protein. SOCS1 is hypermethylated in cervical cancer and renewal of its expression upsurges Rb protein thereby inhibits cell proliferation (Kamio et al., 2004; Sobti et al., 2011). A decrease in E cadherin can be linked to WNT signaling which prevents phosphorylation of SNAIL, allowing it to accumulate and repress cadherin (Loh et al., 2019). Based upon the findings from the present study, it can be proposed that the restoration of transcription in the tumor-suppressor genes plays a crucial role in the anticancer potential of chrysin against HeLa cells, as it can directly influence cell proliferation and cell migration. Our current results are based on the chrysin efficacy on HeLa cells, but can further be extrapolated on other cell lines and animal models.

CONCLUSION

Chrysin appears to be a promising natural chemopreventive agent which is cytotoxic to cancer cells and inhibits migration, diminishes CpG promoter methylation of TSG modulates, and causes re-expression of TSG, and downregulation of genes related to migration and inflammation. Hence, chrysin can be exploited for further use at a clinical setup after experimental validation and checking its pharmacokinetic properties involving human subjects.

DATA AVAILABILITY STATEMENT

The original contributions presented in the study are included in the article, further inquiries can be directed to the corresponding authors.

AUTHOR CONTRIBUTIONS

RR, NA, and AH contributed to conception, design of study, experimental work, and manuscript preparation; AA and SB contributed to data validation and review; SH and SF contributed to data validation and statistical analysis.

ACKNOWLEDGMENTS

The authors are thankful to MAHE DUBAI Internal research grant (R and DP/MAHE DUBAI/RL-02/19) for the financial support. The author (AM) is thankful to the Deanship of Scientific Research, Qassim University, for funding the publication of this project.

REFERENCES

Aggarwal, R., Jha, M., Shrivastava, A., and Jha, A. K. (2015). Natural Compounds: Role in Reversal of Epigenetic Changes. *Biochem. Mosc.* 80, 972–989. doi:10.1134/S0006297915080027

Ahn, M.-Y., and Yoon, J.-H. (2017). Histone Deacetylase 7 Silencing Induces Apoptosis and Autophagy in Salivary Mucoepidermoid Carcinoma Cells. *J. Oral Pathol. Med.* 46, 276–283. doi:10.1111/jop.12560

Ali Khan, M., Kedhari Sundaram, M., Hamza, A., Quraishi, U., Gunasekera, D., Ramesh, L., et al. (2015). Sulforaphane Reverses the Expression of Various Tumor Suppressor Genes by Targeting DNMT3B and HDAC1 in Human Cervical Cancer Cells. *Evidence-Based Complement. Altern. Med.* 2015, 1–12. doi:10.1155/2015/412149

Andrijauskaite, K., Morris, J., and Wargovich, M. J. (2019). "Natural Anticancer Agents," in *Epigenetics of Cancer Prevention* (Elsevier), 49–73. doi:10.1016/b978-0-12-812494-9.00003-2

Baruah, M. M., Khandwekar, A. P., and Sharma, N. (2016). Quercetin Modulates Wnt Signaling Components in Prostate Cancer Cell Line by Inhibiting Cell Viability, Migration, and Metastases. *Tumor Biol.* 37, 14025–14034. doi:10.1007/s13277-016-5277-6

Busch, C., Burkard, M., Leischner, C., Lauer, U. M., Frank, J., and Venturelli, S. (2015). Epigenetic Activities of Flavonoids in the Prevention and Treatment of Cancer. *Clin. Epigenet.* 7, 64. doi:10.1186/s13148-015-0095-z

Carlos-Reyes, Á., López-González, J. S., Meneses-Flores, M., Gallardo-Rincón, D., Ruíz-García, E., Marchat, L. A., et al. (2019). Dietary Compounds as Epigenetic Modulating Agents in Cancer. *Front. Genet.* 10, 1–14. doi:10.3389/fgene.2019.00079

Chakrabarti, A., Oehme, I., Witt, O., Oliveira, G., Sippl, W., Romier, C., et al. (2015). HDAC8: a Multifaceted Target for Therapeutic Interventions. *Trends Pharmacol. Sci.* 36, 481–492. doi:10.1016/j.tips.2015.04.013

Chakravarthy, S., Park, Y.-J., Chodaparambil, J., Edayathumangalam, R. S., and Luger, K. (2005). Structure and Dynamic Properties of Nucleosome Core Particles. *FEBS Lett.* 579, 895–898. doi:10.1016/j.febslet.2004.11.030

Chang, L.-C., and Yu, Y.-L. (2016). Dietary Components as Epigenetic-Regulating Agents against Cancer. *BioMed* 6, 9–16. doi:10.7603/s40681-016-0002-8

Chang, L. C., and Yu, Y. L. (2016). Dietary Components as Epigenetic-Regulating Agents against Cancer. *Biomedicine (Taipei)* 6, 2–8. doi:10.7603/s40681-016-0002-8

Charostad, J., Astani, A., Goudarzi, H., and Faghihloo, E. (2019). DNA Methyltransferases in Virus-Associated Cancers. *Rev. Med. Virol.* 29, e2022. doi:10.1002/rmv.2022

Chatterjee, A., Rodger, E. J., and Eccles, M. R. (2018). Epigenetic Drivers of Tumourigenesis and Cancer Metastasis. *Semin. Cancer Biol.* 51, 149–159. doi:10.1016/j.semcancer.2017.08.004

Chen, R.-J., Shun, C.-T., Yen, M.-L., Chou, C.-H., and Lin, M.-C. (2017). Methyltransferase G9a Promotes Cervical Cancer Angiogenesis and Decreases Patient Survival. *Oncotarget* 8, 62081–62098. doi:10.18632/oncotarget.19060

Chistiakov, D. A. D., Myasoedova, V. A. V., Orekhov, A. N., and Bobryshev, Y. V. (2017). Epigenetically Active Drugs Inhibiting DNA Methylation and Histone Deacetylation. *Cpd* 23, 1167–1174. doi:10.2174/1381612822666161021110827

Crowley, L. C., Marfell, B. J., Scott, A. P., Boughaba, J. A., Chojnowski, G., Christensen, M. E., et al. (2016). Dead Cert: Measuring Cell Death. *Cold Spring Harb. Protoc.* 2016, pdb.top070318–1072. doi:10.1101/pdb.top070318

Daniel, J. A., Pray-Grant, M. G., and Grant, P. A. (2005). Effector Proteins for Methylated Histones: an Expanding Family. *Cell Cycle* 4, 919. doi:10.4161/cc.4.7.1824

Deivendran, S., Marzook, K. H., and Radhakrishna Pillai, M. (2014). The Role of Inflammation in Cervical Cancer. *Adv. Exp. Med. Biol.* 816, 377–399. doi:10.1007/978-3-0348-0837-8_15

Dueñas-González, A., Lizano, M., Candelaria, M., Cetina, L., Arce, C., and Cervera, E. (2005). Epigenetics of Cervical Cancer. An Overview and Therapeutic Perspectives. *Mol. Cancer* 4, 1–24. doi:10.1186/1476-4598-4-38

Ganai, S. A., Sheikh, F. A., Baba, Z. A., Mir, M. A., Mantoo, M. A., and Yatoo, M. A. (2021). Anticancer Activity of the Plant Flavonoid Luteolin against Preclinical Models of Various Cancers and Insights on Different Signalling Mechanisms Modulated. *Phytotherapy Res.* 35, 3509–3532. doi:10.1002/ptr.7044

Ganai, S. A., Sheikh, F. A., and Baba, Z. A. (2021). Plant Flavone Chrysin as an Emerging Histone Deacetylase Inhibitor for Prosperous Epigenetic-based Anticancer Therapy. *Phytotherapy Res.* 35, 823–834. doi:10.1002/ptr.6869

Guo, X.-B., Huang, B., Pan, Y.-H., Su, S.-G., and Li, Y. (2018). ESCO2 Inhibits Tumor Metastasis via Transcriptionally Repressing MMP2 in Colorectal Cancer. *Cmar* 10, 6157–6166. doi:10.2147/cmar.s181265

Guo, Y., Su, Z.-Y., and Kong, A.-N. T. (2015). Current Perspectives on Epigenetic Modifications by Dietary Chemopreventive and Herbal Phytochemicals. *Curr. Pharmacol. Rep.* 1, 245–257. doi:10.1007/s40495-015-0023-0

Hatzimichael, E., and Crook, T. (2013). Cancer Epigenetics: New Therapies and New Challenges. *J. Drug Deliv.* 2013, 529312. doi:10.1155/2013/529312

Heerboth, S., Lapinska, K., Snyder, N., Leary, M., Rollinson, S., and Sarkar, S. (2014). Use of Epigenetic Drugs in Disease: An Overview. *Genet. Epigenet.* 6, GEG.S12270–19. doi:10.4137/GeG.s12270

Herranz, M., and Esteller, M. (2007). "DNA Methylation and Histone Modifications in Patients with Cancer," in *Target Discovery and Validation Reviews and Protocols* (Springer), 25–62.

Herranz, M., and Esteller, M. (2007). DNA Methylation and Histone Modifications in Patients with Cancer: Potential Prognostic and Therapeutic Targets. *Methods Mol. Biol.* 361, 25–62. doi:10.1385/1-59745-208-4:25

Ho, A. S., Turcan, S., and Chan, T. A. (2013). Epigenetic Therapy: Use of Agents Targeting Deacetylation and Methylation in Cancer Management. *Onco Targets Ther.* 6, 223–232. doi:10.2147/OTT.S34680

Huang, B. H., Laban, M., Leung, C. H.-W., Lee, L., Lee, C. K., Salto-Tellez, M., et al. (2005). Inhibition of Histone Deacetylase 2 Increases Apoptosis and p21Cip1/WAF1 Expression, Independent of Histone Deacetylase 1. *Cell Death Differ.* 12, 395–404. doi:10.1038/sj.cdd.4401567

Huang, J., Plass, C., and Gerhauser, C. (2011). Cancer Chemoprevention by Targeting the Epigenome. *Cdt* 12, 1925–1956. doi:10.2174/138945011798184155

Izzo, S., Naponelli, V., and Bettuzzi, S. (2020). Flavonoids as Epigenetic Modulators for Prostate Cancer Prevention. *Nutrients* 12, 1010–1024. doi:10.3390/nu12041010

Jenuwein, T., and Allis, C. D. (2001). Translating the Histone Code. *Science* 293, 1074–1080. doi:10.1126/science.1063127

Jiménez-wences, H., Peralta-Zaragoza, O., and Fernández-tilapa, G. (2014). Human Papilloma Virus, DNA Methylation and microRNA Expression in Cervical Cancer (Review). *Oncol. Rep.* 31, 2467–2476. doi:10.3892/or.2014.3142

Kai, L., Samuel, S. K., and Levenson, A. S. (2010). Resveratrol Enhances P53 Acetylation and Apoptosis in Prostate Cancer by Inhibiting MTA1/NuRD Complex. *Int. J. Cancer* 126, 1538–1548. doi:10.1002/ijc.24928

Kamio, M., Yoshida, T., Ogata, H., Douchi, T., Nagata, Y., Inoue, M., et al. (2004). SOC1 Inhibits HPV-E7-Mediated Transformation by Inducing Degradation of E7 Protein. *Oncogene* 23, 3107–3115. doi:10.1038/sj.onc.1207453

Kanwal, R., Gupta, K., and Gupta, S. (2015). "Aberrant DNA Methylation Is One of the Most Important Epigenetic Modifications in Cancer Cells and it Is Also Associated with Histone Modifications and Their Interaction of Is Crucial to Regulate the Functioning of the Genome by Changing Chromatin Archite," in *Cancer Epigenetics* (Springer), 3–25.

Kanwal, R., Datt, M., Liu, X., and Gupta, S. (2016). Dietary Flavones as Dual Inhibitors of DNA Methyltransferases and Histone Methyltransferases. *PLoS One* 11, e0162956. doi:10.1371/journal.pone.0162956

Kasala, E. R., Bodduluru, L. N., Madana, R. M., V, A. K., Gogoi, R., Barua, C. C., et al. (2015). Chemopreventive and Therapeutic Potential of Chrysin in Cancer: Mechanistic Perspectives. *Toxicol. Lett.* 233, 214–225. doi:10.1016/j.toxlet.2015.01.008

Kedhari Sundaram, M., Raina, R., Afroze, N., Bajbouj, K., Hamad, M., Haque, S., et al. (2019). Quercetin Modulates Signaling Pathways and Induces Apoptosis in Cervical Cancer Cells. *Biosci. Rep.* 39. doi:10.1042/BSR20190720

Kedhari Sundaram, M., Hussain, A., Haque, S., Raina, R., and Afroze, N. (2019). Quercetin Modifies 5′CpG Promoter Methylation and Reactivates Various Tumor Suppressor Genes by Modulating Epigenetic marks in Human

Cervical Cancer Cells. *J. Cel. Biochem.* 120, 18357–18369. doi:10.1002/jcb.29147

Khoo, B. Y., Chua, S. L., and Balaram, P. (2010). Apoptotic Effects of Chrysin in Human Cancer Cell Lines. *Ijms* 11, 2188–2199. doi:10.3390/ijms11052188

Kim, S. O., and Kim, M. R. (2013). (-)-Epigallocatechin 3-gallate Inhibits Invasion by Inducing the Expression of Raf Kinase Inhibitor Protein in AsPC-1 Human Pancreatic Adenocarcinoma Cells through the Modulation of Histone Deacetylase Activity. *Int. J. Oncol.* 42, 349–358. doi:10.3892/ijo.2012.1686

Kogan, E. A., Unanyan, A. L., Kadyrova, A. E., Demura, T. A., Sidorova, I. S., Faizullin, R. I., et al. (2017). Immunohistochemical Analysis of Epigenetic Markers in Cervical Pathologies Associated with Human Papillomavirus Infection. *BioNanoSci.* 7, 284–287. doi:10.1007/s12668-016-0339-1

Koosha, S., Alshawsh, M. A., Looi, C. Y., Seyedan, A., and Mohamed, Z. (2016). An Association Map on the Effect of Flavonoids on the Signaling Pathways in Colorectal Cancer. *Int. J. Med. Sci.* 13, 374–385. doi:10.7150/ijms.14485

Kouzarides, T. (2007). Chromatin Modifications and Their Function. *Cell* 128, 693–705. doi:10.1016/j.cell.2007.02.005

Lachner, M., O'Carroll, D., Rea, S., Mechtler, K., and Jenuwein, T. (2001). Methylation of Histone H3 Lysine 9 Creates a Binding Site for HP1 Proteins. *Nature* 410, 116–120. doi:10.1038/35065132

Li, L-L., and Wang, S-S. (2017). DNA Methyltransferase (DNMTs) Expression in Cervical Cancer Tissues and its Relationship with HPV Infection and Tumor Malignancy. *J. Hainan Med. Univ.* 23, 136–139.

Lim, W., Ryu, S., Bazer, F. W., Kim, S.-M., and Song, G. (2018). Chrysin Attenuates Progression of Ovarian Cancer Cells by Regulating Signaling Cascades and Mitochondrial Dysfunction. *J. Cel. Physiol.* 233, 3129–3140. doi:10.1002/jcp.26150

Lin, Z., Bazzaro, M., Wang, M.-C., Chan, K. C., Peng, S., and Roden, R. B. S. (2009). Combination of Proteasome and HDAC Inhibitors for Uterine Cervical Cancer Treatment. *Clin. Cancer Res.* 15, 570–577. doi:10.1158/1078-0432.CCR-08-1813

Liskova, A., Koklesova, L., Samec, M., Smejkal, K., Samuel, S. M., Varghese, E., et al. (2020). Flavonoids in Cancer Metastasis. *Cancers* 12, 1498. doi:10.3390/cancers12061498

Loh, C.-Y., Chai, J., Tang, T., Wong, W., Sethi, G., Shanmugam, M., et al. (2019). The E-Cadherin and N-Cadherin Switch in Epithelial-To-Mesenchymal Transition: Signaling, Therapeutic Implications, and Challenges. *Cells* 8, 1118. doi:10.3390/cells8101118

Mani, S. A., Yang, J., Brooks, M., Schwaninger, G., Zhou, A., Miura, N., et al. (2007). Mesenchyme Forkhead 1 (FOXC2) Plays a Key Role in Metastasis and Is Associated with Aggressive Basal-like Breast Cancers. *Proc. Natl. Acad. Sci.* 104, 10069–10074. doi:10.1073/pnas.0703900104

McLaughlin-Drubin, M. E., Crum, C. P., and Münger, K. (2011). Human Papillomavirus E7 Oncoprotein Induces KDM6A and KDM6B Histone Demethylase Expression and Causes Epigenetic Reprogramming. *Proc. Natl. Acad. Sci. USA* 108, 2130–2135. doi:10.1073/pnas.1009933108

Mocanu, M.-M., Nagy, P., and Szöllősi, J. (2015). Chemoprevention of Breast Cancer by Dietary Polyphenols. *Molecules* 20, 22578–22620. doi:10.3390/molecules201219864

Mukherjee, N., Kumar, A. P., and Ghosh, R. (2015). DNA Methylation and Flavonoids in Genitourinary Cancers. *Curr. Pharmacol. Rep.* 1, 112–120. doi:10.1007/s40495-014-0004-8

Ong, T. P., Moreno, F. S., and Ross, S. A. (2011). Targeting the Epigenome with Bioactive Food Components for Cancer Prevention. *J. Nutrigenet. Nutrigenomics* 4, 275–292. doi:10.1159/000334585

Pal-Bhadra, M., Ramaiah, M. J., Reddy, T. L., Krishnan, A., Pushpavalli, S., Babu, K. S., et al. (2012). Plant HDAC Inhibitor Chrysin Arrest Cell Growth and Induce P21 WAF1 by Altering Chromatin of STAT Response Element in A375 Cells. *BMC Cancer* 12, 180. doi:10.1186/1471-2407-12-180

Paredes-Gonzalez, X., Fuentes, F., Su, Z.-Y., and Kong, A.-N. T. (2014). Apigenin Reactivates Nrf2 Anti-oxidative Stress Signaling in Mouse Skin Epidermal JB6 P + Cells through Epigenetics Modifications. *AAPS J.* 16, 727–735. doi:10.1208/s12248-014-9613-8

Piyathilake, C., Badiga, S., Borak, S., Weragoda, J., Bae, S., Matthews, R., et al. (2017). A Higher Degree of Expression of DNA Methyl Transferase 1 in Cervical Cancer Is Associated with Poor Survival Outcome. *Ijwh* 9, 413–420. doi:10.2147/IJWH.S133441

Rahman, M. S., Jamil, H. M., Akhtar, N., Islam, R., Abdul-Awal, S. M., Rana, M. M., et al. (2016). Cancer Epigenetics and Epigenetical Therapy. *J. Exp. Integr. Med.* 6, 1. doi:10.5455/jeim.270616.rw.016

Raina, R., Afroze, N., Kedhari Sundaram, M., Haque, S., Bajbouj, K., Hamad, M., et al. (2021). Chrysin Inhibits Propagation of HeLa Cells by Attenuating Cell Survival and Inducing Apoptotic Pathways. *Eur. Rev. Med. Pharmacol. Sci.* 25, 2206–2220. doi:10.26355/eurrev_202103_25253

Ramia, E., Chiaravalli, A. M., Bou Nasser Eddine, F. F., Tedeschi, A., Sessa, F., Accolla, R. S., et al. (2019). CIITA-related Block of HLA Class II Expression, Upregulation of HLA Class I, and Heterogeneous Expression of Immune Checkpoints in Hepatocarcinomas: Implications for New Therapeutic Approaches. *Oncoimmunology* 8, 1548243. doi:10.1080/2162402X.2018.1548243

Ramis-Conde, I., Chaplain, M. A., Anderson, A. R., and Drasdo, D. (2009). Multi-scale Modelling of Cancer Cell Intravasation: the Role of Cadherins in Metastasis. *Phys. Biol.* 6, 016008. doi:10.1088/1478-3975/6/1/016008

Rose, N. R., and Klose, R. J. (2014). Understanding the Relationship between DNA Methylation and Histone Lysine Methylation. *Biochim. Biophys. Acta (Bba) - Gene Regul. Mech.* 1839, 1362–1372. doi:10.1016/j.bbagrm.2014.02.007

Ryu, S., Lim, W., Bazer, F. W., and Song, G. (2017). Chrysin Induces Death of Prostate Cancer Cells by Inducing ROS and ER Stress. *J. Cel. Physiol.* 232, 3786–3797. doi:10.1002/jcp.25861

Salimi Sartakhti, J., Manshaei, M. H., and Sadeghi, M. (2017). MMP-TIMP Interactions in Cancer Invasion: An Evolutionary Game-Theoretical Framework. *J. Theor. Biol.* 412, 17–26. doi:10.1016/j.jtbi.2016.09.019

Shankar, E., Kanwal, R., Candamo, M., and Gupta, S. (2016). Dietary Phytochemicals as Epigenetic Modifiers in Cancer: Promise and Challenges. *Semin. Cancer Biol.* 40-41, 82–99. doi:10.1016/j.semcancer.2016.04.002

Sharma, S., Kelly, T. K., and Jones, P. A. (2009). Epigenetics in Cancer. *Carcinogenesis* 31, 27–36. doi:10.1093/carcin/bgp220

Sobti, R. C., Singh, N., Hussain, S., Suri, V., Nijhawan, R., Bharti, A. C., et al. (2011). Aberrant Promoter Methylation and Loss of Suppressor of Cytokine Signalling-1 Gene Expression in the Development of Uterine Cervical Carcinogenesis. *Cell Oncol.* 34, 533–543. doi:10.1007/s13402-011-0056-2

Soto, D., Song, C., and McLaughlin-Drubin, M. E. (2017). Epigenetic Alterations in Human Papillomavirus-Associated Cancers. *Viruses* 9, 248. doi:10.3390/v9090248

Sun, L.-P., Chen, A.-L., Hung, H.-C., Chien, Y.-H., Huang, J.-S., Huang, C.-Y., et al. (2012). Chrysin: a Histone Deacetylase 8 Inhibitor with Anticancer Activity and a Suitable Candidate for the Standardization of Chinese Propolis. *J. Agric. Food Chem.* 60, 11748–11758. doi:10.1021/jf303261r

Trievel, R. C. (2004). Structure and Function of Histone Methyltransferases. *Crit. Rev. Eukaryot. Gene Expr.* 14, 147–170. doi:10.1615/CritRevEukaryotGeneExpr.v14.i3.10

Wang, J., Wang, H., Sun, K., Wang, X., Pan, H., Zhu, J., et al. (2018). Chrysin Suppresses Proliferation, Migration, and Invasion in Glioblastoma Cell Lines via Mediating the ERK/Nrf2 Signaling Pathway. *Dddt* 12, 721–733. doi:10.2147/dddt.s160020

Wang, X., Jiang, Z., An, J., Mao, X., Lin, F., and Sun, P. (2018). Effect of a Synthetic Inhibitor of Urokinase Plasminogen Activator on the Migration and Invasion of Human Cervical Cancer Cells *In Vitro*. *Mol. Med. Rep.* 17, 4273–4280. doi:10.3892/mmr.2018.8414

Wu, D., Zhao, B., Song, Y., Chi, X., Fu, H., Guan, T., et al. (2021). Nogo-B Receptor Is Required for Stabilizing TGF-β Type Ireceptor and Promotes the TGF-B1-Induced Epithelial-To-Mesenchymal Transition of Non-small Cell Lung Cancer. *J. Cancer* 12, 717–725. doi:10.7150/jca.50483

Xia, Y., Lian, S., Khoi, P. N., Yoon, H. J., Joo, Y. E., Chay, K. O., et al. (2015). Chrysin Inhibits Tumor Promoter-Induced MMP-9 Expression by Blocking AP-1 via Suppression of ERK and JNK Pathways in Gastric Cancer Cells. *PLoS One* 10, e0124007. doi:10.1371/journal.pone.0124007

Xue, G., Restuccia, D. F., Lan, Q., Hynx, D., Dirnhofer, S., Hess, D., et al. (2012). Akt/PKB-Mediated Phosphorylation of Twist1 Promotes Tumor Metastasis via Mediating Cross-Talk between PI3K/Akt and TGF-β Signaling Axes. *Cancer Discov.* 2, 248–259. doi:10.1158/2159-8290.cd-11-0270

Yan, W., Wu, T. H. Y., Leung, S. S. Y., and To, K. K. W. (2020). Flavonoids Potentiated Anticancer Activity of Cisplatin in Non-small Cell Lung Cancer Cells *In Vitro* by Inhibiting Histone Deacetylases. *Life Sci.* 258, 118211. doi:10.1016/j.lfs.2020.118211

Yang, B., Huang, J., Xiang, T., Yin, X., Luo, X., Huang, J., et al. (2014). Chrysin Inhibits Metastatic Potential of Human Triple-Negative Breast Cancer Cells by Modulating Matrix Metalloproteinase-10, Epithelial to Mesenchymal Transition, and PI3K/Akt Signaling Pathway. *J. Appl. Toxicol.* 34, 105–112. doi:10.1002/jat.2941

You, J. S., and Jones, P. A. (2012). Cancer Genetics and Epigenetics: Two Sides of the Same Coin? *Cancer Cell* 22, 9–20. doi:10.1016/j.ccr.2012.06.008

Zam, W., and Khadour, A. (2017). Impact of Phytochemicals and Dietary Patterns on Epigenome and Cancer. *Nutr. Cancer* 69, 184–200. doi:10.1080/01635581.2017.1263746

Zhang, L., Yuan, C., Wang, Y., and Zhao, S. (2016). Histone Deacetylases 3 (HDAC3) Is Highly Expressed in Cervical Cancer and Inhibited by siRNA. *Int. J. Clin. Exp. Pathol.* 9, 3600–3605.

Conflict of Interest: The authors declare that the research was conducted in the absence of any commercial or financial relationships that could be construed as a potential conflict of interest.

Publisher's Note: All claims expressed in this article are solely those of the authors and do not necessarily represent those of their affiliated organizations, or those of the publisher, the editors, and the reviewers. Any product that may be evaluated in this article, or claim that may be made by its manufacturer, is not guaranteed or endorsed by the publisher.

Advantages of publishing in Frontiers

OPEN ACCESS
Articles are free to read for greatest visibility and readership

FAST PUBLICATION
Around 90 days from submission to decision

HIGH QUALITY PEER-REVIEW
Rigorous, collaborative, and constructive peer-review

TRANSPARENT PEER-REVIEW
Editors and reviewers acknowledged by name on published articles

Frontiers
Avenue du Tribunal-Fédéral 34
1005 Lausanne | Switzerland

Visit us: www.frontiersin.org
Contact us: frontiersin.org/about/contact

REPRODUCIBILITY OF RESEARCH
Support open data and methods to enhance research reproducibility

DIGITAL PUBLISHING
Articles designed for optimal readership across devices

FOLLOW US
@frontiersin

IMPACT METRICS
Advanced article metrics track visibility across digital media

EXTENSIVE PROMOTION
Marketing and promotion of impactful research

LOOP RESEARCH NETWORK
Our network increases your article's readership